VOL. **481** NOVEMBER 3, 1989

COMPLETE IN ONE ISSUE

OF

IROMATOGRAPHY

TIONAL JOURNAL ON CHROMATOGRAPHY, ELECTROPHORESIS AND RELATED METHODS

ELSEVIER

JOURNAL OF CHROMATOGRAPHY

Scope. The *Journal of Chromatography* publishes papers on all aspects of chromatography, electrophoresis and related methods. Contributions consist mainly of research papers dealing with chromatographic theory, instrumental development and their applications. The section *Biomedical Applications*, which is under separate editorship, deals with the following aspects: developments in and applications of chromatographic and electrophoretic techniques related to clinical diagnosis or alterations during medical treatment; screening and profiling of body fluids or tissues with special reference to metabolic disorders; results from basic medical research with direct consequences in clinical practice; drug level monitoring and pharmacokinetic studies; clinical toxicology; analytical studies in occupational medicine.

Submission of Papers. Papers in English, French and German may be submitted, in three copies. Manuscripts should be submitted to: The Editor of *Journal of Chromatography*, P.O. Box 681, 1000 AR Amsterdam, The Netherlands, or to: The Editor of *Journal of Chromatography, Biomedical Applications*, P.O. Box 681, 1000 AR Amsterdam, The Netherlands. Review articles are invited or proposed by letter to the Editors. An outline of the proposed review should first be forwarded to the Editors for preliminary discussion prior to preparation. Submission of an article is understood to imply that the article is original and unpublished and is not being considered for publication elsewhere. For copyright regulations, see below.

Subscription Orders. Subscription orders should be sent to: Elsevier Science Publishers B.V., P.O. Box 211, 1000 AE Amsterdam, The Netherlands, Tel. 5803 911, Telex 18582 ESPA NL. The *Journal of Chromatography* and the *Biomedical Applications* section can be subscribed to separately.

Publication. The *Journal of Chromatography* (incl. *Biomedical Applications*) has 37 volumes in 1989. The subscription prices for 1989 are:

J. Chromatogr. + *Biomed. Appl.* (Vols. 461–497):
Dfl. 6475.00 plus Dfl. 999.00 (p.p.h.) (total *ca.* US$ 3428,50)

J. Chromatogr. only (Vols. 461–486):
Dfl. 5200.00 plus Dfl. 702.00 (p.p.h.) (total *ca.* US$ 2707.25)

Biomed. Appl. only (Vols. 487–497):
Dfl. 2200.00 plus Dfl. 297.00 (p.p.h.) (total *ca.* US$ 1145.50).

Our p.p.h. (postage, package and handling) charge includes surface delivery of all issues, except to subscribers in Argentina, Australia, Brasil, Canada, China, Hong Kong, India, Israel, Malaysia, Mexico, New Zealand, Pakistan, Singapore, South Africa, South Korea, Taiwan, Thailand and the U.S.A. who receive all issues by air delivery (S.A.L. — Surface Air Lifted) ' no extra cost. For Japan, air delivery requires 50% additional charge; for all other countries airmail and S.A.L. charges are available upon request. Back volumes of the *Journal of Chromatography* (Vols. 1–460) are available at Dfl. 195.00 (plus postage). Claims for missing issues will be honoured, free of charge, within three months after publication of the issue. Customers in the U.S.A. and Canada wishing information on this and other Elsevier journals, please contact Journal Information Center, Elsevier Science Publishing Co. Inc., 655 Avenue of the Americas, New York, NY 10010. Tel. (212) 633-3750.

Abstracts/Contents Lists published in Analytical Abstracts, ASCA, Biochemical Abstracts, Biological Abstracts, Chemical Abstracts, Chemical Titles, Chromatography Abstracts, Clinical Chemistry Lookout, Current Contents/Physical, Chemical & Earth Sciences, Current Contents/Life Sciences, Deep-Sea Research/Part B: Oceanographic Literature Review, Excerpta Medica, Index Medicus, Mass Spectrometry Bulletin, PASCAL-CNRS, Pharmaceutical Abstracts, Referativnyi Zhurnal, Science Citation Index and Trends in Biotechnology.

See inside back cover for Publication Schedule, Information for Authors and information on Advertisements.

0378-4347/89/$03.50

Printed in The Netherlands

CONTENTS

(Abstracts/Content Lists published in Analytical Abstracts, ASCA, Biochemical Abstracts, Biological Abstracts, Chemical Abstracts, Chemical Titles, Chromatography Abstracts, Current Contents/Physical, Chemical & Earth Sciences, Current Contents/Life Sciences, Deep-Sea Research/Part B: Oceanographic Literature Review, Excerpta Medica, Index Medicus, Mass Spectrometry Bulletin, PASCAL-CNRS, Referativnyi Zhurnal and Science Citation Index)

(Continued overleaf)

(Continued overleaf)

In articles with more than one author, the name of the author to whom correspondence should be addressed is indicated in the article heading by a 6-pointed asterisk (*)

Collect LC peaks in separate tubes

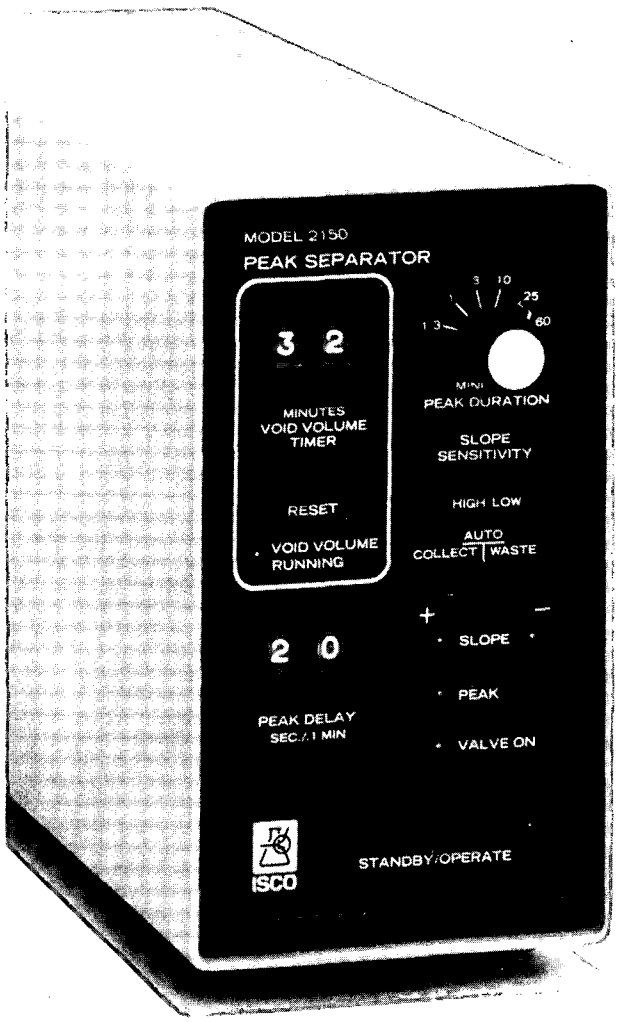

You don't have to choose between diluted peaks or collecting too many small fractions. Isco's peak separator operates with your present UV or other LC detector and fraction collector to put separate peaks into separate test tubes.

Drifting baselines or incomplete resolution are no problem because peaks are identified by their shape, not height. Short HPLC peaks or long prep LC peaks are cut with equal accuracy. A delay timer compensates for the time lag as the peak passes from the flow cell to the fraction collector, and another timer postpones collection until the void volume has eluted. An optional valve lets you collect only peaks, diverting the effluent between peaks to waste or collecting it in a single container for recycling. So isn't it time to stop playing hide and seek with every LC peak?

In the U.S., phone toll free **(800)228-4250** for a complete catalog. In Europe, fax Isco Europe A.G. at **(41-1)920 62 08.**

Isco, Inc.
P.O. Box 5347
Lincoln NE 68505 U.S.A.

Isco Europe AG
Brüschstr. 17
CH8708 Männedorf, Switzerland

ISCO

Distributors • **Austria:** Neuber Gesellschaft mbH • **Belgium:** SA HVL NV • **Denmark:** Mikrolab Aarhus • **Finland:** ETEK OY • **France:** Ets. Roucaire, S.A. • **Germany:** Colora Messtechnik GmbH • **Hungary:** Lasis Handelsges. mbH • **Italy:** Gio. de Vita e C. s.r.l. • **The Netherlands:** Beun-de Ronde B.V. • **Norway:** Dipl. Ing. Houm A.S. • **Spain:** Iberlabo, s.a. • **Sweden:** SAVEN AB • **Switzerland:** IG Instrumenten-Gesellschaft AG • **U.K.:** Life Science Laboratories, Ltd. •

JOURNAL OF CHROMATOGRAPHY

VOL. 481 (1989)

JOURNAL *of* CHROMATOGRAPHY

INTERNATIONAL JOURNAL ON CHROMATOGRAPHY, ELECTROPHORESIS AND RELATED METHODS

ELSEVIER

AMSTERDAM — OXFORD — NEW YORK — TOKYO

0021-9673/89/$03.50

Printed in The Netherlands

Journal of Chromatography, 481 (1989) 1–16
Elsevier Science Publishers B.V., Amsterdam — Printed in The Netherlands

CHROM. 21 775

CORRELATION FOR KOVÁTS RETENTION INDEX OF C_9–C_{26} MONOALKYL AND POLYMETHYL ALKANES AND ALKENES

FARHAD KHORASHEH, MURRAY R. GRAY and MILAN L. SELUCKY*
Department of Chemical Engineering, University of Alberta, Edmonton, Alberta T6G 2G6 (Canada)
(First received March 7th, 1989; revised manuscript received June 30th, 1989)

SUMMARY

Correlations based on graph theoretic indices are proposed for prediction of the Kováts retention index of high-molecular-weight monoalkyl and polymethyl alkanes and alkenes. As a test for the proposed correlations, the Kováts index of monoalkyl hexadecanes in the C_{18}–C_{27} range were experimentally measured and compared with predicted values. Agreement between experimental and predicted values were quite satisfactory with an average error of 8 index units.

INTRODUCTION

The Kováts retention index system[1] is a logarithmic system where the logarithmic retention of a substance is interpolated between those of two standard compounds. Although any homologous series of organic compounds can be used as standards, originally *n*-alkanes were used exclusively. The retention index, I, is defined as:

$$I = 100z + 100\frac{\log t_R(\text{substance}) - \log t_R(z)}{\log t_R(z+1) - \log t_R(z)} \quad (1)$$

where t_R is the net retention time and z represents an *n*-alkane with z carbon atoms. For linear-temperature-programmed gas chromatography, I can be expressed as:

$$I = 100z + 100\frac{t_R(\text{substance}) - t_R(z)}{t_R(z+1) - t_R(z)} \quad (2)$$

Because of the relationship between structure and retention index of organic compounds, Kováts retention index system can be used to identify a component based on its retention behavior. The retention index for a compound depends on the stationary phase, the column temperature, and the structure of the compound. The correlations between structure and retention index for various stationary phases and temperatures have been the subject of many investigations since the initial work by Kováts. All of the methods have one common approach; the retention index is predicted from one or more structural features of the compound.

0021-9673/89/$03.50

Some investigators have taken the group-additivity approach for the prediction of I from structural formula of the compound. Group-additivity methods have been extensively studied by Benson[2] for prediction of thermochemical properties. The main hypothesis is that a property of a compound can be expressed as the sum of additive contributions from every structural group of the molecule.

Takács and co-workers[3–7] in a series of publications developed a scheme for prediction of Kováts retention indexes based on additive index contributions from individual bonds. They gave the index contributions for some 125 different bond types involved in saturated hydrocarbons, 118 bond types involving double bonds, and some 50 bonds involving aromatic and cyclic hydrocarbons. With such a large number of structural parameters, one would expect a high degree of accuracy for the predictive ability of Takács method. The approach of Takács and co-workers, however, has received critical reviews. Vanheertum[8] used the method of Takács to predict the Kováts index of some 80 paraffinic and olefinic compounds. For approximately 20% of the compounds, the error in predicted values was in excess of 10 index units (i.u.). He suggested that the method be expanded to include index contributions from a more complete set of bonds. Such an approach would give rise to even a larger number of structural parameters. Souter[9], on the other hand, criticized the validity of Takács approach. He suggested that predictive methods based on additivity assumption should involve as few groups as possible.

Spivakovskii *et al.*[10] used 28 structural groups for describing aliphatic alcohols and saturated hydrocarbons. The groups considered were structural "fragments" involving several types of bonds rather than a unique bond. The retention index was expressed as the summation of additive index contributions from individual fragments. The individual group contributions were obtained from experimental retention indices of some 97 C_6–C_9 aliphatic alcohols and alkanes on squalane using a least squares regression analysis. They reported a mean square error of 7 i.u. between calculated and experimental values.

Other than additivity schemes, empirical correlations, have been developed, for example by Dimov and Papazova[11–13], for prediction of I for various classes of organic compounds. A detailed list of these investigations is included in ref. 3.

Some investigators, for example Castello *et al.*[14], Schomburg and Dielmann[15] and Kissin and co-workers[16–19], have found it more useful to use group additivity methods for prediction of δI, *i.e.* the difference between the retention index of a compound and that for the corresponding n-alkane. Each structural group has an additive contribution to δI. These methods also require a significant number of structural parameters to accurately predict δI.

Many authors who have published structure–retention relationships, do not claim the correlation to be the only means of identification. Rather, it should be complementary to other identification methods such as gas chromatography–mass spectrometry. The recommendation of Souter[9] is thus reasonable that a predictive method for calculation of Kováts index should include as few structural parameters as possible.

The idea of using a few structural parameters for prediction of physical and thermodynamic properties of organic compounds has been studied by many investigators who have developed property–structure relationships based on graph-theoretic approaches.

GRAPH-THEORETIC APPROACH FOR PREDICTION OF KOVÁTS INDEX

Chemical graphs allow for mathematical representation of molecular structures. A graph is a set of vertices or points which are connected to each other by edges or lines. In a chemical graph, atoms other than hydrogen represent vertices and bonds represent edges. In terms of matrices, a graph can be represented by either an adjacency matrix, A, or by a distance matrix, D. These matrices are square matrices where rows (or columns) represent the atoms (vertices) of a chemical graph. The entries of the distance matrix, d_{ij}, represent the bond distance between vertices i and j. The entry a_{ij} of the adjacency matrix is 1 if i and j are connected by a bond, or 0 if i and j are not connected.

One graph-theoretic approach for prediction of Kováts index is based on topology–information correlations as proposed by Chrétien and co-workers[20–24]. In this approach, molecular structure for a compound in a family of compounds, for example alkenes, is represented by a graph which is generated from a focus point, for example the double bond in alkenes, based on the concept of ELCO (an Environment which is Limited, Concentric and Ordered). Superposition of these graphs gives the characteristic "imprint" for that particular family of compounds. Associated with this "imprint" are topological sites for which perturbation parameters are obtained from regression analysis of the available experimental Kováts indices. Kováts index for a particular compound can thus be predicted based on its structure (topological sites) and the associated perturbation parameters.

The topology–information correlation approach is quite a powerful technique for prediction of retention index. It utilizes a rather small number of parameters (one for each site) and provides an accuracy comparable to the more traditional methods based on additivity principles which use numerous parameters. In the case of *n*-alkenes, for example Dubois *et al.*[20], the retention indices were predicted using a 25-parameter correlation. The correlation coefficient was 0.9999 and standard deviation of 1.64.

Another graph theoretic approach for prediction of retention index, which uses even fewer parameters (as few as one or two), is based on correlations using graph theoretic indices. A graph theoretic index is a single number which mathematically characterizes the pattern of interconnections between atoms. The application of graph indices for property estimation was first realized by Wiener[25] in 1947. Since then, many different indices were proposed and applied for property estimation. Most of these indices are either based on the properties of the adjacency matrix or on the properties of the distance matrix. A review of these indices and their application is given by Rouvray[26].

Randić's connectivity index, χ, and the Wiener index, W, have been used by some investigators for correlating the Kováts retention index of some classes of organic compounds. Such correlations depend on the stationary phase and the column temperature. The connectivity index of Randić[27] is defined as:

$$\chi = \Sigma(v_i v_j)^{-1/2} \tag{3}$$

where v_i and v_j are the degrees of vertices i and j, respectively, and the summation extends over all edges. The degree of vertex i is defined as the number of edges connected to vertex i. From a chemical viewpoint, the degree of vertex i represents the order of the corresponding carbon.

Randić[27,28] showed that Kováts retention index for alkanes can be correlated with the connectivity index. From the properties of the connectivity index and the definition of the Kováts index, such as correlation would be a linear relationship given by the following equation:

$$I = 200(\chi - 1.4142) + 300 \tag{4}$$

The factor of 200 converts the Kováts retention scale to that of the connectivity values while 1.4142 and 300 are connectivity and Kováts indices for propane, respectively. The above equation is exact for the *n*-alkane series, however, deviation from linearity is observed when considering isomeric compounds. Randić[28] suggested that such deviations from linearity were due to interactions between some methyl–methyl fragments in highly branched structures and improved the correlation by introducing a correction factor:

$$I = 200(\chi - 1.4142) + 300 + (T_3)^2 \tag{5}$$

where T_3 is the number of methyl–methyl fragments separated by 3 carbon atoms. With only two structural parameters, namely χ and T_3, the error in the predicted values of I was comparable with more sophisticated predictive methods based on numerous parameters. Several correlations between the retention index and the connectivity index were proposed by Gassiot-Matas and Firpo-Pamies[29] for various classes of compounds, and by Kaliszan and co-workers[30–32] for more complex structures such as pyrazine carbothioamide derivatives, polycyclic aromatics, and complex cyclic alcohols and methyl esters.

One difficulty in applying the Randić approach for alkyl substituted alkanes and alkenes is that the index does not have a high discriminating power for various isomers. For example the position of the alkyl substituent on the chain is not reflected in the index value. The index value for 4-methyl, 5-methyl, 6-methyl, ..., $n/2$-methyl isomers of methyl-*n*-alkane all have the same connectivity index. However, I is strongly affected by the position of branches with respect to the main chain.

Bonchev *et al.*[33] correlated the Kováts retention index of monoalkyl and *o*-dialkylbenzenes on squalane at 413 K with the Wiener index, W. The Wiener index for a structure is obtained from its distance matrix, $\boldsymbol{D}$, and is defined as:

$$W = 1/2\left(\sum_{i,j} d_{ij}\right) \tag{6}$$

W is the total number of bonds existing between all atoms in a molecular graph and it depends on the size and the shape of the skeletal network. The smaller the number is, the more compact is the corresponding structure.

Bonchev *et al.*[33] suggested the following equation for predicting the Kováts retention index, I, for monoalkyl and *o*-dialkylbenzenes in the C_9–C_{16} range:

$$I = 244\, W^{0.3} \tag{7}$$

With the above equation, the error between predicted and measured values of I was in the range of 1 to 20 i.u. with an average error of 7.5 i.u.

Unlike the connectivity index of Randić, the Wiener index has a high discriminating power for isomeric compounds. However, the Wiener index does not distinguish double or aromatic C–C bonds with the corresponding saturated or cyclic bonds. Hence the Wiener indices for alkenes and aromatics are identical to those for the corresponding alkanes and cycloalkanes, respectively. For a high discriminating power, in particular for isomeric compounds, Rouvray[26] suggests the design of so called superindices which are based on the combination of two or more indices.

Even with the problems associated with discrimination of isomeric compounds, a graph-theoretic approach for predicting Kováts retention index seems to be complementary to if not competitive with other emperical and additive methods. As pointed out by Bonchev *et al.*[33], such an approach is very simple to use, and most important, has an accuracy comparable with other approaches that require a significant number of structural parameters. In this study the graph theoretic approach for prediction of Kováts retention index has been extended to high-molecular-weight branched alkanes and alkenes.

RESULTS AND DISCUSSION

Correlations of the type given by eqns. 4 and 7 were developed using the experimental data of Kissin and co-workers[16–19] for the retention indices of monoalkyl and polymethyl alkanes and alkenes in the C_9–C_{26} range. Kissin and co-workers used a fused-silica capillary column coated with cross-linked methylsilicone. The temperature programming was from 40 to 300°C at 5°C/min.

The hydrocarbons considered by Kissin and co-workers can be divided into four categories. These include: (1) monoalkyl alkanes; (2) monoalkyl alkenes; (3) polymethyl alkanes; and (4) polymethyl alkenes.

Correlations of the form given by eqn. 4 for prediction of I from Randić connectivity index, χ, were obtained for each of the above classes of hydrocarbons. Eqn. 4, when rearranged, can be written as:

$$I = a_0 + a_1\chi \tag{8}$$

where a_0 and a_1 are 17.2 and 200, respectively. For the above classes of hydrocarbons, values of a_1 were found to be in the range of 183 to 198. Such correlations were found to be unsatisfactory with standard deviations ranging between 10 and 25 index units. It was thought that addition of a third term (a correction term such as that suggested by Randić[28]) containing the effect of the Wiener index on Kováts index would improve the correlation. However, correlations of the form given by eqns. 9 and 10 did not significantly improve the correlation given by eqn. 8.

$$I = a_0 + a_1\chi + a_2 W \tag{9}$$

$$I = a_0 + a_1\chi + a_2 \log W \tag{10}$$

Fig. 1 shows a plot of Kováts index *versus* Randić index for all hydrocarbons

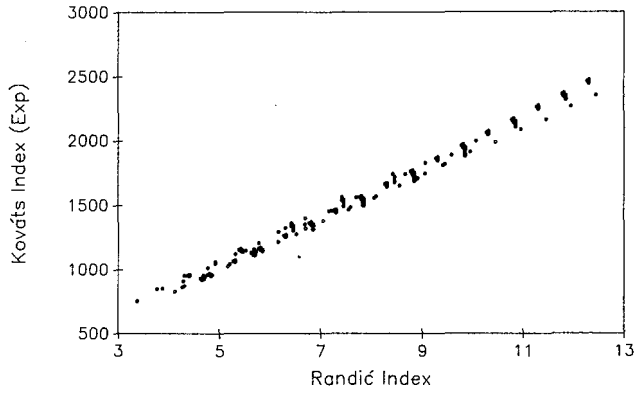

Fig. 1. Plot of Kováts index *versus* Randić index for C_{10} and higher alkanes and alkenes.

considered. Although a linear relationship exists over the entire range of χ values, deviations from linearity for isomeric compounds are significant. Fig. 2 shows the plot of Kováts index *versus* the Wiener index which suggests a smooth correlation in particular when one considers two classes of compounds; monoalkyl compounds and polymethyl compounds (see Figs. 3 and 4).

Correlations of the form suggested by Bonchev *et al.*[33], eqn. 11, were developed for each class of hydrocarbons.

$$I = b_0 W^{b_1} \tag{11}$$

The value of b_0 was found to be in the range of 172 to 192 with exponent b_1 ranging between 0.32 and 0.34. These values are in good agreement with those reported by Bonchev *et al.*[33] for alkyl-substituted benzenes. To distinguish between alkenes and corresponding alkanes, a third term was added to eqn. 11:

$$I = b_0 W^{b_1} \chi^{b_2} \tag{12}$$

The additional term resulted in an improved correlation. For polymethyl and

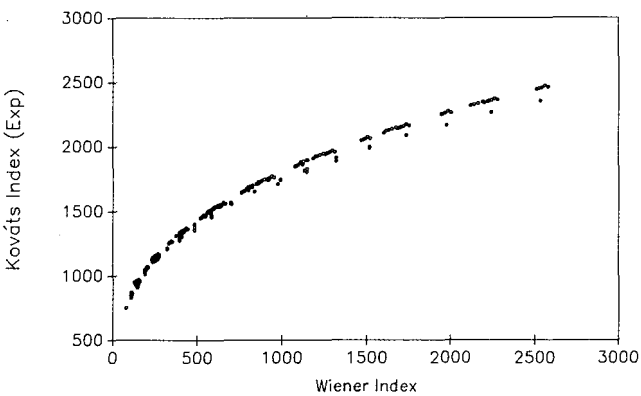

Fig. 2. Plot of Kováts index *versus* Wiener index for C_{10} and higher alkanes and alkenes.

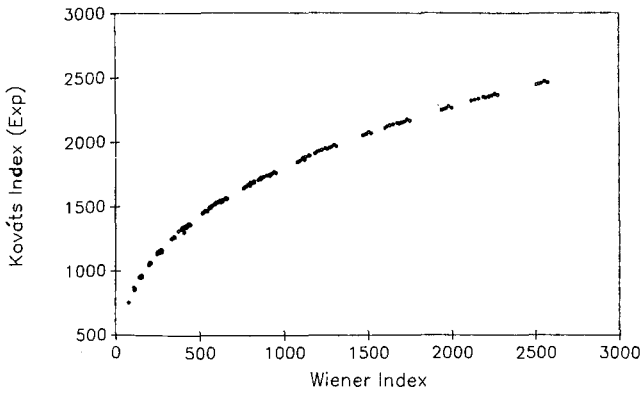

Fig. 3. Plot of Kováts index *versus* Wiener index for C_{10} and higher monoalkyl alkanes and alkenes.

monoalkyl hydrocarbons, the resulting correlations are given by eqns. 13 and 14, respectively.

$$I = 197W^{0.258}\chi^{0.181} \tag{13}$$

$$I = 186W^{0.276}\chi^{0.165} \tag{14}$$

The correlation coefficients for the above correlations were 0.998 and 1.000, respectively. For all the hydrocarbons considered, the experimental values of I are compared with those predicted by eqns. 13 and 14 in Table I. The correlation between experimental and predicted values is shown in Fig. 5.

For monoalkyl hydrocarbons, the error between predicted and experimental values was in the range of 0 to 26 i.u. with an average error of 5.1 i.u. For polymethyl hydrocarbons, the error was in the range of 1 to 29 i.u. with an average error of 10.9 i.u. For all hydrocarbons, the average error was 6.6 index units. The somewhat higher error for polymethyl hydrocarbons may indicate secondary effects (in particular for

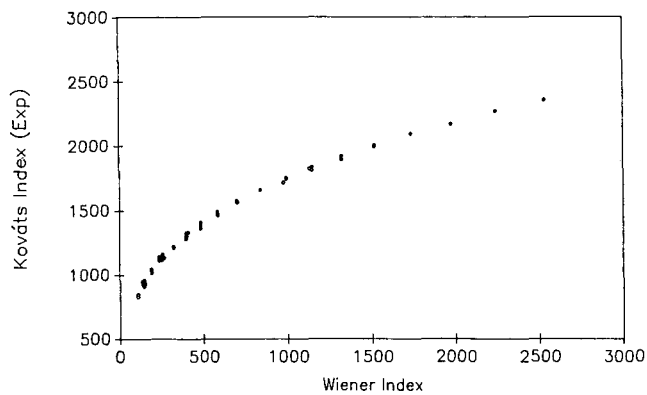

Fig. 4. Plot of Kováts index *versus* Wiener index for C_{10} and higher polymethyl alkanes and alkenes.

TABLE I

EXPERIMENTAL AND PREDICTED VALUES OF KOVÁTS INDEX

I = Kováts index; W = Wiener index; χ = Randić index; Me = methyl; Et = ethyl; Pr = propyl; Bu = butyl.

Compound	*I (Exp)*	*W*	χ	*I (Calc)*	*Difference*
2-Me-C_8	865.0	114	4.270	873.5	8.5
2-Me-C_9	964.0	158	4.770	973.4	9.4
2-Me-C_{10}	1065.0	212	5.270	1073.2	8.2
2-Me-C_{11}	1164.5	277	5.770	1172.8	8.3
2-Me-C_{12}	1265.0	354	6.270	1272.3	7.3
2-Me-C_{13}	1364.5	444	6.770	1371.6	7.1
2-Me-C_{14}	1465.0	548	7.270	1470.9	5.9
2-Me-C_{15}	1564.0	667	7.770	1570.0	6.0
2-Me-C_{16}	1664.5	802	8.270	1669.0	4.5
2-Me-C_{17}	1764.0	954	8.770	1767.9	3.9
2-Me-C_{18}	1864.5	1124	9.270	1866.8	2.3
2-Me-C_{19}	1964.0	1313	9.770	1965.6	1.6
2-Me-C_{20}	2064.5	1522	10.270	2064.3	−0.2
2-Me-C_{21}	2164.0	1752	10.770	2162.9	−1.1
2-Me-C_{22}	2263.5	2004	11.270	2261.5	−2.0
2-Me-C_{23}	2363.0	2279	11.770	2360.1	−2.9
2-Me-C_{24}	2463.0	2578	12.270	2458.6	−4.4
3-Me-C_8	872.0	110	4.308	866.2	−5.8
3-Me-C_9	971.0	153	4.808	966.1	−4.9
3-Me-C_{10}	1071.5	206	5.308	1066.0	−5.5
3-Me-C_{11}	1172.0	270	5.808	1165.8	−6.2
3-Me-C_{12}	1272.0	346	6.308	1265.6	−6.4
3-Me-C_{13}	1372.0	435	6.808	1365.2	−6.8
3-Me-C_{14}	1472.5	538	7.308	1464.7	−7.8
3-Me-C_{15}	1572.0	656	7.808	1564.0	−8.0
3-Me-C_{16}	1673.0	790	8.308	1663.3	−9.7
3-Me-C_{17}	1773.5	941	8.808	1762.5	−11.0
3-Me-C_{18}	1873.5	1110	9.308	1861.6	−11.9
3-Me-C_{19}	1973.7	1298	9.808	1960.6	−13.1
3-Me-C_{20}	2074.0	1506	10.308	2059.5	−14.5
3-Me-C_{21}	2174.0	1735	10.808	2158.4	−15.6
3-Me-C_{22}	2274.0	1986	11.308	2257.2	−16.8
3-Me-C_{23}	2373.7	2260	11.808	2355.9	−17.8
3-Me-C_{24}	2473.7	2558	12.308	2454.6	−19.1
4-Me-C_9	962.0	150	4.808	960.8	−1.2
4-Me-C_{10}	1061.5	202	5.308	1060.2	−1.3
4-Me-C_{11}	1161.0	265	5.808	1159.8	−1.2
4-Me-C_{12}	1261.0	340	6.308	1259.5	−1.5
4-Me-C_{13}	1360.0	428	6.808	1359.1	−0.9
4-Me-C_{14}	1460.5	530	7.308	1458.6	−1.9
4-Me-C_{15}	1560.0	647	7.808	1558.1	−1.9
4-Me-C_{16}	1660.5	780	8.308	1657.5	−3.0
4-Me-C_{17}	1760.0	930	8.808	1756.8	−3.2
4-Me-C_{18}	1860.2	1098	9.308	1856.0	−4.2
4-Me-C_{19}	1960.2	1285	9.808	1955.2	−5.0
4-Me-C_{20}	2060.5	1492	10.308	2054.2	−6.3
4-Me-C_{21}	2160.0	1720	10.808	2153.2	−6.8
4-Me-C_{22}	2259.5	1970	11.308	2252.1	−7.4
4-Me-C_{23}	2359.0	2243	11.808	2351.0	−8.0

TABLE I (*continued*)

Compound	*I (Exp)*	*W*	χ	*I (Calc)*	*Difference*
4-Me-C_{24}	2458.5	2540	12.308	2449.8	−8.7
5-Me-C_9	961.0	149	4.808	959.0	−2.0
5-Me-C_{10}	1058.0	200	5.308	1057.3	−0.7
5-Me-C_{11}	1156.0	262	5.808	1156.2	0.2
5-Me-C_{12}	1255.0	336	6.308	1255.4	0.4
5-Me-C_{13}	1354.0	423	6.808	1354.7	0.7
5-Me-C_{14}	1453.8	524	7.308	1454.0	0.2
5-Me-C_{15}	1553.6	640	7.808	1553.4	−0.2
5-Me-C_{16}	1653.4	772	8.308	1652.8	−0.6
5-Me-C_{17}	1753.2	921	8.808	1752.1	−1.1
5-Me-C_{18}	1853.0	1088	9.308	1851.3	−1.7
5-Me-C_{19}	1953.2	1274	9.808	1950.5	−2.7
5-Me-C_{20}	2053.0	1480	10.308	2049.7	−3.3
5-Me-C_{21}	2153.0	1707	10.808	2148.7	−4.3
5-Me-C_{22}	2252.0	1956	11.308	2247.7	−4.3
5-Me-C_{23}	2352.5	2228	11.808	2346.6	−5.9
5-Me-C_{24}	2453.0	2524	12.308	2445.5	−7.5
6-Me-C_{12}	1254.0	334	6.308	1253.3	− .7
6-Me-C_{14}	1451.0	520	7.308	1451.0	−0.0
6-Me-C_{16}	1650.0	766	8.308	1649.2	−0.8
6-Me-C_{17}	1749.0	914	8.808	1748.4	−0.6
6-Me-C_{18}	1848.0	1080	9.308	1847.6	−0.4
6-Me-C_{20}	2048.0	1470	10.308	2045.8	−2.2
6-Me-C_{21}	2147.5	1696	10.808	2144.9	−2.6
6-Me-C_{22}	2247.0	1944	11.308	2243.9	−3.1
6-Me-C_{24}	2446.5	2510	12.308	2441.8	−4.7
7-Me-C_{13}	1351.0	419	6.808	1351.1	0.1
7-Me-C_{14}	1450.0	518	7.308	1449.4	−0.6
7-Me-C_{15}	1548.0	632	7.808	1548.0	0.0
7-Me-C_{16}	1646.0	762	8.308	1646.8	0.8
7-Me-C_{17}	1745.0	809	8.808	1745.8	0.8
7-Me-C_{19}	1944.0	1258	9.808	1943.7	−0.3
7-Me-C_{21}	2143.0	1687	10.808	2141.7	−1.3
7-Me-C_{23}	2342.0	2204	11.808	2339.6	−2.4
3-Et-C_8	961.0	145	4.846	953.1	−7.9
3-Et-C_{10}	1157.0	258	5.846	1152.5	−4.5
3-Et-C_{12}	1355.0	419	6.846	1352.4	−2.6
3-Et-C_{14}	1554.0	636	7.846	1552.0	−2.0
3-Et-C_{16}	1753.0	917	8.846	1751.2	−1.8
3-Et-C_{18}	1952.0	1270	9.846	1950.1	−1.9
3-Et-C_{20}	2152.0	1703	10.846	2148.6	−3.4
3-Et-C_{22}	2351.5	2224	11.846	2346.7	−4.8
4-Et-C_8	954.0	141	4.846	945.8	−8.2
4-Et-C_{10}	1152.0	250	5.846	1142.6	−9.4
4-Et-C_{12}	1348.0	407	6.846	1341.6	−6.4
4-Et-C_{14}	1548.0	620	7.846	1541.1	−6.9
4-Et-C_{16}	1747.0	897	8.846	1740.6	−6.4
4-Et-C_{18}	1947.5	1246	9.846	1939.8	−7.7
4-Et-C_{20}	2148.0	1675	10.846	2138.8	−9.2
4-Et-C_{22}	2348.0	2192	11.846	2337.4	−10.6
5-Et-C_{10}	1146.0	246	5.846	1137.5	−8.5
5-Et-C_{12}	1341.0	399	6.846	1334.2	−6.8
5-Et-C_{14}	1538.0	608	7.846	1532.8	−5.2

(Continued on p. 10)

TABLE I (*continued*)

Compound	*I (Exp)*	*W*	χ	*I (Calc)*	*Difference*
5-Et-C_{16}	1736.0	881	8.846	1732.0	−4.0
5-Et-C_{18}	1937.0	1226	9.846	1931.2	−5.8
5-Et-C_{20}	2137.0	1651	10.846	2130.3	−6.7
5-Et-C_{22}	2335.0	2164	11.846	2329.1	−5.9
6-Et-C_{12}	1336.0	395	6.846	1330.5	−5.5
6-Et-C_{14}	1533.0	600	7.846	1527.2	−5.8
6-Et-C_{16}	1731.0	869	8.846	1725.4	−5.6
6-Et-C_{18}	1929.0	1210	9.846	1924.2	−4.8
6-Et-C_{20}	2129.0	1631	10.846	2123.1	−5.9
6-Et-C_{22}	2327.0	2140	11.846	2321.9	−5.1
7-Et-C_{14}	1530.0	596	7.846	1524.4	−5.6
7-Et-C_{16}	1727.0	861	8.846	1721.0	−6.0
7-Et-C_{18}	1924.0	1198	9.846	1918.9	−5.1
7-Et-C_{20}	2122.0	1615	10.846	2117.3	−4.7
7-Et-C_{22}	2320.0	2120	11.846	2315.9	−4.1
5-Pr-C_{13}	1516.0	584	7.846	1515.9	−0.1
5-Pr-C_{15}	1712.0	849	8.846	1714.4	2.4
5-Pr-C_{17}	1910.0	1186	9.846	1913.6	3.6
5-Pr-C_{19}	2108.0	1603	10.846	2113.0	5.0
7-Pr-C_{13}	1506.0	572	7.846	1507.2	1.2
7-Pr-C_{15}	1700.0	825	8.846	1700.9	0.9
7-Pr-C_{17}	1898.0	1150	9.846	1897.4	−0.6
5-Bu-C_{10}	1313.0	375	6.846	1311.6	−1.4
5-Bu-C_{12}	1505.0	568	7.846	1504.3	−0.7
5-Bu-C_{14}	1699.0	825	8.846	1700.9	1.9
5-Bu-C_{16}	1896.0	1154	9.846	1899.2	3.2
6-Bu-C_{12}	1498.0	560	7.846	1498.4	0.4
6-Bu-C_{14}	1691.0	809	8.846	1691.7	0.7
6-Bu-C_{16}	1887.0	1130	9.846	1888.2	1.2
7-Bu-C_{14}	1688.0	801	8.846	1687.1	−0.9
7-Bu-C_{16}	1880.0	1114	9.846	1880.8	0.8
6-Me-1-C_7=	752.6	79	3.380	759.5	6.9
7-Me-1-C_8=	853.1	114	3.880	859.7	6.6
5-Me-1-C_9=	951.6	149	4.418	945.7	−5.9
7-Me-1-C_9=	961.1	153	4.418	952.7	−8.4
8-Me-1-C_9=	954.7	158	4.380	959.8	5.1
4-Me-1-C_{10}=	1051.5	202	4.918	1047.0	−4.5
6-Me-1-C_{10}=	1048.1	200	4.918	1044.1	−4.0
8-Me-1-C_{10}=	1061.4	206	4.918	1052.6	−8.8
5-Me-1-C_{11}=	1147.8	262	5.518	1146.4	−1.4
7-Me-1-C_{11}=	1146.2	262	5.418	1143.0	−3.2
9-Me-1-C_{11}=	1161.0	270	5.418	1152.5	−8.5
10-Me-1-C_{11}=	1154.3	277	5.380	1159.3	5.0
4-Et-1-C_{10}=	1143.5	250	5.456	1129.6	−13.9
6-Et-1-C_{10}=	1136.1	246	5.456	1124.6	−11.5
8-Et-1-C_{10}=	1147.3	258	5.456	1139.5	−7.8
7-Me-1-C_{13}=	1340.9	419	6.418	1338.0	−2.9
9-Me-1-C_{13}=	1344.8	423	6.418	1341.5	−3.3
11-Me-1-C_{13}=	1362.2	435	6.418	1351.9	−10.3
4-Et-1-C_{12}=	1342.5	407	6.456	1328.6	−13.9
6-Et-1-C_{12}=	1328.1	395	6.456	1317.7	−10.4
8-Et-1-C_{12}=	1331.4	407	6.456	1328.6	−2.8
6-Bu-1-C_{10}=	1303.7	409	6.456	1330.4	26.7

TABLE I (*continued*)

Compound	*I (Exp)*	*W*	χ	*I (Calc)*	*Difference*
7-Me-1-C_{15}=	1539.2	632	7.418	1535.0	−4.2
9-Me-1-C_{15}=	1538.8	632	7.418	1535.0	−3.8
11-Me-1-C_{15}=	1544.4	640	7.418	1540.3	−4.1
13-Me-1-C_{15}=	1563.1	656	7.418	1550.9	−12.2
4-Et-1-C_{14}=	1538.3	620	7.456	1528.2	−10.1
8-Et-1-C_{14}=	1521.3	596	7.456	1511.6	−9.7
12-Et-1-C_{14}=	1542.8	636	7.456	1539.0	−3.8
6-Bu-1-C_{12}=	1490.7	560	7.456	1485.8	−4.9
8-Bu-1-C_{12}=	1494.8	568	7.456	1491.7	−3.1
13-Me-1-C_{17}=	1743.9	921	8.418	1739.0	−4.9
6-Et-1-C_{16}=	1722.1	869	8.456	1712.6	−9.5
10-Et-1-C_{16}=	1716.2	861	8.456	1708.3	−7.9
6-Bu-1-C_{14}=	1683.3	809	8.456	1679.1	−4.2
8-Bu-1-C_{14}=	1678.3	801	8.456	1674.5	−3.8
10-Bu-1-C_{14}=	1689.2	825	8.456	1688.2	−1.0
2,6-Me_2-1-C_7=	848.0	108	3.770	839.6	−8.4
2,6-Me_2-1-C_8=	954.5	146	4.308	929.7	−24.8
3,7-Me_2-1-C_8=	910.4	146	4.290	929.0	18.6
4,8-Me_2-1-C_9=	1015.0	194	4.774	1019.2	4.2
4,8-Me_2-1-C_{10}=	1120.4	249	5.312	1108.2	−12.2
6,10-Me_2-1-C_{11}=	1208.5	324	5.774	1204.1	−4.4
2,6-Me_2-2-C_{12}=	1324.9	408	6.298	1298.2	−26.7
2,6,10-Me_3-1-C_{11}=	1295.3	397	6.164	1284.1	−11.2
3,7,11-Me_3-1-C_{12}=	1354.1	484	6.684	1371.4	17.3
2,6,10-Me_3-1-C_{12}=	1400.8	484	6.702	1372.0	−28.8
4,8,12-Me_3-1-C_{13}=	1456.4	586	7.168	1459.0	2.6
3,7,11-Me_3-1-C_{13}=	1460.2	583	7.222	1459.1	−1.1
4,8,12-Me_3-1-C_{14}=	1562.1	698	7.706	1546.5	−15.6
7,11,15-Me_3-1-C_{16}=	1741.7	992	8.668	1729.8	−11.9
2,7,11,15-Me_4-1-C_{16}=	1828.8	1147	9.058	1810.2	−18.6
3,8,12,16-Me_4-1-C_{17}=	1888.6	1322	9.578	1896.8	8.2
4,9,13,17-Me_4-1-C_{18}=	2000.0	1518	10.062	1983.3	−16.7
2,3-Me_2-C_8	956.9	143	4.681	938.7	−18.2
2,4-Me_2-C_8	919.8	142	4.664	936.4	16.6
2,5-Me_2-C_8	926.6	143	4.664	938.1	11.5
2,6-Me_2-C_8	936.0	146	4.664	943.1	7.1
2,7-Me_2-C_8	930.6	151	4.626	950.0	19.4
3,5-Me_2-C_8	927.6	138	4.702	930.9	3.3
3,6-Me_2-C_8	942.3	141	4.702	936.1	−6.2
4,5-Me_2-C_8	947.8	135	4.718	926.2	−21.6
2,3-Me_2-C_{10}	1158.0	256	5.681	1129.8	−28.2
2,4-Me_2-C_{10}	1115.2	253	5.664	1125.8	10.6
2,5-Me_2-C_{10}	1118.5	252	5.664	1124.6	6.1
2,6-Me_2-C_{10}	1120.0	253	5.664	1125.8	5.8
2,7-Me_2-C_{10}	1125.7	256	5.664	1129.2	3.5
2,8-Me_2-C_{10}	1136.8	261	5.664	1134.8	−2.0
2,9-Me_2-C_{10}	1130.1	268	5.626	1141.2	11.1
3,5-Me_2-C_{10}	1118.4	245	5.702	1117.8	−0.6
3,6-Me_2-C_{10}	1128.8	246	5.702	1119.0	−9.8
3,7-Me_2-C_{10}	1132.6	249	5.702	1122.5	−10.1
3,8-Me_2-C_{10}	1143.6	254	5.702	1128.3	−15.3
4,5-Me_2-C_{10}	1138.0	238	5.719	1110.1	−27.9
4,6-Me_2-C_{10}	1111.2	239	5.702	1110.7	−0.5

(Continued on p. 12)

TABLE I (*continued*)

Compound	*I (Exp)*	*W*	χ	*I (Calc)*	*Difference*
4,7-Me_2-C_{10}	1120.8	242	5.702	1114.3	−6.5
2,6,10-Me_3-C_{11}	1276.8	397	6.521	1297.2	20.4
2,6,10-Me_3-C_{12}	1380.6	484	7.058	1384.9	4.3
2,6,10-Me_3-C_{13}	1466.6	586	7.558	1473.1	6.5
2,6,10-Me_3-C_{15}	1653.6	839	8.558	1652.8	−0.8
2,6,10,14-Me_4-C_{15}	1711.7	976	8.914	1731.3	19.6
2,6,10,14-Me_4-C_{16}	1816.2	1132	9.452	1818.0	1.8
2,6-Me_2-C_7	830.0	108	4.126	853.4	23.4
2,6-Me_2-C_9	1025.3	194	5.164	1033.8	8.5
3,7-Me_2-C_9	1042.2	192	5.202	1032.4	−9.8
2,6-Me_2-C_{11}	1216.7	324	6.164	1218.5	1.8
3,7-Me_2-C_{12}	1321.2	400	6.702	1306.2	−15.0
3,7,11-Me_3-C_{13}	1485.0	583	7.596	1472.5	−12.5
2,6,10-Me_3-C_{14}	1557.0	704	8.058	1562.5	5.5
3,7,11-Me_3-C_{14}	1570.0	698	8.096	1560.4	−9.6
2,6,10-Me_3-C_{16}	1746.9	992	9.058	1743.6	−3.3
2,6,10,15-Me_4-C_{16}	1806.0	1147	9.414	1822.8	16.8
2,6,10,15-Me_4-C_{17}	1913.8	1322	9.952	1910.0	−3.8
2,6,10,15-Me_4-C_{18}	1989.8	1518	10.452	1997.0	7.2
2,6,10,15-Me_4-C_{19}	2088.5	1736	10.952	2084.9	−3.6
2,6,10,15-Me_4-C_{20}	2165.5	1977	11.452	2173.5	8.0
2,6,10,15-Me_4-C_{21}	2268.0	2242	11.952	2262.6	−5.4
2,6,10,15-Me_4-C_{22}	2354.5	2532	12.452	2352.1	−2.4

adjacent branches and those in α position). These effects may be accounted for by methods such as that suggested by Randić[28].

To test the validity of the correlations, eqn. 14 was used to predict the Kováts retention index for a series of monoalkyl-substituted hexadecanes. The retention data for these compounds were not included in the parameter estimation for the correlations. *n*-Hexadecane was decomposed by thermal cracking at relatively mild

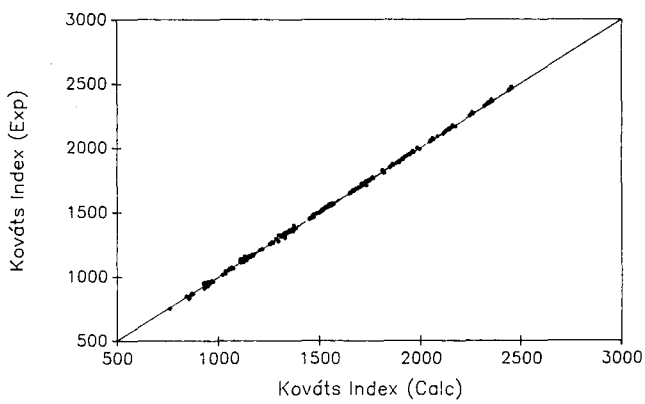

Fig. 5. Plot of experimental (Exp) *versus* predicted (Calc) Kováts index for C_{10} and higher alkanes and alkenes.

temperatures, 400–440°C, and under relatively high pressure (14 MPa). Under the above conditions, the primary decomposition products were a complete series of *n*-alkanes and α-olefins ranging from C_2 to C_{15}. Also present in the products were significant amounts of monoalkyl hexadecanes. Under conditions of high pressure, the bimolecular reactions involving the addition of the parent *n*-hexadecyl radicals to the terminal carbon of the α-olefins become significant. These reactions lead to the formation of saturated alkanes containing a hexadecane backbone and a single branch ranging from ethyl to pentadecyl. Because of the symmetry of *n*-hexadecane, there are seven isomeric secondary *n*-hexadecyl radicals. The resulting monoalkyl hexadecanes have the alkyl branch at position 2–8. Only compounds up to C_{27}'s (undecylhexadecanes) were present in detectable amounts. C_{28+} compounds were only present in trace amounts.

Liquid products were analyzed by a gas chromatograph equipped with a flame ionization detector using a DB-1 column. Temperature programming was as follows: initial temperature of 35°C for 3 min, up to 300°C at 3°C/min, and held at 300°C until complete elution.

Table II lists the high-molecular-weight compounds identified by gas chromatography–mass spectrometry and the corresponding experimental Kováts retention indices and those predicted by eqn. 14. The agreement between predicted and experimental values are quite satisfactory. The difference between experimental and predicted values were within ± 5 i.u. for over 40% of the compounds, and within ± 10 i.u. for over 70% of the compounds. The average error was 8.5 i.u. It is interesting to note that the predicted order of elution of compounds was identical to the experimental observation and, furthermore, the positions of peaks relative to the *n*-alkanes were accurately predicted. For example, among the C_{26} compounds (decylhexadecanes), the 2- and 3-isomers have retention times between those of *n*-C_{25} and *n*-C_{26}, whereas the 4-, 5-, 6-, 7- and 8-decylhexadecanes have retention times between those of *n*-C_{24} and *n*-C_{25}.

Data in Table I show that among isomeric monoalkyl alkanes of same carbon number and same alkyl group, the order of elution is correctly predicted. For example the retention index increases for 7-, 6-, 5-, 4-, 3- and 2-ethyl-C_{22}'s (2-ethyl-C_{22} = 3-methyl-C_{23}). The only exception is for methyl substituted alkanes where the 3-methylalkane has a higher retention index than the corresponding 2-methyl isomer. Also for the dimethyl compounds, the elution order is poorly predicted. In Table III, C_{10} and C_{18} compounds of Table I are listed in decreasing experimental retention index. C_{18} compounds are primarily monoalkyl compounds, for which the predicted order of elution is satisfactory. The C_{10} compounds, however, consist of monoalkyl and dimethyl compounds for which the predicted elution order is rather poor.

CONCLUSIONS

The graph-theoretic approach for estimation of Kováts index of organic compounds provides an easier alternative with same degree of accuracy to the more sophisticated methods based on additivity assumption. The approach of Bonchev *et al.*[33] was extended to high-molecular-weight monoalkyl and polymethyl alkanes and alkenes. Including two indices, W and χ, in the correlation resulted in an improved correlation. For approximately half of the compounds considered, the error in

TABLE II

EXPERIMENTAL AND PREDICTED KOVÁTS INDEX FOR ALKYL HEXADECANES

I = Kováts index; W = Wiener index, χ = Randić index.

Compound	*W*	χ	*I (Exp)*	*I (Calc)*	*Difference*
2-Ethyl-C_{16}	941	8.808	1774.8	1762.5	12.3
3-Ethyl-C_{16}	917	8.846	1769.5	1751.2	18.3
4-Ethyl-C_{16}	897	8.846	1749.3	1740.6	8.7
5-Ethyl-C_{16}	881	8.846	1739.6	1732.0	7.6
6-Ethyl-C_{16}	869	8.846	1733.2	1725.4	7.8
7-Ethyl-C_{16}	861	8.846	1728.0	1721.0	7.0
8-Ethyl-C_{16}	857	8.846	1726.6	1718.8	7.8
2-Propyl-C_{16}	1098	9.308	1859.1	1856.0	3.1
3-Propyl-C_{16}	1062	9.346	1846.9	1840.3	6.6
4-Propyl-C_{16}	1032	9.346	1823.4	1825.8	−2.4
5-Propyl-C_{16}	1008	9.346	1808.9	1813.9	−5.0
6-Propyl-C_{16}	990	9.346	1804.3	1804.9	−0.6
7-Propyl-C_{16}	978	9.346	1800.0	1798.9	1.1
8-Propyl-C_{16}	972	9.346	1798.6	1795.8	2.8
2-Butyl-C_{16}	1274	9.808	1952.7	1950.5	2.2
3-Butyl-C_{16}	1226	9.846	1936.5	1931.2	5.3
4-Butyl-C_{16}	1186	9.846	1911.4	1913.6	−2.2
5-Butyl-C_{16}	1154	9.846	1897.4	1899.2	−1.8
6-Butyl-C_{16}	1130	9.846	1889.7	1888.2	1.5
7-Butyl-C_{16}	1114	9.846	1884.6	1880.8	3.8
8-Butyl-C_{16}	1106	9.846	1883.1	1877.1	6.0
2-Pentyl-C_{16}	1470	10.308	2047.8	2045.8	2.0
3-Pentyl-C_{16}	1410	10.346	2028.3	2023.7	4.6
4-Pentyl-C_{16}	1360	10.346	2000.0	2003.6	−3.6
5-Pentyl-C_{16}	1320	10.346	1987.7	1987.1	0.6
6-Pentyl-C_{16}	1290	10.346	1979.6	1974.6	5.0
7-Pentyl-C_{16}	1270	10.346	1972.8	1966.1	6.7
8-Pentyl-C_{16}	1260	10.346	1971.3	1961.8	9.5
2-Hexyl-C_{16}	1687	10.808	2144.4	2141.7	2.7
3-Hexyl-C_{16}	1615	10.846	2122.9	2117.3	5.6
4-Hexyl-C_{16}	1555	10.846	2094.7	2095.3	−0.6
5-Hexyl-C_{16}	1507	10.846	2080.5	2077.3	3.2
6-Hexyl-C_{16}	1471	10.846	2071.7	2063.5	8.2
7-Hexyl-C_{16}	1447	10.846	2066.0	2054.1	11.9
8-Hexyl-C_{16}	1435	10.846	2064.2	2049.4	14.8
2-Heptyl-C_{16}	1926	11.308	2241.5	2238.1	3.4
3-Heptyl-C_{16}	1842	11.346	2218.4	2212.0	6.4
4-Heptyl-C_{16}	1772	11.346	2189.5	2188.5	1.0
5-Heptyl-C_{16}	1716	11.346	2174.8	2169.2	5.6
6-Heptyl-C_{16}	1674	11.346	2166.0	2154.4	11.6
7-Heptyl-C_{16}	1646	11.346	2160.1	2144.4	15.7
8-Heptyl-C_{16}	1632	11.346	2158.5	2139.3	19.2
2-Octyl-C_{16}	2188	11.808	2339.4	2334.9	4.5
3-Octyl-C_{16}	2092	11.846	2314.9	2307.4	7.5
4-Octyl-C_{16}	2012	11.846	2285.4	2282.7	2.7
5-Octyl-C_{16}	1948	11.846	2270.4	2262.5	7.9
6-Octyl-C_{16}	1900	11.846	2261.2	2246.9	14.3
7-Octyl-C_{16}	1868	11.846	2253.4	2236.4	17.0
8-Octyl-C_{16}	1852	11.846	2251.7	2231.1	20.6
2-Nonyl-C_{16}	2474	12.308	2436.6	2432.1	4.5

TABLE II (*continued*)

Compound	*W*	χ	*I (Exp)*	*I (Calc)*	*Difference*
3-Nonyl-C_{16}	2366	12.346	2411.6	2403.5	8.1
4-Nonyl-C_{16}	2276	12.346	2381.9	2377.9	4.0
5-Nonyl-C_{16}	2204	12.346	2366.3	2356.9	9.4
6-Nonyl-C_{16}	2150	12.346	2357.1	2340.8	16.3
7-Nonyl-C_{16}	2114	12.346	2349.3	2329.9	19.4
8-Nonyl-C_{16}	2096	12.346	2347.5	2324.4	23.1
2-Decyl-C_{16}	2785	12.808	2533.3	2529.4	3.9
3-Decyl-C_{16}	2665	12.846	2508.6	2500.1	8.5
4-Decyl-C_{16}	2565	12.846	2477.9	2473.8	4.1
5-Decyl-C_{16}	2485	12.846	2462.3	2452.3	10.0
6-Decyl-C_{16}	2425	12.846	2452.9	2435.8	17.1
7-Decyl-C_{16}	2385	12.846	2446.7	2424.6	22.1
8-Decyl-C_{16}	2365	12.846	2444.9	2419.0	25.9
2-Undecyl-C_{16}	3122	13.308	2631.7	2627.0	4.7
3-Undecyl-C_{16}	2990	13.346	2606.6	2597.1	9.5
4-Undecyl-C_{16}	2880	13.346	2574.3	2570.3	4.0
5-Undecyl-C_{16}	2792	13.346	2557.8	2548.4	9.4
6-Undecyl-C_{16}	2726	13.346	2547.9	2531.6	16.3
7-Undecyl-C_{16}	2682	13.346	2540.0	2520.3	19.7
8-Undecyl-C_{16}	2660	13.346	2538.4	2514.6	23.8

TABLE III

EXPERIMENTAL AND PREDICTED KOVÁTS INDEX

Me = Methyl; Et = ethyl; Pr = propyl; Bu = butyl.

Compound	*I (Exp)*	*I (Calc)*	*Compound*	*I (Exp)*	*I (Calc)*
C_{10} compounds			*C_{18} compounds*		
3-Me-C_9	971.0	966.1	3.Me-C_{17}	1773.5	1762.5
2-Me-C_9	964.0	973.4	2-Me-C_{17}	1764.0	1767.9
4-Me-C_9	962.0	960.8	4-Me-C_{17}	1760.0	1756.8
7-Me-1-C_9=	961.1	952.7	5-Me-C_{17}	1753.2	1752.1
3-Et-C_8	961.0	953.1	3-Et-C_{16}	1753.0	1751.2
5-Me-C_9	961.0	959.0	6-Me-C_{17}	1749.0	1748.4
2,3-Me_2-C_8	956.9	938.7	4-Et-C_{16}	1747.0	1740.6
8-Me-1-C_9=	954.7	959.8	7-Me-C_{17}	1745.0	1745.8
2,6-Me_2-1-C_8=	954.5	929.7	13-Me-1-C_{17}=	1743.9	1739.0
4-Et-C_8	954.0	945.8	5-Et-C_{16}	1736.0	1732.0
5-Me-1-C_9=	951.6	945.7	6-Et-C_{16}	1731.0	1725.4
4,5-Me_2-C_8	947.8	926.2	7-Et-C_{16}	1727.0	1721.0
3,6-Me_2-C_8	942.3	936.1	6-Et-1-C_{16}=	1722.1	1712.6
2,6-Me_2-C_8	936.0	943.1	10-Et-1-C_{16}=	1716.2	1708.3
2,7-Me_2-C_8	930.6	950.0	5-Pr-C_{15}	1712.0	1714.4
3,5-Me_2-C_8	927.6	930.9	7-Pr-C_{15}	1700.0	1700.9
2,5-Me_2-C_8	926.6	938.1	5-Bu-C_{14}	1699.0	1700.9
2,4-Me_2-C_8	919.8	936.4	6-Bu-C_{14}	1691.0	1691.7
3,7-Me_2-1-C_8=	910.4	929.0	10-Bu-1-C_{14}=	1689.2	1688.2
			7-Bu-C_{14}	1688.0	1687.1
			6-Bu-1-C_{14}=	1683.3	1679.1
			8-Bu-1-C_{14}=	1678.3	1674.5
			2,6,10-Me_3-C_{15}	1653.6	1652.8

predicted values of I was less than 5 i.u., and for approximately 80% of the compounds, the error was less than 10 index units. The correlation for monoalkyl alkanes was tested to predict the retention behavior of monoalkylhexadecanes in the range of C_{18} to C_{27}. Agreement between predicted and experimental Kováts indices was satisfactory.

REFERENCES

1 E. sz. Kováts, *Adv. Chromatogr.*, 1 (1965) 229.
2 S. W. Benson, *Thermochemical Kinetics*, Wiley, New York, 1976.
3 J. M. Takács, C. Szita and G. Tarján, *J. Chromatogr.*, 56 (1971) 1.
4 C. Káplár, C. Szita, J. M. Takács and G. Tarján, *J. Chromatogr.*, 65 (1972) 115.
5 J. M. Takács, Zs. Tálas, I. Bernáth and Gy. Czakó, *J. Chromatogr.*, 67 (1972) 203.
6 J. M. Takács, E. Kocsi, E. Garmavolgyi, E. Eckhart, T. Lombosi, Sz. Nyiredy, I. Borbély and Gy. Krasznai, *J. Chromatogr.*, 81 (1973) 1.
7 J. M. Takács, *J. Chromatogr. Sci.*, 11 (1973) 210.
8 R. Vanheertum, *J. Chromatogr. Sci.*, 13 (1975) 150.
9 P. Souter, *J. Chromatogr. Sci.*, 12 (1974) 418.
10 G. I. Spivakovskii, A. I. Tishchenko, I. I. Zaslavskii and N. S. Wulfson, *J. Chromatogr.*, 144 (1977) 1.
11 N. Dimov, *J. Chromatogr.*, 119 (1976) 109.
12 D. Papazova and N. Dimov, *J. Chromatogr.*, 137 (1977) 259.
13 N. Dimov and D. Papazova, *J. Chromatogr.*, 137 (1977) 265.
14 G. Castello, M. Lunardelli and M. Berg, *J. Chromatogr.*, 76 (1973) 31.
15 G. Schomburg and G. Dielmann, *J. Chromatogr. Sci.*, 11 (1973) 151.
16 Y. V. Kissin, G. P. Feulmer and W. B. Payne, *J. Chromatogr. Sci.*, 24 (1986) 164.
17 Y. V. Kissin, *J. Chromatogr. Sci.*, 24 (1986) 278.
18 Y. V. Kissin and G. P. Feulmer, *J. Chromatogr. Sci.*, 24 (1986) 53.
19 Y. V. Kissin, *Ind. Eng. Chem. Res.*, 26 (1987) 1633.
20 J. E. Dubois, J. R. Chrétien, L. Soják and J. A. Rijks, *J. Chromatogr.*, 194 (1980) 121.
21 J. R. Chrétien and J. E. Dubois, *J. Chromatogr.*, 158 (1978) 43.
22 J. R. Chrétien and J. E. Dubois, *Anal. Chem.*, 49 (1977) 747.
23 J. E. Dubois and J. R. Chrétien, *J. Chromatogr. Sci.*, 12 (1974) 811.
24 J. R. Chrétien and J. E. Dubois, *J. Chromatogr.*, 126 (1976) 171.
25 H. Wiener, *J. Am. Chem. Soc.*, 69 (1947) 2636.
26 D. Rouvray, in R. B. King (Editor), *Chemical Applications of Topology and Graph Theory*, Elsevier, New York, 1983, pp. 159–177.
27 M. Randić, *J. Am. Chem. Soc.*, 97 (1975) 6609.
28 M. Randić, *J. Chromatogr.*, 161 (1978) 1.
29 M. Gassiot-Matas and G. Firpo-Pamies, *J. Chromatogr.*, 187 (1980) 1.
30 R. Kaliszan and H. Lamparczyk, *J. Chromatogr. Sci.*, 16 (1978) 246.
31 R. Kaliszan and H. Foks, *Chromatographia*, 10 (1977) 346.
32 R. Kaliszan, *Chromatographia*, 10 (1977) 529.
33 D. Bonchev, Ov. Mekenjan, G. Protić and N. Trinajstić, *J. Chromatogr.*, 176 (1979) 149.

Journal of Chromatography, 481 (1989) 17–26
Elsevier Science Publishers B.V., Amsterdam — Printed in The Netherlands

CHROM. 21 783

THERMODYNAMIC PROPERTIES OF ENANTIOMERS OF UNDERIVATIZED DIOLS *VERSUS* THE CYCLIC CARBONATES IN GAS CHROMATOGRAPHY ON CHIRASIL-VAL

B. KOPPENHOEFER*
Institut für Organische Chemie der Universität, Auf der Morgenstelle 18, D-7400 Tübingen (F.R.G.)
and
B. LIN
Dalian Institute of Chemical Physics, Chinese Academy of Sciences, Dalian (China)
(Received May 8th, 1989)

SUMMARY

Enantiomers of underivatized vicinal alkyl diols are resolved by capillary gas chromatography on the polymeric chiral stationary phase Chirasil-Val. Owing to intramolecular hydrogen bonding of the type O–H···O, aliphatic 1,2-diols are far less polar than 1,3-diols, and can be separated with only moderate peak tailing on deactivated glass capillaries. Thermodynamic measurements reveal a fairly large difference in the enthalpy of interaction of the enantiomers ($\Delta\Delta H$) but also an unusual high negative (unfavourable) value for the entropy difference) ($\Delta\Delta S$). Hence the extrapolated isoselective temperature (T_s) is intriguingly low, but the resolution is thereby also restricted to the low-temperature range. The corresponding cyclic carbonates, formed by reaction with phosgen in toluene, are also fairly polar and therefore do not offer any significant advantage in terms of peak tailing. The resolution factors (α) are apparently small, owing to the very low values of $-\Delta\Delta H$ and $\Delta\Delta S$, but the isoselective temperature is usually much higher than for the diols.

INTRODUCTION

Chiral aliphatic compounds with several hydroxy groups[1–12] are important as starting compounds for the synthesis of natural products. Diols are formed in high enantiomeric purity by enzymatic conversion of suitable precursors[13–17]. Among different techniques for the determination of the enantiomeric excess (e.e.)[18–20], enantiomer resolution by gas chromatography (GC) of the underivatized hydroxy compounds on a chiral stationary phase[21–23] is the most convenient approach.

However, even on the particularly versatile polymeric phase L-[24] or D-Chirasil-Val[25,a], binaphthol[26], aryl-1,2-ethanediols[26] and aliphatic triols[11] are only separated after perfluoroacylation. Accordingly, trifluoracylation has been applied

[a] Fused-silica capillary columns coated with either L- or D-Chirasil-Val are commercially available from Chrompack (Middelburg, The Netherlands).

0021-9673/89/$03.50

prior to enantiomer resolution of polyols, such as sugar alcohols, on the stationary phase XE-60–L-Val-(*R*)-α-pea[27] and for diols and polyols on modified cyclodextrins[28]. Other methods involve conversion with phosgene or ethyl chloroformate into cyclic carbonates that are separated on XE-60–L-Val-(*R*)-α-pea[27], and the formation of either cyclic boronates or acetals that are separated by complexation GC[29]. N-Trifluoroacetylglycyl chloride has also been used as a promising achiral auxiliary to convert aliphatic 1,2- and 1,3-diols into monoesters with good enantiomer resolution factors (α) on Chirasil-Val[1]. However, all of these approaches have certain drawbacks. Apart from the additional time consumption and safety problems (*e.g.*, with phosgene) during sample preparation, the derivatization reactions may be accompanied by side-reations and racemization.

The purpose of this work was to extend the scope of the direct separation on well deactivated borosilicate glass capillaries coated with Chirasil-Val, previously reported briefly for *trans*-cyclohexane-1,2-diol[23], to other aliphatic diols, and to compare the chromatographic properties of the underivatized diols with those of the corresponding cyclic carbonates in terms of peak resolution and thermodynamic behaviour.

EXPERIMENTAL

Reference compounds

Racemic 1,2-propanediol, 1,2-hexanediol, *trans*-cyclohexanediol and *trans*-cycloheptanediol were purchased from Aldrich and 1,2-butanediol from Fluka. Mixtures of the three stereoisomers of 2,3-butanediol and 2,4-pentanediol were obtained from Fluka and Aldrich, respectively. (2*R*,4*R*)-Pentanediol was purchased from Aldrich. (2*S*,3*S*)-2,3-Butanediol[30] and (*S*)-1,2-propanediol[31] were synthesized according to literature procedures.

Cyclic carbonates

In a 1-ml Reactivial (Macherey, Nagel & Co.), 50 μl of a solution of phosgene in toluene (20%, 1.93 *M*; Fluka) were added to a sample of the diol (1–2 mg). After 1 h at ambient temperature, the reaction mixture was slowly concentrated in a gentle stream of nitrogen. Care should be taken to prevent the loss of volatile cyclic carbonates. Eventually, the oily residue was dissolved in 50 μl of dichloromethane.

Gas chromatography

Samples were eluted from a borosilicate glass (Duran 50; Schott, Mainz, F.R.G.) capillary column (M 174, 22 m × 0.28 mm I.D.), deactivated with diphenyltetramethyldisilazane (DPTMDS)[32], and coated with L-Chirasil-Val (film thickness 0.3 μm). Gas chromatography was performed on a Carlo-Erba Model 2001 AC gas chromatograph with hydrogen as the carrier gas at a constant inlet pressure (typically 0.4 kg cm^{-2}, splitting ratio 1:50) with flame ionization detection. Net retention times (from methane) were measured with a Trivector Trilab II laboratory computer. Calculations were run on an IBM XT computer.

RESULTS AND DISCUSSION

The free vicinal diols were injected on to a well deactivated borosilicate glass column, coated with L-Chirasil-Val. It was found that the peak resolution is strongly temperature dependent. For short-chain compounds, a good compromise between peak resolution and peak retention was reached at *ca.* 50°C. Within the series of terminal diols investigated (up to 1,2-hexanediol, **4a**), the peak resolution of the enantiomeric pairs increased with increasing chain length as a rule, for two reasons. First, as indicated in Table I, the resolution factors (α) are significantly increased in this order. Second, the influence of peak tailing on resolution vanishes for large capacity factors (k'). Similar trends are seen with the alicyclic compounds **5** and **6**, but they can be resolved at much higher temperatures.

The absolute configurations were assigned by using diols of high enantiomeric purity, *i.e.*, (*S*)-1,2-propanediol (**1a**) and (2*S*,3*S*)-butanediol, [(*S*,*S*)-**2a**] [synthesized in six steps from (*R*,*R*)-tartaric acid[30]]. (*R*,*R*)-**2a** and (*R*,*S*)-**2a** were assigned by comparison of the relative peak areas obtained from a synthetic mixture of the three stereoisomers.

The only 1,3-diol investigated, 2,4-pentanediol (**7**), was separated into the diastereoisomers with unlike (*R*,*S*) and like (*S*,*S* and *R*,*R*) configurations. However, the enantiomers of the latter were not resolved. This interesting observation deserves further comment (see below).

TABLE I

ENANTIOMER RESOLUTION OF ALIPHATIC DIOLS ON L-CHIRASIL-VAL

Conditions: capillary column (M 174, 22 m × 0.28 mm I.D., film thickness 0.3 μm); 0.4 kg cm^{-2} hydrogen; U = 28 m min^{-1}; t_0 = 55.5 s at 52°C; flame ionization detection.

No.	*Compound*	*Temperature (°C)*	*Stereo-isomer*	*k'*	α
1a	1,2-Propanediol	52	*S*	6.16	1.023
			R	6.30	
2a	2,3-Butanediol	52	*S,S*	5.07	1.046
			R,R	5.30	
			R,S	6.17	
3a	1,2-Butanediol	52	(1)[a]	12.30	1.056
			(2)[a]	12.99	
4a	1,2-Hexanediol	52	(1)[a]	67.7	1.062
			(2)[a]	71.9	
		72	(1)[a]	14.15	1.032
			(2)[a]	14.60	
5	*trans*-1,2-Cyclohexanediol	72	(1)[a]	14.63	1.030
			(2)[a]	15.07	
6	*trans*-1,2-Cycloheptanediol	92	(1)[a]	14.62	1.030
			(2)[a]	15.06	
7	2,4-Pentanediol	52	*S,S*/*R,R*	15.16	1[b]
			R,S	17.77	

[a] First and second peaks, absolute configuration not assigned.
[b] Not resolved.

TABLE II

ENANTIOMER RESOLUTION OF CYCLIC CARBONATES ON L-CHIRASIL-VAL

Conditions as in Table I.

No.	*Compound*	*Temperature (°C)*	*Stereo-isomer*	*k'*	*α*
1b	1,2-Propylene carbonate	52	*S*	5.90	1.015
			R	5.99	
2b	2,3-Butylene carbonate	52	*S,S*	6.32	1.037
			R,R	6.55	
			R,S	9.04	
3b	1,2-Butylene carbonate	52	(1)[a]	10.98	1.020
			(2)[a]	11.20	
4b	1,2-Hexylene carbonate	72	(1)[a]	15.03	1.028
			(2)[a]	15.45	

[a] First and second peaks, absolute configuration not assigned.

The resolution factors for vicinal diols are comparable to or even better than those of the corresponding carbonates formed by a derivatization reaction with phosgene or ethyl chloroformate, as determined on XE-60–L-Val-(*R*)-α-pea[27]. In order to make a fair comparison, some carbonates were prepared by reaction with a solution of phosgene in toluene and injected on to the same Chirasil-Val column. The chromatographic data are given in Table II. All carbonates investigated could be separated on Chirasil-Val, but in terms of resolution factors and capacity factors there is no point in resorting to this derivatization method. As shown in Fig. 1 for a typical example, **3a** *versus* **3b**, there is no striking advantage in peak shape, and thus peak resolution, of the carbonate on well deactivated Chirasil-Val columns.

In order to gain a better understanding of the chromatographic behaviour, the temperature coefficients of the Kováts retention indices of the diols **1a–4a** were

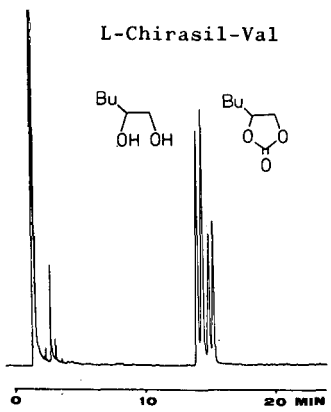

Fig. 1. Comparison of the enantiomer resolution of 1,2-hexanediol **4a** and the corresponding cyclic carbonate **4b** on L-Chirasil-Val with a DPTMDS-deactivated borosilicate glass column (22 m × 0.28 mm I.D.). Conditions: 0.4 kg cm^{-2} hydrogen, 72°C (isothermal), flame ionization detection. Bu = Butyl.

determined and compared with those of the carbonates **1b–3b**. Differences in the retention index–temperature relationship between the two classes of compounds are demonstrated in Fig. 2. In general, the slopes for the cyclic carbonates exceed those for the corresponding diols, thus reflecting the differences in entropy and enthalpy of interaction for the two classes of compounds, as compared with the coeluted hydrocarbons. The lines for the open-chain diols are rather flat; in other words, their enthalpies of interaction are approximately similar to those of the straight-chain hydrocarbons of comparable free enthalpy of interaction. In contrast, the lines for the carbonates are biased considerably. All carbonates have a positive temperature coefficient. Hence, on decreasing the oven temperature they are not retained as much as the coeluted hydrocarbons, owing to their smaller enthalpies of interaction. For a given temperature, they are coeluted with hydrocarbons with much higher $-\Delta H$ values, as the ΔS values are particularly small. In our experience with Chirasil-Val, such a behaviour is typical of cyclic compounds with little capability of hydrogen bonding to the stationary phase.

This interpretation is corroborated by the thermodynamic parameters of interaction of butanediols and the corresponding cyclic carbonates with L-Chirasil-Val, as given in Tables III and IV, respectively. Because of the hydrogen-bonding capability of the hydroxy groups, the enthalpies of interaction between the diols and the stationary phase are larger than those of the corresponding cyclic carbonates. However, owing to the influence of entropy, the free energies of the diols are usually lower than those of the corresponding derivatives, which are therefore eluted later within the temperature range investigated.

Striking dissimilarities between the two classes of compounds are also found in the differences in the thermodynamic parameters $-\Delta\Delta H$, $\Delta\Delta S$ and $-\Delta\Delta G$ (*cf.*, Tables V and VI). In general, the contributions of the (favourable) enthalpy and (unfavourable) entropy of interaction are much larger for the diols than the corresponding carbonates, owing to the contribution of hydrogen bonding to chiral recognition[26]. The differences in the free enthalpy values ($-\Delta\Delta G$), and hence the resolution factors

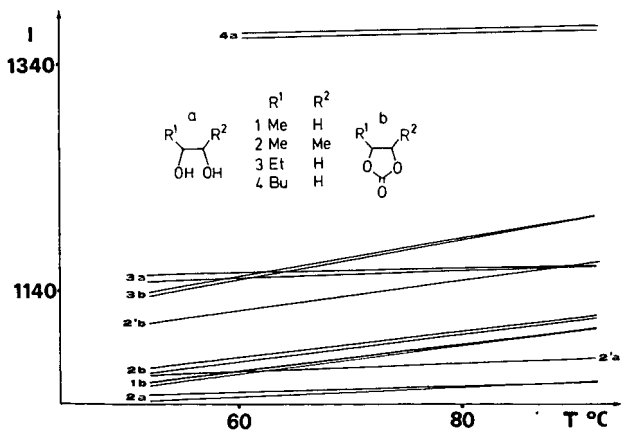

Fig. 2. Comparison of the temperature dependence of the Kováts retention indices of some aliphatic diols and the corresponding cyclic carbonates on L-Chirasil-Val. The notation **2'** refers to the achiral *meso* compound (*R,S*)-**2**.

TABLE III

THERMODYNAMIC PARAMETERS OF INTERACTION OF SOME ALIPHATIC DIOLS WITH L-CHIRASIL-VAL

No.	*Compound*	*Stereo-isomer*	$-\Delta H$ *(kcal mol^{-1})*	$-\Delta S$ *(cal mol^{-1} K^{-1})*	$-\Delta G_{298}$ *(kcal mol^{-1})*	$-\Delta G_{323}$ *(kcal mol^{-1})*	$-\Delta G_{373}$ *(kcal mol^{-1})*
2a	2,3-Butanediol	*S,S*	13.29	27.05	5.23	4.55	3.20
		R,R	13.60	27.93	5.28	4.58	3.18
		R,S	13.77	28.14	5.38	4.68	3.27
3a	1,2-Butanediol	(1)[a]	14.99	30.52	5.90	5.13	3.60
		(2)[a]	15.29	31.37	5.94	5.15	3.58

[a] First and second peak, absolute configuration not assigned.

TABLE IV

THERMODYNAMIC PARAMETERS OF INTERACTION OF SOME CYCLIC CARBONATES WITH L-CHIRASIL-VAL

No.	*Compound*	*Stereo-isomer*	$-\Delta H$ *(kcal mol^{-1})*	$-\Delta S$ *(cal mol^{-1} K^{-1})*	$-\Delta G_{298}$ *(kcal mol^{-1})*	$-\Delta G_{323}$ *(kcal mol^{-1})*	$-\Delta G_{373}$ *(kcal mol^{-1})*
2b	2,3-Butylene carbonate	*S,S*	12.59	24.47	4.69	3.46	2.24
		R,R	12.63	24.52	4.71	3.48	2.26
		R,S	12.75	24.23	5.52	4.92	3.71
3b	1,2-Butylene carbonate	(1)[a]	12.30	22.46	5.04	3.92	2.80
		(2)[a]	12.33	22.53	5.05	3.93	2.80

[a] First and second peak, absolute configuration not assigned.

TABLE V

ENANTIOMER DIFFERENCES IN THERMODYNAMIC PARAMETERS FOR SOME ALIPHATIC DIOLS WITH L-CHIRASIL-VAL

No.	$-\Delta\Delta H$ *(kcal mol^{-1})*	$-\Delta\Delta S$ *(cal mol^{-1} K^{-1})*	$-\Delta\Delta G_{298}$ *(kcal mol^{-1})*	$-\Delta\Delta G_{323}$ *(kcal mol^{-1})*	α_{298}	α_{323}	T_s *(°C)*
2a	227.4	0.6090	45.8	30.6	1.080	1.049	100
	±53.8[a]	±0.1632	±7.5	±3.7	±0.014	±0.006	±14
3a	336.7	0.9277	60.1	36.9	1.107	1.059	90
	±43.8	±0.1336	±7.5	±3.7	±0.014	±0.006	±6
4a	287.7	0.7679	58.8	39.6	1.104	1.063	102
	±33.3	±0.0977	±5.4	±3.1	±0.010	±0.005	±5

[a] Standard deviations after ± signs.

(α), are much higher for the diols at 50°C and even more pronounced at 25°C, but not at elevated temperatures. The reason becomes obvious from the van't Hoff plot of ln α *versus* $1/T$ for the most striking example of **3a** versus **3b** (see Fig. 3). As the ratio of the enthalpy difference and entropy difference, $\Delta\Delta H/\Delta\Delta S$, is particularly small for the free diol **3a**, the isoselective temperature, T_s at which the selectivity is similar for a pair of compounds out of a multitude of sample components, depicted in Fig. 3 as the cross-section of the straight line with the abscissa, is unusually low. Further experiments with extra-long Chirasil-Val columns are in progress in order to demonstrate the expected peak reversal of the enantiomers of **3a** above 90 ± 6°C. Similar phenomena were predicted several years ago[26,33], and independently observed recently in three laboratories[34–36]. The extrapolated isoselective temperature (T_s) for the carbonate **3b** is considerably higher, *i.e.*, 252 ± 36°C, although both $-\Delta\Delta H$ and $\Delta\Delta S$ are much smaller. As expected, the ratio $T_s = \Delta\Delta H/\Delta\Delta S$ is larger for the interaction of the rigid carbonate with the chiral polysiloxane. In view of the different possible conformations of the free diols (see Fig. 4), one can presume in this instance that there is a dedicated change in conformation population during solute–solvent interaction. Such a significant change in the average conformation has been termed "induced fit"[37], in analogy with similar phenomena in enzyme–substrate recognition processes[38]. One should bear in mind, however, that such a change in average conformation, although it may increase the difference in the interaction enthalpies

TABLE VI

ENANTIOMER DIFFERENCES IN THERMODYNAMIC PARAMETERS FOR SOME CYCLIC CARBONATES WITH L-CHIRASIL-VAL

No.	$-\Delta\Delta H$ *(kcal mol^{-1})*	$-\Delta\Delta S$ *(cal mol^{-1} K^{-1})*	$-\Delta\Delta G_{298}$ *(kcal mol^{-1})*	$-\Delta\Delta G_{323}$ *(kcal mol^{-1})*	α_{298}	α_{323}	T_s *(°C)*
3b	37.7	0.0437	24.7	23.6	1.0425	1.0374	589
	±0.7[a]	±0.0021	±0.1	±0.1	±0.0002	±0.0001	±7
4b	33.1	0.0631	14.3	12.7	1.0245	1.0200	252
	±3.6	±0.0109	±0.5	±0.3	±0.0009	±0.0004	±36

[a] Standard deviations after ± signs.

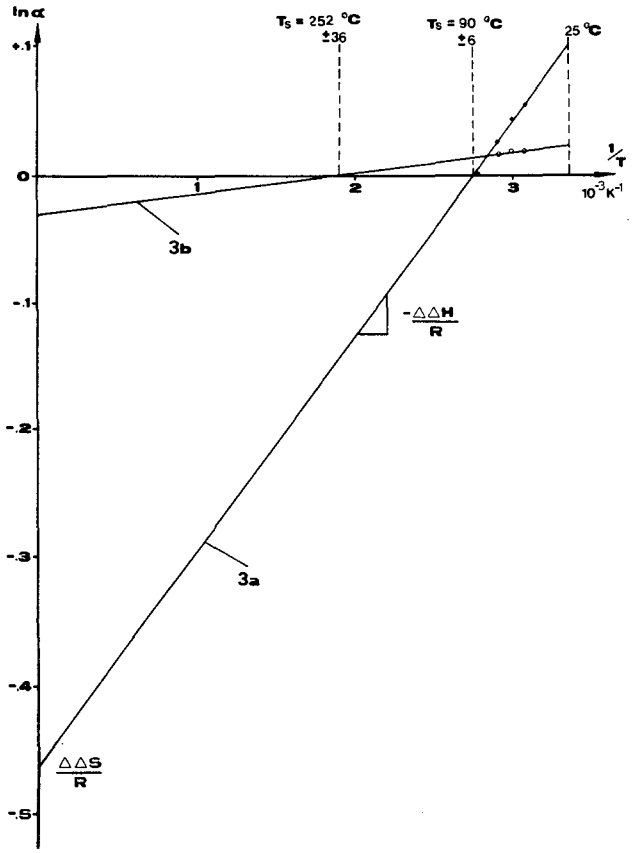

Fig. 3. Comparison of the van't Hoff plots of 1,2-butanediol (**3a**) and the corresponding cyclic carbonate **3b** for enantiomer resolution on L-Chirasil-Val. The extrapolated isoselective temperature, where peak inversion occurs, is marked T_s.

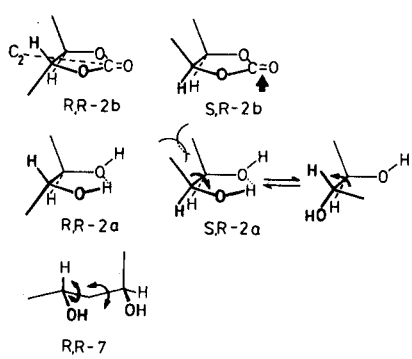

Fig. 4. Possible conformations for the cyclic carbonate **2b** and the free diols **2a** and **7**.

($-\Delta\Delta H$) of the two enantiomers, is very unfortunate in terms of the entropy difference ($\Delta\Delta S$), in particular at elevated temperature. Too much flexibility may even cancel possible differences in the interaction energies of the two enantiomers with the chiral stationary phase, as demonstrated by the non-resolved enantiomeric pair (*S,S*)/(*R,R*)-2,4-pentanediol.

Differences in conformation populations may also account for the relative retentivity of the diastereoisomers of **2a** and **2b**. As demonstrated by IR spectroscopy, the free diol **2a** with *like* configuration of the two stereogenic centres is more likely to undergo intramolecular hydrogen bonding[39] (see Fig. 4). Hence one can conclude that the *unlike* diastereoisomer is more prone to undergo intermolecular hydrogen bonding, and thus is retained more strongly by the stationary phase, which is indeed observed (see Table I). For the cyclic carbonate **2b**, a similar order of the diastereoisomers is found, but the explanation is completely different. The *unlike* diastereoisomer with a *cis* configuration is more readily accessible to the hydrogen-bonding amide moieties of the stationary phase (see arrow in Fig. 4) than the respective like diastereoisomer with a *trans* configuration, and is therefore more strongly retained.

It is noted with interest that the order of emergence of the enantiomers of the diols **1a** and **2a** from L-Chirasil-Val (see Table I) can be correlated with the corresponding simple alcohols[40] formed by replacement of one hydroxy function by an alkyl residue, leaving one residual hydroxy function at the stereogenic centre. Likewise, the derivative **2b** is eluted with an enantiomeric order that is comparable to that of perfluoroacylated arylethanediols[26] and vinyltriols[11].

CONCLUSION

Enantiomers of aliphatic 1,2-diols, in contrast to 1,3-diols, can be separated by gas chromatography on well deactivated glass capillaries coated with L-Chirasil-Val. At low temperature, the resolution factors (α) are even higher than for the corresponding cyclic carbonates. Although the properties of the two classes of compounds seem to be similar around 70°C, detailed studies reveal intriguing differences in their thermodynamic properties, according to the pronounced differences in conformational flexibility and in the mode of the solute–solvent interaction. The surprisingly low isoselective temperature (T_s) found for simple aliphatic 1,2-diols may shed new light on the strong influence of interaction entropy on the separation mechanism. Obviously, rigidity of either the solute or solvent molecules is not a prerequisite for separation, although it may help to keep the resolution at a high level at elevated temperatures. At low temperatures, on the other hand, well designed flexibility may give rise to a good balance between enthalpy and entropy of interaction, and thus to relatively high α values.

ACKNOWLEDGEMENT

Lin Bingcheng is grateful to the Alexander von Humboldt-Stiftung for financial support.

REFERENCES

1 B. Koppenhoefer, M. Walser and E. Bayer, *J. Chromatogr.*, 358 (1986) 159; and references cited therein.
2 D. Seebach and H.-O. Kalinowski, *Nachr. Chem. Tech.*, 24 (1976) 415; and references cited therein.
3 K. Mori, *Tetrahedron*, 32 (1976) 1101.
4 G. L. Baker, S. J. Fritschel and J. K. Stille, *J. Org. Chem.*, 46 (1981) 2960.
5 L. D. Martin and J. K. Stille, *J. Org. Chem.*, 47 (1982) 3630.
6 K. S. Bhat, P. L. Joshi and A. S. Rao, *Synthesis*, (1984) 142.
7 K. Mori, H. Watanabe, K. Yanagi and M. Minobe, *Tetrahedron*, (1985) 3663.
8 P. L. Robinson, C. N. Barry, J. W. Kelly and S. A. Evans, Jr., *J. Am. Chem. Soc.*, 107 (1985) 5210.
9 P. J. Kocienski, S. D. A. Street, C. Yeates and S. F. Campbell, *J. Chem. Soc., Perkin Trans. 1*, (1987) 2171, and subsequent papers.
10 S. Hashimoto, T. Shinoda, Y. Shimada, T. Honda and S. Ikegami, *Tetrahedron Lett.*, 28 (1987) 637.
11 B. Koppenhoefer, M. Walser, D. Schröter, B. Häfele and V. Jäger, *Tetrahedron*, 43 (1987) 2064.
12 A. Yusufoglu, S. Antons and H.-D. Scharf, *Justus Liebigs Ann. Chem.*, (1986) 1119.
13 P. A. Levene and A. Walti, *J. Biol. Chem.*, 94 (1931) 361.
14 D. D. Ridley and M. Stralow, *J. Chem. Soc., Chem. Commun.*, (1975) 400.
15 B. Koppenhoefer, W. Winter and E. Bayer, *Justus Liebigs Ann. Chem.*, (1983) 1986.
16 H. Simon, J. Bader, H. Günther, S. Neumann and J. Thanos, *Angew. Chem.*, 97 (1985) 541; *Angew. Chem., Int. Ed. Engl.*, 24 (1985) 539.
17 D. Wistuba and V. Schurig, *Angew. Chem.*, 98 (1986) 1008; *Angew. Chem., Int. Ed. Engl.*, 25 (1986) 1032.
18 J. A. Dale and H. S. Mosher, *J. Am. Chem. Soc.*, 95 (1973) 512.
19 J. D. Morrison (Editor), *Asymmetric Synthesis, Vol. 1, Analytical Methods*, Academic Press, New York, 1983.
20 M. Zief and L. J. Crane (Editors), *Chromatographic Chiral Separations*, Marcel Dekker, New York, 1988.
21 V. Schurig, *Kontakte (Merck, Darmstadt)*, 1 (1985) 54, and subsequent papers.
22 B. Koppenhoefer and E. Bayer, in F. Bruner (Editor), *The Science of Chromatography*, Elsevier, Amsterdam, 1985, p. 1.
23 B. Koppenhoefer, H. Allmendinger and G. J. Nicholson, *Angew. Chem.*, 97 (1985) 46; *Angew. Chem., Int. Ed. Engl.*, 24 (1985) 48.
24 H. Frank, G. J. Nicholson and E. Bayer, *J. Chromatogr. Sci.*, 15 (1977) 174.
25 E. Bayer, H. Allmendinger, G. Enderle and B. Koppenhoefer, *Fresenius' Z. Anal. Chem.*, 321 (1985) 321.
26 B. Koppenhoefer and E. Bayer, *Chromatographia*, 19 (1984) 123.
27 W. A. König, *The Practice of Enantiomer Separation by Capillary Gas Chromatography*, Hüthig, Heidelberg, Basle, New York, 1987, and references cited therein.
28 W. A. König, S. Lutz and G. Wenz, *Angew. Chem.*, 100 (1988) 989; *Angew. Chem., Int. Ed. Engl.*, 27 (1988) 979.
29 V. Schurig and D. Wistuba, *Tetrahedron Lett.*, 25 (1984) 5633.
30 V. Schurig, B. Koppenhoefer and W. Bürkle, *J. Org. Chem.*, 45 (1980) 538.
31 V. Schurig, B. Koppenhoefer and W. Bürkle, *Angew. Chem.*, 90 (1978) 993; *Angew. Chem., Int. Ed. Engl.*, 17 (1978) 937.
32 G. J. Nicholson, personal communication.
33 B. Koppenhoefer, *Thesis*, University of Tübingen, 1980.
34 B. Koppenhoefer, B. Lin, V. Muschalek, U. Trettin, H. Willisch and E. Bayer, in E. Bayer and G. Jung (Editors), *Proceedings of the 20th European Peptide Symposium, Tübingen (FRG), September 4–9, 1988*, Walter de Gruyter, Berlin, 1989, p. 109.
35 K. Watabe, R. Charles and E. Gil-Av, *Angew. Chem.*, 101 (1989) 195.
36 V. Schurig, J. Ossig and R. Link, *Angew. Chem.*, 101 (1989) 197.
37 B. Koppenhoefer, H. Allmendinger, G. J. Nicholson and E. Bayer, *J. Chromatogr.*, 260 (1983) 63.
38 D. E. Koshland, Jr., *Sci. Am.*, 229, No. 4 (1973) 52.
39 G. Chiurdoglu, R. de Groote, W. Masschelein and M. H. van Risseghem, *Bull. Soc. Chim. Belg.*, 70 (1961) 342.
40 B. Koppenhoefer and H. Allmendinger, *Chromatographia*, 21 (1986) 503.

Journal of Chromatography, 481 (1989) 27–35
Elsevier Science Publishers B.V., Amsterdam — Printed in The Netherlands

CHROM. 21 742

CONVERSION OF A CONVENTIONAL PACKED-COLUMN GAS CHROMATOGRAPH TO ACCOMMODATE MEGABORE COLUMNS

I. EVALUATION OF THE SYSTEM FOR ORGANOPHOSPHORUS PESTICIDES

CLAUDE MALLET and VICTORIN N. MALLET*
Chemistry and Biochemistry Department, Université de Moncton, Moncton, NB E1A 3E9 (Canada)
(First received February 16th, 1989; revised manuscript received July 5th, 1989)

SUMMARY

A conventional packed-column chromatograph was modified for use with a megabore column using a commercial conversion kit, with the intention of developing a multi-residue method for organophosphorus pesticides. The results indicate that the conversion does not affect the resolving power of the megabore column, since fourteen organophosphorus pesticides could be separated in a single injection. The megabore column in such a system proved to be much more efficient than a packed column in terms of resolution and qualitative reproducibility, and comparable with a similar column in a dedicated chromatograph.

However, the conversion did affect the quantitative reproducibility of the system to some degree, as indicated by coefficients of variation between 5 and 27%, although it was determined that the particular nitrogen–phosphorus detector system (filament bead) used in this study was partly responsible for the variation. Nevertheless, calibration curves were obtained down to 0.1 ng per component, and a limit of quantitation of 1.0 ng was established for each component in a sample containing fourteen organophosphorus compounds. The results indicate that the system is sufficiently reproducible to develop a multi-residue method for organophosphorus pesticides in environmental waters.

INTRODUCTION

The technique of gas chromatography has evolved tremendously since its inception in 1951[1]. Initially the instrument was crude and simple, and consisted essentially of a heated injection port, an oven and a thermal conductivity detector. The column was initially made of copper tubing filled with an absorbant, but this was later replaced by glass tubing.

The first capillary (open tubular) column was introduced in 1957 by Golay[2], but its use was somewhat curtailed owing to a lack of capacity and easy breakage. A breakthrough came in 1979 with the introduction of fused-silica columns[3] (0.23 or

0021-9673/89/$03.50

0.32 mm I.D.). They were characterized by inertness, flexibility and ease of handling, and could be prepared with very thin stationary phases. However, column bleed was still a problem[4]. Subsequent studies resulted in a new breed of capillary columns with chemically bonded stationary phases[5–10]. These columns have excellent chemical and thermal stability, although the problem of capacity still remains[11]. Megabore columns (0.53–1.0 mm I.D.) have recently been introduced[12]. They are characterized by speed, inertness, thermal and chemical stability and efficacy (better resolution), but they have much better capacity[11] than conventional capillary (microbore) columns.

Many laboratories are still equipped with conventional packed-column chromatographs since it is only recently that dedicated capillary instruments have been marketed. Thus several authors[13,14] have reported on the conversion of their chromatograph to accept a megabore column for specific applications. Several prototypes of conversion kits have recently been marketed.

This paper reports on the conversion of a packed-column chromatograph to accommodate a megabore column, and on the evaluation of the system for the multiresidue determination of organophosphorus pesticides.

EXPERIMENTAL

Chemicals and apparatus

Organophosphorus pesticide standards were obtained from agriculture Canada (Ottawa, Canada). Stock solutions of 1 mg/ml were prepared in ethyl acetate (Anachemia). A complete list of all the pesticides studied is presented in Table I.

A Tracor 560 gas chromatograph with a Tracor 702 nitrogen–phosphorus detector was used. The chromatograph was modified to accept a megabore column using the "direct injection kit. No. 2" and the "make-up gas adaptor kit No. 2" from Supelco (Bellefonte, CA, U.S.A.).

The borosilicate megabore column (Supelco) was 30 m × 0.75 mm I.D. and contained 1.0-μm SPB-5 (a mixture of 5% dimethylpolysiloxane, 1% vinylmethylsiloxane and 94% diphenylpolysiloxane). The column was inserted 2 cm into the conversion tube (inlet) and 13 cm (outlet) into the detector system, so that the tip of the column came to rest *ca.* 2 mm from the jet. Another megabore column (30 m × 0.75 mm I.D.) containing SPB-1 (1.0 μm) was used for comparison purposes.

The detector source (filament) was operated at 7.5 V with the polarizing voltage at low. The flow-rates of air and hydrogen were set at 125 and 3.0 ml/min, respectively. The helium (carrier gas) flow-rate was set at 5.0 ml/min. A gas purifier operated at 600°C (Demery Lindberg) was installed to remove oxygen and water. Helium was also used as make-up gas when necessary.

Under normal conditions, the chromatograph was programmed as follows: 150°C for 3 min, up to 250°C at 5°C/min, hold for 8 min.

RESULTS AND DISCUSSION

The conversion of a packed-column chromatograph to accept a megabore column is straightfoward. Fig. 1 shows the location of the column in the injection port and the detector. There is some dead volume created by the glass tubing in the injection port and also in the second port, which is used as an inlet for make-up gas.

TABLE I

ADJUSTED RETENTION TIMES OF ORGANOPHOSPHORUS COMPOUNDS STUDIED

N.D. = Not detected.

Common name (trade name)	*Chemical name*	t'_R *(min)*
Acephate (Orthene)	O,S-Dimethyl acetyl-phosphoroamidothioate	9.3
Azinphos-methyl (Guthion)	O,O-Dimethyl S-[(4-oxo-1,2,3-benzotriazine-3(4*H*)-yl)methyl] phosphorodithioate	N.D.
Chlorpyrifos (Dursban)	O,O-Diethyl O-(3,5,6-trichloro-2-pyridyl) phosphorothioate	22.2
Diazinon (Basudin)	O,O-Diethyl O-(2-isopropyl-6-methyl-4-pyrimidyl) phosphorothioate	18.0
Dichlorvos (Nogos)	2,2-Dichlorovinyl dimethyl phosphate	4.5
Dimethoate (Cygon)	O,O-Dimethyl S-(methyl-carbamoylmethyl) phosphorodithioate	16.5
Disulfoton (Disyston)	O,O-Diethyl S-2-(ethylthio)-ethyl phosphorodithioate	18.3
Fenitrothion (Folithion)	O,O-Dimethyl O-(3-methyl-4-nitrophenyl) phosphorothioate	21.3
Bis-fenitrothion	O-methyl-O,O-[di-(3-methyl-4-nitrophenyl)]phosphorothioate	N.D.
S-Methyl-bis-fenitrothion	S-methyl-O,O-di-3-methyl-4-nitrophenyl phosphorothiolate	N.D.
Fensulfothion (Dasanit)	O,O-Diethyl O-[4-(methyl-sulphinyl) phenyl]phosphorothioate	27.3
Fenthion (Baycid)	O,O-Dimethyl O-[3-methyl-4-(methylthio)phenyl]phosphorothioate	21.9
Fonofos (Dyfonate)	O-Ethyl S-phenyl ethyl-phosphonodithioate	17.5
Malathion (Mercaptothion)	O,O-Dimethyl S-1,2-di-(ethoxycarbonyl) ethyl phosphorodithioate	21.6
Methamidophos (Monitor)	O,S-Dimethyl phosphoramidate	4.4
Oxydemeton-methyl (Metosystox-R)	S-[2-(Ethylsulfinyl)ethyl] O,O-dimethyl phosphorodithioate	N.D.
Parathion (Thiophos)	O,O-Diethyl O-*p*-nitrophenyl phosphorothioate	22.2
Phorate (Thimet)	O,O-Diethyl S-(ethyl-thiomethyl) phosphorodithioate	15.9
Phosalone (Zolone)	S-6-Chloro-2,3-dihydro-2-oxobenzoxazol-3-ylmethyl O,O-diethyl phosphorodithioate	N.D.
Phosmet (Imidan)	O,O-Dimethyl-S-phthalimi-domethyl phosphorodithioate	32.7
Temephos (Abate)	O,O,O',O'-Tetramethyl O,O'-thiodi-*p*-phenylene diphosphorothioate	N.D.
Tetrachlorvinphos (Gardonna)	2-Chloro-1-(2,4,5-tri-chlorophenyl)vinyl dimethylphosphate	24.6
Trichlorfon (Dipterex)	Dimethyl-(2,2,2-tri-chloro-1-hydroxyethyl phosphonate	9.8

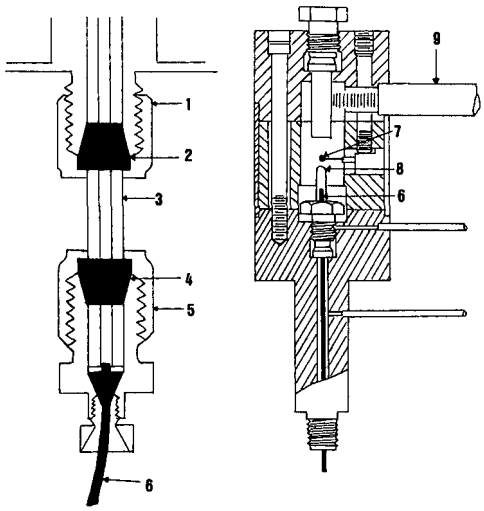

Fig. 1. Location of the column in the injection port (left) and in the Tracor detector (right): 1 = nut; 2 = ferrule; 3 = glass tubing; 4 = ferrule; 5 = nut; 6 = megabore column; 7 = filament and bead; 8 = jet; 9 = collecting electrode.

These two aspects are obvious drawbacks to this particular conversion kit as opposed to those kits that allow on-column injection.

The carrier gas was optimized using fenitrothion as a good representative of the organophosphorus compounds under study. It was found that a flow-rate of 5 ml/min offered good peak symmetry and reasonable retention time (21.3 min.) for fenitrothion. This is in agreement with the results of Lubkowitz *et al.*[15] who showed that the response of the nitrogen–phosphorus detector is at a maximum with a helium flow-rate of 5.0 ml/min. The response of the detector to fenitrothion was best with the air and hydrogen flow-rates set at 120 and 3.0 ml/min, respectively. It was also found that the response was better without make-up gas.

All the organophosphorus compounds available were tested individually under the above conditions. The results given in Table I show that 17 of the 23 compounds gave positive responses, with retention times varying from 4.4 to 32.7 min. However, some were not detected because of lack of volatility, and also several had similar retention times.

Attempts to separate all seventeen organophosphorus compounds by temperature programming failed. For this reason dichlorvos, fenthion and chlorpyrifos were excluded from further studies. Very good resolution was then achieved by temperature programming (140°C for 5 min up to 250°C at 3°C/min) for the remaining fourteen organophosphorus compounds, but the analysis time was unacceptably long at 115 min. Thus the programme time was shortened to 31 min with some loss in resolution (R = 0.78 between peaks 6 and 7, which means 30% overlap), as illustrated in Fig. 2.

Linearity study

Standard mix solutions of the fourteen organophosphorus compounds were

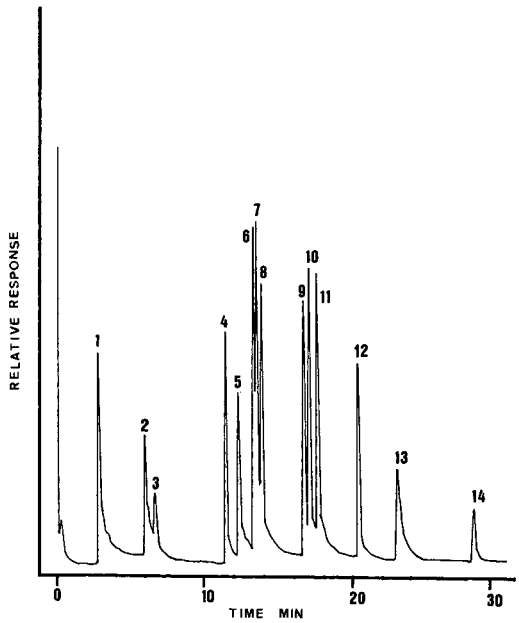

Fig. 2. Chromatogram showing separation of fourteen organophosphorus compounds on Megabore SPB-5. Amount injected, 1 ng of each. Peaks: 1 = methamidophos; 2 = acephate; 3 = trichlorfon; 4 = phorate; 5 = dimethoate; 6 = fonofos; 7 = diazinon; 8 = disulfoton; 9 = fenitrothion; 10 = malathion; 11 = ethyl-parathion; 12 = tetrachlorvinphos; 13 = fensulfothion; 14 = phosmet.

prepared such that 100.0, 10.0, 5.0, 1.0, 0.1 and 0.01 ng/μl of each pesticide were injected. Only a few pesticides, such as diazinon and ethyl-parathion, could be detected at 0.01 ng. Thus further studies with all fourteen organophosphorus were limited to 0.1 ng/μl solutions. A typical cailbration curve for metamidophos is shown in Fig. 3. The slope of the curve is 0.92, which indicates good sensitivity. However, below 1.0 ng, the deviation from linearity becomes excessive. All the other organophosphorus compounds showed similar response curves, with slopes (sensitivity) varying between 0.90 and 1.0; exceptions were phorate and disulfoton, with values of 0.60 and 0.77, respectively.

Reproducibility studies

The reproducibility of a chromatogram in terms of individual retention times in multi-residue analysis is very important for identification purposes. Table II gives the coefficients of variation (C.V., n = 16) of the retention times for the fourteen organophosphorus compounds studied. The variation is slightly higher at low retention values but the average C.V. is only 2%, which is quite acceptable considering that variations between 1 and 10% are common in gas chromatography[16]. Such little variation enables the analyst to detect a particular organophosphorus compound with reasonable accuracy and is a clear indication that the conversion does not adversely affect column performance.

Reproducibility as a function of peak height is more of a problem. C.V. for 1.0

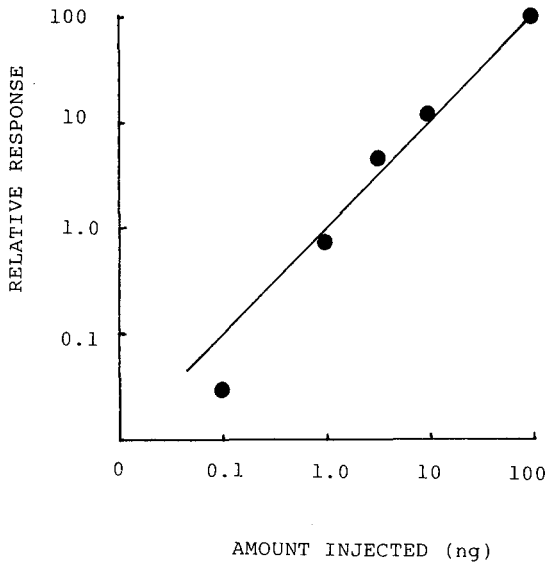

Fig. 3. Calibration curve for methamidophos.

ng of each component in the multi- residue standard are given in Table III. They show a minimum of 5% for ethyl-parathion and a maximum of 27% for phosmet. This variation may be attributed to several reasons. The main one is the greater surface area (due to extra plumbing) that the injected sample comes in contact with before

TABLE II

REPRODUCIBILITY STUDY OF RETENTION TIMES OF A MULTI-RESIDUE STANDARD (1.0 ng)

Organophosphorus compound	*Average (n=16) retention time (min)*	*S.D.*	*C.V. (%)*
Methamidophos	2.9	0.1	4
Acephate	5.9	0.2	3
Trichlorfon	6.4	0.2	3
Phorate	11.1	0.3	2
Dimethoate	12.0	0.3	2
Fonofos	13.1	0.3	2
Diazinon	13.2	0.3	2
Disulfoton	13.5	0.3	2
Fenitrothion	16.3	0.3	2
Malathion	16.7	0.2	1
Ethyl-parathion	17.1	0.2	1
Tetrachlorvinphos	19.9	0.3	1
Fensulfothion	22.6	0.4	2
Phosmet	27.3	0.5	2
		Average	2

TABLE III

REPRODUCIBILITY STUDY OF DETECTOR RESPONSE TO A MULTI-RESIDUE STANDARD (1.0 ng)

Organophosphorus compound	*Average (n = 16) peak height*	*S.D.*	*C.V. (%)*
Methamidophos	12.1	1.8	15
Acephate	2.3	0.4	15
Trichlorfon	6.3	0.6	9
Phorate	21.6	1.6	7
Dimethoate	14.7	2.3	16
Fonofos	34.0	3.8	11
Diazinon	52.1	6.1	12
Disulfoton	38.8	3.8	10
Fenitrothion	42.7	3.0	7
Malathion	36.4	3.4	9
Ethyl-parathion	48.4	2.6	5
Tetrachlorvinphos	30.0	3.3	11
Fensulfothion	6.4	1.6	25
Phosmet	3.9	1.1	27
		Average	12

entering and at the exit of the column, which contributes to band broadening and inevitably affects reproducibility. Another important reason is believed to be detector variability. In the past, while working with packed columns, this particular nitrogen–phosphorus detector (Tracor 702) showed occasional variability, which was related to the particular filament bead in the detector. A third cause of variation is related to the particular organophosphorus compound (for example, tetrachlorovinphos and phosmet), which sometimes lack volatility. This results in broad and unsymmetrical peaks, which have a strong influence on reproducibility.

Limits of detection and quantitation

The limit of detection (LOD) (peak height double the noise) varies with each chemical. In order to detect each compound in the multi-residue standard, a solution of at least 0.1 ng/μl has to be injected. However, considering the variability expressed above for each pesticide, a limit of quantitation (LOQ) of 1.0 ng per analyte (ten times LOD) was chosen (average C.V. 12%) to ensure that all pesticides could be analysed with precision.

Comparison with SPB-1 megabore

The SPB-1 is considered to be less polar than SPB-5. A chromatogram of fourteen organophosphorus compounds at 1.0 ng/μl is shown in Fig. 4. Resolution is better for peaks 8, 9, 10 and 11 than with the SPB-5 column. However, peaks 6 and 7 co-elute and peaks 1 and 2 are not as sharp. Overall, the SPB-5 stationary phase gives better results than the SPB-1.

Sasaki *et al.*[17] have evaluated three megabore columns installed in a dedicated capillary gas chromatograph with a flame photometric detector in a multi-residue study of OPs in agricultural products. All the columns were 0.53 mm I.D., with

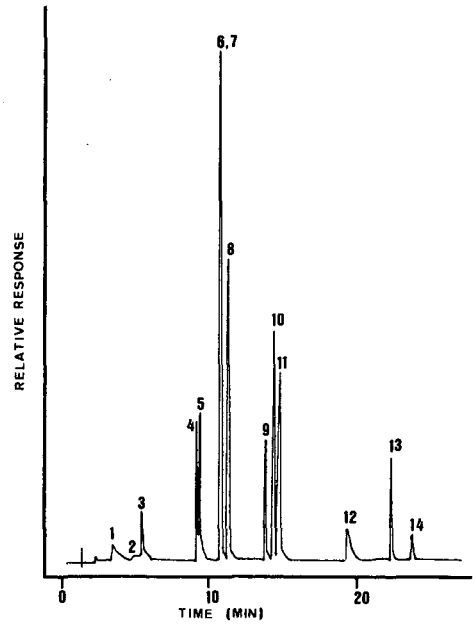

Fig. 4. Chromatogram of fourteen organophosphorus pesticides on SPB-1; amount injected, 1.0 ng of each. Peak numbers as in Fig. 2.

lengths between 10 and 12 m. These authors studied individually 23 organophosphorus compounds on CBP-10, CBP-1 and 5% phenylmethylsilicone. For comparison purposes, only the results with 5% phenylsilicone will be mentioned since this stationary phase compares favourably with SPB-5. The retention times varied from 0.9 min (dichlorvos) to 24.3 min for phosmet. The LOD varied between 0.01 and 0.08, which compares favourably with our data.

CONCLUSION

This study shows the separation of fourteen organophosphorus compounds on a megabore column installed in a conventional gas chromatograph. The results compare well with those obtained with a dedicated capillary gas chromatograph[17]. In comparison, a packed column (1.8 m × 4 mm I.D., OV-101:OV-210) in the same chromatograph can separate only five of the fourteen chemicals. Others co-elute or are simply not volatile under these conditions.

The quantitative data, on the other hand, show more variability, some of which may be caused by the conversion (more dead volume and surface area) of the gas chromatograph to accept megabore columns. However, it is suspected that much of the variability may be due to detector instability in our particular case.

It was felt that the results were sufficiently reproducible to warrant further studies. Thus, the system was used to evaluate several methods for the recovery of organophosphorus compounds from water. The results of this study appear in the following paper.

ACKNOWLEDGMENT

This work was supported by the National Science and Engineering Research Council of Canada and performed under the auspices of the Environmental Research Sciences Centre at the Université de Moncton.

REFERENCES

1 A. J. D. James and A. J. Martin, *Biochemistry*, 8 (1951) vii.
2 M. J. E. Golay, *Anal. Chem.*, 29 (1957) 29.
3 R. Dandeneau and E. H. Zerenner, *J. High Resolut. Chromatogr. Chromatogr. Commun.*, 2 (1979) 351.
4 S. Lipsky and W. J. McMurray, *J. Chromatogr.*, 279 (1983) 59.
5 C. Madini, E. M. Chamboz, M. Rigaud, J. Durand and P. Chebroux, *J. Chromatogr.*, 279 (1983) 59.
6 C. Madini and E. M. Chamboz, *Am. Oil Chem. Soc.*, 58 (1981) 63.
7 L. Bloomberg and J. Wannman, *J. Chromatogr.*, 168 (1979) 81.
8 L. Bloomberg and J. Wannman, *J. Chromatogr.*, 186 (1979) 159.
9 K. Grob, G. Grob and K. Grob Jr., *J. Chromatogr.*, 211 (1981) 243.
10 K. Grob and G. Grob, *J. Chromatogr.*, 213 (1981) 211.
11 R. T. Weidener, S. L. McKinley and T. W. Rende, *Int. Lab.*, May (1986) 69.
12 C. F. Poole, *Contemporary Practice of Chromatography*, Elsevier, Amsterdam, New York, 1984.
13 R. K. Mitchum, W. A. Korfmacher and G. F. Moler, *J. High Resolut. Chromatogr. Chromatogr. Commun.*, 4 (1987) 180.
14 P. Demeatts, J. Vander Verren and A. Heyndrickx, *J. Pharm. Biol. Anal.*, 4 (1987) 105.
15 J. A. Lubkowitz, J. L. Glajch, B. P. Semonian and L. B. Rogers, *J. Chromatogr.*, 133 (1977) 37.
16 D. A. Skoog, *Principles of Instrumental Analysis*, CBS College Publishing, New York, 3rd ed., 1985, p. 749.
17 K. Sasaki, J. Suzuki and Y. Saito, *J. Assoc. Off. Anal. Chem.*, 170 (1987) 460.

Journal of Chromatography, 481 (1989) 37–44
Elsevier Science Publishers B.V., Amsterdam — Printed in The Netherlands

CHROM. 21 743

CONVERSION OF A CONVENTIONAL PACKED-COLUMN GAS CHROMATOGRAPH TO ACCOMMODATE MEGABORE COLUMNS

II. DETERMINATION OF ORGANOPHOSPHORUS PESTICIDES IN ENVIRONMENTAL WATER

CLAUDE MALLET and VICTORIN N. MALLET*
Chemistry and Biochemistry Department, Université de Moncton, Moncton, NB E1A 3E9 (Canada)
(First received February 16th, 1989; revised manuscript received July 5th, 1989)

SUMMARY

Several methods involving solvent extraction or solid extraction (Amberlite XAD resins) were studied for the multi-residue recovery of fourteen organophosphorus compounds in water. It was found that extraction with ethyl acetate in a salted medium provided the most consistent data, both in terms of number of compounds recovered and percentage recovery. Amberlite XAD resins gave consistently high recoveries, and this was attributed to a matrix effect upon the particular nitrogen–phosphorus detector.

The evaluation was made using a megabore column installed in a conventional packed-column chromatograph, and the results show that such a system is amenable to the multi-residue analysis of organophosphorus pesticides at very low cost.

INTRODUCTION

Organophosphorus pesticides form a large class of compounds with various chemical structures. This presents a problem in terms of developing a multi-residue method for their analysis from environmental samples, since extraction and instrumental methods of analysis are not universal. Aqueous samples of organophosphorus pesticides may be extracted with an organic solvent, such as ethyl acetate, benzene, chloroform, dichloromethane or hexane. Suffet *et al.*[1] have determined that proper control of pH and ionic strength is necessary to obtain reproducible recoveries.

Solid phase extraction of aqueous samples has become very common in recent years. Amberlite XAD resin columns have been used for the recovery of fenitrothion and several breakdown products in water[2–4]. This technique has been extended to the recovery of organophosphorus pesticides from tap water by sampling large volumes[5]. Adsorption columns[6] and, more recently, reversed-phased adsorbants[7] have also been used.

The most popular approach to the analysis of organophosphorus pesticides is gas–liquid chromatography (GLC). Until recently mostly packed columns coupled to

0021-9673/89/$03.50

various detectors, such as the flame photometric[8], the thermionic[9], the electron capture[10] and the Hall[11], were used. However, the number of organophosphorous pesticides that may be analysed simultaneously with packed columns is limited by lack of resolution and lack of volatility.

Recently, dedicated capillary chromatographs[12–15] have been used with excellent results in terms of resolution, but limited capacity is a drawback. Megabore columns offer an alternative in the sense that they possess good resolution and capacity[16].

In the first part of this project[17] a packed-column gas chromatograph was converted into a megabore system and used for the analysis of fourteen organophosphorous compounds. In this part of the study the object was to evaluate several approaches to their multi-residue extraction in water using megabore column GLC.

EXPERIMENTAL

Materials and apparatus

These were as described in Part I[17]. The environmental water came from a lake used for drinking water.

Amberlite XAD resin column and extraction

The resin (500 g) in a 1-l beaker was cleaned with ethyl acetate by placing the container in an ultrasonic bath for 15 min. It was filtered, and cleaned again with ethyl acetate, then with methanol followed by purified water.

Columns were prepared as described earlier[2–4]. A 1-l water sample was processed by passage through an XAD resin column (gravity flow) and elution with two 100-ml volumes of ethyl acetate. The final volume was adjusted to 10.0 or 1.0 ml.

Solvent extraction of organophosphorus compounds from water

A 1-l water sample was fortified with the multi-residue standard at the appropriate concentration, and the sample was stirred for 10 min. The sample was then extracted with three 100-ml volumes of solvent (ethyl acetate, dichloromethane or hexane). The extract was dried with anhydrous sodium sulphate, evaporated to a small volume on a rotary evaporator, then adjusted to 10.0 ml. Duplicate extractions were done for each set of conditions. Whenever variation was observed a third or fourth sample was processed until agreement was obtained.

Purified water (pH 5.8) was used as control. A series of samples was also prepared by adjusting the pH to 3.0 using HCl (1.0 *M*). Another set of samples was prepared by adding 50 g of NaCl to purified water.

RESULTS AND DISCUSSION

In Part I[17] it was established that fourteen organophosphorus compounds could be separated on a SPB-5 megabore column and that the limit of quantitation using a multi-residue standard was 1.0 ng. At this level the coefficients of variation (C.V.) varied between 5 and 27%, with an average of 12%. Bearing this in mind, water samples were fortified at the 10 μg/l (ppb) level and extracted using Amberlite XAD-4, Amberlite XAD-7, ethyl acetate, dichloromethane or hexane. Extraction

was also performed under different conditions of pH and salinity. Percentage recoveries were obtained by comparing peak heights with those of a multi-residue external standard of the same concentration.

The results for purified water are presented in Table I. Values for each pesticide are expected to vary according to the respective C.V.[17], which is a parameter indicative of the precision of the gas chromatographic analysis using standard solutions. For instance, the value for fenitrothion recovery with hexane should be 93% ± 7%, that for phosmet should be 118% ± 27%. Several data were outside the normal error range of the method: these are indicated in Table I. This indicates that some additional factor has an influence on the reproducibility. Accuracy, or how close to 100% the recovery values will be, is another matter. It depends on the effectiveness of the recovery step and many factors interfere along the way. At the limit of quantitation of a method the variation may be very high, and it becomes difficult to decide what is acceptable. Thus, in this study, for the purpose of comparison between methods, values within a range of 100% ± 25% will be considered acceptable.

The data for hexane in Table I show that nine pesticides are well recovered, four cannot be detected and one value is too low. This is reflected by the recovery ratios (9:4:1:0), which have been used in this study to compare the effectiveness of the various methods. The recovery ratio for dichloromethane shows that only three recoveries are acceptable (3:3:8:0). Good results were obtained with ethyl acetate with a ratio of 10:2:2:0. With Amberlite XAD-7 the ratio 10:2:1:1 indicates good performance, although the same pesticides are not involved. With Amberlite XAD-4 the

TABLE I

PERCENTAGE RECOVERY OF ORGANOPHOSPHORUS PESTICIDES (10 ppb) FROM PURIFIED WATER (pH 5.8)

ND = Not detected.

Pesticide	*Extractant*				
	Hexane	*Dichloromethane*	*Ethylacetate*	*XAD-7*	*XAD-4*
Methamidophos	ND	ND	ND	ND	16[a]
Acephate	ND	ND	ND	ND	9[a]
Trichlorfon	ND	ND	21[a]	63[a]	104
Phorate	99	70[a]	99	85	95
Dimethoate	ND	51[a]	66[a]	113[a]	161[a]
Fonofos	104	71[a]	110	89	92
Diazinon	93	69[a]	95	89	101
Disulfoton	98	67[a]	101	107	117[a]
Fenitrothion	93	71[a]	93	95	108[a]
Malathion	93	68[a]	102	88	103
Ethyl-parathion	92	68[a]	93	101	105
Tetrachlorvinphos	95	80[a]	91	106	126[a]
Fensulfothion	53[a]	94	90	112[a]	147[a]
Phosmet	118	105	86	213[a]	251[a]
Recovery ratios[b]	9:4:1:0	3:3:8:0	10:2:2:0	10:2:1:1	9:0:2:3

[a] Recovery is outside the C.V. range[17].

[b] Recovery ratio means acceptable recovery:not detected:low value:high value.

recoveries for methamidophos and acephate are out of range because of low results, and three values are excessively high. Overall the results with ethyl acetate and Amberlite XAD-7 are equivalent, although not similar for all pesticides. An explanation for the high values with XAD resins will be offered later.

Some extraction procedures are known to improve at lower pH, particularly when acidic compounds are present. Thus the pH was adjusted to 3.0. The results, presented in Table II, indicate that a decrease in pH has a favourable effect with dichloromethane but very little effect with the other solvents. With XAD resins more of the values are greater than 125%. Some high values are also observed with the organic solvents. Several attempts to increase recoveries were made at pH 7.5, 8.5 and 9.5, but without success.

Sometimes, particularly with slightly water-soluble solvents and to increase the partition coefficient of a solute in an organic solvent, the water sample is saturated with sodium chloride. The results, presented in Table III, show that salt addition favours recovery with organic solvents but with the resins more higher values are obtained.

The overall picture (compare recovery ratios) indicates that, among the three organic solvents, recoveries with ethyl acetate are better and more organophosphorus pesticides are recoverd. Recoveries with hexane are good, with the exception of four compounds. Recoveries with dichloromethane are positive but the values are low. In general, recoveries are better at a lower pH or in a salt-saturated medium. Recoveries with Amberlite XAD resins are sometimes high, particularly at low pH or in a salt medium. However, Amberlite XAD-4, in particular, recovers some part of all the

TABLE II

PERCENTAGE RECOVERY OF ORGANOPHOSPHORUS PESTICIDES (10 ppb) FROM PURIFIED WATER (pH 3.0)

ND = Not detected.

Pesticide	*Extractant*				
	Hexane	*Dichloromethane*	*Ethylacetate*	*XAD-7*	*XAD-4*
Methamidophos	ND	ND	ND	12[a]	ND
Acephate	ND	ND	ND	11[a]	ND
Trichlorfon	ND	ND	25[a]	71[a]	82
Phorate	112[a]	98	95	61[a]	98
Dimethoate	ND	101	80	156[a]	140[a]
Fonofos	122[a]	109	119[a]	89	97
Diazinon	105	95	93	92	100
Disulfoton	109	94	96	15[a]	134[a]
Fenitrothion	115[a]	106	104	127[a]	114[a]
Malathion	117[a]	103	108	97	103
Ethyl-parathion	112[a]	104	100	97	113[a]
Tetrachlorvinphos	118[a]	111	98	115[a]	128[a]
Fensulfothion	88	159[a]	102	143[a]	134[a]
Phosmet	192[a]	171[a]	121[a]	204[a]	236[a]
Recovery ratios	9:4:0:1	9:3:0:2	11:2:1:0	5:0:5:4	7:2:0:5

[a] Recovery is outside the C.V. range[17].

TABLE III

PERCENTAGE RECOVERY OF ORGANOPHOSPHORUS PESTICIDES (10 ppb) FROM PURIFIED WATER SATURATED WITH SODIUM CHLORIDE

ND = Not detected.

Pesticide	*Extractant*				
	Hexane	*Dichloromethane*	*Ethylacetate*	*XAD-7*	*XAD-4*
Methamidophos	ND	ND	ND	ND	10[a]
Acephate	ND	ND	ND	ND	11[a]
Trichlorfon	ND	ND	41[a]	93	112[a]
Phorate	104	79[a]	96	111[a]	92
Dimethoate	ND	66[a]	87	163[a]	175[a]
Fonofos	110	88	105	107	99
Diazinon	105	76[a]	99	108	110
Disulfoton	106	72[a]	96	130[a]	89
Fenitrothion	108	84	99	122[a]	119[a]
Malathion	105	79[a]	96	114[a]	110
Ethyl-parathion	105	81	95	114[a]	111
Tetrachlorvinphos	110	88	98	132[a]	127[a]
Fensulfothion	95	124[a]	102	143[a]	161[a]
Phosmet	133[a]	119[a]	87	215[a]	249[a]
Recovery ratios	9:4:0:1	9:3:4:0	11:2:1:0	7:2:0:5	8:0:2:4

[a] Recovery is outside the C.V. range[17]

organophosphorus pesticides tested. None of the above extraction methods successfully recovered methamidophos or acephate, although Amberlite XAD-4 showed some recovery, and trichlorfon could not be recovered successfully with organic solvents.

The major cause for the high results, which is more pronounced with Amberlite XAD-4, is attributable to a matrix effect. A standard solution of the pesticides was prepared in ethyl acetate that had been eluted through a resin column. The results compared to a regular standard in ethyl acetate are presented in Table IV. They show that the detector response increases tremendously in some cases (300% phosmet), indicating a definite matrix effect. The fault in this case lies mostly with the filament bead of the nitrogen–phophorus detector and not on the XAD resin. If it was not for the matrix effect, Amberlite XAD-4 columns would probably have given quantitative recoveries for twelve out of fourteen pesticides. Therefore Amberlite XAD resin columns should not be discounted as an extraction procedure for organophosphorus pesticides.

To reduce the matrix effect the data were recalculated using the internal standard approach. Usually an internal standard has a structure and chromatographic properties similar to those of the analytes, and the peak must be well resolved. Thus, using tetrachlorvinphos as internal standard gave the results in Table IV for purified water. The results are very similar to those obtained with the external standard (*cf.* Tables I–III) except for dichloromethane, where the values are now mostly in the acceptable range. The use of fenitrothion as internal standard was also tested and the same conclusion was obtained, *i.e.* the internal standard approach can correct for

TABLE IV

EFFECT OF CO-EXTRACTIVES FROM AMBERLITE XAD-4 RESIN ON DETECTOR RESPONSE

Pesticide	*Peak height (cm) of standard in purified methyl acetate*	*Peak height (cm) of standard in ethyl acetate extract*	*Increase (%)*
Methamidophos	13.0	21.5	65.4
Acephate	8.3	14.5	74.7
Trichlorfon	3.8	4.7	23.7
Phorate	21.8	24.5	12.4
Dimethoate	23.2	38.3	65.1
Fonofos	77.8	85.0	9.3
Diazinon	34.5	38.5	11.6
Disulfoton	50.5	58.0	14.9
Fenitrothion	43.3	59.3	37.0
Malathion	67.8	78.5	15.8
Ethyl-parathion	62.5	77.8	24.5
Tetrachlorvinphos	38.8	55.3	42.5
Fensulfothion	12.3	28.3	130
Phosmet	4.0	16.0	300

TABLE V

PERCENTAGE RECOVERY OF ORGANOPHOSPHORUS PESTICIDES (10 ppb) FROM DISTILLED WATER (pH 5.8) WITH TETRACHLORVINPHOS AS INTERNAL STANDARD

ND = Not detected.

Pesticide	*Extractant*				
	Hexane	*Dichloromethane*	*Ethylacetate*	*XAD-7*	*XAD-4*
Methamidophos	ND	ND	ND	ND	12[a]
Acephate	ND	ND	ND	ND	7[a]
Trichlorfon	ND	ND	23[a]	59[a]	82
Phorate	104	88	103	81	74[a]
Dimethoate	ND	64[a]	73[a]	108	128[a]
Fonofos	110	89	121[a]	85	74[a]
Diazinon	97	87	105	84	81
Disulfoton	104	85	112	102	94
Fenitrothion	98	89	102	90	86
Malathion	98	85	113	84	82
Ethyl-parathion	97	86	102	83	84
Tetrachlorvinphos	–	–	–	–	–
Fensulfothion	56[a]	119[a]	100	106	116[a]
Phosmet	124[a]	132[a]	95	200[a]	198[a]
Recovery ratios	8:4:1:0	8:3:1:1	9:2:2:0	9:2:1:1	7:0:4:2

[a] Recovery is outside the C.V. range[17].

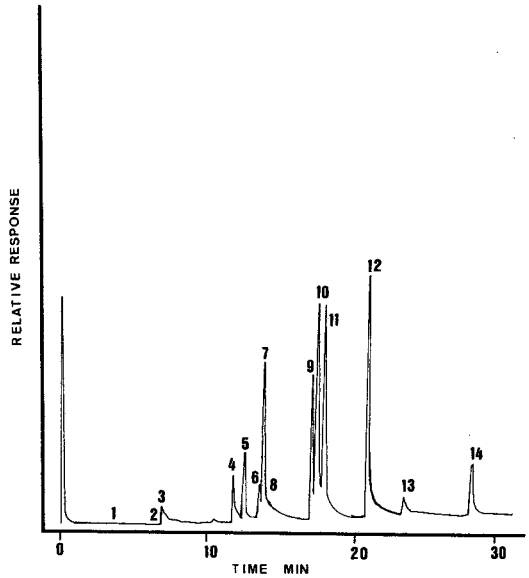

Fig. 1. Chromatogram of an extract of fourteen organophosphorus pesticides in environmental water at 1.0 μg/l. Extraction with ethyl acetate and sodium chloride. Peaks: 1 = methamidophos; 2 = acephate; 3 = trichlorfon; 4 = phorate; 5 = dimethoate; 6 = fonofos; 7 = diazinon; 8 = disulfoton; 9 = fenitrothion; 10 = malathion; 11 = ethyl-parathion; 12 = tetrachlorvinphos; 13 = fensulfothion; 14 = phosmet.

matrix effects in some cases but overall the picture is not much better than with an external standard. This was expected since the detector response to the matrix is not equivalent for each OP (see Table IV).

Determination of the limit of quantitation in environmental water

It has already been established that, at 10 ppb, eleven out of fourteen organophosphorus pesticides may be recovered successfully from water with ethyl acetate in a salt-saturated medium (methamidophos, acephate and trichlorfon are not well recovered). Under the same extraction conditions fonofos, disulfoton and fensulfothion cannot be quantitated at the 1.0 ppb level, as shown in Fig. 1. Only diazinon, fenitrothion, malathion and ethyl parathion may be determined quantitatively using the multi-residue approach.

CONCLUSION

This study confirms that a megabore column installed in a conventional gas chromatograph may be used for the separation and quantitation of organophosphorus compounds from a multi-residue sample of water. Evaluation of a liquid extraction procedure *versus* solid extraction showed that extraction with ethyl acetate in a salted medium gave the most reliable recoveries for eleven compounds out of fourteen. Extraction with Amberlite XAD-4 gave excellent recoveries with twelve out of fourteen compounds, but some of the values were consistantly high, a phenomenon attributed to a matrix effect towards the nitrogen–phosphorus (thermionic) detector.

Sasaki *et al.*[16] have studied the use of megabore columns in a dedicated capillary gas chromatograph for the multi-residue determination of organophosphorus compounds in various crops. They used megabore columns, 10–12 m × 0.53 mm I.D., containing CBP-10, CBP-1 or 5% phenyl methyl silicone. The last stationary phase compares favourably with SPB-5 used in this study. Their results showed a limit of detection five to ten times better than ours with comparable resolution (for those organophosphorus compounds in common) using a flame photometric detector. However, such a limit of detection could be attained with a modified megabore system using the nitrogen–phosphorus detector, provided the latter is performing as it should.

Thus it is fair so say that the megabore dedicated capillary system used by Sasaki *et al.* gave a slightly better performance than the modified conventional megabore system used in this study. However, we feel that the results obtained with the modified system are satisfactory in terms of performance, and the method proposed in this study (extraction with ethyl acetate in salted medium) is applicable to the multi-residue analysis of organophosphorus pesticides in environmental water, although the use of Amberlite XAD-4 should not be discounted. Conversion of a conventional chromatograph to megabore (and back to packed columns) is simple and involves little cost. It is felt that improvements in resolution and quantitation could be made with better conversion kits and a more reliable nitrogen–phosphorus detector.

ACKNOWLEDGEMENT

This work was supported by National Science and Engineering Research Council of Canada and performed under the auspices of the Environmental Research Sciences Centre at the Université de Moncton.

REFERENCES

1 I. H. Suffet, C. Wu and D. T. L. Wong, *ASTM Spec. Tech. Publ.*, 573 (1975) 167.
2 K. Berkane, G. E. Caissie and V. N. Mallet, *J. Chromatogr.*, 139 (1977) 386.
3 V. N. Mallet, G. L. Brun, R. N. Macdonald and K. Berkane, *J. Chromatogr.*, 160 (1978) 81.
4 G. G. Volpé and V. N. Mallet, *Int. J. Environ. Anal. Chem.*, 8 (1980) 291.
5 G. L. Lebel, D. T. Williams, G. Griffith and F. M. Benoit, *J. Assoc. Off. Anal. Chem.* 62 (1979) 241.
6 W. A. Saner and J. Gilbert, *J. Liq. Chromatogr.*, 3 (1988) 1753.
7 P. A. Greve and C. E. Goeuie, *Int. J. Environ. Anal. Chem.*, 20 (1985) 29.
8 K. Sasaki, J. Suzuki and Y. Saito, *J. Assoc. Off. Anal. Chem.*, 70 (1987) 460.
9 J. J. Blaha and P. J. Jackson, *J. Assoc. Off. Anal. Chem.*, 68 (1985) 1095.
10 H. B. Lee, L. Weng and A. S. Y. Chau, *J. Assoc. Off. Anal. Chem.*, 67 (1984) 553.
11 M. A. Luke, *J. Assoc. Off. Anal. Chem.*, 64 (1981) 1187.
12 T. J. Kim, Y. W. Eo and Y. S. Kim, *J. Korean Chem. Soc.*, 30 (1986) 465.
13 H. J. Stan and D. Mrowetz, *J. High Resolut. Chromatogr. Chromatogr. Commun.*, 6 (1983) 235.
14 L. Zenon-Roland, R. Agneessens, P. Nagnicot and H. Jacobs, *J. High Resolut. Chromatogr. Chromatogr. Commun.*, 7 (1984) 136.
15 J. Kjolholt, *J. Chromatogr.*, 325 (1985) 231.
16 K. Sasaki, T. Suzuki and Y. Saito, *J. Assoc. Off. Anal. Chem.*, 70 (1987) 460.
17 C. Mallet and V. N. Mallet, *J. Chromatogr.*, 481 (1989) 27.

Journal of Chromatography, 481 (1989) 45–54
Elsevier Science Publishers B.V., Amsterdam — Printed in The Netherlands

CHROM. 21 751

GAS CHROMATOGRAPHY OF TITAN'S ATMOSPHERE

I. ANALYSIS OF LOW-MOLECULAR-WEIGHT HYDROCARBONS AND NITRILES WITH A PORAPLOT Q POROUS POLYMER COATED OPEN-TUBULAR CAPILLARY COLUMN

L. DO and F. RAULIN*
Laboratoire de Physico-Chimie de l'Environnement, Université Paris XII, 94010 Creteil Cedex (France)
(First received February 14th, 1989; revised manuscript received July 6th, 1989)

SUMMARY

A PoraPLOT Q column was utilized for gas chromatographic analyses of various mixtures of low-molecular-weight saturated and unsaturated hydrocarbons and nitriles, which are plausible constituents of the atmosphere of Titan, the largest satellite of Saturn. This capillary column coated with styrene–divinylbenzene copolymer has a chromatographic behaviour similar to that of a Porapak Q packed column when analyzing these compounds. Its chromatographic behaviour however, is drastically improved by its much higher resolving power. With more than 1000 theoretical plates per metre for nitriles, this column offers a rapid separation of these compounds from C_1–C_8 hydrocarbons, even under isothermal conditions. It appears to be a viable choice for the gas chromatograph–mass spectrometer aboard the Huygens probe of the Cassini mission which is planned to explore Titan's atmosphere.

INTRODUCTION

For the development of space missions involving gas chromatography (GC), rapid GC analyses with good resolution and compatible with the requirements of space instrumentation and planetary missions are now needed. This is the case in particular with the joint NASA-ESA Cassini mission to the Saturn system, planned to be launched in 1996[1].

Cassini and the in situ analysis of Titan's atmosphere

One of the main objectives of the Cassini mission is to explore the atmosphere of Titan, the largest satellite of Saturn, from an atmospheric probe called Huygens. Several of the nine scientific instruments aboard will allow the *in situ* analysis of Titan's atmosphere during the 3-h descent of the probe. These include a gas chromatograph operating in two possible modes: not coupled or coupled to a mass spectrometer. It will be able to analyze gases either directly sampled from the atmosphere, or provided after pyrolysis by an aerosol collector-pyrolyzer experiment[1].

0021-9673/89/$03.50

Titan's atmosphere is mainly composed of nitrogen with a noticeable mole fraction of methane and the likely presence of argon. Several minor constituents have already been detected: at the 1000–10 ppmv level, H_2, CO and C_2H_6; below 10 ppmv, saturated C_2–C_3 hydrocarbons, ethylene, acetylene, propyne and diacetylene, HCN, C_2N_2, HC_3N and CO_2. Several other hydrocarbons and nitriles are expected to be present in this environment[2].

GC requirements

The GC experiment aboard Huygens must be able to analyze simultaneously C_1–C_8 hydrocarbons, C_1–C_4 nitriles and dinitriles, CO, H_2 and CO_2, in the presence of large amounts of N_2 and Ar, within a short enough time frame (less than about 15 min) necessary for several analyses.

However, it must offer a resolution high enough to allow the separation of most of these expected atmospheric constituents, with a column capacity allowing their quantitative analysis in an high dynamic range of concentration.

In order to solve this problem, we are currently developing chromatographic studies in two directions: the use of small and short columns packed with microparticles, and the use of capillary columns. We plan to present the different results of such studies in a series of articles. This article, the first in the series, is devoted to the study of a PLOT (porous-layer open-tubular) capillary column[3].

Capillary GC columns have not yet been used in space instrumentation. However, they can offer a good resolution within a relatively short time of analysis, if they are not too long, and their use simplifies the coupling of the gas chromatograph with a mass spectrometer. With PLOT capillary columns one can combine these advantages with the chromatographic capabilities of adsorption materials such as porous polymers, which can be used as column coatings.

Porous polymers have been largely utilized as packing materials in GC. In particular, styrene polymers or styrene–divinylbenzene or ethylvinylbenzene copolymer packings such as Chromosorb 103 (Manville, Lompoc, CA, U.S.A.) or Porapak Q (Waters, Milford, MA, U.S.A.) have been used intensively in packed GC columns to analyze gaseous mixtures including hydrocarbons and nitriles[4–7]. This type of adsorbent has also been used as a packing material in space gas chromatographs, such as that of the "gas exchange" experiment of the Viking Mission to Mars[8] and the Pioneer-Venus sounder probe gas chromatograph[9,10].

PoraPLOT Q

A fused-silica PLOT capillary column coated with the same kind of porous polymer (styrene–divinylbenzene) named PoraPLOT Q has recently been commercialized (Chrompack, The Netherlands). Detailed studies of the characteristics and chromatographic performances of this column, and comparisons with those of Porapak Q packed columns, have already been published[11,12]. PoraPLOT Q seems to offer the advantages of the Porapak Q column, such as the possibility of separation of permanent gases, and volatile polar and apolar organic compounds, with the high resolution of a capillary column. However, no data were available on the separation of nitriles and very few on that of alkynes with this PLOT column.

We found the close similarities between this capillary column and the column packed with Porapak Q to be particularly interesting. For this reason, we decided to

test the capabilities of PoraPLOT Q in analyzing nitriles and mixtures of nitriles and hydrocarbons (alkanes, alkenes and alkynes). This first paper in the series presents the main results of the above-mentioned study. The next papers will be devoted to similar studies carried out with a Al_2O_3–KCl PLOT capillary column, and with short columns packed with micro-particles.

EXPERIMENTAL

Column and gas chromatograph

The PoraPLOT Q column (Chrompack, Netherlands) was a 10 m × 0.32 mm I.D. PLOT fused-silica capillary column coated with a 10-μm film of styrene–divinylbenzene copolymer. It was mounted in a split mode (splitter ratio: 100/1) on a Carlo Erba Model Fractovap 2150 gas chromatograph equipped with a linear temperature programmer Model LT 232, a flame ionization detector and a Shimadzu Model IRC-1B integrator recorder.

The following conditions were chosen for all the presented results: injector temperature = detector temperature = 225°C. The carrier gas was hydrogen.

Sampling

Both liquid and gas mixtures have been tested. The complex gas mixtures of standard volatile hydrocarbons and nitriles were prepared in a sampling glass reservoir equipped with a septum. This reservoir was connected to a glass vacuum line. It was initially evacuated and isolated from the line. Then constituents of the mixture were successively introduced in the reservoir. This was done by expanding a known and adequate pressure of a pure constituent from the known volume of the vacuum line into the additional known volume of the reservoir (where the pressure before this expansion was also known). Nitriles which are liquids at room temperature were added to the gaseous mixture (at a pressure lower than their saturation vapour pressure) by introducing a calculated volume of liquid in the sampling reservoir through its septum with an Hamilton liquid syringe. The final mixture was sampled from the reservoir with a 1-ml Hamilton gas syringe equipped with a gas-tight stopcock. The concentration of each constituent in the gaseous sample was decreased by a known factor by dilution in air in the syringe itself.

When using liquid mixtures the constituents were diluted in methanol. The final liquid mixture was sampled with a 0.5-μl Hamilton liquid syringe.

Reagents

Allene and cyanogen were from Matheson (East Rutherford, NJ, U.S.A.). Methylacetylene (propyne) and ethylacetylene (1-butyne) were from Baker (Phillipsburg, NJ, U.S.A.). All the other C_1–C_4 hydrocarbons tested were obtained from Alphagaz-L'Air Liquide (Bois d'Arcy, France) and were at least 99% pure.

Pentanes, 2-methyl-2-butene, 1-hexene, *n*-hexane, benzene, cyclohexane, cyclohexene, acetonitrile, acrylonitrile and propionitrile were obtained from Prolabo (Paris, France). 1-Pentene and 3-methylpentane were from Fluka (Buchs, Switzerland). Butyronitrile, isobutyronitrile, methacrylonitrile, cyclopropanecarbonitrile, crotononitrile (mixture of *cis* and *trans* isomers) and 3-butenenitrile were from Riedel-de-Haën (Hannover, F.R.G.).

Hydrogen cyanide was prepared by acidification of sodium cyanide with sulphuric acid[13]. Cyanoacetylene (propynenitrile) was synthesized by the dehydration of propynoic acid amide, and cyanopropyne (2-butynenitrile) was synthesized by the cyanidation of 3-chloropropyne. Details of these syntheses have been published elsewhere[14].

Determination of Van Deemter curves

To determine experimentally the dependence of the height equivalent to a theoretical plate, H, for selected solutes on the linear velocity of the carrier gas, u, we injected the selected solutes and methane at different inlet pressures of the carrier gas. The outlet flow-rate was measured with a soap flow meter.

The value of u was calculated from the relationship $u = L/t_m$, where L is the length of the column and t_m is the retention time of methane.

For the solute selected, H was calculated from the classical relationship

$$H = \frac{L}{5.54} \frac{\omega^2}{(t_R - t_m)^2}$$

where t_R is the retention time of the solute and ω is the half width of its chromatographic peak assumed to be gaussian.

RESULTS AND DISCUSSION

In order to characterize quantitatively the performances of the column and to use optimized flow-rate conditions for analyzing mixtures of hydrocarbons and nitriles, we have determined Van Deemter curves at different temperatures. In the

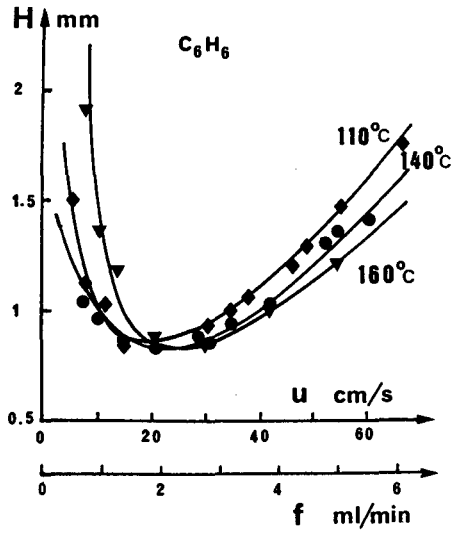

Fig. 1. Benzene: variation of H with the mean linear velocity, u, and outlet flow-rate, f, of the carrier gas (H_2) at 110, 140 and 160°C on a 0.32 mm I.D. PoraPLOT Q fused-silica column (thickness 10 μm). Total quantity injected: 2.2 (110°C) or 1.1 nmol (140 and 160°C). Split mode (100/1).

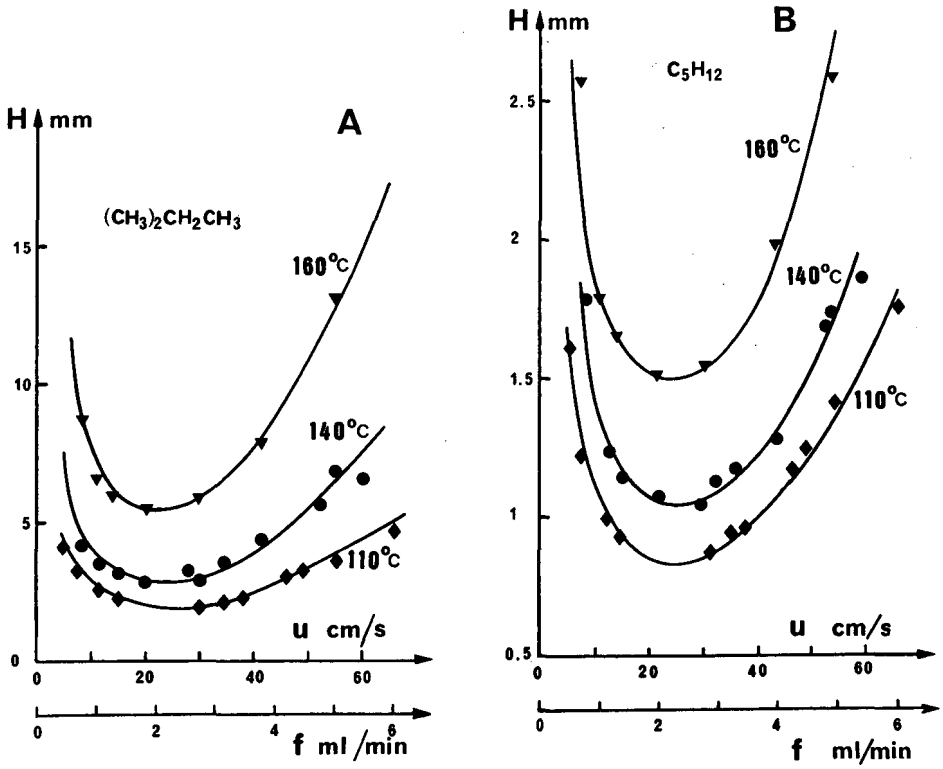

Fig. 2. Isobutane (A) and *n*-pentane (B): variation of H with u and f as in Fig. 1. Total quantity injected: isobutane, 0.9 nmol; *n*-pentane, 0.6 nmol.

following studies, hydrogen was used as a carrier gas, because for equivalent H values, it can provide faster analyses (the retention times are about two times smaller with H_2 as a carrier gas than with He). In addition, the use of H_2 facilitates the coupling with a mass spectrometer.

The results for benzene, isobutane, pentane, acetonitrile and acrylonitrile are given in Figs. 1, 2A, B, 3A and B respectively, for column temperatures of 110, 140 and 160°C. They have been obtained by injecting constant quantities of solute (0.6 to less than 4 nmol) in the injector of the gas chromatograph. In the case of benzene, the value of H is not very temperature dependent, at least for u values higher than about 10 cm/s (corresponding to an outlet flow-rate of about 1 ml/min). For a given flow-rate, a slight decrease in H is observed when the temperature is increased. The minimum of the curve is relatively flat. It is reached for linear velocities of about 20 cm/s (flow-rate of about 2 ml/min). Its value is 0.87 mm, corresponding to 1150 theoretical plates per metre.

The curves obtained with alkanes (Fig. 2A and B) differ significantly from that of benzene. First, H is temperature dependent: for the same carrier gas velocity, H markedly increases with temperature. It is at least two times higher at 160 than at 110°C. With butane, the minimum value of H is about 1.9 mm at 110°C. It is 2.8 mm at 140°C and more than 5 mm at 160°C. With pentane, the corresponding values are about three times smaller: 0.8, 0.9 and 1.5 mm at 110, 140 and 160°C respectively. For

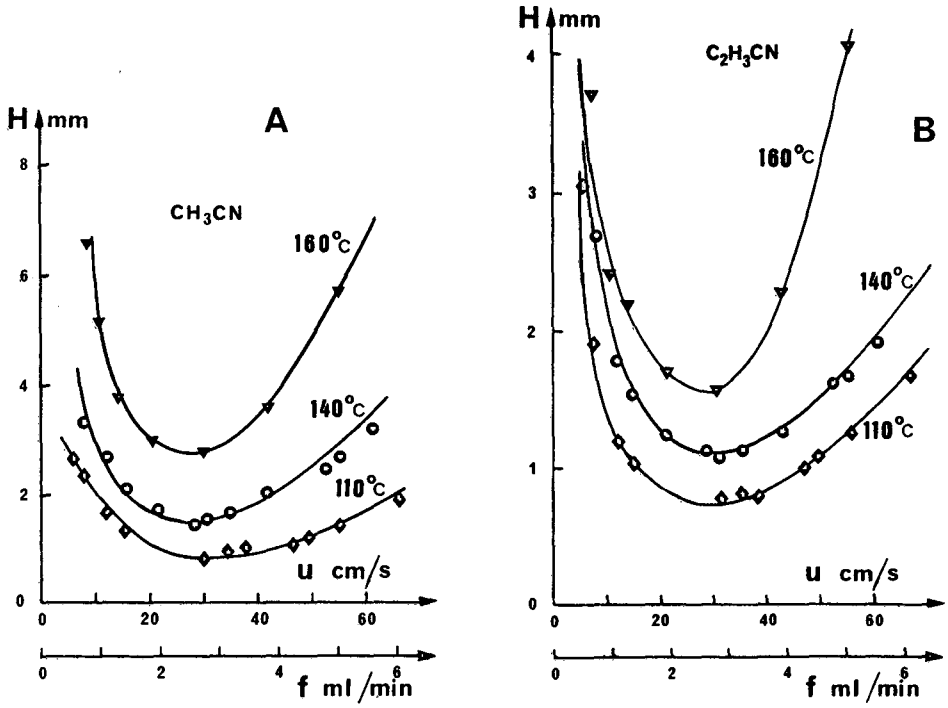

Fig. 3. Acetonitrile (A) and acrylonitrile (B): variation of H with u and f as in Fig. 1. Total quantity injected: acetonitrile, 3.8 nmol; acrylonitrile, 3 (110°C) or 1.5 nmol (140 and 160°C).

these two solutes, the minimum of H is obtained for a u value of about 25 cm/s. In both cases, in the range of temperatures studied, the minimum corresponds to a linear velocity of about 30 cm/s (about 2.5 ml/min). A similar behaviour is observed in the case of nitriles (Fig. 3): H increases markedly with temperature. For acetonitrile, its minimum value is 0.8 mm at 110°C, 1.5 mm at 140°C and 2.7 mm at 160°C. For acrylonitrile, the values are 0.7, 1.1 and 1.6 mm respectively at the same temperatures. Again, the efficiency of the column seems to decrease when the temperature increases. In addition, for the two nitriles, the minimum of H is obtained for a u value of about 30 cm/s.

Thus, there is an observed increase in H with temperature for most solutes, either polar, such as nitriles, or apolar, such as alkanes. This suggests that the retention processes are mainly driven by gas–solid adsorption, and that there is a change in the physical structure of the organic polymer film in the range of temperatures. The particular behaviour of benzene seems to indicate that, for this compound, contrary to the other solutes for which H plots have been determined, the retention process involves mainly solubility phenomena. Effectively, this compound is less volatile than the other solutes considered above, and its chemical structure is very similar to that of the monomers constituting the organic polymer coating. From these results it also appears that with such a column, using H_2 as the carrier gas, the outlet flow-rate should be at least 2 ml/min. We have chosen this value for calibrating the column with hydrocarbons and nitriles.

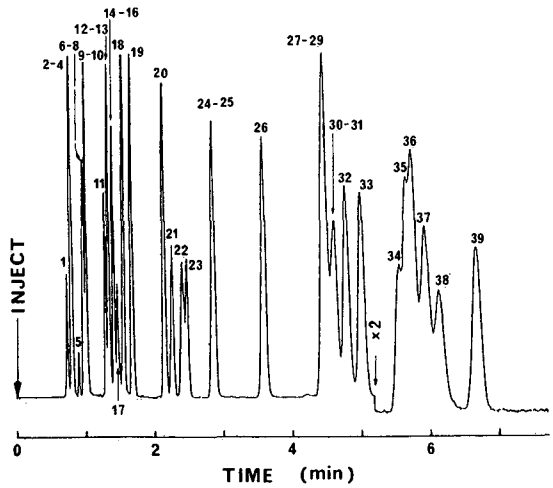

Fig. 4. Gas chromatogram of a gaseous mixture of C_1–C_6 hydrocarbons and C_1–C_4 nitriles on a 10 m × 0.32 mm I.D. PoraPLOT Q fused-silica column at 160°C. Carrier gas: H_2. Outlet flow-rate: 2 ml/min. Injected quantity: 1–3 nmol of each constituent; split mode (100/1). Flame ionization detector. Peaks: 1 = methane; 2 = ethene; 3 = ethyne; 4 = ethane; 5 = cyanogen; 6 = propene; 7 = hydrocyanic acid; 8 = propane; 9 = allene; 10 = propyne; 11 = isobutane; 12 = 1-butene; 13 = isobutene; 14 = butane; 15 = *trans*-2-butene; 16 = 1-butyne; 17 = *cis*-2-butene; 18 = cyanoacetylene; 19 = acetonitrile; 20 = acrylonitrile; 21 = 1-pentene; 22 = *n*-pentane; 23 = 2-methyl-2-butene; 24 = cyclopentane; 25 = propionitrile; 26 = methacrylonitrile; 27 = isobutyronitrile; 28 = 3-methylpentane; 29 = 1-hexene; 30 = cyanopropyne; 31 = *cis*- or *trans*-crotononitrile; 32 = *n*-hexane; 33 = 3-butenenitrile; 34 = benzene; 35 = butyronitrile; 36 = *trans*- or *cis*-crotononitrile; 37 = cyclohexane; 38 = cyclohexene; 39 = cyclopropanecarbonitrile.

Fig. 4 shows a chromatogram of a mixture of C_1–C_6 hydrocarbons and C_1–C_4 nitriles at 160°C. The retention times of hydrocarbons are roughly in the order of their boiling points and increase with the number of carbon atoms in their structures. The chromatographic behaviour of nitriles is somewhat similar, in spite of the polarity of the CN group. With the exception of the non-polar compound C_2N_2 which is eluted very quickly, the retention times of all the nitriles studied increase with the number of carbon atoms, whatever the nature of the carbon chain (saturated, ethylenic or acetylenic). With this isothermal condition of relatively high temperature, many of the hydrocarbons are co-eluted, especially those with a small number of C atoms. There are also several interferences between hydrocarbons and nitriles. Hydrogen cyanide is co-eluted with propane and propene, propanenitrile with cyclopentane, 2-methylpropanenitrile with 3-methylpentane and with 1-hexene. A few nitriles, such as cyanopropyne and *cis*-crotononitrile are not separated. However, the separation is markedly better and faster than that obtained with a Porapak Q column using similar temperature conditions[4]. All the solutes injected are eluted in less than 7 min, and they exhibit symmetrical peaks.

Fig. 5 shows a chromatogram obtained under the same conditions, but at 100°C. Ethane is separated from the other C_2 hydrocarbons, propane from propene. Hydrogen cyanide is still co-eluted, but only with propene. Cyanopropyne and *cis*-crotononitrile again are co-eluted, butanenitrile and *trans*-crotononitrile are no

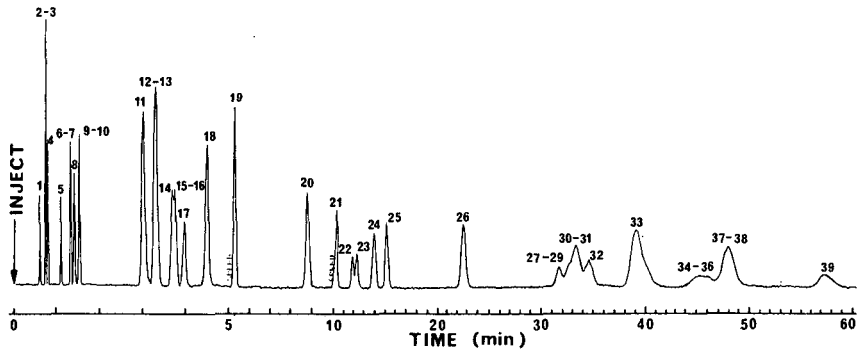

Fig. 5. Chromatogram obtained under the same conditions as in Fig. 4, but at 100°C. For peak identification see Fig. 4.

longer separated and are co-eluted with benzene. Elution of all the constituents of the mixture requires almost 1 h.

The separation can be improved by using programmed column temperatures. Fig. 6 shows as an example the analysis of a mixture of C_1–C_4 hydrocarbons and C_1–C_3 nitriles with a linearly programmed temperature starting from 40°C, isothermal for 2 min, then increased at 20°C/min to 115°C. The entire analysis takes 10 min and allows the separation of all the constituents, with the exception of ethylene and acetylene.

In order to provide a more general view of the behaviour of this column, we have

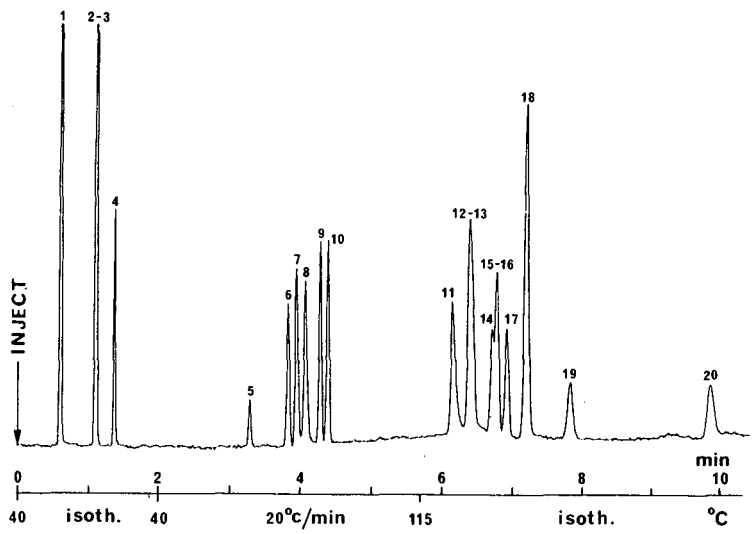

Fig. 6. Gas chromatogram of a gaseous mixture of C_1–C_4 hydrocarbons and C_1–C_3 nitriles. Conditions as in Fig. 4, but programmed temperature of the column: isothermal for 2 min at 40°C, then 20°C/min to 115°C. For peak identification see Fig. 4.

also determined the retention indices, $I(i)$, of the solutes studied, using the Kováts system. The following equation was used

$$I(i) = 100 \cdot \frac{\log t'_{R(i)} - \log t'_{R(P_z)}}{\log t'_{R(P_{z+1})} - \log t'_{R(P_z)}} + 100\,Z$$

where t'_R is the relative retention time, P_z and P_{z+1} correspond to the paraffins with

TABLE I

RETENTION INDICES OF HYDROCARBONS AND NITRILES (*) ON PoraPLOT Q COLUMN AT 100 AND 160°C

Reference alkanes in brackets.

Solute	*Retention index*	
	100°C	*160°C*
(Ethane)	200	200
Cyanogen*	236.8	273
Propene	248.9	300
Hydrogen cyanide*	248.9	300
(Propane)	300	300
Allene	311	315.9
Propyne	311	315.9
Isobutane	380.5	384.7
1-Butene	389	390
Isobutene	389	390
(Butane)	400	400
trans-2-Butene	401.8	400
Butyne	401.8	400
cis-2-Butene	406.9	407.9
Cyanoacetylene*	420.9	423.5
Acetonitrile*	432.3	441.6
Acrylonitrile*	475.6	482.2
1-Pentene	489.2	490.8
(*n*-Pentane)	500	500
2-Methyl-2-butene	503.5	504.1
Cyclopentane	516.1	527
Propionitrile*	523.3	527
Methacrylonitrile*	560.5	559.6
Isobutyronitrile*	592.2	590.4
3-Methylpentane	592.2	590.4
1-Hexene	592.2	590.4
Cyanopropyne*	596.5	595
trans- or *cis*-Crotononitrile*	596.5	595
(*n*-Hexane)	600	600
Allyl cyanide*	611	605.8
Benzene	623.9	619.5
Butyronitrile*	623.9	622.2
cis- or *trans*-Crotononitrile*	623.9	624.0
Cyclohexane	628.8	628.2
Cyclohexene	628.8	628.2
Cyclopropyl cyanide*	645	643.6
(Heptane)	700	700

z and $z + 1$ carbon atoms respectively and i corresponds to a solute the retention time of which is between that of P_z and P_{z+1}. The results are given on Table I, for two different temperatures: 100 and 160°C. It can be checked that, for a given chemical family, the retention index varies linearly with the number of carbon atoms in the solute.

CONCLUSIONS

The analogy between the PoraPLOT Q capillary column and a Porapak Q packed column, already reported for apolar and polar compounds other than nitriles, is also true for these organics. This PLOT column can be used advantageously for analyzing mixtures of hydrocarbons and nitriles, combining the advantages of the high resolution of a capillary column with the ability of styrene–divinylbenzene copolymer to allow the elution of polar and apolar compounds. A 10-m PoraPLOT Q column can provide a good separation of saturated and unsaturated low-molecular-weight hydrocarbons and nitriles, in a relatively short time. Only the separation of HCN and propene seems to be difficult and requires programmed temperature conditions. Such conditions are not convenient for space GC instrumentation, because they increase markedly the duration of the analytical cycle and the complexity of the instrument and its software. In fact, in the case of the Titan probe, the existence of a coupling of GC with MS reduces the importance of the problem of co-elution, especially if the co-eluted compounds have well differentiated chemical properties and consequently mass fragmentation. This is the case of HCN–propene. Thus the PoraPLOT Q column may be a good choice for one of the chromatographic columns of the GC–MS instrument of the Titan probe.

ACKNOWLEDGEMENTS

We thank Dr. C. Vidal-Madjar for her helpful comments during the preparation of this work. This research has been supported by a grant from the Centre National d'Etudes Spatiales (Grant 88/CNES/1283).

REFERENCES

1 *CASSINI Report on the Phase A Study*, European Space Agency, Report Reference SCI (88) 5, 1988.
2 F. Raulin, N. Dubouloz and C. Frère, *Adv. Space Res.*, 9 (6) (1989) 35.
3 J. de Zeeuw, R. C. M. de Nijs and L. T. Henrich, *J. Chromatogr. Sci.*, 25 (1987) 71.
4 G. Toupance, F. Raulin and R. Buvet, *Origins Life*, 6 (1975) 83.
5 F. Raulin and G. Toupance, *Bull. Soc. Chim. Fr.*, (1976) 29.
6 A. Bossard and G. Toupance, *Nature (London)*, 288 (1980) 243.
7 A. Bossard, D. Mourey and F. Raulin, *Adv. Space Res.*, 3 (9) (1983) 39.
8 F. S. Brown, H. E. Adelson, M. C. Chapman, O. W. Clausen, A. J. Cole, J. T. Cragin, R. J. Day, C. H. Debenham, R. E. Fortney, R. I. Gilje, D. W. Harvey, J. L. Kropp, S. J. Loer, J. L. Logan, Jr., W. D. Potter and G. T. Rosiak, *Rev. Sci. Instrum.*, 49 (1978) 139.
9 F. H. Woeller and G. E. Pollock, *J. Chromatogr. Sci.*, 16 (1978) 137.
10 V. I. Oyama, G. C. Carle, F. Woeller, S. Rocklin, J. Vogrin, W. Potter, G. Rosiak and C. Reichwein, *I.E.E. Trans. Geos. Rem. Sens.*, GE-18 (1) (1980) 85.
11 J. de Zeeuw, R. C. M. de Nijs, J. C. Buijten, J. A. Peene and M. Mohnke, *Int. Lab.*, December (198) 52.
12 J. de Zeeuw, R. C. M. de Nijs, J. C. Buijten, J. A. Peene and M. Mohnke, *J. High Resolut. Chromatogr. Commun. Chromatogr.*, 11 (1988) 162.
13 A. Vogel, *Textbook of Practical Organic Chemistry including Qualitative Organic Analysis*, Longman, London, 1978, p. 298.
14 P. Bruston, H. Poncet, F. Raulin, C. Cossart-Magos and R. Courtin, *Icarus*, 78 (1989) 38.

Journal of Chromatography, 481 (1989) 55–61
Elsevier Science Publishers B.V., Amsterdam — Printed in The Netherlands

CHROM. 21 727

DETECTION AND QUANTITATION OF OXALIC ACID BY CAPILLARY GAS CHROMATOGRAPHY

HANS D. GOTTSTEIN[a], MICHAEL N. ZOOK and JOSEPH A. KUĆ*
Department of Plant Pathology, University of Kentucky, Lexington, KY 40546-0091 (U.S.A.)
(First received December 16th, 1988, revised manuscript received June 22nd, 1989)

SUMMARY

Oxalic acid was extracted from plant tissue and quantified by a rapid and accurate procedure using capillary gas chromatography (GC). Samples derived from leaves, stems, and woody plant tissue were extracted with 3 *M* hydrochloric acid. Oxalic acid in these extracts was esterified with diazomethane in ether and determined as dimethyl oxalate by capillary GC. Recoveries of oxalates added to plant preparations ranged from 92 to 105% as compared to a range of 96–102% for oxalate standards added to 3 *M* hydrochloric acid. Oxalate was detected and quantified in cucumber leaves, rhubarb, woody tissue of American chestnut infected with the fungus *Endothia parasitica* and an agar culture of *Endothia parasitica*. This is the first report of the presence of oxalate in cucumber foliage. The new procedure using diazomethane does not require time consuming purification of the extracts before capillary GC analysis. Unlike alcoholysis, it results in complete esterification. The determination limit for this method of oxalate quantitation is approximately 500 pg using a flame ionization detector.

INTRODUCTION

Measurement of oxalic acid has important applications in areas of medical and plant research. Oxalic acid is thought to have a role in renal stone formation[1,2]. Oxalate is also a plant metabolite, and crystalline deposits of calcium oxalate are found in many plant tissues[3]. Recent studies have demonstrated that aqueous solutions of potassium oxalate, applied to the first two leaves of cucumber, induced systemic resistance to several fungal pathogens[4]. Studies of the metabolism of oxalates and their possible role in induced resistance require sensitive methods for the detection of low levels of oxalates.

Spectrophotometric[5], isotope dilution mass spectrometric[6], electrochemical[7], liquid chromatographic[8], high-performance liquid chromatographic (HPLC)[9], (GC)[10–12], ion chromatographic[13] and enzymatic[14,15] methods have been used to

[a] Present address: Institute of Plant Biochemistry of the Academy of Science of the German Democratic Republic, Halle 4050, Weinberg 3, G.D.R.

0021-9673/89/$03.50

separate and quantify oxalic acid. The methods listed above are either less sensitive or inappropriate for crude plant extracts when compared to the method described in this paper.

The present paper describes a simple, rapid, sensitive and reproducible procedure for the detection of oxalates useful for quantitative analyses of these compounds in samples from different origins. The procedures described in this paper include modifications of previously published methods for the extraction of oxalic acid and the derivatization of oxalic acid prior to determination by capillary GC[10–12].

EXPERIMENTAL

Chemicals

All chemicals were of a analytical grade. Diazomethane was generated *in situ* from N-methyl-N-nitroso-*p*-toluenesulfonamide (Sigma) by a standard procedure. Dipropyl oxalate, and diisopropyl oxalate were synthesized by alcoholysis and purified by thin-layer chromatography (TLC) on Silica gel G (0.25 mm) (Analtech). Dimethyl oxalate and diethyl oxalate were obtained from Sigma.

Samples

Cucumber plants (cultivar Wisconsin SMR 58) were grown in a greenhouse. Rhubarb was purchased at a local market. Wood of the American chestnut (*Castanea tentata*) infected with the fungus *Endothia parasitica* was harvested from trees in the Lexington, Kentucky area. *E. parasitica* was grown on an amended potato dextrose agar medium in a standard petri dish[16].

Tissue extraction

A 5 g amount of cucumber leaf tissue was cut into small pieces with a razor blade and homogenized at high speed (Brinkmann, PT 10-35) with 25 ml of 3 *M* hydrochloric acid. The suspension was centrifuged at 25 000 *g* for 5 min and the supernatant filtered through Whatman No. 1 paper. The residue retained by the filter was extracted twice with 15 ml of 3 *M* hydrochloric acid and the combined filtrates were adjusted to 60 ml. Samples (5 g fresh weight) from rhubarb leaves, wood of American chestnut (*Castanea tentata*) infected with the fungus *E. parasitica*, and an agar culture of *Endothia parasitica* were extracted as described above with 60 ml of 3 *M* hydrochloric acid. Aliquots (6 ml) of the 3 *M* hydrochloric acid extracts were used for methyl esterification and subsequent GC analysis.

Alcoholysis of oxalic acid

A 6-ml volume of 3 *M* hydrochloric acid extract was evaporated to dryness under reduced pressure at 40–45°C. Four different oxalic acid esters were made using methanol, ethanol, isopropanol, and *n*-propanol. Dimethyl oxalate was prepared by adding 5 ml of 7% hydrochloric acid in methanol to the evaporated plant extract. The solution was then heated to 60°C for 30 min. Diethyl oxalate and diisopropyl oxalate were prepared by the addition to evaporated plant extract of either 5 ml of 7% hydrochloric acid in ethanol or 5 ml of 7% hydrochloric acid in isopropanol. In the preparation of diethyl oxalate, the solution was heated for 30 min at 70°C, whereas diisopropyl oxalate was prepared by heating the solution for 45 min at 80°C. For the

preparation of dipropyl oxalate, 5 ml of *n*-propanol was added to the evaporated plant extract, and the solution was then heated to 105°C for 3.5 h. After each alcoholysis was complete, 10 ml of water was added. The solution was then extracted with 30 ml (three times at 10 ml each) of chloroform, and the combined chloroform extracts were concentrated by rotory evaporation at 40°C prior to GC and TLC analysis.

Esterification with diazomethane

A 6-ml volume of the 3 *M* hydrochloric acid extract was evaporated to dryness at 40–45°C and 12 mmHg using a vacuum rotary evaporator. Diethyl ether was added to the dry, hydrochloric acid-free residue. The ether solution was then transferred to a graduated 15-ml vial and evaporated under a stream of nitrogen to a volume of 5 ml. To this solution, 10 ml of freshly prepared diazomethane (0.05 mol N-methyl-N-nitroso-*p*-toluenesulfonamide, 3 g potassium hydroxide; 100 ml diethyl ether) was added. The esterification was complete when bubbles were no longer visible and the yellow color of the solution was stable. The vial was closed by a screw cap and stored at 4°C until GC analysis.

TLC

After esterification, solutions derived from plant extracts or pure compounds were chromatographed on silica gel G plates using cyclohexane–ethyl acetate (3:1, v/v) as the mobile phase. Spraying the plates with hydroxylamine hydrochloride–iron (III) chloride resulted in a violet color reaction for mono- and diesters of oxalic acid.

Capillary GC

A Perkin-Elmer Sigma 2000 gas chromatograph equipped with a computer integrator, flame ionization detector and a 25 mm × 0.32 mm fused-silica column coated with methyl silicone (OV-1) at a film thickness of 0.25 μm was used for analyses. A 1-μl aliquot of the 15 ml ether solutions was used for the determination of oxalate content by capillary GC. The split injection port of the instrument was adjusted to a split ratio of 18:82. Nitrogen was used as a carrier gas at a flow-rate of 15 ml/min through the column with an inlet pressure of $1.0 \cdot 10^5$ Pa. The column temperature was held at 70°C initially, then raised at 30°C/min to 220°C with an isothermal hold for 15 min at 220°C. The detector and injector port were set at 270°C. The amount of oxalate in plant extracts was quantitated by comparing the peak areas of the detector response to injections of plant samples and known amounts of a dimethyl oxalate standard. The dimethyl oxalate standard was dissolved in ether prior to injection.

RESULTS

Methods of esterification

Two methods for derivatization of oxalic acid. Alcoholysis resulted in only a partial conversion of oxalic acid to the diester derivative. The relatively high temperatures required for alcoholysis also increased the number of contaminants in plant extracts which often cochromatographed with compounds of interest. Diazomethane was used as an alternative method for esterifying oxalic acid. In contrast to alcoholysis, esterification with diazomethane resulted in the total conversion of oxalic acid to

dimethyl oxalate. Dissolving the evaporated 3 *M* hydrochloric acid extracts in ether before esterification with diazomethane removed many contaminants. This was the only sample cleanup necessary prior to GC analysis.

Capillary GC

Analyses were performed on plant extracts which contained esterified oxalates using different oxalic acid diesters as standards. Fig. 1 shows the chromatogram for dimethyl, diethyl, diisopropyl and dipropyl oxalate at 90°C column temperature. The dimethyl ester of oxalic acid was the most useful ester derivative in quantitating oxalate in plant extracts since peaks of contaminants in plant extracts interferred with the peaks for the diethyl, diisopropyl and dipropyl oxalate, whereas contaminant peaks did not interfere with the peak of dimethyl oxalate. A decrease in the column temperature to 70°C enhanced the separation of the peak of dimethyl oxalate from the solvent front.

Fig. 2 shows chromatograms of dimethyl oxalate obtained from a standard solution and from cucumber leaf extract at 70°C. As shown by this figure, the peak of dimethyl oxalate was well separated from peaks of contaminants in plant extracts.

Recovery of applied oxalates

The results of oxalate recovery studies are shown in Table I. The average recovery for the three different compounds added to cucumber leaf tissue and extracted with 3 *M* hydrochloric acid was 97% and the average recovery for the three compounds added to 3 *M* hydrochloric acid extracts of cucumber leaf tissue was 102%. Treatment of cucumber leaf tissue with 3 *M* hydrochloric acid led to complete extrac-

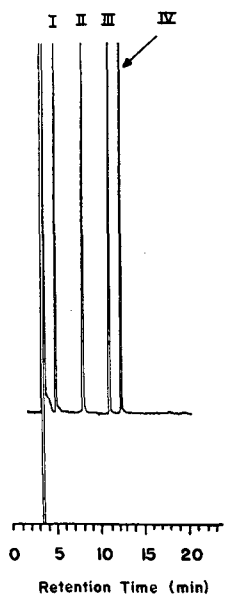

Fig. 1. Chromatogram of different oxalate diesters. Peaks I, II, III, and IV correspond to dimethyl, diethyl, diisopropyl and dipropyl oxalate, respectively.

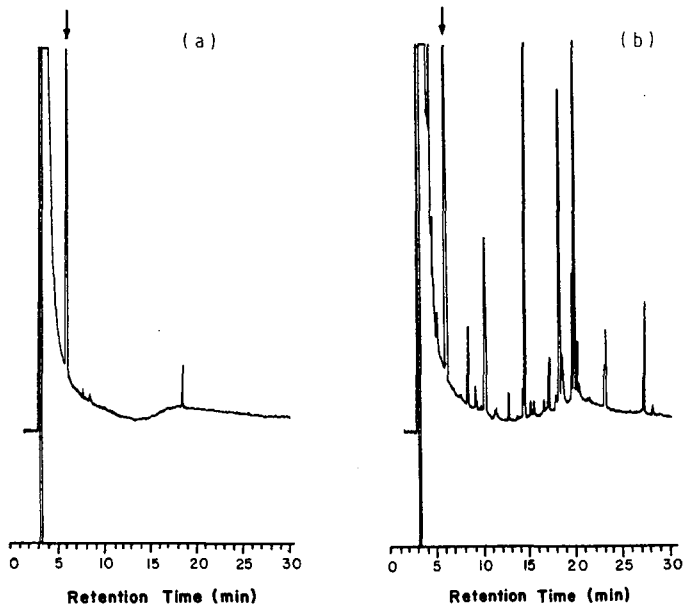

Fig. 2. Chromatograms of dimethyl oxalate standard (A) and derivatized cucumber leaf extract (B). The peaks indicated by the arrow correspond to dimethyl oxalate.

TABLE I

RECOVERY OF POTASSIUM OXALATE, OXALIC ACID AND DIETHYL OXALATE ADDED TO 3 *M* HYDROCHLORIC ACID, AQUEOUS EXTRACTS FROM CUCUMBER LEAVES AND FRESH CUCUMBER LEAF TISSUE

Potassium oxalate, oxalic acid and diethyl oxalate were added separately to three 60-ml aliquots of 3 *M* hydrochloric acid, 3 *M* hydrochloric acid extracts of 5 g (fresh weight) cucumber leaf samples and to three 5-g (fresh weight) freshly harvested cucumber leaf samples. The freshly harvested cucumber leaf samples were extracted with 60 ml of 3 *M* hydrochloric acid. Dimethyl oxalate was prepared with diazomethane and quantified by GC described in the text.

Sample	*Form of oxalate added*	*Amount added (mg)*	*Amount quantified by GC analysis (mg)*	*Recovery (%)*
3 *M* HCl	Potassium oxalate	168	162	96
(60 ml)	Oxalic acid	90	92	102
	Diethyl ester	146	144	99
Extract from	Potassium oxalate	168	168	100
cucumber leaves	Oxalic acid	90	90	100
(60 ml)	Diethyl ester	146	153	105
Fresh cucumber	Potassium oxalate	168	154	92
leaf tissue	Oxalic acid	90	87	97
(5 g fresh weight)	Diethyl ester	146	148	101

tion of oxalates. Repeated extraction of the remaining residue failed to yield detectable levels of oxalate.

Determination of oxalic acid content

The oxalate concentration was determined for different plant samples and the oxalic acid producing fungus *Endothia parasitica* (Table II). The amount of oxalic acid detected in rhubarb, *Castanea tentata* and *Endothia parasitica* was similar to that reported previously[4]. Oxalic acid was also found in cucumber leaves and the amount increased as a function of age (Table II).

DISCUSSION

A capillary GC method has been developed for the rapid and accurate determination of oxalic acid and oxalates. The procedure described in this report is useful for the determination of very low concentrations of these compounds by derivatization to dimethyl oxalate. This technique also does not require time consuming purification steps before analysis.

In order to develop a reliable technique for determination of oxalates, it was necessary to have an efficient method for derivatizing oxalic acid. Different methods of derivatizing oxalic acid were investigated. These methods included alcoholysis with methanol, ethanol, *n*-propanol and isopropanol as well as esterification with diazomethane. Monoesters of oxalic acid were found after alcoholysis, which indicated that the formation of the diesters was not complete. On the other hand, methyl esterification with diazomethane was complete, and therefore, it was the method of choice for quantitative analysis of oxalic acid.

The technique for determination of oxalates outlined in this paper is reliable as evidenced by the high levels of recovery we observed from samples of different origins as well as by the low determination limit for dimethyl oxalate compared to known GC and HPLC methods[4,9,10]. We found that the determination limit of our capillary

TABLE II

DETERMINATION OF OXALIC ACID AND OXALATE IN DIFFERENT PLANT MATERIAL

Sample	*Oxalic acid*[a] *(μg/g fresh weight)*
Rhubarb	980
Cucumber leaf No. 1[b] (2 weeks old)	ND[c]
Cucumber leaf No. 1 (3 weeks old)	57
Cucumber leaf No. 1 (4 weeks old)	217
Castanea tentata, infected with *Endothia parasitica*	5904
Endothia parasitica	4519[d]

[a] One determination.

[b] Refers to the first true leaf. Leaves were from two plants at each age.

[c] None detected.

[d] Data for one agar culture of the fungus representing the total oxalic acid content of agar and fungus.

GC for dimethyl oxalate to be approximately 500 pg, whereas the lowest limit of determination for potassium oxalate was about 200 mg (ref. 4).

Though oxalic acid has been reported previously in spinach, rhubarb, stem material of *Castanea tentata* infected with *E. parasitica* and a culture of *E. parasitica*[4,17], we are not aware of any reports of oxalic acid in cucumber. The data suggest that the oxalate content increases with age in cucumber leaves. Although the exogenous application of oxalate has been demonstrated to induce resistance to fungal diseases in cucumber[4], it is not known what role endogenous oxalates have in the expression of resistance in cucumber.

The procedure described in this paper for the determination of oxalates is simple, rapid, reliable and sensitive. This technique should be useful for the determination of oxalate from a variety of sources.

ACKNOWLEDGEMENTS

The work reported in this paper was supported in part by a grant from the CIBA-GEIGY Corporation. Journal series paper 88.11.328 of the Kentucky Agricultural Experiment Station.

REFERENCES

1 J. M. Barlow, *Clin. Chem.*, 33 (1987) 855.
2 E. R. Yendt and M. Cohanm, *New Engl. J. Med.*, 312 (1985) 953.
3 V. R. Franceshi and H. T. Horner, Jr., *Bot. Rev.*, 46 (1980) 361.
4 N. Doubrava, R. Dean and J. Kuč, *Physiol. Mol. Plant Pathol.*, 33 (1988) 69.
5 I. S. Parkinson, W. L. Sheldon, M. F. Laker and P. A. Smith, *Clin. Chem.*, 33 (1987) 1203.
6 W. Koolstra, B. G. Wolthers, M. Hayer and H. Elzerga, *Clin. Chim. Acta*, 170 (1987) 227.
7 W. J. Mayer, J. D. McCarthy and M. S. Greenberg, *J. Chromatogr. Sci.*, 17 (1979) 656.
8 J. F. Murray, Jr., H. W. Nolen, III, G. R. Gordon and J. H. Peters, *Anal. Biochem.*, 121 (1982) 301.
9 W. Koolstra, B. G. Wolthers, H. Hayer and H. M. Rutgers, *Clin. Chim. Acta*, 170 (1987) 237.
10 H. Ohkawa, *J. Assoc. Off. Anal. Chem.*, 68 (1985) 108.
11 M. A. Gelot, G. Lavone, F. Belleville and P. Nabet, *Clin. Chim. Acta*, 106 (1980) 279.
12 H. A. Moye, M. H. Malagod, D. H. Clarke and C. J. Miles, *Clin. Chim. Acta*, 114 (1981) 173.
13 F. C. Smith and R. C. Chang, *CRC Crit. Rev. Anal. Chem.*, 9 (1980) 197.
14 J. E. Buttery, N. Ludvigson, E. A. Braiotta and P. R. Pannall, *Clin. Chem.*, 29 (1983) 700.
15 L. L. Liao and K. E. Richardson, *Arch. Biochem. Biophys.*, 153 (1972) 438.
16 S. Anagnostakis, *Science (Washington, D.C.)*, 215 (1982) 466.
17 E. A. Havir and S. L. Anagnostakis, *Physiol. Plant Pathol.*, 23 (1983) 369.

Journal of Chromatography, 481 (1989) 63–69
Elsevier Science Publishers B.V., Amsterdam — Printed in The Netherlands

CHROM. 21 754

SUPERCRITICAL FLUID CHROMATOGRAPHY OF BARBITURATES

ROGER M. SMITH* and M. MARSIN SANAGI[a]
Department of Chemistry, Loughborough University of Technology, Loughborough, Leics. LE11 3TU (U.K.)
(First received February 24th, 1989; revised manuscript received June 30th, 1989)

SUMMARY

A number of barbiturates have been separated by supercritical fluid chromatography on columns packed with polystyrene–divinylbenzene or ODS-silica using carbon dioxide containing methanol as a modifier. The effect of the proportion of modifier on the capacity factors, relative capacity factors, and retention indices based on the alkyl aryl ketone scale has been studied.

INTRODUCTION

Over the last few years there has been considerably interest in the application of supercritical fluids as the mobile phase in chromatographic separations using either capillary or packed columns[1–3]. These methods offer an alternative to conventional gas or liquid chromatography but the influence of the separation conditions on the resolution and retention particularly for polar compounds has not yet been fully examined. Much work is still in progress to determine the scope and potential applications of supercritical fluid chromatography (SFC). Although the technique has been applied to the separation of a number of individual drugs and pharmaceutical compounds[1,4,5] and the separation of the opium alkaloids using different stationary phases and modifiers has been studied in detail[6], few other systematic studies of groups of related drugs have been reported.

The separation of the barbiturates by gas–liquid chromatography (GLC)[7,8] and high-performance liquid chromatography (HPLC)[8–10] has been widely examined in therapeutical and toxicological studies because of their widespread application for the treatment of epilepsy. It was therefore of interest to examine their separation by SFC to determine if this method could provide an alternative selectivity that might be advantageous for the confirmation of identification or to improve the resolution in complex mixtures. By using a different mobile phase the relative separation of the barbiturates compared to each other or to other drug groups might be enhanced.

Phenobarbitone had been chromatographed previously by Later *et al.*[4] using capillary SFC with a polymethylsiloxane stationary phase and in an initial study in

[a] Present address, Department of Chemistry, University of Technology, Johor Bahru Malaysia.

0021-9673/89/$03.50

this laboratory[11] a number of barbiturates were examined using a polystyrene–divinylbenzene (PS–DVB) packed column with carbon dioxide as the mobile phase. However, in that case the peak shapes were poor compared to less polar aromatic test compounds and on a ODS-silica column all the barbiturates were totally retained.

In the present paper the use of a modifier in the mobile phase to improve the separation of the barbiturates using these two stationary phases has been examined in detail and the influence of the proportion of modifier on the retention and selectivity has been determined.

EXPERIMENTAL

Chemicals

The alkyl aryl ketones from acetophenone to octadecanophenone were laboratory grade from a range of suppliers. Barbiturates were from the reference collection of the Central Research Establishment, Home Office Forensic Science Service, U.K. Carbon dioxide was industrial grade (99.98%) from British Oxygen Company, U.K.

Equipment

The separations were carried out using a packed column chromatograph[1,12] consisting of a Jasco BIP-1 pump, with cooled check valves and pumping head, operating under constant pressure conditions, a Pye Unicam LC-XPS pump for the addition of modifier, a Rheodyne 7125 injection valve with a 20-μl loop and a Pye 104 gas chromatographic oven (Pye Unicam, Cambridge, U.K.). The analytes were detected at 254 nm using an ACS 750/12 variable-wavelength ultraviolet spectrophotometric detector (Applied Chromatography Systems, Macclesfield, U.K.) fitted with a high-pressure flow cell.

The samples were separated on either a 150 × 4.6 mm column packed with PLRP-S (PS–DVB) 5-μm particles (Polymer Labs., Church Stretton, U.K.) or a 250 × 4.6 mm column packed with Ultrasphere-ODS 5-μm particles (Beckman) and peaks were recorded using a Hewlett-Packard 3390 integrator.

Method

Samples of the barbiturates and alkyl aryl ketones in methanol were injected onto the column and eluted with supercritical carbon dioxide. Selected percentages of methanol by weight were added to the eluent as required. A sample of acetone was used as the column void volume marker.

Capacity factors k' were calculated as $k' = (t_R - t_0)/t_0$ (where t_R = retention time and t_0 = column void volume and the mean of triplicate injections was used in calculations). Retention indices based on the alkyl aryl ketones were calculated as described for HPLC[13] by fitting log k' against carbon number × 100 for the standards to a linear correlation using a least squares routine and then interpolating the log k' values for the test compounds.

RESULTS AND DISCUSSION

In an initial study, it was found that there were problems with the separation of barbiturates on either PS–DVB or ODS bonded-silica columns using unmodified carbon dioxide as the mobile phase[11]. On the ODS-bonded silica column, the barbiturates were totally retained and on the PS–DVB column the peak shapes were poor and considerable tailing was observed. It has been suggested that residual silanol groups on the surface of the silica may be a cause of tailing[4] but the PS–DVB column contains no silanol groups. Other workers have suggested that a more important factor is the solubility of the analyte in the mobile phase and that phenolic, acidic and amide groupings cause particular problems. In both cases it is reported that the effects can be reduced by the addition of a modifier to the mobile phase[14–16].

The addition of methanol to the carbon dioxide eluent in the present study caused a sharpening of the peaks for the barbiturates on the PS–DVB column (Fig. 1) and reductions in their retentions, which were directly dependent of the proportion of modifier (Table I). The capacity factors of all the barbiturates changed markedly but smaller changes were observed for the N-methyl substituted barbiturate, methohexitone. The order of elution differed from that found on HPLC which was generally in the order of increasing molecular size[9,10]. In the SFC separation, talbutal, which contains an unsaturated side chain, was retained much more than amylobarbitone and pentobarbitone, the corresponding isomeric saturated compounds. The cyclic derivatives phenobarbitone and heptabarbitone also were very highly retained.

Retention indices based on the alkyl aryl ketones have been shown to provide a robust method for recording the retentions of the barbiturates by HPLC, which were less dependent than capacity factors on small variations in the operating conditions, such as temperature and eluent composition and in the determination of the column void volume[9,10]. This approach was initially investigated in the earlier study of the SFC separation[11]. In the present work the retentions of the homologous alkyl aryl ketones, acetophenone to heptanophenone were recorded (Table I) and these were used to calculate the retention indices of the barbiturates (Table II). However, the indices were very dependent on the proportion of modifier. This was in agreement with a study of a series of aromatic test compounds on a PS–DVB column in which

Fig. 1. Separation of quinalbarbitone (1) and heptabarbitone (2) on a PS–DVB column. Conditions: mean column pressure, 2200 p.s.i.; temperature, 60°C; eluent, carbon dioxide containing 9% methanol; detection, UV spectroscopy at 254 nm.

TABLE I

CAPACITY FACTORS OF BARBITURATES IN DIFFERENT METHANOL CONCENTRATIONS ON A PS–DVB COLUMN

Conditions; column, PLRP-S; eluent carbon dioxide plus methanol; mean column pressure, 2200 p.s.i.; temperature, 60°C; detection, UV spectroscopy at 254 nm.

Compound	*Capacity factor*			
	Methanol (%, w/w)			
	0	*4.0*	*9.1*	*14.6*
Barbiturates				
Barbitone	5.32	1.34	0.67	0.37
Butobarbitone	6.51	1.73	0.78	0.39
Amylobarbitone	6.55	1.74	0.78	0.40
Pentobarbitone	6.56	1.75	0.79	0.39
Talbutal	7.50	2.06	0.92	0.47
Quinalbarbitone	8.34	2.19	0.95	0.48
Methohexitone	6.16	2.27	1.11	0.69
Phenobarbitone	>24	4.87	1.91	0.91
Heptabarbitone	>24	5.07	1.98	0.98
Alkyl aryl ketones				
Acetophenone	2.27	1.33	0.89	0.67
Propiophenone	2.99	1.70	1.07	0.78
Butyrophenone	3.41	1.85	1.17	0.87
Valerophenone	4.15	2.11	1.36	0.99
Hexanophenone	5.21	2.56	1.59	1.14
Heptanophenone	6.57	3.06	1.85	1.31

TABLE II

RETENTION INDICES OF BARBITURATES IN DIFFERENT METHANOL CONCENTRATIONS ON A PS–DVB COLUMN

Based on alkyl aryl ketone standards, butyrophenone–heptanophenone[17]. Conditions as in Table I.

Compound	*Retention index*			
	Methanol (%, w/w)			
	0	*4.0*	*9.1*	*14.6*
Barbitone	1207	829	641	378
Butobarbitone	1299	974	740	424
Amylobarbitone	1302	976	734	442
Pentobarbitone	1303	978	742	433
Talbutal	1364	1072	848	567
Quinalbarbitone	1412	1106	867	570
Methohexitone	1274	1126	966	842
Phenobarbitone		1558	1321	1040
Heptabarbitone		1582	1342	1089

TABLE III

RELATIVE CAPACITY FACTORS OF BARBITURATES IN DIFFERENT METHANOL CONCENTRATIONS ON A PS–DVB COLUMN

Conditions as in Table I.

Compound	*Relative capacity factor*			
	Methanol (%, w/w)			
	0	*4.0*	*9.1*	*14.6*
Barbitone	63.8	61.2	70.5	77.1
Butobarbitone	78.1	79.0	82.1	81.3
Amylobarbitone	78.5	79.5	82.1	83.3
Pentobarbitone	78.7	79.9	83.2	81.3
Talbutal	89.9	94.1	96.8	97.9
Quinalbarbitone	100	100	100	100
Methohexitone	73.9	104	117	144
Phenobarbitone		222	201	190
Heptabarbitone		232	208	204

the effect of the modifier varied markedly with the nature of the functional groups in the analyte[17]. Changing the proportion of modifier can cause large differences in relative retentions for unrelated compounds, thus because of the structural differences between the alkyl aryl ketone standards and the acidic barbiturates, retention indices are unlikely to be as useful as in HPLC as a method of recording robust retention values. However, the more detailed study of separation on the PS–DVB column found that the retention indices of the test compounds were robust to small changes in the temperature, pressure and density of a unmodified carbon dioxide mobile phase[17].

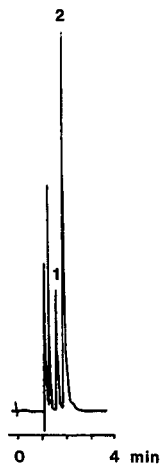

Fig. 2. Separation of amylobarbitone (1) and phenobarbitone (2) on a ODS-silica column. Conditions: mean column pressure, 1950 p.s.i.; temperature, 60°C; eluent, carbon dioxide containing 4.2% methanol; detection, UV spectroscopy at 254 nm.

An alternative method is to record retentions relative to an internal standard closely related to the analytes of interest and this approach was very succesful in the HPLC studies as it compensated for small pH changes in the eluent[18]. The relative retention times were therefore calculated compared to quinalbarbitone as an internal standard (Table III). Although these values showed a smaller variation than capacity factors or retention indices there were still considerable changes with the proportion of methanol. Thus neither relative method of recording retentions would be robust to small changes in the proportion of methanol, such as might be found in using a specified method on different equipment or in different laboratories.

The separation of the barbiturates on an ODS-silica column with methanol as a modifier was then examined. Again the capacity factors and retention indices were determined using different proportions of modifier (Table IV) and the retention times were reduced as the proportion of modifier was increased. Good peak shapes were obtained for most of the compounds (Fig. 2), although the more retained analytes

TABLE IV

CAPACITY FACTORS OF BARBITURATES IN DIFFERENT METHANOL CONCENTRATIONS ON AN ODS-SILICA COLUMN

Conditions: column, Ultrasphere ODS; eluent carbon dioxide plus methanol; mean column pressure, 1950 p.s.i.; temperature, 60°C; detection, UV spectroscopy at 254 nm.

Compound	*Capacity factor*		*Retention index*	
	Methanol (%, w/w)[a]		*Methanol (%, w/w)*[a]	
	4.2	*8.4*	*4.2*	*8.4*
Barbiturates				
Barbitone	0.30	0.16	619	398
Butobarbitone	0.37	0.17	751	437
Amylobarbitone	0.42	0.17	831	467
Pentobarbitone	0.37	0.17	747	437
Talbutal	0.41	0.22	825	631
Quinalbarbitone	0.46	0.24	893	681
Methohexitone	0.51	0.28	953	793
Phenobarbitone	0.65	0.28	1111	793
Heptabarbitone	0.78	0.35	1223	964
Alkyl aryl ketones				
Acetophenone	0.35	0.25	726	722
Propiophenone	0.47	0.32	902	888
Butyrophenone	0.53	0.35	984	970
Valerophenone	0.63	0.42	1090	1088
Hexanophenone	0.75	0.49	1199	1202
Heptanophenone	0.89	0.57	1307	1311
Octanophenone	1.06	0.66	1413	1417
Decanophenone	1.48	0.88	1622	1623
Dodecanophenone	1.93	1.13	1790	1806
Tetradecanophenone	2.76	1.51	2013	2012
Hexadecanophenone	3.73	1.95	2202	2196
Octadecanophenone	4.97	2.50	2382	2374

[a] At 0% methanol all the barbiturates were fully retained[11].

showed some tailing. Generally using a similar pressure of carbon dioxide, the retentions were shorter than on the PS–DVB column probably because of a lower overall retention capacity, which is also found in HPLC[19]. The elution orders of the barbiturates on the two columns were the same except for the closely eluted compounds, amylobarbitone and pentobarbitone. Again the retention indices (Table IV) changed markedly with the proportion of organic modifier and this can be attributed to differences in the selectivity of the separation observed for compounds with different functional groups[20].

CONCLUSION

The barbiturates can be successfully separated by SFC on both PS–DVB and ODS-silica columns by incorporating methanol as a modifier into the mobile phase with a different selectivity to HPLC separations. The proportion of the modifier has a marked effect on the retentions and particular care will be needed to reproduce these separations in different laboratories. Because of the changes in relative retentions with the proportion of modifier, retention indices and relative retention times cannot successfully compensate for small changes in the composition of the eluent.

ACKNOWLEDGEMENTS

Thanks to Polymer Laboratories and Beckman Ltd. for gifts of column materials, to Central Research Establishment, Home Office Forensic Science Service for drug samples and to the University of Technology, Malaysia for a studentship to M.M.S.

REFERENCES

1 R. M. Smith (Editor), *Supercritical Fluid Chromatography (RSC Chromatography Monographs)*, Royal Society of Chemistry, London, 1988.
2 B. A. Carpentier and M. R. Sevenants (Editors), *Supercritical Fluid Extraction and Chromatography: Techniques and applications (ACS Symposium Series,* No. 366), American Chemical Society, Washington, DC, 1988.
3 C. M. White (Editor), *Modern Supercritical Fluid Chromatography,* Hüthig, Heidelberg, 1988.
4 D. W. Later, B. E. Ritcher, D. E. Knowles and M. R. Andersen, *J. Chromatogr. Sci.,* 24 (1986) 249.
5 J. B. Crowther and J. D. Henion, *Anal. Chem.,* 57 (1985) 2711
6 J. L. Janicot, M. Caude and R. Rosset, *J. Chromatogr.,* 437 (1988) 351.
7 D. N. Pillai and S. Dilli, *J. Chromatogr.,* 220 (1981) 253.
8 R. N. Gupta, *J. Chromatogr.,* 340 (1985) 139.
9 R. M. Smith, T. G. Hurdley, R. Gill and A. C. Moffat, *Chromatographia,* 19 (1984) 401.
10 R. M. Smith, T. G. Hurdley, R. Gill and A. C. Moffat, *Chromatographia,* 19 (1984) 407.
11 R. M. Smith and M. M. Sanagi, *J. Pharm. Biomed. Anal.,* 6 (1988) 837.
12 M. M. Sanagi and R. M. Smith, *Anal. Proc.,* 24 (1987) 304.
13 R. M. Smith, *J. Chromatogr.,* 236 (1982) 313.
14 A. L. Blilie and T. Greibrokk, *Anal. Chem.,* 57 (1985) 2239.
15 R. Board, D. McManigill, H. Weaver and D. Gere, presented at *1982 Pittsburgh Conference, Atlantic City, NJ,* 1982.
16 B. W. Wright and R. D. Smith, *J. Chromatogr.,* 355 (1986) 367.
17 R. M. Smith and M. M. Sanagi, *Chromatographia,* 26 (1988) 77.
18 R. Gill, A. C. Moffat, R. M. Smith and T. G. Hurdley, *J. Chromatogr. Sci.,* 24 (1986) 153.
19 R. M. Smith, *J. Chromatogr.,* 291 (1984) 372.
20 R. M. Smith and M. M. Sanagi, *J. Chromatogr.,* in preparation.

Journal of Chromatography, 481 (1989) 71–84
Elsevier Science Publishers B.V., Amsterdam — Printed in The Netherlands

CHROM. 21 757

RETENTION PREDICTION OF ANALYTES IN REVERSED-PHASE HIGH-PERFORMANCE LIQUID CHROMATOGRAPHY BASED ON MOLECULAR STRUCTURE

III. MONOSUBSTITUTED ALIPHATIC COMPOUNDS

ROGER M. SMITH* and CHRISTINA M. BURR
Department of Chemistry, Loughborough University of Technology, Loughborough, Leics. LE11 3TU (U.K.)

(First received April 11th, 1989; revised manuscript received June 30th, 1989)

SUMMARY

A system has been developed to predict retentions in reversed-phase high-performance liquid chromatography based on the molecular structure of the analyte. The contributions of aliphatic functional groups to the retention index of an analyte have been determined based on a series of substituted alkylbenzenes. These contributions are expressed as quadratic equations which relate the contribution to the proportion and type of organic modifier. The influence of phenyl groups in the proximity of the substituents has been examined.

INTRODUCTION

Attempts have been made in a number of laboratories to devise methods to aid the development of high-performance liquid chromatographic (HPLC) separations. These attempts have been primarily based on either the prediction of isocratic conditions from a gradient elution[1] or optimisation methods, which aim to satisfy a set of empirical separation and resolution criteria[2]. Both techniques combine experimental observation with calculations and require no knowledge of the structure of the analyte. However, in many cases the structure or partial structure of the analyte is known or the structural differences between related compounds, such as isomers or metabolites are known.

The aim of the present project has been to develop a retention prediction method for reversed-phase HPLC based on the molecular structure of the analyte[3,4]. A series of studies has therefore been carried out to determine the contributions of different substituents, both aliphatic and aromatic, to the retention of an analyte. The intention is to calculate the retention index (I) as the summation of a series of terms:

$$I = I_P + I_{S,R} + \Sigma I_{S,Al-X} + \Sigma I_{S,Ar-X} + \Sigma I_{I,Y-Z}$$

0021-9673/89/$03.50

These represent the retention index of a parent compound (I_P), a contribution for saturated alkyl chains ($I_{S,R}$), contributions for substituents on saturated aliphatic carbons ($I_{S,Al-X}$), contributions for aromatic substituents ($I_{S,Ar-X}$), and terms to account for any interactions between substituents ($I_{I,Y-Z}$) caused by electronic, hydrogen bonding and steric effects. Each of these terms will be sensitive to eluent composition and the organic modifier in the eluent and will be related to the percentage of modifier using a quadratic equation. Benzene was selected as the parent compound as its substituted derivatives can be readily detected. Retention indices based on the alkyl aryl ketones were used as the basis of the study as they are more robust than capacity factors and can be more readily transferred between systems[5,6]. The coefficients of the regression equations are held in a database which can be interrogated by an expert system program (CRIPES, Chromatographic Retention Index Prediction Expert System) for the calculation of predicted retention indices[7].

So far the coefficients of the equations for benzene and the substituent index coefficients for individual groups attached to an aromatic ring have been described in a range of methanol–pH 7 buffer and acetonitrile–pH 7 buffer eluents[3] and the methods used to ensure the reproducibility of the retention values throughout the study have been reported[8].

The present paper describes the determination of the contributions to the retention of substituents on an aliphatic side chain. By examining side chains of different lengths, it has been possible to examine the effects of interactions of the substituents with a phenyl ring. The magnitude of the contributions have been compared with the contribution of these groups to octanol–water partition constants. Despite considerable previous interest in the contribution of aromatic substituents to retention few studies have examined aliphatic substitution[9].

EXPERIMENTAL

Chemicals, equipment and procedures were as described previously[3].

Calculation of aliphatic substituent indices

The retention index increments for each aliphatic substituent were calculated as the difference between the retention index of the substituted model compound and the calculated retention index in the same eluent for the corresponding alkylbenzene based on the parent index value of benzene (I_P) and contributions for the alkyl side chain. The increments were fitted to a quadratic expression to relate the substituent indices to the proportion of organic modifier.

DISCUSSION

Rather than base a study of the effect on retention of substituents on a saturated carbon by examining substituted aliphatic compounds, which would be difficult to detect spectroscopically, three series of substituted alkylbenzenes have been examined. Because it is possible that the phenyl group could interact with the substituent, alkyl chains of different length were compared. Any effects should decrease with the separation between the groups and would not be expected to be significant for terminal substituents on a propyl side chain.

Retention behaviour of alkylbenzenes

The first step was to examine the retention of the alkylbenzene parent compounds. It was necessary to establish whether the contribution to the retention for a aliphatic methylene group (CH_2 = 100 units), which is defined in the alkyl aryl ketone retention index scale, was also valid to predict the retention of the homologous alkylbenzenes, particularly as it has been suggested that the methylene group increments for different homologous series may differ[10,11].

The capacity factors (Tables I and II) and retention indices (Tables III and IV) of toluene, ethylbenzene, *n*-propylbenzene and *n*-butylbenzene were measured across the eluent ranges methanol–pH 7 buffer (40:60) to (80:20) and acetonitrile–pH 7 buffer (30:70) to (80:20). Using the calculated parent index for benzene[3] as the baseline, the increments for the successive additions of a methylene group to the alkyl side chain can be calculated as $\delta I_{CH_2} = I_{Ph(CH_2)n+1H} - I_{Ph(CH_2)nH}$ (where Ph = phenyl) (Table V). With the exception of the effect of adding the second methylene group

TABLE I

CAPACITY FACTORS FOR COMPOUNDS WITH AN ALIPHATIC SUBSTITUENT ON THE ALKYL CHAIN IN ELUENTS CONTAINING METHANOL

Compound	*Capacity factor (k')*				
	Methanol (%)				
	40	*50*	*60*	*70*	*80*
Toluene	29.51	14.02	7.37	3.37	1.74
Benzyl alcohol	2.31	1.31	0.84	0.56	0.41
Benzyl bromide	31.54	13.40	6.52	2.85	1.56
Benzyl chloride	24.56	10.90	5.51	2.38	1.24
Benzyl cyanide	4.79	2.28	1.31	0.73	0.48
Methyl phenylacetate	10.39	4.68	2.53	1.25	0.74
Phenylacetaldehyde	5.35	2.01	1.13	0.70	0.56
Phenylacetamide	1.36	0.79	0.52	0.38	0.30
1-Phenyl-2-butanone	13.16	5.23	2.67	1.41	0.74
Ethylbenzene	65.28	27.38	13.73	5.02	2.35
Methyl phenylethyl ether	18.39	7.63	3.88	2.00	1.07
Methyl 3-phenylpropionate	24.04	9.58	4.64	1.99	1.06
4-Phenyl-2-butanone	12.60	5.24	2.42	1.35	0.75
2-Phenylethanol	4.11	2.42	1.28	0.74	0.50
2-Phenylethyl bromide	62.88	25.08	11.31	4.30	1.73
2-Phenylethyl chloride	45.99	18.81	8.30	3.49	1.66
3-Phenyl-1-propionamide	2.65	1.38	0.83	0.51	0.36
3-Phenyl-1-propionitrile	6.38	2.99	1.58	0.83	0.52
n-Propylbenzene	165.50	59.57	24.60	8.19	3.38
Methyl 4-phenylbutyrate	51.00	17.98	7.78	2.88	1.40
4-Phenyl-1-butyronitrile	15.22	6.13	2.94	1.32	0.72
3-Phenyl-1-propanol	8.55	3.84	2.06	1.03	0.62
3-Phenyl-1-propyl bromide	163.37	56.07	22.12	7.21	2.92
3-Phenyl-1-propyl chloride	121.95	42.36	15.69	5.86	2.45
n-Butylbenzene	420.37	130.97	46.25	13.55	4.94

TABLE II

CAPACITY FACTORS OF COMPOUNDS WITH ALIPHATIC SUBSTITUENTS ON AN ALKYL SIDE CHAIN IN ELUENTS CONTAINING ACETONITRILE

Compound	*Capacity factor (k')*					
	Acetonitrile (%)					
	30	*40*	*50*	*60*	*70*	*80*
Toluene	28.86	12.74	6.08	3.24	1.97	1.23
Benzyl alcohol	1.75	1.14	0.80	0.57	0.46	0.39
Benzyl bromide	34.10	13.07	5.69	2.84	1.66	1.10
Benzyl chloride	27.63	11.04	4.97	2.53	1.50	0.93
Benzyl cyanide	6.87	3.50	1.92	1.13	0.75	0.52
Methyl phenylacetate	10.63	4.99	2.59	1.47	0.95	0.65
Phenylacetaldehyde	5.30	2.56	1.81	1.17	0.77	0.47
Phenylacetamide	0.93	0.61	0.45	0.34	0.31	0.28
1-Phenyl-2-butanone	15.38	5.89	3.24	1.85	1.10	0.62
Ethylbenzene	59.53	22.38	9.46	4.66	2.67	1.58
Methyl phenylethyl ether	16.39	6.38	3.76	2.19	1.37	0.79
Methyl 3-phenylpropionate	20.39	8.26	3.85	2.04	1.26	0.81
4-Phenyl-2-butanone	13.05	5.05	3.16	1.66	1.01	0.58
2-Phenylethanol	2.71	1.56	1.00	0.68	0.53	0.43
2-Phenylethyl bromide	61.35	20.70	8.18	3.83	2.13	1.23
2-Phenylethyl chloride	47.24	16.74	6.85	3.28	1.86	1.09
3-Phenyl-1-propionamide	1.61	0.90	0.60	0.43	0.36	0.32
3-Phenyl-1-propionitrile	9.47	4.40	2.27	1.27	0.82	0.55
n-Propylbenzene	137.23	42.52	15.83	7.17	3.88	2.15
Methyl 4-phenylbutyrate	38.09	13.35	5.63	2.79	1.64	1.01
4-Phenyl-1-butyronitrile	18.40	7.38	3.41	1.78	1.08	0.69
3-Phenyl-1-propanol	4.90	2.39	1.38	0.87	0.64	0.50
3-Phenyl-1-propyl bromide	–	39.98	14.04	6.10	3.23	1.76
3-Phenyl-1-propyl chloride	106.66	31.94	11.60	5.14	2.76	1.53
n-Butylbenzene	308.86	79.97	26.33	11.02	5.63	2.94

(toluene to ethylbenzene) the increments ranged from 91 to 112 units. The variations from the anticipated values of 100 are generally within the expected experimental error range of ± 10 units for this study determined from the uncertainties in measurement and calculations[8], the only higher deviation being at 80% acetonitrile when measurements are the least reliable because of the short retention times. However, the change from toluene to ethylbenzene was consistently smaller and ranged from 87 to 92 (mean 88) units. A corresponding anomaly can also be seen in the octanol–water partition coefficient substituent constants (π) for the alkyl substituents on benzene (H, 0.0; methyl, 0.56; ethyl, 1.02; propyl, 1.55; butyl, 2.13)[12]. The step between methyl and ethyl of 0.46 is smaller than the other changes which range from 0.56 to 0.58.

Thus in the present study it will be valid to use the defined value of 100 units for the addition of a methylene group to an alkyl chain substituted on benzene but it will be necessary to apply an interaction index correction of −12 units ($I_{I,PhCH_2R}$) if the addition is to a benzylic carbon.

TABLE III

RETENTION INDICES OF ALIPHATIC COMPOUNDS WITH METHANOL ELUENTS

Compound	*Retention index*				
	Methanol (%)				
	40	*50*	*60*	*70*	*80*
Toluene	983	1010	1038	1063	1090
Benzyl alcohol	689	691	698	684	675
Benzyl bromide	991	1004	1019	1030	1059
Benzyl chloride	962	976	992	992	994
Benzyl cyanide	773	766	763	738	722
Methyl phenylacetate	863	862	853	853	846
Phenylacetaldehyde	790	752	745	734	782
Phenylacetamide	627	623	591	598	582
1-Phenyl-2-butanone	884	885	883	877	867
Ethylbenzene	1075	1100	1126	1151	1177
Methyl phenylethyl ether	923	934	945	955	968
Methyl 3-phenylpropionate	960	959	954	953	948
4-Phenyl-2-butanone	888	883	879	871	863
2-Phenylethanol	756	774	759	741	729
2-Phenylethyl bromide	1072	1088	1107	1118	1090
2-Phenylethyl chloride	1033	1049	1066	1074	1077
3-Phenyl-1-propionamide	705	698	667	663	640
3-Phenyl-1-propionitrile	806	802	793	766	742
n-Propylbenzene	1182	1204	1227	1256	1282
Methyl 4-phenylbutyrate	1046	1043	1040	1033	1029
4-Phenylbutyronitrile	907	899	892	866	842
3-Phenyl-1-propanol	840	835	835	813	793
3-Phenyl-1-propyl bromide	1181	1196	1214	1229	1240
3-Phenyl-1-propyl chloride	1147	1159	1175	1184	1190
n-Butylbenzene	1290	1310	1331	1364	1392

Substituent indices of aliphatic substituents

The capacity factors (Tables I and II) of model substituted toluenes, ethylbenzenes and propylbenzenes, measured over the same eluent ranges as the alkylbenzenes, all showed systematic reductions with increased modifier in the eluent. At the pH of the buffer, carboxylic acid groups were ionised and aliphatic amino groups were protonated so these groups were not included in the study. The changes in the retention indices (Tables III and IV, Fig. 1a and b) were not as marked as for the capacity factors but all the compounds showed some dependence on the eluent composition. A number of the substituted toluenes had been examined previously as model substituted aromatic compounds[3] and are reported here for comparison with the longer chain compounds.

The effect of each of the substituents can be determined as a retention index increment (δI, Tables VI and VII). This value is the difference between the retention index and the predicted value of the corresponding unsubstituted alkylbenzene, which is calculated as the sum of the parent index for benzene, the methylene increments and as appropriate the interaction correction for methylene substitution on

TABLE IV

RETENTION INDICES OF ALIPHATIC COMPOUNDS IN ACETONITRILE ELUENTS

Compound	*Retention index*					
	Acetonitrile (%)					
	30	*40*	*50*	*60*	*70*	*80*
Toluene	1005	1021	1033	1042	1050	1056
Benzyl alcohol	654	640	630	624	636	645
Benzyl bromide	1026	1025	1020	1011	1002	986
Benzyl chloride	999	999	993	983	973	956
Benzyl cyanide	825	817	804	789	774	751
Methyl phenylacetate	879	873	864	853	843	829
Phenylacetaldehyde	781	784	781	790	790	782
Phenylacetamide	575	540	516	504	522	535
1-Phenyl-2-butanone	912	910	904	898	888	874
Ethylbenzene	1095	1110	1121	1130	1137	1144
Methyl phenylethyl ether	919	925	932	937	945	957
Methyl 3-phenylpropionate	961	952	942	932	922	907
4-Phenyl-2-butanone	896	889	880	869	864	855
2-Phenylethanol	708	689	675	667	676	682
2-Phenylethyl bromide	1099	1098	1092	1083	1073	1056
2-Phenylethyl chloride	1066	1064	1057	1045	1034	1013
3-Phenyl-1-propionamide	643	602	573	557	568	574
3-Phenyl-1-propionitrile	865	853	837	818	799	771
n-Propylbenzene	1200	1212	1223	1233	1244	1253
Methyl 4-phenylbutyrate	1039	1029	1018	1007	997	984
4-Phenylbutyronitrile	948	935	918	898	879	851
3-Phenyl-1-propanol	782	756	739	728	731	735
3-Phenyl-1-propyl bromide	–	1202	1200	1194	1191	1182
3-Phenyl-1-propyl chloride	1168	1167	1162	1153	1147	1132
n-Butylbenzene	1302	1313	1325	1337	1350	1365

the benzylic carbon ($\delta I_X = I_{Ph(CH_2)n-X} - [I_P + nI_{S,CH_2} + I_{I,PhCH_2R}$ (if $n>1$)]). A number of the substituents, CO_2CH_3, OCH_3, $COCH_2CH_3$ and $COCH_3$, also contained saturated alkyl groups not directly attached to the aromatic ring. The increments for the corresponding functional groups CO_2R, OR and COR have been calculated by subtracting 100 units for each aliphatic methylene group. The size of the increments for the substituents were markedly different from those for the corresponding groups directly attached to aromatic ring[3]. With the exception of the hydroxyl group, the retention index increments calculated from the ethyl- and propylbenzenes showed only small differences. This suggested that there was little interaction in these compounds between the substituent and the aromatic ring.

The coefficients for the quadratic equations (Table VIII) relating the increments to the eluent composition were calculated, for each substituent, based on the model compound with the longest available alkyl chain (indicated by '*a*' in Tables VI and VII). This was usually the substituted *n*-propylbenzene except for the amide and ketone groups which were based on ethylbenzene and the aldehyde group, which was

TABLE V

RETENTION INDEX INCREMENTS FOR THE ADDITION OF A METHYLENE GROUP TO AN ALKYLBENZENE

Compound	*Retention index increment*					
	Organic modifier proportion (%)					
	30	*40*	*50*	*60*	*70*	*80*
Methanol–buffer						
$I_{P,benzene}$[a]		885	913	938	961	982
Benzene–toluene	–	98	97	100	102	108
Toluene–ethylbenzene	–	92	90	88	88	87
Ethylbenzene–propylbenzene	–	107	104	101	105	105
Propylbenzene–butylbenzene	–	108	106	104	105	105
Acetonitrile–buffer						
$I_{P,benzene}$[a]	910	927	940	951	958	963
Benzene–toluene	95	94	93	91	92	95
Toluene–ethylbenzene	90	89	88	88	87	88
Ethylbenzene–propylbenzene	105	102	102	103	107	109
Propylbenzene–butylbenzene	102	101	103	107	106	112

[a] Calculated from ref. 3.

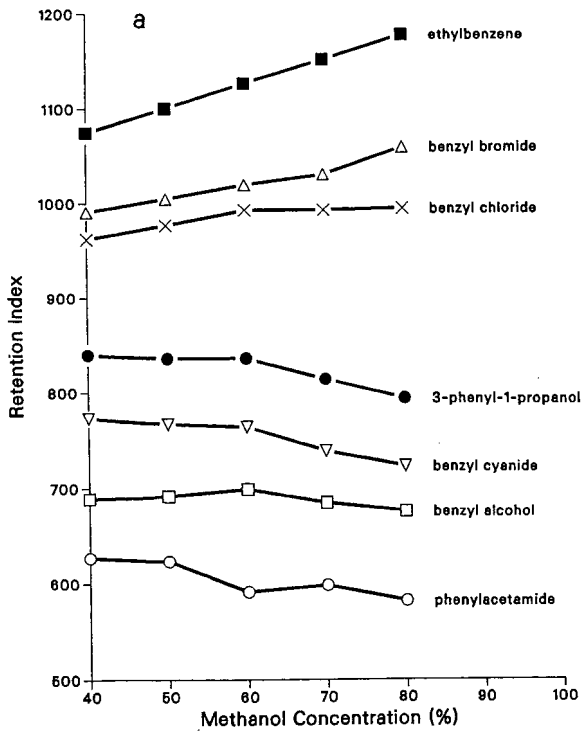

Fig. 1.

(Continued on p. 78)

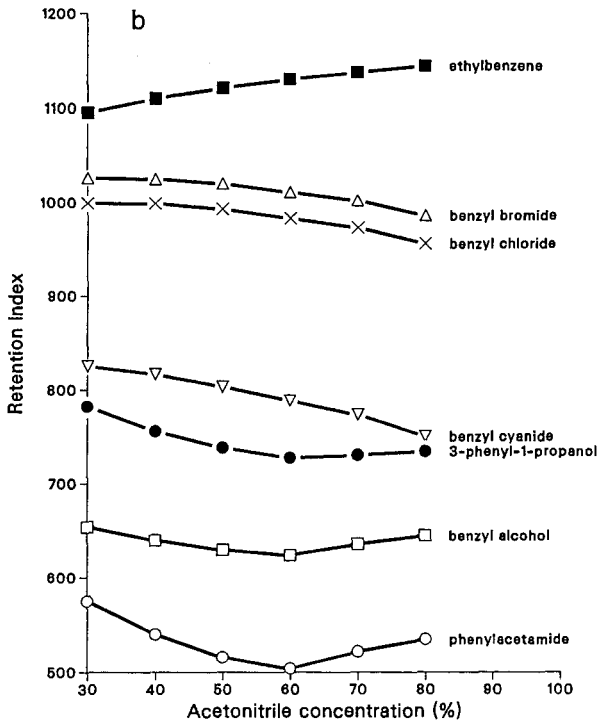

Fig. 1. Retention indices of selected substituted alkylbenzenes with proportion of (a) methanol and (b) acetonitrile.

based on toluene. These coefficients can be used to calculate the substituent indices and in each case there was a good correlation with the experimental values of the retention index increments (Fig. 2a and b) suggesting that within the composition ranges studied, the results would be a good prediction of retention changes.

Interactions of substituents with the phenyl group

The differences between the retention index increments derived from the different alkylbenzenes (Table VI and VII) are assumed to be caused by interactions between the substituents and the phenyl group. These interactions would be expected to depend on the distance of the substituent from the ring and to be strongest with substituents positioned on the benzylic carbon. The interaction increments (δI_I) for the substituted toluenes and ethylbenzenes have been examined by calculating the differences between the calculated substituent index (based on Table VIII) and the measured retention index increment ($\delta I_I = \delta I_X - I_{S,X}$) (Table IX).

The largest interaction increments (+55 to +88 units) were observed for the cyano and hydroxyl groups on the benzylic carbon (1-phenyl, 1–X interactions). These were much reduced for the substituted ethylbenzenes in methanolic eluents (1-phenyl, 2–X interactions) but were still significant for the hydroxyl group with acetonitrile–buffer eluents. Moderate interactions were observed for the amide and ester groups. The substitution of a ketonic carbonyl group on the benzylic carbon

TABLE VI

RETENTION INDEX INCREMENTS FOR ALIPHATIC SUBSTITUENTS IN METHANOL ELUENTS

	Fragmental constant[12]	*Retention index increment*				
		Methanol (%)				
		40	*50*	*60*	*70*	*80*
Substituents on toluene						
Calculated parent I ($I_P + I_{S,CH_2}$)		985	1013	1038	1061	1082
$CONH_2$		−358	−390	−447	−463	−500
OH		−296	−322	−340	−377	−407
CN		−212	−247	−275	−323	−360
CHO[a]	−1.10	−195	−261	−293	−327	−300
CO_2CH_3		−122	−151	−185	−208	−236
(CO_2R[b]		−222	−251	−285	−308	−336)
COC_2H_5		−101	−128	−155	−184	−215
(COR[c]		−301	−328	−355	−384	−415)
Cl		−23	−37	−46	−69	−88
Br		6	−9	−19	−31	−23
Substituents on ethylbenzene						
Calculated parent I ($I_P + 2I_{S,CH_2} + I_{I,PhCH_2R}$)		1073	1101	1126	1149	1170
$CONH_2$[a]	−2.18	−368	−403	−459	−486	−530
OH		−317	−327	−367	−408	−441
CN		−267	−299	−333	−383	−428
$COCH_3$	−1.13	−189	−216	−243	−272	−303
(COR[a,b]		−289	−316	−343	−372	−403)
OCH_3	−1.54	−150	−167	−181	−194	−202
(OR[a,b]		−250	−267	−281	−294	−302)
CO_2CH_3		−113	−142	−172	−196	−222
(CO_2R[b]		−213	−242	−272	−296	−322)
Cl		−40	−52	−60	−75	−93
Br		−1	−13	−19	−31	−80
Substituents on n-propylbenzene						
Calculated parent I ($I_P + 3I_{S,CH_2} + I_{I,PhCH_2R}$)		1173	1201	1226	1249	1270
OH[a]	−1.64	−333	−366	−391	−436	−477
CN[a]	−1.27	−266	−302	−334	−383	−428
CO_2CH_3	−0.72	−127	−158	−186	−216	−241
CO_2R[a,b]		−227	−258	−286	−316	−341)
Cl[a]	0.06	−26	−42	−51	−65	−80
Br[a]	0.20	8	−5	−12	−20	−70

[a] Values used for the calculation of substituent index equations.
[b] 100 subtracted for the methyl group contribution.
[c] 200 subtracted for the ethyl group contribution.

TABLE VII

RETENTION INDEX INCREMENTS FOR ALIPHATIC SUBSTITUENTS IN ACETONITRILE ELUENTS

	Retention index increment					
	Acetonitrile (%)					
	30	*40*	*50*	*60*	*70*	*80*
Substituents on toluene						
Calculated parent I ($I_P + I_{S,CH_2}$)	1001	1027	1040	1051	1058	1063
$CONH_2$	−435	−487	−524	−547	−536	−528
OH	−356	−387	−410	−427	−422	−418
CN	−185	−210	−236	−262	−284	−312
CHO[a]	−229	−243	−259	−261	−268	−281
CO_2CH_3	−131	−154	−176	−198	−215	−234
(CO_2R[b]	−231	−254	−276	−298	−315	−334)
COC_2H_5	−98	−117	−136	−153	−170	−189
(COR[c]	−298	−317	−336	−353	−370	−389)
Cl	−11	−28	−47	−68	−85	−107
Br	16	−2	−20	−40	−56	−77
Substituents on ethylbenzene						
Calculated parent I ($I_P + 2I_{S,CH_2} + I_{I,PhCH_2}$)	1098	1115	1128	1139	1146	1151
$CONH_2$[a]	−455	−513	−555	−582	−578	−577
OH	−390	−426	−453	−472	−470	−469
CN	−233	−262	−291	−321	−347	−380
$COCH_3$	−202	−226	−248	−270	−282	−296
(COR[a,b]	−302	−326	−348	−370	−382	−396)
OCH_3	−179	−190	−196	−202	−201	−194
(OR[a,b]	−279	−290	−296	−302	−301	−294)
CO_2CH_3	−137	−163	−186	−207	−224	−244
(CO_2R[b]	−237	−263	−286	−307	−324	−344)
Cl	−32	−51	−71	−94	−112	−138
Br	1	−17	−36	−56	−73	−95
Substituents on n-propylbenzene						
Calculated parent I ($I_P + 3I_{S,CH_2} + I_{I,PhCH_2R}$)	1198	1215	1228	1239	1246	1251
OH[a]	−416	−459	−489	−511	−515	−516
CN[a]	−250	−280	−310	−341	−367	−400
CO_2CH_3	−159	−186	−210	−232	−249	−267
(CO_2R[a,b]	−259	−286	−310	−332	−349	−367)
Cl[a]	−30	−48	−66	−86	−99	−119
Br[a]	−	−13	−28	−45	−55	−69

[a] Values used for the calculation of substituent index equations.
[b] 100 subtracted for the methyl group contribution.
[c] 200 subtracted for the ethyl group contribution.

TABLE VIII

SUBSTITUENT INDEX EQUATIONS FOR ALIPHATIC SUBSTITUENTS ON AN ALKYL SIDE CHAIN

$I_S = ax^2 + bx + c$; x = % organic modifier.

Substituent	*Coefficients*		
	a	*b*	*c*
Methanol–buffer			
$CONH_2$	0.0079	−5.013	−178
OH	−0.0257	−0.494	−273
CN	−0.0250	−1.050	−185
CHO	0.1314	−18.531	337
CO_2R	0.0071	−3.717	−90
COR	−0.0086	−1.851	−201
OR	0.0136	−2.939	−154
Cl	−0.0021	−1.053	19
Br	−0.0536	4.719	−99
CH_3	0.0	0.0	100
Acetonitrile–buffer			
$CONH_2$	0.0855	−11.786	−179
OH	0.0561	−8.139	−223
CN	0.0002	−2.997	−160
CHO	0.0073	−1.768	−184
CO_2R	0.0130	−3.580	−164
COR	0.0161	−3.654	−206
OR	0.0211	−2.644	−218
Cl	0.0018	−1.962	27
Br	0.0064	−2.161	63
CH_3	0.0	0.0	100

showed a negative interaction contribution in methanol as did the halides on both carbons.

The coefficients relating these interaction increments to the eluent composition were calculated but changes smaller than 10 units across the eluent range were regarded as within experimental error and a single mean value for the c term was used (Table X). Although general comments on the size of the interactions have been made, it was difficult to correlate these with any properties of the substituents.

Relationship between I_S and structural parameters

The substituent indices should be related to the contributions of the substituents to octanol–water partition coefficients and Hansch and Leo[12] have suggested that for aliphatic compounds fragmental constants F_r are a better guide than π constants. If a linear relationship between F_r and I_S exists, it could be useful as it could provide a method to estimate I_S for a substituent not included in the data set such as un-ionised aliphatic amino and carboxylic acid groups. The fragmental contributions (Table VI) have been compared with the substituent index values at different eluent compositions. However, there was only an approximately linear relationship with correlations decreasing from 0.925 to 0.869 in methanol and 0.924 to 0.860 in aceto-

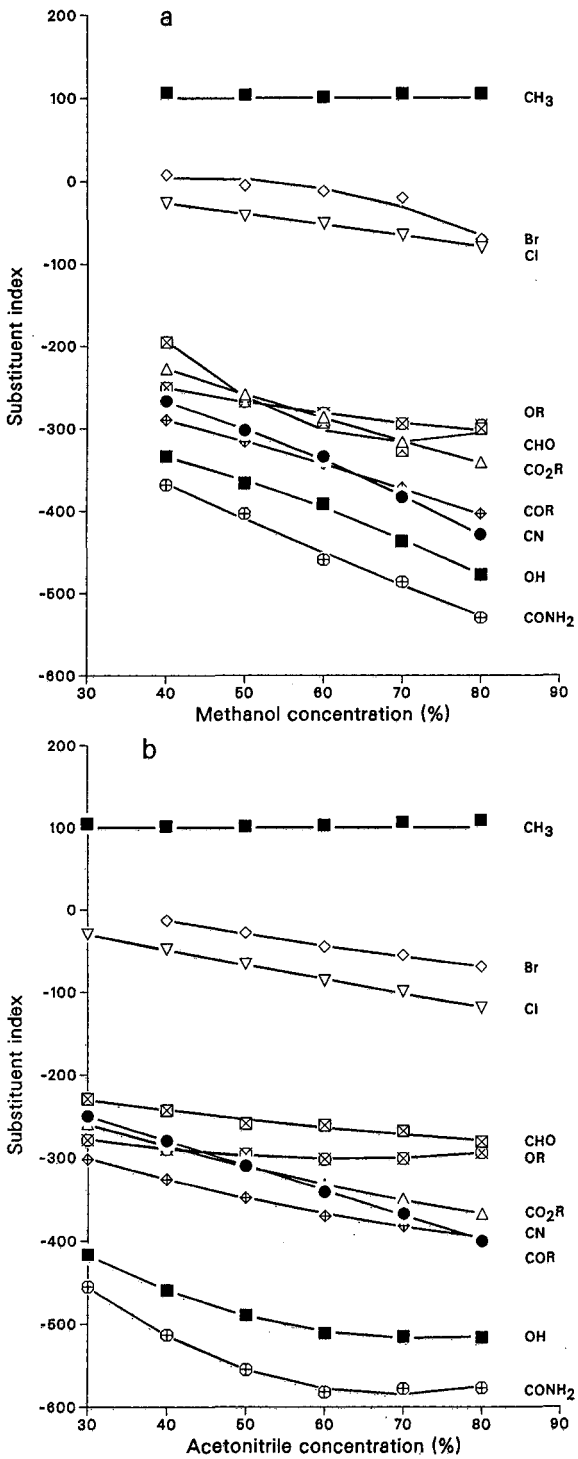

Fig. 2. Comparison of retention index increments for aliphatic substituents groups (points, from Tables VI and VII) with calculated substituents indices (solid line, calculated from Table VIII) in (a) methanol and (b) acetonitrile-containing eluents.

TABLE IX

INTERACTION INCREMENTS FOR INTERACTIONS OF ALIPHATIC SUBSTITUENTS WITH A PHENYL GROUP

Substituent	*Interaction increment*											
	Methanol (%)					*Acetonitrile (%)*						
	40	*50*	*60*	*70*	*80*	*30*	*40*	*50*	*60*	*70*	*80*	
1-phenyl, 1–X interactions ($PhCH_2$–X)												
$\delta I_I = \delta I_{PhCH_2-X} - I_S$												
$CONH_2$	11	19	3	27	28	19	27	30	31	49	47	
OH	38	40	55	67	70	61	72	80	82	96	97	
CN	55	53	53	58	69	65	70	73	77	85	86	
CO_2R	5	7	2	7	6	29	32	35	34	36	33	
COR	−12	−13	−12	−13	−12	3	9	12	14	13	6	
Cl	3	2	5	−4	−9	19	21	20	16	17	11	
Br	2	−11	−10	0	41	12	11	9	4	1	−8	
1-phenyl, 2–X interactions ($PhCH_2CH_2$–X)												
$\delta I_I = \delta I_{PhCH_2CH_2-X} - I_S$												
OH	17	35	28	26	36	27	33	37	37	48	46	
CN	0	−1	−5	2	1	17	18	18	18	22	18	
CO_2R	14	16	15	19	20	23	23	25	25	27	23	
Cl	−14	−13	−8	−10	−14	−2	−2	−4	−10	−10	−20	
Br	−5	−10	−10	0	−15	−3	−4	−5	−12	−16	−26	

TABLE X

COEFFICIENTS OF INTERACTION INDEX EQUATIONS FOR INTERACTIONS BETWEEN ALIPHATIC SUBSTITUENTS AND A PHENYL GROUP

$I_I = ax^2 + bx + c$; x = % organic modifier

Substituent	*Coefficients*					
	Methanol–buffer			*Acetonitrile–buffer*		
	a	*b*	*c*	*a*	*b*	*c*
1-phenyl, 1–X interactions ($I_{1,PhCH_2-X}$)						
$CONH_2$	0.0186	−1.809	56	0.0018	0.395	6
OH	−0.0007	0.996	−3	−0.0046	1.236	29
CN	0.0221	−2.327	113	0	0.440	52
CO_2R	0	0	0	0	0	33
COR	0	0	−12	0	0	10
Cl	−0.0143	1.414	−31	0	0	17
Br	0.0836	−9.139	235	−0.0079	0.479	5
1-phenyl, 2–X interactions ($I_{1,PhCH_2CH_2-X}$)						
OH	−0.0079	1.233	−16	−0.0021	0.636	10
CN	0	0	0	0	0	19
CO_2R	0	0	17	0	0	24
Cl	0	0	−12	−0.0075	0.482	−10
Br	−0.0071	0.757	−26	−0.0101	0.668	−14

nitrile as the proportion of the modifier increased. This trend agrees with previous reports which have suggested that the chromatographic system more closely resembles the octanol–water system when the organic content is lowest[13]. In both cases the correlations were poorer than the corresponding relationship for substituents on an aromatic ring[3].

CONCLUSION

The coefficients of the substituent index and interaction index determined for the aliphatic substituents generally reflect the effect on partitioning and the interaction of the phenyl groups and can be used in the prediction system to predict the retention indices of other substituents.

ACKNOWLEDGEMENTS

The authors thank the Sciences and Engineering Research Council for a research grant and for a studentship to C.M.B. and Phase Separations for a gift of Spherisorb ODS-2.

REFERENCES

1 J. W. Dolan, L. R. Snyder and M. A. Quarry, *Chromatographia*, 24 (1987) 261.
2 J. C. Berridge, *Techniques for the Automated Optimization of HPLC Separations*, Wiley, Chichester, 1985.
3 R. M. Smith and C. M. Burr, *J. Chromatogr.*, 475 (1989) 57.
4 C. M. Burr and R. M. Smith, *Anal. Proc.*, 25 (1988) 46.
5 R. M. Smith, *J. Chromatogr.*, 236 (1982) 313.
6 R. M. Smith, *Adv. Chromatogr.*, 26 (1987) 277.
7 C. M. Burr and R. M. Smith, *Anal. Proc.*, 26 (1989) 24.
8 R. M. Smith and C. M. Burr, *J. Chromatogr.*, 475 (1989) 75.
9 R. Kaliszan, *Quantitative Structure–Chromatographic retention relationships* (*Chemical Analysis*, Vol. 93), Wiley, New York, 1987.
10 A. Tchapla, H. Colin and G. Guiochon, *Anal. Chem.*, 56 (1984) 621.
11 H. Colin and G. Guiochon, *J. Chromatogr. Sci.*, 18 (1980) 54.
12 C. Hansch and A. Leo, *Substituent Constants for Correlation Analysis in Chemistry and Biology*, Wiley, New York, 1979.
13 T. Braumann, *J. Chromatogr.*, 373 (1986) 191.

Journal of Chromatography, 481 (1989) 85–95
Elsevier Science Publishers B.V., Amsterdam — Printed in The Netherlands

CHROM. 21 758

RETENTION PREDICTION OF ANALYTES IN REVERSED-PHASE HIGH-PERFORMANCE LIQUID CHROMATOGRAPHY BASED ON MOLECULAR STRUCTURE

IV. BRANCHED AND UNSATURATED ALKYLBENZENES

ROGER M. SMITH* and CHRISTINA M. BURR
Department of Chemistry, Loughborough University of Technology, Loughborough, Leics. LE11 3TU (U.K.)

(First received April 20th, 1989; revised manuscript received June 30th, 1989)

SUMMARY

As part of a study to predict the retention of analytes in reversed-phase liquid chromatography the effects of isomerisation and unsaturation in alkyl chain substituents on an aromatic ring have been examined. The contributions of the presence of branching and of olefinic groups have been related to the eluent composition in methanol-buffer and acetonitrile–buffer eluents. These results have been applied to a comparison of the influence on retention of primary, secondary and tertiary hydroxyl groups in isomeric phenylpropanols.

INTRODUCTION

A method has been developed to predict the retention of analytes in reversed-phase liquid chromatography based on their molecular structure and the composition of the mobile phase[1]. The retention index (I) of a compound is calculated by the summation of the retention index of a parent structure (I_P, benzene) and substituent index contributions from alkyl groups ($I_{S,R}$), from substituents on the aromatic ring ($I_{S,Ar-X}$) and on aliphatic carbons ($I_{S,Al-X}$), and from interactions between the substituents ($I_{I,Z-Y}$). In previous reports the coefficients of the quadratic equations relating the eluent composition to the contributions for individual aromatic[1] and aliphatic[2] substituent groups have been reported and the steps taken to ensure reproducibility throughout the study have been described[3]. The retention coefficients are held in a database which can be interrogated by an expert system program CRIPES (Chromatographic Retention Index Prediction Expert System)[4]. Throughout the study the retention measurements have been based on retention indices using the alkyl aryl ketone scale to increase the reproducibility and to improve the interchangability of the predictions between columns[5].

Previous studies in a number of laboratories have examined the capacity factors of branched and normal chain alkylbenzenes[6–8], alkylphenols[9] and aliphatic al-

0021-9673/89/$03.50

kanes[10] in reversed-phase liquid chromatography. The presence of secondary and tertiary groups were found to cause a reduction in the retention compared to unbranched compounds and the effect increased with the degree of branching. This suggested that a prediction method could not be based on a simple summation of the number of aliphatic carbon atoms. In an attempt to quantify the changes in phenolic antioxidants Popl *et al.*[9] have calculated the contributions for the different alkyl groups as retention index increments using a scale based on the polycyclic aromatic hydrocarbons. They related the changes to the eluent composition using a linear function and found that the slope of the relationship for *n*- and branched alkyl groups differed and this could be predicted in an additive manner. In a more recent study Knox *et al.*[8] confirmed the relative retentions observed earlier by Smith[6] for the isomeric alkyl- and polymethylbenzenes. Both these studies suggested that although the molecular connectivity of the alkylbenzenes showed a reasonable correlation with retention this was largely a function of the number of carbon atoms and was a poor guide to the relative retentions of isomeric compounds such as iso- and *sec.*-butylbenzene.

In the present paper the effect of branching and unsaturation in alkyl groups substituted on an aromatic ring are examined. The results are then applied to the comparison of isomeric phenylpropanols to determine the contributions from primary, secondary and tertiary hydroxyl groups.

EXPERIMENTAL

The chemical, methods and equipment were as described in Part I[1].

RESULTS AND DISCUSSION

The first step in the prediction of the retention of a compound is to calculate a value for the unsubstituted carbon skeleton as a summation of contributions from the aromatic ring and from the aliphatic carbon side chains. The parent retention index values for benzene have been determined empirically[1] and as the method is based in retention indices each aliphatic carbon atom should by definition make a contribution of 100 units. However, when studying the retention increments for increases in the length of *n*-alkyl group substituted on an aromatic ring, it was found that going from toluene to ethylbenzene caused a smaller change than 100 units in the retention indices, which was ascribed to the effects of hyperconjugation. An interaction index term ($I_{\text{I,PhCH}_2\text{R}} = -12$ units; Ph = phenyl) for alkyl substitution on the benzylic carbon in both methanol–buffer and acetonitrile–buffer eluents was determined. In view of the earlier reports of the differences in the retention of branched alkylbenzenes, it appeared that a similar interaction term might also be needed if secondary and tertiary carbons are present in the analyte.

Isomeric alkylbenzenes

The capacity factors (Table I) of isopropylbenzene and iso-, *sec.*- and *tert.*-butylbenzene were determined over the eluent ranges methanol–buffer (50:50) to (80:20) and acetonitrile–buffer (30:70) to (80:20) and were compared with the capacity factors of ethyl-, *n*-propyl- and *n*-butylbenzene determined previously[2]. The ethyl-

TABLE I

CAPACITY FACTORS OF ISOMERIC ALKYLBENZENES

Compound	*Capacity factor*					
	Modifier (%)					
	30	*40*	*50*	*60*	*70*	*80*
Methanol–buffer						
Ethylbenzene[a]		65.28	27.28	13.73	5.02	2.35
Isopropylbenzene		130.97	51.64	19.16	7.41	3.08
n-Propylbenzene[a]		165.50	59.57	24.60	8.19	3.38
tert.-Butylbenzene		–	76.08	27.61	9.69	3.81
sec.-Butylbenzene		–	95.77	32.85	11.16	4.38
Isobutylbenzene		–	123.12	38.89	12.84	4.72
n-Butylbenzene[a]		–	130.97	41.20	13.37	4.95
Acetonitrile–buffer						
Ethylbenzene[a]	59.53	22.38	9.46	4.66	2.67	1.58
Isopropylbenzene	131.26	35.92	14.36	6.70	3.50	2.06
n-Propylbenzene[a]	137.23	42.42	15.83	7.17	3.88	2.15
tert.-Butylbenzene	216.36	53.09	19.57	8.77	4.07	2.50
sec.-Butylbenzene	290.89	65.43	23.39	10.28	4.69	2.82
Isobutylbenzene	334.41	73.41	25.71	11.01	5.38	3.02
n-Butylbenzene[a]	308.86	79.97	27.39	11.81	5.63	2.94

[a] included from ref. 2 for comparison.

TABLE II

RETENTION INDICES OF ISOMERIC ALKYLBENZENES

Compound	*Retention index*					
	Modifier (%)					
	30	*40*	*50*	*60*	*70*	*80*
Methanol–buffer						
Ethylbenzene[a]		1073	1101	1126	1149	1170
Isopropylbenzene		1154	1179	1202	1224	1246
n-Propylbenzene[a]		1173	1201	1226	1249	1270
tert.-Butylbenzene		–	1251	1269	1290	1313
sec.-Butylbenzene		–	1280	1298	1320	1341
Isobutylbenzene		–	1296	1317	1341	1362
n-Butylbenzene[a]		–	1301	1326	1349	1370
Acetonitrile–buffer						
Ethylbenzene[a]	1098	1115	1128	1139	1146	1151
Isopropylbenzene	1169	1186	1196	1203	1211	1215
n-Propylbenzene[a]	1198	1215	1228	1239	1246	1251
tert.-Butylbenzene	1230	1248	1256	1264	1272	1280
sec.-Butylbenzene	1266	1281	1291	1302	1312	1325
Isobutylbenzene	1283	1299	1310	1322	1333	1344
n-Butylbenzene[a]	1298	1315	1328	1339	1346	1351

[a] Predicted retention indices calculated as in ref. 2.

TABLE III

RETENTION INDEX INCREMENTS FOR METHYL SUBSTITUENTS ON ALKYL CHAINS

Alkylbenzene	*Carbon substituted*	*Retention index increment for each branched methyl*											
		Compared to n-alkylbenzene						*Corrected for* $I_{1\text{-}PhCH_2\text{-}R}$					
		Modifier (%)						*Modifier (%)*					
		30	*40*	*50*	*60*	*70*	*80*	*30*	*40*	*50*	*60*	*70*	*80*
Methanol–buffer													
Isopropylbenzene	1	–	81	78	76	75	76	–	93	90	88	87	88
sec.-Butylbenzene	1	–	–	79	72	71	71	–	–	91	84	83	83
tert.-Butylbenzene[a]	1	–	–	75	71	70	71	–	–	87	83	82	83
Isobutylbenzene	2	–	–	95	91	92	92	–	–	95	91	92	92
Acetonitrile–buffer													
Isopropylbenzene	1	71	71	68	64	65	64	83	83	80	76	77	76
sec.-Butylbenzene	1	68	66	63	63	66	74	80	78	75	75	78	86
tert.-Butylbenzene[a]	1	66	66	64	61	62	64	78	78	76	73	74	76
Isobutylbenzene	2	85	84	82	83	87	93	85	84	82	83	87	93

[a] Change in retention index divided by 2.

and propylbenzenes were also examined at methanol–buffer (40:60). These results were then used to calculate the retention indices (Table II). As expected from the earlier work, as the degree of branching increased from normal to iso or *sec.* to *tert.* groups the capacity factors and retention index values decreased. The elution order agreed with the earlier studies[6,8].

In order to determine the changes due to the addition of the secondary or tertiary methyl group to the alkyl chain, the retentions of the branched compounds were compared with those of the corresponding unsubstituted *n*-alkylbenzenes. Thus isopropylbenzene and *tert.*-butylbenzene were compared with ethylbenzene and isobutylbenzene and *sec.*-butylbenzene with *n*-propylbenzene. In each case the retention index increment for the addition of the branched methyl group (Table III) was calculated by subtracting the predicted retention index for the parent *n*-alkylbenzene derived from the earlier study[2] (given in Table II).

The increments for the secondary and tertiary methyl groups substituted on the benzylic carbon (isopropyl-, *sec.*-butyl- and *tert.*-butylbenzene) were very similar (71–81 units in methanol and 61–74 units in acetonitrile). However, the retention index increments of a methyl group substituted onto the second carbon (91–95 units in methanol and 82–93 units in acetonitrile) were always larger. Both groups therefore made a smaller contribution to retention than that for an increase in a linear alkyl chain by a methylene group (100 units).

It can be assumed that the interactions noted earlier in the *n*-alkylbenzenes for substitution on the benzylic carbon are also present in the branched chain compounds. The retention index increments for the methyl groups substituted on a benzylic carbon should therefore be corrected by adding 12 units to their value. These corrected values (Table III) show only small differences between the increments for secondary and tertiary methyl groups, irrespective of their position.

Thus the presence of a branched carbon reduces the effect of alkyl substitution compared to an unbranched group. This can be accounted for by an interaction index term ($I_{\text{I,branch}}$) whose value can be determined from the difference between the expected increment of 100 units for a methylene group and the corrected retention index increments from Table III. The magnitude of the branching increments vary over only a small range with eluent composition (-7 to -18 units in methanol–buffer and -17 to -27 units in acetonitrile–buffer, Table IV). These changes in the values with eluent composition are within the experimental error margins of $\pm$ 10 retention index units estimated for the study[3]. The mean value for each eluent was therefore used as the interaction increment (methanol, $I_{\text{I,branch}} = -12$ and acetonitrile, $I_{\text{I,branch}} = -20$). With this proposal a *tert.*-butyl group would be considered to contain two branches.

The retention indices of the alkylbenzenes can be correlated with the corresponding Hansch π constants used in the determination of predicted octanol–water partition coefficients[11]. These contributions decrease from *n*-propyl (1.55) to isopropyl (1.53) and from *n*-butyl (2.13) to *sec.*-butyl (2.04) to *tert*-butyl (1.98). However, a value for isobutyl has not been reported[11]. Thus branching decreases the partition coefficients for *tert.*-butyl by nearly twice the value of a single branch.

It is also possible to calculate the molecular connectivity indices for the alkyl chains as described by Kier *et al.*[12]. The indices for the straight chain isomer, *n*-propyl (1.411) is higher than for the corresponding branched chain, isopropyl (1.354). How-

TABLE IV

INTERACTION INCREMENTS FOR A BRANCH IN AN ALKYL GROUP ON AN AROMATIC RING

Interaction increment for branching = corrected retention index increment for branched methyl (from Table III) − 100 (nominal value for methyl). The mean values are used to determine values for $I_{\text{i,branch}}$ (see discussion).

Carbon chain	*Interaction increment branching*[a] *Modifier (%)*					
	30	*40*	*50*	*60*	*70*	*80*
Methanol–buffer						
$CH(CH_3)_2$	–	−7	−10	−12	−13	−12
$C(CH_3)_3$	–	–	−13	−17	−18	−17
$CH(CH_3)CH_2CH_3$	–	–	−9	−16	−17	−17
$CH_2CH(CH_3)_2$	–	–	−5	−9	−8	−8
Mean	–	−7	−9	−14	−14	−14
Acetonitrile–buffer						
$CH(CH_3)_2$	−17	−17	−20	−24	−23	−24
$C(CH_3)_3$	−22	−22	−24	−27	−26	−24
$CH(CH_3)CH_2CH_3$	−20	−22	−25	−25	−22	−14
$CH_2CH(CH_3)_2$	−15	−16	−18	−17	−13	−7
Mean	−19	−19	−22	−23	−21	−17

[a] A *tert.*-butyl group is considered to contain two branches.

ever, as found previously[6,8] although the indices for the butyl groups decrease as the branching increases, *n*-butyl (1.971), isobutyl (1.827), *sec.*-butyl (1.892) and *tert.*-butyl (1.661), they do not agree with the order of elution of the iso- and *sec.*-isomers.

Unsaturated alkyl chains

In early high-performance liquid chromatography studies Shabron *et al.*[13] suggested that the presence of an unsaturated group (–CH = CH–) had a similar effect on retention as a single methylene group and showed that this relationship was valid for a series of polycyclic hydrocarbons. In the present work, the unsaturated alkylbenzenes, 1-phenyl-1-propene ($PhCH = CHCH_3$) and 3-phenyl-1-propene ($PhCH_2CH = CH_2$) have been examined. The capacity factors of these compounds were used to calculate their retention indices (Table V). In both cases the retentions were shorter than for *n*-propylbenzene, the corresponding saturated alkylbenzene (Tables I and II). It was decided that, rather than regarding the olefinic group as part of an alkyl chain, it would be treated as a substituent placed either on the aromatic ring or on an aliphatic side chain. This approach has also been used for other π-bonded carbons such as ketones and esters. The contributions of the olefinic groups were therefore calculated as retention index increments (Table VI) by subtraction of the calculated retention index values for benzene and 100 units for the methylene or methyl group from the indices of the phenylpropenes.

In both eluents the effect of the aliphatic olefinic group [$Ph(CH_2)_nCH = CHR$] was larger than for the aryl conjugated group ($PhCH = CHR$). The range of values

TABLE V

CAPACITY FACTORS AND RETENTION INDICES OF PHENYLPROPENES

Compound	*Capacity factor*						*Retention index*					
	Modifier (%)						*Modifier (%)*					
	30	*40*	*50*	*60*	*70*	*80*	*30*	*40*	*50*	*60*	*70*	*80*
Methanol–buffer												
3-Phenyl-1-propene		91.64	31.68	12.03	5.41	2.39		1105	1133	1151	1166	1186
1-Phenyl-1-propene		112.43	38.39	14.85	6.17	2.80		1128	1156	1176	1194	1220
Acetonitrile–buffer												
3-Phenyl-1-propene	83.52	29.08	10.38	5.06	2.63	1.28	1119	1127	1132	1135	1135	1138
1-Phenyl-1-propene	96.47	32.77	13.13	5.56	2.90	1.43	1136	1144	1149	1157	1163	1175

TABLE VI

RETENTION INDEX INCREMENTS FOR OLEFINIC GROUP –CH=CH–

Retention index increments and coefficients for their relationship to eluent composition: $I_s = ax^2 + bx + c$; x = % modifier.

Compound	*Retention index increment*						*Coefficients of regression equation for* I_s			
	Modifier (%)									
	30	*40*	*50*	*60*	*70*	*80*	*Substituent group*	*a*	*b*	*c*
Methanol–buffer										
3-Phenyl-1-propene		122	118	114	108	83	Aliphatic CH=CH	−0.0314	2.891	74
1-Phenyl-1-propene		145	141	139	136	111	Aromatic CH=CH	−0.0307	2.956	55
Acetonitrile–buffer										
3-Phenyl-1-propene	109	100	92	84	75	78	Aliphatic CH=CH	0.0100	−1.780	154
1-Phenyl-1-propene	126	117	109	106	103	115	Aromatic CH=CH	0.0223	−2.741	189

from 99 to 142 units agreed with the observation[13] that the effect was much less than an ethyl group and was similar to an single methylene group. The coefficients for the substituent indices (I_S) relating the contributions of the substituents to the eluent composition were then calculated (Table VI).

Differences between the allyl and propenyl groups are also seen in the octanol–water partition coefficients (P) of the two alkenes: allylbenzene, log P = 3.23 and 1-phenyl-1-propene, 3.35[11]. Hansch and Leo[11] suggested that conjugation reduced the polarity of the latter alkene and hence it has a higher partition coefficient and longer retention.

Isomeric phenylpropanols

In a previous study[2], we examined the retention of a series of phenyl-*n*-alkanols and determined the contribution of the primary aliphatic hydroxyl group. The extent of the interaction between the phenyl and hydroxyl groups on the same ($I_{I,1\text{-OH}}$, 20–100 units) and adjacent carbon atoms ($I_{I,2\text{-OH}}$, 15–50 units) were also measured[2]. These values and the coefficients of the retention indices for the branched alkyl chains can be used to provide a baseline for the comparison of the effects of primary, secondary and tertiary hydroxyl groups.

The capacity factors and retention indices of five isomeric phenylpropanols were measured (Table VII) The compounds can be divided into those containing primary (3-phenyl-1-propanol and 2-phenyl-1-propanol), secondary (1-phenyl-1-propanol and 1-phenyl-2-propanol) and tertiary hydroxyl groups (2-phenyl-2-propanol). The retention of each isomer differed and the order differed in the two eluents.

The effect of the hydroxyl groups on the retention indices can be determined by subtracting the calculated retention index of the corresponding unsubstituted alkylbenzene and corrections for any interactions between the phenyl and hydroxyl groups

TABLE VII

CAPACITY FACTORS AND RETENTION INDICES OF ISOMERIC PHENYLPROPANOLS

Compound	*Capacity factor*						*Retention index*					
	Modifier (%)						*Modifier (%)*					
	30	*40*	*50*	*60*	*70*	*80*	*30*	*40*	*50*	*60*	*70*	*80*
Methanol–buffer												
2-Phenyl-2-propanol	–	7.83	3.31	1.70	1.01	0.54	–	825	823	819	809	789
2-Phenyl-1-propanol	–	8.15	3.48	1.72	1.02	0.55	–	830	827	821	812	792
1-Phenyl-2-propanol	–	8.18	3.52	1.75	1.02	0.57	–	830	829	824	812	797
3-Phenyl-1-propanol	–	9.12	3.75	1.78	1.03	0.56	–	840	835	828	813	793
1-Phenyl-1-propanol	–	9.81	4.04	1.95	1.11	0.60	–	851	847	842	830	812
Acetonitrile–buffer												
2-Phenyl-2-propanol	4.73	2.29	1.48	0.97	0.66	0.42	772	760	750	745	742	746
2-Phenyl-1-propanol	4.96	2.35	1.45	0.94	0.63	0.42	778	763	746	738	733	740
1-Phenyl-2-propanol	4.61	2.23	1.41	0.92	0.64	0.43	769	755	740	734	734	748
3-Phenyl-1-propanol	5.18	2.37	1.42	0.91	0.62	0.41	782	756	739	728	731	735
1-Phenyl-1-propanol	6.00	2.79	1.74	1.10	0.73	0.47	801	791	780	775	773	777

TABLE VIII

SUBSTITUENT INDEX INCREMENTS CALCULATED FOR HYDROXYL GROUPS

Compound	*Retention index increment*					
	Modifier (%)					
	30	*40*	*50*	*60*	*70*	*80*
Methanol–buffer						
3-Phenyl-1-propanol		−333	−366	−398	−436	−477
2-Phenyl-1-propanol		−339	−376	−411	−444	−486
1-Phenyl-1-propanol		−358	−399	−438	−485	−531
1-Phenyl-2-propanol		−363	−393	−432	−444	−505
2-Phenyl-2-propanol		−360	−399	−437	−482	−521
$\delta I_{sec.\text{-}OH}$ (mean)		−360	−393	−436	−470	−519
Acetonitrile–buffer						
3-Phenyl-1-propanol	−416	−459	−489	−511	−515	−516
2-Phenyl-1-propanol	−415	−452	−487	−509	−526	−527
1-Phenyl-1-propanol	−456	−495	−527	−550	−566	−585
1-Phenyl-2-propanol	−456	−492	−525	−545	−557	−551
2-Phenyl-2-propanol	−456	−494	−526	−549	−565	−584
$\delta I_{sec.\text{-}OH}$ (mean)	−456	−494	−526	−548	−563	−573

on the assumption that these are not dependent on the "type" of hydroxyl group but only on the distance between the groups. For the compounds containing a branched alkyl chain (2-phenyl-2-propanol and 2-phenyl-1-propanol), this calculation should also include the interaction index term for branched alkyl chains ($I_{I,branch}$) as well as the interaction index for the substitution of methyl groups on the benzylic carbon ($I_{I,PhCH_2R}$). Thus for 1-phenyl-2-propanol, which contains a straight alkyl chain with a secondary hydroxyl group substituted on C-2 of the side chain, the predicted retention for the skeleton and interactions can be calculated as ($I_P + 3I_{S,CH_2} + 2I_{I,PhCH_2R} + I_{I,2\text{-}OH}$) and for the more complex tertiary alcohol, 2-phenyl-2-propanol, which contains a branched chain and a tertiary hydroxyl group ($I_P + 3I_{S,CH_2} + 2I_{I,PhCH_2R} + I_{I,1\text{-}OH} + I_{I,branch}$).

TABLE IX

SUBSTITUENT INDEX EQUATIONS FOR SECONDARY AND TERTIARY HYDROXYL GROUPS

The same substituent index value is used for both secondary and tertiary hydroxyl groups. Based on mean values in Table VIII. $I_{S,sec.\text{-}OH} = ax^2 + bx + c$; x = % modifier

Modifier	*Coefficients of regression equation*		
	a	*b*	*c*
Methanol	−0.0164	−1.979	−254
Acetonitrile	0.0371	−6.411	−297

The retention index increments (Table VIII) for the secondary hydroxyl groups in 1-phenyl-1-propanol and 1-phenyl-2-propanol and the tertiary hydroxyl group in 2-phenyl-2-propanol were very similar but all were significantly larger than those for the primary hydroxyl groups in 3-phenyl-1-propanol and 2-phenyl-1-propanol. At each eluent composition most of the values for the secondary and tertiary hydroxyl groups were within a range of ± 10 units and as they are based on the accumulation of multiple interaction terms, they can be considered to be well within the experimental error estimated for the accuracy of the determination of retention indices[3]. The coefficients of a single quadratic equation relating the change in substituent index ($I_{S,sec.\text{-}OH}$) with proportion of organic modifier for both the secondary and tertiary hydroxyl groups has therefore been calculated (Table IX) from the mean retention increments [$\delta I_{sec.\text{-}OH}$ (mean), Table VIII].

CONCLUSIONS

It has been possible to derive coefficients for expressions which represent the effect of branching of the alkyl chain in alkylbenzenes and for the presence of aliphatic and aromatic unsaturated groups. The validity of their use in prediction has been tested by examining isomeric phenylpropanols and the results suggest a distinction between primary hydroxyl and secondary and tertiary hydroxyl groups. Each of the terms has been included in the database for retention prediction.

ACKNOWLEDGEMENTS

The authors thank the Science and Engineering Research Council for a research grant and for a studentship to C.M.B. and Phase-Separations for a gift of Spherisorb ODS-2.

REFERENCES

1 R. M. Smith and C. M. Burr, *J. Chromatogr.*, 475 (1989) 57.
2 R. M. Smith and C. M. Burr, *J. Chromatogr.*, 481 (1989) 71.
3 R. M. Smith and C. M. Burr, *J. Chromatogr.*, 475 (1989) 75.
4 C. M. Burr and R. M. Smith, *Anal. Proc.*, 26 (1989) 24.
5 R. M. Smith, *Adv. Chromatogr.*, 26 (1987) 277.
6 R. M. Smith, *J. Chromatogr.*, 209 (1981) 1.
7 K. Jinno and K. Kawasaki, *Chromatographia*, 17 (1983) 337.
8 J. H. Knox, J. Kriz and E. Adamcova, *J. Chromatogr.*, 447 (1988) 13.
9 M. Popl, I. Vit and F. Smejkal, *J. Chromatogr.*, 213 (1981) 363.
10 J. Burda, M. Kuras, J. Kriz and L. Vodicka, *Fresenius' Z. Anal. Chem.*, 321 (1985) 549.
11 C. Hansch and A. Leo, *Substituent Constants for Correlation Analysis in Chemistry and Biology*, Wiley, New York, 1979.
12 L. B. Kier, L. H. Hall, W. J. Murray and M. Randic, *J. Pharm. Sci.*, 64 (1975) 1971.
13 J. F. Schrabon, R. J. Hurtubise and H. F. Silver, *Anal Chem.*, 49 (1977) 2253.

Journal of Chromatography, 481 (1989) 97–109
Elsevier Science Publishers B.V., Amsterdam — Printed in The Netherlands

CHROM. 21 753

FREE ENERGY CORRELATIONS: DEAD VOLUME AND THE REVERSED-PHASE HIGH-PERFORMANCE LIQUID CHROMATOGRAPHIC CAPACITY FACTOR IN THE INTERACTION INDEX MODEL

A DISCUSSION AND APPLICATION TO A NITROSAMINE SERIES

M. MONTES, J. L. USERO, A. DEL ARCO, C. IZQUIERDO and J. CASADO*
Departamento de Química Física, Facultad de Química, Universidad de Salamanca, E-37008 Salamanca (Spain)
(First received December 23rd, 1988; revised manuscript received July 5th, 1989)

SUMMARY

On the basis of a free energy correlation between distribution coefficients and the number of carbon atoms found in a series of nine nitrosamines, the column dead volume was determined for different column–mobile phase systems, using methanol and acetonitrile as the organic components of the mobile phase. Application of the interaction index model for reversed-phase liquid chromatography yielded a quadratic equation as the expression of the selectivity, α, without it being possible to dispense with the second degree term. It is shown that the variation in the capacity factor, k', with the composition of the organic component cannot be dealt with simplistically, since the relationship between the volumes of the stationary and mobile phases, $\varphi(x)$, varies considerably with composition. The existence of a convergence zone in plots of $\ln k'$ against the number of carbon atoms in the solute chain should not be interpreted as a characteristic property of the series, and may result from a compensation effect of the terms governing the dependence of the capacity factor on the eluent composition.

INTRODUCTION

The investigation of precise correlations between chromatographic parameters and experimental distribution coefficients is proving to be a useful approach to a better knowledge of the hydrophilic–lipophilic behaviour of many chemical species of biological interest[1].

The chemistry of N-nitrosamines has received increasing attention owing to the proven carcinogenic[2,3], mutagenic[4] and teratogenic[5] properties of such substances towards many animal species, including the primates. A report prepared for the Surgeon General of the United States stated that the majority of human cancers are caused by avoidable exposure to carcinogens[6] and recently the Congress of the United States itself published a background paper on the identification and regulation of carcinogens[7].

0021-9673/89/$03.50

Within the framework of research into the mechanisms of the formation and degradation of N-nitroso compounds, *cf.*, refs. 8–12, chromatography, among other techniques[13], has been used for the analysis and monitoring of such species[14].

The scope of this paper lies not so much in the use of chromatography as an analytical tool but rather in its possibilities for the study of the behaviour of N-nitroso compounds in hydrophilic–lipophilic media. Accordingly, results are reported on the correlations between the structures of N-nitrosamines (in terms of their numbers of carbon atoms) and their distribution coefficients in hydrophilic–lipophilic media on the one hand and their capacity factors on the other, and application of the interaction index model to the study of the reversed-phase behaviour of the same N-nitrosamine series.

PROBLEM

Eqn. 1 establishes the relationship between the capacity factor, k', and the distribution coefficient, P, *cf.*, ref. 15

$$\log k' = \log P + \log \varphi \tag{1}$$

where $\varphi(x) = V_s/V_m$, V_s and V_m are the volumes of the stationary and mobile phases (the latter of composition x, as fraction, v/v of organic component) and k' is a function of the dead volume of the column, V_0, and of the elution volume, V_R:

$$k' = (V_R - V_0)/V_0 \tag{2}$$

According to the general equation of Collander[16] between the distribution coefficients, P_a and P_b, of a single species in two different aqueous organic systems, a and b

$$\log P_a = m \log P_b + \tilde{n} \tag{3}$$

where m and $\tilde{n}$ are two characteristic parameters of the working systems. Since P_a and P_b are referred to each organic solvent–water system, the Collander equation involves the use of pure water as the mobile eluting phase in any reversed-phase high-performance liquid chromatography (RP–HPLC) experiment designed to establish correlations between the distribution in a column and the distribution in an aqueous organic system. As this is not practical, efforts have been made to palliate the problem by measuring k' under different mobile phase conditions, then extrapolating to a zero concentration of organic solvent[17]. However, the function $\log k' = f(x)$ is complicated[18,19] and even more so close to 100% water[18]; for most authors this kind of linear extrapolation involves considerable error[20]. As a more feasible solution, the measurement of distribution coefficients by correlation with capacity factors corresponding to conventional mobile phases has been proposed.

A result of such methodology has been the interest in the correct measurement of dead volume. Different techniques have been advanced.

(a) Determination by direct weighing[21], which involves an appreciable degree of error derived from the measurement of a small magnitude such as the difference between much larger terms. The dead volume thus determined is generally considered

as an extreme value, $V_{0_{max}}$, since the amount of organic component that can solvate the stationary phase is not taken into account[22].

(b) Injection of organic or inorganic salts under particular elution conditions[23–25]. This also has drawbacks, mainly owing to repulsion effects between charges that alter the elution time, and hence the measurement of V_0.

(c) Injection of isotopic species of some of the species not retained in the elution; this method requires the use of a differential refractive index detector. It is a technique that has been widely reported, *cf.*, refs. 26–28, and has shown that the value of V_0 does not remain constant with different mobile phase compositions[26] and normally shows a minimum in the range 40–60% of methanol or acetonitrile[29].

In 1985, Knox and Kaliszan[30] reported that none of these methods leads to a rigorous definition of the thermodynamic dead volume and proposed as such the total volume of the eluents present in the column packing; they used labelled isotopic samples and monitored the elution with a scintillation counter.

METHODS

Starting from the extrathermodynamic correlation between the distribution coefficient, P, and the simplest structural index, the number of carbon atoms of the terms of an homologous series, n_c[1]

$$-(\Delta G)/RT = \ln P = An_c + B \tag{4}$$

and taking into account eqns. 1 and 2, one easily arrives at the expression

$$V_R = V_0(1 + k'_0 e^{\alpha' n_c}) \tag{5}$$

where k'_0 represents the capacity factor of the parent molecule of the series. The third parameter, α', is directly related to the selectivity of the system, α, and, in terms of energy, corresponds to the increase in the variation of the free energy associated with the distribution phenomenon during column elution of the two solutes of the homologous series differentiated by one carbon atom in their chains:

$$\alpha' = \ln \alpha = \ln \frac{k'_n}{k'_{n-1}} = \frac{1}{RT}(\Delta G_{n-1} - \Delta G_n) = \frac{-\Delta(\Delta G)}{RT} \tag{6}$$

After searching for correlations of the kind shown in eqn. 4, our aim was to study the relationships of k'_0 and α with the composition of the eluting phase in order to apply these to the calculation of distribution coefficients, with the consequent advantages not only in speed of operation, but also in safety when working with very dangerous species such as the nitrosamines.

In order to investigate the variation in α' with the composition of the eluting phase, the empirical methodology developed by Jandera *et al.*[27] was employed. According to this, reversed-phase chromatography is mainly controlled by the interactions occurring in the mobile phase, such that the energy change during the transference of 1 mol of solute from this phase to the stationary phase will be given by

$$-\Delta E = E^{P}_{(M-M)} - E^{P}_{(M-X)} \tag{7}$$

where the first term on the right is directly associated with the energy of cohesion between the molecules of the mobile phase, M, and the second term corresponds to the solute (X)–mobile phase interaction.

According to this model, the polar interaction energy between two molecular species can be expressed as a function of a pair of parameters characteristic of each: I_i, the interaction index, which is constant for each solute, and C_i, the interaction coefficient, which depends on the nature of the molecular species:

$$E^{p}_{(A-B)} = C_A I_A C_B I_B \tag{8}$$

According to this, the free energy associated with the distribution of 1 mol of solute of n carbon atoms can be expressed as

$$\Delta G_n = -(C_M^2 I_M^2 - C_M I_M C_{X_n} I_{X_n}) V_{X_n} \tag{9}$$

where X_n represents a solute of n carbon atoms and V_{X_n} its molar fraction.

The third and last supporting logistic aspect taken from the methodology of Jandera to develop our treatment lies in expressing the interaction index of the mobile phase as a linear function of its composition, x (in molar fraction of organic compound):

$$I_M = (1 - x) I_{wat} + x I_{org} \tag{10}$$

On the basis of the ideas put forward, α' can be expressed as:

$$\alpha' = -\frac{\Delta(\Delta G)}{RT} = \frac{C_M^2 I_M^2}{RT}(V_{X_n} - V_{X_{n-1}}) - \frac{C_M I_M}{RT}(C_{X_n} I_{X_n} V_{X_n} - C_{X_{n-1}} I_{X_{n-1}} V_{X_{n-1}}) \tag{11}$$

Since the interaction coefficient, C_{X_i}, is constant within an homologous series (the presence of the same functional group), $C_{X_n} = C_{X_{n-1}} = C_{X'}$, and taking into account that both the molar volume and the interaction index are a linear function of the number of carbon atoms, n_c[28]

$$\alpha' = \alpha_0 - \alpha_1 x + \alpha_2 x^2 \tag{12}$$

where

$$\alpha_0 = \frac{C_M}{RT} \cdot I_{wat}[(C_M I_{wat} \Delta V_X) - C_X(I_{0X} \Delta V_X + V_{0X} \Delta I_X)]$$

$$\alpha_1 = \frac{C_M}{RT}(I_{wat} - I_{org})[2C_M \Delta V_X I_{wat} - C_X(I_{0X} \Delta V_X + V_{0X} \Delta I_X)]$$

$$\alpha_2 = \frac{C_M^2}{RT}(I_{wat} - I_{org})^2 \Delta V_X \tag{13}$$

where V_0 and I_0 correspond to the parent molecule.

Applying the same consideration to eqn. 1, one obtains

$$\ln k'_0 = \ln \varphi(x) + \beta_0 - \beta_1 x + \beta_2 x^2 \tag{14}$$

where:

$$\beta_0 = \frac{C_M}{RT} \cdot V_{0X}(C_M I_{wat}^2 - C_X I_{0X} I_{wat})$$

$$\beta_1 = \frac{C_M}{RT} \cdot V_{0X}(I_{wat} - I_{org})(2C_M I_{wat} - C_X I_{0X})$$

$$\beta_2 = \frac{C_M^2}{RT} \cdot V_{0X}(I_{wat} - I_{org})^2 \tag{15}$$

From expressions 12 and 14 one can write:

$$\ln k' = \ln \varphi(x) + (\beta_0 - \beta_1 x + \beta_2 x^2) + (\alpha_0 - \alpha_1 x + \alpha_2 x^2) n_c \tag{16}$$

Eqn. 16 now allows us to express the capacity factor as a function of n_c and of the mobile phase composition.

EXPERIMENTAL

A Model 500A HPLC chromatograph (Konik Instruments, Barcelona, Spain) was used with a Rheodyne 20-μl injector, a guard column Phase Sep Spherisorb S5CN (5 cm × 4.6 mm; 5 μm) just before a column of Phase Sep. Spherisorb S5CN (10 cm × 4.6 mm; 5 μm) (a type of column frequently employed in the chemistry of N-nitroso compounds[31,32]) and a double beam VIS–UV 757 detector (Kratos Analytical Instruments, Ramsey, NJ, U.S.A.). The detector signal was programmed with an SP 4290 integrator (Spectra Physics, San José, CA, U.S.A.).

The mobile phase was prepared by mixing water (doubly distilled in glass with addition of potassium permanganate) with the organic solvents at the required volume ratio. Methanol, acetonitrile and isooctane were "HPLC solvents" from Farmitalia, Carlo Erba (Milan, Italy).

The homologous series of N-nitrosamines were all from Sigma Chemical Co. (St. Louis, MO, U.S.A.).

Experiments for determining the distribution coefficients of N-nitrosamines were carried out by analyzing the composition of the aqueous phase by an HPLC technique, working at 30°C; the P values, expressed as quotients of molar fractions, were the means of six determinations for each N-nitrosamine.

Retention volumes, V_R, were calculated as the arithmetic means from three injections.

DATA TREATMENT

The V_0, k'_0 and α' values were obtained as fitting parameters in the optimization

TABLE I

RETENTION VOLUMES (TIME, s) OF N-NITROSAMINES IN METHANOL–WATER AND ACETONITRILE–WATER MOBILE PHASES

Guard column: Phase Sep Spherisorb S5CN (5 μm, 5 cm). Column: Phase Sep Spherisorb S5CN (5 μm, 10 cm). Solvent flow-rate: 1 ml min^{-1}.

Nitrosamine	*% (v/v) Methanol*							*% (v/v) Acetonitrile*							
	30	*35*	*40*	*45*	*50*	*55*	*60*	*20*	*25*	*30*	*35*	*40*	*45*	*50*	*55*
NDMA	3.59	3.48	3.41	3.36	3.31	3.25	3.19	3.42	3.37	3.31	3.27	3.21	3.19	3.13	3.09
NMEA	4.07	3.83	3.67	3.57	3.46	3.35	3.27	3.75	3.65	3.54	3.46	3.37	3.32	3.23	3.15
NDEA	4.85	4.35	4.04	3.85	3.67	3.48	3.35	4.27	4.07	3.87	3.73	3.58	3.49	3.36	3.24
NMPA	4.81	4.34	4.05	3.84	3.66	3.49	3.35	4.26	4.05	3.87	3.73	3.58	3.49	3.35	3.23
NDPA	8.27	6.35	5.36	4.73	4.23	3.85	3.56	6.32	5.53	4.92	4.53	4.15	3.93	3.65	3.43
NMBA	6.24	5.24	4.63	4.26	3.93	3.65	3.45	5.14	4.71	4.35	4.11	3.85	3.69	3.49	3.32
NEBA	8.46	6.51	5.42	4.79	4.29	3.85	3.56	6.44	5.62	4.96	4.57	4.16	3.93	3.65	3.42
NPBA	12.33	8.60	6.65	5.56	4.73	4.11	3.71	8.61	7.00	5.85	5.17	4.55	4.24	3.85	3.54
NDBA	19.71	12.27	8.67	6.76	5.45	4.47	3.89	12.76	9.44	7.23	6.06	5.09	4.59	4.05	3.67

of eqn. 5 using the Gauss–Newton algorithm with statistical weights, ω_i, accumulated over the dependent variable. Taking into account that the main source of error in the retention time is not so much in the flow-rate but rather in the phenomenon of retention itself in the stationary phase, and that less strongly retained species should not be weighted as much as those which are strongly retained, we employed weighting factors inversely related to the difference in retention time in the stationary phase ($V_R - V_0$), *i.e.*, the difference between the retention time and the apparent dead volume. In these terms the function to be minimized is:

$$S = \sum_i [V_{R_i} - V_0(1 + k'_0 e^{\alpha' n_{c_i}})]^2 \omega_i \tag{17}$$

Expressions similar to this have been used by different authors[25,29].

RESULTS AND DISCUSSION

The methodology described above was applied to a series of nine nitrosamines: N-nitrosodimethylamine (NDMA), N-nitrosomethylethylamine (NMEA), N-nitrosodiethylamine (NDEA), N-nitrosomethyl-*n*-propylamine (NMPA), N-nitrosodi-*n*-propylamine (NDPA), N-nitrosomethyl-*n*-butylamine (NMBA), N-nitrosoethyl-*n*-butylamine (NEBA), N-nitroso-*n*-butyl-*n*-propylamine (NPBA) and N-nitrosodi-*n*-butylamine (NDBA), after verifying fulfilment of correlation[5] with different organic solvents. Fig. 1 shows this correlation when working with isooctane.

Table I shows the values found for the retention volumes in different mobile phases. On subjecting these results to the above-described fitting (eqns. 5 and 17), the optimum parameters shown in Table II were obtained. Regarding the results, it is interesting that the contribution of the carbon chain to the value of the distribution coefficient is independent of its position (see Fig. 1: two pairs of linear isomers whose coefficients coincide have been included). The data shown in Table I point to a similar kind of behaviour with respect to the elution times of these isomers. Although in the case of NDPA and NEBA (both with $n_c = 6$) the retention of NDPA in weak mobile phases is less than their NEBA, suggestive of a subtle effect of the position of the

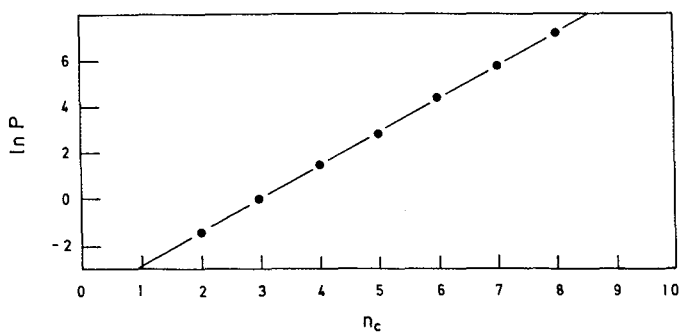

Fig. 1. Correlation between experimental isooctane–water distribution coefficients (ln P) and the number of carbon atoms, n_c, in a series of nitrosamines: 2 (NDMA); 3 (NMEA); 4 (NMPA and NDEA); 5 (NMBA); 6 (NDPA and NEBA); 7 (NPBA); 8 (NDBA).

TABLE II

VALUES OF V_0, ln k'_0 AND α' DETERMINED BY LINEAR REGRESSION (EQNS. 5 AND 17) OF EXPERIMENTAL RETENTION VOLUMES (TIME, s) SHOWN IN TABLE I AGAINST THE NUMBER OF CARBON ATOMS, n_c, BY THE GAUSS–NEWTON ALGORITHM

	% (v/v) Methanol						
	30	*35*	*40*	*45*	*50*	*55*	*60*
V_0	2.97±0.02	2.94±0.02	2.90±0.02	2.89±0.02	2.89±0.02	2.87±0.02	2.85±0.02
$-\ln k'_0$	2.64±0.04	2.60±0.04	2.54±0.04	2.50±0.04	2.51±0.04	2.48±0.05	2.49±0.05
α'	0.543±0.006	0.467±0.005	0.401±0.005	0.347±0.004	0.296±0.004	0.237±0.005	0.184±0.005

carbon atoms on the chain, the fact that the elution times are coincident in strong mobile phases ($\geqslant$55% methanol) points to the notion that such differences might simply be due to the optimum conditions (with higher resolving power of the column) when working with mobile phases with high percentages of water and long elution times. Furthermore, the relative variation of the optimized values of V_0 with the eluent composition is concordant with the fact[33] that the amount of organic component adhering to the stationary phase varies as a function of the nature and percentage of this phase.

The optimized values of $\alpha'(x)$ were fitted by the least squares algorithm to a second degree polynomial expression (eqn. 12); the results are shown in Table III.

A usual practice is the first degree reduction of equations of this kind[28,34,35]. To analyze this kind of protocol, our experimental data were fitted to a linear function (Table III). Application of the F test shows that the second degree is significant with respect to the first degree at the 95% level when working with methanol and at 99% when working with acetonitrile. We believe that these results preclude the possibility of carrying out this simplification that is normally done in lower composition ranges of the mobile phase and at high concentrations of the organic component[28] (see Figs. 2 and 3).

Moreover, the results obtained confirm the expected effect (eqn. 13) of the

TABLE III

VALUES OF α_0, α_1, α_2 DETERMINED BY THE LEAST SQUARES ALGORITHM AT USING THE SECOND DEGREE POLYNOMIAL EXPRESSION (EQN. 12) AND α_0, α_1 DETERMINED BY THE SQUARE ALGORITHM OF THE LINEAR FUNCTION (FIRST DEGREE)

Application of the F test shows that the second degree is significant with respect to the first at the 95% (methanol) and 99% levels (acetonitrile).

Degree		*Methanol*	*Acetonitrile*
1	α_0	0.88 ± 0.01	0.67 ± 0.03
	α_1	$(-1.17 \pm 0.03) \cdot 10^{-2}$	$(-1.04 \pm 0.07) \cdot 10^{-2}$
	Residual	$4.08 \cdot 10^{-4}$	$2.85 \cdot 10^{-3}$
2	α_0	1.02 ± 0.05	0.88 ± 0.02
	α_1	$(-1.8 \pm 0.2) \cdot 10^{-2}$	$(-2.2 \pm 0.1) \cdot 10^{-2}$
	α_2	$(7.4 \pm 2.4) \cdot 10^{-5}$	$(1.6 \pm 0.2) \cdot 10^{-4}$
	Residual	$1.18 \cdot 10^{-4}$	$1.50 \cdot 10^{-4}$

% (v/v) Acetonitrile							
20	*25*	*30*	*35*	*40*	*45*	*50*	*55*
2.92±0.02	2.86±0.02	2.76±0.02	2.68±0.02	2.58±0.03	2.57±0.03	2.48±0.04	2.59±0.03
2.75±0.05	2.55±0.05	2.30±0.05	2.10±0.04	1.87±0.06	1.82±0.07	1.64±0.08	1.92±0.09
0.490±0.006	0.419±0.006	0.346±0.005	0.291±0.005	0.230±0.006	0.197±0.007	0.148±0.006	0.130±0.007

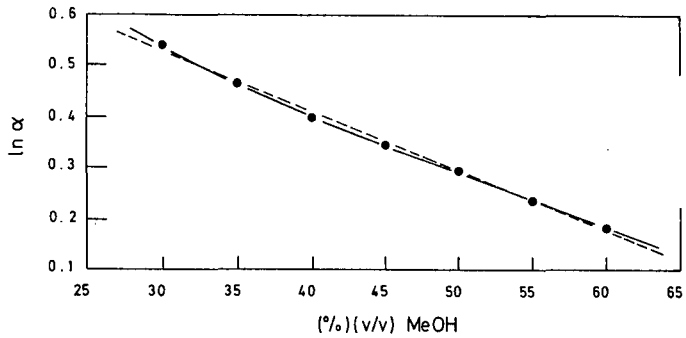

Fig. 2. Plots of the ln α of eqn. 5 against the concentration, x (%, v/v), of methanol in the mobile phase for the homologous series of nitrosamines. Fitting of data to a second degree polynomial expression (———) eqn. 12) and a linear function (---------).

strength of the organic solvent on the second degree term (Table III), since methanol, which is weaker, results in less curvature.

Another interesting aspect is that, according to the interaction index model, the profile of the function relating the values of ln k'_0 with those of the mobile phase composition should be quadratic (like that of ln α) as long as the relationship between the phases is considered constant. In our case it was not possible to observe this kind of

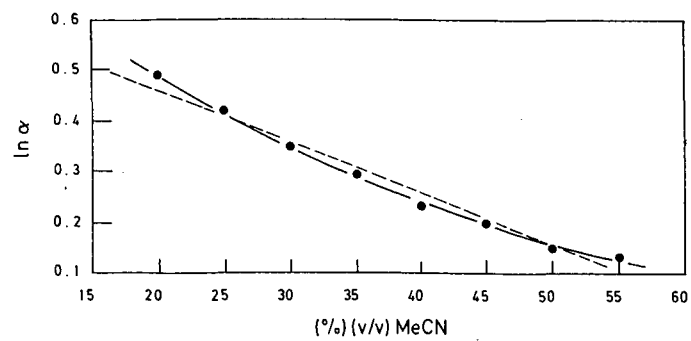

Fig. 3. Plots as in Fig. 2 but for acetonitrile in the mobile phase.

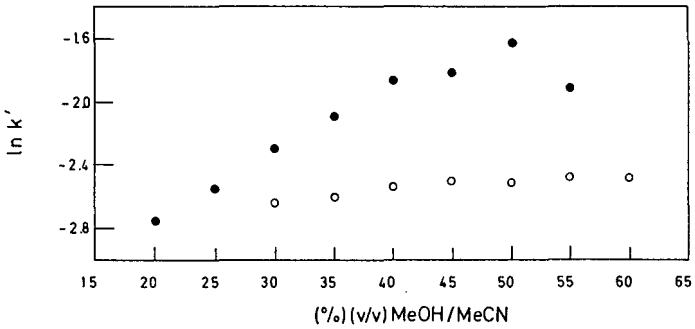

Fig. 4. Logarithmic plots of capacity factors k', of N-nitrosamines against the concentration, x (%, v/v), of methanol–water (○) and acetonitrile–water (●) as the mobile phase on a Phase Sep. Spherisorb S5CN (5 μm) column.

behaviour; by contrast, we observed a variation depending on the sign of the derivative of the dead volume. Thus, as V_R decreases, in φ (and hence in k'_0) should increase, as is shown in Fig. 4. As a result of such findings, we believe that the function φ cannot be considered constant with respect to x (at least under the working conditions used in this study), and therefore there is no point in attempting to fit the data to a polynomial equation, whether of first or second degree.

Using the optimized values of V_0 the k' values were calculated are represented logarithmically against the number of atoms in the carbon chain. Figs. 5 and 6 reveal similar correlations to those obtained with the distribution coefficient, together with another aspect that is worthy of note. This is the appearance of a convergence zone in the sheaf of straight lines. Some authors[28,36] consider this to be characteristic of the homologous series and of each mixture of the mobile phase. However, on recalling the foregoing considerations, the presence of this convergence zone implies that at a certain value, n^*, of n_c, the value of the capacity factor is independent of the mobile

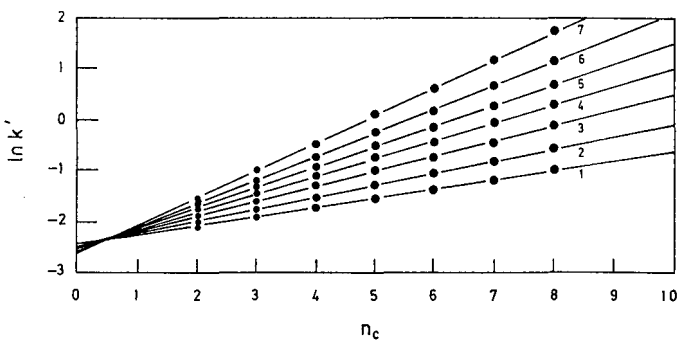

Fig. 5. Logarithmic plots of capacity factors, k', of N-nitrosamines against the numbers of carbon atoms in methanol–water containing 60 (1), 55 (2), 50 (3), 45 (4), 40 (5), 35 (6) and 30% (v/v) (7) of methanol.

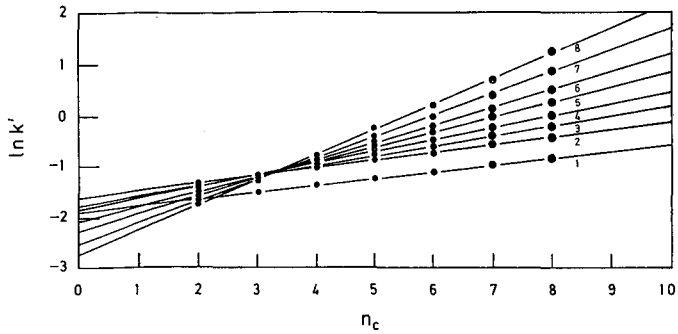

Fig. 6. Logarithmic plots of capacity factors, k', of N-nitrosamines against the numbers of carbon atoms in acetonitrile–water containing 55 (1), 50 (2) 45 (3), 40 (4), 35 (5), 30 (6), 25 (7) and 20% (v/v) (8) of acetonitrile.

phase composition, k^* thus being constant

$$\ln k^* = \ln k'_0(x) + n_c^* \ln \alpha(x) = \text{constant} \tag{18}$$

in other words:

$$\ln k^* = \ln \varphi(x) - \frac{\Delta G_0}{RT} - \frac{\Delta(\Delta G_0)}{RT} \cdot n_c^* = \text{constant} \tag{19}$$

Accordingly, we feel that the appearance of this point (or rather zone) of intersection may simply be the result of a compensation of the variations of the three summands of eqn. 19 and as consequence we cannot attribute to it any well defined physical significance. However, this opinion is not *sensu stricto*, in disagreement with the idea that the intersection zone is characteristic of the homologous series. Nevertheless it is no less true that, while we cannot find the explicit characteristic of the function $\varphi(x)$, we shall not be able to give to the intersection point any other meaning.

CONCLUSIONS

The values of the column dead volume, V_0, for a given column–mobile phase system can be determined from the experimental retention volumes, V_R, of an homologous series of compounds for which there is a free energy correlation between their distribution coefficients and some structural index, such as the number of carbon atoms n_c. The variations occurring in the values of V_0 thus calculated with the mobile phase composition are in excellent agreement with the laboratory results.

Application of the interaction index model to reversed-phase liquid chromatography yields a quadratic equation for the logarithm of the selectivity ($\ln \alpha$), in good concordance with the experimental results. In none of the cases studied (methanol, acetonitrile) is it possible to leave out the quadratic term within the concentration range studied.

The variation in k' with x cannot be dealt with as assumed by the interaction index model, since considerable variations of φ with x are detected. Regarding this point, it should be noted that the possible omission of the quadratic term in the $\ln k'/x$

eqn. 16 is only a question of the use to which it is to be put. Thus, although from a rigorous point of view the problem of having no knowledge of the explicit characteristic of the function $\varphi(x)$ is inevitable, when equations like 16 are used for predictive purposes it is clear that the quadratic term can be neglected.

Finally, and according to our own criteria, the existence of a convergence zone in the linear plots of ln k' against n_c for different compositions should not necessarily be understood as a specific property of the series, but rather as a result of a compensation of the terms governing the dependence of the capacity factor on the eluent composition.

ACKNOWLEDGEMENTS

J.C. thanks the Spanish Comisión Interministerial de Ciencia y Tecnología, CICYT, for supporting the research reported as part of an investigation into Structure/Reactivity Correlations in the Chemistry of N-nitroso compounds (Grant No. PA86/0111). Thanks are also due to the referees for their kind comments and suggestions.

REFERENCES

1 R. Kaliszan, *Quantitative Structure Chromatographic Retention Relationships*, Wiley, New York, 1987.
2 B. Pignatelli, G. Descotes and H. Bartsch, *Actual. Chim.*, 10 (1985) 33.
3 C. E. Searle (Editor), *Chemical Carcinogens*, American Chemical Society Monographs No. 182, Washington, DC, 2nd ed., 1985.
4 F. K. Zimmermann, *Biochem. Pharmacol.*, 20 (1971) 985.
5 H. Druckrey, *Xenobiótica*, 3 (1973) 271.
6 *Evaluation of Environmental Carcinogens*, U.S. Dept. of Health and Human Services, Nat. Cancer Institute, *Ad hoc* Committee on the Evaluation of Low Level of Environmental Chemical Carcinogens, Report to the Surgeon General, Washington, DC, 1987.
7 *Identifying and Regulating Carcinogens*, Background Paper, Congress of the United States, Office of Technology Assessment, OTA-BP-H-42, Washington, DC, 1987.
8 J. M. Cachaza, J. Casado, A. Castro and M. A. López Quintela, *Z. Krebsforsch.*, 91 (1978) 279.
9 J. Casado, A. Castro, J. R. Leis, M. Mosquera and E. Peña, *J. Chem. Soc.*, Perkin Trans., 2 (1985) 1859.
10 J. Casado, A. Castro, M. A. López Quintela and F. M. Lorenzo Barral, *Bull. Soc. Chim. Fr.*, (1987) 401.
11 P. Motilva, A. Del Arco, J. L. Usero, C. Izquierdo and J. Casado, *Int. J. Biochem.*, 20 (1988) 41.
12 M. A. López Quintela and J. Casado, *J. Theor. Biol.*, 139 (1989) 129.
13 D. Ruiz López, C. López Martínez and R. García Villanova, *Anal. Chem.*, 58 (1986) 2646.
14 J. L. Usero, A. Del Arco, C. Izquierdo, M. Montes and J. Casado, *J. Chromatogr.*, 407 (1987) 355.
15 A. J. P. Martin, *Biochem. Soc. Symp.*, 3 (1950) 4.
16 R. Collander, *Acta Chem. Scand.*, 5 (1951) 774.
17 M. C. Pietrogrande, C. B. Bighi, P. A. Borea, A. M. Barbaro, M. C. Guerra and G. L. Biagi, *J. Liq. Chromatogr.*, 8 (1985) 1711.
18 P. J. Schoenmakers, H. A. H. Billiet and L. de Galan, *J. Chromatogr.*, 282 (1983) 107.
19 W. Melander, B.-K. Chen and Cs. Horváth, *J. Chromatogr.*, 318 (1985) 1.
20 T. L. Hafkenscheid and E. Tomlinson, *Int. J. Pharm.*, 16 (1983) 225.
21 E. H. Slaats, J. C. Kraak, W. J. T. Brugman and H. Poppe, *J. Chromatogr.*, 149 (1978) 255.
22 G. E. Berendsen, Pl. J. Schoenmakers, L. de Galan, G. Vigh, Z. Varga-Puchony and J. Inczedy, *J. Liq. Chromatogr.*, 3 (1980) 1669.
23 P. J. Schoenmakers, H. A. H. Billiet, R. Tijssen and L. de Galan, *J. Chromatogr.*, 149 (1978) 519.
24 Cs. Horváth, W. Melander and I. Molnár, *J. Chromatogr.*, 125 (1976) 129.
25 O. A. G. Van der Houwen, J. A. A. Van der Linden and A. W. M. Indemans, *J. Liq. Chromatogr.*, 5 (1982) 234.
26 H. Engelhardt, H. Müller and B. Dreyer, *Chromatographia*, 19 (1984) 240.

27 P. Jandera, H. Colin and G. Guiochon, *Anal. Chem.*, 54 (1982) 435.
28 P. Jandera, *J. Chromatogr.*, 314 (1984) 13.
29 A. M. Krstulovic, H. Colin and G. Guiochon, *Anal. Chem.*, 54 (1982) 2438.
30 J. H. Knox and R. Kaliszan, *J. Chromatogr.*, 349 (1985) 1341.
31 S. J. Kubacki, D. C. Havery and T. Fazio, in I. K. O'Neill, R. C. von Borstel, C. T. Miller, J. Long and H. Bartsch (Editors), *N-Nitroso Compounds: Occurrence, Biological Effects and Relevance to Human Cancer*, IARC, Lyon, 1984, pp. 145–158.
32 R. N. Loeppky, W. Tomasik and T. G. Millard, in I. K. O'Neill, R. C. von Borstel, C. T. Miller, J. Long and H. Bartsch (Editors), *N-Nitroso Compounds: Occurrence, Biological Effects and Relevance to Human Cancer*, IARC, Lyon, 1984, pp. 353–363.
33 R. M. McCormick and B. L. Karger, *Anal. Chem.*, 52 (1980) 2249.
34 P. Jandera, *J. Chromatogr.*, 352 (1986) 91.
35 P. Jandera, *J. Chromatogr.*, 352 (1986) 111.
36 E. Grushka, H. Colin and G. Guiochon, *J. Chromatogr.*, 248 (1982) 325.

Journal of Chromatography, 481 (1989) 111–120
Elsevier Science Publishers B.V., Amsterdam — Printed in The Netherlands

CHROM. 21 661

HIGH-SPEED ANALYTICAL SENSOR FOR IN-LINE MONITORING OF DISSOLVED ANALYTES FLOWING IN A TUBE EMPLOYING A COMBINATION OF LIMITED DIFFUSION, LAMINAR FLOW AND PLUG SOLVENT INJECTIONS

CONRAD N. TRUMBORE*, LEIA M. JACKSON, STEVEN BENNETT and ANDREW THOMPSON
Department of Chemistry and Biochemistry, University of Delaware, Newark, DE 19716 (U.S.A.)
(First received August 24th, 1988; revised manuscript received May 24th, 1989)

SUMMARY

A fast molecular weight sensor is described in which pure solvent is introduced as a plug into an analyte-containing mobile phase undergoing laminar flow within a capillary tube. If diffusion of the mobile phase analyte is limited, a complex concentration *vs.* time profile of capillary effluent is observed. Molecular weight and quantitative information regarding the analyte dissolved in the mobile phase is obtained from such profiles in a minute or less. Anomalous results due to analyte adsorption are avoided in this technique by cleaning the injection system with organic as well as aqueous solvents.

INTRODUCTION

Previous papers[1,2] have described a rapid method for determining molecular weights of single components[1] and polymers and mixtures of polymers[2] dissolved in a liquid phase. Our original method relies on injection of a liquid plug of analyte solution into a capillary containing a mobile phase which is flowing with a laminar flow profile. Concentrations *vs.* time profiles of the effluent from this capillary reveal two peaks or one peak and a shoulder, even for a single component, when radial diffusion of the analyte is limited in comparison with axial transport.

For a given temperature, the unique shapes of these concentration *vs.* time profiles of the analyte effluent measured at the exit of the capillary are dependent upon the inner diameter of the capillary, the flow-rate, the length of the capillary, and the diffusion coefficient(s) of the analyte(s) contained in the injected liquid plug. The anticipated profile shapes have been calculated by Atwood and Golay[3] and others (see refs. 4 and 5 and the references cited in refs. 1 and 2) as two component peaks or peak plus shoulder when there is limited radial diffusion in comparison with the axial transport of the injected analyte. Our method relies on the smoothly changing ratio of analyte effluent concentrations representing these two concentration *vs.* time profile components as the diffusion coefficient of the analyte changes, when all the other experimental variables are held constant.

0021-9673/89/$03.50

Analysis of the shapes of capillary effluent analyte concentration *vs.* time profiles in terms of a ratio (R) of concentrations at two characteristic times following injection of the analyte allows the empirical determination of molecular weights on the basis of a standard curve relating this concentration ratio R to molecular weight. Interpolation of R value data for a material of unknown molecular weight on the resulting standard curve can be used to yield molecular weights of biopolymers[1] or number-average molecular weights of synthetic polymers[2] in a minute or less. The type of analyte which can be investigated in this manner is limited only by its ability to undergo diffusion without physical entanglement or molecular aggregation in a liquid phase under laminar flow conditions, by the absence of significant adsorption of analyte components on the walls of the capillary, and by the existence of an appropriate standard curve for the analyte.

We report in this paper a new application of the same basic technique as described above, except that in the work reported here, we *employ the analyte solution as the mobile phase and inject a plug of pure solvent.* Such an experiment allows a quantitative determination of both the concentration and an empirical determination of the molecular weight of the analyte contained in the mobile phase. Thus, the analyte concentration *vs.* time profiles obtained in this system consist of *negative* rather than positive concentration *vs.* time traces, since the injected, initially analyte-free, pure solvent plug can only have an analyte concentration lower than that of the mobile phase as it emerges from the capillary and passes through the concentration detector.

The success of this new method depends on the absence of significant analyte adsorption to the inner surface of the injection system capillary surface. In this "negative profile mode" of our empirical molecular weight method, there are significant complications owing to analyte adsorption, even with low-molecular-weight compounds. This adsorption is especially important in the injection system of the apparatus. We have shown that such adsorption problems in the injection system can be eliminated or at least minimized in order to achieve reproducible results by a thorough cleaning of the injection system before loading[6]. This cleaning is accomplished by a combination of organic and aqueous solvents, the organic solvent flush being a critical phase of the cleaning process.

EXPERIMENTAL

The apparatus employed is essentially the same as reported previously[1,2] except for the use in some experiments of either a Harvard Model 909 or an ISCO μLC 500 syringe pump as the mobile phase pump. The system is essentially a conventional liquid chromatographic arrangement, except that the packed column is replaced with an untreated length (30–100 cm) of stainless-steel capillary (0.25–0.75 mm I.D.). Chemicals were reagent grade and were used without further purification. The Valco injection valve was flushed between injections with approximately 20 ml each of 2-propanol, methanol and Milli-Q water, in that order. If only water was used as the wash, different often irreproducible results were obtained, and positive peaks were obtained where negative peaks were expected[6]. We tentatively attribute these positive peaks to flow sensitive, metastable absorbed analyte in the injection system which is released under the zero flow condition while the injection system is loaded[6]. Further studies of these phenomena are needed.

RESULTS AND DISCUSSION

Concentration vs. time profiles of low-molecular-weight compounds in the positive profile mode

Our method[1,2] involving injection of a liquid analyte into a liquid mobile phase containing no analyte and yielding positive analyte concentration *vs.* time profiles, will hereafter be referred to as the "positive profile mode". Previous investigations, involving synthetic[2] and biopolymers[1] and employing the positive profile mode, demonstrated concentration *vs.* time profiles of the type predicted by Atwood and Golay[3]. In our previous studies no low-molecular-weight species were investigated.

In this paper, we demonstrate similar positive mode profiles, as seen in Fig. 1, for three different low-molecular-weight compounds at three different flow-rates. Fig. 1 illustrates the method used previously[1,2] for empirical determinations of molecular weights with one modification. For low-molecular-weight compounds, the ratio R is defined as

$$R = \frac{h_{1.35t_b}}{h_{2.0t_b}}$$

where h represents the positive (or negative) height above (or below) the baseline value of the concentration *vs.* time profile at either 1.35 or 2.0 times the breakthrough time, t_b, defined as the time interval between injection and first compound from the injection emerging from the capillary at the detector. The above definition of R is slightly different from that previously reported in that an empirical value of 1.35 is used in the numerator rather than the previously employed value[1] of 1.2 t_b. This higher value is an empirical fitting coefficient used to locate the top of the first sharp peaks on the left sides of the two component profiles illustrated in Fig. 1. This empirical coefficient is apparently different for very-high- and very-low-molecular-weight compounds. The constant 2.0 in the denominator of the above expression is theoretical in origin, since it can be used to locate the time of the maximum in a gaussian absorbance *vs.* time curve which represents the case where radial diffusion is rapid in comparison with axial transport.

Fig. 2 illustrates the dependence on molecular weight and mobile phase flow-rate of R values calculated as indicated above from the data of Fig. 1. In agreement with our previous work, R values are approximately linear with flow-rate for a single compound[2] and smoothly increasing functions of molecular weight[1,2]. These studies, in combination with our earlier observations with polymers, serve to emphasize the wide dynamic molecular weight range of the positive profile mode of our empirical molecular weight method since the same type of quantitative behavior of R values is observed over more than three orders of magnitude in molecular weight. This would be expected if the R value is primarily a reflection of the diffusion properties of the dissolved analyte(s).

Pure solvent injection into mobile phase containing analyte —the negative profile mode

When pure solvent is injected as a plug into an analyte-containing mobile phase in laminar flow in a capillary, there is diffusion of the analyte into the pure solvent plug as it assumes a laminar profile and is transported through the capillary. The shape of

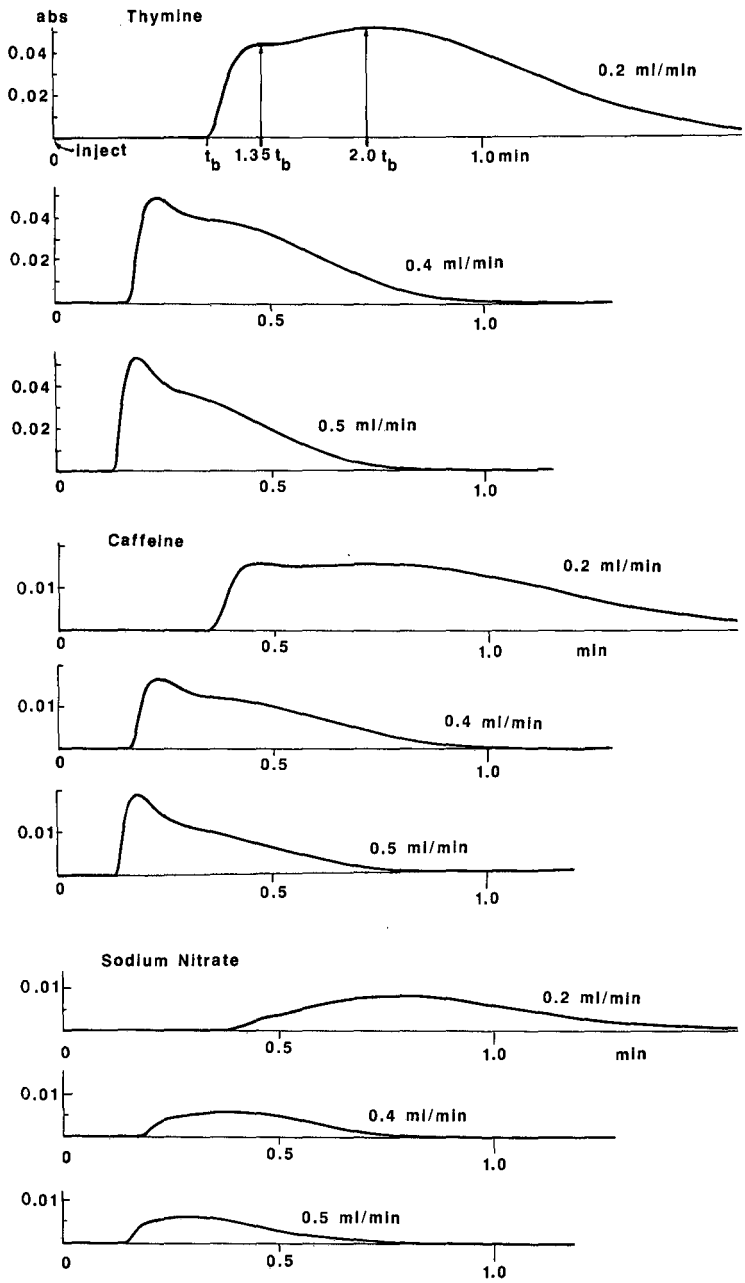

Fig. 1. Effect of molecular weight and flow-rate on concentration *vs.* time profiles from solutions of low-molecular-weight compounds injected into water mobile phase and passed through a capillary tube under laminar flow conditions where radial diffusion is limited in comparison with axial transport through the tube (90 cm × 0.5 mm I.D.). An ISCO μLC 500 syringe pump was used. Solutions concentrations: caffeine, 0.24 m*M*; thymine, 0.056 m*M*; $NaNO_3$, 0.090 m*M*. Absorbance monitored at 254 nm.

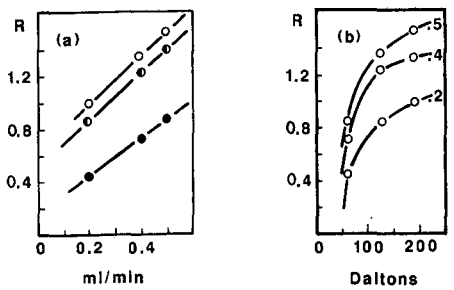

Fig. 2. Variation of R values (ratios of capillary effluent analyte concentration at two selected times after a plug injection of an analyte solution) with: (a) molecular weight; (b) flow-rate (values shown in ml/min on the right). ○ = Caffeine; ◐ = thymine; ● = $NaNO_3$. Data taken from Fig. 1.

the resulting negative concentration *vs.* time profile of the effluent should be dependent on the same experimental parameters as with the positive profile mode. This type of experiment will be designated as the "negative profile mode" of our empirical molecular weight method.

Fig. 3 illustrates the results of switching caffeine solution and pure solvent (water) as the injected phase and mobile phases in positive and negative mode experiments. The positive profile is obtained by injecting a plug of 8 μl of the caffeine solution into water mobile phase. The negative profile is obtained by injecting an 8-μl volume of pure water into a caffeine solution mobile phase with the same caffeine concentration used to obtain the positive profile under otherwise identical conditions of flow-rate and temperature, employing the same stainless-steel capillary and experimental system.

Within experimental error, the positive and negative peaks are scaled mirror images of one another, except near the last third of the profile. Fig. 3 illustrates this point by plotting the inverted negative profile (dashed line) on the same coordinates with the positive profile. A crossing of the curves is noted in the right-hand portion of the profiles. Calculated R values, using either the 1.2 or the 1.35 numerator coefficient, are within experimental error of one another for the positive and the negative profiles, indicating quantitative peak scaling in the region of the profiles used in R value calculations. The lack of quantitative peak scaling in the trailing edge of the profiles may be due to wall adsorption effects, since molecules in the tail segment have a higher probability of colliding with the wall.

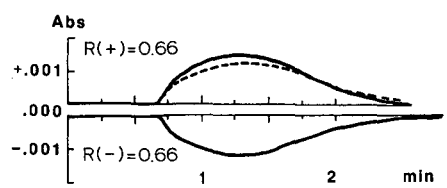

Fig. 3. (Solid lines) Comparison of positive profile mode (analyte solution injected into water mobile phase) and negative profile mode (water injected into mobile phase solution containing analyte) employing the same analyte, a 0.24 mM caffeine solution. (Dashed line) Inversion of negative mode profile for direct comparison with positive profile mode result. Capillary: 100 cm × 0.75 mm I.D.; flow-rate: 0.3 ml/min; ISCO μLC 500 syringe pump.

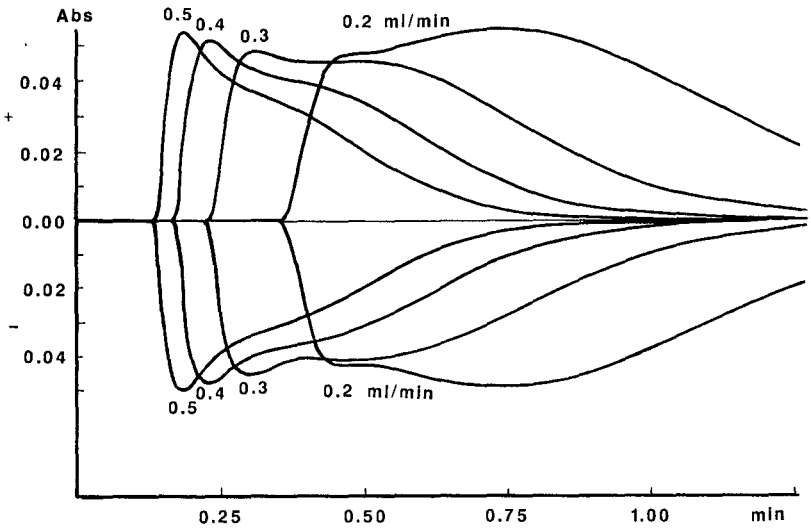

Fig. 4. Effect of flow-rate on positive and negative profile mode results from the injection of 10 μl of a 0.05 m*M* thymine solution into water (or 10 μl water into 0.05 m*M* thymine mobile phase) flowing in a 30 cm × 0.5 mm I.D. capillary. Flow-rates indicated; Altex 100A pump.

Results similar to those in Fig. 3 are observed in Fig. 4 in which a thymine solution is analyzed in the positive and negative profile modes at different flow-rates. Again, the early portions of the negative profiles are almost exact scaled mirror images of the positive profiles. In Fig. 5, the negative peaks from Fig. 4 are inverted (dashed line) and compared directly with the positive peaks. Once more, there is a non-quantitative scaling of the negative and positive profiles at later times as is the case with Fig. 3. The slight quantitative differences between absolute absorbances in the positive and negative profiles for a given flow-rate may arise because of adsorption problems which have been encountered[6]. However, *R* values calculated from the above data comparing positive and corresponding negative profiles are again within experimental error, as illustrated in Table I. Thus, the ability to switch injected and mobile phases without

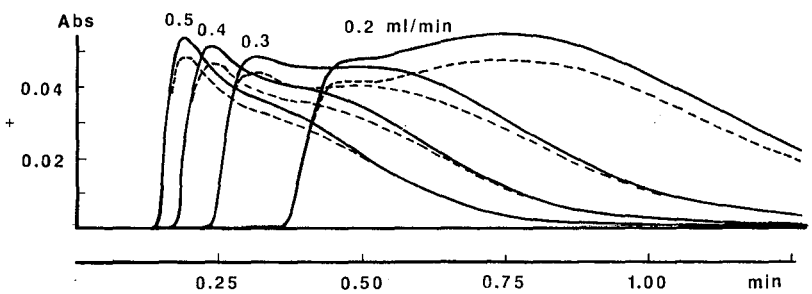

Fig. 5. Inverted negative profile mode results from Fig. 4 (dashed line) compared with positive profile mode results from Fig. 4.

TABLE I

COMPARISON OF *R* VALUES FROM POSITIVE AND NEGATIVE PROFILE MODES

Data taken from Fig. 4.

Flow-rate (ml/min)	*R (positive mode)*	*R (negative mode)*
0.2	0.86	0.88
0.3	1.11	1.16
0.4	1.21	1.24
0.5	1.43	1.39

changing the *R* value apparently does not depend on flow-rate for low molecular weight samples in the molecular weight range and flow-rate ranges reported.

Molecular weight dependence of R values —the negative profile mode

As might be expected from the above data and our previous experience with the positive profile mode results, the negative profile mode should be useful in providing empirical determinations of molecular weights employing the *R* value concept. Fig. 6 illustrates the dependence of *R* values, calculated from a large number of data taken

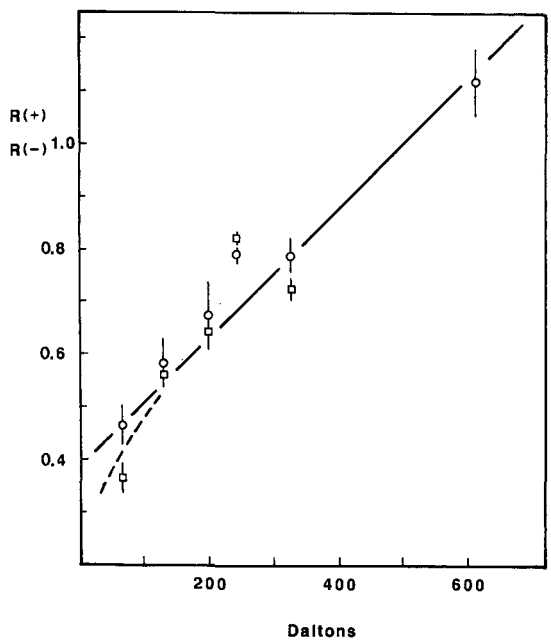

Fig. 6. Effect of molecular weight on positive (○) and negative (□) profile mode *R* values. Average values taken from different runs made on different days with the same 90 cm × 0.75 mm I.D. capillary. Solution concentrations varied over a factor of 4–8 with no apparent correlations of *R vs.* concentration. Altex pump; flow-rate, 0.3 ml/min; injections, 10 μl; solvent, water.

from parallel positive and negative profile mode experiments, done on the same equipment and at the same flow-rate, on molecular weight for a number of low-molecular-weight substances. The data in Fig. 6 were obtained over an extended period of time but employed the same capillary tubing. Smaller experimental error in obtaining a standard curve for either the positive or the negative mode would be expected than that shown in Fig. 6 if the standard curve were prepared and compared with the unknown within a shorter time span. Both molecular weight discrimination and day-to-day reproducibility of R values obtained with this method are on the order of 10–15% with the system employed. These two values could be reduced by the use of a more reliable pump than the one used to gather the data in Fig. 6.

The positive and negative mode R values shown in Fig. 6 are nearly within experimental error of one another. The near linear dependence of R on molecular weight is reminiscent of our previous data on biopolymers[1]. The reason for the relatively large deviation of 2′-deoxyadenine (molecular weight 269) from the linear portion of the figure may arise from the severe adsorption problems encountered with this compound in other experiments in which careful washing of the injection system was not carried out. The wide scatter noted for nitrate data can be traced to the near-Gausssian shape of the nitrate profiles, with which R value calculations are difficult because of the uncertainty in determination of breakthrough times. Gaussian or near-Gaussian peaks should not be used for analysis in this method and can be avoided by increasing the flow-rate. A shift to a higher flow-rate would increase all R values in Fig. 6 but the near-linear relationship may not be retained[1,2]. Values for R at a single flow-rate were independent of analyte concentration over a factor of 4 to 8 for a number of different compounds. These points were included in calculating the experimental scatter.

Peak shapes in the positive profile mode of our technique have been shown in all cases not involving adsorption problems to give those shapes calculated from the assumption of limited diffusion and laminar flow. These positive profile mode peak shapes have been independent of molecular weight, provided the flow-rate is adjusted to maintain the same, limited degree of diffusion, *i.e.* slow flow for high-molecular-weight substances and faster flow for lower-molecular-weight substances. In this paper, we have demonstrated that the profiles obtained for the same analyte in the positive and negative profile modes are, for the most part *scaled*, mirror images of one another, especially in the early portions of the profiles. Deviations from an exact mirror image relationship between positive and negative profiles may be due to adsorption problems, even for low-molecular-weight compounds. Thus, in the absence of significant wall adsorption, we predict that our negative profile mode technique, described and illustrated in this paper, can be used to quickly characterize *any* molecules or particles of *any* molecular weight where those species are capable of free diffusion in a liquid undergoing laminar flow. However, because absorption problems may be more serious with increased molecular weight[7], each individual molecular system would have to be investigated in both the positive and negative modes to determine the extent of adsorption problems encountered when continuously passing the analyte through the capillary system, including the injection port region. These added exploratory investigations may be worth the extra effort, if the reward is an analysis system which requires no sample to be withdrawn from a stream and allows *in situ* analysis.

Even though all of the examples we have shown in this paper are for single molecular species, we believe that both positive and negative profile methods can be used to characterize or monitor mixtures of molecules by measuring or monitoring profile shapes. Since the technique assumes free diffusion of molecular species, profiles should be linearly dependent on analyte concentration, providing the absorbance is in the Beer's law range, and individual profiles for each analyte should be additive for mixtures of analytes. Analyte solutions could be monitored for impurities, provided the diffusion and extinction coefficients of the impurity or impurities allow such an analysis to be sensitive enough to detect the impurity through changes in the positive or negative profile shape.

CONCLUSIONS

We conclude from the above results that the same type of empirically determined molecular weight information may be obtained in very short times through both the positive and the negative profile modes of our capillary method, *i.e.*, by either injecting analyte solution into pure solvent mobile phase or by injecting pure solvent into analyte solution employed as the mobile phase. Discrimination of small differences (less than about 15%) in molecular weight cannot easily be accomplished with either the positive or the nagative profile modes of this method. The method is employed to greatest advantage when there are significant changes in molecular weights to be quickly characterized.

The experimental information obtained from either mode contains two different pieces of information. First, with proper calibration, the integrated area of the positive or negative profile gives quantitative information on the amount of material present. Secondly, the shape of the positive or negative profile reflects the diffusion characteristics and therefore also the molecular weight of the dissolved species, provided shape and solvent interaction characteristics of a series of compounds in the standard curve are similar.

POSSIBLE APPLICATIONS OF THE METHOD

The methods described above are most useful in a situation in which the composition of a solution is to be quickly and repetitively monitored for *changes in composition or concentration* over an extended period of time. Given the low cost, the wide dynamic range, and the speed of the positive and negative profile methods, we suggest the following as logical applications of these empirical molecular weight methods.

A side stream from a pipe or a continuously recycling sampling stream from a stirred reactor could be fed through either the loop of an injector or through the system capillary. Since it has been shown[2] that our capillary method yields number average molecular weights, it is anticipated that the method can be used as a fast sensor for *changes* in number-average molecular weight of a polymer solution. The method could use a capillary shunt which continuously draws off material for sampling from a process container or pipeline, with periodic injections of the appropriate solvent. Fast computer feedback from the concentration detector could be sent to an alarm device when any deviation from a standard profile is observed and standard analytical

methods could be employed for pinpointing specifically what chemical changes triggered the profile difference-based alarm.

Water from a municipal water supply or waste water from an industrial source can be monitored for purity by continuing to pass this water through either the injection loop or through the capillary. A mobile phase of pure water could be passed through the capillary system or through the loop and a periodic injection could be made to check for positive or negative profiles which quickly characterizes the number-average molecular weight of an impurity in addition to providing quantitative information regarding the amount of impurity present.

When there are solubility problems in which there can be drastic changes in the average molecular weight of a substance beause of changing experimental variables, the positive or negative profile methods would provide a valuable means of quickly observing the changing average molecular weights which might precede precipitation or colloid formation. We believe with proper development this technique is capable of determining molecular weights in the order of tens of seconds.

Such complex biological fluids as blood and urine often need to be monitored for sudden changes in composition. For example, kidney failure, in which high-molecular-weight biopolymers are suddenly found in the urine could be be monitored with either the positive or negative profile methods. Monitoring of dialysis fluids also would appear to be another possible application. Blood monitoring may be possible but also may present special problems. The limits of our method at the very high end of the moleular weight range have yet to be tested. Preliminary experiments in our laboratory with very high molecular weight biological systems appear to be quite promising.

Thus, many applications of this new method can be envisioned for a wide range of molecular weight compounds including industrial polymers and waste water, biopolymers and clinical samples, provided there are not significant problems of wall adsorption. For higher-molecular-weight compounds, these problems may be minimized by increasing the capillary tube diameter and decreasing the flow-rate.

ACKNOWLEDGEMENTS

We wish to thank Drs. E. C. Hermann, J. J. Kirkland, D. B. Wetlaufer, S. D. Brown and A. Lenhoff for discussions regarding this work. We also thank the ISCO Corporation for the loan of the pump used in part of this work. This work was supported by the University of Delaware.

REFERENCES

1 F. M. Kelleher and C. N. Trumbore, *Anal. Biochem.*, 137 (1984) 20.
2 C. N. Trumbore, M. Grehlinger, M. Stowe and F. M. Kelleher, *J. Chromatogr.*, 322 (1985) 443.
3 J. G. Atwood and M. J. E. Golay, *J. Chromatogr.*, 218 (1981) 97.
4 J. S. Vrentas and C. M. Vrentas, *AIChE J.*, 34 (1988) 1423.
5 J. S. Yu, *ASME J. Appl. Mech.*, 48 (1981) 217.
6 C. N. Trumbore and L. M. Jackson, unpublished results.
7 C. N. Trumbore, R. D. Tremblay, J. T. Penrose, M. Mercer and F. M. Kelleher, *J. Chromatogr.*, 280 (1983) 43.

Journal of Chromatography, 481 (1989) 121–133
Elsevier Science Publishers B.V., Amsterdam — Printed in The Netherlands

CHROM. 21 772

OPTIMIZATION IN PHOTOCHEMICAL REACTION DETECTION

APPLICATION TO HIGH-PERFORMANCE LIQUID CHROMATOGRAPHY–PHOTOLYSIS–ELECTROCHEMICAL DETECTION

WILLIAM J. BACHMAN* and JAMES T. STEWART
Department of Medicinal Chemistry and Pharmacognosy, College of Pharmacy, University of Georgia, Athens, GA 30602 (U.S.A.)
(First received January 17th, 1989; revised manuscript June 6th, 1989)

SUMMARY

Chemometric techniques have been applied to optimization of response in photochemical reaction detection. Multivariate optimization using a factorial experimental design was employed to assess the effects of mobile phase pH and UV irradiation time on the amperometric response obtained by high-performance liquid chromatography–photolysis–electrochemical detection for four cardiovascular drugs. The procedure is more representative of the dynamic analytical conditions encountered in photochemical reaction detection than previous methods employing univariate optimization or off-line static methods. Stepwise multiple linear regression with backward elimination was used to fit the experimental data to empirical reduced third-order polynomial models. Plots of response were used to determine optimum conditions and visualize the interactions between pH and irradiation time. The design and construction of a low-cost on-line photochemical reactor for high-performance liquid chromatography is also discussed.

INTRODUCTION

Photochemical reaction detection is a variation of on-line post-column derivatization which has found particular usefulness in pharmaceutical and forensic analysis. It is employed to extend the sensitivity and selectivity of detection in high-performance liquid chromatography (HPLC) and to minimize sample preparation. Reviews of photochemical reaction detection in HPLC have been published[1–4]. Combining photoderivatization with electrochemical detection techniques allows rapid and unique photochemical reactions to be advantageously coupled with the high selectivity and sensitivity of electrochemical detection[5]. Krull and co-workers[6–14] have extensively studied HPLC–photolysis ($h\nu$)–electrochemical detection (ED) using conventional thin-layer amperometric cell detectors.

In the previously reported $h\nu$–ED methods, optimization of electrochemical response with respect to solution pH has been performed off-line using photolysis–cyclic voltammetry[12–14], on-line, but independently of irradiation time or flow-

0021-9673/89/$03.50

rate[7,8], or the pH dependence was either not reported or not optimized[9–11]. Although static off-line methods such as cyclic voltammetry (CV) are useful for scouting purposes and indicating trends, the results may not accurately represent the actual dynamic conditions of the on-line photochemical reactor (PCR) employing amperometric detection. We have observed situations in which a compound may show no activity at a glassy carbon electrode by CV, yet produce an electrochemical response by HPLC–amperometric detection under similar conditions. In both experiments, the same solvent was used for CV and as the HPLC mobile phase. Slow electron transfer under the CV conditions may be responsible for this phenomenon. Alternatively, the enhanced mass transfer of electroactive species to the electrode under hydrodynamic conditions of HPLC–amperometry may result in the greater sensitivity observed[15].

With respect to both the off-line and on-line optimization procedures, these methods have systematically varied one experimental variable of the analytical system at a time while holding all others constant (univariate optimization). Conditions were optimized for pH then optimized for irradiation time. Because the influences of these parameters on the formation of electroactive photoderivatives are not mutually independent, both parameters should be varied simultaneously (multivariate optimization).

In the previous hν–ED methods, irradiation time was evaluated by altering the flow-rate incrementally to produce a range of residence times within an irradiation coil of fixed length. The peak areas or heights representing the electrochemical responses as a function of flow-rate (residence time) were used as a measure of optimum irradiation time. A new coil was then constructed corresponding to the length required to give an equivalent residence time at the flow-rate desired for the chromatographic separation. However, for concentration-dependent detectors such as amperometric detectors, variation in flow-rate has a pronounced effect on the observed response[16]. The area response for a constant amount of electroactive compound is inversely proportional to the flow-rate. The peak height is inversely proportional to the standard deviation of the peak, which in turn is influenced by flow-rate. When a post-column reactor is added to an HPLC system, additional factors resulting from dispersion in the reactor further compound the effect of flow-rate on response. In light of these influences, it is apparent that variation of flow-rate to optimize irradiation time incorporates response factors related to flow-rate that are unresolved from the effect of irradiation on electrochemical response. A better approach to optimization of irradiation time requires that the flow-rate required by the chromatographic separation be maintained and the reactor length and pH be varied simultaneously. Alternatively, a system might be employed in which the flow-rate and reactor length remain constant and the photon flux and pH are varied.

The application of hν–ED to the analysis of antihypertensive drugs in dosage forms and biological fluids is currently being investigated in our laboratory. One of the objectives of the study has been to demonstrate the utility of chemometric techniques in the optimization of electrochemical response obtained by photochemical reaction detection. This paper describes a multivariate optimization procedure in which the mobile phase pH and irradiation time parameters are simultaneously varied under the actual dynamic conditions of analysis. A rigorous statistically based factorial experimental design was employed. No previous papers employing multivariate chemometric techniques to optimize response in photochemical reaction detection have been reported.

EXPERIMENTAL

Standards, reagents and test solutions

Spironolactone, hydrochlorothiazide, clonidine, and chlorthalidone reference standards were all obtained from the United States Pharmacopeial Convention (Rockville, MD, U.S.A.). Reagent-grade sodium dihydrogen phosphate, sodium hydroxide, and phosphoric acid were obtained from J. T. Baker (Phillipsburg, NJ, U.S.A.). HPLC-grade methanol was purchased from Burdick & Jackson Labs. (Muskegon, MI, U.S.A.).

Stock solutions (0.25 mg/ml) of spironolactone, hydrochlorothiazide, clonidine and chlorthalidone were prepared in methanol. Working standard solutions (12.5 μg per ml) were prepared by diluting a 5-ml aliquot of the stock solution to 100 ml with 42% aqueous methanol.

Mobile phase solutions were prepared from a bulk solution containing methanol–0.1 *M* NaH_2PO_4 (45:55). A set of eight mobile phases within the pH range 2.0–8.0 was prepared from portions of the bulk solution by adjusting the pH with concentrated phosphoric acid or 50% aqueous sodium hydroxide to the required pH. All mobile phases were degassed before use in an ultrasonic bath.

Instrumentation

Fig. 1 illustrates the arrangement of the HPLC–hν–ED system components. The system included a Beckman Model 110B solvent delivery module (Fullerton, CA, U.S.A.) delivering a flow-rate of 1.0 ml/min and a Rheodyne Model 7125 loop injector with a 20-μl loop. An Uptight guard column (Upchurch Scientific, Oak Harbor, WA, U.S.A.) packed with Vydac reversed-phase packing, 30–40-μm pellicular particles (Universal Scientific, Atlanta, GA, U.S.A.) was used. The analytical column was a Zorbax CN Reliance cartridge column, 5-μm spherical particles, 8 cm × 4 mm I.D. (DuPont, Wilmington, DE, U.S.A.). The photochemical reactor was constructed using a Model SC3-9 low-pressure mercury discharge lamp with a Model SCT-4 power supply (UVP, San Gabriel, CA, U.S.A.). A set of five irradiation coils of different length was knitted from PTFE tubing 0.3 mm I.D. × 1.59 mm O.D. (Anspec, Ann Arbor, MI, U.S.A.) corresponding to irradiation times of 4.17, 8.35, 16.70, 25.05 and 33.40 s at a flow-rate of 1.0 ml/min. A 7.62-cm diameter fan (Rotron, Woodstock, NY, U.S.A.) provided air cooling for the reactor. Reactor components were contained in a 31.5 × 16.5 × 15.5 cm box constructed from galvanized sheet steel and perforated masonite. The bottom and back sides were perforated to improve

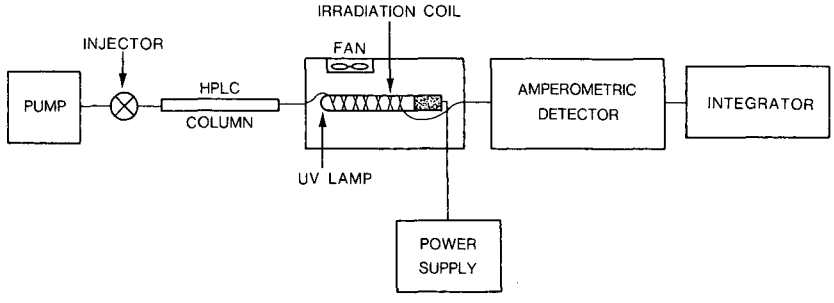

Fig. 1. Diagram of HPLC–photolysis–electrochemical detection system.

air flow for cooling purposes. The detector used was a BAS LC-4B amperometric controller and LC-17 thin-layer transducer with glassy carbon working electrode and Ag/AgCl reference electrode (Bioanalytical Systems, West Lafayette, IN, U.S.A.). The operating potential was +1.0 V and a range of 20 nA was used. Connections between the analytical column, irradiation coil and the thin-layer transducer were all made with Upchurch Fingertight fittings (Upchurch Scientific). Area responses were recorded using an HP 3392A Integrator (Hewlett-Packard, Avondale, PA, U.S.A.).

Optimization procedure

Electroactive photoderivative formation was determined simultaneously as a function of irradiation time and mobile pH for spironolactone, hydrochlorothiazide, chlorthalidone and clonidine. Irradiation time was varied by changing the coil length in the photoreactor using one of the five coils in the set. Working standard solutions of the model compounds were injected in duplicate into the HPLC–hν–ED system. Amperometric responses were recorded for each coil and also with the UV lamp of the reactor off to provide response values without irradiation. This time series was repeated in each of the eight mobile phases.

RESULTS AND DISCUSSION

Experimental design, data analysis and mathematical modeling

Chemometric techniques similar to those used in the optimization of chromatographic resolution[17] may be used to optimize analyte response. In fact, many of the same variables affecting resolution also influence photoderivatization: mobile phase pH, per cent and type of organic modifier, presence of inorganic salts, etc. The additional parameter which must be considered in hν–ED is the irradiation time or photon flux. In general, optimization includes the selection of optimization criteria and the parameters to optimize, selection of an experimental design, and evaluation and interpretation of the results. In hν–ED, of course, the criterion to optimize is the photoinduced electrochemical response (peak area or height). On a practical level, the basic reaction conditions are constrained by the general chromatographic limitations (pH range 2–8 for silica-based columns, choice of solvents, etc.), the specific requirements of a given separation (*e.g.* conditions for reversed-phase or ion-pair chromatography as dictated by the analyte), and the need for a suitable electrolyte for hν–ED. Frequently, existing HPLC methods have been adapted to use hν–ED. Considering these restrictions, the parameters to optimize are usually limited to the mobile phase pH and irradiation time.

A factorial experimental design was implemented in which the photoinduced amperometric response was acquired at eight levels of mobile phase pH and six levels of irradiation time. This 8 × 6 factorial design parameter space encompasses the region of pH 2–8 recommended for silica-based HPLC columns and the irradiation times (coil lengths) possible with the UV lamp used in the study (0–33.4 s). A factorial type design was chosen rather than a simplex design because it was desired to obtain an accurate representation of the response surfaces encountered in HPLC–hν–ED over the entire parameter space and because no information of this type has been reported. The possibility also existed that the surfaces contained local optima, a situation in which simplex or univariate techniques may fail to find the best response

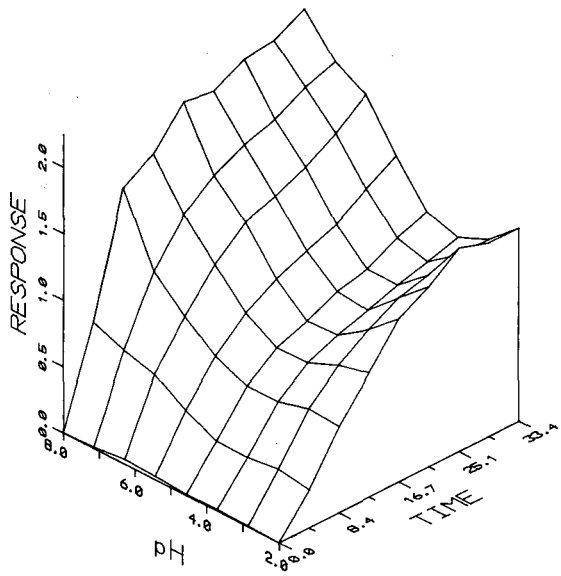

Fig. 2. Experimental amperometric response surface as a function of irradiation time and mobile phase pH for spironolactone. Time in s.

conditions or global optimum. It was also desired to establish the extent of interaction between pH and irradiation time.

Fig. 2 is a plot of the response surface constructed from the experimental data for spironolactone. Spironolactone is electro-inactive in the absence of UV irradiation as indicated by zero response along the pH axis at zero time. Photoinduced response generally increased with increasing pH and irradiation time. The global optimum is found at a pH of 8.0 and irradiation time of 33.4 s. A depression is evident in the surface along values collected at pH 4.0. Response at pH 2.0 and 33.4 s represents a local optimum within the parameter space.

The hydrochlorothiazide response surface is given in Fig. 3. Hydrochlorothiazide is electroactive without irradiation. The left forward edge of the surface (time zero) represents the effect of the observed native amperometric response of hydrochlorothiazide. As is well known, a significant enhancement in response for electroactive compounds is possible by optimizing the mobile phase pH. At a pH of 8.0, the response is constant regardless of irradiation time (relative standard deviation of $\pm 3.5\%$). Equivalent responses are attainable at any irradiation time at this pH. At low pH values where hydrochlorothiazide has no native electroactivity, the response can be increased by UV irradiation.

Chlorthalidone, like spironolactone, is inactive without irradiation. The response surface (Fig. 4) is similar to that of spironolactone with the exception that a ridge occurs rather than a depression. Optimum response is found along this ridge at pH 6.0 and 33.4 s. The clonidine data produced a response surface (Fig. 5) which indicated low-level response only at high pH and no significant response at low or intermediate pH. However, a large enhancement in response with increasing irradiation time is observed at high pH.

Empirical polynomial models of photoinduced electrochemical response as a

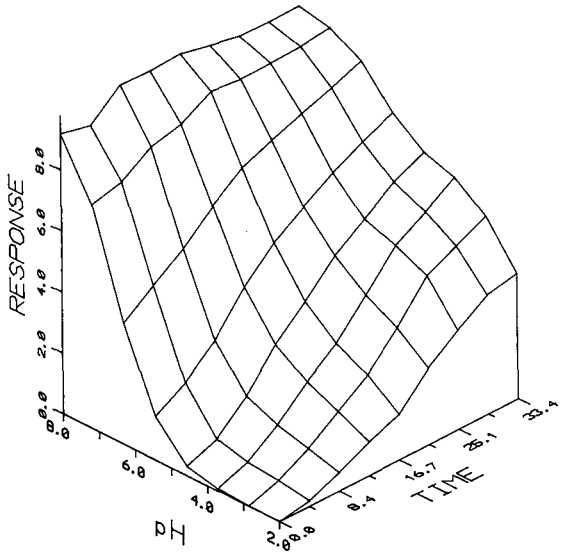

Fig. 3. Experimental amperometric response surface as a function of irradiation time and mobile phase pH for hydrochlorothiazide. Time in s.

function of pH and irradiation time were fit to the experimental data using matrix least squares regression analysis. Polynomial models allow interaction effect terms to be included in the model. A full second-order polynomial was first employed because they are frequently useful in describing response surfaces of phenomena over limited factor domains[18]. The resulting regression equation is:

$$R = a + bt + c\text{pH} + dt^2 + e\text{pH}^2 + ft\text{pH}$$

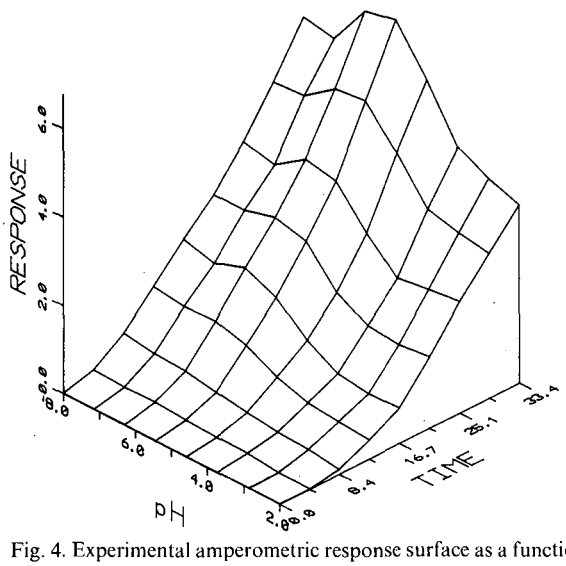

Fig. 4. Experimental amperometric response surface as a function of irradiation time and mobile phase pH for chlorthalidone. Time in s.

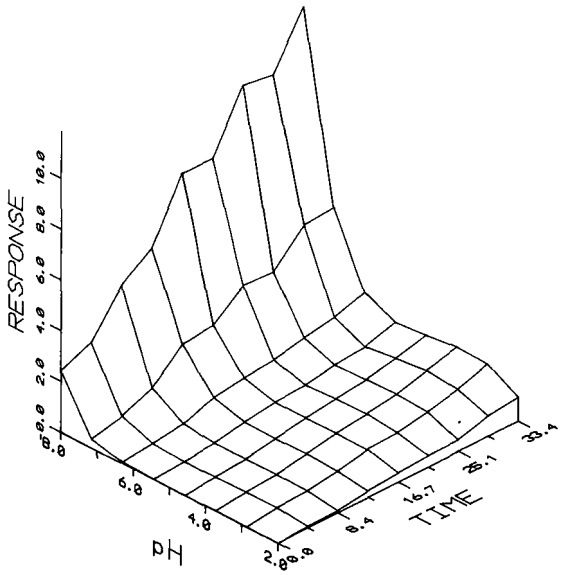

Fig. 5. Experimental amperometric response surface as a function of irradiation time and mobile phase pH for clonidine. Time in s.

where R is the amperometric response, t is the irradiation time in seconds, pH is the mobile phase pH and a–f are the estimated numerical coefficients of the equation. Values obtained for the numerical coefficients and the coefficients of determination (R^2) for the second-order model for each compound are given in Table I. Adequacy of the models was assessed using the coefficients of determination and the F-test for the significance of regression[18]. In three of the four sets of experimental data, an R^2 of 0.941 or greater was obtained which indicates that the second-order model accounts for 94.1% (or more) of the variation in the data. In the fourth case, the data for clonidine, the model explained only 80% of the variance of the data. For cloni-

TABLE I

ESTIMATED REGRESSION COEFFICIENTS, COEFFICIENTS OF DETERMINATION (R^2) AND STANDARD ERROR OF ESTIMATE (S.E.E.) FOR SECOND-ORDER POLYNOMIAL MODEL

Coefficient	*Spirono-lactone*	*Hydrochloro-thiazide*	*Chlorthal-idone*	*Clonidine*
a	0.721	−1.721	−0.850	6.150
b	0.085	0.298	−0.036	−0.093
c	−0.399	−0.311	0.369	−3.086
d	−0.002	−0.001	0.004	0.000
e	0.045	0.206	−0.035	0.327
f	0.004	−0.026	0.010	0.035
R^2	0.941	0.944	0.968	0.800
S.E.E.	0.162	0.815	0.374	1.176

dine, the change in photoinduced amperometric response *versus* pH and irradiation time was less gradual than the three other compounds. Response increased sharply at high pH and with increasing irradiation time. The rapid changes in response within a small area of the parameter space resulted in a poorer fit using the second-order equation for clonidine.

In order to develop a model that encompassed all the compounds studied, higher-order polynomials were investigated. Although it is always possible to make R^2 large by adding more terms to the model, the new model is not necessarily a better description of the experimental data unless the error sum of squares in the new model is reduced by an amount equal to the original error mean square[19]. If it is not, the new model will have a larger error mean square than the old model due to the loss of degrees of freedom for error. It is also recommended that the order of the model be kept low to eliminate higher order oscillations. In order to obtain a model that explains the data with minimal error yet does not contain a large number of non-significant terms, an alternative technique, stepwise multiple regression using backward elimination was employed[19]. The initial regression equation was a full third-order model:

$$R = a + bt + c\text{pH} + dt^2 + e\text{pH}^2 + ft\text{pH} + gt^3 + h\text{pH}^3 + it^2\text{pH} + jt\text{pH}^2$$

where R, t and pH are as previously defined and a–j are the estimated regression coefficients. Backward elimination attempts to find a good model with a small set of significant variables by starting with a model containing all the terms to be considered and eliminating them one at a time. In each step, the partial F-statistic is calculated for each term in the model as if it were the last variable to enter the model. The smallest of the partial F-statistics is compared with a user-selected F-to-remove. The term is removed from the model if the F-statistic is smaller than the F-to-remove. Using this technique, third-order models reduced in the number of terms from the full model were obtained. In all cases, R^2 values (adjusted for degrees of freedom) were greater than 0.952. Because of the variety of response surfaces that are possible, the number of terms in the model and the particular terms retained in the model as well as the signs and values are different for each compound. The coefficients of determination corrected for degrees of freedom were greater using this reduced third-order model than the full second-order model and were not statistically different from R^2 values for a full third-order regression. Coefficients of determination and the estimated regression coefficients for the reduced third-order model are found in Table II.

Model response surfaces generated from the regression coefficients for the reduced third-order model more accurately approximated the shapes of the experimental response surfaces than using the full second-order coefficients. Response surfaces generated from the model equations for spironolactone and hydrochlorothiazide are shown in Figs. 6 and 7,. respectively.

Chromatographic results

Mixtures containing spironolactone and hydrochlorothiazide or chlorthalidone and clonidine were analyzed by HPLC–hν–ED using the optimal conditions determined by visual inspection of the experimental response surface plots. For the four compounds studied, mathematical analysis of the model equations could not be used

TABLE II

ESTIMATED REGRESSION COEFFICIENTS, COEFFICIENTS OF DETERMINATION (R^2) AND STANDARD ERROR OF ESTIMATE (S.E.E.) FOR REDUCED THIRD-ORDER MODEL

E designates term eliminated from regression model.

Coefficient	*Spirono-lactone*	*Hydrochloro-thiazide*	*Chlorothal-idone*	*Clonidine*
a	0.458	2.261	2.370	-11.890
b	0.102	E	-0.125	0.220
c	-0.248	-2.200	-1.693	9.259
d	$-3.43 \cdot 10^{-3}$	E	$4.46 \cdot 10^{-3}$	E
e	$2.62 \cdot 10^{-2}$	0.391	0.345	-2.143
f	E	0.109	$5.19 \cdot 10^{-2}$	-0.109
g	$6.20 \cdot 10^{-5}$	E	E	E
h	E	E	$-2.13 \cdot 10^{-2}$	0.151
i	$-2.75 \cdot 10^{-4}$	$-2.66 \cdot 10^{-4}$	E	E
j	$1.28 \cdot 10^{-3}$	$-1.26 \cdot 10^{-2}$	$-4.16 \cdot 10^{-3}$	0.014
R^2	0.966	0.977	0.977	0.952
S.E.E.	0.124	0.525	0.316	0.577

to predict optimal responses because the functions did not maximize within the experimental parameter space. These pairs of drugs were analyzed because they occur in commercially available diuretic–antihypertensive combination dosage forms.

Fig. 8 shows the chromatograms obtained for spironolactone and hydrochlorothiazide using a pH 8.0 mobile phase without the PCR and with the PCR containing a 33.40-s irradiation coil. As indicated by the response surfaces, spironolactone

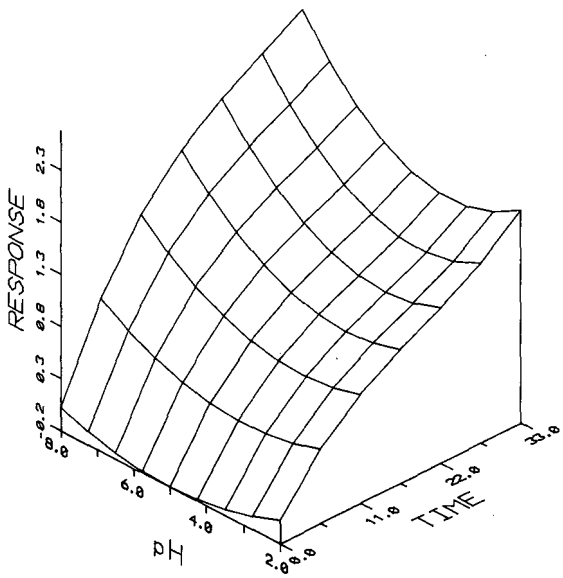

Fig. 6. Reduced third-order regression model response surface as a function of irradiation time and mobile phase pH for spironolactone. Time in s.

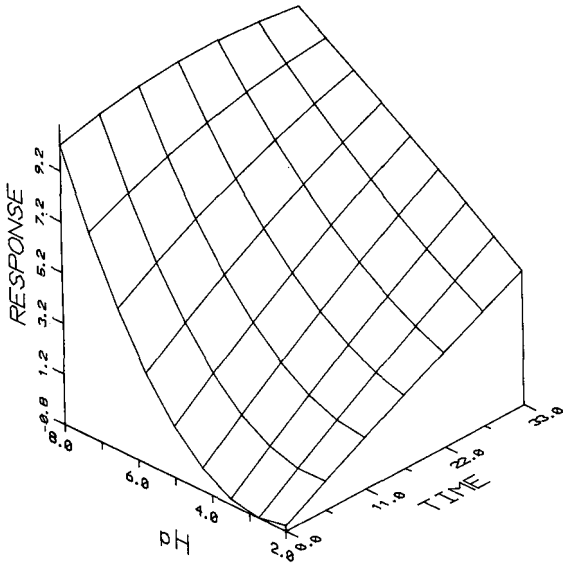

Fig. 7. Reduced third-order regression model response surface as a function of irradiation time and mobile phase pH for hydrochlorothiazide. Time in s.

produces an amperometric response only on irradiation and the response for hydrochlorothiazide remains unchanged under these conditions. The chromatograms for chlorthalidone and clonidine are given in Fig. 9. Irradiation results in an amperometric response for chlorthalidone and a 390% increase in the response for clonidine. A cyano-bonded phase was used in this study because it provided good separations for mixtures containing compounds of widely different lipophilicity while maintaining shorter analysis times than C_{18}-bonded phase columns.

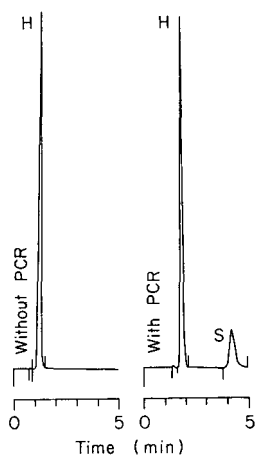

Fig. 8. Chromatograms of a solution containing hydrochlorothiazide (H) and spironolactone (S) without the on-line photochemical reactor (PCR) and with PCR and 33.4-s irradiation coil. Conditions: methanol–0.1 *M* NaH_2PO_4 pH 8.0 (45:55), 1.0 ml/min, Zorbax CN cartridge column, BAS glassy carbon electrode, + 1.0 *vs.* Ag/AgCl, 20 nA range.

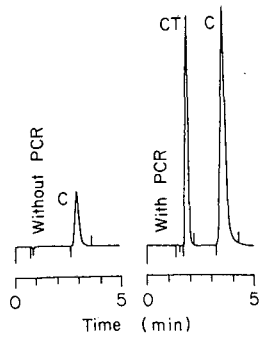

Fig. 9. Chromatograms of a solution containing chlorthalidone (CT) and clonidine (C) without the on-line photochemical reactor (PCR) and with PCR and 33.4-s irradiation coil. Conditions as in Fig. 8.

Photochemical reactor design

Because there are no commercially available PCRs for HPLC–photochemical reaction detection, a large variety of individual reactor designs have appeared in the literature. These designs employ irradiation sources ranging from high-intensity mercury or xenon arc lamps to medium- and low-pressure mercury or zinc lamps. The irradiation coils have been made of either quartz or PTFE and a number of different coil geometries have been proposed.

Although the majority of previous reactor designs have employed medium- and high-pressure lamps, a low-pressure mercury discharge lamp was selected for use. The factors involved in the lamp selection included the desire to decrease the size, complexity and cost of the photoreactor relative to existing designs. Low-pressure mercury lamps have a number of advantages for use in photochemical reactors. They generate much less heat and infrared radiation than high-pressure arc lamps and therefore do not require complicated liquid cooling systems. Air cooling is usually sufficient. High temperatures within the irradiation coil can result in unwanted side reactions such as polymerization. Temperature fluctuations can decrease system reproducibility. Low-pressure lamps have a very stable output over long periods and lamp life is longer also contributing to system reproducibility. Compared to high-pressure arc lamps, these lamps emit a higher percentage of ultraviolet light and very low heat loss. 85% of the radiation is emitted at 254 nm, a wavelength useful for many photochemical reactions[20]. Because low-pressure lamps do not require d.c. power or high current ratings, the power supplies are small and inexpensive. Finally, use of high-pressure sources can shorten the lifetime of PTFE irradiation coils which become brittle on prolonged exposure to high-intensity UV light. The particular lamp selected was chosen because it provided a large irradiated cylindrical surface (23 cm long × 0.95 cm diameter) onto which the irradiation coil could be directly placed for efficient transfer of radiant energy to the coil. The irradiation coils can be quickly changed by sliding off one coil and sliding on another. If size, cost and complexity are not considerations, the decision to incorporate either a high-pressure arc lamp or low pressure discharge lamp in a PCR is ultimately dependent on the reaction kinetics of the particular system under study. Both the intensity of the source and the length of irradiation time influence the concentrations of intermediate short-lived radicals and excited molecules[2]. These concentrations in turn influence the concentrations of the

various photoproducts that result from the multiple reaction pathways that often exist in photochemical reactions. The desired detectable species is produced in highest yield using the appropriate combination of high or low intensity and long or short irradiation time and is dependent on the analyte-specific kinetics. On a more pragmatic level, neither the kinetics nor the reaction products need be known as long as the post-column photochemical reaction is reproducible and results in enhanced sensitivity or selectivity of detection. However, elucidation of the electroactive photochemical reaction products is currently being investigated because knowledge of the mechanism and structural requirements will aid in optimization procedures and allow extension to other analytes.

The advantages of PTFE reaction coils in photochemical reaction detectors were reported by Scholten *et al.*[21]. PTFE provides good transparency in the 200–300 nm region and is readily available in a variety of internal and external diameters. PTFE tubing is less expensive, less fragile and easier to connect to systems than quartz. Knitted PTFE open tubular reactors exhibit minimal dispersion in comparison to coiled reactors of identical dimensions due to the deformed flow pattern they produce within the tubing. The geometry used in the irradiation coils in this study is a modification of a design published by Engelhardt and Neue[22]. Their original design was knitted on a device with four pins that produces a coil with four distinguishable sides. Our coils were knitted on a device with six pins placed on the corners of a regular hexagon. The six-sided design was chosen in order to maximize the surface area of the coil exposed to the UV lamp. The coils require no external support and slide directly onto the surface of the lamp in a "sleeve-like" manner.

All the components of the PCR fit within a relatively small box. The bottom and rear panels of the reactor box were made from 3-mm perforated masonite ("peg board") to provide improved ventilation and to facilitate the mounting of the lamp and cooling fan and the routing of irradiation coil entrance and exit tubing and electrical connections to the lamp and fan. The remaining sides were fabricated from thin gauge sheet steel.

Reproducibility of the HPLC–hν–ED system as measured by repeatability of injection ($n = 6$) was determined by making replicate injections of a working standard solution containing hydrochlorothiazide and spironolactone. Relative standard deviations were $\pm 0.9\%$ for hydrochlorothiazide and $\pm 1.7\%$ for spironolactone.

CONCLUSIONS

An improved procedure for optimization in HPLC–hν–ED has been presented that more accurately represents the dynamic analytical conditions than static off-line methods or dynamic methods that vary flow-rates. The factorial design allows the entire response surface to be constructed and provides a better representation of the effect of experimental conditions than simplex or univariate techniques. Graphical representation of response surfaces indicates visually the best condititons and the interaction between parameters. The ruggedness of experimental conditions can be judged by whether an optimum occurs on a narrow ridge or a wide plateau.

Stepwise multiple linear regression was found to be a useful statistical technique for developing mathematical models for analytical response phenomena. It produces models which adequately describe the experimental data while minimizing the num-

ber of terms and maximizing the degrees of freedom for estimation of the error in the model. If the model equation maximizes within the experimental parameter space, mathematical analysis can be used to predict the optimum experimental conditions.

The results of this optimization study will be used in the development of analytical methods for these four drugs in dosage forms and in biological fluids. It is anticipated that the high selectivity of HPLC–hν–ED will be of particular value in the determination of pharmaceuticals in biological fluids. The high selectivity of this technique results from the conditions that the analyte: (1) possesses a specific retention time, (2) absorbs radiation from the UV source, and (3) undergoes a photoreaction to produce an electroactive species which is oxidized at the specific electrode and operating potential. The probability that an interfering component will meet all three of these criteria is quite low.

ACKNOWLEDGEMENTS

W. J. B. gratefully acknowledges the support of the United States Pharmacopeial Convention, Inc. and the American Foundation for Pharmaceutical Education. The authors also thank Linda J. Pennington, U.S. Food and Drug Administration, for helpful comments in reviewing this manuscript.

REFERENCES

1 J. T. Stewart, *Trends Anal. Chem.*, 1 (1982) 170.
2 J. W. Birks and R. W. Frei, *Trends Anal. Chem.*, 1 (1982) 361.
3 R. W. Frei and J. F. Lawrence, *Chemical Derivatization in Analytical Chemistry*, Plenum Press, New York, 1981.
4 I. S. Krull, *Reaction Detection in Liquid Chromatography*, Marcel Dekker, New York, 1986.
5 W. R. LaCourse and I. S. Krull, *Trends Anal. Chem.*, 4 (1985) 118.
6 I. S. Krull, X-D. Ding and C. M. Selavka, *LC, Mag. Liq. Chromatogr. HPLC*, 2 (1984) 215.
7 I. S. Krull, X-D. Ding and C. M. Selavka, *J. Forens. Sci.*, 29 (1984) 449.
8 X-D. Ding and I. S. Krull, *J. Agric. Food Chem.*, 32 (1984) 622.
9 C. M. Selavka, I. S. Krull and I. S. Lurie, *J. Chromatogr. Sci.*, 23 (1985) 499.
10 I. S. Krull, C. M. Selavka, R. J. Nelson, K. Bratin and I. S. Lurie, *Current Sep.*, 7 (1985) 11.
11 C. M. Selavka, I. S. Krull and K. Bratin, *J. Pharm. Biomed. Anal.*, 4 (1986) 83.
12 C. M. Selavka, I. S. Krull, *Anal. Chem.*, 59 (1987) 2699.
13 C. M. Selavka, I. S. Krull, *Anal. Chem.*, 59 (1987) 2704.
14 C. M. Selavka, K-S. Jiao, I. S. Krull, P. Sheih, W. Yu and M. Wolf, *Anal. Chem.*, 60 (1988) 250.
15 P. T. Kissinger and W. R. Heineman, *Laboratory Techniques in Electroanalytical Chemistry*, Marcel Dekker, New York, 1984, p. 111.
16 Y. T. Shih and P. W. Carr, *Anal. Chim. Acta*, 167 (1985) 137.
17 C. E. Goewie, *J. Liq. Chromatogr.*, 9 (1986) 1431.
18 D. L. Massart, B. G. M. Vandeginste, S. N. Deming, Y. Michotte and L. Kaufman, *Chemometrics: A Textbook*, Elsevier, Amsterdam, 1988.
19 D. C. Montgomery and E. A. Peck, *Introduction to Linear Regression Analysis*, Wiley, New York, 1982.
20 *Pen Ray Lamps, Bulletin No. 103*, UVP, San Gabriel, CA, 1988.
21 A. H. M. T. Scholten, P. L. M. Welling, U. A. Th. Brinkman and R. W. Frei, *J. Chromatogr.*, 199 (1980) 239.
22 H. Engelhardt and U. D. Neue, *Chromatographia*, 15 (1982) 403.

Journal of Chromatography, 481 (1989) 135–146
Elsevier Science Publishers B.V., Amsterdam — Printed in The Netherlands

CHROM. 21 823

TEMPERATURE-INDUCED CHANGES IN REVERSED-PHASE CHROMATOGRAPHIC SURFACES

C_8 AND C_9 POLYMERIC LIGANDS

J. W. CARR[a] and J. M. HARRIS*
Department of Chemistry, University of Utah, Henry Eyring Building, Salt Lake City, UT 84112 (U.S.A.)
(First received July 28th, 1988; revised manuscript received July 26th, 1989)

SUMMARY

The temperature-dependent polarity of polymeric C_8 and C_9 stationary phases, preconditioned with acetonitrile and then contacted with water, is studied using the fluorescence of sorbed pyrene as a probe. The fluorescence vibronic band ratio, sensitive to the polarity of the probe surroundings, shows a temperature-dependent hysteresis which is indistinguishable from the retention behavior of these materials. The stationary phase polarity decreases when passing through the hysteresis, which is consistent with the loss of conditioning solvent from the interface but inconsistent with an extended structure for the alkyl ligands. Solvent retention in the stationary phase and its temperature dependence appear to require local ordering of the polymeric phase.

INTRODUCTION

One of the more challenging aspects of developing a comprehensive model for reversed-phase liquid chromatography has been to determine the role of the alkylated surface in the selective retention of solute molecules. While mobile phase effects dominate solute retention[1,2], the contribution of the surface to retention has been the subject of intensive investigation and interest[3–13]. These chromatographic experiments have provided insight into the structure and behavior of bonded hydrocarbon layers and have extended our ideas of the stationary phase beyond a homogeneous, hydrocarbon layer. A picture of the stationary phase as a dynamic surface, responding to conditions in the mobile phase and affecting solute retention, is beginning to emerge.

Models of the stationary phase as an alkyl "grass" or "bristles"[5] attached to the solid support, or as a hydrocarbon "blanket" covering the silica gel[3] are being replaced by models of a heterogeneous surface incompletely covered by chemically bonded alkyl ligands. Lochmüller and Wilder[4] have suggested a microdroplet configuration for the bonded layer, where alkyl ligands are aggregated by hydrophobic interactions

[a] Present address: IBM Watson Research Center, Yorktown Heights, NY 10596, U.S.A.

0021-9673/89/$03.50

into clusters of organic material. If the solute is sufficiently small to be contained within these clusters, the stationary phase would appear as islands of non-polar material distributed on a polar silica surface. The organization of bound ligands appears to influence shape selectivity of retention[11,12] and depends on the bonding to the silica surface, the degree of surface coverage, and the underlying substrate. Distribution of solvent components into the stationary phase has also been studied, and the resulting effects on solute retention have been described[6–10].

Transfer of organic modifier from the mobile phase into the stationary phase is responsible for changes in the environment of a solute sorbed to the bound layer[13–16] and for changes in the phase volumes[6,9]. The intercalation of organic modifier into the stationary phase may, in addition to a change in the polarity of the bonded layer, be responsible for conformational changes in the surface as well. While studying the effects of temperature and conditioning solvent on polymeric C_8, C_9 and C_{10} stationary phases with a totally aqueous mobile phase, Gilpin and Squires[7] noted an interesting hysteresis in the temperature dependence of solute retention, following preconditioning with organic solvent. They showed in a subsequent study that organic modifier, initially retained by the stationary phase when the mobile phase is abruptly changed from neat organic modifier to water, is released[8] when a sufficiently high temperature is reached. The temperature at which the solvent was released correlated with the alkyl chain length and functionality of the organic solvent[7,17]. A mechanism proposed to account for the observed behavior was that solvent molecules were trapped in the stationary phase by collapse of the alkyl ligands[7] into an aggregated, metastable state[17] when exposed to water. Raising the temperature of the stationary phase above a transition temperature was postulated to cause restructuring of the surface ligands into an extended or "bristle" configuration[7,8], releasing trapped organic modifier which is replaced by water molecules between the hydrocarbon chain, now in an extended, more stable surface structure[17].

In the present work, the surface environments of C_8 and C_9 polymeric stationary phases, under conditions of the above temperature-dependent hysteresis, are examined using the fluorescence emission of sorbed pyrene as a probe. The vibronic band structure of the fluorescence from pyrene is quite sensitive to the polarity of the molecule's local environment[18]. As the solvent polarity around pyrene is increased, the intensity of the vibronic origin of the weak, highest energy L_b transition (band I at 374 nm) is increased due to symmetry lowering perturbations from the solvent environment which allow mixing with the much stronger L_a transition dominating the third vibronic peak (band III at 385 nm)[19]. As a result, the ratio of the intensities of the third and first peaks, III:I, varies inversely with increases in the polarity of microenvironment of the pyrene probe[14,18]. The vibronic band ratios of pyrene fluorescence have been used to study the interfacial microenvironments of polymeric and monomeric C_{18} stationary phases by sorption of the probe to the hydrophobic surface[14–16]. The results of these studies showed the effects on C_{18} stationary phases of organic modifier and the heterogeneity of the sorption environments as a function of overlaying solvent. In the present work, the polarity of polymeric C_8 and C_9 stationary phases, preconditioned with acetonitrile and then contacted with water, is investigated as a function of temperature using sorbed pyrene as a probe. The results indicate that the polarity of the stationary phase *decreases* upon heating, which is not consistent with an extended structure for alkyl ligands in contact with the totally aqueous mobile phase.

EXPERIMENTAL

Chemicals

Pyrene was obtained from Aldrich and used after recrystallization from ethanol–water solution. Reversed-phase high-performance liquid chromatography (HPLC) analysis of the compound using a 10-cm × 4.6 mm I.D., 10-μm particle column revealed no resolvable impurities. Acetonitrile (HPLC grade) was obtained from MCB and Burdick & Jackson. Water was purified in-house using a Corning still (MP-1) and a Barnstead, four-cartridge Nanopure system. Decane and 1,2-ethanediol were obtained from Fisher and used without further purification. Polymeric C_8 and C_9 stationary phases were prepared in-house by reacting either *n*-octyltrichlorosilane or *n*-nonyltrichlorosilane with 10-μm irregular silica (Partisil-10) having a surface area of approximately 320 $m^2\ g^{-1}$ and a mean pore diameter of 9.6 nm before derivatization. The trichlorosilane reagents were obtained from Petrarch and used without further purification. The silica was stirred in water-saturated toluene for 2 h. After filtering, dry toluene and the silane reagent were added to the silica and refluxed for 2 h. Carbon loading of the resulting polymer phase was determined to be 8.4 and 7.5% for C_8 and C_9, respectively, by M-H-W Laboratories (Phoenix, AZ, U.S.A.).

Column preparation

The stationary phase was contained in a 43 × 1.5-mm I.D. precision bore quartz tube (Wilmad Glass). The quartz microcolumn was supported in a brass cuvette assembly. Both the cell and the packing procedure have been described in detail in earlier publications[15,20].

Before an experiment, the stationary phase was conditioned by passing large volumes of acetonitrile through the column (approximately 50 ml or 2000 column volumes) at a flow-rate of 1 ml min^{-1}. Pyrene was introduced to the column with acetonitrile–water (50:50, v/v) as the mobile phase. The concentration of pyrene in the mobile phase was adjusted to a value of *ca.* 3.0 μM, which gives a surface concentration low enough to avoid excimer formation (to assure that no probe–probe interactions are present) but high enough to emit a strong fluorescence signal with a small fraction of shot noise. When the pyrene concentration on the column reached equilibrium (as determined by a steady-state fluorescence signal), the mobile phase was changed to 100% water for the remainder of the experiment. The contributions to the fluorescence signal from pyrene in the mbile phase were extremely small due to the high capacity factor conditions for 100% water mobile phase conditions. Using *in situ* fluorescence measurement of the frontal elution of pyrene through a spectroscopic microcolumn, the capacity factor (k') for pyrene on a C_{18} phase has been measured to be $6.0 \cdot 10^3$ (refs. 21 and 22). While the lower carbon loading of the C_8 and C_9 stationary phases studied here would result in a factor of two smaller k', the mass fraction of pyrene in the mobile phase under these conditions would still be less than 0.1%.

Fluorescence measurements

Emission spectra of pyrene sorbed onto the stationary phase were measured at 2.5 nm resolution on a Farrand Model 201 spectrofluorimeter (Farrand Optical, New York, NY, U.S.A.). The excitation wavelength used through the experiment was 335 nm. Fluorescence emission spectra were recorded on a strip chart. To obtain a measure

of the stationary phase polarity, the intensity ratio of the third vibronic band to the highest energy, first band was calculated. The reported results were typically obtained from the average of seven spectra. At a particular temperature, the precision of the vibronic band intensity ratios was normally 0.3% relative standard deviation.

The brass cuvette, when placed in the spectrometer, was in thermal contact with a circulating fluid bath (Haake, Model L). The temperature of the cell could be set between 10 and 110°C (± 0.25°C) using a Haake temperature controller (Model D3). In a typical experiment, the column would be raised from 14 to 65°C and then cooled down to approximately 15°C. A series of spectra were recorded every 2.5–5.0°C when the temperature was being increased and every 5.0–15.0°C when the sample was cooling down. The magnitude of the temperature change between the series of spectra was determined by the behavior of the stationary phase; *i.e.* the rate of change of surface polarity. After a series of spectra at a particular temperature were recorded the system was allowed to reach the next temperature and kept there for 10 min to ensure satisfactory equilibration; during this period the solvent flow was discontinued. Aqueous moble phase at a flow-rate of 1.0 ml min^{-1} was then pumped through the column for 2 min to remove any released organic modifier. The flow-rate was reduced to 0.5 ml min^{-1} while the spectra were being recorded.

The temperature dependence of pyrene vibronic bands was also measured in free solution in four different solvents in a standard 1-cm quartz fluorescence cel (Wilmad Glass). The solvents used covered a wide range of polarity: decane, 1,2-ethanediol, acetonitrile and water. The conditions were the same as on-column experiments except

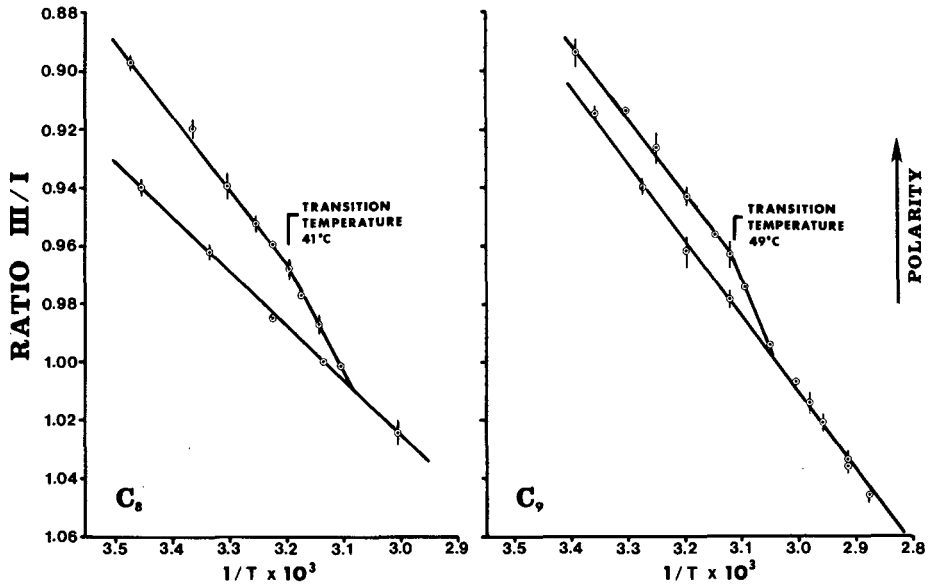

Fig. 1. Temperature-dependent stationary phase polarity as measured by the fluorescence vibronic band ratios of pyrene sorbed to C_8 and C_9 polymeric surfaces in contact with 100% aqueous mobile phase. Upper curve represents surface polarity immediately after preconditioning with acetonitrile. Lower curve represents surface polarity following temperature excursions above 41°C for C_8 and 49°C for C_9, respectively.

that the solution was not flowing. Spectra were obtained from 15 to 105°C for decane and 1,2-ethanediol, between 15 and 75°C for acetonitrile and between 15 and 95°C for water.

RESULTS AND DISCUSSION

Temperature dependence of stationary phase polarity

The effect of temperature (T) on the fluorescence vibronic band ratio of pyrene sorbed to a C_8 or C_9 polymeric surface in contact with water is plotted *versus* $1/T$ in Fig. 1 for comparision with the retention behavior. When the temperature of the stationary phase, preconditioned with acetonitrile, was being raised, the change in polarity of the surface was linear with $1/T$. This behavior was followed at a higher temperature, by a sigmoidal transition of the surface polarity towards less polar values. At still higher temperatures, the surface polarity again varied linearly with $1/T$. Upon cooling, the surface polarity increases with a linear dependence for temperatures as small as the initial conditions. Since the non-linear portion of the curve is not repeated, the stationary phase at the end of the experiment is less polar than at the beginning. The temperature where the surface polarity undergoes a non-linear change is dependent on the chain length of the surface-bound hydrocarbons. The temperatures characteristic of the on-set of this non-linear region are 41 and 49°C ($\pm$ 1°C) for the C_8 and C_9 polymeric surfaces, respectively.

Gilpin and co-workers[7,8,17] have noted a similar temperature dependence in the retention of phenol and resorcinol on C_8, C_9 and C_{10} stationary phases. Following preconditioning with pure organic modifier and elution with a totally aqueous mobile phase, increasing temperature causes the log of the capacity factor, ln k', to decrease linearly with $1/T$; at a chain length-dependent transition temperature ln k' undergoes a sigmoidal drop in magnitude. Following this transition, ln k' again varies linearly with $1/T$, along a line which is offset from the original temperature dependence. Two examples of the temperature dependent retention behavior of phenol and resorcinol from ref. 7 have been reproduced in Fig. 2, which allow the similarity between the retention data and the surface polarity to be compared (see Fig. 1). Further verification of the strong correlation between these two experiments is the agreement of the transition temperatures which were observed; the on-set temperatures for the non-linear decrease in ln k' were reported to be 40.7 and 51.8°C ($\pm$ 1.5°C) for the C_8 and C_9 stationary phases, respectively[7]. The transition temperatures for surface polarity and solute retention, therefore, agree within their uncertainty bounds.

Surface structural changes with temperature

The temperature-dependent hysteresis in surface polarity and solute retention appears to be related to the preconditioning with organic modifier, in this case acetonitrile. By collecting and analyzing fractions of the aqueous mobile phase following the transition temperature, Gilpin *et al.*[8] have showed that the conditioning solvent was initially retained in the alkyl layer and released upon heating. In interpreting this observation, however, the authors suggested that solvent retention is by physical entrapment and that its release was associated with a significant rearrangement of the alkyl chain conformation. They assert that the chains evolve from a "collapsed state" with "solvent entrapment within the bonded hydrocarbon

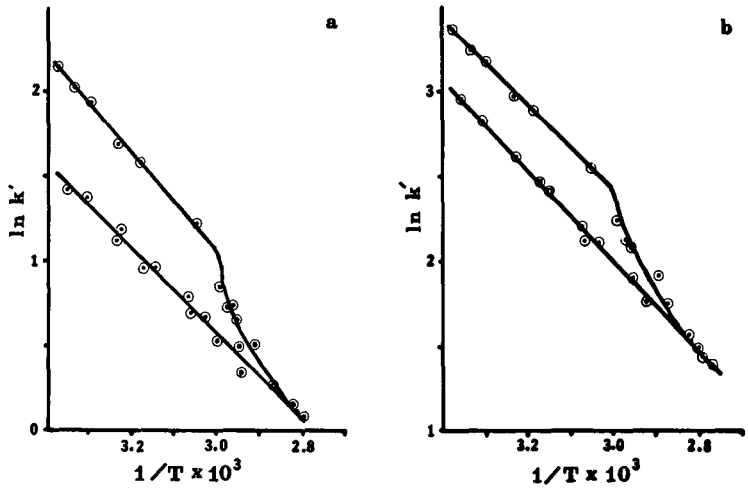

Fig. 2. Temperature-dependent retention of (a) phenol and (b) resorcinol on C_{10} polymeric reversed phases with 100% aqueous mobile phase; surfaces were preconditioned with acetonitrile. Data are replotted from Figs. 1c and 2c of ref. 7.

layer during formation" to a more stable, chain-extended or "bristle" configuration where "entrapped" conditioning solvent is released and replaced by water[8,17].

The surface polarity change indicated by sorbed pyrene fluorescence is consistent with the observed loss of conditioning solvent from the interface, but *not* with a chain conformation where alkyl ligands extend into the aqueous solution. Although less polar than water, the preconditioning solvent is considerably more polar than the bound hydrocarbonaceous ligands. Removal of solvent molecules from the bound layer would decrease the average polarity of the stationary phase as observed in the pyrene fluorescence. The irreversible decrease in polarity which takes place in the transition region can, therefore, be attributed to the departure of intercalated solvent from the stationary phase leaving a less polar environment. This interpretation is consistent with other spectroscopic studies of the effects of conditioning solvent on stationary phase environments[13,15,16]. On the other hand, the observed decrease in polarity upon heating confirms that the conditioning solvent is not replaced by water, at least in regions of the stationary phase occupied by a sorbed, hydrophobic solute. These results cast doubt about the existence of a extended chain or "bristle" configuration for the stationary phase layer under aqueous moble phase conditions. Instead, the surface environment both before and after the transition temperature appears to exist in a collapsed state[4], where environment differences are primarily determined by the presence or absence of the preconditioning solvent. This interpretation appears to be reasonable in terms of hydrophobic interactions between the hydrocarbon ligands and water, and the capability of amphiphilic molecules such as typical reversed-phase organic modifiers to reduce surface tension at hydrophobic layer–water and hydrophobic layer–silica interfaces.

In addition to the non-linear decrease in surface polarity accompanying the loss of conditioning solvent, a systematic lowering of the stationary phase polarity is observed as the system temperature is increased. This trend is observed both before

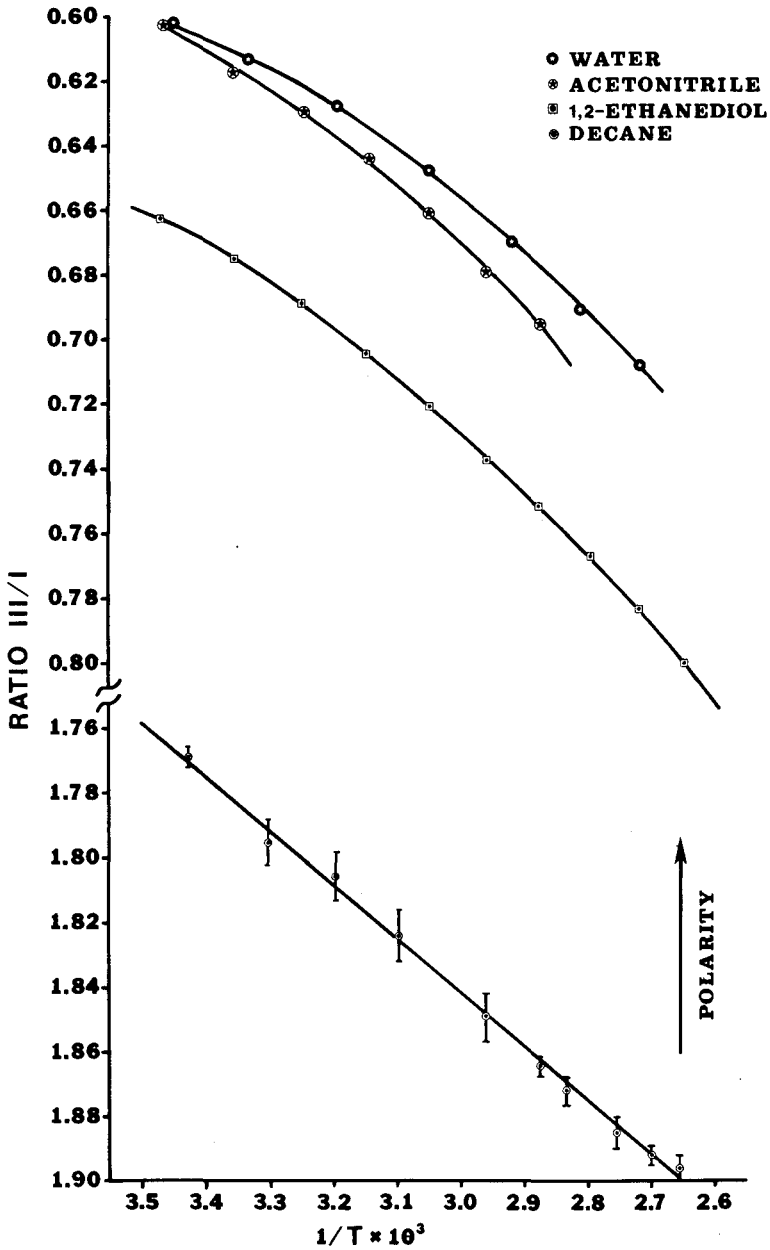

Fig. 3. Fluorescence vibronic band ratios of pyrene as a function of temperature in four solvents: water, acetonitrile, 1,2-ethanediol and decane. Precision of the data in the curves for water, acetonitrile and 1,2-ethanediol is about the size of the plotted points; reproducibility of the data in the decane is indicated by the error bars.

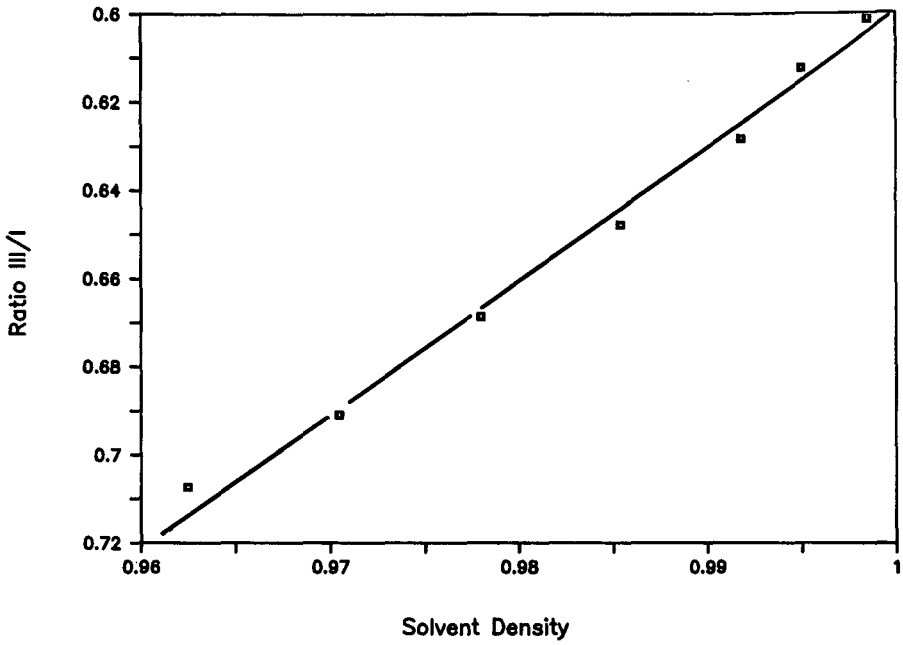

Fig. 4. Fluorescence vibronic band ratios of pyrene *versus* temperature-induced changes in the density of the solvent. The solvent is water, and the temperature range is identical to that shown in Fig. 3.

and after the loss of conditioning solvent at the interface. To better understand this trend, the effect of temperature on the vibronic band ratios of pyrene fluorescence was measured in four solvents of differing polarity, and the results are plotted in Fig. 3. For each of the solvents, a similar reduction in the environmental polarity of the probe is observed with increasing temperature. This trend would indicate a lowering of solvent-induced perturbations which are responsible for mixing the weak L_b transition, which dominates the highest energy vibronic band, with the much stronger L_a transition in pyrene[18,19]. The observed trends in polarity with temperature likely corresponds to the decrease in the density of the solvents at higher temperature temperature. The reduction in density would effectively increase the size of the solvent cage or the free volume of the solvent and thereby increase the average distance between pyrene and its perturbing neighbors, the final result being a decrease in the dielectric constant of the probe's immediate surroundings.

The density dependence of the vibronic band ratios for pyrene fluorescence has been included in an empirical response model by Stahlberg and Almgren[14] where the III to I intensity ratio of pyrene in a solvent was found to correlate well with the solvent's dipole moment divided by its molecular volume. This model also appears to be valid for temperature-induced changes in solvent density as shown in Fig. 4, where the III to I ratio of pyrene in water varies linearly with density over the same temperature range as the data in Fig. 3. A similar decrease in the apparent dielectric constant with increasing temperature is also observed in both sets of stationary phase data. The slopes of the surface environment curves in Fig. 1 are of the same magnitude

as the slopes of the free solution curves in Fig. 3. While the stationary phase layer would not duplicate the behavior of free solution, the similarities in response are enough to suggest an analogy. The environment of pyrene sorbed to a polymeric stationary phase responds to a change in temperature in a manner analogous to thermal expansion of a bulk solvent. Studies of the temperature dependence of monomeric stationary phases[23], on the other hand, reveal quite different behavior for these surfaces, where little sensitivity to temperature change is observed following loss of conditioning solvent. The lack of a response to temperature for the monomeric stationary phase is consistent with a symmetry perturbation of pyrene's excited states which is interfacial in nature and thus depends less significantly on the density of its surroundings. If differences in this behavior are similarly interpreted, then the slope of the C_9 polymer stationary phase temperature dependence being steeper than C_8 in Fig. 1 could relate to how much of the probe's environment is of bulk *versus* interfacial character. Differences in the temperature dependence of surface environments, therefore, appear to carry information about surface structures and sorption mechanisms. More complete discussion of these issues follows in a separate article[23].

Organic modifier in alkylated silica environments

The lowering of the polarity of C_8 and C_9 stationary phases upon loss of conditioning solvent provides strong evidence that the surface structure does not evolve from a collapsed to an extended configuration upon heating. As a result, a mechanism other than "physical entrapment" for the retention and loss of the conditioning solvent must be considered. Regardless of changes in alkyl chain conformation, physical entrapment of organic solvent by an alkyl layer is not a likely mechanism for solvent retention because of molecular diffusion. Taking the viscosity of the stationary phase from excimer formation rates to be 19 cP (ref. 24)[a], and the thickness of the hydrocarbon layer to be less than 2.0 nm, diffusion rates through the alkyl layer are fast. Even if the solubility of organic solvent in the hydrocarbonaceous overlayer were only 0.01% of its concentration at the underlying silica surface, the diffusion rate calculated from this viscosity and solubility reveals that more than 99% of "trapped" organic solvent would diffuse from the stationary phase into the mobile phase in less than 1 ms. Even if transport of the solvent through the stationary phase were as slow as molecular diffusion through a crystalline hydrocarbon solid[26], trapped solvent would still be released in less than 1 s. Physical entrapment, therefore, cannot account for solvent retention in the stationary phase, independent of changes in ligand conformation.

Another mechanism which could account for the retention of an amphiphilic solvent under these conditions relates to the reduction in surface tension of the alkyl chain–water interface and possibly the alkyl chain–surface silanol interface. The addition of mutually miscible solvent molecules at these interfaces lowers the surface free energy, and interfacial excess concentrations are, therefore, selectively adsorbed[27]. If this process were a simple two-phase adsorption equilibrium, however, the lack of organic modifier in the totally aqueous mobile phase would cause its slow but

[a] More recent studies using pressure jump and nuclear magnetic resonance relaxation methods place the value closer to 2 cP (ref. 25).

eventual loss from the stationary phase for any finite values of the adsorption equilibrium constant. An abrupt decrease in the concentration of retained solvent upon increasing the temperature could only arise if the enthalpy of adsorption were unrealistically large in magnitude.

These two observations, the stable retention of organic solvent and the well-defined temperature at which the solvent is lost from the surface phase, strongly suggest ordering of the solvated interface. While the irregular, porous structure of the underlying silica substrate would prevent long-range order of bound ligands, nevertheless, short-range ordering of alkyl chains and intercalated solvent could support a stable, nematic phase which minimizes the surface energy. An analogy could be drawn between the short-range order of these bonded chains and the local intramolecular ordering of polymer molecules containing relatively long, linear side-chains; in free solution, these macromolecules have no long-range orientational order as in the porous silica matrix, but there exists strong correlation in the conformations of neighboring side-chains[28]. Above a particular temperature, one would expect such a system to exhibit a nematic–isotropic phase transition where conformational order is lost together with, in this case, the intercalated solvent.

Considerable evidence exists in polymeric reversed-phase chromatographic materials for surface structures which have local conformational order. In Gilpin and Squires' pioneering observations[7] of temperature dependent retention hysteresis in C_8, C_9 and C_{10} phases, it was found that observation of the hysteresis required a significant surface coverage by alkyl chains, and that the magnitude of the hysteresis increased dramatically with increasing carbon percentage above a critical coverage. Studies of the effects of temperature on densely-grafted C_{22} (ref. 29) and C_{28} (ref. 30) polymer phases showed similar, persistent effects of conditioning solvent on elution with aqueous mobile phase and temperature-dependent hysteresis in retention.

Wise and co-workers[11,12,31] have showed that C_{18}, polymer stationary phases grafted at high-carbon loadings on large-pore silica supports produce unusually large selectivity for planar solutes compared to monomeric phases; drawing on an analogy to retention on liquid crystalline phases in gas chromatography, they conclude that such polymeric phases are considerably more "ordered". The relationship between the observed selectivity and the pore diameter of the substrate argues for conformational order over a significant range. Such ordering also requires a high density of alkyl ligands with a surface configuration produced by polymeric bonding of the phase. Similar conclusions can be drawn from a comparison of the temperature-dependent retention and sorption environment hysteresis in C_6, C_7 and C_8 monomeric stationary phases, where *neither* the persistent retention of conditioning solvent nor a distinct transition temperature for its accelerated loss are observed[23].

From differences in solute retention[7] as shown in Fig. 2, stationary phase affinity for solutes is affected by the retention of solvent. Since the mobile phase is identical for both upper and lower curves of Fig. 2, differences in retention (after correcting for changes in the phase volume ratio) reflect only changes in the partial molar free energy of a solute in the stationary phase[29,30]. From the effects of the acetonitrile on the surface polarity, one might expect that the enthalpy of sorption of molecules such as phenol and resorcinol would be increased by the presence of acetonitrile the hydrocarbon layer. The slopes of the straight-line portions of the upper and lower curves of Fig. 2, however, do not differ from each other by more than the error of

estimation when fit to a linear equation[32]. The partial molar enthalpy of sorption of these molecules, therefore, does not change significantly upon loss of the conditioning solvent.

In contrast to the negligible differences in slope, in the intercepts of the straight-line portions of respective upper and lower curves of Fig. 2 are statistically distinguishable. The differences are equivalent to a lowering of the partial molar entropy of sorption by $-2.0 (\pm 1.0)$ cal. mol^{-1} K^{-1} not counting changes in the phase volume ratio. Using quantitative data for the amount of lost solvent[8], the carbon loading of the stationary phase and an estimate of its mass from the column size and packing method[7], the relative change in volume of the stationary phase due to loss of organic solvent is less than 5%, corresponding to a 2% gain in mobile phase volume. The resulting change in the phase ratio accounts for less than -0.2 cal mol^{-1} K^{-1} of the change in partial molar entropy of sorption upon loss of solvent.

The lowering of the sorption entropy upon loss of the preconditioning solvent supports the existence of a more ordered stationary phase in the presence of the adsorbed organic solvent. Under these conditions, the effect of a solute molecule in the stationary phase layer is to locally disrupt this order and to increase the overall entropy of the system. Above the transition temperature, when the conditioning solvent is lost, the effect of solute sorption on the stationary phase order is less and the partial molar entropy of sorption is lowered. Thus, thermodynamic data available from temperature-dependent retention of solutes also support the model of a structured, polymeric stationary phase layer in the presence of a conditioning solvent. Monomeric stationary phases, on the other hand, show distinctly different behavior, more characteristic of disordered structures; a comparative study of monomeric surfaces will consider the differences in more detail[23].

ACKNOWLEDGEMENTS

This work was supported in part by the Office of Naval Research. Fellowship funds (to J.M.H.) from the Alfred P. Sloan Foundation are also acknowledged.

REFERENCES

1 Cs. Horváth, W. Melander and I. Molnár, *J. Chromatogr.*, 125 (1976) 129.
2 B. Karger, J. R. Grant, A. Hartkopf and P. Welner, *J. Chromatogr.*, 128 (1976) 65.
3 H. Hemetsberger, W. Maasfeld and H. Ricken, *Chromatographia*, 9 (1976) 303.
4 C. H. Lochmüller and D. R. Wilder, *J. Chromatogr. Sci.*, 17 (1979) 574.
5 R. P. W. Scott and C. F. Simpson, *J. Chromatogr.*, 197 (1980) 11.
6 R. M. McCormick and B. L. Karger, *J. Chromatogr.*, 199 (1980) 259.
7 R. K. Gilpin and J. A. Squires, *J. Chromatogr. Sci.*, 19 (1981) 195.
8 R. K. Gilpin, M. E. Gangoda and A. E. Krishen, *J. Chromatogr. Sci.*, 10 (1982) 345.
9 C. R. Yonker, T. A. Zwier and M. F. Burke, *J. Chromatogr.*, 241 (1982) 257.
10 D. Morel and J. Serpinet, *J. Chromatogr.*, 248 (1982) 231.
11 S. A. Wise and W. E. May, *Anal. Chem.*, 55 (1983) 1479.
12 S. A. Wise and L. C. Sander, *J. High Resolut. Chromatogr. Chromatogr. Commun.*, 8 (1985) 248.
13 C. H. Lochmüller, D. B. Marshall and D. R. Wilder, *Anal. Chim. Acta*, 130 (1981) 31.
14 J. Stahlberg and M. Almgren, *Anal. Chem.*, 57 (1985) 817.
15 J. W. Carr and J. M. Harris, *Anal. Chem.*, 58 (1986) 626.
16 J. W. Carr and J. M. Harris, *Anal. Chem.*, 59 (1987) 2546.
17 S. S. Yang and R. K. Gilpin, *J. Chromatogr.*, 394 (1987) 295.

18 D. C. Dong and M. W. Winnik, *Photochem. Photobiol.*, 35 (1984) 17.
19 F. W. Langkilde, E. W. Thulstup and J. Michl, *J. Chem. Phys.*, 78 (1983) 3372.
20 C. H. Lochmüller, A. S. Colborn, M. L. Hunnicutt and J. M. Harris, *Anal. Chem.*, 55 (1983) 1344.
21 J. W. Carr and J. M. Harris, *Anal. Chem.*, 60 (1988) 698.
22 J. W. Carr, *Ph.D. Dissertation*, University of Utah, Salt Lake City, UT. 1986.
23 J. W. Carr, A. J. Rauckhorst and J. M. Harris, *J. Chromatogr.*, submitted for publication.
24 R. G. Bogar, J. C. Thomas and J. B. Callis, *Anal. Chem.*, 56 (1984) 1080.
25 D. B. Marshall, University of Utah, Salt Lake City, UT, personal communication.
26 A. V. Chadwick, in F. Beniere and C. R. Catlow (Editors), *Mass Transport in Solids*, Plenum Press, New York, 1983, pp. 285–320.
27 J. J. Kipling, *Adsorption from Solutions of Non-Electrolytes*, Academic Press, New York, 1965, Ch. 10 and 14.
28 V. N. Tsvetkov, E. I. Rjumtsev and I. N. Shtennikova, in A. Blumstein (Editor), *Liquid Crystalline Order in Polymers*, Academic Press, New York, 1978, Ch. 2.
29 D. Morel and J. Serpinet, *J. Chromatogr.*, 248 (1982) 241.
30 W. E. Hammers and P. B. A. Verschoor, *J. Chromatogr.*, 282 (1983) 41.
31 L. C. Sander and S. A. Wise, *J. Chromatogr.*, 316 (1984) 163.
32 N. R. Draper and H. Smith, *Applied Regression Analysis*, Wiley, New York, 2nd ed., 1981, Ch. 2.

Journal of Chromatography, 481 (1989) 147–157
Elsevier Science Publishers B.V., Amsterdam — Printed in The Netherlands

CHROM. 21 733

PERFORMANCE OF POLYMER-COATED SILICA C_{18} PACKING MATERIALS PREPARED FROM HIGH-PURITY SILICA GEL

THE SUPPRESSION OF UNDESIRABLE SECONDARY RETENTION PROCESSES

YUTAKA OHTSU*, YOSHIHIRO SHIOJIMA, TATSUYA OKUMURA, JUN-ICHI KOYAMA, KIYOSHI NAKAMURA and OKITSUGU NAKATA

Shiseido Toxicological and Analytical Research Center, 1050 Nippa-Cho, Kohoku-ku, Yokohama 223 (Japan)

and

KAZUHIRO KIMATA and NOBUO TANAKA

Kyoto Institute of Technology, Department of Polymer Science and Engineering, Matsugasaki, Sakyo-ku, Kyoto 606 (Japan)

(First received May 22nd, 1989; revised manuscript received June 27th, 1989)

SUMMARY

Coating with silicone polymer of silica surfaces was shown to be very effective in suppressing the undesirable peak tailing in reversed-phase liquid chromatography caused by hydrogen bonding, ion-exchange and chelate formation processes. Silica particles containing various amounts of metal impurities were derivatized to octadecylsilylated (ODS) silica phases with or without subsequent trimethylsilylation, and to a polymer-coated phase with subsequent introduction of octadecyl groups. The performance of endcapped ODS phases prepared from high-purity silica gel was satisfactory for hydrogen-bond acceptors and protonated amines, but not acceptable for chelating compounds. The extent of tailing seen with chelating compounds depends on the solute structure and the metal content of silica particles. Coating with silicone polymer was more effective than trimethylsilylation of ODS phases for the suppression of tailing for chelating compounds, and afforded alkyl-bonded silica packing materials free from undesirable secondary effects by using metal-free silica particles.

INTRODUCTION

Alkylsilylated silica packing materials such as octadecylsilylated silica gels are used for the separation of a wide range of substances in reversed-phase liquid chromatography (RPLC). These stationary phases, however, sometimes give poor results for compounds containing a protonated amino group, a chelating group or a group capable of forming an hydrogen bond. Improvements have been made in the prep-

0021-9673/89/$03.50

aration procedure of RPLC packing materials to eliminate the secondary effects and to enhance the performance of alkylsilylated silica packing materials.

The complexities of silica surface composition have been pointed out[1–8]. The undesirable stationary phase effects were attributed to neutral silanols[9–11], metal impurities[3,12,13] and ion-exchange sites existing on the silica surfaces[2]. The ion-exchange sites can be provided by the dissociation of silanols, especially those of higher acidity than ordinary silanols[4–7,14] or they can be related to metal impurities in silica structures[13].

Kohler *et al.*[14] reported the better surface coverage and the longer life of the stationary phase when chemical bonding is carried out after full hydroxylation of silica surfaces. Thus they showed the possibility of achieving an optimized stationary phase by applying a dense surface coverage on a fully hydroxylated silica gel with a minimum amount of metal impurities.

The current status of silica-based packing materials was recently reviewed by Nawrocki and Buszewski[6] who showed examples of so-called silanol effects and the effect of metal impurities. Some commercially available silica C_{18} packing materials exhibit such problems[15–22]. The utilization of silanol effects for achieving separation is sometimes recommended[10,23]. In general, however, the presence of secondary effects is not desirable for both column efficiency and stationary phase stability.

The importance of stationary phase optimization for RPLC is increasing, because of the increasing demand for separations of substances of biological importance. The separations of these substances often require optimized stationary phases without secondary retention as well as severe separation conditions which sometimes decompose silica-based packing materials. Although some of the undesirable effects may be avoided by using so-called silanol blocking reagents such as amines, there still remain problems due to the complicated mobile phase and irreproducible retention.

Here we report a comparison of the methods of preparation of C_{18}-type silica packing materials with respect to their performance for solutes which are known to interact with silanols, ion-exchange sites or metals. A silicone-polymer coating was found to be more effective in shielding the secondary retention processes than conventional ODS phases with endcapping. The use of pure silica gel with a minimum amount of metal impurities along with polymer coating resulted in a stationary phase that enabled facile elution of protonated amines and chelating compounds.

EXPERIMENTAL

The HPLC system consisted of an LC-6A pump, SPD-6A UV detector and CR-3A data processor (all from Shimadzu, Kyoto, Japan). The column temperature was maintained at 30°C with a water-bath.

Two silica gel batches (particle size 5 μm; Shiseido, Tokyo, Japan) were employed; one (S-I) contained a considerable amount of metal impurities, and the other (S-III) was one of the purest silica gels available. S-III was prepared similary to S-I, after the purification of sodium silicate. S-I and S-III silicas were treated with 2 *M* hydrochloric acid at reflux-temperature for 16 h to produce silica gels of much lower metal contents, S-II and S-IV, respectively.

The metal contents of silica particles were examined by inductively coupled plasma-atomic emission spectrometry (Jobin Ivon, Longjumeau, France). The sur-

face areas and pore size distributions of silica particles were measured with a nitrogen sorption system, Autosorb I (Quantachrome, Syosset, NY, U.S.A.). The pH of silica particles was measured as a 1% (w/w) suspension in water, as described by Engelhardt and Muller[24].

Octadecylsilylation and trimethylsilylation (endcapping) were carried out as described previously[25]. Maximum coverages with octadecylsilyl groups were achieved by repeating the octadecylsilylation (the stationary phases are abbreviated as ODS), and the resulting ODS phases were further trimethylsilylated to produce the ODS-TMS phases. Coating with silicone polymer and subsequent introduction of octadecyl groups were carried out, as previously reported for commercially available Capcellpak C_{18}, to produce polymer-coated C_{18} (PC-C_{18}) phases[26]. Each packing material was packed into a stainless-steel column (10 cm × 4.6 mm I.D.).

The solutes employed in this study to illustrate the contribution of secondary effects include caffeine and theophylline for the hydrogen-bonding effect of neutral silanols, amines including aniline, N-methylaniline and N,N-dimethylaniline, procainamide (PA) and N-acetylprocainamide (NAPA) for the ion-exchange effect. Solutes such as acetylacetone and 8-quinolinol which can form chelates with metals were also used. The structures of some of the solutes are shown in Fig. 1.

The mobile phases were methanol–water mixtures, with buffers for the study of ion-exchange effects and chelate formation. The retention time of uracil was used as dead time t_0. Although uracil is slightly retained in a mobile phase of low methanol content, it has essentially no effects on the comparisons among the stationary phases.

RESULTS AND DISCUSSION

Silica particles and chemical bonding

The surface properties of silica gels and their metal contents are listed in Table I. Acid treatment of silica particles S-I and S-III removes a considerable portion of metal impurities, but not completely, with little effects on the surface area and pore size parameters. Repeated acid treatment of S-II did not reduce the metal content significantly. The remaining metals are supposed to be embedded in the silica structure. The pH value of S-II was lower than that of S-I, implying that silanol metal salts were converted into neutral silanols. The pH values of silicas with low metal contents, S-III and S-IV, were similar to each other. Acid treatment of S-III afforded an extremely pure silica gel, S-IV.

These four kinds of silica gels were derivatized to ODS, ODS-TMS and PC-C_{18}, in order to compare how the purities of silica gel and the chemical bonding method affect the appearance of the secondary retention processes in RPLC. Octadecylsilyla-

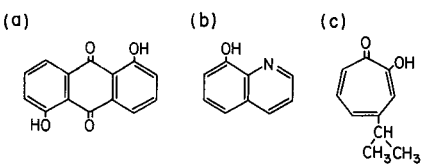

Fig. 1. Structures of solutes capable of chelate formation. (a) 1,5-Dihydroxyanthraquinone, (b) 8-quinolinol, (c) hinokitiol.

TABLE I

PROPERTIES OF SILICA GELS USED

Silica	*Pore diameter (Å)*	*Pore volume (ml/g)*	*Surface area (m^2/g)*	*pH*[a]	*Metal content (ppm)*[b]							
					Na	*Mg*	*Al*	*K*	*Ca*	*Ti*	*Fe*	*Zr*
S-I	134	0.83	273	7.1	308	11	264	42	16	230	154	11
S-II	132	0.86	286	4.9	0	8	188	0	13	162	33	13
S-III	108	0.76	307	5.2	6	0.1	8	0	1	10	15	3
S-IV	113	0.76	281	5.2	0	0	6	0	0	7	1	3

[a] pH of suspension in water.
[b] Other metals were not found in 10 ppm for S-I.

tion was repeated twice under conditions that would achieve maximum surface coverages as reported previously[25]. The surface coverages of the ODS phases, lower than those reported as maximal, may imply the abundance of much smaller pores than average in silica gel.

The first step of the preparation of PC-C_{18} includes the polymerization of 1,3,5,7-tetramethylcyclotetrasiloxane on the silica surface followed by the introduction of octadecyl groups in the presence of a soluble platinum catalyst[26]. Table II lists the carbon contents of the bonded phases. Although the increases in carbon content from silicone polymer-coated silica to PC-C_{18} were similar to those associated with octadecylsilylation, PC-C_{18} phases from pure silicas contained slightly less octadecyl groups than those from silicas with metal impurities prepared under the same reaction conditions.

TABLE II

CARBON CONTENTS OF ALKYLSILYLATED SILICA GEL

Stationary phase	*Silica gel*	*Carbon content (%)*	*Surface coverage (μmol/m^2)*
ODS	S-I	13.63	2.5
	S-II	13.48	2.4
	S-III	14.58	2.4
	S-IV	14.29	2.6
ODS-TMS	S-I	14.47	–
	S-II	14.67	–
	S-III	14.73	–
	S-IV	14.46	–
PC-C_{18}[a]	S-I	15.74	–
	S-II	13.85	–
	S-III	12.64	–
	S-IV	12.32	–

[a] Increases in carbon content associated with octadecylation are listed, after the polymer coating which resulted in *ca.* 2% carbon contents in each stationary phase.

Hydrogen-bonding effect

The effect of neutral silanols on retention via hydrogen bonding is clearly seen with caffeine as a solute[21]. Caffeine does not have a formal charge in methanol–water mobile phases, but possesses functional groups capable of hydrogen bonding. A correlation between the retention of polar compounds on various C_{18} phases in non-polar eluents in normal-phase mode and the retention of caffeine in reversed-phase mode has been reported[21].

As shown in Table III and in Fig. 2, ODS phases without endcapping resulted in strong retention of caffeine with peak tailing and loss of column efficiency regardless of the starting silica gel. Trimethylsilylation, or so-called endcapping, reduced the retention of caffeine with improvement in the peak shape, as seen with the ODS-TMS phases prepared from any of the silica packings, regardless of the pretreatment or the metal content. Polymer coating was as effective as trimethylsilylation in reducing the silanol effect via hydrogen bonding, although PC-C_{18} from S-IV silica showed a

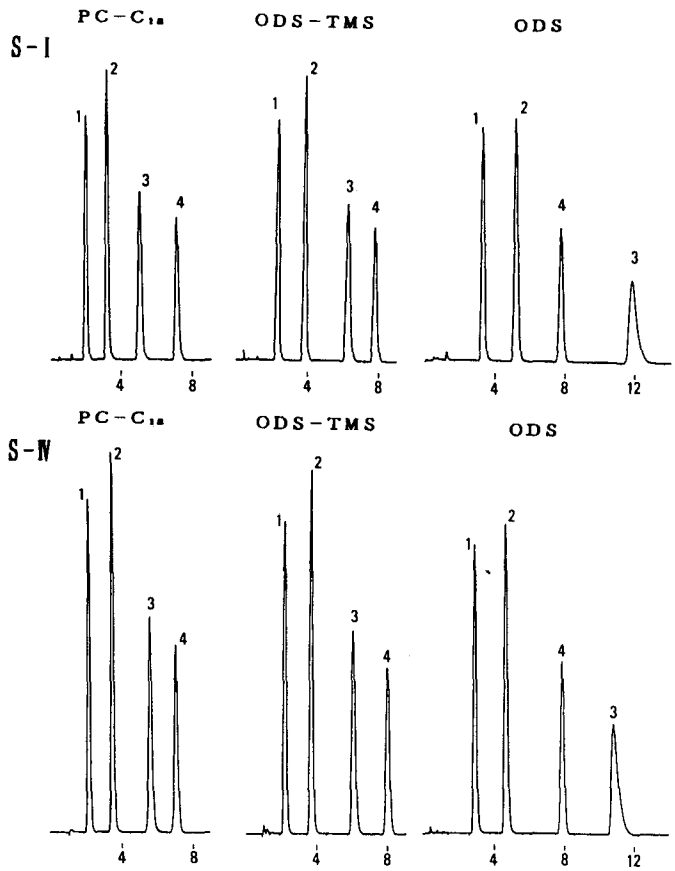

Fig. 2. The effect of the preparation method on the elution of hydrogen-bond acceptors. Mobile phase: methanol–water (20:80). Solutes 1 = theobromine; 2 = theophylline; 3 = caffeine; 4 = phenol. Flow-rate: 1 ml/min. Time scale in min.

TABLE III

RETENTION OF THEOPHYLLINE AND CAFFEINE INDICATING HYDROGEN BONDING

Stationary phase	*Starting silica gel*	*k'(α)*[a]	
		Theophylline	*Caffeine*
ODS	S-I	3.78 (0.61)	9.94 (1.61)
	S-II	4.16 (0.60)	10.7 (1.53)
	S-III	3.68 (0.55)	9.86 (1.47)
	S-IV	3.60 (0.53)	9.60 (1.42)
ODS-TMS	S-I	2.54 (0.41)	4.77 (0.77)
	S-II	2.77 (0.40)	5.46 (0.79)
	S-III	2.58 (0.38)	4.93 (0.73)
	S-IV	2.54 (0.38)	4.85 (0.72)
PC-C_{18}	S-I	2.18 (0.36)	4.03 (0.67)
	S-II	2.17 (0.38)	3.98 (0.69)
	S-III	2.31 (0.40)	4.18 (0.72)
	S-IV	2.50 (0.42)	4.60 (0.76)

[a] Mobile phase: methanol–water (20:80). The α values were calculated by dividing the capacity factor (k') of each compound by the k' value of phenol.

slightly larger $\alpha_{caffeine/phenol}$ value, reflecting the slightly lower surface density of octadecyl groups on this stationary phase.

Cation-exchange effect

As pointed out frequently, a serious secondary effect often termed as the "silanol effect" is observed with protonated amines as the solutes. Since silanols on the silica surface dissociate partially at neutral pH of the mobile phase, the ODS phases containing considerable amounts of residual silanols showed strong retention of protonated amines with severe tailing regardless of the batch of silica gel, as shown in Fig. 3. This is due to the slow ion-exchange process in the hydrophobic stationary phase.

Note that the packing material ODS-TMS from S-I silica showed tailing for PA and NAPA in Fig. 3 in spite of its good performance for caffeine in Fig. 2. The severe tailing with relatively small retention of the amines on ODS-TMS from S-I silica suggests that the slow ion-exchange process is taking place at a small number of ion-exchange sites. The poor accessibility of displacing ions to the ionic sites in hydrophobic stationary phase causes severe tailing[27], unless these ionic sites are completely shielded by the surface alkylsilyl groups. The ODS-TMS phases prepared similarly from S-II, S-III and S-IV silicas showed much better performance for the protonated amines at the neutral pH than the one from S-I silica. This suggests that the cation-exchange effect was not caused only by the participation of silanols.

PC-C_{18} from S-I silica showed much better performance than the corresponding ODS-TMS phase for PA and NAPA, which are alkylamines with pK_a above 9. Polymer coating seems to be more effective than endcapping of the ODS phases in shielding the secondary retention caused by the surface properties of silica gel.

As is the case with the performance of the ODS-TMS phase for PA and NAPA

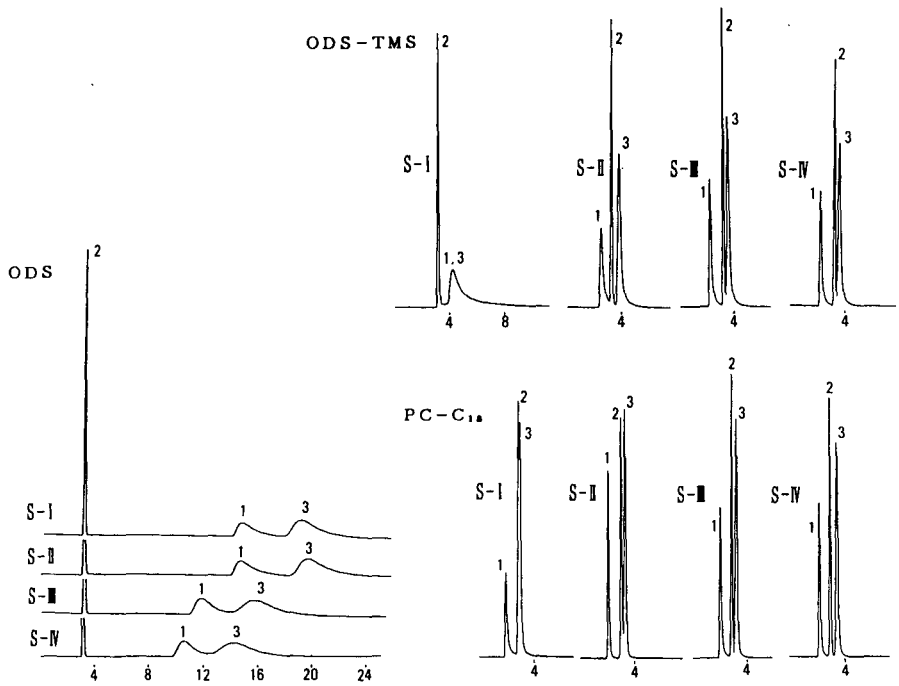

Fig. 3. Chromatograms of procainamide (PA) and N-acetylprocainamide (NAPA). Mobile phase: 0.02 *M* phosphate buffer–methanol (60:40), pH 7.6. Solutes: 1 = PA; 2 = phenol; 3 = NAPA. Flow-rate: 1 ml/min. Time scale in min.

at pH above 7, the results of amine elution at pH below 3 cannot simply be explained by the participation of ordinary silanols. At pH below 3, very few silanols should dissociate, because the pK_a of silica is reported[6] to be about 7.1. At the acidic pH values, the peak shapes of aniline derivatives having pK_a of 4–5 were worst on the ODS phase from S-I silica among the twelve stationary phases. Interestingly, the peak shape was much better on the ODS stationary phases prepared from S-II, S-III and S-IV silicas in this order, as shown in Fig. 4. This was also the case with ODS-TMS phases. It appears that the performance for protonated amines at acidic pH is related more to the amount of metals than to the number of silanols[21]. Note that all the ODS-TMS phases showed good performance for caffeine, implying the presence of few residual silanols, as shown in Fig. 2 and Table III.

As shown in Fig. 4, the ODS phases prepared from S-III and S-IV showed much better performance than those prepared from S-I and S-II in spite of the similar amount of residual silanols on these phases, as indicated by the similar hydrogen-bonding effects in Fig. 2 and the similar ion-exchange effects in Fig. 3 for all the ODS phases without endcapping. The results imply that ordinary silanols are not responsible; rather some other ion-exchange sites are responsible for the peak tailing of protonated amines at pH below 3. The ion-exchange sites can be provided by the presence of the metals[13] or silanols of higher acidity than ordinary silanols[4–7,14].

As simple acid treatment is reported to be inadequate to remove isolated sila-

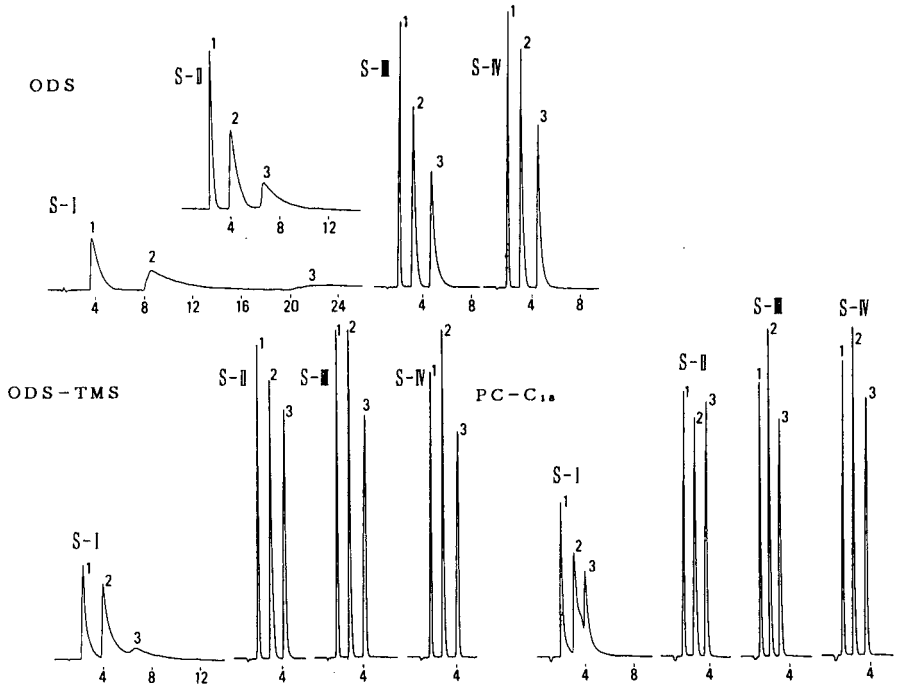

Fig. 4. Chromatograms of aniline derivatives. Mobile phase: 0.02 *M* phosphate buffer–methanol (95:5), pH 2.7. Solutes: 1 = aniline; 2 = N-methylaniline; 3 = N,N-dimethylaniline. Flow-rate: 1 ml/min. Time scale in min.

nols[14], the present results, revealing the better performance with acid-treated silica gels, seem to show that tailing of protonated amines at pH below 3 is related, al least partially, to the metal impurities on the silica surface. This is possible if the presence of metal impurities increases the acidity of silanols[13], or the acidity is provided on the basis of binary metal oxide structures[28,29]. Further studies are required to elucidate the source of the ion-exchange sites at acidic pH, whether they are provided by isolated silanols or by the presence of metal impurities.

The PC-C_{18} phase from any silica gel performed better than the corresponding ODS-TMS phase, indicating that polymer coating can shield the effect of ion-exchange sites on the silica surface more effectively than simple endcapping. Figge *et al.*[30] also reported an excellent performance of polymer-coated silica packing materials for basic substances.

Chelate formation

Verzele and Dewaele[31] reported that metal impurities in silica gel contributed to the peak tailing of carboxylic acids, based on the electrostatic interaction as well as chelate formation. The present results show that metal impurities give rise to the most serious secondary effect by chelate formation.

As shown in Fig. 5, ODS and ODS-TMS phases from S-I and S-II silicas did not give reasonable peak shape for solutes that form chelates, such as 1,5-dihydroxyan-

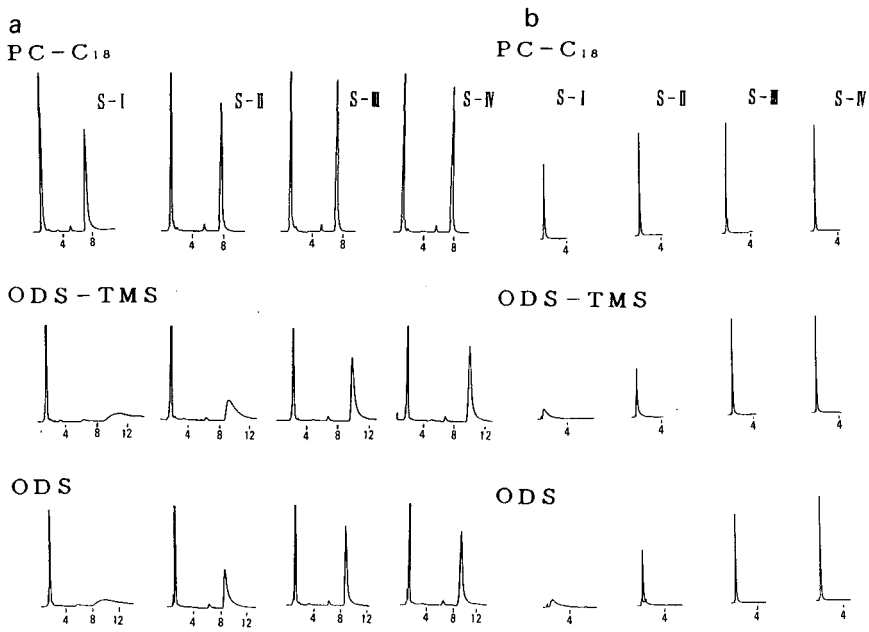

Fig. 5. Chromatograms of chelating compounds. (a) 1,5-Dihydroxyanthraquinone; (b) Acetylacetone. Mobile phase: 0.02 *M* phosphate buffer–methanol (30:70), pH 7.6. Flow-rate: 1 ml/min. Time scale in min.

thraquinone or acetylacetone. The ODS-TMS phases were not better than the ODS phases. This is understandable, because alkylsilylation reactions occur on the silanols and attached alkylsilyl groups cannot directly cover the metals which are supposed to be embedded in the silica structure. Note that undesirable peak tailing was related to the amount of metal impurities in silica gel. ODS and ODS-TMS phases prepared from S-III and S-IV silicas gave acceptable results. Here again the PC-C_{18} phase showed much better results than the corresponding ODS-TMS phase, indicating the better shielding of metal sites by the polymer layer.

The extent of peak distortion by chelate formation depends strongly on the type of solutes. Some of the worst examples can be seen in Fig. 6. Hinokitiol and 8-quinolinol were not eluted from any of the ODS and ODS-TMS phases as acceptable peaks. As hinokitiol does not contain any potentially basic nitrogen atoms, this solute specifically reveals the effect of chelate formation with surface metals, while those containing aromatic nitrogen atoms may interact with highly acidic silanols.

In the case of secondary retention processes in RPLC, very poor results were usually obtained when the solute possesses polar groups at only one part of the molecule able to interact with silica surface sites and the rest of the molecule is hydrophobic. When two pairs of polar groups are located at the opposite ends of the molecule, or when the molecule is not so hydrophobic, the effect of chelate formation is relatively small, as seen in Fig. 5.

Such a case is seen with the ion-exchange process in the chromatography of protonated amines. At pH below 3, PA and NAPA, with polar groups at both ends of the molecule, can be eluted without much peak tailing from ODS phases prepared

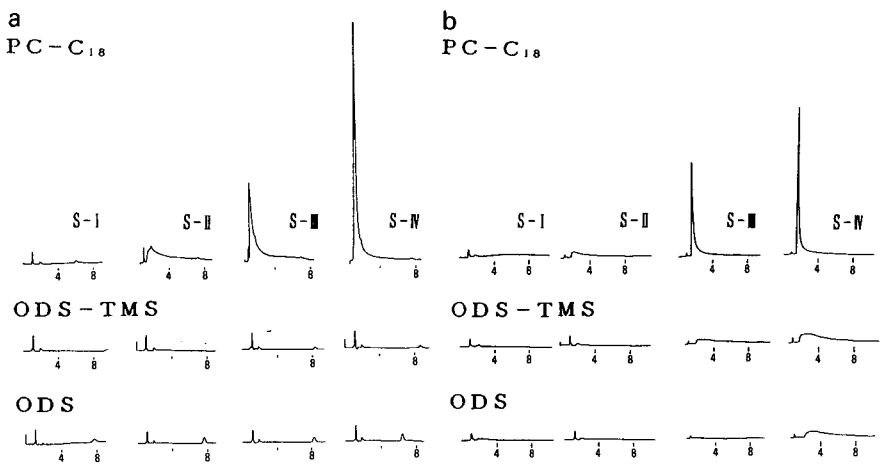

Fig. 6. Chromatograms of chelating compounds. (a) 4-Isopropylcycloheptatrienolone (hinokitiol); (b) 8-quinolinol. Mobile phase: 0.02 *M* phosphate buffer–methanol (30:70), pH 7.6. Flow-rate: 1 ml/min. Time scale in min.

from S-II, S-III and S-IV, whereas the peaks of aniline derivatives with a polar group at one end of the molecule were accompanied by tailing on these stationary phases at the same pH, as shown in Fig. 4. These observations are related to the stability of the ion pair or the chelate in the hydrophobic environment in the stationary phase. Localization of polar groups within a molecule causes an excessive secondary effect, if the interaction between the polar groups and the surface site on the silica is possible. The elution of solutes used in Fig. 6 represents the most sensitive test for stationary phases with respect to the presence and the shielding of metal impurities on alkylsilylated silica packing materials.

The results in Fig. 6 indicate that the polymer coating of silica gel containing a minimum amount of metal impurities and subsequent octadecylation seems to be the way to eliminate the most serious secondary effects of metal impurities in silica gel. Such stationary phases are free from the effects of hydrogen bonding with silanols, electrostatic interactions with ion-exchange sites and chelate formation with metal impurities, and are expected to be suitable for most separations in reversed-phase chromatography.

CONCLUSION

Coating with silicone polymer is more effective than trimethylsilylation of ODS phase, in suppressing the secondary retention processes in RPLC. A polymer-coated C_{18} phase prepared from silica gels with a minimum amount of metal impurities showed excellent performance for compounds known to interact with conventional silica-ODS stationary phases via hydrogen bonding, electrostatic interaction and chelate formation.

REFERENCES

1 K. K. Unger, *Porous Silica*, Elsevier, Amsterdam, 1979, Ch. 3.
2 S. G. Weber and W. G. Tramposch, *Anal. Chem.*, 55 (1983) 1771.
3 M. Verzele, M. De Potter and J. Ghysels, *J. High Resolut. Chromatogr. Chromatogr. Commun.*, 2 (1979) 151.
4 M. Mauss and H. Engelhardt, *J. Chromatogr.*, 371 (1986) 235.
5 J. Nawrocki, *J. Chromatogr.*, 407 (1987) 171.
6 J. Nawrocki and B. Buszewski, *J. Chromatogr.*, 449 (1988) 1.
7 J. Kohler and J. J. Kirkland, *J. Chromatogr.*, 385 (1987) 125.
8 G. B. Cox and R. W. Stout, *J. Chromatogr.*, 384 (1987) 315.
9 A. Nahum and C. Horvath, *J. Chromatogr.*, 203 (1981) 53.
10 K. E. Bij, Cs. Horváth, W. R. Melander and A. Nahum, *J. Chromatogr.*, 203 (1981) 65.
11 N. Tanaka, H. Goodell and B. L. Karger, *J. Chromatogr.*, 158 (1978) 233.
12 P. C. Sadek, P. W. Carr and L. W. Bowers, *J. Liq. Chromatogr.*, 8 (1985) 2369.
13 P. C. Sadek, C. J. Koester and L. D. Bowers, *J. Chromatogr. Sci.*, 25 (1987) 489.
14 K. Kohler, D. B. Chase, R. D. Farlee, A. J. Vega and J. J. Kirkland, *J. Chromatogr.*, 352 (1986) 275.
15 P. C. Sadek and P. W. Carr, *J. Chromatogr. Sci.*, 21 (1983) 314.
16 M. Verzele and C. Dewaele, *Chromatographia*, 18 (1984) 84.
17 M. J. Walters, *J. Assoc. Off. Anal. Chem.*, 70 (1987) 465.
18 B. Walczak, L. Morin-Allory, M. Lafosse, M. Dreux and J. R. Chretien, *J. Chromatogr.*, 395 (1987) 183.
19 E. Bayer and A. Paulus, *J. Chromatogr.*, 400 (1987) 1.
20 M. F. Delaney, A. N. Papas and M. J. Walters, *J. Chromatogr.*, 410 (1987) 31.
21 K. Kimata, K. Iwaguchi, S. Onishi, K. Jinno, R. Eksteen, K. Hosoya, M. Araki and N. Tanaka, *J. Chromatogr. Sci.*, in press.
22 Y. Ohtsu, unpublished results.
23 W. S. Hancock and J. T. Sparrow, *J. Chromatogr.*, 206 (1981) 71.
24 H. Engelhardt and H. Muller, *J. Chromatogr.*, 218 (1981) 395.
25 K. Jinno, S. Shimura, N. Tanaka, K. Kimata, J. C. Fetzer and W. R. Biggs, *Chromatographia*, 27 (1989) 285.
26 Y. Ohtsu, H. Fukui, T. Kanda, K. Nakamura, M. Nakano, O. Nakata and Y. Fujiyama, *Chromatographia*, 24 (1987) 380.
27 B. A. Bidlingmeyer, J. K. Del Rios and J. Korpi, *Anal. Chem.*, 54 (1982) 442.
28 C. L. Thomas, *Ind. Eng. Chem.*, 41 (1949) 2564.
29 K. Tanabe, T. Sumiyoshi, K. Shibata, T. Kiyoura and J. Kitagawa, *Bull. Chem. Soc. Jpn.*, 47 (1974) 1064.
30 H. Figge, A. Deege, J. Kohler and G. Schomburg, *J. Chromatogr.*, 351 (1986) 393.
31 M. Verzele and C. Dewaele, *J. Chromatogr.*, 217 (1981) 399.

Journal of Chromatography, 481 (1989) 159–174
Elsevier Science Publishers B.V., Amsterdam — Printed in The Netherlands

CHROM. 21 807

PREPARATION AND CHARACTERIZATION OF ADSORBENTS FOR USE IN HIGH-PERFORMANCE LIQUID AFFINITY CHROMATOGRAPHY

A. G. LIVINGSTON and H. A. CHASE*
Department of Chemical Engineering, University of Cambridge, Pembroke Street, Cambridge CB2 3RA (U.K.)
(First received March 21st, 1989; revised manuscript received July 20th, 1989)

SUMMARY

Adsorbents suitable for use in high-performance liquid chromatography were produced by covalently immobilizing Procion Blue MX-R to microporous silica. The adsorption capacities of the resulting materials were investigated. It was found that a Langmuir isotherm gave the best fit to data obtained for the adsorption of lactate dehydrogenase, while a Freundlich isotherm best described adsorpion of lysozyme. A 12-μm diameter silica with 28-nm diameter pores and a bound ligand concentration of 7 μmol (Procion Blue MX-R)/g (silica) had a capacity of 8.7 mg (lactate dehydrogenase)/g and 40.0 mg (lysozyme)/g. The rate of the overall adsorption process was found to be rapid. A model which assumes instantaneous equilibrium between solid and liquid phases was used to describe chromatography performed on these adsorbents. This gave a good approximation to the breakthrough and washout profiles.

INTRODUCTION

High-performance liquid affinity chromatography (HPLAC) is a technique that has been developed for the separation and purification of biomolecules. It combines the high specificity of affinity chromatography with the advantages of high-performance liquid chromatography (HPLC). A review of the technique has been presented by Larsson *et al.*[1]. Applications of HPLAC have been presented in papers by Clonis *et al.*[2], who used HPLAC for the process-scale purification of lactate dehydrogenase (LDH) from a crude extract, and by Chase[3], who showed that HPLAC can be used in monitoring various bioprocesses.

Adsorbents for HPLAC have to be rigid, to withstand the high pressure drops associated with a packed bed of small diameter particles without suffering from deformation. They must also present a high surface area for adsorption and have properties which allow suitable affinity ligands to be attached to their surface. Microporous silica has been used extensively as a solid phase as it meets the above criteria. Typical pore sizes range from 5 to 500 nm, and particle diameters from 2 to 20 μm. Protein diameters range from 2 to 25 nm, and so judicious choice of the silica

0021-9673/89/$03.50

properties ensures that the pore size will not hinder the diffusion of the proteins to the adsorpion sites. In addition, it is possible to modify the surface of the silica so that non-specific protein–adsorbent interactions due to charged groups are eliminated.

Ligands used in affinity chromatography can be chosen to be extremely specific, *e.g.* antibody–antigen systems. Such a choice results in a high degree of purification but suffers the drawback that once a packing material is prepared it is useful for only one type of separation. An alternative is to use "group-specific" ligands that mimic the behaviour of biomolecules. Triazine textile dyes such as Cibacron Blue F3G-A and Procion Blue MX-R have been found to engage in biospecific interactions with certain proteins[1,4]. These dyes can be attached to the surface of microporous silica and the resulting adsorbent used for a range of separations.

In this study Procion Blue MX-R is attached to the surface of microporous silica and the resulting adsorbents are characterized with regard to their capacity to bind lysozyme and lactate dehydrogenase. The effects of bound dye concentration, buffer ionic strength and pH on the equilibrium capacity are studied. The kinetics of this adsorption are investigated and a simple model is proposed to predict the breakthrough and washout profiles produced when lysozyme is applied to a column packed with adsorbent. Breakthrough profiles obtained under varying inlet lysozyme concentrations and varying column flow-rates are compared to predictions made using the simple model.

THEORY

Adsorption isotherms

An adsorption isotherm is used to characterize the capacity of an affinity adsorbent to bind protein[5]. It provides a relationship between the concentration of the protein in the bulk solution and the amount of protein adsorbed to the solid phase when the two phases are at equilibrium. Two types of adsorption isotherm are typically used in describing affinity systems. These are the:

Langmuir which assumes that the molecules are adsorbed at a fixed number of well defined sites each of which can only hold one molecule. These sites are also assumed to be energetically equivalent, and far enough apart on the surface so that there are no interactions between molecules adsorbed to adjacent sites. This results in the following relationship between equilibrium concentrations in the two phases (for definitions of symbols, see Symbols section at the end of the paper):

$$q^* = \frac{c^* q_{\max}}{K_d + c^*} \tag{1}$$

and *Freundlich* which is an empirical isotherm corresponding to the assumption that the enthalpy of adsorption varies exponentially among the available sites.

$$q^* = k(c^*)^n \tag{2}$$

Neither of these isotherms gives any information on the rate at which equilibrium is approached. It is possible to obtain the constants in the above equations from a series of batch experiments in which fixed quantities of adsorbent are allowed to reach equilibrium with varying amounts of protein[5].

Local equilibrium theory

It is desirable to be able to model the performance of fixed bed adsorption processes from the point of view of optimizing the process and also for scaling up purposes. The simplest model used to describe fixed bed adsorption assumes there are no mass transfer or kinetic limitations on the process. Thus the solute in the adsorbed and liquid phases reaches equilibrium instantaneously, and ignoring the effects of axial dispersion, the equation of motion for a chromatographic column is[6]

$$U_0 \frac{\partial c}{\partial z} + \varepsilon \frac{\partial c}{\partial t} + \rho_b \frac{\partial q}{\partial t} = 0 \tag{3}$$

This is a first-order partial differential equation and it can be shown[6] that concentration is constant along lines in the z–t plane given by

$$\frac{z}{t} = \frac{U_0}{\varepsilon + \rho_b f'(c)} \tag{4}$$

Where $f'(c)$ is dq^*/dc^*, the slope of the isotherm at the concentration of interest. This leads to the following results.

Adsorption. When a front of protein is applied to the column and the concentration of protein in the buffer leaving the bed is plotted as c/c_0 against a dimensionless throughput parameter Γ given by

$$\Gamma = \frac{Q\left(t - \frac{\varepsilon L}{U_0}\right)}{\rho_b q_0 V} \tag{5}$$

local equilibrium theory predicts a step change in c/c_0 from 0 to 1 when $\Gamma = 1$.

Washing. When protein-free buffer ($c = 0$) enters a saturated column ($c = c_0$) at time $t = 0$, the shape of the bed exit profile is governed by the shape of the isotherm describing the system. In this study the Freundlich isotherm describes the lysozyme–Procion Blue system used in the chromatographic runs, and for a Freundlich isotherm[7]

$$\frac{c}{c_0} = \frac{1}{c_0} \left[\frac{\left(\frac{U_0 t}{\varepsilon L} - 1\right)\varepsilon}{k n \rho_b} \right]^{\left(\frac{1}{1-n}\right)} \tag{6}$$

EXPERIMENTAL

Preparation of adsorbents

The adsorbents used in this work were prepared by attaching Procion Blue MX-R to microporous silica. All silicas used were supplied by Dr. K. Jones (Phase Separations, U.K.) whose assistance is gratefully acknowledged. Three separate batches of adsorbent were prepared. Henceforth these are referred to as adsorbents a, b and c, respectively. The first two of these were prepared by the authors as detailed

below. The silica used in preparing these was spherical, had a nominal pore size of 28 nm and a nominal diameter of 12 μm. The third was the gift of Y. Clonis and was prepared by a procedure which is detailed elsewhere[2]. This material had a particle diameter of 20 μm and a nominal pore size of 30 nm.

Adsorbent a. In order to silanize the surface of the silica, 10 g of silica was suspended in 100 ml of 0.01 *M* sodium acetate buffer, adjusted to pH 5.5 and containing 5% (v/v) 3-glycidoxypropyltrimethoxysilane (Aldrich, U.K.). This provides a silane in a four-fold excess to the amount stoichiometrically required for complete coverage of the silica surface, as recommended by Dean *et al.*[8]. The buffer was heated to 70°C, and the silane added followed immediately by the silica. The flask was placed in an ultrasonic bath for 3 min to remove air from the pores in the silica, and then placed in an oil bath at 90°C for 4 h. The silica was kept in suspension by stirring with a magnetic bar. The resulting epoxy silica was then washed with 500 ml water on a Buchner funnel through a Whatman filter paper and was then placed in a flask with 450 ml of 1 m*M* hydrochloric acid. The mixture was stirred at 90°C for 1 h to hydrolyse it to the corresponding diol. The diol-silica was then washed with 500 ml water followed by 500 ml acetone and placed in an oven (110°C) for 45 min. Procion Blue MX-R (2 g) was dissolved in 100 ml 0.1 *M* sodium bicarbonate and the diol-silica introduced to the flask. The suspension was sonicated for 2 min, then placed in an oil bath at 38°C for 18 h with an overhead stirrer to provide agitation. The blue silica was washed with water (500 ml) until the blue colour of the unbound dye was washed out, followed by 500 ml acetone prior to being dried in the oven. All steps were carried out at atmospheric pressure.

Adsorbent b. A 50-g amount of silica was prepared in this batch. The ratios of reagents (*i.e.* 10 ml/g for silanization and incubation, 0.2 g dye/g silica) were the same as for adsorbent a, except for hydrolysis (adsorbent a 45 ml/g, adsorbent b 20 ml/g). The times and temperatures of all the steps were the same as for adsorbent a. All reactions were carried out in a rotary evaporator flask rotating at 130 rpm and at atmospheric pressure.

Determination of bound ligand loading

Following the method of Lowe *et al.*[4] approximately 20-mg samples of adsorbent were weighed into test tubes. The silica was solubilized by adding 5 ml 1 *M* NaOH to each test tube and placing the test tubes in a water bath at 60°C for 30 min. The pH was then adjusted to 6–7 using 1 m*M* HCl and the solution volume made up to between 15 and 25 ml with water. The absorbance was measured at 620 nm against a blank prepared in the same fashion but using an unmodified silica. Assuming the molar extinction coefficient of Procion Blue MX-R is 10.5 ml mol^{-1} cm^{-1} (Clonis *et al.*[2]), the loading of bound ligand (μmol/g) can be found from

$$\frac{\text{Absorbance} \cdot \text{final volume (ml)}}{10.5 \text{ ml mol}^{-1} \text{ cm}^{-1} \cdot \text{mass of silica (g)}} \tag{7}$$

The molar extinction coefficient of Procion Blue MX-R is taken as 10.5 ml mol^{-1} cm^{-1} (Clonis *et al.*[2]).

Determination of diol content of diol-bonded silica

The diol content of the diol-bonded silica was determined following the modified periodate oxidation method outlined by Dean *et al.*[8].

Adsorbent capacities

A known mass of adsorbent was placed into buffer containing a known concentration of solute. The change in solute concentration (after allowing 1 h for equilibrium to be attained) can be equated to the amount of solute adsorbed by the solid, and by using varying starting solute concentrations, equilibrium data is obtained. When values of c^* *vs.* q^* have been obtained it is necessary to determine which theoretical isotherm best fits the data. For the Langmuir, a plot of c^*/q^* *vs.* c^* should yield a straight line with a slope of $1/q_{max}$ and with an intercept on the c^*-axis at $c^* = -K_d$. For the Freundlich, a plot of $\ln q^*$ *vs.* $\ln c^*$ should yield a straight line of slope n and intercept $\ln k$. Fitting straight lines to the transformed data using the method of least squares, it can be determined which theoretical isotherm gives the best fit to the experimental data.

The capacity of the adsorbent for two proteins was investigated; these were LDH and lysozyme.

Lactate dehydrogenase. Data were obtained using adsorbents a and c and both pure and crude extracts of LDH. Pure LDH was purchased from Boehringer (F.R.G.; product No. 127 876) and crude LDH from Sigma (U.S.A.; product No. L-2375). The desired concentration of the stock solution for the experiments was 300–400 units/ml of enzyme activity. (One unit will convert 1 μmol of phospho(enol)pyruvate to pyruvate per minute at pH 7.0 at 25°C.) This was obtained by dialysing 500 μl of pure or 1000 μl of crude enzyme at a ratio of 500:1 in 0.05 *M* pH 7.0 phosphate buffer overnight and making the extract up to a total volume of 2 ml.

Varying dilutions of the stock enzyme solution were added to 1.5 ml Eppendorf tubes containing approximately 0.02 g of adsorbent, keeping the total volume of solution at 400 μl. The samples were placed in a water bath at 20°C for 1 h, being removed at intervals to agitate and re-suspend the silica. For each experiment a control was carried out at half the concentration of the stock solution to check the enzyme suffered no loss of activity during the experiment. The Eppendorf tubes were then centrifuged, the supernatant removed, and the concentration of LDH determined by assaying enzyme activity.

LDH was assayed by following the reaction of pyruvate in the presence of NADH. An assay solution of 0.1 *M* phosphate buffer pH 7.0 containing 0.18 mg/ml NADH (nicotinamide–adenine dinucleotide, reduced; Boehringer) and 0.115 mg/ml sodium pyruvate (BDH, U.K.) and having an absorbance > 1.3 a.u. (path length 1 cm) was prepared. For each assay 50 μl of sample were added to 2.95 ml of assay solution and the absorbance monitored at a wavelength of 320 nm and 25°C on a Pye Unicam (U.K.) PU8160 kinetics spectrophotometer. Samples were diluted as necessary so that the decrease of absorbance with time could be followed accurately. The concentration of LDH in mg/ml is then calculated from:

$$c^* = \frac{\Delta A_{min} \cdot 3 \cdot \text{dilution}}{6.22 \cdot 655} \tag{8}$$

The molar extinction coefficient of NADH is 6220 l mol^{-1} cm^{-1}; the specific activity of pure LDH, measured from assays at 25°C, is 655 units/mg, and the adsorbent phase loading is then calculated from:

$$q^* = \frac{(c_{\text{initial}} - c^*) \cdot 0.4}{w} \tag{9}$$

Lysozyme. Known amounts (approximately 0.1 g) of adsorbent were weighed into 1.5 ml Eppendorf test tubes. Lysozyme (Sigma) solution in 0.05 *M* pH 7.0 phosphate buffer (except where stated) was prepared as a stock solution at 0.8 mg/ml and diluted to yield solutions at varying concentrations. Of each of these solutions 1 ml was added to an Eppendorf tube containing silica, 1 ml to an Eppendorf tube not containing silica to act as a control and for use in determining the calibration curve to relate optical density to lysozyme concentration. The tubes were placed in a water bath at 20°C for 1 h with agitation at regular intervals. The Eppendorf tubes were then centrifuged and the supernatant removed. These liquid samples were then diluted by factors between 7 and 15 and the absorbance measured at a wavelength of 280 nm using a 1-cm path length. Phosphate buffer was used as a blank and a calibration curve prepared from linear regression of the absorbance/concentration data provided by the control samples. The solid phase concentration was then calculated from:

$$q^* = \frac{(c_{\text{initial}} - c^*) \cdot 1.0}{w} \tag{10}$$

Adsorption kinetics

The equilibrium isotherms give no information on the rate of the adsorption reaction. The theoretical model used in this work assumes that equilibrium is instantaneously achieved between the two phases. In order to test whether the adsorption reaction is indeed fast enough for this assumption to be valid, batch tests to ascertain the rate of adsorption were undertaken.

Lactate dehydrogenase. A 800-μl volume of pure LDH was dialysed overnight in pH 7.0 0.05 *M* phosphate buffer and further diluted to a total volume of 5 ml after dialysis. Adsorbent a (0.5 g) was suspended in 15 ml of phosphate buffer and held in suspension by a magnetic stirrer in a 25 ml beaker surrounded by a water jacket at 25°C. At time zero the LDH solution was introduced into the beaker. Samples (50 μl) were taken at regular intervals, centrifuged and the supernatant removed and assayed for enzyme activity, as described earlier.

Lysozyme. A 40-ml volume of 0.05 *M* pH 7.0 phosphate buffer containing 1 mg/ml of lysozyme was agitated using a magnetic stirrer. Adsorbent b (2 g) was suspended in 10 ml of the same buffer and added to the beaker at time zero. Samples were removed using syringes with filters attached so that no centrifuging was necessary. The absorbance was measured at 280 nm and the concentration of lysozyme in the liquid phase determined.

Chromatographic performance

Affinity chromatography was studied using a column packed with adsorbent b

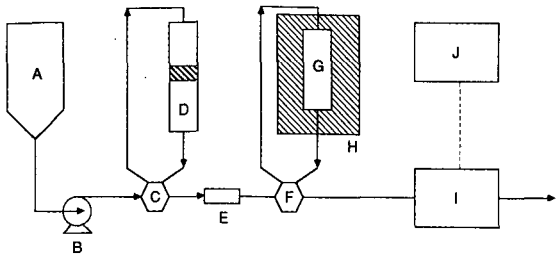

Fig. 1. Chromatography apparatus. A = Buffer reservoir; B = pump; C = valve; D = sample loop; E = guard column; F = valve; G = column; H = water bath; I = spectrophotometer; J = microcomputer. ——— = Fluid flows; – – – – = data flow.

and lysozyme as a solute. Breakthrough profiles were obtained when a front of protein was applied to the column and washout profiles were obtained when protein free buffer was applied to a protein saturated column.

Apparatus. A diagram of the apparatus is shown in Fig. 1. Two sample injection valves were used to divert the flow to the sample loop and column as required. It was necessary to use a sample loop to forestall problems associated the passage of protein through the pump and resulting in fouling onto the internal valves. The sample loop was designed and constructed by the authors and consisted of a 1.6 cm I.D. stainless-steel pipe approximately 40 cm long (Fig. 2) with a working volume of 70 ml. An internal piston separates the protein and buffer and has a length of polished steel

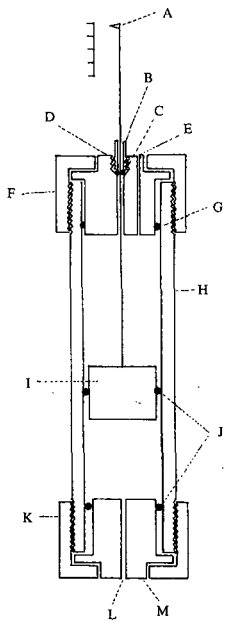

Fig. 2. Sample loop used for applying protein to column. A = Indicator; B = sealing nut; C = "O"-ring seal; D = end piece; E = liquid entry; F = retaining cap; G = "O"-ring seal; H = 16 mm I.D. stainless-steel tube; I = piston; J = "O"-ring seal; K = retaining cap; L = liquid exit; M = end piece.

wire attached which protrudes from the sample loop and acts as an indicator of the piston position. An "O"-ring seal prevents the protein and buffer from mixing. As buffer is pumped behind the piston, it moves down the tube and forces the liquid ahead of it out and through the column.

The column was 0.86 cm in diameter and 5.86 cm long, giving a volume of 3.4 ml. The cell used in the spectrophotometer was a low-volume HPLC type designed to give minimal dispersion. Tubing throughout the system was 0.76 mm I.D. HPLC tubing.

Packing columns. In preparation for column packing, adsorbent (3 g) was slurried in 75 ml of methanol ("Hipersolve", BDH, U.K.), sonicated for 5 min to remove air and then poured into a packing bomb. The column (with a frit at one end) was screwed onto the bomb and an upward flow of methanol was maintained through the column at sequential backpressures of 1500, 2500 and 3000 p.s.i. for periods of 5 min each. The column was removed, the cake adhering to the end was broken off and packed down smoothly with a spatula, and a frit screwed on. The mass of silica initially slurried was measured, and the mass of silica not packed into the column at the end of the packing process was also determined. The difference between these two figures gives the mass of silica packed into the column. Thus the bulk density was determined as 0.44 g/ml.

Column runs. All buffers used in the column experiments were filtered through a 0.22-μm filter and then degassed under vacuum. The column was suspended in a water bath at 20°C. All runs were carried out using 0.05 *M* phosphate buffer. At the end of each run the column was eluted with 1 *M* KCl solution to ensure that the protein was completely removed before the next run.

Column void volume. The system delay due to the volume of tubing, valves and guard column, *i.e.* the time delay between switching valve 1 to pump through the sample loop and the spectrophotometer registering an increase in concentration, was estimated using runs where the column was bypassed. The additional dead time due to the tubing between the column and valve 2 was added to this delay time.

The column void volume is an important parameter and occurs in eqns. 3–6. It was estimated in this work by three separate methods:

(1) When 1 *M* KCl is applied to a loaded column containing adsorbed protein the affinity interaction is greatly reduced and protein is desorbed from the column. The time lag between salt being applied to the base of the column and protein appearing at the exit is proportional to the void volume of the column, $\varepsilon V/Q$. This gave a mean value of $\varepsilon = 0.59$.

(2) The mass of silica packed into the column was 1.5 g. The density of solid silica is 2.34 g/ml. This gives a value of $\varepsilon = 0.81$.

(3) The actual volume occupied by solid silica was measured by mixing 1 g of silica and 5 ml of methanol in a 10-ml measuring cylinder and noting the increase in volume. This was 0.6 ml/g, giving $\varepsilon = 0.73$.

The average value for ε was taken to be 0.7. This assumes that lysozyme can enter all the pores of the silica. The nominal pore size is 30 nm and the molecular diameter of lysozyme is 4 nm, so provided the pore size distribution is not too wide this should be the case.

RESULTS AND DISCUSSION

Bound ligand loading

The results of the analysis of the bound ligand loading are given in Table I. A separate analysis by the same technique on adsorbent a gave 8.1 μmol/g and Clonis *et al.*[2] arrived at 2.9 μmol/g for adsorbent c. Thus these values have errors of ±1 μmol/g. It can be seen that there is a large variation in the final loading of bound ligands on the silica. The reason why adsorbent c has a low bound ligand loading is possibly due to the low dye/silica ratio used in the final derivatization step (0.05 g Procion Blue/g silica, *vs.* 0.2 g Procion Blue/g silica for adsorbents a and b). Adsorbents a and b, however, were produced by the authors in the same laboratory by ostensibly the same process, except for the ratio of 1 m*M* HCl used during the hydrolysis step. The difference in the final surface loading of bound ligands may be due to varying degrees of surface coverage of the silica by diol groups following the hydrolysis step. A diol-bonded silica was produced following an identical procedure to that used in preparing adsorbent b up to the end of the hydrolysis step. This was analysed for diol content and found to have a diol loading of 601 μmol/g. The surface area of the silica was determined using a BET machine (Sorptomatic Series 1800, Carlo Erba) as being 210 m^2/g. The theoretical monolayer coverage of diol is[8] 2.3 μmol/m^2, and so a monolayer coverage of this material would yield a diol loading of 489 μmol/g. The actual diol loading of 610 μmol/g indicates that there are more than sufficient diol groups present to form a monolayer, and that in places there is a multilayer covering of diol groups. However the aqueous procedures used herein for the derivatization process are known to result in a polymeric diol layer[8] and so it is still possible that significant areas of the silica surface may not be covered with diol groups and so are unable to bind dye molecules in the ligand attachment step. To investigate the effect of the acid/silica ratio during the hydrolysis step further, small amounts of adsorbents were produced in four separate batches, using identical conditions. All reagent quantities and steps were the same as for adsorbents a and b except the hydrolysis ratio, which was 10 ml 1 m*M* HCl/g silica. Bound ligand loading was analysed by the same method. The four samples were found to have a mean ligand loading of 4.3 μmol/g with a standard deviation between samples of 0.6 μmol/g. Thus there is no significant difference between the ligand loading on these samples and adsorbent b. The reason for adsorbent a having a higher bound ligand loading is not understood and needs to be investigated further, so that high bound ligand loadings can be obtained consistently.

TABLE I

BOUND LIGAND LOADING FOR ADSORBENTS a, b AND c

Adsorbent	*Bound ligand loading (μmol/g)*
a	7.0
b	3.8
c	1.7

Adsorbent capacities

Lactate dehydrogenase. The data for the adsorption of LDH from a crude extract binding onto adsorbents a and c are shown in Fig. 3. Each experimental point is the average of two enzyme assays for that sample. The error in the assay was found to be less than 25% between two repetitions. The Langmuir isotherm was found to give a better fit than the Freundlich, and to give a good fit to the data. Table II lists the binding parameters for the adsorption of both pure and crude LDH.

The reduced binding capacity for LDH of both adsorbents with crude rather than pure LDH extract is possibly due to the "wide band" specificity of the Procion Blue MX-R as a ligand, *i.e.* many of the available sites could be engaging in affinity reactions with proteins other than LDH which are present in the crude extract.

The data also shows that adsorbent a has a higher maximum binding capacity than adsorbent c. The ratios q_{max} (adsorbent a)/q_{max} (adsorbent c) are 1.7 and 3.2 for pure and crude LDH, respectively. The ratio of bound ligand loading on adsorbent a/adsorbent c is in the region 2.8 to 4.1. Thus it is probable that the higher capacity of adsorbent a is due to the larger number of available sites. The molecular weight of LDH is 140 000 g/mol. Thus the figure of 8.7 mg LDH/g can be equated to 0.062 μmol LDH/g which corresponds to less than 1% of the total ligand sites being occupied. This could be due to steric hindrance of the LDH molecules in some of the pores or to only a small fraction of the ligands being "active" in terms of binding LDH. The molecular diameter of LDH is[1] 8 nm. Thus if several LDH molecules are bound to ligands at the mouth of the pore, there may be insufficient room for any additional LDH molecules to pass the pore mouth. It should also be bourne in mind that the length of the ligand will further reduce the effective pore diameter. The nature of the affinity interaction may thus be critical in determining whether the LDH can penetrate the pores of the

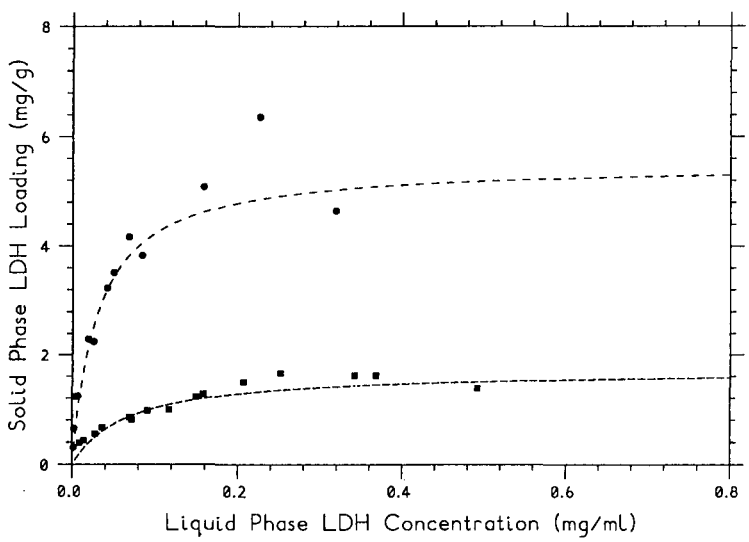

Fig. 3. Equilibrium adsorption of crude LDH onto silicas derivatized with Procion Blue MX-R; 20°C, 0.05 *M* pH 7 phosphate buffer. ● = Adsorbent a (7.0 μmol ligand/g silica); ■ = adsorbent c (1.7 μmol ligand/g silica). Langmuir isotherms fitted with the following constants: Adsorbent a (– – – –); q_{max} = 5.50 mg/g, K_d = 0.023 mg/ml; adsorbent c (- - - - - - - -); q_{max} = 1.70 mg/g, K_d = 0.053 mg/ml.

TABLE II

BINDING PARAMETERS FOR LDH

	K_d (mg/ml)	q_{max} (mg/g)
Pure LDH and adsorbent a	0.031 ± 0.005	8.70 ± 0.52
Pure LDH and adsorbent c	0.107 ± 0.040	5.25 ± 0.88
Crude LDH and adsorbent a	0.023 ± 0.007	5.51 ± 0.32
Crude LDH and adsorbent c	0.053 ± 0.012	1.70 ± 0.09

adsorbent. If an LDH molecule binds itself irreversibly to a ligand until the conditions are altered to elute the material, there may be no further penetration of the pores after the pore mouth is blocked by the first few molecules. If the LDH–ligand interaction is a reversible process during which the protein is periodically adsorbed/desorbed it is possible that there will be a migration of protein along the length of the pore. The figure of 8.7 mg/g for the maximum capacity of adsorbent a for LDH is in agreement with the data of Larsson *et al.*[1] who measured 6 and 9 mg/g for LDH binding to NAD-derivatized silicas with pore diameters of 10 and 100 nm, respectively. Their results also indicate that steric hindrance may be a problem in LDH adsorption, as 10-nm pore size silica has ostensibly a far greater surface area for adsorption than 100-nm silica, and yet they measured the 100-nm silica as having the larger capacity.

Lysozyme. A Freundlich isotherm was found to fit these data more accurately than the Langmuir, and a good fit was obtained with the experimental data. Fig. 4 shows the experimental values with the fitted isotherm drawn in as well. Table III lists

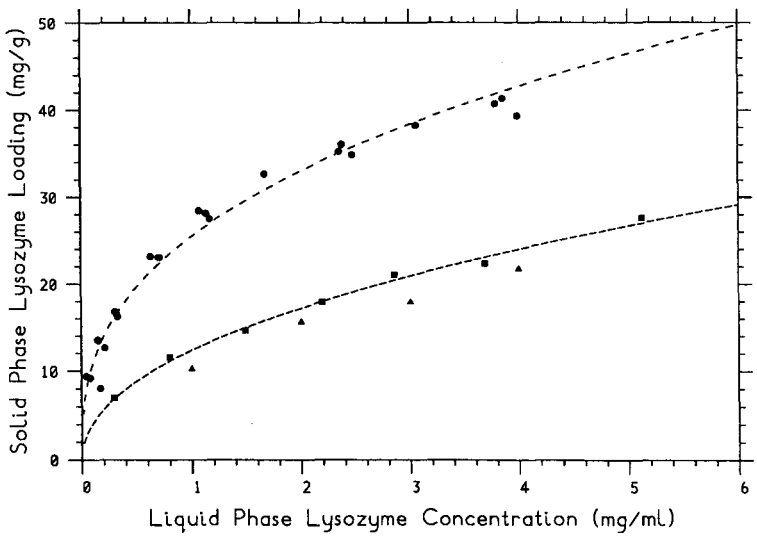

Fig. 4. Equilibrium adsorption of lysozyme onto silicas derivatized with Procion Blue MX-R; 20°C, 0.05 *M* pH 7 phosphate buffer. ● = Adsorbent a (7.0 μmol ligand/g silica); ■ = adsorbent b (3.8 μmol ligand/g silica); ▲ = adsorbent b results from breakthrough profiles. Freundlich isotherms fitted with the following constants: Adsorbent a (-----); k = 25.4 ml/g, n = 0.375; adsorbent b (--------); k = 12.3 ml/g, n = 0.481.

TABLE III

BINDING PARAMETERS FOR LYSOZYME

Adsorbent	k ($mg^{(1-n)}$ ml^n/g)	n
a	25.4 ± 1.0	0.37 ± 0.02
b	12.3 ± 1.0	0.48 ± 0.01

the binding parameters for adsorbents a and b. It is unclear why a Freundlich isotherm gives a better fit to this data. A Freundlich isotherm implies no theoretical limit exists for the maximum capacity of the adsorbent for lysozyme. This is obviously unrealistic in practice because the adsorbents used have physical limits as to how much protein can attach itself to its inner pore surface. It is possible that at higher concentrations of lysozyme than used in this work the solid phase loading would have reached a constant value. It is also possible that there is an affinity binding effect taking place between the ligand and the lysozyme, and at the same time there is also some kind of non-specific interaction occuring between the ligand and the lysozyme. The Freundlich isotherm may be the best representation of the superposition of these two effects. Whatever the reason, the utility of the isotherm lies in its use as a tool for quantifying adsorbent capacity. The Freundlich isotherm, while causing theoretical difficulties, serves this purpose well.

The ratio of binding capacity for different adsorbents is a function of liquid phase concentration for the Freundlich isotherm, *e.g.* q^* (adsorbent a)/q^* (adsorbent b) = 2.1 $(c^*)^{-0.11}$. Over the range of concentrations in these experiments this is equal to approximately 1.9. The ratio of bound ligand loadings is approximately 2.0. Thus it seems reasonable to assume for the adsorption of lysozyme the capacity is limited by the number of ligands available at the adsorbent surface. Lysozyme has a molecular weight of 13 930 g/mol[9] and a molecular diameter of 4 nm[10]. This equates to 3 μmol lysozyme/g adsorbent for adsorbent a, or approximately 40% of the available sites being used, assuming that one ligand binds one lysozyme molecule. If it were assumed that more than one dye molecule is required to bind a lysozyme molecule, or that 40% of the bound ligands are available to adsorb lysozyme, the equivalence in the ratio of capacity to bound ligand loading is explained. Data for the adsorption of lysozyme onto Blue Sepharose[11] show a maximum binding capacity of 16 mg lysozyme/ml settled adsorbent. Adsorbent b was measured to have a packed volume of 2.3 ml/g. Thus 40 mg/g corresponds to 17 mg/ml (packed volume) which is of the same order as the capacity of the Blue Sepharose. These results cannot be directly compared because the immobilized ligand used on Blue Sepharose is Cibacron Blue F3G-A, and the two adsorbents have different surface areas. However, it is interesting to consider the relative capacities of the two adsorbents with view to scale up and process economics.

The ionic strength of the liquid phase significantly effects the capacity of the adsorbent (Fig. 5). The pH of the solution however does not have a significant effect over the range 6.5–7.5, while a liquid phase concentration of 1 *M* KCl was found to reduce the bound protein loading by an order of magnitude. Tests (results not shown) on diol-silica showed that it is effectively "sealed off" and binds no lysozyme, while the unmodified silica was found to bind protein irreversibly. As discussed earlier, the

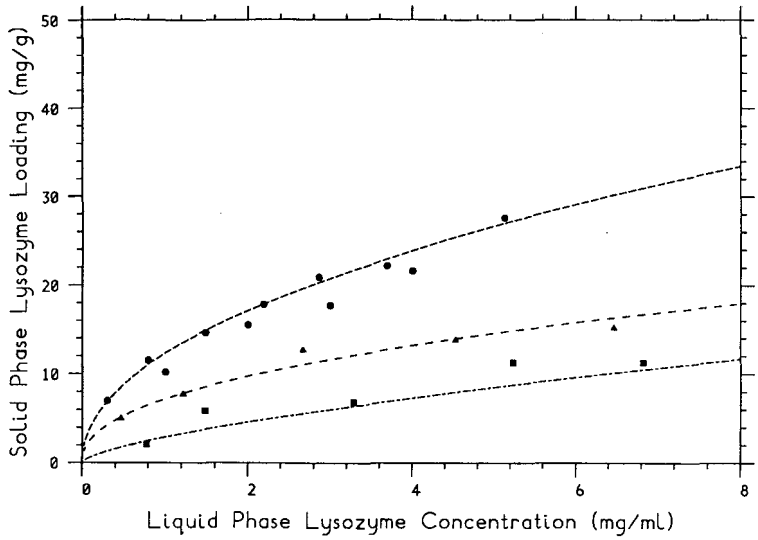

Fig. 5. Effect of buffer ionic strength on equilibrium adsorption of lysozyme to adsorbent b; 20°C. Phosphate buffer pH 7: ■ = 0.2 *M*; ▲ = 0.1 *M*; ● = 0.05 *M*. Freundlich isotherm fitted with the following constants: (-·-·-·-·-) 0.2 *M* buffer; $k = 2.9, n = 0.67$; (– – – –) 0.1 *M* buffer; $k = 7.2, n = 0.44$; (- - - - - - - - -) 0.05 *M* buffer; $k = 12.3, n = 0.48$.

diol-silica was analysed for diol loading and found to contain diol groups excess to the requirement for a monolayer. The fact that there was no binding of lysozyme to the diol silica indicates that the diol groups present probably constitute a monolayer covering most of the silica surface, as opposed to a patchwork of polymeric diol layers. The approximate coverage of available surface area on the adsorbents can be calculated. For LDH, 0.062 μmol/g corresponds to a projected area of 1.9 m^2/g. Similarly for lysozyme 3 mmol/g corresponds to 22 m^2/g. The surface area of adsorbent a was 210 m^2/g so that if the molecules are spread out on the surface uniformly the lysozyme molecules may be close enough together to limit the capacity due to steric hindrance, since the surface coverage is 10% of the total available surface. However, the LDH molecules would be some distance apart, as they cover only 0.8% of the total available area. However, as mentioned above, the capacity of the adsorbent for LDH may well be limited by adsorbed molecules at the pore mouth hindering the passage of other molecules past them to the empty sites.

Adsorption kinetics

The results of the kinetics experiments on LDH are shown in Fig. 6. Equilibrium was reached in under 2 min. For lysozyme, the rate of adsorption was so rapid as to be almost instantaneous compared to the resolution obtainable by the method described here (15 s), and this data is not shown on the plot. The faster rate of adsorption for lysozyme may be due to the greater diffusivity of lysozyme (the diffusivities of the proteins in water at 20°C are $1.12 \cdot 10^{-7}$ and $0.45 \cdot 10^{-7}$ cm^2/s for lysozyme and LDH, respectively[9]) which allows it to make its way down the pores more quickly. Alternatively, the larger size of the LDH molecule may hinder diffusion due to collisions and interactions with the pore walls and adsorbed LDH molecules.

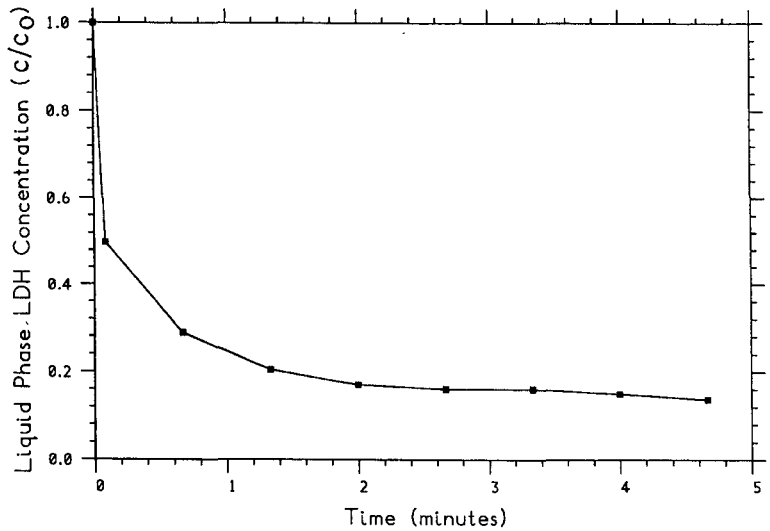

Fig. 6. Rate of adsorption of LDH onto adsorbent a in a stirred beaker; 20°C, 0.05 *M* pH 7 phosphate buffer. ■ = Experimental data.

Chromatographic performance

Plots of breakthrough curves for varying inlet concentrations and flow-rates are shown in Figs. 7 and 8. The dimensionless concentration c/c_0 is plotted against Γ, the dimensionless throughput parameter. The area behind the breakthrough curve, from $\Gamma = 0.0$ to the point where $c/c_0 = 1.0$ should be equal to 1.0. Equilibrium theory predicts a step change in c/c_0 from 0 to 1 at $\Gamma = 1.0$. The results show that breakthrough generally occurs slightly before this and that the breakthrough profile is not affected very much by either flow-rate or inlet concentration over the range of

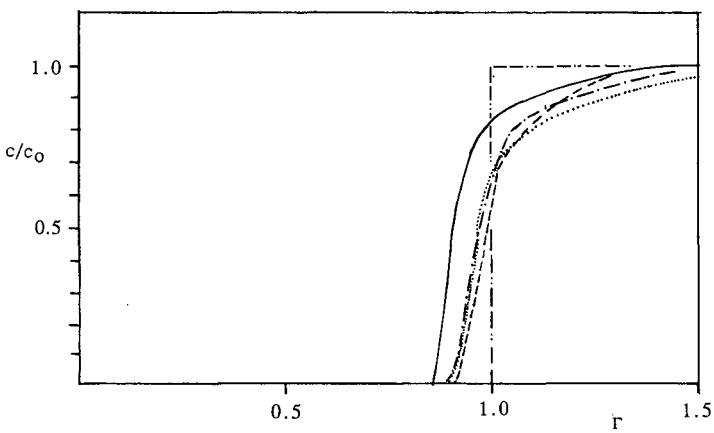

Fig. 7. Breakthrough profiles for lysozyme on adsorbent b at varying inlet concentrations. Superficial velocity = 3.7 cm/min, 20°C, 0.05 *M* pH 7 phosphate buffer. –··–··–, Local equilibrium theory; ———, c_0 = 1 mg/ml; ·····, c_0 = 2 mg/ml; –·–·–, c_0 = 3 mg/ml; – – – –, c_0 = 4 mg/ml.

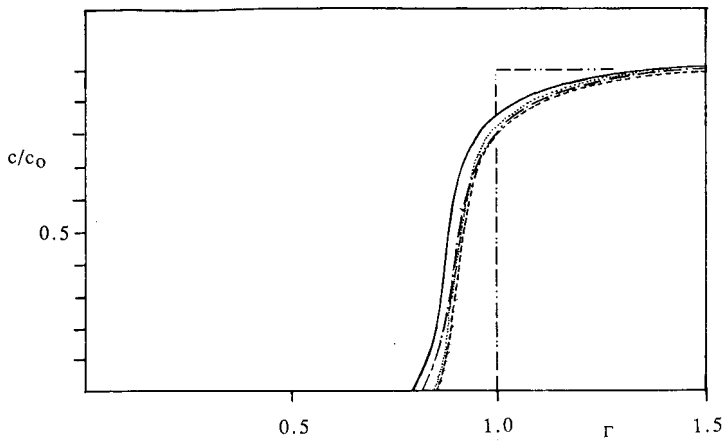

Fig. 8. Breakthrough profiles for lysozyme on adsorbent b at varying superficial velocities. Inlet concentration (c_0) = 1 mg/ml, 20°C, 0.05 *M* pH 7 phosphate buffer. – · – · –, Local equilibrium theory; · – · – ·, superficial velocity (U_0) = 3.7 cm/min; ———, U_0 = 5.2 cm/min; – – – –, U_0 = 7.2 cm/min; · · · · · · · · ·, U_0 = 8.6 cm/min.

values used in this work. The broadening that is evident is thought to be due primarily to dispersive and mixing effects within the column and pipework.

Using eqn. 6 and the values for the Freundlich isotherm parameters obtained previously for adsorbent b (Table III), theoretical washing curves can be obtained. These are shown superimposed on the experimentally determined curves in Fig. 9 and show a good agreement. The apparent offset in the theoretical and experimental curves may be due to the uncertainty in estimating the system delay time. Thus for both breakthrough and wash situations the local equilibrium model, which makes no allowance for any rate determining steps, can be seen to give a reasonable approximation of the performance of the column. This is due to the rapidity with which equilibrium is approached using the small-diameter HPLAC adsorbents. Obtaining the equilibrium adsorption parameters required to make predictions of column performance using the local equilibrium model requires a minimum of

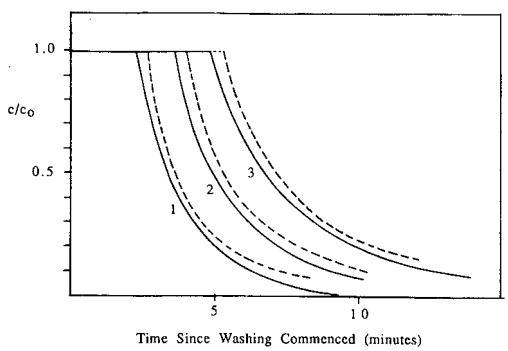

Fig. 9. Washout profiles obtained when protein-free buffer is applied to a protein-saturated column; 20°C, 0.05 *M* pH 7 phosphate buffer. **1**, Superficial velocity (U_0) = 5.2 cm/min, inlet concentration (c_0) = 1 mg/ml; **2**, U_0 = 3.7 cm/min, c_0 = 2 mg/ml; **3**, U_0 = 3.7 cm/min, c_0 = 1 mg/ml. ——— = Experimental; – – – – – = predicted from eqn. 6.

experimental work. This model is thus useful for process evaluation and scale up studies.

The area behind the breakthrough curve can be used to calculate the solid phase concentration that is in equilibrium with the liquid feed concentration. This has been done for the various feed concentrations employed herein and the isotherm data obtained in this fashion are shown plotted with the results from the batch tests discussed previously (Fig. 4). These two methods for obtaining isotherm data agree very well, thus confirming the validity of the method used herein.

SYMBOLS

ΔA_{min}	rate of change of absorbance (a.u./min)
c	liquid phase concentration (mg/g)
c^*	equilibrium liquid phase concentration (mg/g)
$c_{initial}$	liquid phase concentration at the start of the isotherm experiment
c_0	liquid phase concentration in column feed (mg/g)
K_d	Langmuir isotherm dissociation constant (mg/g)
k	Freundlich isotherm constant ($mg^{(1-n)}$ ml^n/g)
L	column length (cm)
n	Freundlich isotherm exponent (dimensionless)
q	adsorbent phase loading (mg/g)
q^*	equilibrium adsorbent phase loading (mg/g)
q_{max}	Langmuir isotherm maximum capacity constant (mg/g)
q_0	solid phase loading in equilibrium with column feed (mg/g)
Q	flow-rate through column (cm^3/min)
t	time (min)
U_0	liquid phase superficial velocity (cm/min)
V	volume of column (ml)
w	mass of silica used in batch tests (g)
z	length variable along column axis (cm)
Γ	dimensionless throughput parameter
ε	void fraction of column
ρ_b	packed density of adsorbent (g/ml)

REFERENCES

1 P. D. Larsson, M. Glad, L. Hansson, M. O. Mansson, S. Ohlson and K. Mosbach, *Adv. Chromatogr.*, 21 (1983) 41.
2 Y. D. Clonis, K. Jones and C. R. Lowe, *J. Chromatogr.*, 363 (1986) 31.
3 H. A. Chase, *Biosensors*, 2 (1986) 269.
4 C. R. Lowe, M. Glad, P. O. Larsson, S. Ohlson, D. A. P. Small, T. Atkinson and K. Mosbach, *J. Chromatogr.*, 215 (1981) 303.
5 H. A. Chase, *J. Chromatogr.*, 297 (1984) 179.
6 T. R. Sherwood, R. L. Pigford and C. R. Wilke, *Mass Transfer*, McGraw-Hill/Kogakusha Ltd., Tokyo, 1975.
7 R. Aris and N. R. Amundson, *Mathematical Methods in Chemical Engineering, Vol. 2, First Order Partial Differential Equations with Applications*, Prentice-Hall, Englewood Cliffs, NJ, 1973.
8 P. D. G. Dean, W. S. Johnson and F. A. Middle, *Affinity Chromatography—A Practical Approach*, IRL Press, Oxford, Washington, DC, 1985.
9 H. A. Sober, *Handbook of Biochemistry*, Chemical Rubber Co., Cleveland, OH, 1986.
10 L. Stryer, *Biochemistry*, Freeman, San Francisco, CA, 2nd ed., 1981.
11 B. J. Horstmann, C. N. Kenny and H. A. Chase, *J. Chromatogr.*, 361 (1986) 179.

Journal of Chromatography, 481 (1989) 175–186
Elsevier Science Publishers B.V., Amsterdam — Printed in The Netherlands

CHROM. 21 523

HIGH-PERFORMANCE ADSORPTION CHROMATOGRAPHY OF PROTEINS ON DEFORMED NON-POROUS AGAROSE BEADS COATED WITH INSOLUBLE METAL COMPOUNDS

I. COATING: FERRIC OXYHYDROXIDE WITH STOICHIOMETRICALLY BOUND PHOSPHATE

S. HJERTÉN*, I. ZELIKMAN, J. LINDEBERG, J.-l. LIAO, K.-O. ERIKSSON and J. MOHAMMAD
Institute of Biochemistry, University of Uppsala, Biomedical Center, P.O. Box 576, S-751 23 Uppsala (Sweden)

(First received January 4th, 1989; revised manuscript received June 30th, 1989)

SUMMARY

A new support for adsorption chromatography of proteins based on cross-linked agarose gels containing ferric (hydr)oxide is described. Two methods have been used for immobilization of the ferric (hydr)oxide on agarose beads; namely,entrapment of preformed ferric oxide particles in connection with the preparation of macroporous agarose beads and precipitation of ferric oxyhydroxide on and in preformed non-porous agarose beads. In the former method many of the adsorption sites of the ferric oxide may become sterically blocked, resulting in chromatographic properties which are similar to those of cation exchangers. Therefore, attention was focused on the second method. Upon using compressed beds of non-porous agarose beads the resolution became independent of the flow-rate, even when the bead diameter was relatively large. When ferric oxyhydroxide agarose is equilibrated with phosphate buffer, some phosphate becomes stoichiometrically and irreversibly bound to the matrix. The separation mechanism of this ferric oxyhydroxide phosphate agarose is discussed. It differs from those of ion-exchange, hydrophobic-interaction, and molecular-sieve chromatography. One characteristic is that phosphate buffers are the most efficient eluting agents. Chromatography on ferric oxyhydroxide phosphate–agarose is accordingly a good complement to these three conventional methods. Some chromatographic properties of the adsorbents are described (resolution as a function of gradient time, flow-rate and protein load; and the pH dependence of the adsorption). A successful separation of a model mixture of six proteins was achieved. Purification of a commercial preparation of β-glucosidase is also presented.

INTRODUCTION

Macromolecules, such as proteins, bind to many insoluble metal salts, oxides and hydroxides, which are therefore potential chromatographic adsorbents. These metal compounds often appear in the form of gelatinous precipitates or as very fine,

0021-9673/89/$03.50

mechanically unstable particles. For this reason they give high resistance against hydrodynamic flow, which in practice prevents their direct use as chromatographic bed materials for column operation. This problem can be overcome by entrapping the adsorbing particles in a macroporous gel, for instance agarose[1–3]. However, this latter method may have the drawback that many of the adsorption sites become sterically blocked by the gel polymer chains. To avoid this, we have developed a technique based on direct precipitation of the metal compound in and on the surface of preformed gel beads. As a matrix we have used non-porous agarose beads because, following compression of the bed, they have the important property of giving a high resolution which is independent of the flow-rate even when their diameter is large[4–6].

In this paper we report the application of ferric oxide, Fe_2O_3, and ferric oxyhydroxide, FeO(OH), immobilized on beads of non-porous cross-linked agarose to the separation of proteins. Some characteristic features of those chromatographic materials are described. Chromatographic supports based on aluminium and zirconium (hydr)oxides will be presented in a forthcoming paper[7].

EXPERIMENTAL AND RESULTS

Chemicals and equipment

Ferric oxide particles (Fe_2O_3) were Bayferrox Red special grade 1120 Z of size 0.1 × 0.8 μm from Bayer (Leverkusen, F.R.G.). Agarose was a kind gift from Dr. R. Armisén, Hispanagar S.A., Spain. All salts were of analytical grade from Merck (Darmstadt, F.R.G.) Ovalbumin (molecular weight, MW = 43 000, p*I* 4.7), bovine serum albumin (MW 69 000, p*I* 4.9), carbonic anhydrase (MW 30 000, p*I* 5.9), α-chymotrypsinogen A (MW 25 000, p*I* 8.8), ribonuclease (MW 13 700, p*I* 8.9), aldolase (MW 158 000, p*I* 9.1), cytochrome *c* (MW 12 200, p*I* 9.2) and lysozyme (MW 14 600, p*I* 10) were from Sigma (St. Louis, MO, U.S.A.). β-Glucosidase from sweet almonds and 3-nitrophenyl-β-glucopyranoside were obtained from Serva (Heidelberg, F.R.G.). Thyroglobulin (MW 670 000, p*I* 4.5) was obtained from Pharmacia (Uppsala, Sweden). Human transferrin (p*I* 5.5) and human serum albumin (p*I* 4.9) were from Kabi (Stockholm, Sweden). Haemoglobin A_{1c} (p*I* 6.9) was from Bio-Rad (Richmond, CA, U.S.A.). Before use all buffer solutions were filtered through a 0.22-μm Millipore filter and degassed.

The chromatographic system, including a Model 2150 HPLC pump, a Model 2152 gradient controller, a Model 2151 variable-wavelength UV monitor and a Model 2220 reporting integrator, was obtained from LKB (Bromma, Sweden) and the HPLC sample injector from Rheodyne (Berkeley, CA, U.S.A.).

Free zone electrophoresis was performed in a 400 mm × 3 mm I.D. quartz tube which was rotated around its long axis at a speed of 40 rpm for stabilization against convection[8].

Preparation of Fe_2O_3–agarose by entrapment of ferric oxide particles into macroporous agarose beads

Agarose beads were prepared by an emulsion-gelation method[9] with some modificatons: 1 g of ferric oxide (Fe_2O_3) powder was added to the hot 12% aqueous agarose solution before the addition of the heated organic phase containing the emulsifier and the suspension was agitated extensively for 10 min before cooling. The

beads containing Fe_2O_3 were sized by elutriation in water[10]. Beads with diameters in the range 15–20 μm were collected and cross-linked twice with γ-glycidoxypropyltrimethoxysilane by a procedure described previously[4]. This material will be referred to as Fe_2O_3–agarose. The Fe_2O_3–agarose beads were packed in water at a constant flow-rate of 2 ml/min into a Plexiglas column with an inner diameter of 6 mm.

Preparation of non-porous agarose beads

Beads of 12% agarose were prepared by the emulsion-gelation method described earlier[9] and were sized by elutriation in water[10]. Beads with diameters of 15–20 μm were collected and shrunk in an organic solvent according to a previous method[5] and then cross-linked twice with γ-glycidoxypropyltrimethoxysilane[4] or butanediol diglycidyl ether[5]. Upon shrinkage, the diameters of the beads decreased to 10–15 μm. A microscopic investigation of the shrunken and cross-linked agarose beads removed from the column immediately after packing at 2 ml/min revealed that the beads had become deformed upon compression, leading to tight contact between their surfaces and to a decrease in the void volume of the bed.

To investigate indirectly the change in pore size of the agarose beads as a result of the shrinkage, a column (30 mm × 6 mm I.D.) was packed with the shrunken agarose beads cross-linked with γ-glycidoxypropyltrimethoxysilane. The following substances were applied separately on each column: potassium chromate (MW 194), ribonuclease (MW 13 700), chymotrypsinogen A (MW 25 000), bovine serum albumin (MW 69 000), aldolase (MW 158 000) and thyroglubilin (MW 670 000); 0.3 *M* potassium phosphate buffer, pH 7.0, was used for elution.

The retention times were plotted against the molecular weights (Fig. 1). It is evident that the shrunken beads were impermeable to proteins, at least to those with molecular weights higher than about 10 000, since the retention times of the proteins were independent of their molecular weights. Similar results were obtained when the experiment was repeated with shrunken agarose beads cross-linked with butanediol diglycidyl ether (Fig. 1). The shrunken, cross-linked beads will be referred to as non-porous agarose beads. Agarose beads cross-linked with γ-glycidoxypropyltrimethoxysilane were used in all the experiments described below, unless otherwise stated.

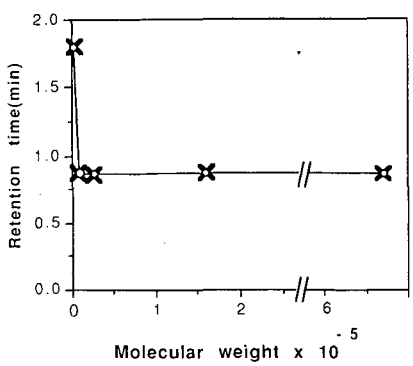

Fig. 1. Retention times of proteins with different molecular weights on a column of deformed non-porous agarose beads. ○ = cross-linked with γ-glycidoxypropyltrimethoxysilane; × = cross-linked with butanediol diglycidyl ether.

Precipitation of ferric oxyhydroxide onto preformed non-porous agarose beads

A 5-g amount of sedimented non-porous agarose beads was incubated for 15 min in 10 ml of water in which 1 g of $FeCl_3$ had been dissolved. The beads were then collected by centrifugation and a 10-ml volume of 2 *M* NH_4OH was added. The suspension was mixed thoroughly and shaken for 5 min. The beads became dark brown, indicating the formation of ferric oxyhydroxide, FeO(OH). To eliminate ferric oxyhydroxide not bound to agarose, the suspension was washed six times with water by centrifugation at 800 *g* until the supernatant became clear or until no free oxyhydroxide clusters were observed by light microscopy.

The beads were packed in distilled water into a Plexiglas column, 6 mm in diameter, to a height of 30–35 mm under such a high pressure (corresponding to a flow-rate of 2 ml/min) that the beads became deformed. The upper piston of the column tube was then pressed down to make contact with the surface of the agarose bed. Otherwise, the bed will expand when the experiments are performed at a lower flow-rate (= lower pressure).

The mechanical properties of FeO(OH)–agarose beads

Two columns with the same total volume were packed: one containing non-porous cross-linked agarose beads, the other containing identical beads coated with ferric oxyhydroxide. Both columns were equilibrated with 0.3 *M* potassium phosphate buffer, pH 7.0, at flow-rates ranging from 0.7 to 5 ml/min. The relationship between the flow-rate and pressure was the same for the two columns. The continuous use of flow-rates above 3 ml/min resulted in some leakage of the ferric oxyhydroxide coating.

Free zone electrophoresis of ferric oxyhydroxide and ferric oxide

Ferric oxyhydroxide was prepared as described under *Precipitation of ferric oxyhydroxide onto preformed non-porous agarose beads* but in the absence of agarose beads. Electrophoresis was performed in both 0.01 *M* potassium phosphate, pH 6.0, and 0.01 *M* sodium cacodylate, pH 6.0, using 1500 V and 3 mA for 15 min. The experiment was repeated with particles of ferric oxide suspended in the same buffers. In both buffers, ferric oxyhydroxide and ferric oxide migrated toward the positive electrode.

Elemental analysis of ferric oxyhydroxide-coated agarose beads

A column of ferric oxyhydroxide agarose was equilibrated with phosphate buffer (phosphate buffers were used for desorption), washed overnight with water and then analyzed for iron and phosphorus. The elemental analysis showed that phosphate had become irreversibly bound to the adsorbent at a molar metal-to-phosphate ratio of 2:1. Since some of the ligands of the ferric ions accordingly are replaced by the phosphate ions and these ions are used for equilibration and elution, it is appropriate to designate the adsorbent ferric oxyhydroxide phosphate by the *simplified* notation $FeO(OH)(PO_4)$.

Chromatographic characterization of Fe_2O_3– and $FeO(OH)(PO_4)$–agarose

Two columns were packed with Fe_2O_3–agarose and $FeO(OH)(PO_4)$–agarose, respectively, to a total volume of 2.5 ml each and equilibrated with 0.005 *M* potassium

phosphate buffer, pH 7.0. These columns were used to investigate the influence of different ions on the elution of proteins. A sample containing 75 μg each of the proteins myoglobin, chymotrypsinogen A and cytochrome *c* dissolved in the equilibration buffer was applied onto each column. In another set of experiments a sample containing 75 μg each of the proteins ovalbumin, human serum albumin and human transferrin was applied to each column. The columns were washed with the equilibration buffer and then eluted with the same buffer using a gradient in salt concentration from 0 to 0.2 *M* over 30 min. The following salts were used: sodium, potassium and ammonium chloride, ammonium hydrogencarbonate, sodium EDTA and ammonium acetate. An experiment was also performed with only a gradient in potassium phosphate concentration from 0.005 to 0.2 *M* over 30 min (without adding any salt). The same experiments were then performed on both columns equilibrated with 0.01 *M* sodium acetate buffer, pH 5.5, or 0.01 *M* sodium borate buffer, pH 9.1, instead of 0.005 *M* potassium phosphate buffer, pH 7.0. In brief, the above experiments gave the following results.

Proteins with p*I* values below the pH of the equilibration buffer did not adsorb to the ferric oxide–agarose column. The adsorbed proteins were eluted in the order of increasing p*I* values (for p*I* values, see the *Chemicals and equipment* section). There was no significant difference between the elution patterns of the proteins eluted with gradients formed by the different salts.

Equilibration of the column with acetate buffer at pH 5.5 instead of phosphate buffer, pH 7.0, resulted in stronger adsorption of the proteins. Upon equilibration with borate buffer at pH 9.1, cytochrome *c* was the only protein bound. The ferric oxide–agarose column thus had cation-exchange properties.

Similarly, proteins were eluted from ferric oxyhydroxide phosphate agarose roughly in the order of increasing p*I* values, but only with a gradient in potassium phosphate concentration and not by the other salts. Of the proteins tested, only ovalbumin did not adsorb to the column. Successful separations were not obtained when the column was equilibrated with 0.01 *M* sodium acetate buffer at pH 5.5, owing to very strong adsorption of the proteins. After equilibration with sodium borate buffer at pH 9.1, the resolution of more acidic proteins was unsatisfactory, due to weak adsorption. Some further experiments indicated that equilibration with a cacodylate buffer, pH 6.0, gave a moderate adsorption and this buffer was therefore used in all subsequent experiments.

The above experiments indicated that Fe_2O_3–agarose had chromatographically less interesting properties than $FeO(OH)(PO_4)$–agarose. Therefore, no further experiments with the former material were designed.

Fig. 2a shows the chromatography of a model protein mixture on the column of $FeO(OH)(PO_4)$–agarose equilibrated with 0.002 *M* potassium phosphate buffer, pH 6.0, and eluted with a 30-min linear gradient in potassium phosphate concentration from 0.002 to 0.2 *M* (pH 6.0). Since dihydrogenphosphate has a pK_a value of 7.2 and therefore a relatively low buffering capacity at pH 6.0 (the pH to be preferred, see above), we repeated the experiment in the presence of a "background buffer" of sodium cacodylate (pK_a 6.27). The column was equilibrated with 0.01 *M* sodium cacodylate buffer, pH 6.0, and eluted with a linear gradient in potassium phosphate concentration from 0 to 0.2 *M* over 30 min in the presence of the equilibration buffer (Fig. 2b). A comparison of Fig. 2a and b shows that somewhat more narrow peaks were obtained in the presence of cacodylate.

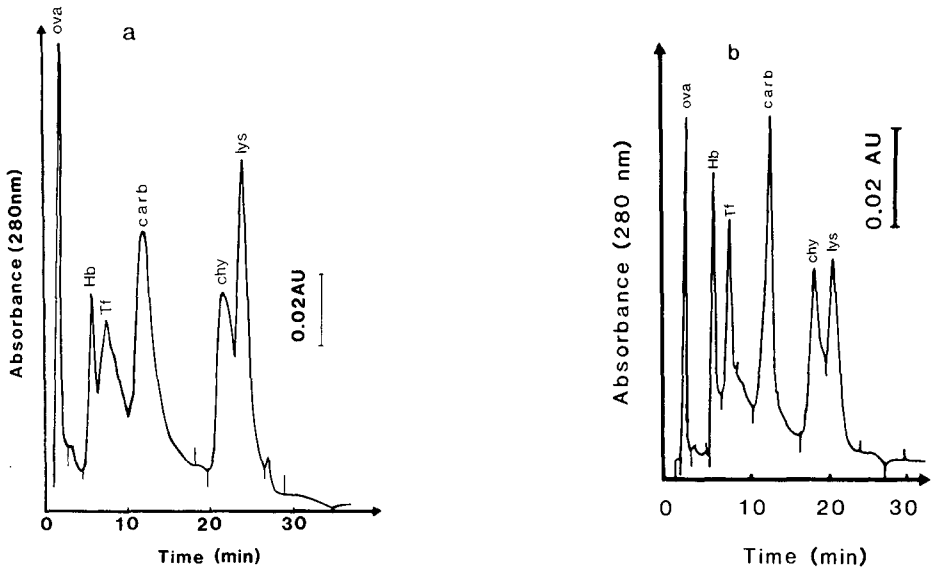

Fig. 2. Chromatography of a model protein mixture on a $FeO(OH)(PO_4)$–agarose column. Column dimensions: 60 mm × 6 mm I.D. Flow-rate: 1 ml/min. Sample: 75 μg of each of the following proteins in a total volume of 60 μl: ovalbumin (ova), haemoglobin A_{1c} (Hb), human transferrin (Tf), carbonic anhydrase (carb), chymotrypsinogen A (chy) and lysozyme (lys). Elution: (a) a linear gradient in potassium phosphate from 0.002 to 0.2 *M* over 30 min, pH 6.0; (b) a linear gradient in potassium phosphate from 0 to 0.2 *M* over 30 min in 0.01 *M* sodium cacodylate, pH 6.0. Sharper peaks were obtained in the presence of cacodylate.

In all experiments to be discussed we used cacodylate as a buffering ion (and phosphate as a desorbing ion) on ferric oxyhydroxide phosphate–agarose columns (*i.e.*, FeO(OH)–agarose equilibrated with phosphate). The cacodylate ions alone did not desorb the proteins.

Resolution as a function of some different chromatographic parameters

The influence of different experimental conditions on the resolution of two proteins on a $FeO(OH)(PO_4)$–agarose column was investigated. Eqn. 1 was used for the calculation of the resolution, R_s, between two components (α-chymotrypsinogen A and carbonic anhydrase),

$$R_s = \frac{t_2 - t_1}{0.5\,(t_{w2} + t_{w1})} \tag{1}$$

where t_2 and t_1 are the retention times and t_{w2} and t_{w1} are the peak widths at half the height of the peaks (in time units) of α-chymotrypsinogen A and carbonic anhydrase, respectively.

Gradient time. Aliquots containing 50 μg each of α-chymotrypsinogen A and carbonic anhydrase dissolved in 100 μl of the equilibration buffer (0.01 *M* sodium cacodylate, pH 6.0), were applied onto the $FeO(OH)(PO_4)$–agarose column and eluted with a gradient in potassium phosphate concentration from 0 to 0.15 *M* in the presence

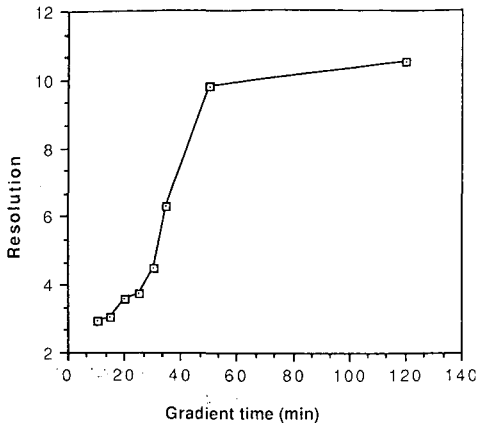

Fig. 3. Resolution of chymotrypsinogen A and carbonic anhydrase *versus* gradient time on a column of $FeO(OH)(PO_4)$–agarose. For details see the Experimental and results section.

of the cacodylate buffer to get a higher buffering capacity. Gradient times were varied between 10 and 120 min. The flow-rate was kept constant at 1 ml/min. Fig. 3 shows that the resolution increased with the gradient time up to about 50 min.

Flow-rate. The same sample as described under *Gradient time* was applied on the column and eluted with the same gradient at flow-rates ranging from 0.2 to 3 ml/min. The total volume of the gradient was kept constant at 25 ml and the gradient times were changed in proportion to the flow-rates to keep dc/dv constant, *i.e.*, the concentration gradient with respect to volume[5]. Fig. 4 shows that there was little, if any, dependence of the resolution on the flow-rate. The recorder chart speed was chosen proportional to the gradient time to give all of the chromatograms the same width, thereby facilitating visual comparison of the separation patterns.

Protein load. Samples containing different amounts of α-chymotrypsinogen A and carbonic anhydrase, ranging from 50 to 1250 μg of each protein dissolved in the equilibration buffer, were applied onto a $FeO(OH)(PO_4)$–agarose column with a total volume of 1 ml equilibrated with 0.01 *M* sodium cacodylate, pH 6.0. Proteins were eluted with the same gradient as described under *Gradient time* over 10 min. The

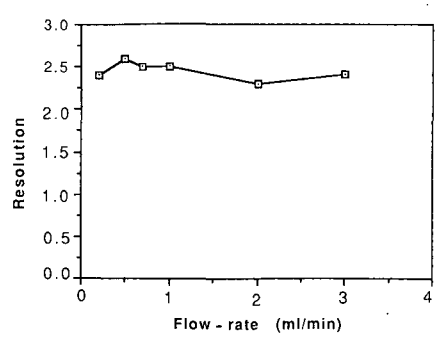

Fig. 4. Resolution of chymotrypsinogen A and carbonic anhydrase *versus* flow-rate on a column of $FeO(OH)(PO_4)$–agarose. For details see the Experimental and results section.

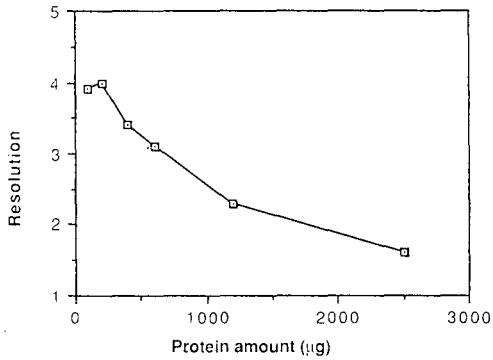

Fig. 5. Resolution of chymotrypsinogen A and carbonic anhydrase *versus* total amount of protein in the sample on a column of $FeO(OH)(PO_4)$–agarose. For details see the Experimental and Results section.

flow-rate was kept constant at 1 ml/min. Fig. 5 shows the decrease in resolution observed when the load of protein was increased.

Chromatography of a commercial preparation of β-glucosidase on $FeO(OH)(PO_4)$–agarose

β-Glucosidase (50 μg) dissolved in 50 μl of the equilibration buffer was applied onto the ferric oxyhydroxide phosphate–agarose column equilibrated with 0.01 *M* sodium cacodylate buffer, pH 6.0. The column was eluted with a gradient in concentration of potassium phosphate from 0 to 0.3 *M* over 30 min in the presence of 0.01 *M* sodium cacodylate, pH 6.0, at a flow-rate of 1 ml/min. Fractions of 1 ml were collected. The activity of β-glucosidase in each fraction was measured with 3-nitrophenyl-β-glucopyranoside as a substrate as described previously[11]. Fig. 6 shows several components without β-glucosidase activity and one peak containing 97% of the initial enzyme activity, indicating an extensive purification of the commercial preparation of β-glucosidase.

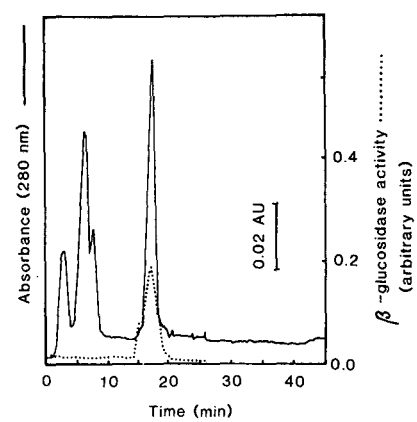

Fig. 6. Chromatography of a commercial preparation of β-glucosidase on a column of $FeO(OH)(PO_4)$–agarose. Elution: a gradient in potassium phosphate from 0 to 0.3 *M* over 30 min in 0.01 *M* sodium cacodylate, pH 6.0. Column dimensions: 60 mm × 6 mm I.D. Flow-rate: 1 ml/min. Sample: 50 μg of β-glucosidase dissolved in 50 μl of the equilibration buffer; substrate: 3-nitrophenyl-β-glucopyranoside.

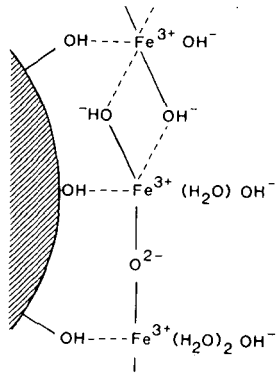

Fig. 7. Proposed possible structure of the ferric oxyhydroxide coating on agarose beads. The coordination number of ferric ions is six. One or more of the coordination sites is thought to be occupied by hydroxyl groups of the agarose. The remaining sites are coordinating water molecules or hydroxide ions, the ratio between these depending on the pH of the surrounding liquid. The hydroxide ions can be shared by other ferric ions forming double hydroxy bridges or, upon rearrangement of water molecules, oxy bridges. In this way a network of ferric oxyhydroxide is formed on and in the agarose bead. After equilibration with phosphate buffer and washing with distilled water overnight, some of the phosphate ions cannot be removed, but are irreversibly bound in a molar ratio between iron and phosphate close to 2.0. How these are incorporated into the ferric oxyhydroxide agarose is not known.

DISCUSSION

The phenomenon that proteins adsorb to ferric (hydr)oxides can be utilized in different ways. For instance, particles of ferric oxide with antibodies or antigens adsorbed on their surfaces have been used for batch affinity separation of proteins[12] and in immunoagglutination assays for the detection of the corresponding antigen or antibody[13]. The separation mechanism of ferric oxyhydroxide phosphate is unknown. We know, however, that it differs from those of ion-exchange, hydrophobic-interaction and molecular-sieve chromatography, since it is not in a simple way related to the charge, hydrophobicity or size of the proteins. Chromatography on ferric oxyhydroxide phosphate–agarose columns in combination with one of these other methods can therefore be expected to give a high purification.

When iron trichloride is dissolved in water, the ferric ion coordinates six aquo groups[a]. One or more of these can probably be displaced by hydroxyl groups on and in the agarose beads in the same way as hydrated titanium oxide is bound by polysaccharides[14]. A layer of ferric ions coordinating OH^- or aquo groups may thus form on the surface and other accessible parts of agarose beads (Fig. 7). This formation may also be stabilized by hydrogen bonding between the coordinated water and the hydroxyl groups of the agarose. To a certain extent, some of the adsorbed water molecules spontaneously lose a proton to the bulk solution, thereby forming hydroxide ions. This deprotonation is strongly facilitated when the pH is raised by the addition of ammonium hydroxide to the solution. The deprotonated water molcules form double hydroxy bridges between ferric ions[15]. This process continues in three

[a] Chloride ions are also coordinated to the ferric ions in solution, but they are omitted in the text and the figure.

dimensions until the agarose beads become covered by a network of ferric ions coordinating water molecules and binding to each other by shared hydroxyl groups.

Upon aging, the hydroxy bridges lose water molecules to form a ferric polyoxy complex on and in the bead[15]. Depending on the pH of the surrounding solution, the remaining coordinated water molcules can lose more protons, thus giving the ferric oxyhydroxide layer a negatively charged surface.

Elemental analysis of phosphate-treated FeO(OH)–agarose shows that some phosphate is irreversibly bound in a molar metal-to-phosphate ratio of 2:1. This is further evidence that the outer layer of the bead should have negative charges.

In free zone electrophoresis in cacodylate and phosphate buffers of pH 6.0, ferric oxyhydroxide migrated towards the positive electrode, which showed that the surface of the oxyhydroxide is negatively charged. It should therefore not be surprising that this support shows pronounced ion-exchange properties. However, the binding of acidic proteins to ferric oxyhydroxide phosphate agarose shows that mechanisms other than ion exchange also take part in the adsorption of proteins to the matrix. The bed material differs from ion exchangers also in that, among the ions tested, only phosphate ions desorb proteins. On the other hand, the elution order of proteins is roughly in accord with their p*I* values.

Certain groups on the protein molecule might have the ability to displace aquo groups coordinated to the ferric ions (Fig. 7). These groups are the carboxyl groups of the C-terminus, aspartyl and glutamyl residues, the phenoxy groups of tyrosyl residues, the imidazole groups of histidyl residues, the guanidinium groups of arginyl residues, the thiol groups of cysteinyl residues and the amino groups of the N-terminus and lysyl residues[14]. Another mode of adsorption might involve an ionic interaction between the negatively charged hydroxide and phosphate ions of ferric oxyhydroxide and positively charged amino acid residues in the protein. If all of the above interactions occur, ferric oxyhydroxide may display both anionic and cationic properties.

Such a combination of different modes of adsorption might explain the differences between chromatography on $FeO(OH)(PO_4)$–agarose and the more conventional methods mentioned above.

In Fe_2O_3–agarose, protein groups may be prevented from displacing water coordinated to ferric ions by steric hindrance arising from the tight contact between the surface of the ferric oxide particles and the carbohydrate chains of the agarose which is created during the preparation of the beads. However, it is likely that the negatively charged surface of the metal oxide can still attract positive groups in the protein, thus allowing Fe_2O_3–agarose to funtion as a cation exchanger. Although the application of this bed material is limited, it was used successfully for the separation of γ-globulin from human serum[2] and for the enrichment of gp70, an envelope protein from the cell culture fluid of feline leukemia virus[3].

Comparison of Fig. 2a and b shows that sharper peaks were obtained when the elution was performed in the presence of cacodylate ions to increase the buffering capacity. A stable pH is essential, since the adsorption is pH dependent (see *Chromatographic characterization of Fe_2O_3- and $FeO(OH)(PO_4)$-agarose*). However, we cannot exclude the possibility that cacodylate ions have some specific desorbing properties analogous to those of "modifiers" used in reversed-phase chromatography.

Chromatography of a model protein mixture on non-shrunken macroporous cross-linked agarose beads coated with ferric oxyhydroxide phosphate gave broader peaks as compared to chromatography on $FeO(OH)(PO_4)$-coated shrunken non-porous cross-linked agarose beads (results not shown). This is not surprising, since the use of non-porous agarose beads prevents zone broadening caused by diffusion of proteins in and out of the beads. We have increased the resolution further by compressing the beds so that the diffusion paths between them are reduced[4-6,16]. The favourable effects of shrinkage, non-porosity and compression of the beads are discussed briefly in refs. 4–6.

The resolution on columns packed with compressed non-porous agarose beads is independent of the flow-rate (Fig. 4 and refs. 4–6), which permits short analysis times without loss of resolution.

Probably the ferric oxyhydroxide on the surface of a bead extends into the cavities of the bead. This anchorage of the ferric oxyhydroxide, together with the proposed mechanism for the binding of ferric oxyhydroxide to agarose, may explain why no leakage from the column was observed at moderate flow-rates. However, continuous use of flow-rates above 3 ml/min on ferric oxyhydroxide–agarose should be avoided owing to mechanical loss of ferric oxyhydroxide.

We have shown herein that ferric oxyhydroxide phosphate agarose under suitable conditions can yield a good separation of proteins. The mechanism of this separation, although not completely understood, is obviously different from that of conventional chromatographic media. It therefore seems appropriate to describe this new adsorbent even at this early stage of development. However, more data should be collected concerning the specificity of ferric oxyhydroxide phosphate for different proteins and other groups of biological substances and the applicability of this new chromatographic material for their separation.

ACKNOWLEDGEMENTS

This work was financially supported by the Swedish Natural Science Research Council and the Knut and Alice Wallenberg, Carl Trygger and Bengt Lundqvist Memorial Foundations.

REFERENCES

1 S. Hjertén, I. Zelikman, I. Kourteva and J. Lindeberg, presented at *6th International Symposium on HPLC of Proteins, Peptides and Polynucleotides, Baden-Baden, October 20–22, 1986*, Abstract No. 113.
2 S. Hjertén and I. Zelikman, *J. Biochem. Biophys. Methods*, 17 (1988) 67–74.
3 I. Zelikman, L. Åkerblom, S. Hjertén and B. Morein, *Biotech. Appl. Biochem.*, 11 (1989) 209–216.
4 S. Hjertén, Y. Kunquan and J.-l. Liao, *Makromol. Chem.*, 17 (1988) 349–357.
5 S. Hjertén and J.-l. Liao, *J. Chromatogr.*, 457 (1988) 165–174.
6 J.-l. Liao and S. Hjertén, *J. Chromatogr.*, 457 (1988) 175–182.
7 S. Hjertén, I. Zelikman, J. Lindeberg and M. Lederer, *J. Chromatogr.*, 481 (1989) 187–199.
8 S. Hjertén, *Chromatogr. Rev.*, 9 (1967) 122–219.
9 S. Hjertén, *Biochim. Biophys. Acta*, 79 (1964) 393–398.
10 S. Hjertén, in M. T. W. Hearn (Editor), *HPLC of Proteins, Peptides and Polynucleotides*, VCH, Weinheim, in press.
11 W. Hössel and A. Nahrstedt, *Hoppe-Seyler's Z. Physiol. Chem.*, 356 (1975) 1265–1275.
12 I. Giaevert, *U.S. Pat.*, 4 018 886 (1977).

13 I. Zelikman and S. Hjertén, *J. Immunol. Meth.*, 114 (1988) 267–273.
14 J. F. Kennedy, *Chemical Soc. Rev.*, 8 (1979) 221–257.
15 A. Müller, *Arzneim.-Forsch.*, 17 (1967) 920–931.
16 S. Hjertén, Z.-q. Liu and D. Yang, *J. Chromatogr.*, 296 (1984) 115–120.

Journal of Chromatography, 481 (1989) 187–199
Elsevier Science Publishers B.V., Amsterdam — Printed in The Netherlands

CHROM. 21 734

HIGH-PERFORMANCE ADSORPTION CHROMATOGRAPHY OF PROTEINS ON DEFORMED NON-POROUS AGAROSE BEADS COATED WITH INSOLUBLE METAL COMPOUNDS

II. COATING: ALUMINIUM AND ZIRCONIUM (HYDR)OXIDE WITH STOICHIOMETRICALLY BOUND PHOSPHATE

S. HJERTÉN*, I. ZELIKMAN and J. LINDEBERG
Institute of Biochemistry, University of Uppsala, Biomedical Center, P.O. Box 576, S-751 23 Uppsala (Sweden)
and
M. LEDERER
Institut de Chimie Minérale et Analytique, Université de Lausanne, Place du Château 3, CH-1005 Lausanne (Switzerland)
(First received January 4th, 1989; revised manuscript received June 30th, 1989)

SUMMARY

Two novel supports for adsorption chromatography of biomolecules, based on deformed non-porous cross-linked agarose beads coated with aluminium or zirconium (hydr)oxide, were prepared. Some fundamental chromatographic properties of these bed materials are discussed, including the adsorption mechanism and high-resolution separations of mixtures of proteins, nucleotides and coenzymes. Both aluminium and zirconium (hydr)oxide agarose irreversibly and stoichiometrically bind phosphate ions, thus some of the chromatographic properties resemble those of calcium phosphate and hydroxyapatite. Fractionation of a β-glucosidase preparation into two components possessing enzymatic activity was achieved on the aluminium (hydr) oxide phosphate agarose, whereas chromatography on zirconium (hydr)oxide phosphate–agarose removed several inactive contaminants but gave only one peak associated with enzyme activity. This finding indicates that the adsorption mechanisms of the two adsorbents are not identical, although other experiments show that there are several analogies. For instance, model proteins chromatographed on these two supports were eluted in the same order, although the relative retention times differed, *i.e.*, the chromatograms did not have the same appearance. Compressed beds of cross-linked non-porous agarose beads, including those coated with aluminium and zirconium (hydr)oxide, have the unique feature that the resolution is roughly independent of flow-rate and that there is no need for small beads of narrow size distribution.

0021-9673/89/$03.50

INTRODUCTION

Transition metals, such as titanium, zirconium, iron, tin and vanadium have been used to activate the surfaces of various matrices, for instance cellulose, nylon, glass and chitin[1,2] to give derivatives to which proteins, cells and antibiotics can be attached[1–5]. Such activated matrices have been shown to be useful tools in biotechnology, one application being the preparation of enzyme reactors[6].

Zirconium phosphate has been employed earlier as a chromatographic support[7].

The use of aluminium oxide (alumina) for chromatographic purposes was reported long ago. Its high capacity for the adsorption of different biological substances makes it an attractive alternative to the bed materials based on silica or polymers. Adsorption on aluminium oxide has been described for chromatographic separation of biological macromolecules[8,9], for purification of cyclic nucleoside monophosphates[10], steroid hormones[11] and polypeptides[12]. Aluminium oxide for high-performance liquid chromatography (HPLC) can be obtained commercially (5 μm Spherisorb A5Y from Chrompack). In this form it is macroporous and permits separation of proteins by size exclusion.

Amorphous (hydr)oxides of aluminium and zirconium are known to adsorb proteins[4,13], but unfortunately there is no possibility to use these materials directly for chromatographic experiments because of their poor flow properties. To overcome this problem we coated non-porous cross-linked agarose beads with aluminium and zirconium (hydr)oxides, respectively. This approach combines the adsorption characteristics of these (hydr)oxides with the good flow properties of the agarose support. The simplicity and relatively low cost of preparation also make these supports attractive. The subtitles used in this paper are analogous to those employed in the preceding paper (Part I[14]) on ferric oxyhydroxide phosphate agarose in order to facilitate comparison of the chromatographic properties of the adsorbents.

CHEMICALS AND EQUIPMENT

Agarose was a kind gift from Dr. R. Armisén (Hispanagar, Burgos, Spain), human transferrin (p*I* 5.5) from Dr. L.-O. Andersson, (KabiVitrum, Stockholm, Sweden) and γ-glycidoxypropyltrimethoxysilane from Mr. H. Gustafsson (Sikema, Stockholm, Sweden). Ovalbumin (p*I* 4.7), carbonic anhydrase (p*I* 5.9), conalbumin (p*I* 5.9), myoglobin from horse muscle (p*I* 7.3), α-chymotrypsinogen A (p*I* 8.8), cytochrome *C* (p*I* 9.2), lysozyme (p*I* 10), AMP, ADP, ATP, oxidized nicotinamide-adenine dinucleotide (NAD) and oxidized nicotinamide-adenine dinucleotide phosphate (NADP) were obtained from Sigma (St. Louis, MO, U.S.A.). β-Glucosidase from sweet almonds and 3-nitrophenyl-β-glucopyranoside were from Serva (Heidelberg, F.R.G.). All salts were of analytical grade from Merck (Darmstadt, F.R.G.).

Before use all buffer solutions were filtered through a 0.22-μm Millipore filter and degassed.

The chromatographic equipment was as described in Part I[14]. The charge of the metal (hydr)oxides was studied by free zone electrophoresis in an horizontal quartz tube rotating around its long axis (40 rpm) to eliminate disturbing convection[14,15].

EXPERIMENTAL AND RESULTS

Preparation of non-porous agarose beads

The procedure was the same as that described in Part I[14]. γ-Glycidoxypropyltrimethoxysilane was used as a cross-linker.

Precipitation of aluminium and zirconium (hydr)oxide onto non-porous agarose beads

We followed the method employed for the preparation of FeO(OH)–agarose (see Part I[14]) with the exception that the ferric chloride solution was replaced by 10 ml of an aqueous solution of 1 *M* $AlCl_3$ or 0.65 *M* $ZrCl_4$. The columns were packed in distilled water and the beds were compressed as outlined in Part I[14]. The mechanical properties of both adsorbents (including the relationship between flow-rate and back pressure) were similar to those of FeO(OH) agarose (Part I[14]).

Elemental analysis of aluminium and zirconium (hydr)oxide-coated agarose beads

The samples for elemental analysis were taken from columns equilibrated with potassium phosphate and then washed with water as described for $FeO(OH)(PO_4)$–agarose in Part I[14]. The metal-to-phosphate molar ratio in this case was also close to 2:1. Since phosphate ions are thus irreversibly bound it may be appropriate to introduce the terms aluminium (hydr)oxide phosphate and zirconium (hydr)oxide phosphate in analogy with the notation ferric oxyhydroxide phosphate used in Part I[14]. In this paper we also use the expressions $Al(OH)(PO_4)$ and $Zr(OH)(PO_4)$, in analogy with $FeO(OH)(PO_4)$ in Part I[14].

Chromatographic characterization of $Al(OH)(PO_4)$–agarose

A separation of a model protein mixture of ovalbumin, human transferrin, myoglobin, conalbumin, lysozyme and cytochrome *c* was performed on a column of $Al(OH)(PO_4)$–agarose under the different equilibration and elution conditions described below. The following buffers were used for equilibration: 0.01 *M* sodium acetate, pH 5.5; 0.01 *M* sodium cacodylate, pH 6.0 and 7.0; 0.01 *M* Tris–HCl, pH 7.5; 0.01 *M* potassium phosphate, pH 7.0 and 0.01 *M* sodium borate, pH 9.1. After equilibration of the column the sample was applied (75 μg of each of the above proteins dissolved in 80 μl of the equilibration buffer). In an attempt to elute the proteins we chose a linear 30-min salt gradient (0–0.2 *M*) in the equilibration buffer. The gradient was created by potassium chloride and sodium salts of chloride, sulphate, EDTA and cacodylate. These salts appeared to have little or no eluting power. However, all proteins were desorbed easily by a concentration gradient of potassium phosphate, pH 7.0, from 0.002 to 0.2 *M* in the absence of other salts (Fig. 1a). It should be added that equilibration of the column at high pH (0.01 *M* borate buffer, pH 9.1) gave a very weak adsorption of acidic proteins, whereas equilibration at low pH (0.01 *M* acetate buffer, pH 5.5) caused very strong adsorption of all proteins tested except ovalbumin.

We also equilibrated the column with 0.01 *M* sodium cacodylate buffer, pH 7.0, and eluted with the same buffer containing a linear gradient in potassium phosphate from 0 to 0.2 *M*, pH 7.0 (Fig. 1b). A comparison of Fig. 1a and b shows that this second elution procedure including sodium cacodylate gave sharper peaks in the chromatogram and thus a better separation, which is in analogy with the experiments on $FeO(OH)PO_4$, presented in Part I[14].

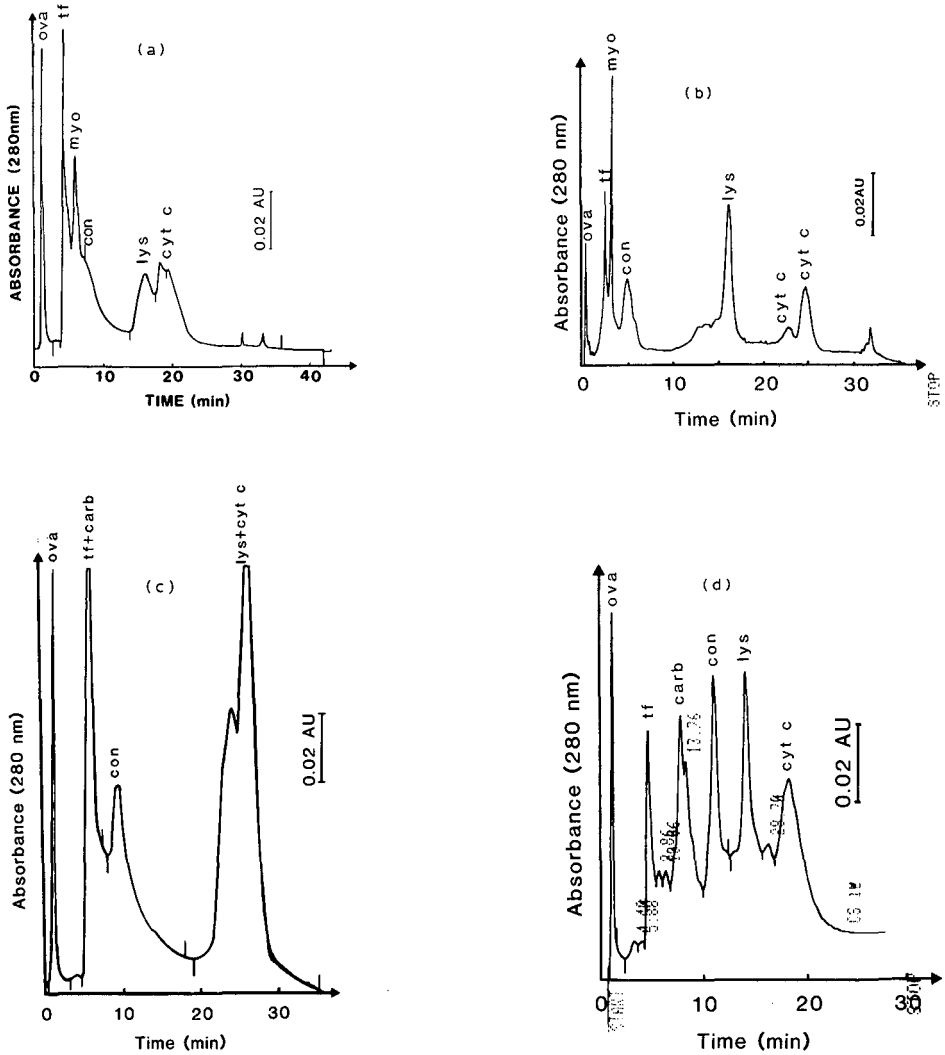

Fig. 1. Chromatography of model proteins on aluminium and zirconium (hydr)oxide phosphate agarose. Column dimensions: 30 mm × 6 mm I.D. Flow-rate: 1.0 ml/min. (a) $Al(OH)(PO_4)$–agarose. Sample: 75 μg each of the following proteins in a total volume of 80 μl: ovalbumin (ova); transferrin (tf); myoglobin (myo); conalbumin (con); lysozyme (lys); cytochrome *c* (cyt c). Elution: a linear gradient of potassium phosphate from 0.002 to 0.2 *M* over 30 min (pH 7.0). (b) $Al(OH)(PO_4)$–agarose. Sample as in (a). Elution: a linear gradient of potassium phosphate from 0 to 0.2 *M* over 30 min in 0.01 *M* sodium cacodylate, pH 7.0. (c) $Zr(OH)(PO_4)$–agarose. Sample as in (a) with the difference that myoglobin was exchanged for carbonic anhydrase (carb). Elution: a linear gradient of potassium phosphate, pH 6.0, from 0.002 to 0.2 *M* over 30 min. (d) $Zr(OH)(PO_4)$–agarose. Sample as in (c). Elution: a linear gradient of potassium phosphate from 0 to 0.2 *M* over 30 min in the presence of 0.01 *M* sodium cacodylate, pH 6.0. A comparison of (a) with (b) and (c) with (d) shows the favourable effect of cacodylate ions on the resolution.

Chromatographic characterization of $Zr(OH)(PO_4)$–agarose

The experiment was performed as discussed above for aluminium (hydr)oxide phosphate–agarose with the exception that myoglobin in the model protein mixture was exchanged for carbonic anhydrase (transferrin and carbonic anhydrase coeluted in all experiments except that shown in Fig. 1d). In Fig. 1c a chromatogram is presented for a column of zirconium (hydr)oxide phosphate–agarose following equilibration with 0.002 *M* potassium phosphate, pH 6.0, and elution with a linear 30-min gradient in potassium phosphate (pH 6.0) from 0.002 to 0.2 *M*. An higher resolution was obtained, however, by equilibration of the same column with 0.01 *M* sodium cacodylate buffer, pH 6.0, and elution with a 30-min gradient in potassium phosphate (pH 6.0) from 0 to 0.2 *M* in the equilibration buffer (Fig. 1d).

The pH dependence of the protein adsorption was similar to that described above for $Al(OH)(PO_4)$–agarose. Other similarities were: (1) among the eluting agents tested only phosphate ions can be used for desorption; (2) there was no obvious correlation between the p*I*-values of the proteins and their order of elution and (3) model proteins were eluted in the same order from aluminium and zirconium (hydr)oxide phosphate–agarose (Fig. 1).

In all subsequent experiments on columns of aluminium and zirconium (hydr)-oxide phosphate–agarose, *i.e.*, metal (hydr)oxide agarose equilibrated with phosphate we used a cacodylate buffer for equilibration and a phosphate buffer for elution.

Resolution on aluminium and zirconium (hydr)oxide phosphate–agarose as a function of different chromatographic parameters

The aluminium (hydr)oxide phosphate–agarose column was equilibrated with 0.01 *M* sodium cacodylate buffer (pH 7.0) and eluted with a concentration gradient of potassium phosphate (pH 7.0) from 0 to 0.2 *M* in the presence of the equilibration buffer. The same buffers were employed for the zirconium (hydr)oxide phosphate–agarose column, but the pH was 6.0 instead of 7.0. Eqn. 1 in Part I[14] was used for calculation of the resolution between the same model proteins (chymotrypsinogen A and carbonic anhydrase) as were used for the $FeO(OH)(PO_4)$–agarose bed[14].

Resolution versus gradient time. About 50 μg of each of the above two model proteins were dissolved in 100 μl of the equilibration buffer. Using a constant flow-rate of 1 ml/min, the resolution was determined at different gradient times for both the aluminium (Fig. 2a) and the zirconium (hydr)oxide phosphate–agarose column (curve 1 in Fig. 2b). Since the latter column exhibited a time-dependent adsorption, we performed two additional sets of experiments in which the column with the proteins adsorbed was washed with the equilibration buffer for 20 and 50 min, respectively, before the start of the gradient elution. The results are presented in Fig. 2b as curves 2 and 3, respectively. A comparison between these curves and curve 1 in the same figure indicates that the resolution as a function of gradient time is dependent on the residence time of the proteins.

Resolution versus flow-rate. The total gradient volume was constant at 7 ml. The gradient times were inversely proportional to the flow-rates. For other details, see Part I[14]. Curves (a) and (b) in Fig. 3 show that the resolution varies only slightly with the flow-rate.

Resolution versus protein load. The samples consisted of 25–1500 μg of each of the model proteins dissolved in 100 μl of the equilibration buffer. The flow-rate was 1

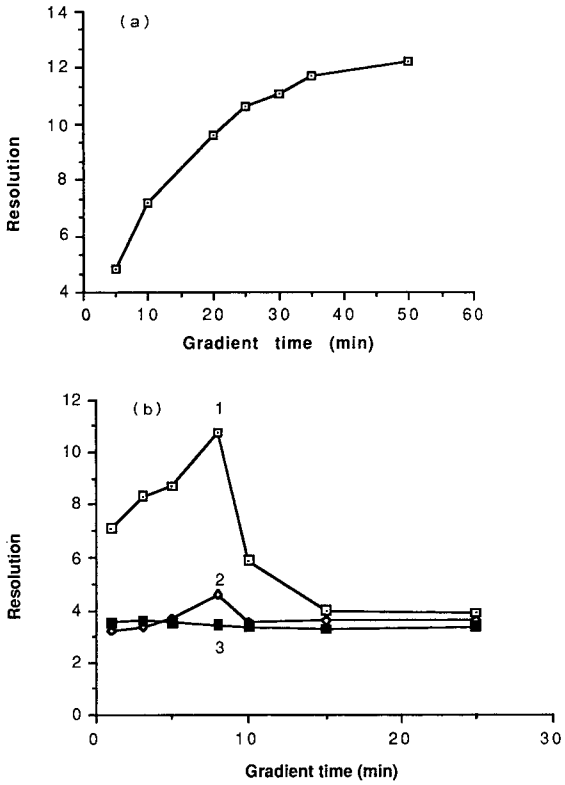

Fig. 2. Resolution (R_s) of chymotrypsinogen A and carbonic anhydrase *versus* gradient time on aluminium and zirconium (hydr)oxide phosphate–agarose. For details see Experimental and Results. (a) Al(OH)-(PO_4)–agarose; (b) Zr(OH)(PO_4)–agarose. Residence times: 0 (1), 20 (2), 50 min (3).

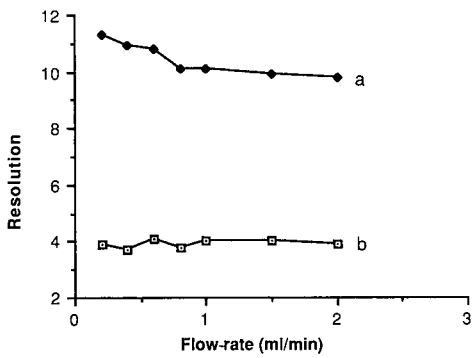

Fig. 3. Resolution of chymotrypsinogen A and carbonic anhydrase *versus* flow-rate on aluminium and zirconium (hydr)oxide phosphate–agarose. For details see Experimental and Results. (a) Al(OH)(PO_4)–agarose; (b) Zr(OH)(PO_4)–agarose.

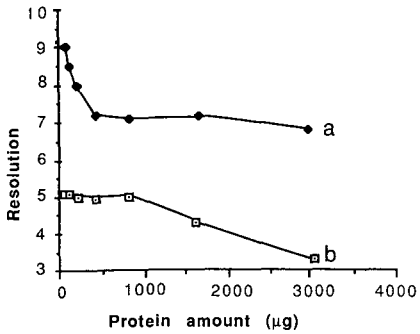

Fig. 4. Resolution of chymotrypsinogen A and carbonic anhydrase *versus* amount of protein in the sample on aluminium and zirconium (hydr)oxide phosphate–agarose. For details see Experimental and Results. (a) $Al(OH)(PO_4)$–agarose; (b) $Zr(OH)(PO_4)$–agarose.

ml/min and the gradient time 10 min. From Fig. 4 one can conclude that the resolution was relatively little impaired upon an increase in the total protein load up to as much as 6 mg.

Chromatography of a commercial preparation of β-glucosidase on aluminium and zirconium (hydr)oxide phosphate–agarose columns

The experimental conditions were similar to those used for the purification of the same preparation of β-glucosidase on $FeO(OH)(PO_4)$–agarose (Part I[14]) with the

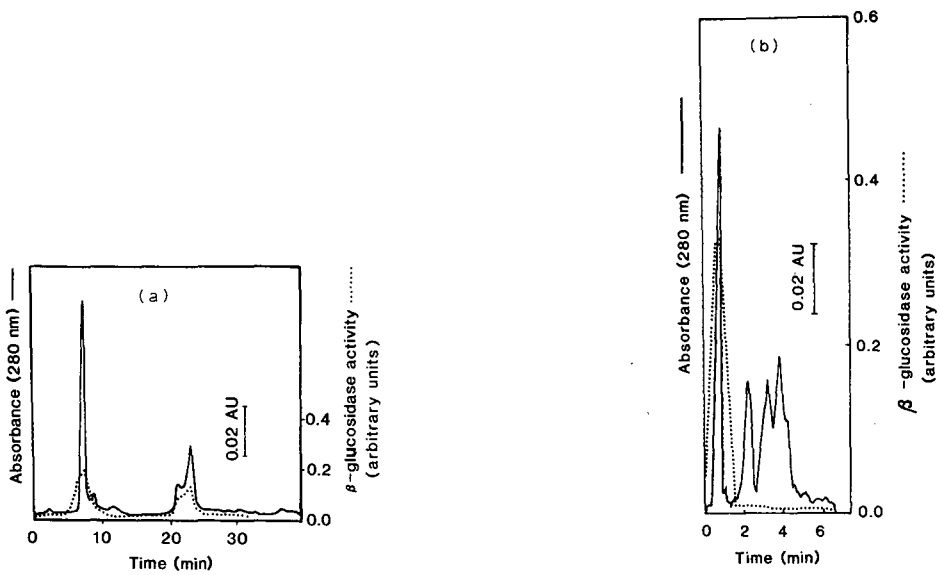

Fig. 5. Chromatography of a commercial preparation of β-glucosidase on aluminium and zirconium (hydr)oxide phosphate–agarose. Column dimensions: 30 mm × 6 mm I.D. Flow-rate: 0.5 ml/min. Sample: β-glucosidase, 50 μg dissolved in 50 μl of equilibration buffer. (a) $Al(OH)(PO_4)$–agarose: elution with a linear gradient of potassium phosphate from 0 to 0.35 *M* over 20 min in 0.01 *M* sodium cacodylate, pH 7.0. (b) $Zr(OH)(PO_4)$–agarose: elution with a linear gradient of potassium phosphate from 0 to 0.2 *M* over 30 min in 0.01 *M* sodium cacodylate, pH 6.0.

exception that the buffer concentrations were somewhat different (see the legend to Fig. 5). The gradient times for the $Al(OH)(PO_4)$–agarose and $Zr(OH)(PO_4)$–agarose were 20 and 30 min, respectively, at a flow-rate of 1 ml/min. The UV pattern for the former adsorbent showed two main peaks, both with enzyme activity (Fig. 5a), whereas the latter adsorbent showed several peaks of which only that corresponding to the void volume showed enzyme activity (Fig. 5b). The recovery of the enzyme activity was 98% on the $Al(OH)(PO_4)$–agarose column and 99% on the $Zr(OH)$-(PO_4)–agarose column.

Separation of nucleotides and coenzymes on $Al(OH)(PO_4)$–agarose

An $Al(OH)(PO_4)$–agarose column was equilibrated with 0.01 *M* sodium cacodylate buffer, pH 7.0. A sample was applied containing 50 μg each of adenosine monophosphate (AMP), diphosphate (ADP) and triphosphate (ATP) dissolved in 150 μl of the equilibration buffer. The column was washed for 10 min with this buffer and then eluted in the presence of the same buffer with a linear gradient of potassium phosphate from 0 to 0.4 *M* over 30 min. Fig. 6a shows three well resolved peaks of the nucleotides. AMP was not adsorbed to the column and ADP and ATP were eluted at potassium phosphate concentrations of 0.16 and 0.21 *M*, respectively.

In another experiment the sample consisted of 50 μg each of NAD and NADP dissolved in 100 μl of the equilibration buffer. The elution conditions were the same as mentioned above, with the difference that the gradient time was 20 instead of 30 min. The chromatogram is presented in Fig. 6b. NAD was not adsorbed to the column, whereas NADP required a potassium phosphate concentration of 0.29 *M* for desorption.

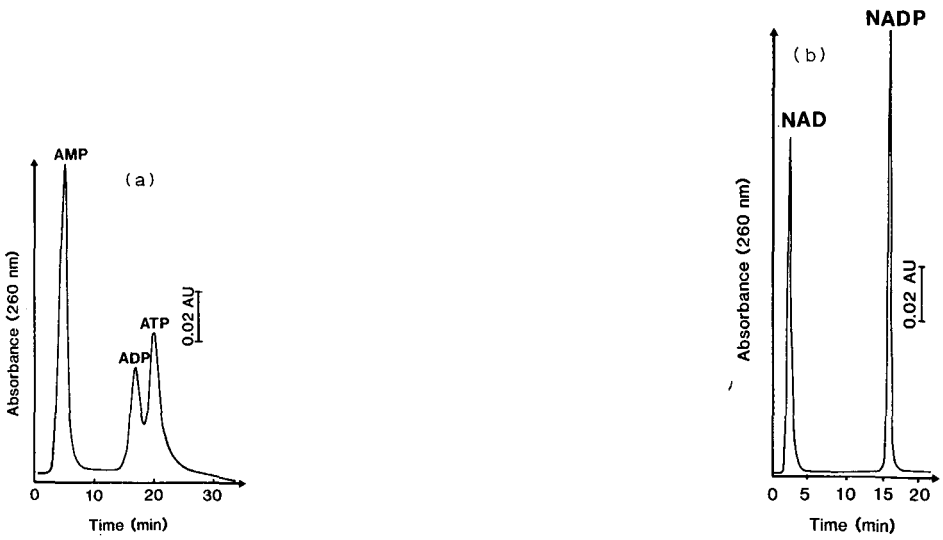

Fig. 6. Chromatography of nucleotides and coenzymes on aluminium (hydr)oxide phosphate–agarose. Column dimensions: 30 mm × 6 mm I.D. Flow-rate: 1 ml/min. (a) Sample: 50 μg of each nucleotide (AMP, ADP and ATP) in a total volume of 150 μl. Elution: a linear gradient of potassium phosphate from 0 to 0.4 *M* over 30 min in 0.01 *M* sodium cacodylate, pH 7.0. (b) Sample: 50 μg of each coenzyme (NAD and NADP) in a total volume of 100 μl. Elution: a linear gradient of potassium phosphate from 0 to 0.4 *M* over 20 min in 0.01 *M* sodium cacodylate, pH 7.0.

DISCUSSION

Aluminium (hydr)oxide phosphate–agarose

In acidic solutions aluminium ions coordinate water. Some of these water molecules may be displaced by hydroxyl groups on and in the agarose bead. As the solution becomes less acidic a successive deprotonation takes place to yield $Al(OH)^{2+}$ and $Al(OH)_2^+$; of course, free hydroxide ions are also created by deprotonation of bulk water molecules and coordinate to the aluminium ion. This process terminates in the formation predominantly of $Al(OH)_3$ when the pH approaches neutrality[16].

At this stage $Al(OH)_3$ gives colloidal (amorphous) complexes of indefinitely large size. When aluminium trichloride is used in the preparation of aluminium hydroxide some of the chloride ions may be present in the $Al(OH)_3$ complex formed. Whether this complex changes upon ageing as proposed for the formation of $FeO(OH)(PO_4)$–agarose is not known.

Upon free zone electrophoresis in the presence of cacodylate and phosphate buffers (pH 7.0), aluminium hydroxide did not migrate, which confirms the existence of uncharged hydroxide in neutral solutions. The amphoteric nature of aluminium hydroxide makes possible an interaction with anions and cations by exchange[17]. It is also known that compounds containing phosphate groups can be specifically adsorbed to aqueous aluminium oxide under conditions where non-phosphorylated compounds show no interaction. Therefore, it is not surprising that specific elution can be obtained by an aqueous solution of inorganic phosphates[17]. Indeed, elemental analysis shows that some phosphate is irreversibly bound at a metal-to-phosphate ratio of 2:1.

Most of the proteins adsorbed on the column of $Al(OH)(PO_4)$–agarose could not be eluted by increasing the ionic strength of the elution buffer, except with regard to phosphate. This adsorbent is thus not a true cation exchanger, although proteins were eluted from the column roughly according to their p*I* values. Unsuccessful separations due to strong adsorption of the proteins to $Al(OH)(PO_4)$–agarose equilibrated at low pH (acetate buffer pH 5.5) and weak adsorption when the column was equilibrated at high pH (borate buffer pH 9.1) suggests that $Al(OH)(PO_4)$–agarose has ion-exchange properties. However, they must be complemented by other mechanisms of adsorption, since, as mentioned, only phosphate ions can effect desorption.

This effectiveness of phosphate ions as an eluting agent indicates that phosphate groups in biomolecules may play an important rôle in the interaction with $Al(OH)(PO_4)$–agarose. This conclusion is supported by our finding that AMP, ADP and ATP are eluted from an aluminium (hydr)oxide phosphate–agarose column in the order of increasing number of phosphate groups (Fig. 6a) and that NADP, but not NAD, is adsorbed (Fig. 6b).

To summarize, our experiments provide support for the idea that several of the above-mentioned mechanisms of adsorption to aluminium (hydr)oxide phosphate agarose may function in combination.

Zirconium (hydr)oxide phosphate agarose

$Zr(OH)(PO_4)$–agarose was prepared in a similar way to $Al(OH)(PO_4)$–agarose and the earlier reported $FeO(OH)(PO_4)$–agarose[14]. When zirconium tetrachloride is dissolved in water, the zirconium ion should coordinate eight water molecules. How-

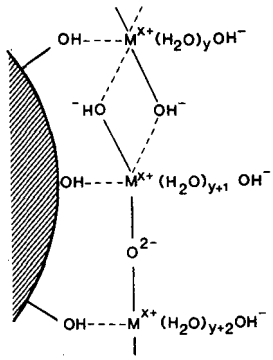

Fig. 7. Proposed structure of the metal (hydr)oxide coating on agarose beads. The two types of connections between metal ions (M^{x+}) thought to be involved in the structure are both drawn, *i.e.*, oxy bridges and double hydroxy bridges. The number of water molecules bound by the metal depends on the coordination number of the metal of interest. The proportion of deprotonated water molecules depends on the pH of the surrounding liquid and the charge of the metal ion. These hydroxide ions can in turn be shared with other metal ions, thus increasing the metal (hydr)oxide layer in all directions. When the metal (hydr)oxide agarose is equilibrated with phosphate buffer, some of the phosphate ions become irreversibly bound with a molar ratio between metal and phoshate close to 2.0. How these phosphate ions are incorporated into the structure is not known, but probably they replace some of the water molecules or hydroxide ions.

ever, even in acidic solution, zirconium salts hydrolyze to form a polymeric aggregate, which has been shown in ultracentrifuge studies to have a molecular weight of about 30 000[18].

These polymeric forms adsorb strongly to dextran, presumably by forming several complexes with vicinal hydroxyl pairs on the dextran surface[19]. Both in solution and adsorbed onto dextran, these polymers readily form outer-sphere complexes with especially divalent and polyvalent anions such as chromate and phosphate[20]. We assume that agarose behaves like dextran in these respects. A proposed structure of the metal (hydr)oxide coating on agarose beads valid for aluminium, zirconium and ferric ions is presented in Fig. 7. Upon equilibrating the column with phosphate buffer, a layer of irreversibly bound phosphate is formed similar to that observed with Al(OH)(PO_4)–agarose and with FeO(OH)(PO_4)–agarose in Part I[14]. This phosphate is bound in a metal-to-phosphate ratio of 2:1.

Electrostatic interaction between the negatively charged phosphate and hydroxide ions on the surface of the metal (hydr)oxide and positively charged groups of the protein might occur, thereby giving the zirconium (hydr)oxide phosphate agarose cation-exchange properties like those of the well known zirconium phosphate cation exchangers[7]. Such a mode of protein adsorption is indicated by the fact that proteins were adsorbed strongly to the column of Zr(OH)(PO_4)–agarose at low pH and hardly at all at high pH; upon free zone electrophoresis in phosphate and cacodylate buffers (pH 6.0), zirconium (hydr)oxide migrated towards the positive electrode, supporting the hypothesis that the surface of the (hydr)oxide is covered with negatively charged hydroxide groups. Adsorbed proteins may also displace coordinated water molecules, *cf.*, the analogous discussion in Part I[14] on protein interaction with FeO(OH)(PO_4)–agarose. The elution of the adsorbed proteins (not in the order of their p*I* values) together with the ineffectiveness of high salt concentrations (with the exception of

potassium phosphate) for elution of proteins from the zirconium (hydr)oxide phosphate–agarose suggest the combined action of the mechanisms described above. Unlike the other two metal (hydr)oxide phosphate-coated agarose supports investigated, *i.e.*, those based on $FeO(OH)(PO_4)$[14] and $Al(OH)(PO_4)$, zirconium (hydr)oxide phosphate–agarose exhibited time-dependent adsorption of proteins (Fig. 2b).

General

The high recovery of the enzymatic activity of β-glucosidase upon chromatography on ferric, aluminium and zirconium (hydr)oxide phosphate–agarose indicates that adsorption to the agarose coated with metal (hydr)oxide phosphate does not change the biological activity of the enzyme.

The use of non-porous agarose beads prevents zone-broadening caused by diffusion of proteins into and out of the bead. Upon compression of the beds the resolution becomes almost independent of the flow-rate[21,22] which permits high flow-rates without lowering the resolution. Some decrease in resolution is observed, however, for aluminium (hydr)oxide phosphate–agarose, which may be explained by the assumption that aluminium (hydr)oxide forms a thicker layer than zirconium (hydr)-oxide and that this layer is permeable to proteins. This hypothesis receives some support from our finding that the former adsorbent has an higher protein capacity (Fig. 4). An alternative explanation may be that the adsorption/desorption proceeds more slowly on $AlOH(PO_4)$–agarose.

The same columns of ferric, aluminium and zirconium (hydr)oxide phosphate–agarose were used over a period of 3 months. More than 200 analyses were performed on each using different buffers over a wide range of pH values and concentrations. No changes in performance or "leakage" of ferric, aluminium and zirconium (hydr)oxide phosphate from the columns was noticed during this time, as judged from the binding of different proteins and capacity studies. This testifies to the high stability of the gel material, which may be explained in terms of binding to vicinal hydroxyl groups and anchorage of the coating in the same way as proposed for $FeO(OH)(PO_4)$–agarose[14].

One of the main technical advantages of agarose beads coated with insoluble metal compounds is that large amounts of gel containing (hydr)oxides and salts of different metals can be prepared from a stock of shrunken and cross-linked agarose beads in a comparatively short time. The procedure does not require any expensive and time-consuming chemical modification of the agarose matrix.

Although the binding mechanisms of the three adsorbents which are based on deformed cross-linked non-porous agarose beads coated with (hydr)oxides of different metals (Fe, Al, Zr) and which have been described in this series of articles are not known in detail, there should be some analogies, since the adsorbents have many similar chromatographic properties. For instance, phosphate from the buffer was irreversibly bound at a metal-to-phosphate molar ratio of 2:1 in all three cases. Furthermore, proteins adsorbed to the columns were eluted only by a concentration gradient of phosphate and not by several other salts tested. From these points of view the adsorbents resemble brushite, $CaHPO_4 \cdot 2H_2O$[23], and hydroxyapatite, $Ca_{10}(PO_4)_6(OH)_2$[24]. (Hydroxyapatite has a metal-to-phosphate molar ratio of 1.67:1.) One should also observe that the elution order of AMP, ADP and ATP is the same on hydroxyapatite[25] and aluminium (hydr)oxide phosphate–agarose (Fig. 6). This may indicate that the number of available phosphate groups in the solute plays

some rôle in the adsorption to aluminium (hydr)oxide phosphate–agarose, as has been proposed for hydroxyapatite[25]. It should be mentioned that AMP, ADP and ATP show little or no adsorption to ferric and zirconium (hydr)oxide phosphate–agarose. In addition, the following proteins are eluted in the same order on hydroxyapatite[24], ferric[14], aluminium (Fig. 1b) and zirconium (hydr)oxide phosphate–agarose (Fig. 1d): ovalbumin, transferrin, lysozyme and cytochrome *C*.

The resolution of the proteins eluted can be improved by the addition of sodium cacodylate (pK_a 6.3) to the buffers, but the reason for this is not yet clear. Its better buffering capacity at pH 6.0 may be important in the case of zirconium (hydr)oxide phosphate–agarose, but this was not valid for aluminium (hydr)oxide phosphate–agarose, where the pH of the buffers is 7.0, *cf.*, columns of hydroxyapatite which give higher resolution of tRNA and proteins when the phosphate buffer is supplemented with sodium chloride[26].

The obvious differences observed are the chromatograms obtained in the purification of β-glucosidase (Fig. 6 in ref. 14, and Fig. 5 herein), the time-dependent adsorption of proteins to zirconium (hydr)oxide phosphate–agarose (Fig. 2b) and the somewhat higher capacity of the aluminium (hydr)oxide phosphate–agarose (Fig. 4 herein and Fig. 5 in ref. 14). An effective purification of proteins should be obtainable upon combining two or three of the adsorbents studied. For example, if the β-glucosidase preparation is first purified on zirconium (Fig. 5b) or ferric (hydr)oxide phosphate–agarose (Fig. 6 in Part I[14]) a considerable fraction of the inactive material can be removed. The peak which is enzymatically active can then be subjected to chromatography on aluminium (hydr)oxide phosphate–agarose for further purification and particularly for fractionation of β-glucosidase into two enzymatically active components.

ACKNOWLEDGEMENTS

This work was supported by the Swedish Natural Science Research Council, the Knut and Alice Wallenberg Foundation and the Bengt Lundqvist Memorial Foundation.

REFERENCES

1 S. A. Barker, A. Emery and J. Novais, *Process Biochem.*, 6 (1971) 11–13.
2 J. F. Kennedy and C. Doyle, *Carbohydr. Res.*, 28 (1973) 89–92.
3 J. F. Kennedy, V. Pike and S. A. Barker, *Enzyme Microb. Technol.*, 2 (1980) 126–132.
4 J. F. Kennedy, S. A. Barker and J. D. Humphreys, *Nature (London)*, 261 (1976) 242–244.
5 A. Kittaha, Y. Sugano, M. Otsuka, Y. Sugira and H. Umerawa, *Tetrahedron Lett.*, 27 (1986) 3631–3634.
6 P. Robinson, P. Dunnil and M. Lilly, *Biotechnol. Bioeng.*, 15 (1973) 603–606.
7 A. Clearfield, in *Inorganic Ion-Exchange Materials*, CRC Press, Boca Raton, FL, 1982, p. 60.
8 S. Colowik, *Methods Enzymol.*, 1 (1955) 90–98.
9 B. Solomon and Y. Levin, *Biotechnol. Bioeng.*, 17 (1975) 1323–1333.
10 A. White and T. Zenser, *Anal. Biochem.*, 41 (1971) 372-396.
11 M. Medina and D. Schwarz, *J. Agric. Food Chem.*, 34 (1986) 907–910.
12 M. Graf, B. Saegesser and G. Schoenenberger, *Anal. Biochem.*, 157 (1986) 295–299.
13 R. B. Martin, *Clin. Chem.*, 32 (1986) 1797–1806.
14 S. Hjertén, I. Zelikman, J. Lindeberg, J.-l. Liao, K.-O. Eriksson and J. Mohammad, *J. Chromatogr.*, 481 (1989) 175–186.

15 S. Hjertén, *Chromatogr. Rev.*, 9 (1967) 122–219.
16 T. L. MacDonald and R. B. Martin, *Trends Biochem. Sci.*, 13 (1988) 15–19.
17 M.-A. Coletti-Previero, M. Pugnière, H. Mattras, J. C. Nicolas and A. Previero, *Biosci. Rep.*, 6 (1986) 477–483.
18 J. S. Johnson and K. A. Kraus, *J. Am. Chem. Soc.*, 78 (1956) 3937–3943.
19 M. Sinibaldi, *J. Chromatogr.*, 76 (1973) 280–284.
20 M. Sinibaldi, G. Matricini and M. Lederer, *J. Chromatogr.*, 129 (1976) 412–414.
21 S. Hjertén and J.-l. Liao, *J. Chromatogr.*, 457 (1988) 165–174.
22 J.-l. Liao and S. Hjertén, *J. Chromatogr.*, 457 (1988) 175–182.
23 A. Tiselius, *Ark. Kemi*, 7 (1954) 443–449.
24 A. Tiselius, S. Hjertén and Ö. Levin, *Arch. Biochem. Biophys.*, 65 (1956) 132–155.
25 G. Bernardi, *Nature (London)*, 206 (1965) 779–783.
26 J. Lindeberg, T. Srichaiyo and S. Hjertén, *J. Chromatogr.*, in press.

Journal of Chromatography, 481 (1989) 201–210
Elsevier Science Publishers B.V., Amsterdam — Printed in The Netherlands

CHROM. 21 810

PREPARATION OF SEVERAL TYPES OF RPC-5-LIKE RESINS AND THEIR USE FOR THE SEPARATION OF OLIGONUCLEOTIDES AND MONONUCLEOTIDES BY HIGH-PERFORMANCE LIQUID CHROMATOGRAPHY

HIROAKI SAWAI
Department of Chemistry, Faculty of Engineering, Gunma University, Kiryu 376 (Japan)
(First received March 29th, 1989; revised manuscript received July 3rd, 1989)

SUMMARY

Improved alternative packing materials to RPC-5 were prepared from granular polychlorotrifluoroethylene of several different particle sizes and trioctylmethylammonium chloride, and used for the separation of mononucleotides and oligonucleotides in high-performance liquid chromatography. High resolution was obtained when particles of 4–8 μm diameter were used, whereas coarser materials (40–90 or 10–40 μm) gave poor resolution. The greater the amount of the quaternary ammonium salt coated, the smaller was the elution volume for the same sample. Oligonucleotides up to a chain length of 75 could be successively separated in less than 2 h under the optimum conditions. Resolution of mononucleotides and short-chain oligonucleotides was accomplished with the resin coated with a minimum amount of the quaternary ammonium salt. A variety of oligonucleotides could be separated depending on the chain length, the differences in the internucleotide linkage and the differences in the base sequence.

INTRODUCTION

The efficient separation of DNA fragments, oligonucleotides and mononucleotides is very important in nucleic aid chemistry and genetic engineering. Up to now the separation and analysis of oligonucleotides have generally been accomplished by high-performance liquid chromatography (HPLC) on a reversed-phase column (ODS-silica gel) or a silica gel-based anion-exchange column[1]. However, these columns cannot be used under alkaline conditions, and are generally inadequate for the separation of long oligonucleotides. Several polymer-based gels have been developed for the separation of oligonucleotides and nucleic acids to overcome the drawbacks of silica gel-based packing materials. For example, Kato and co-workers reported a bonded anion-exchange column based on polymer gel (TSK gel DEAE-5PW) for the separation of oligodeoxyribonucleotides[2] or ribosomal RNA[3].

RPC-5 column chromatography has proved useful for the separation of t-RNA[4–6], DNA restriction fragments[7–9], plasmid DNA[8,10] phage RNA[11] and long oligonucleotides[7,12], since the introduction of RPC-5 by Pearson *et al.*[4]. RPC-5 gives

0021-9673/89/$03.50

a high resolution of long-chain oligonucleotides; it is mechanically strong and chemically inert under strongly acidic and alkaline conditions. However, the original RPC-5 material requires a long time for separations and was not commercially available in high quality, although some alternative materials have been devised. Usher[13] used Kel-F powder as a support for RPC-5 and separated oligouridylates and oligoadenylates. We have now prepared RPC-5-like resins from polychlorotrifluoroethylene with several different particle sizes by modifying the coating and packing methods and have investigated the separation of long- and short-chain oligonucleotides and mononucleotides. The influence of the particle size and amount of coating of trioctylmethylammonium chloride on the resolution and retention volume was studied. This paper reports the usefulness of these RPC-5-like resins for the separation of short-chain oligonucleotides and mononucleotides.

EXPERIMENTAL

Materials

All chemicals were of analytical reagent grade. Buffer solutions were prepared from distilled water and filtered through a 0.22-μm membrane filter.

Oligonucleotides

3′–5′-Linked oligoadenylates containing 5′-terminal phosphate were prepared by partial digestion of polyadenylic acid (Poly A) with nuclease SW[14]. The enzyme digestion was carried out in a solution (1.5 ml) containing Poly A (10 mg), 0.05 *M* carbonate buffer (pH 10.3), 0.1 *M* sodium chloride, 1.5 m*M* magnesium chloride and nuclease SW (100 units) at 37°C. Aliquots of 200 μl were taken after 30 min and 1, 2 and 4 h and stored in a freezer until analysis by HPLC. The chain length of the resulting oligoadenylates depended on the reaction time. Linkage isomers of oligoadenylates and oligouridylates were prepared by lead ion-catalysed polymerization of adenosine-[15] and uridine-5′-phosphorimidazolide[16], respectively. Synthetic oligodeoxyribonucleotides, which were prepared by the phosphotriester method, were a gift from Professor Hata of Tokyo Institute of Technology.

Packing materials

Coarse and fine granular polychlorotrifluoroethyelene (Neosorb ND) were supplied by Nishio Kogyo. Coarse materials were dry-sieved through 100-, 200- and 400-mesh stainless-steel sieves successively to fractionate them into three portions, 100–200 mesh (IV), 200–400 mesh (III) and 400+-mesh (II) particles. A 100-g amount of each fraction was suspended in 200 ml of dichloromethane in a measuring cylinder for sedimentation. The contaminated fine particles in the fraction, which settled slowly, were discarded by suction. Fine materials (I) with a small and uniform particle size had an average particle size of 5–6 μm. The particle size distributions of the materials I, II, III and IV were analysed by the balance sedimentation method in a suspension of isobutyl alcohol. The analyses were carried out by Sumika Analytical Center. The polychlorotrifluoroethylene particles were non-porous, with a nearly spherical to irregular shape with a rough surface which was observed with a microscope. The surface area of material I was 2.47 m^2/g, as measured by the fluidized BET method with a Shimazu Flowsorb 2300 apparatus (Shimazu Techno Research). Table I lists the particle-size distribution of materials I, II, III and IV.

TABLE I

PARTICLE SIZE DISTRIBUTIONS OF POLYCHLOROTRIFLUOROETHYLENE POWDERS

Size range (μm)	*Mass-%*			
	I	*II*	*III*	*IV*
1–2	3			
2–4	36			
4–8	56			
8–10	5			
10–20	0	9		
20–30		36	5	
30–40		55	71	9
40–50		0	18	17
50–60			6	24
60–80			0	29
80–100				21

Coating of Neosorb ND with trioctylmethylammonium chloride was carried out by a modification of the method described by Pearson *et al.*[4]. The original RPC-5 contains 4.0 ml of trioctylmethylammonium chloride per 100 g of Plaskon (polychlorotrifluoroethylene) powder. In our experiments, 100 g of material I were coated with 12, 6 and 3.8 ml of trioctylmethylammonium chloride to prepare RPC-5-like materials Ib, Ia and Ic, respectively. The materials II, III and IV were coated with 6 ml of trioctylmethylammonium chloride.

A slurry of the coated materials in 0.5 *M* sodium perchlorate containing 10 m*M* Tris–acetate (pH 7.5) and 1 m*M* EDTA was packed into a stainless-steel column (25 cm × 4 mm I.D.) with a magnetically stirred slurry packer at a flow-rate of 5.0 ml/min. The pressure rose during packing to 250 kg/cm^2 for the materials prepared from I. The flow was continued for 1 h at a constant pressure of 250 kg/cm^2 to obtain cross packings. The column for the separation of mononucleotides was prepared by coating the polychlorotrifluoroethylene powder with trioctylmethylammonium chloride at 3.5 ml per 100 g, followed by washing with distilled water for 2 h at a flow-rate of 1.0 ml/min to remove the weakly bound trioctylmethylammonium chloride. Emulsified turbid water came out first, then turned clear.

High-performance liquid chromatography

A Hitachi 638 high-performance liquid chromatograph was used with a UV detector at 260 nm. The column was equilibrated with an initial eluting solution and eluted with a linear gradient of sodium perchlorate solution buffered with Tris–acetate (pH 7.5) or sodium hydroxide (pH 12) containing EDTA at a flow-rate of 1.0 ml/min. The relative concentrations of sodium perchlorate, Tris buffer and EDTA were varied. Typical back-pressures of the columns were 5, 15, 35 and 120 kg/cm^2 from materials IV, III, II and I, respectively. The material from I was used in the usual operations, except in the experiment to investigate the influence of particle size on resolution.

RESULTS AND DISCUSSION

The column performance was greatly affected by the particle size of the resin, the coating method and the packing procedure. The finest materials gave the best resolution of the oligonucleotides. In most instances we used material I coated with 6 ml of trioctylmethylammonium chloride per 100 g of the resin (Ia). The retention time and resolution of the oligonucleotides changed during the first five injections partly because of the loss of the weakly bound coating from the new column. We therefore conducted a blank operation a few times with a newly packed column; the column performance became stable after this simple pretreatment. Gradients of acetate, chloride and perchlorate salt solution have previously been used as an eluent in RPC-5 column chromatography[7,13]. The column performance differs greatly with the different types of salt. We investigated solutions of sodium chloride, perchlorate and acetate as eluents and confirmed that sodium perchlorate is the most suitable. The advantages of sodium perchlorate are as follows: (1) perchlorate solution does not corrode stainless-steel HPLC equipment, whereas chloride solution is corrosive; (2) perchlorate solution has a high ionic strength and is a strong eluent[17]; sodium perchlorate solution eluted oligonucleotides at concentrations three to ten time lower than sodium chloride or acetate solution; and (3) sodium perchlorate can be removed more easily than sodium chloride from the recovered oligonucleotide solution by ethanol precipitation, as sodium perchlorate is far more soluble than sodium chloride in organic solvents. The recovered oligonucleotides after desalting retain their susceptibility to enzymes such as nucleases, polynucleotide kinase and T_4 ligase.

Fig. 1 shows a typical separation of oligoadenylates containing 5'-terminal phosphate, which was prepared by partial digestion of poly A with nuclease SW for 30 min. Oligoadenylates up to the 75-mer were successively separated in less than 2 h by HPLC on column Ia. After the enzyme digestion of the poly A for 4 h, long oligoadenylates diminished and only short-chain oligoadenylates were detected by HPLC (data not shown). The time course of the enzyme digestion of nucleic acid was monitored by HPLC.

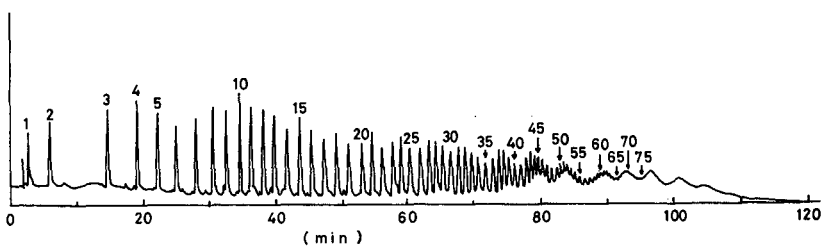

Fig. 1. Separation of oligoadenylates on an RPC-5-like column (Ia) The column (250 × 4 mm I.D.) was eluted with a gradient of $NaClO_4$ solution from 0.01 to 0.05 *M* in 30 min, then to 0.1 *M* in 50 min and finally to 0.15 *M* in 40 min, at a flow-rate of 1.0 ml/min and at 22°C. The buffer used was 10 m*M* Tris–acetate (pH 7.5) and 1 m*M* EDTA. Oligoadenylates, which were prepared by partial digestion of polyadenylates with nuclease SW for 30 min, were applied to the column without purification. The eluate was monitored by UV absorption at 260 nm. The numbers on the peaks denote the chain length of the oligoadenylate.

We investigated the effect of the particle size of the packing materials on the resolution of the oligonucleotides. Fig. 2 shows the elution profiles of the oligoadenylates when packing materials II, III and IV were used. The elution conditions were the same as in Fig. 1. The difference in particle size of the packing materials did not influence the retention time, but had a great effect on the resolution. A smaller and more uniform size of the material gave better resolution. Oligoadenylates up to the 30-mer were separated with packing material III whereas IV gave very poor resolution. Hence the material obtained by sieving between 100 and 200 or 200 and 400 mesh was found to be unsuitable for the HPLC use.

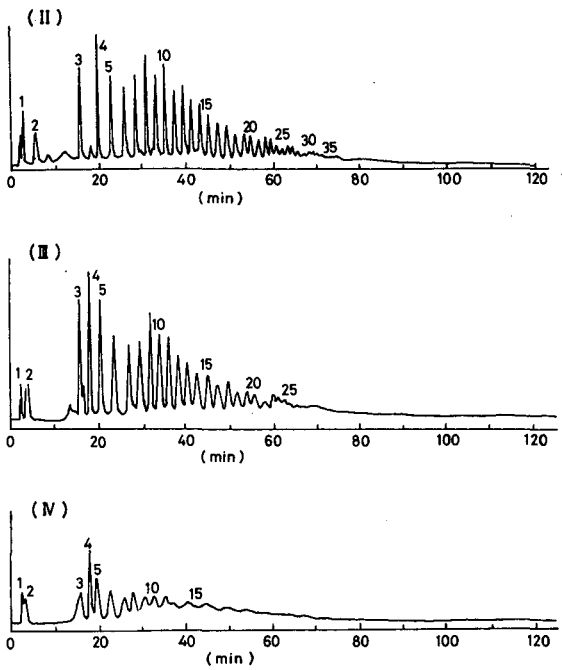

Fig. 2. Effect of particle size of RPC-5-like material on the resolution of oligoadenylates. Particle size: II, 10–40; III, 20–60; IV, 30–100 μm. Column size and elution conditions as in Fig. 1. Oligoanylates, which were prepared by partial digestion of polyadenylates with nuclease SW for 1 h, were used as samples. The numbers on the peakes denote the chain length of the oligoadenylates.

The influence of the amount of coating of trioctylmethylammonium chloride on the elution of oligoadenylates is shown in Fig. 3. Elution of the oligonucleotides was faster when a larger amount of trioctylmethylammonium chloride was used. It is interesting that the retention time decreases as the amount of stationary phase increased. Polychlorotrifluoroethylene particles have a strong hydrophobic character and bind oligonucleotides tightly[13]. Trioctylmethylammonium chloride decreases the hydrophobic binding of oligonucleotides to the polymer, although it promotes the electrostatic interactions with oligonucleotides. The packing material prepared by washing with water after coating contained a minimum amount of trioctylmethylammonium chloride, and eluted the oligonucleotides slowly. Despite previously published suggestions that RPC-5 should not be exposed to low salt concentrations or

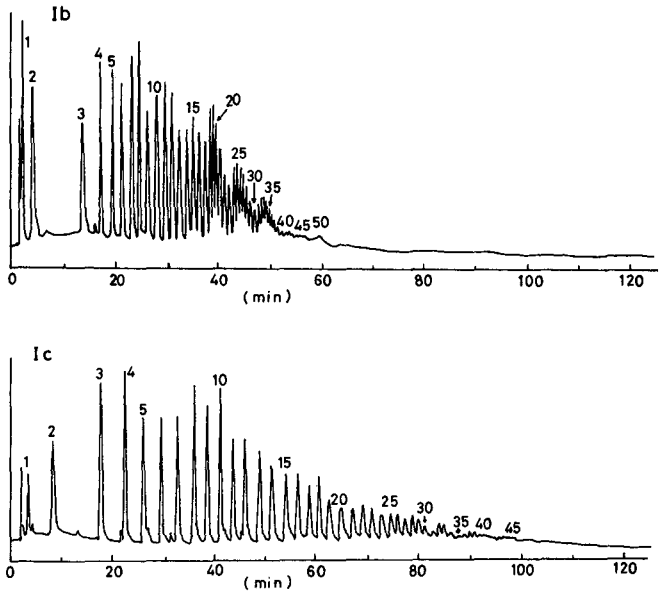

Fig. 3. Effect of amount of coating of trioctylmethylammonium chloride on RPC-5-like materials on the separation of oligoadenylates. Coating amount: Ib, 14 ml of trioctylmethylammonium chloride per 100 g of polychlorotrifuoroethylene; Ic, 3.8 ml per 100 g. Column size, elution conditions and sample as in Fig. 2.

water[7,12], we found that pretreatment of the RPC-5-like resin with water had a good effect on the separation of mononucleotides and short-chain oligonucleotides, as their retention times became longer. Adenosine, 5′-AMP, 2′-AMP, 3′-AMP, ADP and ATP were separated in less than 15 min with the prewashed column, as shown in Fig.

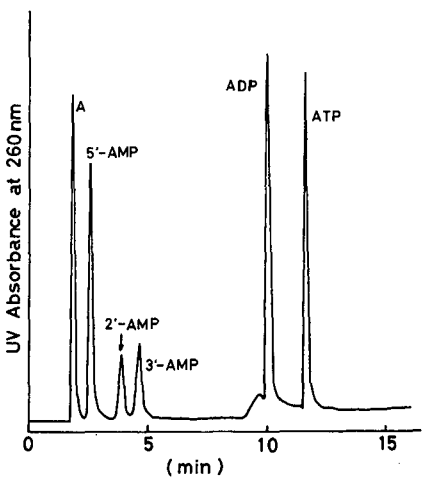

Fig. 4. Separation of adenine mononucleotides on an RPC-5-like column (Ic). The column (250 × 4 mm I.D.), pretreated with water, was eluted with a linear gradient of 0–0.01 *M* $NaClO_4$ in 15 min at a flow-rate of 1.0 ml/min and at 24°C. The buffer used was 2.5 m*M* Tris-acetate and 0.1 m*M* EDTA (pH 7.5). The eluate was monitored by UV absorption at 260 nm.

4. Compounds with more phosphate residues tend to elute later as the column has an anion-exchange character.

The separation of 2′–5′- and 3′–5′-linked isomers of oligoadenylates with the column Ic is shown in Fig. 5a. Two dimers, four trimers and four tetramers were well separated. Similarly linked isomers of oligouridylates, oligoinosinates and oligocytidylastes were resolved in a short time. Fig. 5b shows the elution profiles of the linked isomers of oligouridylates. 2′–5′-Linked isomers eluted earlier than the corresponding 3′–5′-linked isomers. Linked isomers containing both 3′–5′ and 2′–5′ linkages eluted between fully 2′–5′- and 3′–5′-linked isomers.

Four base-sequence isomeric oligodeoxyribonucleotides, GGCC, CCGG, GCGC and CGCG, showed different chromatographic patterns, as shown in Fig. 6. The mobility of the isomers was altered on changing the pH of the eluent from 7.5 to 12. The results suggest that the tetramers have different conformations which can be

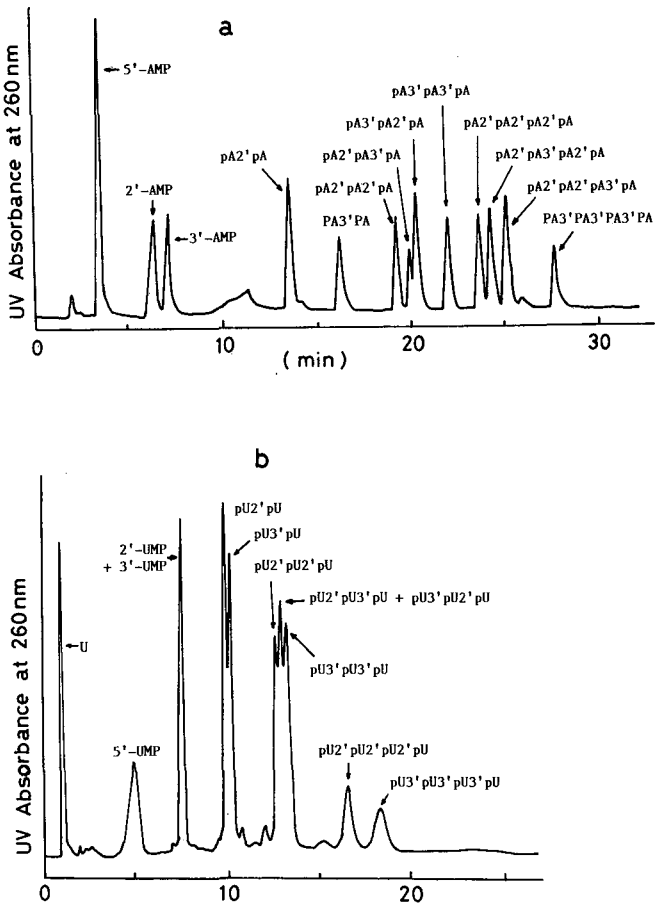

Fig. 5. Resolution of lined isomers of short-chain oligoribonucleotides. The column (Ic, 250 × 4 mm I.D.) was eluted with a linear gradient of 0–0.02 *M* $NaClO_4$ in 30 min at a flow-rate of 1.0 ml/min and at 22°C. The buffer was 2.5 m*M* Tris–acetate and 0.1 m*M* EDTA (pH 7.5). The elutate was monitored by UV absorption at 260 nm. (a) Linked isomers (2′–5′ and 3′–5′) of oligoadenylates; (b) linked isomers (2′–5′ and 3′–5′) of oligouridylates.

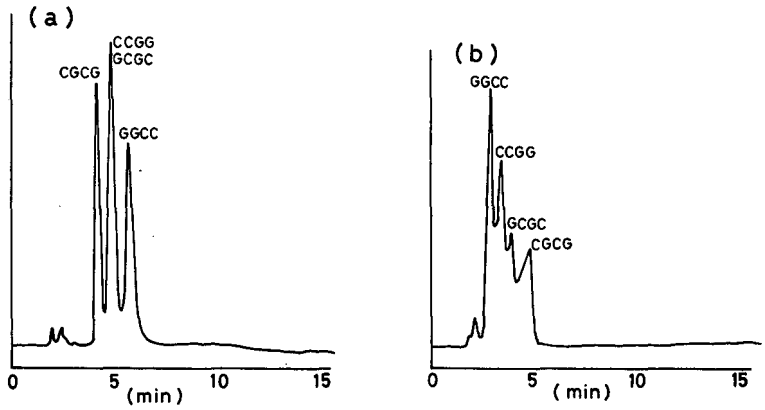

Fig. 6. Separation of sequence isomers of tetradeoxyribonucleotides, CGCG, GCGC, GGCC and CCGG, on an RPC-5-like column (Ia). The column (250 × 4 mm I.D.) was eluted with a gradient of 0.01–0.025 *M* $NaClO_4$ in 15 min at a flow-rate of 1.0 ml/min and at 22°C. Buffer (a) 10 m*M* NaOH and 1 m*M* EDTA (pH 12); (b) 10 *M* Tris–acetate and 1 m*M* EDTA (pH 7.5). The eluate was monitored by UV absorption at 260 nm.

recognized on the surface of the resin. Different elution patterns depending on the base sequence were also obversed with other sequence isomers containing AT bases, as shown in Fig. 7.

RPC-5 has generally been used for the separation of long-chain oligonucleotides such as DNA restriction fragments and t-RNA. Our results demonstrate that RPC-5 is also useful for the separation of mononucleotides and short-chain oligonucleotides. The capacity of the resin is several to ten times smaller than that of ODS-silica gel with the same column size, as the polychlorotrifluoroethylene particles are non-porous and the surface area is smaller than that of silica gel. Up to twenty A_{260} units of oligoadenylates from the dimer to decamer could be loaded on the column without a decrease in the resolution under the normal operating conditions. The

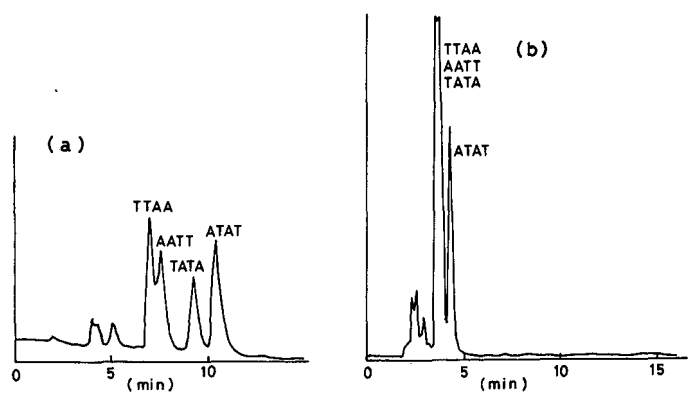

Fig. 7. Separation of sequence isomers of tetradeoxyribonucleotides, ATAT, TATA, TTAA and AATT, on an RPC-5-like column. Column and elution conditions as in Fig. 6. The minor impurities eluted in front of the tetramers.

loading capacity of the oligodeoxyribonucleotides on the resin is smaller than that of oligoribonucleotides. Up to five A_{260} units of dATAT could be chromatographed on the column with satisfactory resolution. When the samples were overloaded, the resolution became worse and the retention time became shorter.

The recoveries of the samples from the column were usually over 70%; 95% of 3′–5′-linked $(pA)_4$ was recovered when one A_{260} unit of the sample was chromatographed, as calculated from the ratio of the UV absorption of the recovered sample to that of the injected sample. The recovery of synthetic DNA oligomers, dATAT and the 25-mer, was 60–90% when 0.01 *M* sodium hydroxide solution was used as the eluting buffer. Resolution of the oligonucleotides was achieved, depending on the differences in chain length, internucleotide linkage, base sequence and phosphate residues. RPC-5 has been reported to separate DNA fragments based on chain length and base composition[7]. DNA, which is rich in AT, eluted slowly[18]. These complexities of the separation mode make the use of RPC-5-type materials difficult for identifying the size of the oligonucleotides. The separation of oligonucleotides can be accomplished based on size alone by gel electrophoresis or size exclusion chromatography with a gel filtration HPLC column[19]. On the other hand, gel electrophoresis cannot separate oligonucleotides of the same chain length but with different base compositions or different base sequences. The separation of oligonucleotides by HPLC on the RPC-5 column may complement separations by gel electrophoresis or size exclusion chromatography. A particle size of about 5 μm is most suitable in an RPC-5 HPLC column and gives rapid separations. The column can be used at least several tens of times without a decrease in resolution. The RPC-5 column has a shorter life than bonded-phase columns. Nevertheless, the RPC-5-type resin is still useful for the separation of short- and long-chain oligonucleotides, as it has a wide range of column performance depending on the operating conditions. The resolution of long-chain DNA and RNA using RPC-5-like resin will be described in a later paper.

REFERENCES

1 G. Zon and J. A. Thompson, *Biochromatography*, 1 (1986) 22.
2 H. Ozaki, H. Wada, T. Takeuchi, K. Makino, T. Fukui and Y. Kato, *J. Chromatogr.*, 332 (1985) 243.
3 Y. Kato, K. Nakamura and T. Hashimoto, *J. Chromatogr.*, 266 (1983) 385.
4 R. L. Pearson, J. F. Weiss and A. D. Kelmer, *Biochim. Biophys. Acta*, 228 (1971) 770.
5 B. Roe, K. Marcu and B. Dudock, *Biochim. Biophys. Acta*, 319 (1973) 25.
6 R. P. Singhal, *J. Chromatogr.*, 266 (1983) 359.
7 R. D. Wells, S. C. Hardies, G. T. Horn, B. Klein, J. E. Larson, S. K. Neuendorf, N. Panayotatos, R. K. Patient and E. Selsing, *Methods Enzymol.*, 65 (1980) 327.
8 J. A. Thompson, R. W. Blakesley, K. Doran, C. J. Hough and R. D. Wells, *Methods Enzymol.*, 100 (1983) 368.
9 W. Hillen, R. D. Klein and R. D. Wells, *Biochemistry*, 20 (1981) 3748.
10 A. N. Best, D. P. Allison and G. D. Novelli, *Anal. Biochem.*, 114 (1981) 235.
11 C. Campbell, S. M. Arfin and E. Goldman, *Anal. Biochem.*, 102 (1980) 153.
12 B. W. Shum and D. M. Crothers, *Nucleic Acids Res.*, 5 (1978) 2297.
13 D. A. Usher, *Nucleic Acids Res.*, 6 (1979) 2289.
14 J.-I. Mukai, *Biochim. Biophys. Res. Commun.*, 21 (1965) 562.
15 H. Sawai, T. Shibata and M. Ohno, *Tetrahedron*, 37 (1981) 481.
16 H. Sawai and M. Ohno, *Chem. Pharm. Bullo.*, 29 (1981) 2237.
17 D. A. Usher and J. A. Rosen, *Anal. Biochem.*, 92 (1979) 276.

18 R. K. Patient, S. C. Hardies, J. E. Larson, R. B. Inman, L. E. Maque and R. D. Wells, *J. Biol. Chem.*, 254 (1979) 5548.
19 Y. Kato, M. Sasaki, T. Hashimoto, T. Murotsu, S. Fukushige, and K. Matsubata, *J. Chromatogr.*, 266 (1983) 341.

Journal of Chromatography, 481 (1989) 211–219
Elsevier Science Publishers B.V., Amsterdam — Printed in The Netherlands

CHROM. 21 665

NEW ULTRAVIOLET LABELLING AGENTS FOR HIGH-PERFORMANCE LIQUID CHROMATOGRAPHIC DETERMINATION OF MONOCARBOXYLIC ACIDS

KOICHI FUNAZO*
Department of Chemistry, Osaka Prefectural College of Technology, Saiwai-cho, Neyagawa, Osaka 572 (Japan)
and
MINORU TANAKA, YUTA YASAKA, HIROSHI TAKIGAWA and TOSHIYUKI SHONO
Department of Applied Chemistry, Faculty of Engineering, Osaka University, Yamada-oka, Suita, Osaka 565 (Japan)
(Received April 14th, 1989)

SUMMARY

New UV-labelling agents have been synthesized, which are designed to convert monocarboxylic acids into their highly UV-absorbing derivatives for enhancement of the sensitivities of UV detection in high-performance liquid chromatography. The reagents are *p*-nitrobenzyl, 3,5-dinitrobenzyl and 2-(phthalimino)ethyl *p*-toluenesulphonates. Each has been prepared by reaction of *p*-toluenesulphonyl chloride with *p*-nitrobenzyl alcohol, 3,5-dinitrobenzyl alcohol or N-(hydroxyethyl)phtalimide, respectively, in the presence of sodium hydroxide, and they are stable in the solid state for at least 6 months. Monocarboxylic acids were derivatized to their *p*-nitrobenzyl, 3,5-dinitrobenzyl or 2-(phthalimino)ethyl esters with each of the above reagents, respectively, then determined by high-performance liquid chromatography with UV detection. In the UV-labelling with each reagent, 18-crown-6 was used as the catalyst. The effects of the reaction solvent, reaction temperature and time and the concentrations of each reagent and the catalyst were also examined.

INTRODUCTION

By the introduction of ion chromatography[1,2], analyses using high-performance liquid chromatography (HPLC) have been widely extended. Ion chromatography has unmatched ability to determine trace inorganic anions[3], since a conductivity detector is used. However, it is diffucult to determine trace amounts of organic anions by ion chromatography because of their low electric conductivities. In the HPLC determination of organic anions a labelling technique has usually been used for enhancement of the sensitivity of UV or fluorescence detection, and various labelling agents have been developed[4,5]. For carboxylic acids, frequently used were O-(*p*-nitrobenzyl)-N,N′-diisopropylisourea[6], tolyltriazene derivatives (such as 1-benzyl-[7] and

0021-9673/89/$03.50

1-*p*-nitrobenzyl-3-*p*-tolyltriazene[8]) and halomethyl compounds (such as substituted phenacyl bromide (*p*-bromo- and *m*-methoxyphenacyl bromide)[9–11], 9-chloromethylantracene[12], N-chloromethyl-4-substituted phthalimide[13–14] and 7-acetoxy- and 7-methoxy-4-bromomethylcoumarins[15]). To our knowledge, only one report has been published with regard to sulphonate-type labelling agents for HPLC[16]. In this method, carboxylic acids were treated with 4′-bromophenacyl trifluoromethanesulphonate and derivatized to *p*-bromophenacyl esters which were subsequently determined by HPLC with UV detection.

Previously, we developed a derivatizing technique for gas chromatography with a new agent, pentafluorobenzyl *p*-toluenesulphonate[17–19], which is now commercially available. This reagent is designed to introduce the pentafluorobenzyl moiety into the analyte molecules in order to enhance not only their volatility but also their sensitivity.

In this work, three *p*-toluenesulphonate-type UV-labelling agents for HPLC have been synthesized; *p*-nitrobenzyl *p*-toluenesulphonate (TsO-PNB), 3,5-dinitrobenzyl *p*-toluenesulphonate (TsO-DNB) and 2-(phthalimino)ethyl *p*-toluenesulphonate (TsO-PE). Their applicabilities to UV labelling and the HPLC determination of monocarboxylic acids have been examined, as shown in Scheme 1.

EXPERIMENTAL

Apparatus

When using TsO-PNB or TsO-DNB as the reagent, the HPLC system comprised a Model KHD-W-52 pump, a Model KHG-250L pressure gauge, a Model KHP-UI-130 high-pressure universal injector (Kyowa Seimitsu, Tokyo, Japan), a special damper (Gasukuro Kogyo, Tokyo, Japan) and a Model UVD-2 fixed-wavelength (254 nm) UV absorption detector (Shimadzu, Kyoto, Japan). The separation column, YMC A-302 ODS (15 cm × 4.6 mm I.D., particle size 5 μm), was obtained from Yamamura Chemical Labs. (Kyoto, Japan).

When using TsO-PE, the system consisted of a Model 880-PU pump (Japan

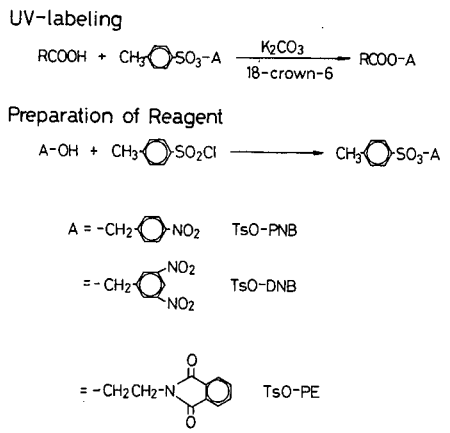

Scheme 1. Preparation of *p*-toluenesulphonate UV-labelling agents.

Spectroscopic, Tokyo, Japan), a Model 7125 syringe loading sample injector (Rheodyne, Cotati, CA, U.S.A.) and a Model 875-UV variable-wavelength UV absorption detector (Japan Spectroscopic) operating at 222 nm. The separation column (15 cm × 4.6 mm I.D.) packed with Tosoh (Tokyo, Japan) ODS-80TM (particle size 5 μm) was used together with a precolumn (3 cm × 4.6 mm I.D.) containing Chemco (Osaka, Japan) Nucleosil 50B anion exchanger, to remove *p*-toluenesulphonic acid and other by-products interfering with the detection at 222 nm.

In both cases, the mobile phase was acetonitrile at a constant flow-rate of 0.5 ml/min. A Shimadzu Chromatopac C-R6A data processor was used as the recorder and integrator.

An Hitachi RMU-6E mass spectrometer was employed with an ionization source temperature of 200°C and an acceleration energy of 1.8 kV.

Reagents

Analytical reagent grade 18-crown-6 was obtained from Aldrich (Milwaukee, WI, U.S.A.), and monocarboxylic acids used were of analytical reagent grade from Wako (Osaka, Japan) and Tokyo Kasei (Tokyo, Japan). Acetonitrille was distilled before use for the labelling-reaction solvent, and it was further filtered with a Millipore FH 0.5-μm membrane filter (Millipore, Bedford, MA, U.S.A.) for the mobile phase.

Syntheses of UV-labelling agents

Each of the three new UV-labelling agents was prepared from reactions between *p*-toluenesulphonyl chloride and corresponding alcohols by modifying the literature method[20] as follows.

TsO-PNB. *p*-Nitrobenzyl alcohol (10 g), *p*-toluenesulphonyl chloride (20 g) and tetra-*n*-butylammonium hydrogensulphate (1 g) were dissolved in 300 ml of toluene, and the toluene solution was stirred in a water-bath at 10°C. Then 5 *M* NaOH (25 ml) was added carefully lest the temperature of the reaction mixture should exceed 15°C. After the addition, stirring was continued for 5 h, keeping the temperature below 15°C. After the filtration of the precipitate liberated during the reaction, the toluene layer was separated from the water layer, washed three times with 200 ml of water, dried on anhydrous magnesium sulphate and evaporated. By recrystallizing the resulting solid from methanol, TsO-PNB was obtained as white needles (yield: 40%).

TsO-DNB. 3,5-Dinitrobenzyl alcohol (1.58 g) and *p*-toluenesulphonyl chloride (2.2 g) were dissolved in 1,4-dioxane (15 ml), and then 40% NaOH (4 g) was added slowly to the solution stirred in an ice-bath. After stirring for 7 h, the reacted solution was poured into 500 ml of cold water. The resulting solid was collected on a glass filter (3G5), washed with methanol and then recrystallized from ligroin. TsO-DNB was obtained as yellow needles (yield: 80%).

TsO-PE. Two pyridine solutions were prepared by dissolving 2 g of N-(hydroxyethyl)phthalimide and 2.4 g *p*-toluenesulphonyl chloride in 10 ml of pyridine, respectively. The *p*-toluenesulphonyl chloride solution was added dropwise to the N-(hydroxyethyl)phthalimide solution which was maintained at −10°C with a mixture of ice and sodium chloride. After stirring for 8 h, pyridine hydrochloride was removed by filtration. The filtrate was diluted in chloroform and washed with water. The chloroform solution dried on anhydrous magnesium sulphate was placed on a

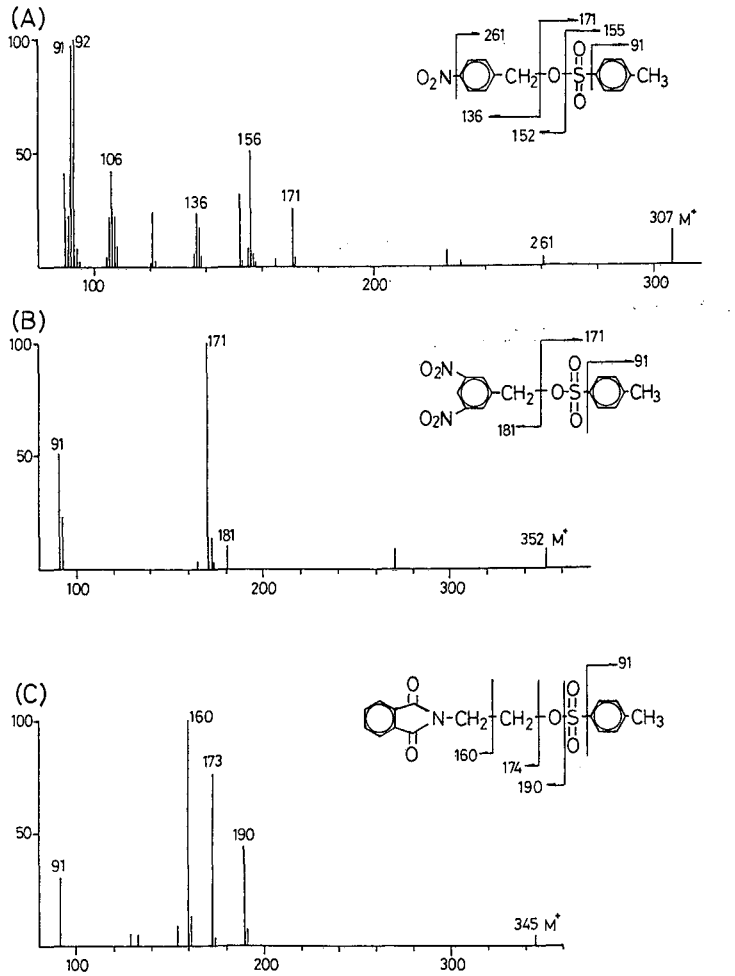

Fig. 1. Mass spectra of TsO-PNB (A), TsO-DNB (B) and TsO-PE (C).

column (5 cm × 5 cm I.D.) of silica gel (C-300, 200–300 mesh) obtained from Wako. TsO-PE eluted with chloroform was recrystallized from ethanol and obtained as white needles (yield : 75%).

The three *p*-toluenesulphonates thus synthesized were identified by mass and infrared spectrometry. Fig. 1 shows their mass spectra, and the infrared spectrum of TsO-PNB is given in Fig. 2.

Procedure

The recommended procedure for UV-labelling of monocarboxylic acids with each of the three reagents was as follows. A brown test-tube with a screw cap (*ca.* 10 ml) was used as the reaction vessel in order to protect the contents from light. To 1.00 ml of a reference standard solution of monocarboxylic acids was added a solution (1.5 ml) containing the reagent and 18-crown-6 as the catalyst. As the solvent of the

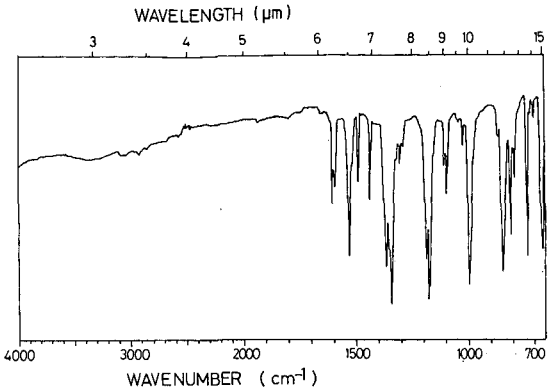

Fig. 2. Infrared spectrum of TsO-PNB.

reference standard and the reagent solutions, acetone, acetonitrile and propionitrile were used in the UV-labelling with TsO-PNB, TsO-DNB and TsO-PE, respectively (Table I). The concentrations of the agent and 18-crown-6 in the solution were dependent on the labelling agent as shown in Table I. Then a small amount of anhydrous potassium carbonate was added, and the mixture was stirred at a fixed temperature for a fixed time. After the reaction period, the reacted solution was filtered with a Minisart SRP 15 disposable filter holder in which an 0.45-μm pore size hydrophobic membrane filter was fitted (Sartorius, Göttingen, F.R.G.). An aliquot (10 μl) of the filtrate was injected into the high-performance liquid chromatograph. The optimum reaction temperature and reaction time for each reagent are given in Table I.

RESULTS AND DISCUSSION

Preparation of reagents, and UV-labelling

Fig. 1 shows the mass spectra of TsO-PNB, TsO-DNB and TsO-PE synthe-

TABLE I

OPTIMUM CONDITIONS AND CALIBRATION

	TsO-PNB	*TsO-DNB*	*TsO-PE*
Reaction solvent	Acetone	Acetonitrile	Propionitrile
Reaction temperature (°C)	Room temp.	50	85
Reaction time (min)	30	20	60
Reagent concentration (m*M*)	15	5	20
18-Crown-6 concentration (m*M*)	2.5	2.5	Not used
Wavelength of UV detection (nm)	232 (254)[a]	272 (254)[a]	222
Determination level (μ*M*)[b]	25–250	10–100	1.0–10.0
Correlation coefficient of calibration graph[b]	0.9989	0.9991	0.9988

[a] In this work, the fixed-wavelength (254 nm) UV detector was used.
[b] These values were obtained for myristic acid.

sized. The mass peak at 307, 352 or 345 corresponds to the parent ion of TsO-PNB, TsO-DNB or TsO-PE, respectively, and other peaks are equivalent to the fragment ions of the *p*-toluenesulphonates. Fig. 2 shows the infrared spectrum of TsO-PNB. Two bands at 1180 and 1350 cm^{-1} are characteristic of the symmetric and anti-symmetric vibrations of $S(=O)_2$, respectively. The other two reagents give similar infrared spectra in this region.

Myristic acid was selected as the model monocarboxylic acid, and it was UV-labelled with each of the three reagents according to the procedure described in the Experimental section. In each case the HPLC peak corresponding to the *p*-nitrobenzyl (PNB), 3,5-dinitrobenzyl (DNB) or 2-(phthalimino)ethyl (PE) derivative was observed. The authentic sample of each derivative was synthesized by scaling up the reaction system and isolated. By mass spectrometry of the authentic samples, the PNB, DNB and PE derivatives were identified as PNB, DNB and PE esters of myristic acid, respectively.

Optimum derivatization conditions

The derivative of myristic acid labelled with each reagent should be detected at a wavelength corresponding to the absorption maximum of the derivative. In order to determine the wavelength, the reacted solution with each reagent was detected at different wavelengths (Fig. 3). The peaks of the PE derivative are much larger than those of the PNB and DNB derivatives. In Fig. 3, therefore, the peak areas of the PE derivative are shown separately from those of the other two derivatives; *i.e.*, the ordinate of Fig. 3 is shown by assigning the maximum peak areas of PE and DNB derivatives as 100. The wavelength which gives the maximum peak area of the PE derivative is 218 nm, and the peak area detected at 254 nm is much less than the maximum peak area. For the PNB and DNB derivatives, on the other hand, the

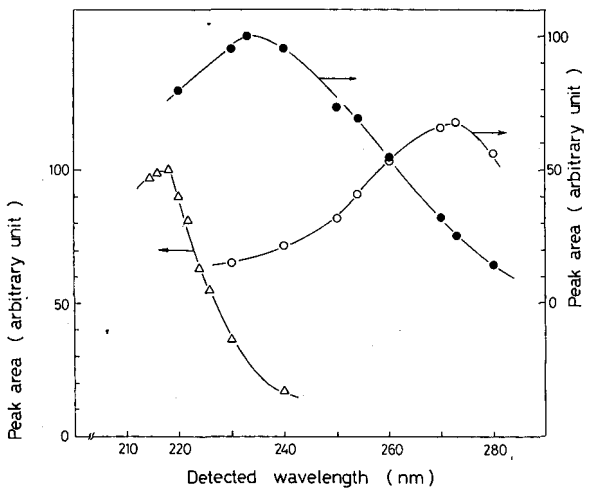

Fig. 3. Effect of wavelength on the peak area of PNB (○), DNB (●) and PE (△) derivatives of myristic acid. The peak area on the ordinate is shown by assigning the maximum peak areas of DNB and PE derivatives as 100.

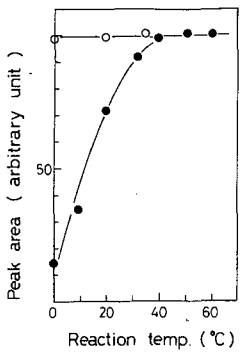

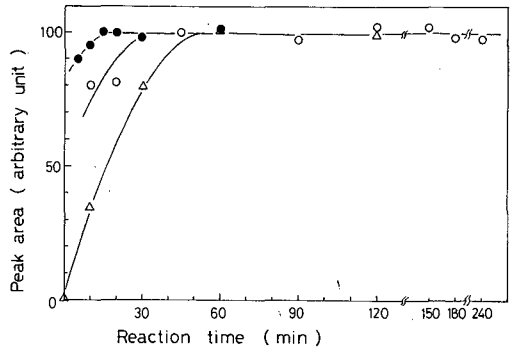

Fig. 4. Effect of reaction temperature on the labelling with TsO-PNB (○) and TsO-DNB (●).

Fig. 5. Effect of reaction time on the labelling with TsO-PNB (○), TsO-DNB (●) and TsO-PE (△).

wavelengths are 273 and 233 nm, respectively, and the peak areas of the derivatives detected at 254 nm are relatively high. In this work, an fixed-wavelength (254 nm) UV detector was used for the analysis of PNB or DNB derivatives. The variable-wavelength UV detector was used at 222 nm for the analysis of PE derivatives, because the noise at 222 nm is much less than that at 218 nm.

The UV-labelling of myristic acid was performed in several organic solvents frequently used. From the results, acetone gives the highest peak area of the derivative for the labelling with TsO-PNB, even if the labelling is carried out at room temperature. For the labelling with TsO-DNB, on the other hand, the yield is highest at 50°C in acetonitrile. For TsO-PE, the best results were obtained using propionitrile as the solvent at 85°C.

The effect of the reaction temperature was studied with the optimum labelling system and solvent. Fig. 4 shows the results for the labelling with TsO-DNB, together with TsO-PNB. In Fig. 4 or 5, the peak area on the ordinate is exhibited by assigning the maximum peak area of the derivative labelled with each reagent as 100. The peak area of the DNB derivative increases with increasing reaction temperature to a constant value beyond 40°C, while that of the PNB derivative is constant, independent of the reaction temperature. Therefore, the reaction temperature was fixed at 50°C for the labelling with TsO-DNB and at room temperature for that with TsO-PNB. From the results of similar measurements, the labelling with TsO-PE was performed at 85°C.

We have also tested the effect of the reaction time on the labelling. From these results, shown in Fig. 5, the reaction times were fixed as given in Table I.

Next, the effect of the concentration of the reagent in the solution added to the reference standard solution was examined. From the results, the optimum concentrations of TsO-PNB, TsO-DNB and TsO-PE are 15, 5 and 20 m*M*, respectively. Furthermore, the effect of the catalyst, 18-crown-6, concentration in that solution on the labelling was examined. To perform the labelling with TsO-PNB or TsO-DNB, 2.5 m*M* 18-crown-6 solution is necessary, while the derivative peak area does not vary regardless of the presence of 18-crown-6 in the labelling with TsO-PE. Therefore, the optimum concentrations of the catalyst were fixed as given in Table I.

Analytical calibrations and chromatograms

After the optimum reaction conditons for the labelling with each reagent had been established, the derivatization yields for myristic acid were evaluated as follows. The peak area of the derivative of myristic acid labelled with each agent was compared with that of the standard solution of the authentic derivative mentioned above. The yields of the labelling reactions with TsO-PNB, TsO-DNB and TsO-PE are 105, 94 and 94%, respectively.

A calibration graph was constructed by analyzing ten reference standard solutions of myristic acid with each agent and by plotting the concentration of myristic acid *vs.* the peak area of the derivative. Three straight lines passing through the origin were obtained with correlation coefficients nearly equal to 1, as shown in Table I. The determination levels are primarily dependent on the strengths of the absorption of the derivatives labelled with the agents. When the detection of PNB and DNB derivatives is carried out at the optimum wavelength (PNB, 272 nm; DNB, 232 nm), the determination levels should be reduced down to about half of those given in Table I. The sensitivity of the labelling method with TsO-PE is very high, but the detection at 222 nm is apt to be obstructed by many compounds.

Fig. 6 shows the chromatograms obtained for the determination of several

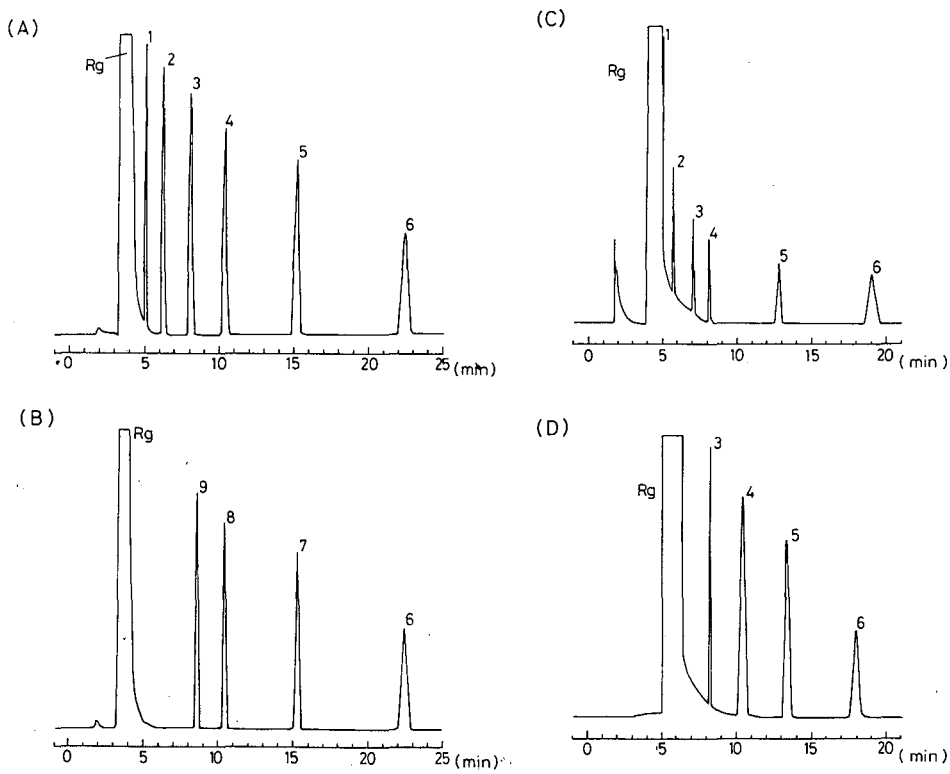

Fig. 6. Chromatograms of a mixture of monocarboxylic acids labelled with TsO-PNB (A,B), TsO-DNB (C) and TsO-PE (D). Peaks: Rg = reagent; 1 = caprylic acid; 2 = capric acid; 3 = lauric acid; 4 = myristic acid; 5 = palmitic acid; 6 = stearic acid; 7 = oleic acid; 8 = linolic acid and 9 = linolenic acid.

monocarboxylic acids. The separation of the peaks of the derivatives of lower monocarboxylic acids from that of the reagent is somewhat improved by using acetonitrile solution containing small quantities of water as the mobile phase. With these reagents, unsaturated monocarboxylic acids can also be labelled, together with saturated ones. Fig. 6B shows the chromatogram obtained when three unsaturated monocarboxylic acids (carbon number: 18) were labelled with TsO-PNB. The retention times for linolenic, linolic and oleic acids are close to those for lauric, myristic and palmitic acids, respectively. Under these HPLC conditions, the separation of the PNB derivatives of myristic and linolic acids is impossible, while the derivatives of lauric and linolenic acids can be separated almost entirely. The derivatives of palmitic and oleic acids can be separated slightly under these conditions. The separation of the derivatives of saturated and unsaturated monocarboxylic acids will be further studied by changing the mobile phase and/or the separation column.

For the HPLC determination of monocarboxylic acids, three *p*-toluenesulphonate-type UV-labelling agents have been developed, which bear tagging groups for UV detection. Various tagging groups will also be introduced for fluorescence detection in a similar fashion. Further work is now in progress to develop a polystyrene-type polymeric UV-labelling agent, in order to facilitate the separation of the reagent from the derivatives, and to avoid the coinjection of the reagent and the contamination of the separation column.

REFERENCES

1 H. Small, T. S. Stevens and W. S. Bauman, *Anal. Chem.*, 47 (1975) 1801.
2 D. T. Gjerde, J. S. Fritz and G. Schmuckler, *J. Chromatogr.*, 186 (1979) 509.
3 J. S. Fritz, D. T. Gjerde and C. Pohlandt, *Ion Chromatography*, Hüthig, Heidelberg, 1982.
4 J. F. Lawrence and R. W. Frei, *Chemical Derivatization in Liquid Chromatography*, Elsevier, Amsterdam, 1976.
5 J. F. Lawrence and R. W. Frei, *Chemical Derivatization in Analytical Chemistry*, Vols. 1 and 2, Plenum, New York, 1981.
6 D. R. Knapp and S. Krueger, *Anal. Lett.*, 8 (1975) 603.
7 I. R. Politzer, G. W. Griffin, B. J. Dowty and J. L. Laseter, *Anal. Lett.*, 6 (1973) 539.
8 S. Okuyama, *Chem. Lett.*, (1976) 679.
9 H. D. Durst, M. Milano, E. J. Kikta, S. A. Connelly and E. Grushka, *Anal. Chem.*, 47 (1975) 1797.
10 F. A. Fitzpatrick, *Anal. Chem.*, 48 (1976) 499.
11 R. A. Miller, N. E. Bussell and C. Ricketts, *J. Liq. Chromatogr.*, 1 (1978) 291.
12 W. D. Korte, *J. Chromatogr.*, 243 (1982) 153.
13 W. Lindner, *J. Chromatogr.*, 176 (1979) 55.
14 W. Lindner, *J. Chromatogr.*, 198 (1980) 367.
15 W. Dunges, *Anal. Chem.*, 49 (1977) 442.
16 S. T. Ingalls, P. E. Minkler, C. L. Hoppel and J. E. Nordlander, *J. Chromatogr.*, 299 (1984) 365.
17 K. Funazo, M. Tanaka, K. Morita, M. Kamino, T. Shono and H.-L. Wu, *J. Chromatogr.*, 346 (1985) 215.
18 K. Funazo, M. Tanaka, K. Morita, M. Kamino and T. Shono, *J. Chromatogr.*, 354 (1986) 259.
19 K. Funazo, M. Tanaka and T. Shono, *Anal. Sci.*, 3 (1987) 257.
20 A. H. Blatt (Editor), *Organic Syntheses*, Coll. Vol. 1, Wiley, New York, 1956, p. 145.

Journal of Chromatography, 481 (1989) 221–231
Elsevier Science Publishers B.V., Amsterdam — Printed in The Netherlands

CHROM. 21 731

IDENTIFICATION OF PEPTIDES, FROM A PEPTIC HAEMOGLOBIN HYDROLYSATE PRODUCED AT PILOT-PLANT SCALE, BY HIGH-PERFORMANCE LIQUID CHROMATOGRAPHY AND MASS SPECTROMETRY

JEAN-MARIE PIOT*, DIDIER GUILLOCHON and QUIYU ZHAO
Laboratoire de Technologie des Substances Naturelles, IUT A-Lille I, B.P. 179, 59653 Villeneuve d'Ascq Cedex (France)
GUY RICART
Laboratoire de Spectrométrie de Masse, Lille I, 59655 Villeneuve d'Ascq Cedex (France)
BERNARD FOURNET
Laboratoire de Chimie Biologique, Lille I, U.A. 217 du C.N.R.S., 59655 Villeneuve d'Ascq Cedex (France)
and
DANIEL THOMAS
Laboratoire de Technologie Enzymatique, E.R.A. 423 du C.N.R.S., Université de Technologie de Compiègne, B.P. 649, Compiègne Cedex (France)
(First received February 3rd, 1989; revised manuscript received June 19th, 1989)

SUMMARY

Gel-permeation high-performance liquid chromatography (HPLC) and reversed-phase HPLC were used to separate a mixture of peptides, produced at pilot-plant scale by peptic hydrolysis of bovine haemoglobin. Volatile buffers were employed in both HPLC techniques in order to get an easy recovery of peptides for further applications. The method is more rapid than low-pressure gel filtration. Amino acid analysis and fast atom bombardment mass spectrometry confirmed the purity, and allowed accurate molecular weights to be determined, for isolated peptides. These data demonstrate that such efficient techniques, usually used to resolve hydrolysates obtained in batch with pure substrates and highly specific enzymes, can be employed to resolve complex enzymatic hydrolysates of crude protein.

INTRODUCTION

Protein hydrolysates have been used as food ingredients for many years[1]. Additional applications have been investigated within the past few years[2], such as nutritional therapy[3,4], research on biological activity[5,6], stimulating effect on fermentation[7]. Such applications require very well defined and reproducible hydrolysates, especially when they are produced on a large scale. In order to gain a better understanding of the peptide population of such complex hydrolysates, precise analytical methods must be employed.

Since the initial uses of high-performance liquid chromatography (HPLC) for

0021-9673/89/$03.50

protein digest mapping[8,9], this method has been largely applied as a means of separating small to medium sizes peptides (less than 100 amino acids)[10–13]. Currently reversed-phase HPLC is most frequently used for peptide fractionation[14–16], because excellent resolutions are obtained. Gel-permeation HPLC is seldom employed, because it appears not to have so high a resolution for peptides separated from complex hydrolysates[17] as for pure standard peptides[18]. The major problem connected with gel-permeation HPLC is the unpredictable behaviour of peptides because complex mechanisms including size exclusion, hydrophobic adsorption and electrostatic interactions operate[13].

As for the determination of accurate peptide molecular weights, a new approach is offered by fast atom bombardment mass spectrometry (FAB-MS)[19–21]. This technique, therefore, allows a direct comparison of the molecular weights of the peptides, expected from the proposed structure after specific enzymatic or chemical cleavage, with those weights experimentally determined by FAB-MS[20].

We report here work on the analysis of a peptic haemoglobin digest, obtained at pilot-plant scale by an ultrafiltration process[22]. Studies on the applications of this hydrolysate are now being undertaken in many areas such as nutritional therapy and the isolation of biologically active peptides. Preliminary studies were successfully confirmed with microbiological culture experiments[23]. The aim of this work is accurately to determine the composition and molecular weight of any peptide in this complex haemoglobin hydrolysate. Peptide fractionation and purification are performed by using reserved-phase HPLC to supplement gel-permeation HPLC separation. The molecular weight of each peptide estimated from the amino acid composition is compared with the value determined by FAB-MS. The results demonstrate that it is possible to know precisely any peptide from a very complex peptic hydrolysate, produced at pilot-plant scale. The efficiency of the procedure is discussed and compared with previous values.

EXPERIMENTAL

Materials

All common reagents were of analytical reagent grade from Merck (Darmstadt, F.R.G.). Acetonitrile was of HPLC grade. Water was obtained from a Waters (Saint-Quentin, France) Milli-Q water system. Standard peptides were insulin A, bacitracin, bradykinin, actinomycin and PZ-Pro-Leu-Gly-Pro-Arg (where PZ is 4-phenylazobenzyloxycarbonyl), from Serva (Heidelberg, F.R.G.). The amino acids standard kit H was from Pierce (Rockford, IL, U.S.A.). All aqueous HPLC eluents were filtered prior to use on Sartorius (Palaiseau, France) 0.45-μm filters, and degassed with helium (Air Liquide, Bois d'Arcy, France) during analysis.

High-performance liquid chromatography

The HPLC apparatus was a Waters 600 E pump-system controller with a Waters Model U6K injector and a Waters Model 445 detector set at 215 nm and connected with a Waters Model 745 integrator.

Gel-permeation HPLC. The elutions were performed on a TSK (LKB, Bromma, Sweden) G2000SW column (600 mm × 7.6 mm I.D.) with 10 m*M* ammonium acetate buffer adjusted to pH 6.0 with acetic acid. Hydrolysate powder samples of 8.5

mg were dissolved in 85 μl of the same buffer before being applied to the column. The flow-rate was 0.75 ml/min. Fractions were collected, and freeze dried. The gel was calibrated with standard peptides under the same conditions.

Reversed-phase HPLC. Analyses of the peptidic fractions eluted from the TSK G2000SW column were performed by reversed-phase HPLC on an LKB ODS-120T-C_{18} column (300 mm × 7.8 mm I.D.). Elutions were accomplished with eluent A, 10 m*M* ammonium acetate pH 6.0, and eluent B, 50% (v/v) acetonitrile in eluent A. The gradient applied was 0–80% B in 80 min and 15 min reequilibration at 0% B between each analysis. The flow-rate was 1.5 ml/min. Samples were dissolved in eluent A (10 mg/ml) and 200 μl were injected. Each peak eluted from the column was collected manually.

Amino acid analysis

Amino acids were analysed using a Waters "Picotag Work Station". Peptides (0.1–10 μg) were hydrolysed by constant boiling HCl containing 1% phenol, for 24 h at 110°C. Precolumn derivatization of amino acids with phenyl isothiocyanate and HPLC separation of derivatized amino acids on a Waters RP-Picotag column (150 mm × 3.9 mm I.D.) were performed according to Bidlingmeyer *et al.*[24]. The wavelength was 254 nm and the flow-rate 1.0 ml/min.

Fast atom bombardment mass spectrometry

A Kratos MS 50 RF high resolution mass spectrometer equipped with a DS 90 (DGDG/30) data system was used. The mass spectrometer was operated at an 8-keV accelerating potential. An Ion Tech Model B 11 NF saddle field fast atom source energized with the B 50 current-regulated power supply was used with xenon as the bombarding atom (operating conditions: 7.3 kV, 1.2 mA). Peptides were dissolved in water (250 μg in 50 μl) and 1 μl of the solution was loaded on the copper tip with thioglycerol as a matrix. In this case the source housing was not heated. The mass range was scanned at 10 s/decade with a mass resolution of 3000. Caesium ionide was the standard for mass calibration.

Peptic haemoglobin hydrolysis

Decolorized bovine haemoglobin hydrolysate was obtained at pilot-plant scale by peptic proteolysis in an ultrafiltration reactor followed by decolorization with magnesia, desalting and atomization as described in ref. 22. The nitrogen content determined by the kjeldahl method allowed us to evaluate amounts of peptides in the hydrolysate greater than 90% (N × 6.25).

RESULTS AND DISCUSSION

Gel permeation HPLC separations

Fig. 1 shows the elution positions of the peptide standards for the TSK G2000SW column. The plot of the logarithms of their molecular weights as a function of the elution volumes is linear in the range from 800 to 2500 according to Richter *et al.*[18]. The gel-permeation HPLC analysis of 8.5 mg of the peptic digest of haemoglobin is shown in Fig. 2. Twenty elutions were performed and gave the same elution patterns. Peaks corresponding to fractions I–VII were collected and pooled. The

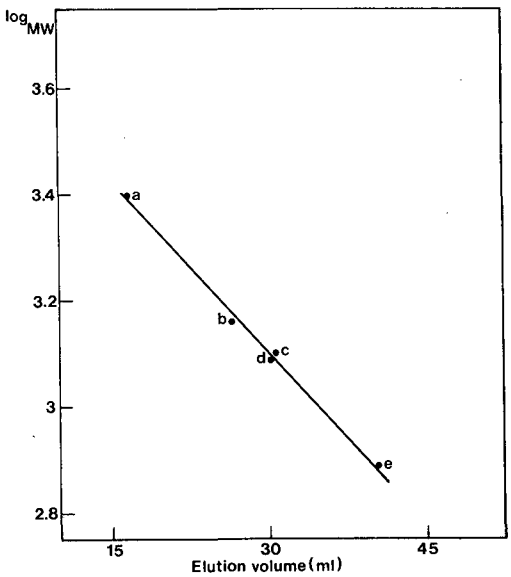

Fig. 1. Calibration plots of peptides using the TSK G2000SW column: (a) insulin A; (b) bacitracin; (c) actionomycin; (d) bradykinin; (e) Pz-Pro-Leu-Gly-Pro-Arg. Eluent: 10 m*M* ammonium acetate buffer (pH 6.0); flow-rate 0.75 ml/min. Detection: UV (215 nm).

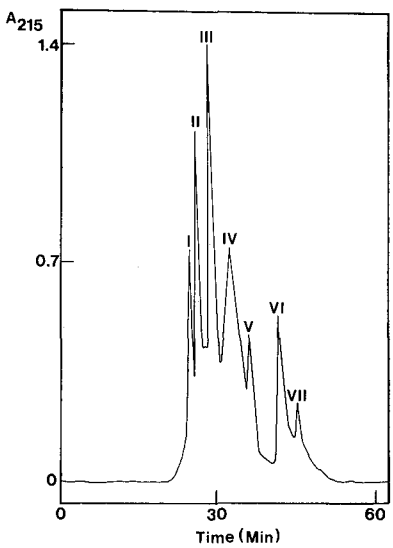

Fig. 2. Elution profile of total decolorized peptic hydrolysate, from bovine haemoglobin, using the TSK G2000SW column. Conditions as in Fig. 1.

TABLE I

APPARENT MOLECULAR WEIGHT DISTRIBUTION OF PEPTIDES SEPARATED BY TSK G2000SW AND QUANTITIES RECOVERED IN EACH FRACTION

	Fractions						
	I	*II*	*III*	*IV*	*V*	*VI*	*VII*
TSK G2000 estimated MW	2200	2100	1950	1650	1430	1170	1050
Efficiency of recovery of peptides (%)	8.8	14.1	25.6	27.9	10.8	9.0	3.8

quantities of peptides recovered in each fraction and their estimated molecular weights, in regard to the calibration curve, are shown in Table I. The use of gel-permeation HPLC provides a good separation for this complex hydrolysate in comparison with a casein hydrolysate, for example[17]. Concerning the elution time, this technique is more effective than conventional low-pressure gel filtration often used for such hydrolysates analysis[25–27]. Therefore gel-permeation HPLC can be performed principally in order to obtain a good and rapid resolution of peptide fractions for further reversed-phase HPLC analysis, and for roughly assessing the reproducibility of the peptidic hydrolysate. Moreover studies have been undertaken in our laboratory in order to follow continuously, by gel-permeation HPLC, the evolution of the elution pattern of a protein hydrolysate, in an enzymatic ultrafiltration reactor at laboratory scale.

Reversed-phase HPLC

For the reversed-phase HPLC peptide mapping, a wide variety of buffers have been investigated in attempts to combine the desirable characteristics of UV transparency and volatility, and it appeared that ammonium acetate–acetonitrile gradient elution provides one of the most efficient systems due to its excellent volatility and the high solubility of many peptides in the buffer. The wavelength selected is 215 nm for both HPLC techniques because it corresponds to an isosbestic point at which the absorptions of random and helical peptide bonds are equal[28].

Whereas single reversed-phase HPLC of the total haemoglobin peptic hydrolysate is inadequate for a complete peptide separation (data not shown), the use of reversed-phase HPLC shows excellent separation of any fraction obtained by gel-permeation HPLC. Fig. 3a–g shows the elution profile of each of the seven fractions separated from the TSK G2000 column. Elutions with linear gradients give optimal separations of peptides having largely different hydrophobicities. With regard to tryptic peptides of haemoglobin[29], the peptic hydrolysate exhibits greater complexity. This is principally due to the lower selectivity of pepsin for peptide bond cleavage[30].

The objective of this publication is to demonstrate the use of FAB-MS to identify components separated by HPLC and gel filtration chromatography in the monitoring of an enzyme hydrolysis reaction. Because the protein is well known, it is not necessary completely to analyze all the components as separated by chromatogra-

phy, but merely to use the MS technique to verify the composition of selected chromatographic fractions to confirm that the hydrolysis is proceeding as expected. In this case, fractions II, III, V–VII have been arbitrarily selected for analysis of the amino amino acids and accurate molecular weight determination by FAB-MS as described in the text. One or two of the peptides have been collected at random in each fraction and named according to the process of isolation as follows: II_8 for fraction II, III_3 and III_{21} for fraction III, V_{16} for fraction V, VI_4 and VI_6 for fraction VI, VII_4 and VII_6 for fraction VII.

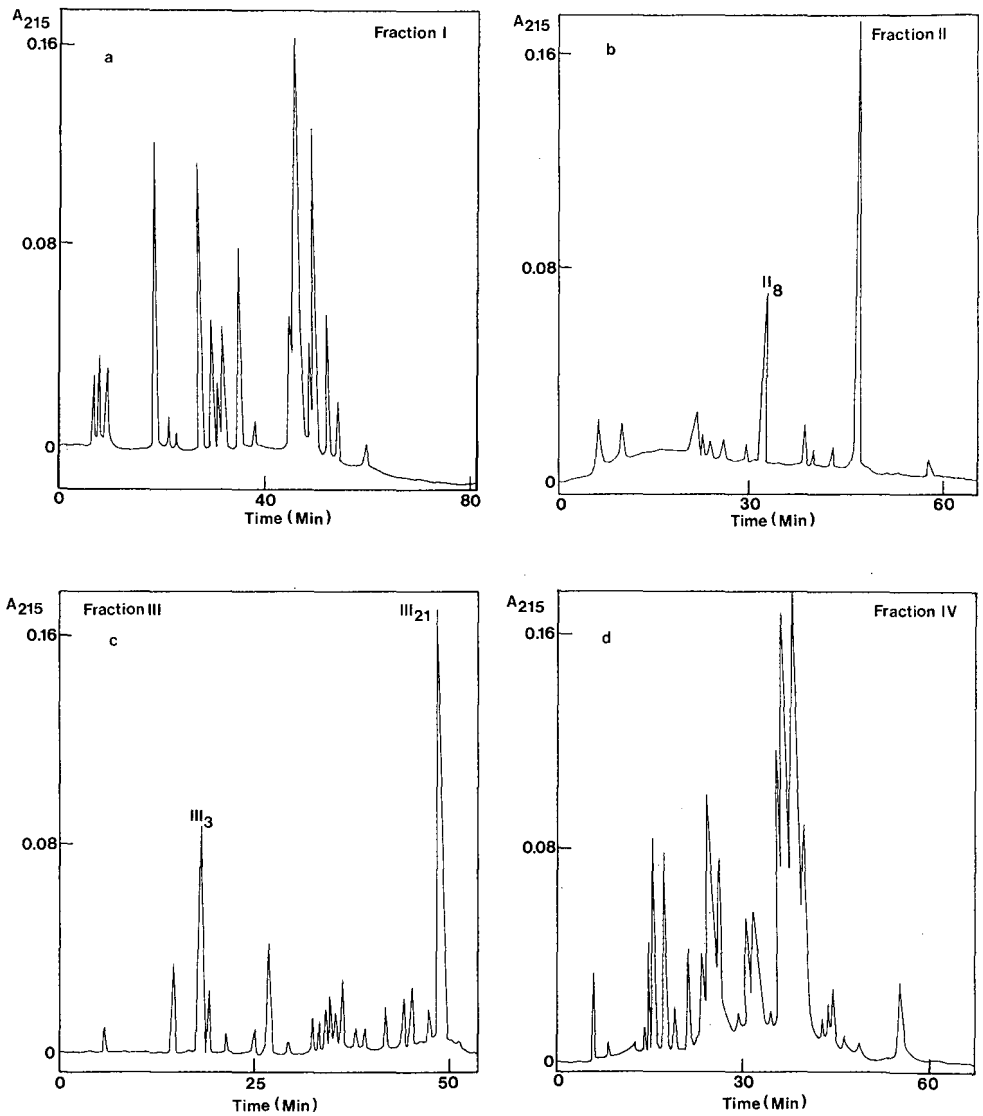

Fig. 3.

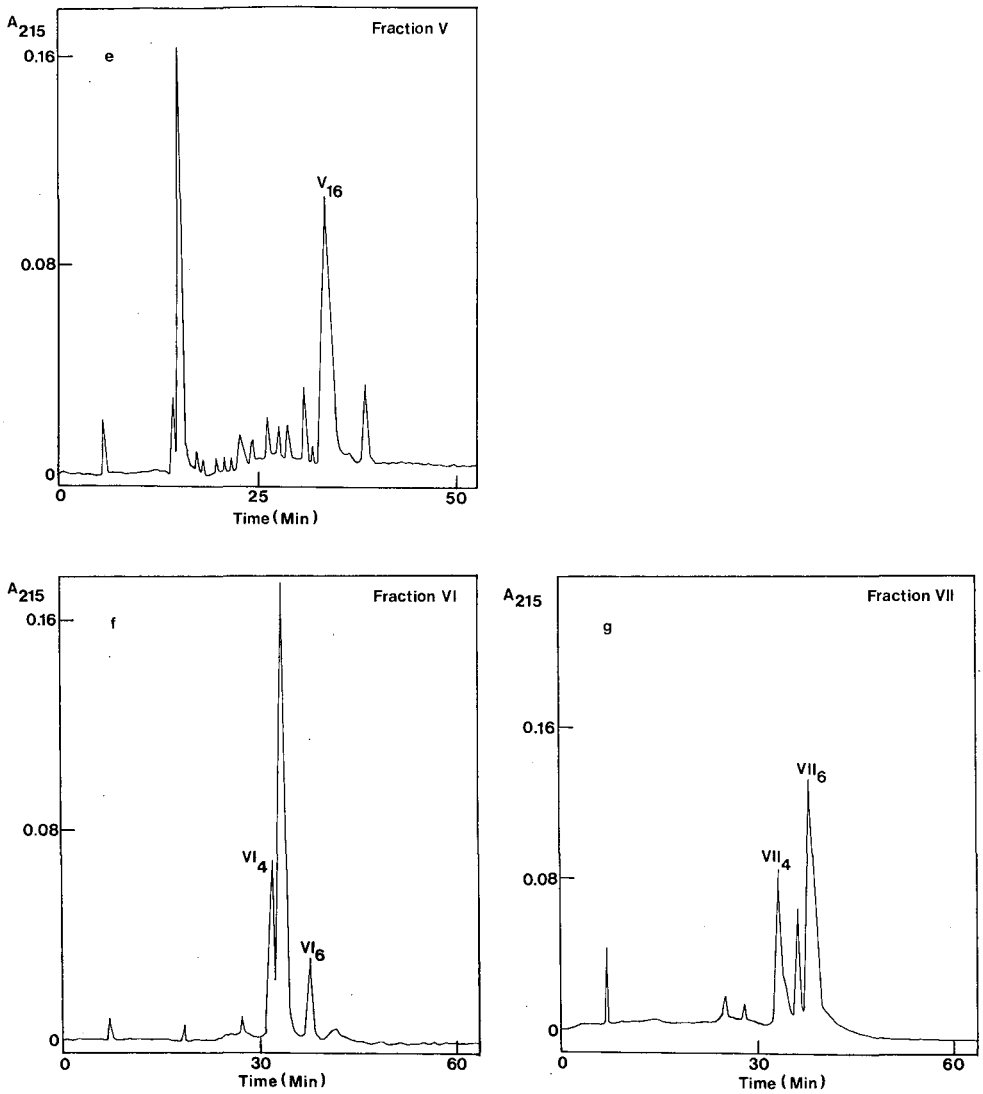

Fig. 3. (a)–(g) Elution profiles of each of the seven peptidic fractions separated from the TSK G2000SW column (Fig. 2). Conditions: column ODS-120 T-C 18; gradient, (A) 10 m*M* ammonium acetate (pH 6.0), (B) 50% (v/v) acetonitrile in eluent A, 0–80% B in 80 min; flow-rate 1.5 ml/min; detection, UV (215 nm).

Amino acid analysis and mass spectrometry

The amino acid compositions and deduced molecular weights of the eight peptides isolated are shown in Table II. Furthermore, owing to their amino acid composition, the peptides can be located in the well known globin sequence (Fig. 4). These data indicate a reasonable purity of these peptides. In Fig. 4 parentheses are used to enclose regions of the globin chain for which the sequence of amino acids has not been established but has been inferred from the amino acid composition by homology

TABLE II

MOLECULAR WEIGHTS OF THE EIGHT PEPTIDES ISOLATED DEDUCED FROM AMINO ACID COMPOSITION AND FROM MASS SPECTROMETRY

N.D. = Not detected.

Amino acid	II_8	III_3	III_{21}	V_{16}	V_4	VI_6	VII_4	VII_6
Asp		1.23(1)	1.33(1)	0.61(1)				
Glu	1.17(1)					1.17(1)		
Ser			2.74(3)					0.83(1)
Gly	1.04(1)			1.07(1)				
His			1.89(2)		0.97(1)		1.04(1)	1.07(1)
Arg						1.06(1)		
Thr			0.86(1)		2.82(3)	1.19(1)	2.60(3)	2.51(3)
Ala	1.76(2)		2.57(3)					
Pro			1.95(2)		2.04(2)	1.27(1)	1.96(2)	1.94(2)
Tyr	0.88(1)				1.03(1)	1.22(1)	0.96(1)	0.92(1)
Val			0.99(1)	1.00(1)		1.52(2)		
Met								
Cys								
Ile								
Leu	0.90(1)		1.83(2)	2.86(3)		0.93(1)		1.16(1)
Phe		0.91(1)	1.01(1)	0.93(1)	1.95(2)	1.24(1)	1.78(2)	2.72(3)
Lys		0.86(1)		1.42(1)	1.30(1)		1.21(1)	0.78(1)
Trp						N.D.(1)		
Deduced MW	622	408	1648	902	1237	1307	1237	1585
Mass spectrometry deduced MW	622	408	1648	902	1237	1307	1237	1585

with known sequences[31]. It seems that some peptides are broken down to others, *e.g.*, VII_6 into VII_4 (Fig. 4). Moreover, the same peptide can be eluted in different fractions during gel-permeation HPLC, *e.g.*, VII_4 to VI_4.

FAB-MS is particularly suitable for peptide analysis because it is capable of analyzing polar and ionic compounds without chemical derivatization. Moreover, it offers the additional advantage of being performed on liquid samples[32]. An highly viscous solvent (thioglycerol) is used in order to keep the sample in the liquid state during insertion into the high-vacuum source of the instrument and throughout the analysis.

As an example, Fig. 5 is the FAB-MS spectrum of a selected peptide (V_{16}). Accurate molecular weights of the eight peptides selected, determined by FAB-MS, are shown in Table II. The use of a FAB ion source in a mass spectrometer allows the m/z values of $(M+H)^+$ or $(M-H)^-$ ions of a peptide to be detected[33]. In our study only the $(M-H)^-$ ions are detected. The molecular weight of any peptide deduced from amino acid composition is rigorously the same as that determined mass spectrometrically. This indicates unambiguously the purity of the peptides isolated.

Important differences, between the accurate molecular weights of the peptides (Table II) determined by FAB-MS and those determined by gel-permeation HPLC (Table I), can be observed. So we can emphasize the failure of gel-permeation HPLC

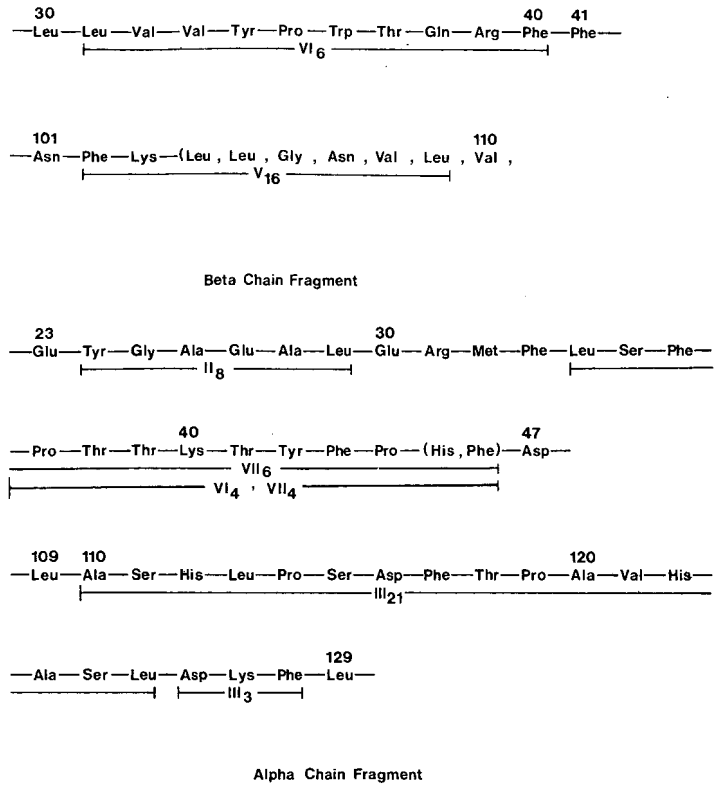

Fig. 4. Location of isolated peptides in the primary structure of bovine haemoglobin (α and β chain fragments).

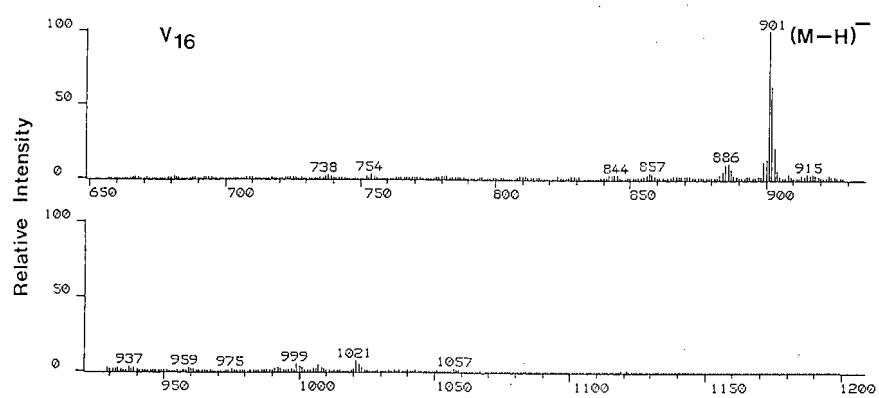

Fig. 5. Negative FAB-MS spectrum of peptide V_{16}. Experimental conditions are given in the text.

to give accurate molecular weights of peptides from such a complex enzymatic hydrolysate. However, in regard to this kind of complex peptidic population from a pilot-plant scale process, the combination of gel-permeation HPLC with reversed-phase HPLC has proven effective for a rapid fractionation and purification of peptides.

FAB-MS, coupled with amino acid analysis and those two simple HPLC methods, seems to be the best choice for determining the accurate composition of such a mixture. Thus, FAB-MS can be efficiently used for some peptides shown, by preliminary experiments, to be active for specific applications in areas such as cell culture or pharmacology. Tandem mass spectrometry (MS–MS) may be a powerful tool for sequencing these peptides[20]. Moreover, owing to the scale of hydrolysate production and its reproducibility[22], preparative gel-permeation HPLC and reversed-phase HPLC can be considered for such peptides.

Recently HPLC techniques have been combined with FAB-MS for the mass specific detection of mixtures of peptides produced by proteolytic hydrolysis of proteins in batch[32]. In the field of enzymatic ultrafiltration reactors, similar studies can be undertaken in order to get a better knowledge of the hydrolysis mechanism.

In conclusion, the results of this investigation show that HPLC and FAB-MS can be used to identify peptides from a complex haemoglobin hydrolysate produced at pilot-plant scale. FAB-MS can provide reliable molecular weight information by direct off-line analysis of HPLC fractions. This procedure should improve the technology of quality control for monitoring the enzymatic hydrolysis of proteins.

REFERENCES

1 D. P. Cuthbertson, *J. Sci. Food Agric.*, 1 (1950) 35.
2 A. Kilara, *Process Biochem.*, 21 (1983) 149.
3 M. L. G. Gardner, *Nutr. Health*, 314 (1985) 163.
4 D. B. A. Silk, *Proc. Nutr. Soc.*, 44 (1985) 63.
5 A. Hasegawa, H. Yamashita, S. Kondo, T. Kiyota, H. Hayashi, H. Yoshizaki, A. Muraki, M. Shiratsuchi and T. Mori, *Biochem. Biophys. Res. Commun.*, 150 (1988) 1230.
6 D. Migliore-Samour and P. Jolles, *Experientia*, 44 (1988) 188.
7 B. Tchorbanov and G. Lazarova, *Biotechnol. Appl. Biochem.*, 10 (1988) 301.
8 W. S. Hancock, C. A. Bishop, R. L. Prestidge and T. W. Hearn, *Anal. Biochem.*, 89 (1978) 203.
9 C. S. Fullmer and R. H. Wasserman, *J. Biol. Chem.*, 254 (1979) 7208.
10 P. Böhlen and G. Kleeman, *J. Chromatogr.*, 205 (1981) 65.
11 T. W. Hearn, F. E. Regnier and C. T. Wehr, *Int. Laboratory*, 1 (1983) 16.
12 C. S. Fullmer, *Anal. Biochem.*, 142 (1984) 336.
13 H. Yoshida and S. Najo, *Anal. Biochem.*, 159 (1986) 273.
14 K. J. Wilson, E. Van Wieringen, S. Klauser and M. W. Berchtold, *J. Chromatogr.*, 237 (1982) 407.
15 W. S. Hancock and D. R. K. Harding, in W. S. Hancock (Editor), *Handbook of HPLC for the Separation of Amino Acids, Peptides, and Proteins*, Vol. II, CRC Press, Boca Raton, FL, 1984, p. 3.
16 R. E. H. Wettenhall and M. J. Quinn, *J. Chromatogr.*, 336 (1984) 51.
17 M. A. Vijayalakshmi, L. Lemieux and J. Amiot, *J. Liq. Chromatogr.*, 16 (1986) 3559.
18 W. O. Richter, B. Jacob and P. Schwandt, *Anal. Biochem.*, 133 (1983) 288.
19 R. M. Caprioli and T. Fan, *Biochem. Biophys. Res. Commun.*, 141 (1986) 1058.
20 K. Biemann and S. A. Martin, *Mass Spectrom. Rev.*, 6 (1987) 1.
21 M. Castognola, L. Cassiano, R. De Cristofaro, R. Landolfi, D. V. Rossetti and G. B. Marini Bettolo, *J. Chromatogr.*, 440 (1988) 231.
22 J. M. Piot, D. Guillochon, D. Leconte and D. Thomas, *J. Chem. Technol. Biotechnol.*, 42 (1988) 147.
23 D. Dive, J. M. Piot, F. Sannier, D. Guillochon, P. Charet and S. Lutrat, *Enzyme Microb. Technol.*, 11 (1989) 165.

24 B. A. Bidlingmeyer, S. A. Cohen and T. L. Tarvin, *J. Chromatogr.*, 336 (1984) 93.
25 J. Amiot, G. J. Brisson, J. Delisle, G. Goulet, L. Savoie and J. D. Jones, *Nutr. Rep. Int.*, 24 (1981) 513.
26 P. Masson, D. Tomé and Y. Popineau, *J. Sci. Food. Agric.*, 37 (1986) 1223.
27 B. Vallejo-Cordoba, S. Nakai, W. D. Powrie and T. Beveridge, *J. Food Sci.*, 51 (1986) 1156.
28 W. S. Hancock and D. R. K. Harding, in W. S. Hancock (Editor), *Handbook of HPLC for the Separation of Amino Acids, Peptides, and Proteins*, Vol. 1, CRC Press, Boca Raton, FL, 1985, p. 190.
29 J. B. Wilson, M. Lam, P. Pravatmuang and T. H. J. Huisman, *J. Chromatogr.*, 179 (1979) 271.
30 F. A. Boveg and S. S. Yanari, *Enzymes*, 4 (1960) 63.
31 M. O. Dayhoff, L. T. Hunt, P. J. Mc Laughin and W. C. Barker, in M. O. Dayhoff (Editor), *Atlas of Protein Sequence and Structure*, Vol. 5, National Biomedical Research Foundation, Washington, DC, 1972, p. D61.
32 R. M. Caprioli, W. T. Moore, B. Da Gue and M. Martin, *J. Chromatogr.*, 443 (1988) 355.
33 R. M. Caprioli, *Biochemistry*, 27 (1988) 513.

Journal of Chromatography, 481 (1989) 233–243
Elsevier Science Publishers B.V., Amsterdam — Printed in The Netherlands

CHROM. 21 669

THE SEPARATION OF PANCREATIC PROCARBOXYPEPTIDASES BY HIGH-PERFORMANCE LIQUID CHROMATOGRAPHY AND CHROMATOFOCUSING

FRANCISCO J. BURGOS, ROGER PASCUAL, JOSEP VENDRELL, CLAUDI M. CUCHILLO and FRANCESC X. AVILÉS*

Departament de Bioquímica i Biologia Molecular, i Institut de Biologia Fonamental, Universitat Autònoma de Barcelona, 08193 Bellaterra (Barcelona) (Spain)

(First received January 23rd, 1989; revised manuscript received June 7th, 1989)

SUMMARY

Different experimental conditions and chromatographic supports have been selected for the most efficient and rapid purification of procarboxypeptidases from porcine and human pancreas by different high-performance liquid chromatography (HPLC) variants (anion exchange, reversed phase and gel filtration). Anion-exchange chromatography was found to be the most capable and permitted the isolation, in a single step, of three different porcine procarboxypeptidases (2A + 1B forms) and five different human procarboxypeptidases (2B + 3A forms) in a native and pure state from whole pancreas extracts. Other pancreatic proproteases are also cleanly isolated in the same step. Reversed-phase chromatography under mild conditions separated porcine or human procarboxypeptidases A from other pancreatic proteins in a very short time but was unable further to subfractionate the same proteins. The sequential use of gel filtration (or anion-exchange) and reversed-phase HPLC chromatography permitted, in a simple way, the isolation and dissociation of the strongly bound components of the binary complexes between procarboxypeptidases A and proproteinase E in either porcine or human pancreas extracts. Chromatofocusing on a fast protein liquid chromatographic support was also found to be a very efficient technique, showing a slightly lower capability to separate procarboxypeptidases than anion-exchange HPLC though in a much shorter time and in larger quantities.

INTRODUCTION

The fractionation of pancreatic proteins requires the use of rapid and mild methodologies in order to avoid their cross- and auto-degradation due to their great proteolytic potential and easy activation[1]. In certain species such as the human, only the use of electrophoresis and electrofocusing in the presence of inhibitors and denaturing agents allowed the analytical separation of the different pancreatic proteins in their undegraded forms[2–4]. Making use of this method, Scheele *et al.*[2–5] were the first to succeed in a reliable visualization and quantification of a large number of these proteins.

0021-9673/89/$03.50

However, the above electrophoretic methods are not appropriate for the isolation of these proteins at the preparative level and in a native state. This is particularly true for procarboxypeptidases due to the similar physico-chemical properties of their subspecies[2,3,5], their existence in complexes with other proproteinases or related proteins[6] and their low degree of renaturation once they have been denatured[7]. High-performance liquid chromatography (HPLC) may be particularly well suited to this task given its usual rapidity of operation and high separative powers. Taking advantage of this, several methods have been reported for the isolation of pancreatic hydrolases by HPLC[8–10]. In the case of procarboxypeptidases, a reversed-phase method which allows the isolation of their subfractions together with other pancreatic proteins has also been reported for porcine extracts[11]. Unfortunately, in this case the proteins isolated are denatured since the separation is carried out at low pH.

The present work describes the application of different HPLC variants (anion exchange, reversed phase, gel filtration) to the preparative separation of porcine and human procarboxypeptidases in their native states. The different properties of these variants permit their alternative use in the simple separation of all or of selected procarboxypeptidase subfractions and other pancreatic proproteases. Of particular interest is the isolation of a previously unreported binary complex between human procarboxypeptidase A and proproteinase E. The great potential of the procedures proposed in the general fractionation of pancreatic proteins is also examined. Finally, a procedure for the fractionation of these proteins based on chromatofocusing on fast protein liquid chromatography (FPLC) support is described and compared with the above-mentioned HPLC procedures.

MATERIALS AND METHODS

Pancreatic extracts

Porcine and human pancreas were defatted by treatment with acetone and diethyl ether as described by Folk and Schirmer[12]. Aqueous extracts of pancreatic powders were made in 20 m*M* Tris–HCl (pH 8.0), containing 50 μM bovine pancreatic trypsin inhibitor, for 1 h, at 4°C. Extracts were either precipitated or not with 43% (w/v) ammonium sulphate prior to their chromatographic analysis. In the former case, they were subsequently dialysed against 20 m*M* Tris–HCl (pH 8.0) overnight.

Enzymatic measurements

The free and potential proteolytic activities were measured spectrophotometrically against synthetic substrates: benzoylglycyl-L-arginine (BGA) for carboxypeptidase B[13]; benzoylglycyl-L-phenylalanine (BGP)[12] or furylacryloyl-L-phenylalanyl-L-phenylalanine (FAPP)[14] for carboxypeptidase A; succinyltrialanine-*p*-nitroanilide Suc-(Ala)3-pNA[15] for proteinase E; benzoylarginine ethyl ester (BAEE)[16] for trypsin; acetyltyrosine ethyl ester (ATEE)[16] for chymotrypsin and elastine-congo red for elastase[17]. To measure the potential activities of the respective zymogens, these were treated for 30 min at 37°C with porcine enterokinase (Sigma E-1256) in the case of trypsinogens, and with porcine trypsin (Sigma T-0134) for the analysis of other proproteases, at a zymogen/protease ratio of 10/1 (w/w) in both cases.

Anion-exchange chromatography

A TSK-DEAE column (particle size 10 μm, 100-nm pore, 7.5 cm × 0.75 cm, from LKB) with a guard column packed with the same support was used throughout. The buffers used were: A, 20 m*M* Tris–HCl (pH 8.0); B, 20 m*M* Tris–HCl, 0.8 *M* ammonium acetate (pH 8.0). Elution was achieved by two different gradients: from 19 to 57% B in 110 min for porcine extracts and from 0 to 40% B in 160 min for human extracts. Chromatography was carried out at a flow-rate of 0.5 ml/min, at 20°C.

Reversed-phase chromatography

An Ultrapore C_3 column (particle size 5 μm, 30-nm pore, 10 cm × 0.45 cm, from Beckman) was used, protected by a guard column packed with Perisorb C_2 from Merck. The two elution systems used were: (a) water–acetonitrile, both containing 0.1% trifluoroacetic acid (TFA); (b) water–isopropanol, both containing 10 m*M* piperazine adjusted to pH 6.5 with TFA. Chromatography was carried out at a flow-rate of 0.5 ml/min, at 20°C.

Gel filtration chromatography

A TSK G3000SW gel filtration column (particle size 10 μm, 100-nm pore, 30 cm × 0.75 cm, from Beckman) protected with a Spherogel-TSK GPWH guard column (particle size 10 μm, 7.5 cm × 0.75 cm) was used. Chromatography was carried out in 25 m*M* Tris–HCl, 0.2 *M* NaCl (pH 6.8) at a flow-rate of 0.1 ml/min and 20°C. The column was calibrated with glycogen phosphorylase, bovine serum albumin, chicken egg albumin, carbonic anhydrase, myoglobin and bovine pancreatic trypsin inhibitor.

Chromatofocusing

Chromatofocusing was performed on either a 20 cm × 0.5 cm or in a 5 cm × 0.5 cm Mono P FPLC column (from Pharmacia). The equilibration buffer was 25 m*M* Bis-Tris–HCl (pH 7.1). The pH gradient was achieved by using 10% Polybuffer 74–HCl (Pharmacia) (pH 4.0) as the eluting agent. Under these conditions, a linear gradient between pH 7.0 and 4.0 was formed in about 40 min, at a flow-rate of 0.5 ml/min. Alternatively, and with the longer column, a gradient between pH 5.5 and 4.0 was achieved by using 25 m*M* piperazine (pH 5.8) as the equilibration buffer. The temperature was kept at 20°C. The system was calibrated with standard proteins of known isoelectric points.

Electrophoresis

Electrophoretic analyses were carried out in slab gels of either 12 or 15% polyacrylamide, following Laemmli's method[18], either in the presence of sodium dodecyl sulphate (SDS) (denaturing conditions) or in its absence (non-denaturing conditions).

RESULTS

Anion-exchange HPLC

When an aqueous extract of porcine or human pancreas was made 20 m*M* in Tris–HCl, adjusted to pH 8.0, and subjected to chromatography in a DEAE-TSK

column, a complete separation of the different procarboxypeptidases was observed when they were eluted with a gradient from 0 to 0.32 *M* ammonium acetate. As shown in Figs. 1a and b, two porcine procarboxypeptidases A, the monomer and the binary complex with proproteinase E, and one procarboxypeptidase B were separated in the case of porcine extracts, and three procarboxypeptidases A, two monomers (A2, A1) and the binary complex with proproteinase E (A3), and two procarboxypeptidases B (B2, B1) were separated in the case of human extracts.

The number of the separated subfractions and their molecular properties (see Table I) coincide with those previously observed by our group[1,19] and by others[3–5,20], using different methods. Thus, in the case of the porcine proenzymes, two procarboxypeptidases A, the monomer and the binary complex with proprotei-

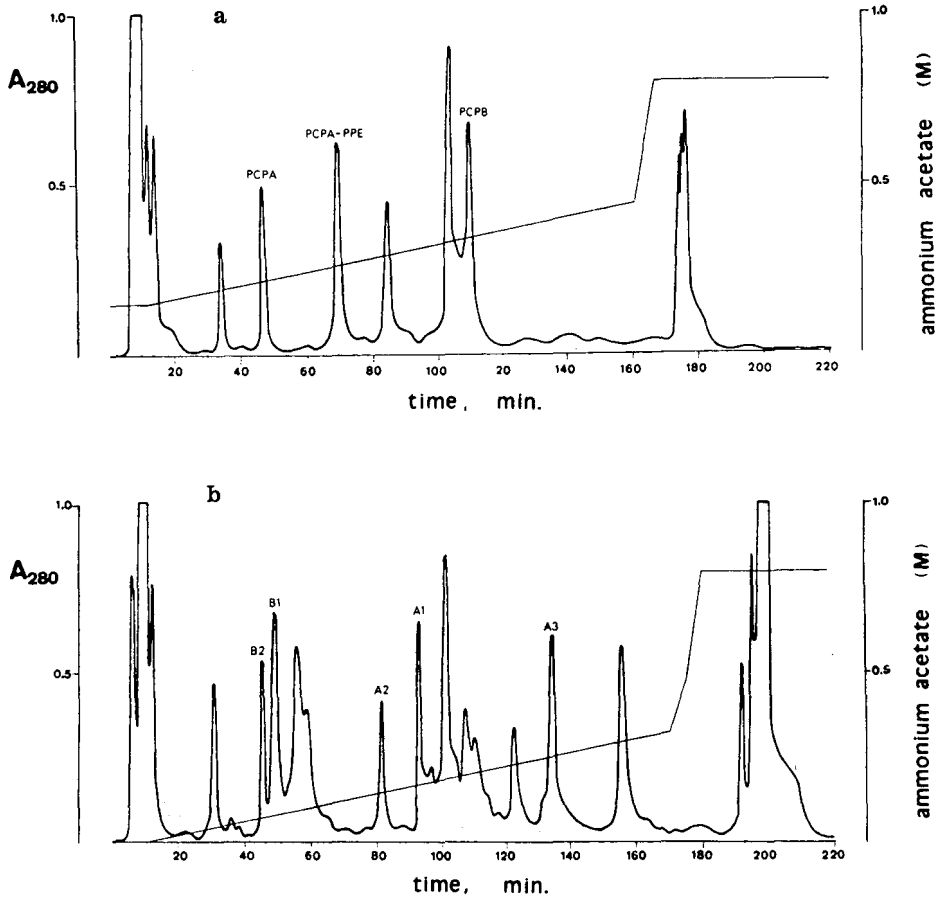

Fig. 1. Chromatographic fractionation of pancreatic proteins in an anion-exchange HPLC column, TSK-DEAE type (7.5 cm × 0.75 cm). Pancreatic extracts were made from 0.2 g of defatted acetone powder: (a) porcine pancreatic extract; (b) human pancreatic extract. Elution was carried out with gradients of ammonium acetate, in the presence of 20 m*M* Tris–acetate buffer (pH 8.0). Flow-rate 0.5 ml/min, temperature 20°C. Assignment of pancreatic procarboxypeptidases was made on the basis of the electrophoretic behaviour of the different fractions and enzymatic measurements, and in agreement with previous reports[2,4,19,20]. See Table I for abbreviations.

nase E, and one procarboxypeptidase B show molecular properties similar to those isolated by Kobayashi *et al.*[20] and by our own group[1,19] using conventional and complex chromatographic methods. In the case of the human proenzymes, procarboxypeptidases B2, B1, A2 and A1 have molecular properties coincident with the same proenzymes as detected and numbered by Scheele *et al.*[3–5] using their two-dimensional electrophoretic method. In addition, a new subfraction, the A3, which is composed of a binary complex between procarboxypeptidase A and proproteinase E from human pancreas is described for the first time. The nature of these proteins was ascertained by electrophoresis in polyacrylamide gels in the presence and absence of SDS determination of their isoelectric points by electrofocusing, analysis of their behaviour in gel filtration HPLC (see below) and by measurement of their actual and potential activity against several synthetic substrates (see Methods). Some of these properties are listed in Table I.

The existence of the binary complex of human procarboxypeptidase A and proproteinase E was demonstrated by its behaviour as a single entity in non-denaturing separative methodologies (electrophoresis, electrofocusing, anion exchange and gel filtration HPLC) and its splitting into two entities when subjected to separative methodologies under denaturing conditions (electrophoresis in SDS or urea, two dimensional electrophoresis in urea gradients, reversed-phase HPLC) (not shown). The identification of proproteinase E as the protein accompanying procarboxypeptidase A was made on the basis of the agreement with properties previously reported for this protein[21–24] and those found for that complex, such as the detection of its activity against Suc-(Ala)3-pNA and the lack of activity against elastin after being treated with trypsin, and the analysis of its N-terminal sequence.

TABLE I

SOME MOLECULAR PROPERTIES OF ZYMOGENS FROM PORCINE AND HUMAN PANCREAS SEPARATED IN THIS WORK BY VARIOUS HPLC TECHNIQUES

The active forms were generated by treatment of the isolated fractions with 0.75 mg/ml of porcine trypsin for 30 min, or with 0.5 mg/ml of enteropeptidase (in the case of trypsinogens) for 30 min, at 25°C. Abbreviations: IEP = isoelectric point; N.D. = not determined; PCPA = monomeric procarboxypeptidase A; PCPA–PPE = binary complex of procarboxypeptidase A and proproteinase E; PCPB = procarboxypeptidase B; CHTn = chymotrypsinogen; Tn = trypsinogen.

Species	*Protein*	M_r, *SDS-PAGE*	*Apparent* M_r, *gel filtration*	*IEP*	M_r *active form, SDS-PAGE*	*Molar activity* (s^{-1})
Pig	PCPA	45 000	29 800	4.7	34 800	9.2
	PCPA–PPE	45 000 + 27 000	53 700	4.7	34 800 + 27 000	10.4–1.38
	PCPB	47 000	29 200	4.4	36 000	114
	CHTn	29 000	18 700	4.2	29 000	48
	Tn	26 000	22 600	N.D.	26 000	31
Human	PCPA2	47 000	33 300	5.1	33 300	60
	PCPA1	44 500	30 800	4.9	33 700	118
	PCPA3	44 500 + 33 000	49 600	4.9	33 700 + 33 000	98–1.26
	PCPB2	47 300	28 700	7.1	35 500	64
	PCPB1	47 300	29 400	6.6	35 500	53
	CHTn	30 000	21 000	7.5	30 000	51
	Tn	31 300	19 400	4.7	31 300	10

All the subfractions isolated using the present method show an almost absolute purity as indicated by subsequent analysis by SDS electrophoresis. Only porcine procarboxypeptidase B and the human procarboxypeptidase A–proproteinase E binary complex require a rechromatography under the same conditions when they are obtained at high loadings of the pancreas extract. In addition, all the subfractions show a complete native state as shown by their easy activation with trypsin and by the high specific activities reached after activation, which compare well with those we have previously reported for the porcine proenzymes[1,23]. It is important to note that, in certain cases the human A3 binary complex obtained by this method was contaminated by trypsin from the preceding chromatographic peak. The quick removal of this contaminant by rechromatography was found to be absolutely necessary to avoid autolysis of A3.

Besides procarboxypeptidases, other pancreatic proproteases are also cleanly isolated in the same chromatographic procedure. Thus, porcine chymotrypsinogen C is cleanly eluted after the binary complex of porcine procarboxypeptidase A and proproteinase E (at 84 min, as shown in Fig. 1a). On the other hand, human chymotrypsinogen is eluted immediately after human procarboxypeptidase B1 and two human anionic trypsinogen are eluted in the peaks before and after human procarboxypeptidase A3 (at 122 and 157 min, respectively, as shown in Fig. 1b). Many other pancreatic proteins can also be purified by slightly changing the elution conditions (not shown). It is also important to note that the above separation of procarboxypeptidases and accompanying proteins can benefit from an improvement in resolution and safety when the pancreas extract is previously fractionated by a salting out precipitation with 43% ammonium sulphate, which removes an important fraction of chymotrypsinogens and trypsinogens from the medium. The supernatant, after an overnight dialysis against 20 m*M* Tris–HCl (pH 8.0), is loaded onto the HPLC column. In this case, the addition of 50 μM bovine trypsin inhibitor to the supernatant to avoid degradation during the long dialysis is advisable.

Reversed-phase and gel filtration HPLC

When a porcine or a human pancreas extract was loaded onto a reversed-phase propyl-bonded HPLC-based column (30-nm pore), equilibrated with 10 m*M* piperazine–HCl (pH 6.5), the pancreatic proteins were eluted in three sharp peaks after application of a linear gradient of increasing isopropanol concentration (0–50%) (results not shown). The last peak contained only a mixture of procarboxypeptidases A, while the penultimate peak contained proproteinase E and other serine proproteinases. The yield of recovery of porcine and human procarboxypeptidases A using this method was found to be inversely dependent on the residence time of these proteins in the column. Thus, after application of a 0–50% isopropanol gradient in 15 min, a 95% recovery of these proteins was noted but the yield decreased to 20% when the same gradient was applied in 30 min. The recovery was even poorer when acetonitrile instead of isopropanol was used as the eluting agent.

Under the above conditions at intermediate pH, both porcine and human procarboxypeptidases B require a much higher percentage of organic solvent to be detached from the column, in which they are eluted at low yield. In contrast, when the chromatography is carried out in 0.1% trifluoroacetic acid but at low pH (pH 2), both procarboxypeptidases A and B (either porcine or human) can be separated from each

other and recovered at a yield which is again dependent upon the residence time of the proteins in the column. However, the intrinsic and potential activity of these isolated proteins, after being equilibrated at intermediate pH and freed of organic solvent by dialysis, is very low ranging from 5 to 20%, in agreement with other reports[25]. It is also worth mentioning that the above chromatographic procedure at low pH dissociates the binary complexes between either porcine or human procarboxypeptidases A and proproteinase E, which can be independently recovered.

Gel filtration HPLC on a silica-based column (TSK G3000SW) was found to be able to separate serine proproteases trypsinogens, chymotrypsinogens, proelastases, etc. from procarboxypeptidases when a porcine or an human pancreatic extract was used a a source of these proteins (data not shown). This was accomplished in spite of an anomalous behaviour of all these proteins which showed a delayed elution and, therefore, an apparent molecular weight lower than expected (see Table I). This behaviour, which can be attributed to non-specific interactions with the support, was not prevented by the use of intermediate ionic strength in the eluting buffer (25 m*M* Tris–HCl, 0.2 *M* NaCl). It was also evident from enzymatic measurements along the chromatographic profiles that in both porcine and human species proproteinase E was present only as a binary complex with procarboxypeptidase A, under a wide range of chromatographic conditions. Unfortunately, other pancreatic proteins of higher molecular weights, such as amylases or lypases were also coeluted with these complexes under the same conditions.

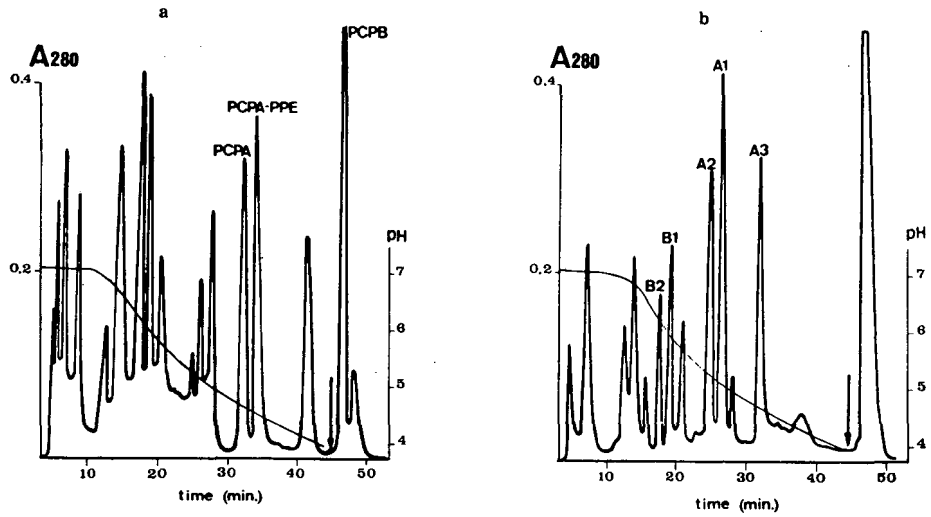

Fig. 2. Chromatofocusing of proteins from a porcine (a), or an human (b), pancreatic extract (each from 16 mg of acetone powder) on a Mono P FPLC column (20 cm × 0.5 cm). Samples were equilibrated against 25 m*M* Bis-Tris (pH 7.1) buffer by dialysis, loaded onto the column and eluted by application of 10% Polybuffer 74–HCl (pH 4.0). Flow-rate 0.5 ml/min, temperature 20°C. Elution of the different procarboxypeptidases and proproteinase E, specifically labelled on the chromatogram, was detected by enzymatic and electrophoretic methods. Arrows on the chromatogram indicate the application of 1.5 *M* sodium acetate (pH 7.1). See Table I for abbreviations.

Chromatofocusing

Chromatofocusing of extracts of porcine or human pancreas in a short FPLC column (Mono P, 5 cm × 0.5 cm, from Pharmacia) gave a good, but not complete, separation of pancreatic proteins when a decreasing gradient between pH 7.0 and 4.0 was applied. However, a complete separation for all these proteins was obtained in a long column (20 cm × 0.5 cm). Thus, as shown in Fig. 2, monomeric procarboxypeptidase A, the procarboxypeptidase A binary complex with proproteinase E and the single procarboxypeptidase B from porcine pancreas extracts are cleanly isolated from each other and from the rest of pancreatic proteins at the end of the chromatography.

A fractionation can also be accomplished for the corresponding proteins from human pancreas but in a more grouped way due to the larger number of isoforms found in this species: a separate doublet of peaks for B2 and B1 is eluted at the first third of the chromatography, a second separate doublet of peaks for A2 and A1 at the middle and A3 is eluted as a single peak before column washing with a high concentration of salt. Enzymatic measurements, polyacrylamide gel electrophoresis (PAGE) and HPLC anion-exchange analysis confirmed the above assignments. It is interesting that the elution order of the A and B forms of procarboxypeptidases is reversed in both species and is in agreement with the important changes observed in the isoelectric points of the B forms (see table I). It is also worth mentioning that a better separation for human procarboxypeptidases A2 and A1 can be accomplished if a restricted gradient between pH 5.8 and 4.0 is applied. However, under these conditions procarboxypeptidases B2 and B1 are eluted together and contaminated with other pancreatic proteins.

DISCUSSION

A systematic survey has been made to study the ability of different new generation chromatographic supports to separate pancreatic procarboxypeptidases. HPLC anion-exchange chromatography on an organic polymeric support has been found to be a particularly appropriate system for separating all subfractions of the above proteins from porcine and human species. Its great separative power, speed and mildness of operation suggest that this system may become a standard method to isolate the above proteins and many other pancreatic proproteases, just as two-dimensional electrophoresis has become at the analytical level[2–5]. The anion-exchange HPLC method is particularly appropriate for isolating pancreatic proproteases, in a native state, at a 100–500 μg level in analytical columns (5 cm × 0.7 cm). This should be sufficient for the characterization of many properties of these proteins by modern procedures. The complementary use of automatic programmers for elution and of autosamplers permits the extension of this separative capability at the milligram level or the consecutive analysis of many samples of different origins. The latter possibility may be very useful in the analysis of the alellomorphism or pathological variants in pancreatic zymogens from different individuals. Moreover, the use of on-line high sensitivity UV detectors allows the detection of pancreatic proteins at an analytical level ($\approx$5 μg) which is similar to that reached by two-dimensional electrophoretic techniques with coomassie blue staining.

Other chromatographic variants tested in this work showed a much lower sep-

arative power than anion-exchange HPLC but are still very useful as complementary techniques. Thus, reversed-phase HPLC on a short alkyl-bonded support is unable to fractionate the different species of procarboxypeptidases A. However, this support permits the rapid dissociation and isolation of the components of the binary complex between procarboxypeptidase A and proproteinase E, either from porcine or from human pancreas. This is an absolute requirement for the independent characterization of these components and led in the past to elaborate methodologies for performing similar tasks[6,20,23]. Besides, reversed-phase HPLC is a convenient and very rapid method of concentrating procarboxypeptidases A or eliminating their accompanying salts or low-molecular-weight contaminants. The last application is very convenient for extended N-terminal sequence analysis of procarboxypeptidases, usually contaminated by amino acids and peptides.

Gel-filtration HPLC showed a low general ability to separate pancreatic proteins from porcine or human extracts. Nevertheless, this technique gives useful information about the interaction between pancreatic proteins. Thus, the stabilities of the procarboxypeptidase A–proproteinase E binary complexes over a wide range of ionic strengths and the existence of the human complex have been demonstrated by this technique. Moreover, this technique can be quickly applied to an extract from human pancreas before anion exchange or chromatofocusing in order to remove serine proproteinases from the procarboxypeptidase A–proproteinase E binary complex. This procedure decreases very much the possibility of autolysis of this labile complex whilst facilitating its ionic equilibration before the next chromatography.

The anomalous hydrodynamic behaviour noted for different pancreatic proteins in the HPLC gel-filtration columns used, a fact already reported by other authors and by ourselves with related chromatographic supports[19,26–28], did not seriously affect the studies on the molecular state of these proteins. The results indicate that all the zymogens of porcine and human pancreatic proteases investigated behave as monomers under the elution conditions selected, except those included in the binary complex between procarboxypeptidase A and proproteinase E. Even more important is the observation that proproteinase E activities appear associated only with the peak containing its binary complex with procarboxypeptidase A, a fact also obseved by means of anion-exchange chromatography. This suggests that proproteinase E is not secreted as a monomer. Probably the expression of its gene is coordinated with that of a procarboxypeptidase A, or the latter protein is expressed in excess with respect to proproteinase E and always maintains this protein in a binary complex after binding to it.

Chromatofocusing on an FPLC support also appears an efficient technique for separating pancreatic procarboxypeptidases. The resolution obtained with the long column is lower than that obtained with anion-exchange HPLC but is complete for all porcine or human procarboxypeptidases. In addition, the resolution for human procarboxypeptidases A is greatly increased by application of a narrow pH gradient. Chromatofocusing has the additional advantage of showing shorter elution times, very sharp peaks and a much larger loading capacity which permits the isolation of milligrams of procarboxypeptidases in half an hour. It also offers the advantage over anion-exchange HPLC of a cleaner separation of anionic trypsin (a possible dangerous contaminant at high loadings) from human procarboxypeptidase A3. However, this method suffers from the disadvantage of the need to remove, (*i.e.*, by gel fil-

tration) the Polybuffer for some applications, such as microsequencing or detailed functional analysis.

The isolation of the native binary complex between procarboxypeptidase A and proproteinase E from human extracts exemplifies the efficiency and mildness of the separative methods reported here. Scheele *et al.*[3–5] did not visualize this binary complex using two-dimensional electrophoresis since this was carried out under denaturing conditions which probably dissociated the complex. Even the proproteinase E protomer is not seen by this electrophoretic method, probably because it suffers from autodegradation in the presence of SDS, as suggested by Sziegoleit[29], or when subjected to unfolding conditions prior or during the analysis. The addition of inhibitors of serine proteinases or high concentrations of urea, recommended procedures in Scheele's method[3–5], do not prevent auto-degradations of this protein as we have shown in our laboratory[30].

The demonstration of the existence of a binary complex between procarboxypeptidase A and proproteinase E in human pancreas suggests some ideas about the future research on the state of proproteinases in the pancreas of mammals. According to previous reports[6], procarboxypeptidases occur in non-ruminants mainly as monomers but also as binary complexes with chymotrypsinogen C, as shown in whale[3], or with proproteinase E, as shown in pig[19,20] and now in humans. However, the occurrence of the last complex may be more frequent if the above difficulties in the separation and detection of proproteinase E also appeared in the analysis of the complement of pancreatic proteins carried out in different non-ruminants, such as guinea pig[2], dog[5], hen[32], etc. This would be in agreement with the reports of Sziegoleit and Linder[33] which claim that proproteinase E-like proteins are present in many mammals. The application of the anion-exchange HPLC or chromatofocusing methods described here to the analysis of pancreatic extracts of these species may answer the above questions.

ACKNOWLEDGEMENTS

This work was supported by grant 0385/84 from the CAICYT, Ministerio de Educación y Ciencia (Spain) and by grant AR/86-14 from the CIRIT, Generalitat de Catalunya (Spain). R. P. is a recipient of a fellowship from Fondo de Investigaciónes Sanitarias (FIS) (Ministerio de Sanidad, Spain), and F. J. B. is a recipient of a fellowship from PFPI (Ministerio de Educación, Spain). We are indebted to Drs. Quintanilla and Espinel from the Unidad de Transplantes, Hospital Valle del Hebrón, Barcelona, for supplying human pancreas.

REFERENCES

1 M. Vilanova, J. Vendrell, M. T. López, C. M. Cuchillo and F. X. Avilés, *Biochem. J.*, 229 (1985) 605–609.
2 G. Scheele, *J. Biol. Chem.*, 250 (1975) 5375–5385.
3 G. Scheele, D. Bartelt and W. Bieger, *Gastroenterology*, 80 (1981) 461–473.
4 W. Bieger and G. Scheele, *Anal. Biochem.*, 109 (1980) 222–230.
5 G. Scheele, in V. L. W. Go, J. D. Gardner, F. P. Brooks, E. Lebenthal, E. P. Dimagno and G. A. Scheele (Editors), *The Exocrine Pancreas*, Raven Press, New York, 1986, pp. 185–192.
6 A. Puigserver, C. Chapus and B. Kerfelec, in P. Desnuelle, H. Sjöstrom and O. Noren, (Editors), *Molecular and Cellular Basis of Digestion*, Elsevier, Amsterdam, 1986, pp. 235–247.

7 J. M. Sánchez, J. L. López, P. L. Mateo, M. Vilanova, M. A. Serra and F. X. Avilés, *Eur. J. Biochem.*, 176 (1988) 225–230.
8 K. Titani, T. Sasagawa, K. Resing and K. A. Walsh, *Anal. Biochem.*, 123 (1982) 408–412.
9 H. Tojo, T. Teramoto, T. Yamano and M. Okamoto, *Anal. Biochem.*, 137 (1984) 533–537.
10 S. A. Cohen, K. Benedek, Y. Tapuhi, J. C. Ford and B. L. Karger, *Anal. Biochem.*, 144 (1985) 275–284.
11 P. J. Padfield, M. Griffin and R. M. Case, *J. Chromatogr.*, 369 (1986) 133–141.
12 J. E. Folk and E. W. Schirmer, *J. Biol. Chem.*, 238 (1963) 3384–3394.
13 J. E. Folk, K. A. Piez, W. R. Carrol and J. A. Gladner, *J. Biol. Chem.*, 235 (1960) 2272–2277.
14 L. M. Peterson, B. Holmquist and J. L. Bethune, *Anal. Biochem.*, 125 (1982) 420–426.
15 J. A. Bieth, B. Spiess and C. G. Wermuth, *Biochem. Med.*, 11 (1974) 350–357.
16 G. W. Schwert and Y. Takenaka, *Biochim. Biophys. Acta*, 16 (1955) 570–576.
17 D. M. Shotton, *Methods Enzymol.*, 19 (1970) 113–140.
18 U. K. Laemmli, *Nature (London)*, 227 (1970) 680–685.
19 M. C. Martinez, F. X. Avilés, B. San Segundo and C. M. Cuchillo, *Biochem. J.*, 197 (1981) 141–147.
20 R. Kobayashi, Y. Kobayashi and C. H. W. Hirs, *J. Biol. Chem.*, 253 (1978) 5526–5530.
21 P. A. Mallory and J. Travis, *Biochemistry* 14 (1975) 722–730.
22 A. Sziegoleit, D. Linder, M. Schüter, M. Ogawa, F. Nishibe and K. Fujimoto, *Eur. J. Biochem.*, 151 (1985) 595–599.
23 J. Vendrell, F. X. Avilés, B. San Segundo and C. M. Cuchillo, *Biochem. J.*, 205 (1982) 449–452.
24 W. F. Shen, T. S. Fletcher and C. Largman, *Biochemistry*, 26 (1987) 3447–3452.
25 J. F. Riordan and B. L. Vallee, *Biochemistry*, 2 (1963) 1460–1469.
26 D. Gratecos, O. Guy, M. Rovery and P. Desnuelle, *Biochim. Biophys. Acta*, 175 (1969) 82–96.
27 A. S. Delk, P. R. Durie, T. S. Fletcher and C. Largman, *Clin. Chem.*, 31 (1985) 1294–1300.
28 E. Fioretti, M. Angeletti, G. Citro, D. Barra and F. Ascolli, *J. Biol. Chem.*, 262 (1987) 3586–3589.
29 A. Sziegoleit, *Biochem. J.*, 219 (1984) 735–742.
30 R. Pascual, F. J. Burgos, M. Salvà, F. Soriano, E. Mendez and F. X. Avilés, *Eur. J. Biochem.*, 179 (1989) 609–616.
31 T. Yoneda, *Compr. Biochem. Physiol.*, 67B (1980) 81–86.
32 G. Marchis-Mouren, M. Charles, A. Ben-Abdeljlil and P. Desnuelle, *Biochim. Biophys. Acta*, 50 (1961) 186–188.
33 A. Sziegoleit and D. Linder, *Biol. Chem. Hoppe-Seyler*, 367 (1986) 527–531.

Journal of Chromatography, 481 (1989) 245–254
Elsevier Science Publishers B.V., Amsterdam — Printed in The Netherlands

CHROM. 21 723

HIGH-PERFORMANCE LIQUID CHROMATOGRAPHIC DETERMINATION OF δ-(L-α-AMINOADIPYL)-L-CYSTEINYL-D-VALINE IN COMPLEX MEDIA BY PRECOLUMN DERIVATISATION WITH DANSYLAZIRIDINE

COLIN D. ORFORD*, DAVID PERRY and MAXWELL W. ADLARD
School of Biotechnology, Polytechnic of Central London, 115 New Cavendish Street, London W1M 8JS (U.K.)
(First received January 26th, 1989; revised manuscript received June 20th, 1989)

SUMMARY

A novel method is described for the trace level quantitation of the tripeptide δ-(L-α-aminoadipyl)-L-cysteinyl-D-valine (ACV) in complex fermentation media, using a high-performance liquid chromatographic, pre-column derivatisation technique. The procedure is based upon the reaction of the ACV monomer with 5-dimethylaminonaphthalene-1-sulphonylaziridine (dansylaziridine) and produces a highly fluorescent product. Reaction conditions between the reagent and tripeptide were investigated and optimal conditions established. Linear calibration graphs were obtained over the ranges 227–0.56 μg/ml and 227–5.6 ng/ml. The extracellular ACV levels produced in fermentation broths of several different fungal strains and species were determined using this technique. The method was compared using ACV standards in buffer solutions for ease of use, sensitivity and selectivity with two other pre-column derivatisation procedures, using dithionitrobenzoic acid and monobromobimane, which also exploit the reaction with the sulphydryl group of the ACV monomer.

INTRODUCTION

The nature of the intermediates involved in the biosynthetic pathways of both penicillins and cephalosporins has been well established[1], but only recently have attempts been made to quantitate levels of these compounds in fermentation broths by the application of high-performance liquid chromatography (HPLC)[2,3]. The tripeptide δ-(L-α-aminoadipyl)-L-cysteinyl-D-valine (ACV) undergoes an unusual cyclisation reaction, catalysed by the enzyme isopenicillin N synthetase, to produce the first bioactive intermediate in the pathway, isopenicillin N[4,5]. The enzyme only accepts the sulphydryl form of the tripeptide as substrate and not the disulphide[5]. When excreted into aerated fermentation broths the ACV readily dimerises into the disulphide, but the monomeric form can be produced by reduction of the disulphide bond by mild reducing agents like dithiothreitol (DTT) or one of the alkali metal borohydrides[6,7].

The lack of a suitable chromophore in this tripeptide makes trace level detec-

0021-9673/89/$03.50

tion in fermentation broths difficult. Reversed-phase analytical HPLC has been employed by several workers to assay levels of either the monomeric or the dimeric form of ACV[2,3,8,9] along with other β-lactam intermediates. The methods employed for this purpose have involved the covalent derivatisation of ACV to introduce a chromophore or fluorophore into the molecule. The resultant product may then be monitored at a wavelength at which very few other broth components absorb and also may have an extremely high extinction coefficient making analysis both more convenient and more sensitive.

Several well established methods for the pre-column reactions currently exist for the assay of small peptides and amino acids. Fluorescent products are regarded as preferable because of their greater detection sensitivity and relative freedom from interference. The assay of ACV has been carried out by pre-column derivatization to yield fluorescent products by reaction of its primary amino group[2,3]; using these methods it is possible to monitor both the monomeric and dimeric forms of the tripeptide. More recently ACV has been derivatised via the sulphydryl group[10] and hence greater selectivity has been achieved. This approach has the added advantage of allowing assay of ACV in a form suitable as a substrate for isopenicillin N synthetase. We now report the new use of a specific thiol derivatising reagent, dansylaziridine, which produces stable fluorescent products[11] and is particularly suited to the trace level analysis of this important biosynthetic intermediate by HPLC. We have also compared this procedure with two existing methods for the quantitation of ACV under similar conditions.

EXPERIMENTAL

Materials and methods

Dansylaziridine (5-dimethylaminonaphthalene-1-sulphonylaziridine), glutathione (reduced form), L-cysteine, sodium borohydride and 5,5′-dithiobis-(2-nitrobenzoic acid) (DTNB) were supplied by Sigma (Poole, U.K.). Glacial acetic acid, ethylenediaminetetraacetic acid (EDTA) and potassium hydroxide were obtained from BDH (Poole, U.K.) and were all analytical reagent quality (AnalaR). Analytical reagent grade sodium acetate and potassium dihydrogenphosphate were purchased from Fisons (Loughborough, U.K.). HPLC grade acetonitrile and methanol were acquired from Rathburn Chemicals (Walkerburn, U.K.). Monobromobimane (3,7-dimethyl-4-bromo-
ethyl-6-methyl-1,5-diazobicyclo[3.3.0]-octa-3,6-diene-2,8-dione) was supplied by Calbiochem-Behring (Cambridge, U.K.) and the ACV was kindly donated by Glaxo Group Research (Greenford, U.K.). All aqueous buffers were prepared in deionised water obtained using a Nanopure II system (Fisons).

Equipment

HPLC was performed using a single 2150 HPLC pump connected to a 2152LC controller and a 11300 Ultragrad mixer (LKB, Milton Keynes, U.K.) to produce the gradient. Integration was performed on a 4290 integrator (Spectra Physics, St. Albans, U.K.) and detection was carried out using a RF-530 fluorescence spectrophotometer (Shimadzu, Columbia, MD, U.S.A.). Ultra-violet detection was conducted using a Shimadzu SPD-2AM detector.

Chromatographic separations were carried out on a 5-μm, reversed-phase, C_{18}, 25 cm × 0.46 cm column obtained from Hichrom (Reading, U.K.). A 5 cm × 0.46 cm guard column (cartridge system) containing the same stationary phase was used to protect the analytical column and was supplied by Chrompack (Middleburg, The Netherlands). Fermentations were carried out in a MK X, LH incubator shaker (LH Fermentations, Stoke Poges, U.K.).

Fungal strains and growth media

Penicillium chrysogenum strain numbers P2 and NRRL1951 (Pan Laboratories) and SC6140 (kindly donated by Professor Sir E. P. Abraham and originally from Squibb Institute for Medical Research, New Jersey, U.S.A.) were grown in Jarvis and Johnson[12] defined medium. A mutant strain of *Cephalosporium acremonium*, N2 (a gift from Glaxo Group Research) was grown as described by Shirafuji *et al.*[13]. *Aspergillus niger* IMI17454 and strains G3 and GH52 of *Aspergillus nidulans* were grown in Aspergillus Complete Medium[14] for 5 days. The broth from the former organism was used as a blank (no ACV could be detected; *A. niger* has not been reported as a β-lactam producer).

Sample preparation

Broths were harvested by centrifugation (5600 *g*, 20 min, 4°C), treated with a two-fold excess of acetone and left for 20 min to allow protein precipitation. The resultant suspension was centrifuged and the supernatant passed through a 0.45-μm filter (Millipore, Bedford, MA, U.S.A.). The sample was treated with an excess of solid sodium borohydride (approximately 3.5 mg borohydride per ml of broth) and incubated at 60°C for 30 min. The excess reducing agent was subsequently destroyed by the addition of 20 μl of glacial acetic acid until the pH of the solution reached a value of 4 (usually 20 μl of acid per ml of broth). Degradation of the borohydride was judged to be complete when the effervesence ceased (approximately 5 min). The pH of the broth was readjusted to that required for the reaction by the addition of 2 *M* potassium hydroxide. Buffer samples containing ACV were treated identically, except no protein precipitation step was needed. The reaction involving monobromobimane was conducted with ACV dimer which had been reduced by dithiothreitol. The dimer was dissolved in phosphate buffer at pH 7.4, in contrast to the other two derivatising procedures where the ACV was prepared in water.

Preparation of derivatising reagents and mobile phases

DTNB solution (1 m*M*) was prepared by dissolving the solid in a phosphate buffer (0.1 *M*, pH 8.0). The reagent was prepared daily and kept in the dark when not in use. The mobile phase for HPLC separations consisted of acetate buffer (0.02 *M*, pH 5.8) and acetonitrile run as a linear gradient at a flow-rate of 1 ml/min.

Monobromobimane (2 m*M*) was prepared as a stock solution in HPLC grade acetonitrile. A similar mobile phase to that described by Newton *et al.*[15] was used. Buffer A consisted of 90% (v/v) water containing EDTA (0.5 m*M*), acetic acid (0.04 *M*) and 10% (v/v) acetonitrile. The buffer was then adjusted to a pH of 3.6 with 10 *M*

potassium hydroxide. Buffer B was composed of 90% acetonitrile, 10% water and was brought to a pH of 3.6 with glacial acetic acid. The two buffers were mixed in a step gradient over 30 min using a flow-rate of 1.5 ml/min.

Dansylaziridine (3 m*M*) was prepared in HPLC grade methanol. Once again a gradient elution programme was employed. This time the mobile phase consisted of acetate buffer (0.02 *M*, pH 4.0) containing EDTA (0.5 m*M*) and acetonitrile (Fig. 2a) and separations were effected at a flow-rate of 1 ml/min.

Derivatisation methods

ACV Standards

Fresh stock solutions of ACV (1 m*M*) were produced on a daily basis as described under Sample preparation. These stock solutions were then serially diluted prior to use in the following procedures.

DTNB procedure. A sample of the ACV monomer (10 μl, 1 m*M*) was reacted with DTNB (30 μl, 1 m*M*) at pH 8.0 for 10 min at room temperature. The resultant solution containing the derivatised peptide was injected onto the column (injection volume 20 μl). Detection was by UV absorbance at 310 nm. (This wavelength had previously been determined to correspond to the maximum absorbance of the mixed disulphide.)

Monobromobimane procedure. ACV dimer (20 μl, 0.9 m*M*) was reacted with DTT (20 μl, 2 m*M*) for 5 min. The resultant solution was treated with monobromobimane stock solution (20 μl, 2 m*M*) and after shaking was left to stand for 20 min in the dark at 20°C. HPLC detection was carried out by spectrofluorimetry using the excitation and emission wavelengths of 380 and 477 nm respectively. HPLC was effected using an injection volume of 20 μl.

Dansylaziridine procedure. A solution of ACV (20 μl, 1 m*M* at the pH stated) was reacted with an equal volume of dansylaziridine stock solution. The mixture was incubated at 60°C for 30 min and then cooled to 20°C. A 20-μl sample was injected onto the HPLC column.

The aziridine derivatisation procedure was also carried out on other thiols known to be present in fermentation media, namely glutathione and cysteine. A 1 ml solution containing glutathione (0.21 m*M*), L-cysteine (0.3 m*M*) and reduced ACV (0.1 m*M*) was assayed similarly.

Biological samples

Filtered, deproteinised fermentation broths were obtained and treated with sodium borohydride as described previously to produce the monomeric form of ACV. The pH of each sample was adjusted to 8.8 and an aliquot (50 μl) was reacted with an equal volume of dansylaziridine stock solution. The reaction mixtures were incubated at 60°C for 30 min followed by rapid cooling to 20°C. As in previous experiments an injection volume of 20 μl was employed for HPLC.

RESULTS AND DISCUSSION

Optimisation of the derivatisation procedure

The analytical procedure based upon derivatisation with dansylaziridine was

optimised with respect to excitation and emission wavelengths, reaction time with ACV, molar ratio of reagent to analyte and temperature of the reaction.

Excitation and emission wavelengths were selected by manual scanning of the monochromator, under stopped flow conditions. The maxima for absorption and emission were found to be at wavelengths of 339 and 540 nm respectively.

The pH dependency of the reaction of the aziridine with ACV is shown in Fig. 1a (using a 60-min incubation at 60°C). A working pH of 8.8 was adopted for all subsequent analyses. This pH represented a compromise between product yield and signal-to-noise ratio which decreased with increasing pH. Furthermore the use of samples at a pH greater than 8.9 was incompatible with the buffering capacity of the mobile phase. At these pH's variable retention times, loss of resolution and increased reagent hydrolysis peak were all noted.

The incubation temperature used for the derivatisation was varied between 20 and 70°C (using a 60-min incubation at pH 8.8). As shown in Fig. 1b the yield of fluorescent product increased with temperature. A working temperature of 60°C was adopted in order to maximise the sensitivity since above this temperature the signal-to-noise ratio decreased dramatically.

Reaction times at 60°C were studied and it was found that the product peak area increased rapidly with time up to 30 min but thereafter increased only slowly, reaching a maximum at approximately 400 min. Since the reaction after 30 min was 95% of that after 60 min the former reaction time period was adopted for the incubation in the standard procedure.

The optimal molar ratio of reagent to analyte was investigated for an ACV concentration of 1 m*M*. It was found that it was necessary to use at least a three-fold reagent excess to ensure complete reaction at the time and temperature specified. When working with broth samples, the standard derivatisation employed a concen-

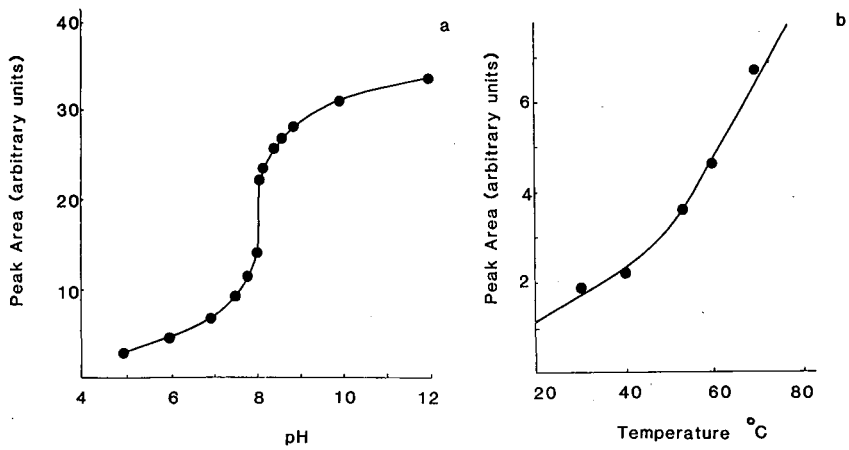

Fig. 1. Optimisation of pH and temperature for the dansylaziridine derivatisation procedure. Chromatographic conditions as described in the Experimental section; detector sensitivity 32; injection volume 20 μl. (a) The effect of reaction pH on peak area was examined using phosphate buffers (50 m*M*) at the appropriate pH (60°C, 60 min) incorporating reagent and ACV at 1.5 and 0.14 m*M* (100 μg/ml) concentrations respectively. (b) The influence of temperature on peak area was examined in phosphate buffer (50 m*M*) at pH 8.8 containing ACV and dansylaziridine at concentrations of 0.14 and 1.5 m*M* respectively.

tration of dansylaziridine (1.5 m*M*) which represented a large molar excess compared to the total thiol concentration in all the complex broths we have studied.

Calibration and detection limits

Two calibration graphs of ACV concentrations were constructed using optimised conditions for the derivatisation as previously described. Regression analysis showed that both plots were linear for ACV concentrations in acetate buffer between 227 and 0.56 μg/ml and 227 and 5.6 ng/ml respectively, and passed through the origin. However, a detection limit of 120 pg/ml for a signal-to-noise ratio of 2:1 was achievable. The regression equations for the two plots were:

Range 1 (227–0.56 μg/ml)
Peak area (arbitrary units) = 3.58 + 0.63 × concentration (μg/ml)

Standard deviation = 2.9
R-squared = 98%

Range 2 (227–5.6 ng/ml)
Peak area (arbitrary units) = 0.52 + 55.43 × concentration (ng/ml)

Standard deviation = 0.223
R-squared = 99.4%

A study of the stability of the product was made. After derivatisation, the reaction mixture was cooled to 20°C and allowed to stand at this temperature for various periods of time prior to HPLC analysis using an injection volume of 20 μl. No variation in peak area was detected after stand-times up to 1250 min (20.8 h). Reproducibility was determined by repeat injections (n = 10) of the same derivatised ACV solution (0.25 m*M*). The standard deviation was found to be 2%.

Comparison with other derivatising reagents

For comparative purposes, assays involving the alternative derivatising reagents DTNB and monobromobimane were carried out using solutions of ACV prepared in acetate buffer. Using the former derivatising reagent good chromatographic resolution was easily obtainable employing a simple gradient and detection at 310 nm. However, the low extinction coefficient of the mixed disulphide did not permit satisfactory detection of ACV below 10 μg/ml in buffer solutions even when maximum detector sensitivity was employed. For this reason, further work in fermentation media was not attempted. The advantages of derivatisation with DTNB are the rapid reaction rates under ambient conditions, and good overall reproducibility in the HPLC analysis. Consequently this method is useful for the assay of thiols in non-complex media.

The use of monobromobimane in the quantitation of thiols from biological sources has been well documented[15–17]. The reagent reacts rapidly with ACV at room temperature and yields highly fluorescent products. Although other workers have reported its use in the study of β-lactam biosynthesis using cell-free extracts[10], when applied to the determination of ACV in fermentation broths problems were encountered in the development of suitable HPLC elution programmes. Additional

problems included the appearance of a very intense peak in the chromatogram attributable to hydrolysed reagent. Other peaks were also obtained which may arise from the reaction of monobromobimane with non-thiol containing broth components. For solutions in buffer, ACV was detectable at concentrations down to 2.5 μg/ml but reproducibility was poor due to poor resolution and the detection limit in broths was subsequently an order of magnitude lower. However, we have developed a procedure for the qualitative visualisation of ACV on paper and thin-layer plates based upon the reaction with monobromobimane and irradiation with UV light (unpublished work).

In conclusion dansylaziridine is the favoured derivatising reagent for the trace analysis of ACV in fermentation samples by an HPLC procedure, on the basis of its selectivity and superior sensitivity when spectrofluorometric detection is employed (Fig. 2a). Detection may also be achieved by the absorption of UV light at 245 nm but this method is considerably less sensitive. Further work was conducted with the dansylaziridine to investigate its applicability to ACV assay in the presence of high levels of other potentially interfering compounds (Fig. 2b). Good resolution between ACV and the likely principle sulphydryl containing metabolites, glutathione and cysteine, was achieved. When equi-molar concentrations of these three metabolites were analysed by the dansylaziridine procedure, a greater signal sensitivity was obtained for cysteine than the two peptides.

Applications of the analytical method to crude fermentation broths

The method has been applied to the measurement of the levels of ACV produced extracellularly in fermentation broths by various fungal species grown under different fermentation conditions. These data are presented in Table I. Broth samples

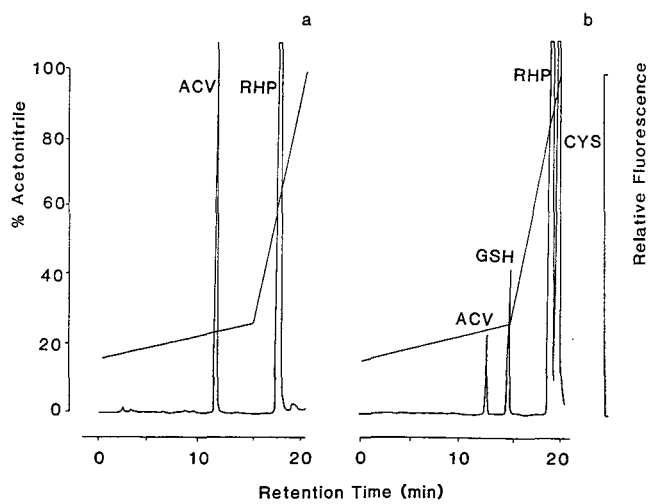

Fig. 2. Reversed-phase HPLC chromatograms of dansylaziridine derivatives. Chromatographic and derivatisation conditions as described in the Experimental section: detector sensitivity 16; injection volume 20 μl. (a) ACV standard at a concentration of 0.07 m*M* (50 μg/ml), showing the reagent peak (RHP). (b) A mixture of glutathione (GSH), cysteine (CYS) and ACV (0.014 m*M*) in a molar ratio 2:3:1 at derivatisation.

TABLE I

DETERMINATION OF ACV CONCENTRATIONS IN CULTURE BROTHS OF FILAMENTOUS FUNGI

After growth of the fungi in the stated complex media for a fixed time, ACV concentrations were determined using the appropriate regression line given in the Results section. Values are the average of duplicate determinations. Media abbreviations used: ACM = *Aspergillus* complete medium; PLFM = *Penicillium* fermentation medium from Pan Labs.; J&J = Jarvis and Johnson defined medium; CSM = *Cephalosporium* sporulation medium.

Species	*Strain*	*Time of assay (h)*	*Media*	*ACV (μg/ml)*
A. nidulans	G3	120	ACM	0.16
A. nidulans	Wild type	120	ACM	0.08
P. chrysogenum	SC6140	0	PLFM	0.13
P. chrysogenum	SC6140	60	PLFM	4.1
P. chrysogenum	NRRL1951	72	J&J	0.00036
P. chrysogenum	P2	120	J&J	1
C. acremonium	N2	120	CSM	4.3

from the fermentation of wild-type *Aspergillus niger* were used as blanks because these were shown to contain no detectable ACV (Fig. 3a). For each fungal species tested several fermentations were carried out and HPLC analyses were made after harvesting broth at fixed times. A typical chromatogram of a given species and fermentation medium is shown (Fig. 3c). ACV concentrations were found to vary according to species, type of liquid culture medium and duration of fermentation prior to assay. To confirm identity of the ACV peaks in the chromatograms from fermentation broths a series of experiments was conducted as follows.

(i) Spiking with standard ACV stock solutions was performed using standard additions calculated to increase the ACV concentration in broth from *P. chrysogenum* SC6140 fermentation by two-, three- and four-fold over the original concentration. This process was also used to confirm the calibration plots described previously.

(ii) Standard additions into spent fermentation broths of *A. niger* (which originally gave no peak at the position corresponding to the ACV derivative) gave an ACV peak which increased in proportion to concentration (Fig. 3a and b).

(iii) When broths treated with and without sodium borohydride were compared, the HPLC of the latter showed no peak corresponding to the ACV derivative. These procedures confirmed the identity of the ACV-dansylaziridine peak in complex media.

Aspergillus nidulans species produced significantly lower ACV levels than the other species, which is consistent with the low penicillin titres obtained from these organisms. This appears to be an intrinsic species trait.

When *P. chrysogenum* strain P2 was grown in defined media with and without the penicillin precursor phenoxyacetic acid (POA) it was observed that addition of POA resulted in reduction of ACV levels by over 50%. There was a concomitant increase in the penicillin V (phenoxymethylpenicillin) titre (unpublished work).

In conclusion, the use of dansylaziridine as a pre-column derivatisation reagent for the HPLC analysis of ACV in fermentation broths has been demonstrated. The method has been shown to be selective and sensitive, with calibrations which are

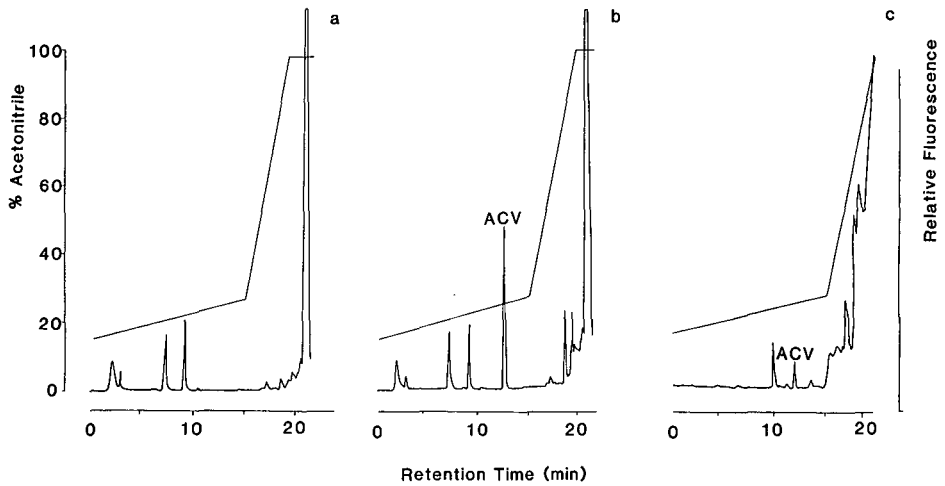

Fig. 3. Reversed-phase HPLC chromatograms of fermentation broth samples after derivatisation with dansylaziridine. Chromatographic procedure, culture conditions and sample derivatisation as described in the Experimental section; detector sensitivity 8; injection volume 20 μl. (a) *A. niger* wild type (IMI17454), 120 h into the fermentation. (b) *A. niger* wild type (IMI17454), 120 h into the fermentation containing a standard addition of ACV (5 μl, 220 μg/ml into 105 μl broth to give a final concentration of 10 μg/ml). (c) *P. chrysogenum* strain SC6140, 60 h into the fermentation.

linear over a wide dynamic range. Dansylaziridine as a derivatising reagent was found to have several advantages over both dithionitrobenzoic acid and monobromobimane, which also react specifically with the sulphydryl group of the ACV monomer.

We believe this is the first direct comparison of broth concentrations of ACV produced extracellularly by the fermentation of different fungal species. In on-going work the procedure is being used to study the influence of media constituents on ACV production in time course studies of fermentations of *A. nidulans*, *P. chrysogenum* and *C. acremonium*. It is intended to monitor both intra- and extracellular levels of the key biosynthetic intermediate, ACV.

ACKNOWLEDGEMENT

This work was funded by a grant from the S.E.R.C. Biotechnology Directorate.

REFERENCES

1 P. B. Loder and E. P. Abraham, *Biochem. J.*, 123 (1971) 471.
2 A. Shah and M. W. Adlard, *J. Chromatogr.*, 424 (1988) 325.
3 J. J. Usher, M. Lewis and D. W. Hughes, *Anal. Biochem.*, 149 (1985) 105.
4 E. P. Abraham, J. A. Huddleston, G. S. Jayatilake, J. O'Sullivan and R. L. White, *Spec. Publ. Chem. Soc.*, 38 (1981) 125.
5 R. L. White, E.-M. John, J. E. Baldwin and E. P. Abraham, *Biochem. J.*, 203 (1982) 791.
6 W. L. Zahler and W. W. Cleland, *J. Biol. Chem.*, 243 (1968) 716.
7 K. Bir, J. C. Crawhill and D. Mauldin, *Clin. Chim. Acta*, 30 (1970) 189.
8 J. Cortes, P. Liras, J. M. Castro and J. F. Martin, *J. Gen. Microbiol.*, 132 (1986) 1805.
9 J. Kupka, Y.-Q. Shen, S. Wolfe and A. L. Demain, *Can. J. Microbiol.*, 29 (1983) 488.
10 G. Banko, S. Wolfe and A. L. Demain, *Biochem. Biophys. Res. Commun.*, 137 (1986) 528.

11 W. H. Scouten, R. Lubcher and W. Baughman, *Biochim. Biophys. Acta*, 336 (1974) 421.
12 F. G. Jarvis and M. J. Johnson, *J. Bacteriol.*, 59 (1950) 51.
13 H. Shirafuji, Y. Fujisawa, M. Kide, T. Kanzaki and M. Yoneda, *Agric. Biol. Chem.*, 43 (1979) 155.
14 G. Pontecarvo, J. A. Roper, L. M. Hemnons, K. D. Macdonald and A. W. Bufton, *Adv. Genet.*, 5 (1953) 141.
15 G. L. Newton, R. Dorian and R. C. Fahey, *Anal. Biochem.*, 114 (1981) 383.
16 R. C. Fahey, G. L. Newton, R. Dorian and E. M. Kowoser, *Anal. Biochem.*, 111 (1981) 357.
17 R. C. Fahey and G. L. Newton, *Methods Enzymol.*, 143 (1987) 85.

Journal of Chromatography, 481 (1989) 255–262
Elsevier Science Publishers B.V., Amsterdam — Printed in The Netherlands

CHROM. 21 726

SEPARATION AND IDENTIFICATION OF RETINOIC ACID PHOTOISOMERS

M. G. MOTTO*, K. L. FACCHINE, P. F. HAMBURG, D. J. BURINSKY, R. DUNPHY, A. R. OYLER and M. L. COTTER

R. W. Johnson Pharmaceutical Research Institute, Ortho Pharmaceutical Corporation, Raritan, NJ 08869-0602 (U.S.A.)

(First received March 21st, 1989; revised manuscript received June 21st, 1989)

SUMMARY

Retinoic acid was isomerized in ethanol–water (90:10) with fluorescent light. Reversed-phase high-performance liquid chromatography (HPLC) on a 3-μm ODS-2 column with a highly specific mobile phase allowed simultaneous determination of ten retinoic acid isomers that were produced during the photoisomerization. Nine of the isomers were isolated by HPLC and characterized by spectroscopic methods (^{1}H NMR, mass spectrometry and UV). The variation of product distribution with time was determined over the course of the reaction (21 h).

INTRODUCTION

Retinoic acid [**1**, (all-*E*)-3,7-dimethyl-9-(2,6,6-trimethyl-1-cyclohexen-1-yl)-2,4,6,8-nonatetraenoic acid, tretinoin] and its analogues (retinoids) are an important class of biomolecules. Retinoids are involved in many biological functions including such processes as epithelial cell growth and differentiation[1] and vision[2]. Retinoids are also used therapeutically for the treatment of acne[3] and photo-damaged skin[4] and have shown potential use as cancer chemotherapeutic agents[5].

In general, retinoids are know to isomerize by chemical methods, with heat, and, most importantly, by the action of light[6,7]. In particular, the photoisomerization of retinoids plays an important role in vision (11-*cis*-retinal isomerization in retinyl opsins) and in some bacterial proton transport (13-*cis*-retinal isomerization in bacteriorhodopsin)[2]. Due to the importance of retinal in these biological systems, photoisomerization of this molecule has been very well documented in the literature[6–8] along with the analytical methodology for the separation and identification of retinal photoisomers[7,9,10]. However, the photoisomerization of retinoic acid has not been as well documented. Previous literature reports of retinoic acid photoisomerization[11,12] did not contain analytical methodology capable of separating all of the retinoic acid isomers. To overcome this deficiency, the isomer mixtures were derivatized to give the methyl retinoates which were more easily resolved by high-performance liquid chromatography (HPLC). After derivatization, eight isomers of retinoic acid were observ-

0021-9673/89/$03.50

ed and characterized as their methyl esters by McKenzie *et al.*[11] and seven isomers by Curley and Fowble[12]. In both papers, chromatography of the retinoic acid mixtures themselves gave poor resolution with much peak overlap. This paper presents an improved reversed-phase method for the separation of retinoic acid isomers, the identification of these isomers by isolation and spectroscopic characterization and an analysis of the time-dependence of photoisomerization.

EXPERIMENTAL

Retinoic acid and 13-*cis*-retinoic acid were purchased from Eastman Kodak (Rochester NY, U.S.A.) and used without further purification. Acetonitrile, methanol and isopropanol were HPLC grade and purchased from Burdick and Jackson (Muskegon, MI, U.S.A.). Acetic acid (glacial) was purchased from Fisher Scientific (Fair Lawn, NJ, U.S.A.). Water for HPLC was obtained using a Milli-Q water purification system from Millipore Corporation (Bedford, MA, U.S.A.). Absolute ethanol was purchased from Pharmco (Bayonne, NJ, U.S.A.).

Separations were performed on an Spherisorb 3-μm ODS-2 (150 mm $\times$ 4.6 mm) HPLC column (Alltech, Deerfield, IL, U.S.A.). We found that a minimum plate count of 60 000 plates/m, based on the manufacturer's test chromatogram, was necessary to achieve the desired separation. The HPLC system consisted of a Perkin-Elmer (Norwalk, CT, U.S.A.) Series-4 quaternary solvent gradient pumping system equipped with a Hewlett-Packard (Palo Alto, CA, U.S.A.) photodiode array (1040M) detection system, with the detection wavelengths set at 345, 290 and 235 $\pm$2 nm. Integration was performed by the HP photodiode array system at each of the wavelengths. Sample injection was accomplished by using a programmable autosampler (WISP; Water Assoc., Milford, MA, U.S.A.).

Proton NMR spectra were obtained in C^2HCl_3 or [$^2H_6$]acetone on a Varian XL-400 (Varian, Palo Alto, CA, U.S.A.) or a GE QE-300 spectrometer (General Electric, Freemont, CA, U.S.A.). Mass spectra were obtained on a Finnigan MAT 8230 mass spectrometer (Finnigan, San Jose, CA, U.S.A.) by desorption electron impact (DEI) or desorption chemical ionization (DCI). DCI spectra were obtained with isobutane as reagent gas. UV spectra were recorded on the Hewlett-Packard 1040M diode array HPLC detector as the compounds were eluting from the HPLC column.

Photoisomerization was carried out by irradiation of a solution of retinoic acid ($1.67 \cdot 10^{-3}$ *M*) in ethanol–water (90:10). The solution was placed in a quartz vessel and purged with argon. The vessel was then placed within the chamber of a Rayonet photochemical reactor (Southern New England Ultraviolet Co., Hamden, CT, U.S.A.) and irradiated with visible light (cool-white fluorescent F6T5/CW; Philips Lighting, Somerset, NJ, U.S.A.). Samples of the solution were periodically removed and analyzed by HPLC.

RESULTS AND DISCUSSION

Retinoic acid and related retinoids have been shown to isomerize in the presence of light to give a photostationary isomer mixture[6,7,11–14]. Theoretically, each of the double bonds in the chain portion of retinoic acid can undergo isomerization to

give both mono *cis* and multiple *cis* isomers resulting in a total of sixteen double-bond isomers. Eight additional isomers are possible due to cyclization of the 7-*cis* isomers of retinoic acid. Therefore a total of twenty-four photoisomers are possible. Due to steric hindrance, some of these isomers may be unstable at room temperature and thermally isomerize to more stable compounds, as was observed for the isomers of retinal[8,15]. In the present study, nine photoisomers of retinoic acid were isolated and characterized by spectroscopic methods and a tenth unidentified isomer was observed in the reversed-phase chromatogram. The structures of these isomers are shown in Fig. 1.

Reversed-phase HPLC separation of retinoic acid isomers

Separation of the retinoic acid photoisomers was accomplished on a 3-μm reversed-phase HPLC column at a flow-rate of 1.2 ml/min with an isocratic mobile phase consisting of 30% acetonitrile, 25% methanol, 15% isopropanol and 30% water each containing 1.2% (v/v) of acetic acid. This HPLC method was found to give an improved separation of the retinoic acid isomers when compared to literature method[11,12]. Typical chromatograms for the photostationary state mixture after 3 h irradiation and for a long term irradiation mixture (7 days) are shown in Figs. 2 and 3, respectively. Resolution of all eight double-bond isomers that were identified in this study was achieved and a minor product that was assumed to be a 7-*cis* isomer of retinoic acid was observed. Complete resolution of one of the two photocyclized isomers was obtained and selective wavelength monitoring allowed observation of the other photocyclized isomer (which overlapped the double-bond isomers). The photocyclized isomers were found to have a maximum absorption at *ca.* 290 nm and to have almost no absorbance at 345 nm. Therefore, quantitation of all of the retinoic acid double-bond isomers was achieved at 345 nm without interference from the photocyclized compounds.

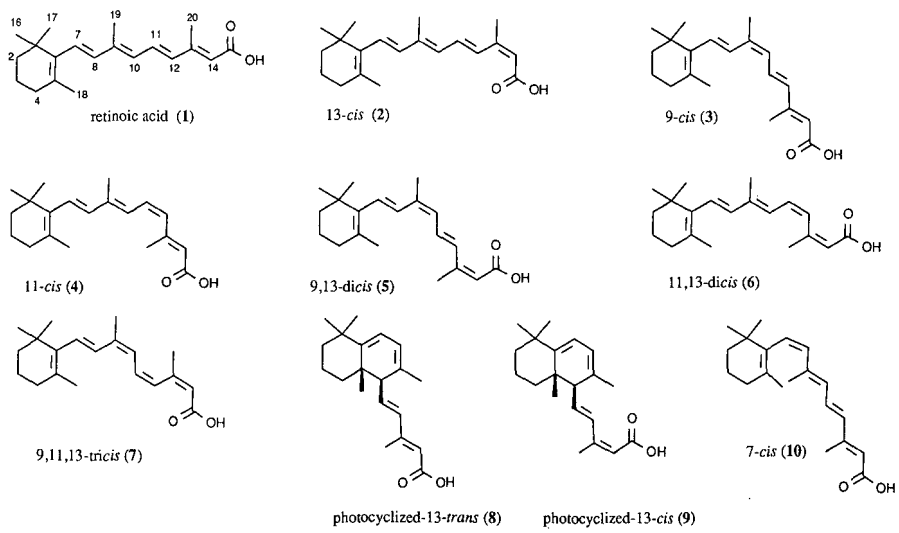

Fig. 1. Retinoic acid isomers observed in this study.

TABLE I

SPECTRAL DATA FOR RETINOIC ACID ISOMERS

Compound	*UV*[a] λ_{max} *(nm)*	*NMR assignments (ppm)*[b]													*Coupling constants (Hz)*[c]		
		16,17-CH_3	*18-CH_3*	*19-CH_3*	*20-CH_3*	*2-CH_2*	*3-CH_2*	*4-CH_2*	*7-H*	*8-H*	*10-H*	*11-H*	*12-H*	*14-H*	$J_{7,8}$	$J_{10,11}$	$J_{11,12}$
1	357	1.032	1.716	2.010	2.367	1.471	1.619	2.025	6.299	6.147	6.157	7.046	6.313	5.798	16.0	11.4	15.0
2	360	1.035	1.719	2.004	2.102	1.472	1.622	2.030	6.29[j]	6.18[j]	6.264	7.026	7.737	5.655	16.1	11.5	15.3
3	352	1.044	1.751	2.008	2.349	1.489	1.644	2.053	6.293	6.651	6.064	7.128	6.248	5.797	16.0	11.5	15.0
4	347	1.027	1.715	1.973	2.357	1.467	1.616	2.018	6.285	6.142	6.533	6.588	5.913	5.897	16.1[g]	13.0[g]	11.2[g]
5[e]	353	1.049	1.752	1.99[d]	2.1[d]	1.496	1.641	2.0[d]	6.347	6.793	6.175	7.207	7.780	5.70	16.0	11.5	15.3
6	350	1.022	1.707	1.964	2.207	1.465	1.613	2.015	6.283	6.121	6.404	6.645	6.966	5.721	16.0	12.6	11.6
7	340	1.031	1.732	1.992	2.199	1.47[f]	1.62[f]	2.031	6.29[f]	6.671[f]	6.29[f]	6.729[f]	6.865	5.724	16.0	11.5[h]	12.0
8	265	1.126[k], 1.141[k]	0.977[k]	1.679	2.328	1.45[f]	1.45[f]	1.45[f]	5.768	5.836	2.795	6.253	6.201	5.7[i]	5.7[g]	10.5[g]	15.3[g]
9	268	1.121[k], 1.136[k]	0.972[k]	1.686	2.059	1.40[f]	1.40[f]	1.40[f]	5.758	5.825	2.889	6.237	7.609	5.660	5.6	10.7	15.7

[a] UV spectra were recorded by the HPLC detector as the peaks eluted from the column, spectral resolution was ±2 nm.

[b] Spectra were recorded at 400 MHz at 25°C for a C^2HCl_3 solution with tetramethylsilane (TMS) as an internal standard, chemical shifts are reported in ppm downfield of TMS with an estimated error of ±0.005 ppm.

[c] Estimated error ±0.3 Hz.

[d] Resonance overlapped with solvent.

[e] Solvent was [$^2H_6$]acetone with TMS as internal standard.

[f] Unresolved or overlapped resonances.

[g] Assignment confirmed by spectral simulation.

[h] Estimated from unresolved resonances.

[i] Estimated error ±0.1 ppm.

[j] Estimated error ±0.01 ppm.

[k] Assignments may be reversed.

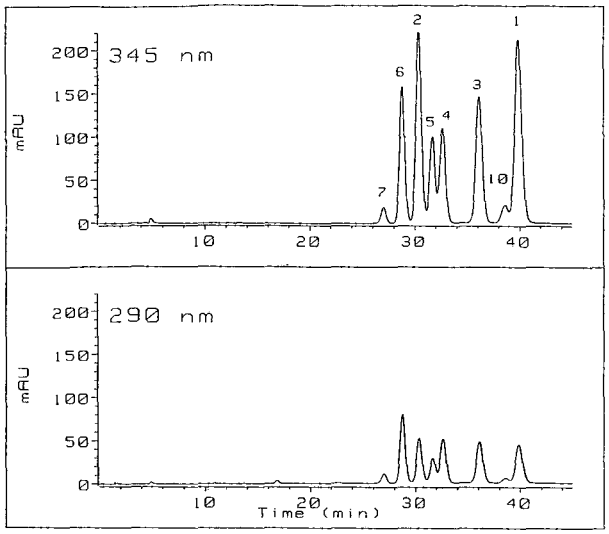

Fig. 2. Reversed-phase HPLC chromatogram of retinoic acid isomer mixture on an Altex Spherisorb ODS-2 3-μm column. The column was eluted with acetonitrile–methanol–isopropanol–water (30:25:15:30) containing 1.2% acetic acid at a flow-rate of 1.2 ml/min. The detection wavelengths were set at 345 and 290 nm. The isomer mixture was produced by irradiation of retinoic acid for 3 h in ethanol–water (90:10) with fluorescent light.

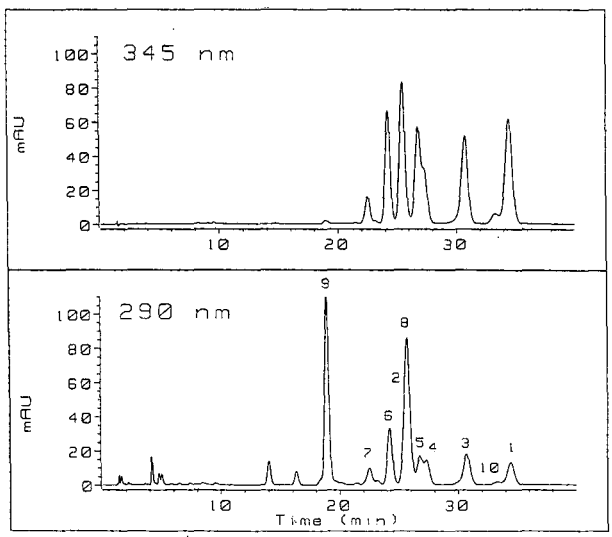

Fig. 3. Reversed-phase HPLC chromatogram of retinoic acid isomer mixture after long term irradiation with fluorescent light (7 days). HPLC conditions as in Fig. 2.

Identification of photoisomers of retinoic acid

Each of the compounds observed in the analytical HPLC chromatogram was isolated by preparative HPLC and its structure determined by a combination of spectral methods that included MS, UV and ^{1}H NMR. ^{1}H NMR spectroscopy, due to its sensitivity to retinoid stereochemistry, has been the method of choice for identifying retinoid isomers[7]. The proton chemical shift assignments and coupling constants and the observed UV maximum for each of the photoisomers are shown in Table I. The spectral data were consistent with those reported in the literature for similar retinoids (retinal[7,16] and methyl retinoate[13]). The stereochemistry of the cyclized isomers was determined by comparison of the NMR spectral data with that for similar compounds reported in literature[13,14,17]. Additionally, a small nOe (nuclear Overhauser enhancement) was observed for the 11-proton upon irradiation of the 18-CH_3 protons in compound **9**. This observation suggests that the 18-CH_3 and the side chain are in a *cis* configuration.

Time-dependence of retinoic acid photoisomerization

The time dependence of retinoic acid photoisomerization ($1.67 \cdot 10^{-3} M$ in 90% ethanol) with visible light was determined by reversed-phase HPLC. The concentrations of the double-bond isomers and the photocyclized isomers were calculated in mole percent based on the observed area counts at 345 and 290 nm, respectively. Calibration curves were obtained for retinoic acid and 13-*cis*-retinoic acid at 345 nm. The concentrations of the remaining double-bond isomers were based on the assumption that the responses for these compounds at 345 nm were similar to that of the 13-*cis* isomer. The response for each of the photocyclized isomers was calculated relative to that for the all-*trans* isomer at 290 nm. Table II gives the concentration of

TABLE II

RETINOIC ACID ISOMER CONCENTRATION AFTER 3 h IRRADIATION WITH VISIBLE LIGHT

Obtained by irradiation of a $1.67 \cdot 10^{-3} M$ solution of retinoic acid in ethanol–water (90:10).

Compound	*Mole-%*[a]
1	18
2	19
3	16
4	10
5	13
6	15
7	3.7
8	1.7
9	1.7[b]
10	2.5

[a] The concentrations of the double-bond isomers (**1**–**7**,**10**) were calculated in mole % based on the observed area counts at 345 nm. Calibration curves were obtained for **1** and **2** with the concentrations of the remaining double-bond isomers based on the assumption that the responses for these compounds at 345 nm were similar to **2**. The concentration for the cyclized compounds **8** and **9** were based on area counts at 290 nm and a response calculated for a pure sample **8** relative to a pure sample of **1**.

[b] The percentage of **9** was approximated due to some peak overlap.

each of the photoisomers present in the retinoic acid solution at the photostationary state.

When retinoic acid was irradiated with visible light at room temperature under an argon atmosphere it quickly isomerized to give a mixture of ten isomers. The mole-percent of each of the isomers is shown in Fig. 4. Within the first 10 min of irradiation all of the double-bond isomers were formed and observed by HPLC. Initially, the 13-*cis* and the 11-*cis* isomers increased rapidly to a point (about 30 min irradiation) where they each made up about 18% of the product mixture. After that time, the remaining isomers increased and the 11-*cis* isomer decreased. The eight double-bond isomers reached a photostationary state mixture after about 3 h of irradiation. This mixture remained essentially unchanged over the next few hours of irradiation. The only subsequent change observed was an increase in the two photocyclized isomers and a concurrent decrease in all the double-bond isomers. After prolonged irradiation, the photocyclized isomers were the two major compounds remaining in the product mixture (Fig. 3). A similar observation has been reported by Halley and Nelson[14] for the methyl ester of retinoic acid. In the cited paper and in a previous paper[13], the authors concluded that the photocyclized isomers are formed by cyclization of the 7-*cis* and 7,13-di*cis* isomers of methyl retinoate. This conclusion was also supported by studies with other similar polyenes[17]. None of the 7-*cis* isomers were isolated in this work. These isomers may be present in the mixture at very low levels, and lead to the formation of the cyclized products. The low level peak (**10**) seen in the reversed-phase chromatogram is believed to be a 7-*cis* isomer. Peak **10** elutes just before the retinoic acid peak and has a UV maximum at 345 nm consistent with a double-bond isomer of retinoic acid.

The HPLC method shows the power of using small particle size colums for the analysis of closely related molecules. This high resolution column and the use of the

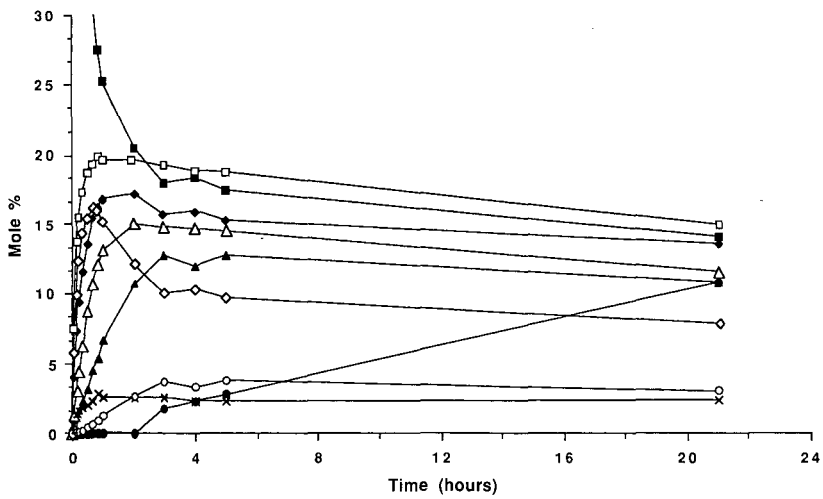

Fig. 4. Time dependence of retinoic acid photoisomerization over 21 h. Retinoic acid ($1.67 \cdot 10^{-3} M$) in ethanol–water (90:10) irradiated with cool-white fluorescent light. ■, retinoic acid; □, 13-*cis*; ◆, 9-*cis*; ◇, 11-*cis*; ▲, 9,13-di*cis*; △, 11,13-di*cis*, ○, 9,11,13-tri*cis*; ●, cyclized isomers (*cis* and *trans*); ×, 7-*cis* (tentative assigment).

specified mobile phase has enabled us to obtain complete separation of the ten isomers observed in this study. We found that the mobile phase selection was extremely important, as small variations in composition caused considerable loss of resolution as well as changes in elution order. In our studies we found that increasing the percentage of acetonitrile relative to the percentage of methanol caused a reversal in the elution order of peaks associated with compounds **4** and **5** and resulted in deteriorated resolution. However, this modified mobile phase gave higher resolution between the peak for retinoic acid and that of compound **10**. The selectivity achieved by small variations in mobile phase can be used as an advantage during the isolation of compounds by HPLC and was employed to help with the isolation of pure retinoic acid isomers.

REFERENCES

1 A. B. Roberts and M. B. Sporn, in M. B. Sporn, A. Roberts and D. S. Goodman (Editors), *The Retinoids*, Vol. 2, Academic Press, Orlando, 1984, Ch. 12, p. 210.
2 C. D. B. Bridges, in M. B. Sporn, A. Roberts and D. S. Goodman (Editors), *The Retinoids*, Vol. 2, Academic Press, Orlando, 1984, Ch. 10, p. 125.
3 S. Mandy and E. Thorne, *Adv. Ther.*, 1 (1984) 404.
4 J. Weis, C. Ellis, J. Headington, T. Tincoff, T. Hamilton and J. Voorhees, *J. Am. Med. Assoc.*, 259 (1988) 527.
5 R. C. Moon and L. M. Itri, in M. B. Sporn, A. Roberts and D. S. Goodman (Editors), *The Retinoids*, Vol. 2, Academic Press, Orlando, 1984, Ch. 14, p. 327.
6 F. Frickel, in M. B. Sporn, A. Roberts and D. S. Goodman (Editors), *The Retinoids*, Vol. 1, Academic Press, Orlando, 1984, Ch. 2, p. 30.
7 R. S. H. Liu and A. E. Asato, *Tetrahedron*, 40 (1984) 1931.
8 R. S. H. Liu and A. E. Asato, *Methods Enzymol.*, 88 (1982) 506.
9 R. C. Bruening, F. Derguini and K. Nakanishi, *J. Chromatogr.*, 361 (1986) 437.
10 P. V. Bhat and P. R. Sundaresan, *CRC Crit. Rev. Anal. Chem.*, 20 (1988) 197 and references within.
11 R. M. McKenzie, D. M. Hellwege, M. L. McGregor, N. L. Rockley, P. J. Riquetti and E. C. Nelson, *J. Chromatogr.*, 155 (1978) 379.
12 R. W. Curley, Jr. and J. W. Fowble, *Photochem. Photobiol.* 47 (1988) 831.
13 B. A. Halley and E. C. Nelson, *J. Chromatogr.*, 175 (1979) 113.
14 B. A. Halley and E. C. Nelson, *Int. J. Vit. Nutr. Res.*, 42 (1979) 347.
15 A. Kini, H. Matsumoto and R. S. H. Liu, *J. Am. Chem. Soc.*, 101 (1979) 5078.
16 D. J. Patel, *Nature (London)*, 221 (1969) 825.
17 V. Ramanurthy and R. S. H. Liu, *J. Org. Chem.*, 41 (1976) 1862.

Journal of Chromatography, 481 (1989) 263–273
Elsevier Science Publishers B.V., Amsterdam — Printed in The Netherlands

CHROM. 21 764

HIGH-PERFORMANCE LIQUID CHROMATOGRAPHIC METHOD FOR ISOLATING COPROSTANOL FROM SEDIMENT EXTRACTS

MARGARET M. KRAHN*, CATHERINE A. WIGREN, LESLIE K. MOORE and DONALD W. BROWN

Environmental Conservation Division, Northwest Fisheries Center, National Oceanic and Atmospheric Administration, 2725 Montlake Boulevard East, Seattle, WA 98112 (U.S.A.)

(First received April 4th, 1989; revised manuscript received June 27th, 1989)

SUMMARY

We report a rapid, largely automated high-performance liquid chromatographic (HPLC) method, which uses an HPLC column packed with alkylnitrile-substituted secondary alkylamine (aminocyano) bonded phase, to isolate coprostanol from interfering compounds in sediment extracts. Coprostanol is then quantitated, as the trimethylsilyl ether, by gas chromatography with flame ionization detection. Results from using the HPLC method to analyze a sediment reference material for coprostanol were statistically comparable to a previously used gravity-flow column method. We also report the coprostanol concentrations in several sediment samples from the California coast which reflect a range of sewage contamination (62–15 000 ng/g).

INTRODUCTION

Continuous discharge of municipal sewage effluents and sludges into the oceans has resulted in the need to monitor the dispersion of sewage-related contaminants throughout the marine environment. Over the past decade, coprostanol (5β-cholestan-3β-ol) has been recognized as a good biochemical indicator of sewage pollution[1]. Coprostanol is formed by the enzymatic hydrogenation of cholesterol in the intestine of higher animals[2,3]. Coprostanol and cholesterol are the major sterols in human feces[3]; however, cholesterol occurs naturally in aquatic environments, limiting its usefulness as a sewage tracer[4].

Many analytical methods for determining coprostanol in sediment have been published over the past decade; all are time-consuming and laborious[1]. For example, typical methods[5–10] involve several steps: (a) freeze- or oven-drying of the sediment; (b) Soxhlet extraction followed by concentration of the extract; (c) saponification; (d) thin-layer or gravity-flow chromatographic cleanup on silica or alumina; (e) derivatization; and (f) quantitation by gas chromatography (GC) with flame ionization (FID) or mass spectrometric (MS) detection.

As the demand for coprostanol analyses grows with increased awareness of the potential environmental impact of ocean dumping, methods must be simplified and improved to lower the costs and to increase the efficiency of these analyses. For

example, McCalley *et al.*[11] report that saponification of the sediment releases only small additional amounts (12–18%) of coprostanol, so they eliminate this step to save time. Furthermore, many laboratories routinely perform determinations of aromatic hydrocarbons (AHs), chlorinated hydrocarbons (CHs) and coprostanol on the same sediment extracts, so a single extraction procedure, such as that reported by Readman *et al.*[10], would prove cost-effective. Our laboratory also uses a sediment extraction procedure which combines the extraction of AHs, CHs and coprostanol; in addition, drying and extraction are combined into a single step[12].

In this manuscript, we report further improvements in the determination of coprostanol in sediment. A rapid high-performance liquid chromatographic (HPLC) separation and fractionation, using two normal-phase columns, isolates coprostanol from interfering compounds. Then, a simple derivatization procedure prepares the sample for GC quantitation. We report the results of analyses for coprostanol in a sediment reference material and in selected sediments acquired as part of the National Oceanic and Atmospheric Administration's (NOAA) National Status and Trends (NS&T) Program, a multiyear national program to measure the quality of our nation's coastal environment[13].

EXPERIMENTAL[a]

Preparation of standards

The following standard solutions were prepared for coprostanol analyses: 5α-androstan-17-β-ol (androstanol; 50.0 ng/μl; Sigma, St. Louis, MO, U.S.A.), the internal standard for quantitating coprostanol; [$^2H_{12}$]benzo[*e*]pyrene (56.5 ng/μl; MSD Isotopes, St. Louis, MO, U.S.A.), the HPLC internal standard for calculating the fraction of the extract used for HPLC; hexamethylbenzene (HMB, 76.1 ng/μl; Aldrich, Milwaukee, WI, U.S.A.), the GC internal standard for calculating the recovery of androstanol and [$^2H_{12}$]benzo[*e*]pyrene; an HPLC calibration standard containing coprostanol (180 ng/μl; Supelco, Bellefonte, PA, U.S.A.) and [$^2H_{12}$]benzo[*e*]pyrene (10 ng/μl) for calibrating fraction collection; and a GC calibration standard containing HMB (3.8 ng/μl), coprostanol (4.7 ng/μl), androstanol (2.5 ng/μl) and [$^2H_{12}$]benzo[*e*]pyrene (4.8 ng/μl). Epicoprostanol (5β-cholestan-3α-ol; 5 ng/μl; ICN Biochemicals, Plainview, NY, U.S.A.) was chromatographed to obtain its GC retention time and mass spectrum.

Collection of sediments

Sediments were collected with a modified Van Veen grab (see ref. 14). Subsamples were taken from the top 2 cm of three replicate grabs at each of three stations per site, and each replicate was put into a clean glass jar. The samples were returned to the laboratory on ice, frozen, and then thawed before the replicates were composited in the laboratory. Each site (*e.g.* South San Diego Bay) had three stations (A, B and C) located within a 2-km radius. The California sites are a subset of those sam-

[a] Mention of trade names is for information only and does not constitute endorsement by the U.S. Department of Commerce.

pled for NOAA's NS&T Program[13] and represent a range of coprostanol concentrations. The Kellogg Island (Seattle, WA, U.S.A.) sediment is a highly contaminated sediment which had been found by a previous analytical procedure[15] to contain compounds that interfered with analyses for coprostanol. We analyzed this sediment by the HPLC method to demonstrate the efficiency of this procedure in isolating coprostanol from interfering compounds.

Selection of the reference material

A sediment reference material from the Duwamish River (Seattle, WA, U.S.A) was collected and stored as described previously[16]. This Duwamish III reference material has been used in intercalibration exercises (AHs and CHs)[17] for the NS&T Program and currently serves as one of the quality assurance control materials for AHs, CHs and coprostanol in our laboratory. Thus, this material has been analyzed repeatedly.

Extraction of sediment

Sediment samples were extracted to obtain AHs, CHs and coprostanol by a tumbling method as described previously[12]. The sediment extract in methylene chloride was reduced to about 20 ml by evaporation. Then, to eliminate particulate matter which could plug the HPLC system, the extract was filtered through a glass-wool plug packed into a 25-ml disposable pipette. The volume of the filtered extract was reduced by evaporation to 1 ml, and 100 μl of the HPLC recovery standard [$^2H_{12}$]benzo[*e*]pyrene was added to determine the percentage of extract used in the HPLC step.

Instrument conditions for HPLC cleanup

A Spectra-Physics (San Jose, CA, U.S.A.) Model 8800 HPLC equipped with a recorder-integrator (Spectra-Physics, Model 4270), an ultraviolet (UV) detector (Spectra-Physics, Model 8450, set at 254 nm) and a refractive index (RI) detector (Model LC-25, Perkin-Elmer, Norwalk, CT, U.S.A.) were interfaced to a Gilson (Middleton, WI, U.S.A.) Model 231/401 autosampler. Two HPLC columns, 250 × 4.6 mm stainless steel, each packed with Partisil 10-μm PAC (alkylnitrile-substituted secondary alkylamine bonded phase, "amino-cyano"; Phenomenex, Torrance, CA, U.S.A.) were connected in series after a 2-μm in-line filter (Model 7302, Rheodyne, Cotati, CA, U.S.A.). The HPLC columns were connected to a six-port valve (Rheodyne, Model 7000) to allow for a reversal of solvent flow to the columns (backflush). The HPLC solvent, methyl *tert.*-butyl ether (MTBE, "high purity solvent", American Burdick & Jackson, Muskegon, MI, U.S.A.), was reported by Miller[18] to be compatible with chromatographing polar compounds on the amino-cyano columns. However, we found that MTBE caused leaks in some PTFE seals, apparently because this solvent shrinks PTFE[19], so we used Kel-F seals when possible. The MTBE was degassed with helium delivered by a regulator equipped with a stainless-steel diaphragm. The helium was passed through an in-line charcoal filter (200-ml "hydrocarbon trap", Alltech, Deerfield, IL, U.S.A.) to eliminate contaminants which may be transferred by the helium to the HPLC solvent.

Cleanup of sediment extracts

MTBE (2 ml) was added to the sediment extract, and the solvent (methylene

TABLE I

MEAN CONCENTRATIONS OF COPROSTANOL [$\bar{x}$, ng/g, DRY WEIGHT (RELATIVE STANDARD DEVIATION, R.S.D., %)] AND MEAN PERCENT RECOVERIES OF THE INTERNAL STANDARD, ANDROSTANOL, BOTH UNDERIVATIZED AND AS TRIMETHYLSILYL ETHERS, IN SEDIMENT SAMPLES AFTER HPLC CLEANUP OF SEDIMENT EXTRACTS

Sample and quantitation method	*Underivatized*		*Trimethylsilyl ethers*		*n*
	Coprostanol, $\bar{x}$ (R.S.D.)	*Androstanol, % recovery (R.S.D.)*	*Coprostanol, $\bar{x}$ (R.S.D.)*	*Androstanol, % recovery (R.S.D.)*	
Duwamish III reference material					
GC–FID	990[a] (15)	84 (14)	920 (17)	84 (7)	5
GC–MS			910[d]	74	1
Kellogg Island sediment					
GC–FID	44 400[b] (2)	87 (1)	33 800 (7)	87 (11)	5
GC–MS	43 400[c]	120	35 000	97	1

[a] Not different by paired Student's *t*-test from concentrations of coprostanol in derivatized samples.
[b] Different by paired Student's *t*-test from concentrations of coprostanol as the trimethylsilyl ether. Sum of coprostanol and epicoprostanol; see Discussion.
[c] Sum of coprostanol and epicoprostanol; see Discussion.
[d] Only a small amount of epicoprostanol was detected.

chloride) was displaced by the MTBE as the volume was reduced to 1 ml. A portion of this extract (100 μl) was injected onto the columns using the autosampler. The elution was isocratic, 100% MTBE at a flow of 2 ml/min for 18 min. The Gilson automatic fraction collector (Model 201C; equipped with a collection valve containing Kel-F seals, Neptune Research, Northbrook, MA, U.S.A.) was calibrated to collect a fraction from the beginning of the [$^2H_{12}$]benzo[*e*]pyrene elution to the end of the coprostanol elution (from 4.2 to 5.8 min). The coprostanol fraction was collected into a conical centrifuge tube (part No. 73785, Kimble Glass, Toledo, OH, U.S.A.). The HPLC columns were backflushed at the completion of fraction collection (from 6 to 16 min) to rapidly remove the remaining polar components from the column.

Hexane (2 ml) was added to the coprostanol fraction and the solvent (MTBE) was displaced by the hexane as the volume was reduced by evaporation to 1 ml. Then, 10 μl of the GC internal standard (HMB) was added, and the volume was further reduced, under nitrogen, to about 100μl.

Preparation of trimethylsilyl ether derivatives

Bis(trimethylsilyl)-trifluoroacetamide (BSTFA with 1% TMCS, Regisil RC-Z; 100 μl; Regis, Morton Grove, IL, U.S.A.) was added to 50 μl of the coprostanol fraction (in hexane), and the mixture was heated on a vial heating module (Pierce, Rockford, IL, U.S.A.) at 60°C for 1 h[20,21]. This mixture was stored in the freezer until GC analyses could be conducted.

Analysis by GC–FID or GC–MS of the sediment fractions

The coprostanol fraction from the sediment extracts and the derivatized fractions were analyzed by capillary GC–FID or GC–MS. A 30 m × 0.25 mm DB-5 capillary column (J & W Scientific, Folsom, CA, U.S.A.) was used in a Hewlett-Packard Model 5880A GC system. The sample (3 μl) was injected splitless, and the split valve was opened after 30 s. An oven temperature of 50°C was held for 1 min and then programmed at 4°C/min to 210°C, at 2°C/min to 280°C and at 8°C/min to 300°C. Helium was the carrier gas, and the flow-rate was set to 30 cm/s at 300°C. Quantitation was made using androstanol as the internal standard.

RESULTS

Analyses by GC–FID and GC–MS for coprostanol in sediment extracts

Extracts from Duwamish III and Kellogg Island sediments (n = 5 for each sediment) were cleaned up by HPLC, and the resulting fractions were analyzed for coprostanol by GC–FID. A portion of each fraction was derivatized with BSTFA and was analyzed for the trimethylsilyl ether of coprostanol. The results are shown in Table I.

One underivatized and one derivatized fraction from the Kellogg Island sediment and one derivatized fraction from the Duwamish III reference material were also analyzed by GC–MS to search for any compounds which could interfere with the quantitation of coprostanol and also to compare the quantitations by GC–FID and GC–MS (Table I). The GC–MS determinations of coprostanol agreed well with the GC–FID results for all the samples (Table I).

In a previous analysis of the Kellogg Island sediment by the column chroma-

tographic procedure of MacLeod *et al.*[15], a "cholestadienol" interferent was found which coeluted with coprostanol on the DB-5 GC column. This cholestadienol interferent had the same molecular weight (384) and fragment ions (*m/z* 367, 351, 255 and 213) as cholesta-5,22-dien-3β-ol, which was tentatively identified (from the mass spectrum) by Matusik *et al.*[22]. No cholestadienol interferent was found in any of the sediment fractions cleaned up by HPLC, indicating a satisfactory separation of this compound from coprostanol.

Epicoprostanol, a product of bacterial action on sewage sludge during digestion[11], coeluted with coprostanol on the DB-5 capillary column (see Discussion). This was unexpected because in previous analyses (*ca.* 1–2 years earlier), the DB-5 columns in use separated the epimers by about 0.8 min. Because coprostanol and epicoprostanol have similar mass spectra, neither selected ion monitoring nor the full-scan mode could effectively distinguish the coeluting epimers. FID also would be unable to differentiate between these compounds. GC–MS chromatograms of one Kellogg Island fraction, both before (Fig. 1A) and after derivatization (Fig. 1B), are shown in order to demonstrate the resolution of the epimers after derivatization.

Statistical comparisons of amounts of coprostanol in derivatized vs. underivatized sediment extracts

When concentrations of coprostanol in underivatized fractions from Kellogg Island sediment were compared by Student's *t*-test (paired) to those in portions of the same fractions derivatized with BSTFA, a significant difference was found; the underivatized fractions had larger concentrations of coprostanol (Table I). In contrast, the concentrations of coprostanol in underivatized and derivatized extracts of Duwamish III reference sediments (Table I) were not significantly different by Student's *t*-test (paired).

Statistical comparisons of amounts of coprostanol in Duwamish III sediment reference material cleaned up by two different methods

Concentrations of coprostanol in samples of Duwamish III sediment reference material analyzed by the HPLC cleanup ($n = 15$) were compared statistically to those in Duwamish III samples cleaned up by the column chromatography method of MacLeod *et al.*[15] (quality assurance for NS&T, 1984–1985; $n = 29$); no differences were found (Table II).

Analyses for coprostanol in sediment samples from California

Several sediments samples, collected in California for the NS&T Program, were extracted, cleaned up by the HPLC method, derivatized, and analyzed for coprostanol (Table III). These samples were chosen, based on analyses for coprostanol in sediments collected at these sites in earlier years, to include a range of coprostanol contamination levels. The lowest coprostanol concentrations were found at the non-urban site, Dana Point, located between San Diego and Los Angeles, while the highest levels were in Santa Monica Bay, adjacent to the Hyperion sewer outfall (Table III). San Pedro Outer Harbor and South San Diego Bay showed intermediate levels of contamination. The variability among the three stations from each site is due to the individual samples taken at each station rather than to analytical method variability; note that the duplicate samples (San Pedro Outer Harbor-C) were in good agreement.

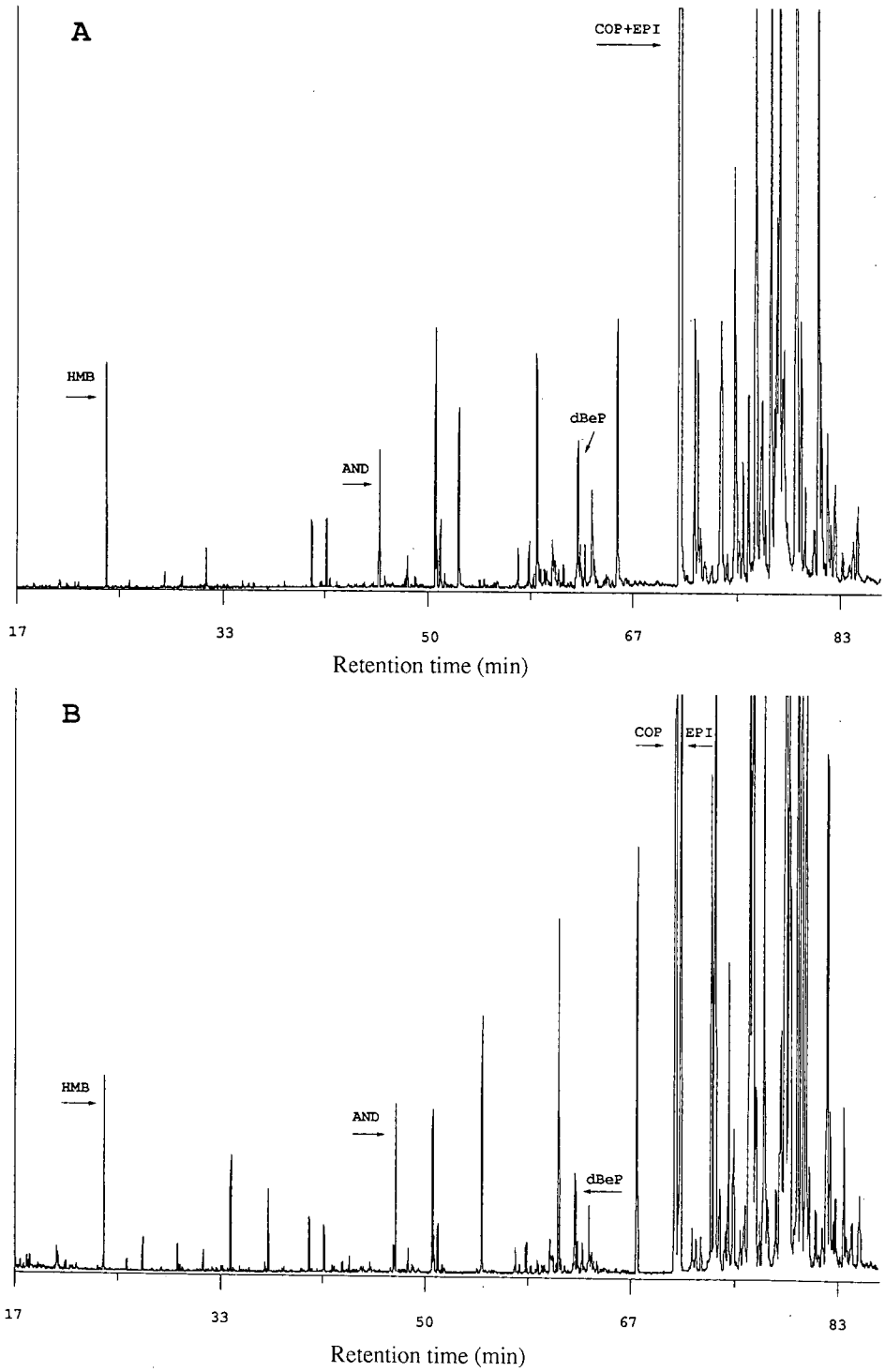

Fig. 1. GC–MS chromatogram of the sediment extract from Kellogg Island after HPLC cleanup and fractionation (see Experimental for details). (A) Prior to derivatization, coprostanol and epicoprostanol coelute. (B) The fraction resulting from HPLC cleanup was derivatized with BSTFA and the epimers were resolved. Abbreviations: HMB = hexamethylbenzene; AND = androstanol; dBeP = [$^2H_{12}$]benzo[*e*]pyrene; COP = coprostanol; EPI = epicoprostanol.

TABLE II

COMPARISON OF MEAN CONCENTRATIONS OF COPROSTANOL [$\bar{x}$, ng/g, DRY WEIGHT, (R.S.D., %)] AND MEAN PERCENT RECOVERIES OF THE INTERNAL STANDARD, ANDROSTANOL, IN DUWAMISH III REFERENCE MATERIAL SEDIMENTS CLEANED UP BY HPLC AND BY A COLUMN CHROMATOGRAPHIC METHOD

Cleanup + quantitation method	*Coprostanol*[a] *$\bar{x}$ (R.S.D.)*	*Androstanol % recovery (R.S.D.)*	*n*
HPLC + GC–FID[b]	900 (24)	89 (27)	15
Column chromatography + GC–FID[c]	860 (28)	86 (20)	29

[a] The concentrations of coprostanol found by the two methods were not statistically different by Student's *t*-test.

[b] All samples were analyzed by the HPLC cleanup method described in this manuscript. Ten samples were part of the quality assurance program for NS&T Program (1986–1988)[13].

[c] Analyzed by an earlier column chromatographic cleanup method[15] as a part of the quality assurance for the NS&T Program (1984–1985).

The limit of detection for coprostanol was $<14 \pm 9$ ng/g, dry weight ($n=7$, from methods blanks). For the spiked blanks ($n=3$), mean percent recoveries of coprostanol were 98 ± 12 and the mean percent recoveries of androstanol were 90 ± 23.

DISCUSSION

The largely automated HPLC method for isolating coprostanol from interfering compounds in sediment extracts is a significant advance over previous methods which used either thin-layer or column chromatographic cleanup steps[5–10]. Although our method is more efficient (less time per sample) than our previous procedure[15], accuracy and precision are maintained as demonstrated by comparing results from analyzing the Duwamish III reference material for coprostanol by both procedures (Table II).

Other advantages of the HPLC method are decreased costs of solvents and the ability to monitor instrument conditions. For example, smaller quantities of highly pure solvent are needed for the cleanup step, *i.e.*, from 10–40% of the solvent used for typical column chromatographic cleanups[5,6,15]. Also, the ability to monitor the UV signal and the system pressure during the HPLC cleanup alerts the operator to problems with the system and reduces the need to rechromatograph the extracts.

In the first two years of the Benthic Surveillance Project of the NS&T Program (1984–1985), we conducted analyses for coprostanol in sediment by a laborious column chromatographic procedure[15]. For samples collected in the years since then, we have used our HPLC procedure to analyze for coprostanol. Data are given for four sites sampled in 1986 from among the 50 NS&T sites (Table III). The degree of sewage contamination reflects the location of these sites with respect to sources of sewage. For example, relatively remote sites such as Dana Point show low levels (62 to 96 ng/g) of coprostanol contamination. In contrast, Santa Monica Bay, which is within a short distance of major urban sewage outfalls, has high levels of coprostanol from sewage (4700–15 000 ng/g). Coprostanol levels in sediments from more typical urban sites fall between these concentrations. The urban South San Diego Bay and

TABLE III

CONCENTRATIONS OF COPROSTANOL (AS THE TRIMETHYLSILYL ETHER) AND RECOVERIES OF THE INTERNAL STANDARD, ANDROSTANOL, IN SEDIMENT SAMPLES

Sediments were sampled in 1986 at sites chosen for the NS&T Program[13]. Individual sediment samples were obtained within a site at each of three stations (A–C) located within a 2 km diameter (see Experimental).

Site	*Coprostanol (ng/g, dry weight)*			*Recovery of androstranol (%)*			*Source of contamination*
	Station			*Station*			
	A	*B*	*C*	*A*	*B*	*C*	
Dana Point	82	96	62	110	120	100	Non-urban site
South San Diego Bay	360	310	370	110	100	100	Urban harbor
San Pedro Outer Harbor	880	700	990	120	120	120	5 miles from the Los Angeles County
			1000[a]			120	sewer outfalls at Palos Verdes
Santa Monica Bay	15 000	10 000	4700	100	100	140	1–2 miles from the Los Angeles city sewer outfalls (Hyperion)

[a] Replicate sample.

San Pedro Outer Harbor sites, receiving general urban runoff and vessel sewage inputs, have coprostanol concentrations from 310 to 1000 ng/g.

The range of coprostanol concentrations found in sediments at these California sites is typical of those reported by researchers working in other locations. Hatcher and McGillivary[23] report a range of 56 to 5200 ng/g coprostanol in sediment for sites in the New York Bight; Readman *et al.*[10] found a range of 1400 to 9000 for estuaries in the U.K.; Goodfellow *et al.*[5] report levels of 3 to 13 500 ng/g for Clyde Estuary in Glasgow, U.K.; and Itoh and Tatsukawa[24] find coprostanol levels of 300 to 3600 ng/g in sediments from Osaka Bay, Japan.

Some of these earlier coprostanol measurements may not be strictly comparable with our results. For example, coprostanol determinations, especially those obtained from packed GC columns, may be artificially high due to coeluting compounds, such as cholesta-5,22-dien-3β-ol and epicoprostanol. Although we separated cholestadienol from coprostanol in the HPLC cleanup step, epicoprostanol was only partially resolved. Therefore, it was necessary to assure the separation of the epimers in the GC analysis. Before derivatization, the coprostanol concentration in the Kellogg Island extract –a sum of the concentrations of the epimers– was 30% high (Table I). After a simple derivatization with BSTFA, the trimethylsilyl ethers of the epimers were resolved on the DB-5 GC column (Fig. 1B).

In conclusion, the HPLC cleanup method for isolating coprostanol is rapid, precise and efficient. Also, the cleanup can be totally automated. Use of this method will permit environmental managers to assess the extent of sewage pollution more rapidly and less expensively. Derivatization of the coprostanol fraction from the cleanup step is recommended because: (a) epicoprostanol is often present in samples in significant amounts; (b) coprostanol and epicoprostanol are reliably separated on the DB-5 GC column only when derivatized; and (c) the condition of the GC column is not as critical in obtaining sharp peaks and good resolution from derivatized compounds.

ACKNOWLEDGEMENTS

We are indebted to Drs. Usha Varanasi and Sin-Lam Chan, Director and Deputy Director of the Environmental Conservation Division, for their support of this research. We appreciate the skillful technical assistance of Douglas Burrows, Ronald Pearce, Jennie Bolton, Karen Tilbury, Susan Pierce and Jonathan Joss. We thank Dr. Carol-Ann Manen, formerly of the Anchorage office of the Ocean Assessment Division and currently of their Washington, DC office, for helpful discussions. We also appreciate the manuscript review and suggestions of Drs. William MacLeod, Jr., Cheryl Krone and Ed Casillas. This study was funded in part by the Minerals Management Service through an Interagency Agreement with NOAA and in part by the Ocean Assessment Division.

REFERENCES

1 R. W. Walker, C. K. Wun and W. Litsky, *CRC Crit. Rev. Environ. Control*, 12 (1982) 91–112.
2 J. Ferezou, E. Gouffier, T. Coste and F. Chevallier, *Digestion*, 18 (1978) 201–212.
3 P. Eneroth, K. Hellstrom and R. Ryhage, *J. Lipid Res.*, 5 (1964) 245–262.

4 R. B. Schwendinger and J. G. Erdman, *Science, (Washington, D.C.)*, 144 (1964) 1575.
5 R. M. Goodfellow, J. Cardoso, G. Eglinton, J. P. Dawson and G. A. Best, *Mar. Poll. Bull.*, 8 (1977) 272–276.
6 P. G. Hatcher, L. E. Keister and P. A. McGillivary, *Bull. Environ. Contam. Toxicol.*, 17 (1977) 491–498.
7 D. V. McCalley, M. Cooke and G. Nickless, *Bull. Environ. Contam. Toxicol.*, 25 (1980) 374–381.
8 R. C. Brown and T. L. Wade, *Water Res.*, 18 (1984) 621–632.
9 R. H. Pierce and R. C. Brown, *Bull. Environ. Contam. Toxicol.*, 32 (1984) 75–79.
10 J. W. Readman, M. R. Preston and R. F. C. Mantoura, *Mar. Poll. Bull.*, 17 (1986) 298–308.
11 D. V. McCalley, M. Cooke and G. Nickless, *Water Res.*, 15 (1981) 1019–1025.
12 M. M. Krahn, C. A. Wigren, R. W. Pearce, L. K. Moore, R. G. Bogar, W. D. MacLeod, Jr., S.-L. Chan and D. W. Brown, *NOAA Technical Memorandum NMFS F/NWC-153*, National Oceanic and Atmospheric Administration, Seattle, WA, 1988; available from the National Technical Information Service of the U.S. Department of Commerce, 5285 Port Royal Road, Springfield, VA 22161, U.S.A.; PB-89-12497.
13 U. Varanasi, S.-L. Chan, B. B. McCain, M. H. Schiewe, R. C. Clark, D. W. Brown, M. S. Myers, J. T. Landahl, M. M. Krahn, W. D. Gronlund and W. D. MacLeod, Jr., *NOAA Technical Memorandum NMFS F/NWC-156*, National Oceanic and Atmospheric Administration, Seattle, WA, 1988; available from the National Technical Information Service of the U.S. Department of Commerce, 5285 Port Royal Road, Springfield, VA 22161, U.S.A.
14 J. Q. Word, in W. Bascom (Editor), *Annual Report, Southern California Coastal Water Research Project*, Southern California Coastal Water Research Project, Long Beach, CA, 1976, pp. 189–194.
15 W. D. MacLeod, Jr., D. W. Brown, A. J. Friedman, D. G. Burrows, O. Maynes, R. W. Pearce, C. A. Wigren and R. G. Bogar, *NOAA Technical Memorandum NMFS F/NWC-92*, National Oceanic and Atmospheric Administration, Seattle, WA, 1985; available from the National Technical Information Service of the U.S. Department of Commerce, 5285 Port Royal Road, Springfield, VA 22161, U.S.A.; PB-86-147873.
16 M. M. Krahn, L. K. Moore, R. G. Bogar, C. A. Wigren, S.-L. Chan and D. W. Brown, *J. Chromatogr.*, 437 (1988) 161–175.
17 W. D. MacLeod, Jr., A. J. Friedman and D. W. Brown, *Mar. Environ. Res.*, 26 (1988) 209–221.
18 R. Miller, *Anal. Chem.*, 54 (1982) 1742–1746.
19 Perkin-Elmer Corp., personal communication.
20 C. J. W. Brooks, W. J. Cole, J. H. Borthwick and G. M. Brown, *J. Chromatogr.*, 239 (1982) 191–216.
21 M. M. Krahn, D. G. Burrows, M. S. Myers and D. C. Malins, *Xenobiotica*, 14 (1984) 633–646.
22 J. E. Matusik, G. P. Hoskin and J. A. Sphon, *J. Assoc. Off. Anal. Chem.*, 71 (1988) 994–999.
23 P. G. Hatcher and P. A. McGillivary, *Environ. Sci. Technol.*, 13 (1979) 1225–1229.
24 J. Itoh and R. Tatsukawa, *Chikyu Kagaku*, 12 (1978) 9–17.

Journal of Chromatography, 481 (1989) 275–285
Elsevier Science Publishers B.V., Amsterdam — Printed in The Netherlands

CHROM. 21 732

DETERMINATION OF PHENOXYACID HERBICIDES IN WATER

POLYMERIC PRE-COLUMN PRECONCENTRATION AND TETRABUTYLAMMONIUM ION-PAIR SEPARATION ON A PRP-1 COLUMN

RENÉ B. GEERDINK*, CONNIE A. A. VAN BALKOM and HENDRIK-JAN BROUWER
Institute for Inland Water Management and Waste Water Treatment, P.O. Box 17, 8200 AA Lelystad (The Netherlands)

(First received December 16th, 1988; revised manuscript received June 26th, 1989)

SUMMARY

Optimum conditions for preconcentration of phenoxyacid herbicides from water on polymeric material and separation on an analytical column (PLRP-S and PRP-1 respectively) have been achieved. The method consists of (a) an on-line preconcentration at pH 3, (b) clean-up with four (precolumn) bed volumes of acetonitrile–water (30:70) at pH 3 and (c) isocratic analytical separation at pH 11 with 0.01 mol/l tetrabutylammonium as the ion-pair reagent and acetonitrile–water (30:70) as the eluent. Data on the repeatability of the method, sample flow dependence and sorption capacity are reported. For reliable integration of the chromatogram a clean-up step was introduced. This washing procedure however is more effective for tap-water than for surface water samples. The results of the method are promising and indicate that 10–50 ml of surface water can be applied to the precolumn without breakthrough. Detection limits in surface water samples are 0.1–0.5 μg/l whereas those in tap-water are 10–50 ng/l. The applicability of the method was tested. The results of this method were in good agreement with gas chromatographic–mass spectrometric results, and only *ca.* 0.1 μg/l lower over the entire range, whereas the analysis time was much shorter. The potential of this technique for automation was demonstrated using a microprocessor-controlled column-switching unit, resulting in a reduction of the total analysis time to *ca.* 20 min.

INTRODUCTION

Phenoxyacid herbicides are widely used to control the growth of broad-leaf weeds. Although they are not extremely poisonous and/or environmentally persistent, their widescale production necessitates an analysis method capable of low detection limits of these herbicides.

In our institute the chlorophenoxy carboxylic acid herbicides 4-chloro-2-methylphenoxyacetic acid (MCPA), (2,4-dichlorophenoxy)acetic acid (2,4-D), 2-(4-chloro-2-methylphenoxy)propionic acid (MCPP), 2-(2,4-dichlorophenoxy)propionic acid (2,4-DP) and (2,4,5-trichlorophenoxy)acetic acid (2,4,5-T) are determined in

0021-9673/89/$03.50

industrial waste-water by gas chromatography (GC) after conversion into the corresponding methyl esters using methanol–BF_3. This method is very cumbersome, poorly repeatable and time consuming because of the many steps such as liquid–liquid extraction, concentration and derivatization with or without additional clean-up. Solid-phase extraction is an attractive alternative for enrichment of environmental samples prior to quantitation. Effective preconcentration is demonstrated for many components or groups[1–4] and detection limits for real (water) samples are often in the low μg/l range.

Åkerblom[5] reported upon a simple precolumn sample enrichment system for acid herbicides in which the sample loop was replaced by a precolumn. Samples were introduced by a syringe into the precolumn, which was packed with *ca.* 40 μm C_{18} silica gel. Smith and Pietrzyk[6] used an auxiliary pump to deliver the sample to the precolumn which was packed with 10- or 20-μm PRP-1. Separations were performed on a PRP-1 analytical column which provided good efficiencies for separation of complex mixtures like chlorophenols and phenoxyacetic acid herbicides.

In a previous paper[7] the simultaneous preconcentration on various materials of fourteen polar (chloro- and methyl-substituted) anilines from surface water was reported. In this paper, a procedure is described for the preconcentration and analysis of some polar phenoxyacid herbicides from water. Enrichment conditions have been studied on a macroporous polystyrene–divinylbenzene copolymer (PLRP-S). This material was chosen because of its good adsorption properties. Desorption and analysis were performed at high pH using tetrabutylammonium (TBA) ion-pair separation on a PRP-1 analytical column. The automated method developed utilizes a microprocessor-controlled valve-switching unit by which the total analysis time is reduced to *ca.* 20 min. To overcome an high background in the chromatogram after the desorption step, a "washing" step was introduced prior to desorption of the herbicides.

EXPERIMENTAL

Reagents

HPLC-grade acetonitrile and water were obtained from Mallinckrodt (St. Louis, MO, U.S.A.) and HPLC-grade methanol, sodium hydroxide and perchloric acid from Baker (Deventer, The Netherlands). All chlorophenoxy carboxylic acids were obtained from Riedel-de Haën (Hannover, F.R.G.) and tetrabutylammonium hydrogensulphate from (Fluka, Buchs, Switzerland).

Apparatus

The HPLC equipment to deliver the wetting solvent, the aqueous sample and the precolumn washing solvent included two LKB (Bromma, Sweden) Model 2150 pumps; an LKB system controller Model 2152, LKB low- and high-pressure mixing valves, Models 2040-203 and 2154-400. A Pye-Unicam (Philips, Eindhoven, The Netherlands) LC-XPC pump was used to deliver the mobile phase. The variable-wavelength UV absorbance detector was a Pye-Unicam Model 4110, set at 230 or 280 nm. The Model SPH 99 column thermostat was from Spark (Emmen, The Netherlands).

The microprocessor-controlled autoinjector (Spark, Model Promis) with two additional valves was used to inject standard samples and to control the flow scheme during analysis. Chromatograms were recorded and integrated by a data station (Millipore, Milford, MA, U.S.A.) with Baseline 810 software.

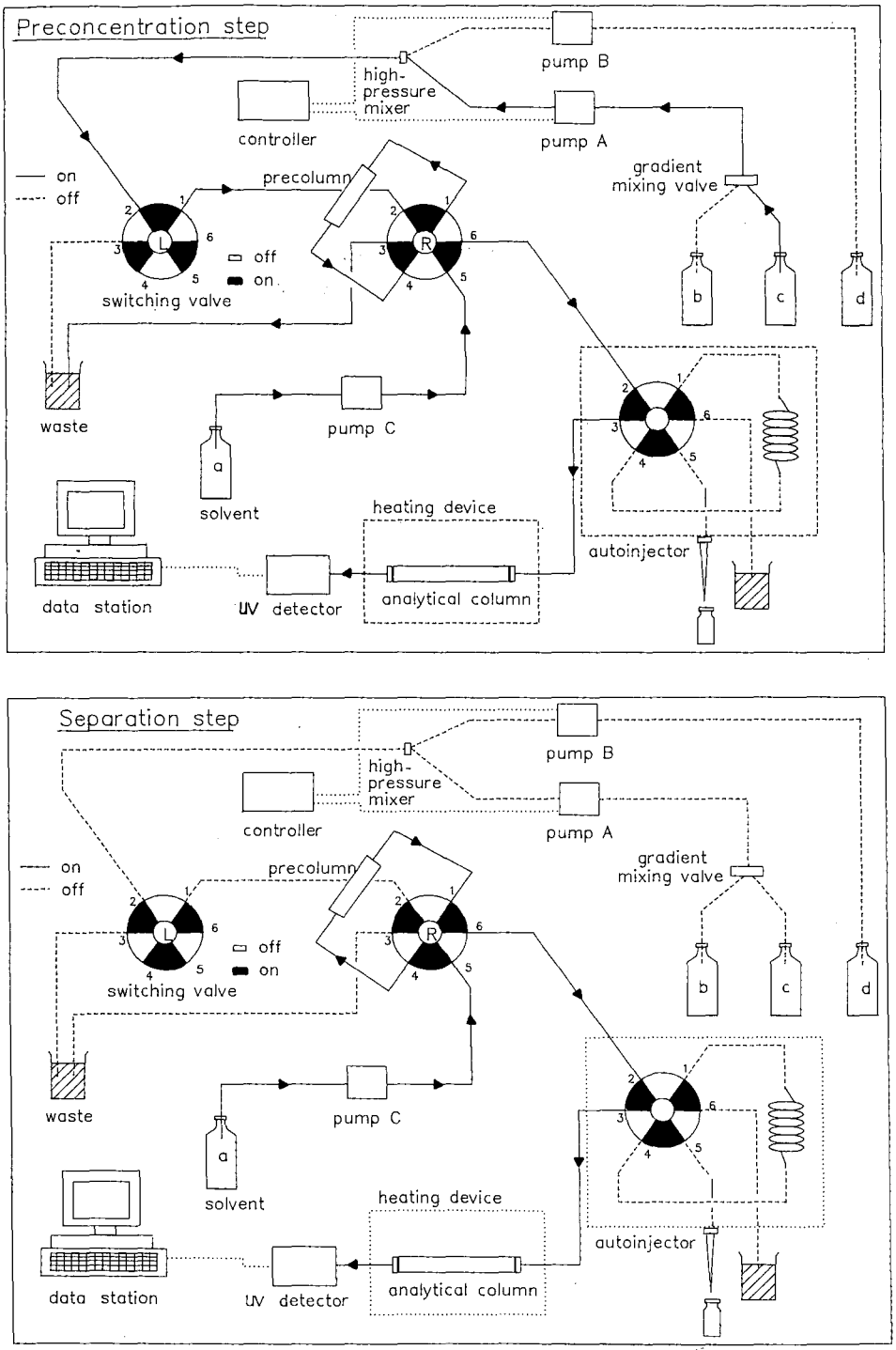

Fig. 1. Experimental set-ups for the on-line enrichment and separation of water samples: a = mobile phase, acetonitrile–water (30:70), 0.010 mol/l at pH 11; b = wetting solvent, 0.02 mol/l $HClO_4$; c = water sample; d = washing solvent, acetonitrile–water (30:70) at pH 3. Analytical column: 150 mm × 4.1 mm I.D. PRP-1; precolumn 10 mm × 2 mm I.D. PLRP-S. The autoinjector is used to inject a standard (loop) sample.

The experimental set-up for the on-line enrichment and separation of water samples is shown in Fig. 1.

Procedures

Stock solutions of the chlorophenoxy herbicides were prepared by weighing *ca.* 5 mg of each component followed by dissolution in 50 ml of methanol. These solutions were diluted in tap-water to obtain standard solutions as well as mixed standard solutions.

Sample solutions were preparad by diluting the stock solutions in tap-water or surface water and acidified to pH 3 with 0.1 mol/l $HClO_4$. Precolumns (10 mm × 2 mm) were manually packed using a microspatula with 15–25 μm PLRP-S (Polymer Laboratories, Shropshire, U.K.) and activated with 30 ml (2 ml/min) of 0.02 mol/l $HClO_4$ and 30 ml (2 ml/min) of 0.001 mol/l $HClO_4$ prior to preconcentration of the samples.

Separations were carried out at 50°C on a 150 mm × 4.1 mm I.D. column, prepacked with 10-μm PRP-1 (Hamilton, Reno, NV, U.S.A.) using acetonitrile–water (30:70), 0.010 mol/l of tetrabutylammonium (TBA), pH 11 (adjusted with 5 mol/l NaOH) at a flow-rate of 1.0 ml/min as the mobile phase, which also served as the desorption phase of the precolumn. Conditions during sample concentration are described below, and illustrated in Fig. 1. Time programming of the automated autoinjector and system controller is described in ref. 8.

RESULTS AND DISCUSSION

Chromatography

Solid phase extraction of polar compounds, such as acid herbicides with polymeric materials, has been shown to be successful from acidified samples[5,6]. Earlier experiments[8,9] showed that desorption of the acid herbicides from PLRP-S is favoured by (a) a high eluent pH and/or (b) a high eluent content of organic solvent. Separation, however, on analytical columns with a related type of material (PRP-1) was hardly achieved up to now because of the general lack of efficiency of those columns in general.

Optimization of the separation conditions, for the acetic acid derivatives MCPA and 2,4-D and the propionic acid derivatives MCPP and 2,4-DP, was adequately effected only using TBA as an ion-pair reagent. Other ion-pair reagents such as ammonium, caesium, tetradecyltrimethylammonium (cetrimide) and tetramethylammonium were not suitable in this respect. High molarity (0.05 mol/l) TBA increased the capacity factor, k', but did not improve the separation, while low molarity (0.010 mol/l) TBA gave higher selectivity, especially for the aforementioned pairs. Raising the temperature to 50°C further improved the separation. Separations therefore were carried out under the optimum isocratic conditions described in Experimental.

Sample flow dependence

In order to determine the dependence of the adsorption of acid herbicides from tap-water on the sample flow-rate, the flow-rate was varied between 1 and 20 ml/min. Recovery percentages of the acid herbicides were determined by comparing the peak areas of a loop injecton with those after enrichment and desorption from the

TABLE I

DEPENDENCE OF THE RECOVERY FROM TAP-WATER ON THE SAMPLE FLOW-RATE AND THE CONTACT TIME

Conditions: flow-rate = 1, 2 or 5 ml/min, sample = 5 ml, 50 μg of component/l; flow-rate = 10, 15 or 20 ml/min, sample = 10 ml, 25 μg of component/l.

Flow-rate (ml/min)	*Contact time[a] (s)*	*Recovery (%)*				
		MCPA	*2,4-D*	*MCPP*	*2,4-DP*	*2,4,5-T*
1	1.20	103	107	89	105	95
2	0.60	103	106	84	108	96
5	0.24	112	122	90	109	99
10	0.12	86	86	85	85	100
15	0.08	107	108	87	89	99
20	0.06	113	101	84	100	100

[a] Contact time = $\frac{\text{precolumn void volume}}{\text{flow-rate}} = 0.64\pi r^2 L/F$

where 0.64 = column porosity factor, $\varepsilon_u{}^{10}$, r = inner radius (dm), L = column length (dm) and F = flow-rate (l/s).

precolumn. From Table I it is seen that, even with a very short contact time of 0.06 s, in the case of a flow-rate of 20 ml/min, the recoveries of all five acid herbicides investigated are over 84%. Moreover no breakthrough occurred in the case of a 10-ml sample. The precolumn was the same during all these experiments. During all other experiments, however, the sample flow-rate was kept constant at 5 ml/min, and new precolumns were used.

Sample pH dependence

The dependence of the retention on sample pH was studied in the range pH 3–7 in order to determine the affinity of the acid herbicides for the hydrophobic adsorbent surface. It might be expected that the acid herbicides (pK_a 2.6–3.0) are more efficiently trapped in their acidic forms by PLRP-S and related materials than are their conjugated bases. Surprisingly, from Table II it is seen that the recoveries from

TABLE II

DEPENDENCE OF RECOVERY ON SAMPLE pH

Conditions: sample = 10 ml of tap-water, 25 μg of component/l; flow-rate = ml/min.

pH	*Recovery (%)*				
	MCPA	*2,4-D*	*MCPP*	*2,4-DP*	*2,4,5-T*
3	97	104	70	89	100
4	96	102	68	88	102
5	100	106	68	94	99
6	101	107	73	82	96
7	94	109	72	95	99

tap-water for all five herbicides investigated, over the entire pH range, are good. Recoveries from surface water (not shown in the table) with a sample pH 7 however are poor (11–41%), whereas at pH 3 the recoveries from surface water for all five herbicides are good ($\geq 70\%$). This means that PLRP-S is able to adsorb charged and uncharged organics, but that the adsorption of the neutral solute is stronger. Breakthrough at pH 7 with surface water might also be aided by competitive sorption by humic substances[11]. Recoveries at pH 3 might further be improved by adding sodium chloride (salting out effect) to the sample[5,12].

Repeatability and washing procedure

The repeatability was tested by applying five spiked tap-water samples on a precolumn. From Table III it is seen that the repeatability is satisfactory, *e.g.*, standard deviation (S.D.) $\approx 12\%$. The mean recovery of MCPP however is 70%. This can be attributed to peak integration errors of the chromatogram, obtained after desorption of the acid herbicides from the precolumn: a chromatogram of a blank shows, especially in the region of MCPP, a sharp irregular dip resulting in a less reliable integration in this region.

In the case of sample loop injections, baselines are straight and chromtogram integration is easily achieved.

During the enrichment step, not only the (spiked) acid herbicides and other unknown compounds are adsorbed, but water is also trapped by the macroporous resin. Desorption of the components and, more slowly, the release of water from the precolumn causes a large unretained peak, which only slowly and irregularly returns to the baseline. Therefore a washing step has been introduced to clean-up the precolumn and to remove interfering compounds and to "recalibrate" the polymer with the organic phase. This is done by delivering acetonitrile–water (30:70) at pH 3 at a constant, but low flow-rate by time programming the LC pump during the preconcentration step (see also Fig. 1A).

From Table IV it is seen that with washing volumes of 70 and 140 μl the recoveries are good and, moreover, the recovery of MCPP is in the same order, due to reliable integration.

TABLE III

REPEATABILITY OF PRECONCENTRATION FROM TAP-WATER

Conditions: as in Table II.

n	*Recovery (%)*				
	MCPA	*2,4-D*	*MCPP*	*2,4-DP*	*2,4,5-T*
1	82	81	79	91	119
2	104	102	77	97	109
3	102	105	72	95	136
4	106	110	52	94	103
5	108	108	70	98	104
Mean	100	101	70	95	114
S.D.	10	12	11	3	14

TABLE IV

DEPENDENCE OF RECOVERY ON WASHING VOLUME

Washing solvent: acetonitrile–water (30:70), pH 3, flow-rate = 0.1 ml/min. Other conditions as in Table II.

No. of bed volumes	*Volume (µl)*	*Recovery (%)*				
		MCPA	*2,4-D*	*MCPP*	*2,4-DP*	*2,4,5-T*
2	70	81	81	79	80	79
4	140	81	81	93	92	87
6	210	48	33	79	77	70

At this point it is also noticeable that manually packing of the precolumns contributes to some extent to the recovery percentages. Commercial, disposable cartridges showed better reproducibility[13] and will be used in our future work.

The low flow-rate of the washing solvent (0.1 ml/min) not only ensures reproducibility of the total volume applied to the precolumn, but also displacement of the water from the inner polymer structure. With 210 µl of washing solvent (six bed volumes), breakthrough of MCPA and 2,4-D is apparent. Fig. 2 demonstrates the effect of the washing step on the chromatogram baseline.

Sorption capacity and detection limits from tap-water and surface water

The sorption capacity of the PLRP-S polymer was measured by applying equal volumes of sample to the precolumn with varying herbicide concentrations (25–5000

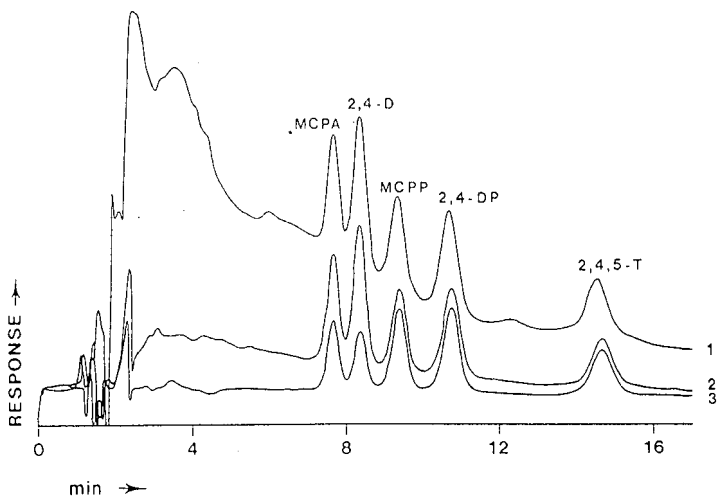

Fig. 2. HPLC chromatograms of acid herbicides after preconcentration: (1) without clean-up step; (2) after clean-up with four precolumn bed volumes and (3) after clean-up with six precolumn bed volumes. Preconcentration conditions: 10 ml of tap-water, 25 µg of component/l; sample flow-rate 5 ml/min; washing solvent, acetonitrile–water (30:70) pH 3, flow-rate 0.1 ml/min. System: 10 mm × 2 mm I.D. precolumn packed with 20 µm PLRP-S, 150 mm × 4.1 mm I.D. analytical column packed with 10 µm PRP-1; eluent, acetonitrile–water (30:70), 0.010 mol/l TBA, pH 11; flow-rate = 1.0 ml/min; UV detection at 280 nm.

TABLE V

RECOVERIES FROM TAP-WATER

Conditions: sample = 10 ml; flow-rate = 5 ml/min.

Concn. (mg of component/l)	*Absolute amount (μg of component)*	*Recovery (%)*				
		MCPA	*2,4-D*	*MCPP*	*2,4-DP*	*2,4,5-T*
0.025	0.25	104	102	79	89	92
0.05	0.50	91	87	75	75	89
0.10	1.00	95	94	88	88	99
0.20	2.00	93	91	84	82	101
0.40	4.00	101	100	91	85	98
1.00	10.00	98	96	90[a]	90[a]	96
2.00	20.00	89	93	89[a]	89[a]	102
5.00	50.00	88[a]	88[a]	88[a]	88[a]	95

[a] Recovery estimated by dividing the peak area of two coinciding components by two.

μg/l). From Table V it is seen that the capacity of the precolumn, determined by the affinity of the herbicides to PLRP-S, is good and not a limiting factor in enrichment of the herbicides from tap-water.

Comparing Tables V and VI, it is seen that breakthrough of MCPA from surface water occurs at concentrations 50 times lower than for tap-water. For surface water, also the other herbicides, except 2,4-D and 2,4,5-T, tend to breakthrough at higher concentrations.

In environmental surface waters, however, the concentrations are commonly below 1 μg/l and so the concentration of 0.5 μg of component applied to the precolumn, at which concentration, *i.e.*, 50 μg/l recoveries are still good, is far above the analyte concentration in practical environmental analysis. This means that the capacity of the PLRP-S material for surface water is sufficient.

With real surface water samples however the clean-up procedure as outlined above is not sufficient to eliminate the "injection peak" as in the case of tap-water samples (see also Fig. 2). This means that the first peaks eluted are more difficult to integrate, due to this injection peak. Moreover, if the sample volume is raised from 10 to 50–100 ml, the injection peak will also increase too.

TABLE VI

RECOVERIES FROM SURFACE WATER

Conditions as in Table V.

Concn. (mg of component/l)	*Absolute amount (μg of component)*	*Recovery (%)*				
		MCPA	*2,4-D*	*MCPP*	*2,4-DP*	*2,4,5-T*
0.025	0.25	95	101	86	85	95
0.05	0.50	94	93	95	98	99
0.10	1.00	51	90	91	97	103
0.20	2.00	40	75	75	77	101
0.40	4.00	32	95	63	64	99

TABLE VII

DEPENDENCE OF RECOVERY ON SAMPLE VOLUME (TAP-WATER)

Flow-rate = 1 ml/min.

Concn. (μg of component/l)	*Preconcn. volume (ml)*	*Recovery (%)*				
		MCPA	*2,4-D*	*MCPP*	*2,4-DP*	*2,4,5-T*
5	10	91	87	75	75	89
0.5	100	71	77	67	81	83
0.12	400	67	46	53	67	56

From Table VII it is seen that the recovery of the phenoxyacid herbicides decreases only slowly with increasing sample volume. With an 100-ml sample and 0.5 μg component/l, the recoveries are acceptable and detection limits of 10–50 ng/l (signal-to-noise ratio 3) were calculated. This, of course, is true only for tap-water samples. Surface water samples were, up to now, limited to 50 ml with detection limits of 0.1–0.5 μg/l (signal-to-noise ratio 3). However, without (off-line) clean-up procedures like gel permeation chromatography (GPC), ultrafiltration or dialysis before concentration of the analytes, lower detection limits for surface water are not expected.

Currently, the behaviour of humic substances (1–5 mg/l surface water) is studied with on-line GPC and off-line SPE techniques in order to improve the sample to be concentrated and to improve the efficiency of the clean-up procedure. The results will be presented in a future paper.

Application to surface water samples

On September 9th, 1988 an accidental spill of 2,4-DP (dichlorprop) (0.5–1 ton) in the river Rhine near Ludwigshafen (F.R.G.) was reported to the authorities. About half of the Dutch drinking water is prepared from surface water, so a monitoring

TABLE VIII

CONCENTRATION AND CALCULATED AMOUNT OF 2,4-DP IN RHINE SAMPLES AFTER ACCIDENTAL SPILL

Sample[a]	*Date*	*Time (h)*	*Concn. (μg/l)*	*Amount (ton)*
1	12-09-88	20.00–24.00	0.5	0.01
5	13-09-88	08.00–12.00	1.5	0.04
7	13-09-88	12.00–16.00	2.2	0.05
9	13-09-88	16.00–20.00	3.0	0.07
11	13-09-88	20.00–24.00	2.7	0.06
13	14-09-88	00.00–04.00	3.2	0.07
15	14-09-88	04.00–08.00	3.1	0.06
16	14-09-88	08.00	2.5	——
			Total =	0.36

[a] Composite or grab samples.

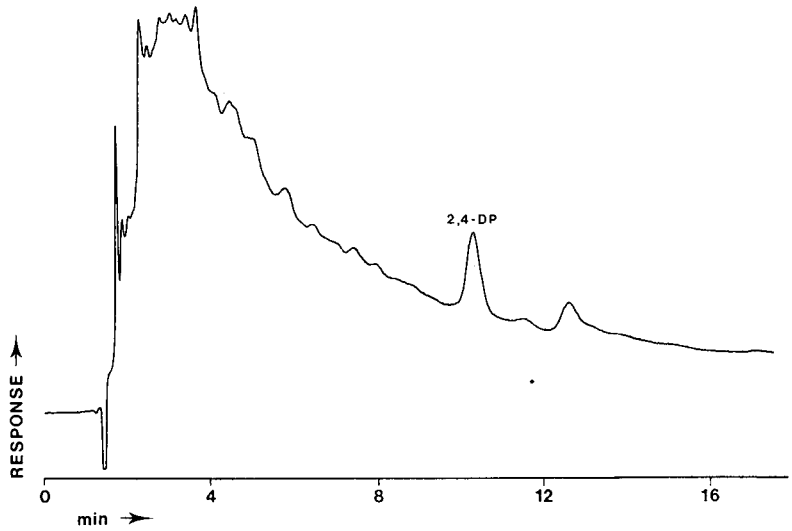

Fig. 3. HPLC chromatogram of a river Rhine sample after an accidental spill. Conditions: see text and Fig. 2; UV detection at 230 nm.

programme, with the aforementioned method, was started. At Lobith, the entrance of the Rhine in The Netherlands, samples were collected and analyzed in our laboratory. From the results the total amount of 2,4-DP can be determined.

From Table VIII it is seen that the maximum concentration was *ca.* 3.2 μg/l 2,4-DP and that the measured amount of 2,4-DP, during the measuring time, was *ca.* 0.4 ton; this fits well with the statement from the factory.

The results were in good agreement with the results of the Water Transport Company[14] (WRK, Nieuwegein) and only slightly lower (*ca.* 0.1 μg/l over the entire range) than their gas chromatographic–mass spectrometric (GC–MS) method, which essentially consists of (a) preconcentration of 0.5 l surface water on a C_{18} cartridge, (b) drying of the cartridge with nitrogen, (c) desorption with 2 ml methanol, (d) methylation with diazomethane, (e) evaporation with nitrogen to 50 μl and (f) injection of 2 μl for GC–MS.

In Fig. 3 a chromatogram is shown of the river Rhine sample using the aforementioned method, except for the washing step, which was omitted.

CONCLUSIONS

Separation of the acid herbicides MCPA, 2,4-D, MCPP, 2,4-DP and 2,4,5-T on a styrene–divinylbenzene copolymer (PRP-1) analytical column has been achieved with the ion-pair reagent tetrabutylammonium under isocratic conditions.

Solid phase extraction was studied on the polymeric material PLRP-S. The herbicides were applied to the precolumn in tap-water or surface water matrices. The results for the tap-water samples indicate that the sorption capacity of the precolumn (with a volume of *ca.* 35 μl) is excellent and that recoveries at pH 3 with various flow-rates (1–20 ml/min) are over 80%. The repeatability of the method is acceptable (S.D. $\approx$12%; 25 μg of component/l).

To overcome the interference of a large unretained peak, which results in a partly less reliable integration of the chromatogram, a clean-up step was introduced which essentially consists of a slow delivery of four bed volumes of acetonitrile–water (30:70) at pH 3. This procedure however, is not sufficient to eliminate the injection peak in the case of surface water samples. Due to a high humic content, an additional clean-up step before preconcentration is considered necessary.

Also the results for the surface water samples indicate that the competitive sorption capacity of the sample matrix is a limiting factor for the sorption capacity of the precolumn. Breakthrough of the first herbicides eluted occurs for surface water 50 times more rapidly than for tap-water samples. Still at least 10–50 ml of surface water can be applied to the precolumn without breakthrough. Detection limits from tap-water are calculated to be 10–50 ng/l (signal-to-noise ratio 3) and those from surface water are 0.1–0.5 μg/l (signal-to-noise ratio 3).

The easy handling of aqueous samples, the low detection limits obtainable and the potential of this technique for automation are very promising.

REFERENCES

1 C. E. Werkhoven-Goewie, W. M. Boon, A. J. J. Praat, R. W. Frei, U. A. Th. Brinkman and C. J. Little, *Chromatographia*, 22 (1982) 53.
2 M. W. F. Nielen, U. A. Th. Brinkman and R. W. Frei, *Anal. Chem.*, 57 (1985) 806.
3 J. Sherma, *J. Liq. Chromatogr.*, 9 (1986) 3433.
4 F. A. Maris, J. A. Ståb, G. J. de Jong and U. A. Th. Brinkman, *J. Chromatogr.*, 445 (1988) 129.
5 M. Åkerblom, *J. Chromatogr.*, 319 (1985) 427.
6 R. L. Smith and D. J. Pietrzyk, *J. Chromatogr. Sci.*, 21 (1983) 282.
7 R. B. Geerdink, *J. Chromatogr.*, 445 (1988) 273.
8 H.-J. Brouwer, *Technical Report*, Institute for Inland Water Management and Wastewater Treatment, Lelystad, 1988.
9 C. A. A. van Balkom, *Technical Report*, Institute for Inland Water Management and Wastewater Treatment, Lelystad, 1988.
10 D. P. Lee and J. H. Kindsvater, *Anal. Chem.*, 52 (1980) 2425.
11 G. E. Carlberg and K. Martinsen, *Sci. Total Environ.*, 25 (1982) 245.
12 B. A. Bidlingmeyer and F. V. Warren, Jr., *Anal. Chem.*, 54 (1982) 2351.
13 B. Ooms, *poster presented at 4th Symposium Handling of Environmental and Biological Samples in Chromatography, Basle, 1988.*
14 R. de Groot, personal communication.

Journal of Chromatography, 481 (1989) 287–297
Elsevier Science Publishers B.V., Amsterdam — Printed in The Netherlands

CHROM. 21 805

REVERSED-PHASE HIGH-PERFORMANCE LIQUID CHROMATOGRAPHY OF METAL–BENZYLPROPIONITRILE DITHIOCARBAMATE COMPLEXES

YONG J. PARK and JAMES K. HARDY*
Department of Chemistry, University of Akron, Akron, OH 44325 (U.S.A.)
(First received April 4th, 1989; revised manuscript received July 18th, 1989)

SUMMARY

A new dithiocarbamate, benzylpropionitrile dithiocarbamate (BPDTC), has been synthesized for use in metal analysis. The high-performance liquid chromatography behavior of metal chelates of BPDTC has been investigated for the simultaneous determination of antimony, cadmium, chromium, copper, mercury, nickel, lead, selenium, thallium, and zinc, all of which are on the U.S. Environmental Protection Agency's list of priority pollutant metals. Metals are extracted into dichloromethane as BPDTC chelates, and then separated on a C_{18} column. Cobalt is added as an internal standard. The effects of pH and of three organic modifiers (methanol, acetonitrile, tetrahydrofuran) of the mobile phase on retention time have been investigated. Addition of dichloromethane to the mobile phase increases solubility and chelate stability, and improves the separation of metal BPDTC complexes. BPDTC is added to the aqueous mobile phase to reduce on-column dissociation of the complexes. Detection limits at 260 nm are in the range of 0.1 to 3 μg/l depending on the metal species.

INTRODUCTION

Dithiocarbamates (DTCs) are useful reagents for the extraction, separation, and spectrophotometric detection of many metals due to their abilities to form stable complexes[1,2]. In recent years, disubstituted DTC chelates have been studied by high-performance liquid chromatography (HPLC), with the resultant separation forming the basis for the simultaneous methods of analysis for the metals[3–13]. A variety of separation conditions, detectors, and a number of different DTCs have been used. Both reversed-phase[3–8] and normal-phase[9,10] chromatographic techniques have been utilized. Electrochemical[11,12], argon-plasma emission spectroscopic[13], and atomic spectrometric detection[14] have been evaluated to some extent, but UV–VIS absorption[3–10] is by far the most used detection method.

Reversed-phase HPLC analysis of metal benzylpropionitrile dithiocarbamate (BPDTC) complexes has been investigated. The metals analyzed in this work are those identified by the U.S. Environmental Protection Agency (EPA) as priority

0021-9673/89/$03.50

pollutants[15]. Included in the list of pollutant metals are antimony, arsenic, beryllium, cadmium, chromium, copper, mercury, nickel, lead, selenium, silver, thallium and zinc. Beryllium was not evaluated since it has a very limited solubility in water under normal pH conditions due to the formation of insoluble $Be(OH)_2$, and, thus, is associated with the particulate rather than the dissolved components of natural systems[15]. Arsenic and silver were also excluded because of the low complexation ability and high precipitation power with halides, respectively. Since chromium exists in two stable oxidation states in aqueous systems, Cr(VI) and Cr(III) were both evaluated, though Cr(VI) is the most environmentally significant. The most common oxidation states of selenium are +4 and +6, represented respectively by selenite and selenate. However, only selenium(IV) was included in this work as selenium occurs in natural water predominantly in the form of selenite[16]. Similarly, due to low solubility of mercurous salts in water[17], only mercury(II) was included in this work among the two oxidation states of mercury. One ppm of cobalt was added in this work as an internal standard. The very low concentration of cobalt in natural water[18] allows its use as an internal standard.

Organic substituents of DTCs do not influence the metal–sulfur bonding, but change some analytical properties of the complexes. The use of BPDTC chelates offers advantages over the other commonly used DTC derivatives due to the characteristics of the two substituents. First, using a benzyl group as a chromophore in the BPDTC results in higher molar absorptivities. Second, disturbance by an excess of the reagent extracted into the organic phase should not be observed, since a propionitrile group of BPDTC allows the reagent, Na–BPDTC, to be readily soluble in water, but very slightly soluble in the organic solvents such as carbon tetrachloride, chloroform, and dichloromethane.

EXPERIMENTAL

Reagents

All chemicals used were of analytical-grade purity unless otherwise stated. Each stock 1000 mg/l metal ion solution was made by dissolution of the respective metal compound in water or diluted nitric acid. The metal compounds used for the stock solutions consisted of three different chemical forms: oxide forms for chromium(VI), selenium(IV) and zinc(II); chloride forms for antimony(III), cadmium(II) and mercury(II); and nitrate forms for chromium(III), cobalt(II), copper(II), lead(II), nickel(II) and thallium(I). Aqueous solutions were made with distilled water filtered through a Barnstead NANOpure II deionization system (Boston, MA, U.S.A). HPLC-grade solvents (acetonitrile, tetrahydrofuran, methanol, dichloromethane) from Fisher Scientific were employed for the chromatographic work to minimize the background absorbance.

Na–BPDTC was not available commercially but was readily prepared in the laboratory by a modification of the procedure described by Moore[19]. All reagents were chilled below 5°C prior to use. A 31-ml volume of 3-(benzylamino)propionitrile was dissolved in 50 ml of a tretrahydrofuran–acetone (1:1) solution. A solution consisting of 12 ml of carbon disulfide in 13 ml of a tetrahydrofuran–acetone (1:1) solution was slowly added with constant stirring. A 20-ml volume of 5.5 *M* NaOH was added dropwise to the solution, while maintaining the temperature below 5°C, and

then the solution was stirred for 30 min. The majority of the solvents (tetrahydrofuran, acetone, water) were removed using a Rotavaporator. A 50-ml aliquot of anhydrous diethyl ether was added and the evaporation is continued. The ether evaporation step was repeated until crystallization occurs. The material was then filtered and washed several times with anhydrous diethyl ether. A 77% yield of pale yellowish white crystals with a melting point of 65–66°C was obtained.

Equipment

Liquid chromatography was carried out using a Hewlett-Packard 1084B liquid chromatograph equipped with an autoinjector and scanning UV–VIS detector. A direct-connect cartridge system (Alltech, Avondale, PA, (U.S.A.) with an Econospere C_{18} reversed-phase cartridge (250 mm × 4.6 mm I.D., 5 μm particle size) was used as the analytical column. The operating conditions were as follows unless otherwise stated: injection volume, 10 μl; detection wavelength, 260 nm; mobile phase temperature, 40°C; column temperature, 35°C. An IBM 9420 spectrophotometer was used to obtain UV–VIS spectra of the complexes and a Perkin-Elmer 4000 Series atomic absorption spectrophotometer was used to evaluate the partition behavior of the metal complexes which were prepared by solvent extraction. A Varian EM-360A NMR spectrometer was used to verify the structure of the BPDTC reagent.

Preparation of metal complexes

Liquid-liquid extraction was used for preconcentration of metals as chelates. Aqueous samples were initially buffered with either 1 *M* phosphate buffer(pH 8) or acetate buffer(pH 5) depending on the metal species. A 1-l aliquot of the sample solution was transferred into a 2-l separatory funnel, to which 1 ml of a 0.2 *M* Na–BPDTC aqueous solution was added. The sample was then agitated for 1 min. For the extraction of Cr(III), the reaction temperature was elevated to 40°C for 15 h. A 1-g amount of sodium nitrate, if needed, was added to the solution to break down colloids which can form in the presence of excess ligand. A 25-ml volume of dichloromethane was then added as the extractant solvent, and the mixture was shaken for 2 min and left to separate for 4–5 min. The organic phase is then recovered and reduced to 1 ml under vacuum. A 10-μl volume of the dichloromethane layer was then injected into the C_{18} column described above. Capacity factors (k') were measured after 1 h of system equilibration. The k' values were calculated assuming that each mobile phase solvent was an unretained substance.

RESULTS AND DISCUSSION

Characterization of BPDTC and metal complexes

The proton NMR spectrum of the free BPDTC has been recorded in deuterated methanol. The resonance signals for phenyl protons in the benzyl group lay in the range δ 7.1–7.3, while the signal for methyl protons in the benzyl group appeared at δ 5.6. The triplet signals for two adjacent CH_2 in the acetonitrile group were in the range δ 2.5–2.9 and δ 3.8–4.2, respectively. The signal appearing at δ 4.67 is due to the trace hydroxyl proton in deuterated methanol or moisture in the sample.

The UV-VIS spectra of free BPDTC solution and metal–BPDTC complexes were obtained in water and dichloromethane, respectively. The molar absorptivities

of free BPDTC ligand at 259.0 nm (λ_{max}) was 19,500. The significant differences in wavelength of maximum absorbance of the most intense bands for metal diethyldithiocarbamate (DDTC) complexes have been reported[20,21]. The spectroscopic properties of BPDTC and DDTC complexes were compared in Table I. It is evident that the benzyl group in BPDTC imparts higher absorptivities to the complex compared to DDTC and the absorptivity of each metal BPDTC complex at 260 nm was reasonably consistent from metal to metal. Thus, it was possible to achieve multi-component determinations at one wavelength.

Extraction behavior of BPDTC complexes

Extraction of metal ions by DTCs is known to depend on several factors such as extractant solvent, chemical form of the metal ion, pH of the solution and shaking time[22,23]. Dichloromethane was selected as the extractant solvent because of its high extraction efficiency. The effect of pH on the extraction of metals has been investigated. Copper and cobalt exhibited extraction efficiencies of 100% over the entire pH range. The pH 5 was preferred for the extraction of selenium and chromium(VI), while the optimum pH for quantitative extraction of the remaining metal species investigated was around pH 8. Shaking time for the extraction of metal–DTC complexes into dichloromethane was studied at an adjusted pH as described above. All twelve metal species were extracted sufficiently within 2 min except for chromium(III). The chromium(III)–BPDTC complex was not readily formed under the normal conditions. To produce the Cr(III) complex, the reaction temperature was raised to 40°C at pH 5 and 15 h was allowed for the complex formation reaction to proceed before the addition of the extractant solvent. Under this condition, other group I metal species showed good stabilities. Reaction temperature above 50°C, however, caused decomposition of the chelating agent.

TABLE I

COMPARISON OF UV SPECTROSCOPIC DATA FOR METAL–BPDTC AND –DDTC COMPLEXES

Species	*Molar absorptivity (mol^{-1} cm^{-1} l)*	
	BPDTC at 260 nm	*DDTC at (λ_{max})*
Sb(III)	74 500	25 000 (504 nm)[20]
Cd(II)	128 500	
Cr(VI)	29 590	
Cr(III)	24 600	
Co(II)	38 110	23 300 (323 nm)[21]
Cu(II)	53 800	13 000 (436 nm)[21]
Pb(II)	96 750	
Hg(II)	125 500	
Ni(II)	43 050	34 200 (326 nm)[21]
Se(IV)	137 400	
Tl(I)	90 350	
Zn(II)	58 650	

Eluent behavior of BPDTC complexes

An initial chromatogram of BPDTC complexes of twelve metal species was obtained using the binary system methanol–water (75:25), which did not sufficiently resolve the first five metal peaks (antimony, cadmium, lead, thallium, zinc). The solvent strength of the mobile phase was increased in order to improve the separation of the five metals which overlapped at the beginning of the chromatogram. However, the late eluting metals such as chromium(III), mercury and copper exhibited poor peak shape. To adequately separate all twelve species, it was necessary to divide them in two groups as follows: group I [chromium(III), chromium(VI), cobalt, copper, mercury, nickel, selenium], group II (antimony, cadmium, lead, thallium, zinc).

Chromium(VI), which reacted quickly with BPDTC, produced two peaks. However, using the conditions described earlier under which chromium(III) formed a complex, the chromium(III) produced only one peak. The appearance of the second peak of chromium(VI) is presumably because a fraction of the dichromate ion is reduced by the chelating agent to chromium(III) ion which forms a BPDTC complex during the extraction. According to Hope *et al.*[24] the first peak is expected as $Cr(S_2CNRR')_2(OS_2CNRR')$ and the second peak is $Cr(S_2CNRR')_3$, where R is the acetonitrile group (CH_2CH_2CN) and R′ is the benzyl group ($CH_2C_6H_5$). Experimentally, the second peak was identified as Cr(III)–BPDTC complex directly made from Cr(III). The standard curve for two peaks from Cr(VI) and one peak from Cr(III) showed good linearity. Since the ratios between the areas of two peaks from Cr(VI) were constant at different concentrations, the area of the first peak from Cr(VI) can be used to extrapolate the contribution to the second peak area and subsequently determine the real amount of Cr(III) in the mixture sample of Cr(VI) and Cr(III).

The separation of the metal complexes was assessed using a variety of methods. The effect of the pH of mobile phase was examined. Even though the retention time of group I was independent of the pH of the mobile phase, the change in pH produced a great effect on the group II metal complexes. Decreasing the pH of the mobile phase resulted in increasing retention time of group II and so exhibited more desirable results. Although lower pH was preferred for the separation of group II, a mobile phase pH less than 4.5 resulted in reagent dissociation[25]. A pH of 4.9 exhibited the best separation for the group II metal species.

The effect of organic solvent as a mobile phase was studied to determine the best chromatographic selectivities according to Snyder[26,27]. A single-solvent system consisting of methanol, acetronitrile or tetrahydrofuran, a binary solvent system (methanol–acetonitrile, acetonitrile–tetrahydrofuran, tetrahydrofuran–methanol) and a ternary solvent system (methanol–acetonitrile–tetrahydrofuran) were investigated, while the volume fraction of organic solvents and water was set to keep the solvent strength[28] of the mobile phase constant. An 0.05 *M* acetate buffer, pH 4.9, was used as an aqueous mobile phase. Using a different solvent system as a mobile phase was effective for the separation of group I metals as shown in Fig. 1. Although large changes in selectivity values among the various mobile phase were exhibited, either single or binary organic solvent systems did not provide the solvent power to separate all of the components in the mixture. Increasing acetonitrile content in the mobile phase improved the separation of mercury–chromium(III), mercury–selenium, and copper–selenium, while increasing tetrahydrofuran content contributed to

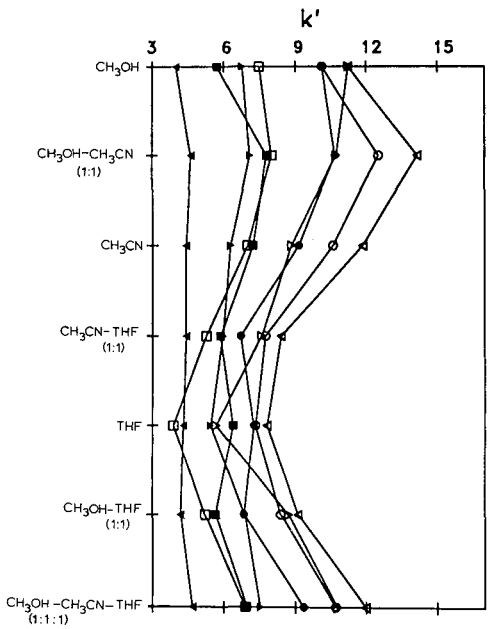

Fig. 1. Effect of organic solvent as a mobile phase on capacity factor for BPDTC complexes of group I metals. THF = Tetrahydrofuran. Metals: ○ = Co; ● = Cu; △ = Hg; ▲ = Se; □ = Ni; ■ = Cr(VI); ▽ = Cr(III); ▼ = decomposition product.

reducing capacity factors of nickel and mercury. Separation of the first three metal species [chromium(VI), selenium, nickel] was improved by increasing methanol content in the mobile phase. A ternary organic solvent system was therefore desirable for the separation of group I metal species. Although using a different solvent system as a mobile phase was effective for the separation of group I metals, it yielded poor results for the separation of group II. However, the peak shapes of group II metal complexes, which were broad and tailed with methanol–water as mobile phase system, were improved with the addition of small volume of acetonitrile and tetrahydrofuran in the mobile phase.

Ichinoki and Yamazaki[8] used chloroform as a stabilizer of some hexamethyleneammonium hexamethylenedithiocarbamate (HMAHMDTC) chelates for the separation of HMAHMDTC chelates of Cd, Ni, Pb, Zn, Cu, Hg, Co and Bi. Dichloromethane was used in this work because of its lower absorptivity at 260 nm. The effect of dichloromethane content in the mobile phase on elution behavior for BPDTC complexes of group I and group II metals is shown in Figs. 2 and 3, respectively. It is apparent that the addition of DCM in the mobile phase is very effective for the separation of BPDTC complexes of both group I and II. For the best separation, the preferred composition of the mobile phase includes 12% DCM in the organic mobile phase for group I and 6% for group II.

The effect of BPDTC in the mobile phase was also examined. The chromatograms with and without BPDTC under the same conditions were compared. The addition of BPDTC to the mobile phase in the concentration range of 0.004 *M*–0.006

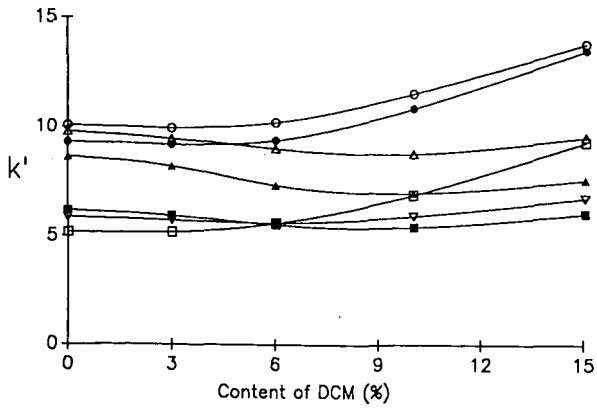

Fig. 2. Effect of dichloromethane (DCM) content in the mobile phase on the capacity factor for BPDTC complexes of group I metals. Mobile phase: methanol–water–DCM ($75-0.75x$:25:$0.75x$) (x = percent of dichloromethane in methanol). Other conditions are given in the text. Metals: ○ = Cr(III); ● = Co(II); △ = Hg(II); ▲ = Cu(II); □ = Cr(VI); ■ = Ni(II); ▽ = Se(IV).

M enhanced the peak reproducibilities and peak shapes of the group II metal complexes which was relatively poor initally with the methanol–water mobile phase system. It is concluded that addition of BPDTC to the mobile phase prevents on-column decomposition of the complexes. However, a high concentration of BPDTC (more than 0.01 *M*) made chelate detection difficult at 260 nm.

The final separation involved an aqueous mobile phase containing 0.005 *M* BPDTC and 0.01 *M* acetate buffer (pH 4.9), and an organic mobile phase of ternary solvents (methanol, acetonitrile, tetrahydrofuran) with additional 12% (v/v) dichloromethane for group I and 6% for group II. Column temperature was kept at 35°C for both group metal species. When a mobile phase of methanol–acetonitrile–tetrahydrofuran–dichloromethane-water (47.6:10.2:2.04:8.16:32.0) was used, group I

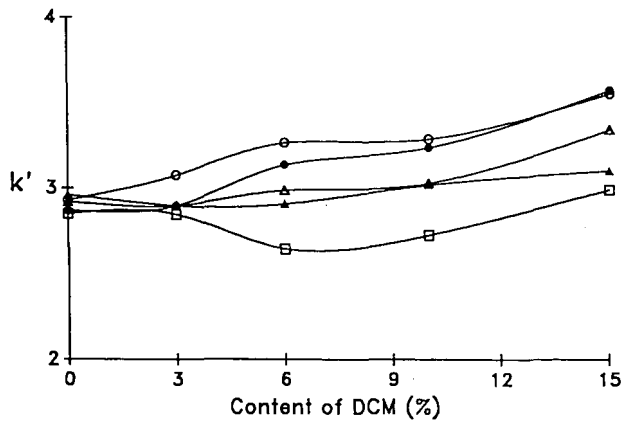

Fig. 3. Effect of dichloromethane content in the mobile phase on capacity factor for BPDTC complexes of group II metals. Conditions as in Fig. 2. Metals: ○ = Tl(I); ● = Sb(III); △ = Zn(II); ▲ = Pb(II); □ = Cd(II).

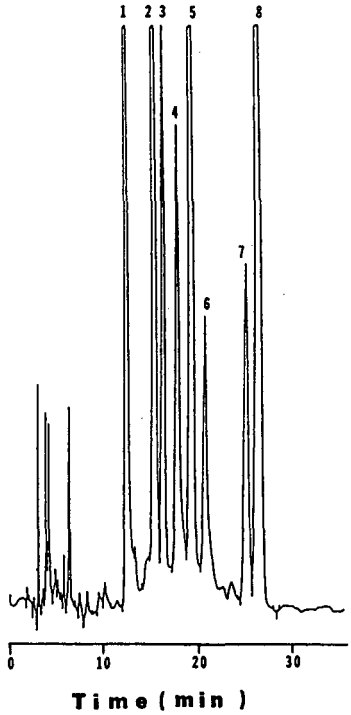

Fig. 4. Separation of a mixture of group I metals. Mobile phase: methanol–acetonitrile–tetrahydrofuran–dichloromethane–water (47.6:10.2:2.04:8.16:32.0) Peaks: 1 = Se; 2 = Ni; 3 = decomposition product; 4 = Cu; 5 = Cr(VI); 6 = Hg; 7 = Co; 8 = Cr(III).

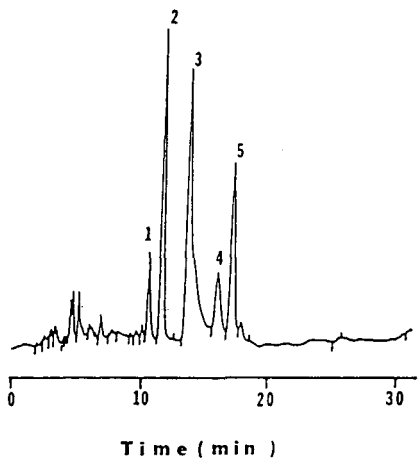

Fig. 5. Separation of a mixture of group II metals. Mobile phase: methanol–acetonitrile–tetrahydrofuran–dichloromethane–water (39.68:12.4:6.2:3.72:38.0). Peaks: 1 = Cd; 2 = Pb; 3 = Zn; 4 = Sb; 5 = Tl.

TABLE II

THE NUMBER OF THEORETICAL PLATES (N) AND THE CAPACITY FACTORS (k') FOR GROUP I AND GROUP II METAL SPECIES

Group	*Species*	*N*	*k'*
I	Se(IV)	3338	3.09
	Ni(II)	4356	4.05
	Cu(II)	4773	4.87
	Cr(VI)	5720	5.38
	Hg(II)	7744	5.86
	Cr(III)	8710	7.75
II	Cd(II)	5518	2.49
	Pb(II)	4910	3.07
	Zn(II)	2566	3.39
	Sb(III)	6084	3.97
	Tl(I)	6720	4.32

chelates were well resolved (Fig. 4). Group II metals were separated using the mobile phase composed of methanol–acetonitrile–tetrahydrofuran–dichloromethane-water (39.68:12.4:6.2:3.72:38.0) (Fig. 5). The number of theoretical plates and the capacity factors of eleven metal species are listed in Table II.

It is clearly evident that simultaneous determination is possible for each of the two groups (six metal species in one group and five in the other group) of BPDTC complexes. Although two injections of the sample mixture under two different mobile phase conditions were required for the determination of eleven pollutant metal species, the separation of each group of metal species were achieved within 30 min without having any interference of other group metal presence. The linearity for each metal species was determined over the range of its detection limit to 5 ppm, which is the concentration range of interest in many environmental samples. The detection

TABLE III

DETECTION LIMITS AND AMBIENT WATER CRITERIA FOR THE METAL SPECIES INVESTIGATED

Species	*Detection limit (μl/g)*	*Ambient water criteria (μl/g)*
Sb(III)	0.2	146
Cd(II)	0.1	10
Cr(III)	3.0	170 000
Cr(VI)	0.7	50
Cu(II)	0.1	1 000
Pb(II)	0.2	50
Hg(II)	0.7	0.14
Ni(II)	0.2	13.4
Se(IV)	0.4	10
Tl(I)	0.2	13
Zn(II)	0.3	5 000

TABLE IV

ANALYTICAL RESULTS OF STANDARD REFERENCE MATERIAL WATER SAMPLE FROM NATIONAL BUREAU OF STANDARDS

ND = Not detected.

Metal	*Concentration reported (μl/g)*	*Concentration found[a] (μl/g)*	*Relative error (%)*
Sb	0	ND	–
Cd	94.0	93.6 ± 20.8	−0.43
Cr	18.6	17.8 ± 5.9	−4.30
Cu	21.9	20.9 ± 5.0	−4.50
Pb	23.7	24.4 ± 7.5	+2.95
Hg	0	ND	–
Ni	49.0	50.6 ± 13.4	+3.27
Se	9.7	10.2 ± 1.7	+5.15
Tl	8.0	8.3 ± 2.0	+3.75
Zn	66.0	62.4 ± 15.6	+2.95

[a] 95% Confidence limits, $n = 3$.

limit of the method was expressed as the amount of metal required to give a peak area of 2000 units which could provide a detectable signal-to-noise ratio of 2 for the last eluting compound [chromium(III)], using a 10-μl injection. The EPA's ambient water criteria[29] for the protection of human health from the toxic properties of pollutant metals ingested through water and contaminated aquatic organisms are compared with the detection limits of our methods in Table III. The detection limits of our method are lower than the current ambient water criteria in all cases except mercury(II). Analytical results of the Standard Reference Material (1643b) issued by the National Bureau of Standards (Washington, DC, U.S.A.) are summarized in Table IV. Results were in good agreement with the standard concentrations, with the average relative error of ± 2.95%.

REFERENCES

1 G. D. Thorn and R. A. Ludwig, *The Dithiocarbamates and Related Compounds*, Elsevier, Amsterdam, New York, 1962, pp. 157–168.
2 A. Hulaniki, *Talanta*, 14 (1967) 1371–1392.
3 R. M. Smith, *Anal. Proc.*, 21 (1984) 73–75.
4 H. Irth, G. J. de Jong, U. A. Th. Brinkman and R. W. Frei, *Anal. Chem.*, 59 (1987) 98–101.
5 J. N. King and J. S. Fritz, *Anal. Chem.*, 59 (1987) 703–708.
6 R. M. Smith, A. M. Butt and A. Thakur, *Analyst (London)*, 110 (1985) 35–37.
7 B. J. Mueller and R. J. Lovett, *Anal. Chem.*, 57 (1985), 2693–2699.
8 S. Ichinoki and M. Yamazaki, *Anal. Chem.*, 57 (1985) 2219–2222.
9 M. Moriyasu and Y. Hashimoto, *Anal. Lett. Part A*, 11 (1978) 593–602.
10 O. Liška, J. Lehotay, E. Brandšteterová, G. Guiochon and H. Colin, *J. Chromatogr.*, 172 (1979) 384–387.
11 A. M. Bond and G. G. Wallace, *Anal. Chem.*, 55 (1983) 718–723.
12 A. M. Bond and G. G. Wallace, *Anal. Chem.*, 56 (1984) 2085–2090.
13 P. C. Uden and I. E. Bigley, *Anal. Chim. Acta.*, 94 (1977) 29–34.
14 J. N. King and J. S. Fritz, *Anal. Chem.*, 57 (1985) 1069–1020.

15 *Water-Related Environmental Fate of the 129 Priority Pollutants, Volume I, Introduction and Technical Background, metals and Inorganics, Pesticides, and PCBs*, U.S. Environmental Protection Agency, Office of Water Planning and Standards, Office of Water and Waste Management, Washington, DC, 1979.
16 R. A. Minear and L. H. Keith (Editor), *Water Analysis, Volume I, Inorganic Species*, Part 1, Academic Press, New York, 1982, pp. 33–35.
17 *Ambient Water Quality Criteria for Mercury*, U.S. Environmental Protection Agency, Office of Water Regulation and Standards, Criteria and Standards Division, Washington, DC, October 1980.
18 W. A. Pettyjohn, *Water Quality in a Stressed Environment–Reading in Environmental Hydrology*, Burgess Publishing Co., Minneapolis, MN, 1972, 227–234.
19 R. V. Moore, *Anal. Chem.*, 54 (1982) 895–897.
20 R. H. Merry and B. A. Zarcinas, *Analyst (London)*, 105 (1980) 558–563.
21 H. Bode, *Z. Anal. Chem.*, 144 (1955) 165–186.
22 L. Danielsson and B. Magnusson and S. Westerlund, *Anal. Chim. Acta.*, 98 (1978) 47–57.
23 B. Magnusson and S. Westerlund, *Anal. Chim. Acta.*, 131 (1981) 63–72.
24 J. M. Hope, R. L. Martin and D. Taylor, *J. Chem. Soc., Chem. Comm.* (1977) 99–100.
25 A. M. Bond and G. G. Wallace, *Anal. Chim. Acta.*, 164 (1984) 223–232.
26 L. R. Snyder, *J. Chromatogr.*, 92 (1974) 223–230.
27 L. R. Snyder, *J. Chromatogr. Sci.*, 116 (1978) 223–234.
28 P. J. Schoenmakers, H. A. H. Billiet and L. de Galan, *J. Chromatogr.*, 218 (1981) 261–284.
29 *Fed. Reg.* 45 (Nov. 28) (1980) 79318.

Journal of Chromatography, 481 (1989) 299–313
Elsevier Science Publishers B.V., Amsterdam — Printed in The Netherlands

CHROM. 21 756

EXCHANGE OF THE CATION AND ANION OF THE SAMPLE (SODIUM OR POTASSIUM CHLORIDE) WITH THE CATION AND ANION OF THE ELUENT (SODIUM OR POTASSIUM PHOSPHATE BUFFER) AND THEIR ELUTION, FROM A SEPHADEX G-15 COLUMN, IN SEPARATE FRACTIONS

TOSHIHIKO OKADA* and KEIKO SUGATA
The First Department of Biochemistry, Kanazawa Medical University, Uchinada, Ishikawa 920-02 (Japan)
YASUKO NAKABAYASHI and KOHEI TERAOKA
Central Clinical Laboratory, Kanazawa Medical University Hospital, Uchinada, Ishikawa 920-02 (Japan)
and
MINORU MIYAKOSHI and MASAO INOUE
Central Research Laboratory, Kanazawa Medical University, Uchinada, Ishikawa 920-02 (Japan)
(First received February 8th, 1989; revised manuscript received May 12th, 1989)

SUMMARY

Various concentrations of sodium and potassium chloride were eluted with sodium or potassium phosphate buffer (0.025 *M*, pH 7.0) in various sample–buffer combinations from a Sephadex G-15 column. A more acidic buffer (pH 6.0) or a more concentrated buffer (0.125 *M*) were also used as the eluent. By observing the elution behaviour of all ions in the eluate, it was found that the cation from the sample accompanied by phosphate ion from the eluent was eluted in earlier fractions, and the chloride ion from the sample accompanied by the eluent's cation was eluted in later fractions in all homocationic and heterocationic sample–eluent combinations employed. The mechanism assumed was that chloride ion from the sample was eluted slowly and the phosphate ion from the eluent rapidly, resulting in the occurrence of cation-exchange reactions between the sample and the eluent.

INTRODUCTION

The chromatographic behaviour of inorganic compounds has been explained in terms of steric exclusion or the sieving effect in the gel phase. The size of the hydrated ions or lyotropic number affects the steric exclusion; the larger the solute molecule, the smaller is the elution volume[1–3]. However, many workers reported that, when inorganic compounds are eluted from Sephadex, various side effects are observed; they include both solute–gel matrix interactions, such as ion exchange[4–6] and adsorption[5,7–9] as well as solute–solute interactions[5,6,10] such as complexation[4,7] and ion exclusion (the Donnan exclusion effect)[4,5,11] (for a review see ref. 1). These effects alter the elution volumes predicted from the size of the hydrated ions. Such phenomena were also observed with cellulose gel (Cellulose-20)[12] and Bio-Gel P-2[4,13]).

0021-9673/89/$03.50

Experiments on the elution behaviour of inorganic compounds on Sephadex were extensively carried out during the period from early 1960 to late 1970. However, pure water was used as an eluent in some experiments and in others the sample and eluent differed either in the cation or anion. When samples and eluents which differed in both the cation and anion were used, only the refractive index curves or the elution behaviours of either the anion or the cation were observed, thus the eluates were not totally characterized. Therefore, side effects in the elution behaviour on Sephadex were not completely elucidated.

In our experiments, when 0.20 *M* potassium chloride was eluted with 0.025 *M* sodium-phosphate buffer (pH 7.0) (heterocationic and heteroanionic system) from a Sephadex G-15 column, a complex refractive index curve of the eluate was observed. We then determined the concentration distribution of all of the ions in the eluate and found that the potassium and chloride ions from the sample were eluted in different fractions, *i.e.*, the potassium ion from the sample was accompanied by the phosphate ion from the eluent and eluted in the earlier fractions, and the chloride ion from the sample was accompanied by sodium ion from the eluent and eluted in the later fractions. Therefore, we examined the behaviour of each ion in relation to the counter ion in all combinations of sample (potassium chloride and sodium chloride) and eluent (potassium phosphate and sodium phosphate) under various conditions. This report describes the results and discusses the mechanism of the phenomenon observed.

EXPERIMENTAL

Chemicals

All reagents were of analytical grade from Wako Pure Chemical Industries (Osaka, Japan). Sodium-22 chloride (^{22}NaCl, 61.60 mCi/mg; 99% pure) was obtained from New England Nuclear (Boston, MA, U.S.A.).

Samples

Various concentrations of sodium chloride and/or potassium chloride dissolved in the eluent were used as sample solutions. In some experiments, the sample was ^{22}NaCl (see Chemicals) sometimes diluted in cold NaCl. The radioactivity of ^{22}NaCl was 0.03 μCi in 0.6 ml of sample solution applied.

Eluents

Distilled water and the following buffers were used as eluents. A 0.025 *M* sodium or potassium phosphate buffer (pH 7.0) was used for most experiments. An acidic buffer, 0.025 *M* sodium phosphate pH 6.0 and a concentrated pH 7.0 buffer, 0.125 *M* sodium phosphate, were also used.

Procedure

Sephadex G-15 (Pharmacia; dry particle diameter, 40–120 μm) was packed according to a standard procedure in two kinds of glass tube: column I (300 × 13 mm; bed height, 25 cm; glass fibre support) and column II (Excel Type SE-1000, 1000 × 19 mm; bed height, 90 cm; porous polystyrene support). Sephadex G-25 (Pharmacia; dry particle diameter, 50–150 μm) packed in the longer glass tube was also used (Fig. 8).

A peristaltic pump (LKB, gear box 3:250) was inserted between the eluent reservoir and the top of the column to maintain a constant flow-rate (12 ml/h). Volumes of 0.1 and 0.6 ml of the sample solution were applied to the tops of columns I and II respectively, and the eluate was continuously monitored with a Refractomonitor (Mitsumi Scientific Co., Japan; Model SF-1107). The eluate was collected in 10-min fractions using an LKB7000 Ultrorac fraction collector. All columns were operated at 4°C.

Four sample–eluent systems, two homocationic (sodium chloride–sodium phosphate buffer, and potassium chloride–potassium phosphate buffer) and two heterocationic (sodium chloride–potassium phosphate buffer, and potassium chloride–sodium phosphate buffer), were employed.

Quantitation of ions

The amounts of sodium ion (Na^+) and potassium ion (K^+) were determined in a Na–K flame photometer (Corning Eel Co., U.K.; Model 450). Chloride ion (Cl^-) was measured with a Chloride-Meter (Corning Eel, Model 920). Phosphate ion (P^-) was determined by the method of Fiske and Subbarow[14]. $^{22}Na^+$ was counted in an Auto-Well Gamma System Model JDC-751 (Aloca, Japan).

RESULTS

NaCl and/or KCl eluted with distilled water

When 0.68 *M* NaCl or 0.54 *M* KCl was eluted from column I with distilled water, the refractive index curves showed single peaks which were found to contain both the anion and cation from the sample. The elution volume of NaCl was slightly less than that of KCl. When a mixed solution of NaCl and KCl was applied to the column, the elution volume of each salt did not change appreciably and a divided peak appeared (data not shown). In order to analyze the elution profile of each ion, the mixed solution was eluted with distilled water from column II (Fig. 1). The earlier peak consisted mainly of Na^+, and the later peak mainly of K^+. The Na^+ was a little skewed toward the latter, while a portion of the K^+ accumulated in the earlier fractions, possibly because of ion–ion interaction. The Cl^- was eluted in two peaks, and accompanied both the Na^+ and K^+.

The Na^+ was eluted earlier than K^+, because hydrated Na^+ (3.58 Å) is larger than K^+ (3.31 Å)[2]. It is not likely to be due to stronger adsorption of K^+ to contaminating substances in the gel, because gel washed sequentially with Tween 80, distilled water, 1,4-dioxane and ethanol gave the same elution profile.

Elution profiles of ions in homocationic systems

When 0.68 *M* NaCl was eluted from column I with sodium phosphate buffer, the refractive index curve showed two peaks (Fig. 2A). The later (higher) peak consisted of almost all of the Na^+ and Cl^-, and the earlier (lower) peak contained some of the Na^+ accompanied by P^-.

When 0.54 *M* KCl was eluted with potassium phosphate buffer, similar refractive index curves and elution profiles were obtained (Fig. 2B), *i.e.*, the later peak consisted of most of the K^+ and Cl^- while the earlier peak contained the remaining K^+ and P^-. Thus, in both homocationic systems, most of the cation and anion from the sample are apparently eluted together.

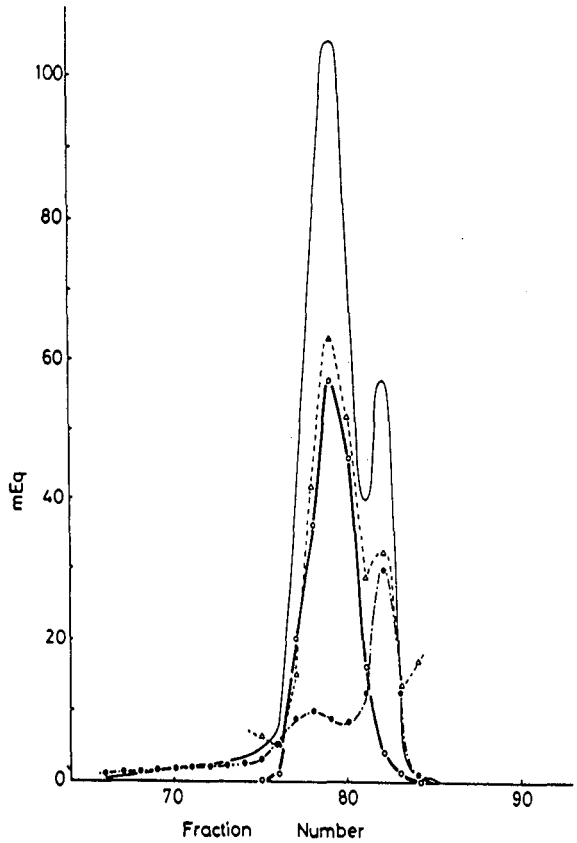

Fig. 1. Refractive index curve (—) and elution profiles of Na^+ (○), K^+ (●) and Cl^- (△) when a mixed solution of 0.72 *M* NaCl and 0.56 *M* KCl was eluted with distilled water from Sephadex G-15 column II.

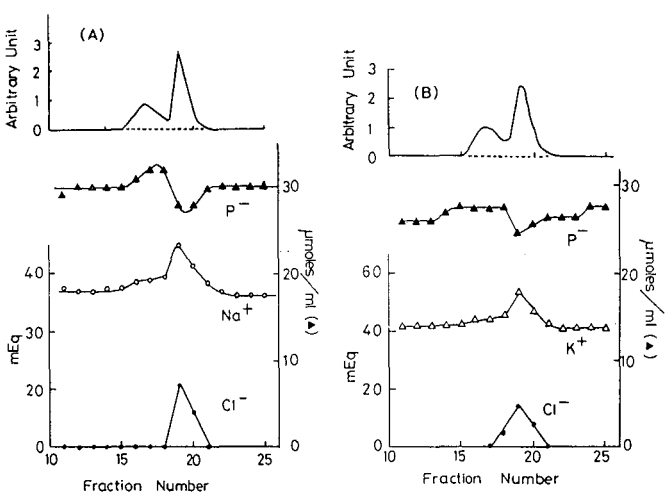

Fig. 2. Refractive index curves and elution profiles of each ion from column I, (A) when 0.68 *M* NaCl was eluted with sodium phosphate buffer, and (B) when 0.54 *M* KCl was eluted with potassium phosphate buffer.

Elution profiles of ions in heterocationic systems

When 0.68 *M* NaCl was eluted from column I with potassium phosphate buffer, the refractive index curve of the eluate showed two peaks with a negative peak in between. Contrary to the results obtained in homocationic systems, the elution profiles of each ion showed that the Na^+ and Cl^- from the sample were eluted in different fractions. The Na^+ accompanied by P^- was eluted first followed by K^+ and Cl^- (Fig. 3A).

When 0.20 *M* KCl was eluted from column I with sodium phosphate buffer, the refractive index curve showed one small negative peak followed by two positive peaks (Fig. 3B). The elution profiles of each ion revealed that the K^+ and Cl^- from the sample were completely separated from each other. The K^+ accompanied by P^- appeared in the first positive peak; Na^+ and Cl^- appeared in the second. Thus, in both heterocationic systems, the cation from the sample was accompanied by the anion (P^-) from the eluent and was eluted in early fractions; the anion (Cl^-) from the sample was accompanied by the cation from the eluent and was eluted in late fractions. This elution profile, which was quite different from that obtained by the use of distilled water as an eluent (Fig. 1), indicated that the differential elution of the cation and anion from the sample was caused by the interaction between the ions derived from the sample and eluent.

Effect of sample concentrations on the elution profiles of ions in heterocationic systems

When various concentrations of NaCl were eluted from column II with potassium phosphate buffer, the refractive index curves of the eluates were complicated and varied with the concentration of the sample (Fig. 4A). The higher the concentration, the later the fractions to which Na^+ spread. The K^+ from the eluent was apparently excluded from the earlier sodium fractions to the late fractions where it made a peak. At high sample concentrations (2.16, 2.87*M*), a sharp trailing spike of Na^+ appeared in fractions a little bit earlier than those in which the potassium peak occurred (Fig.

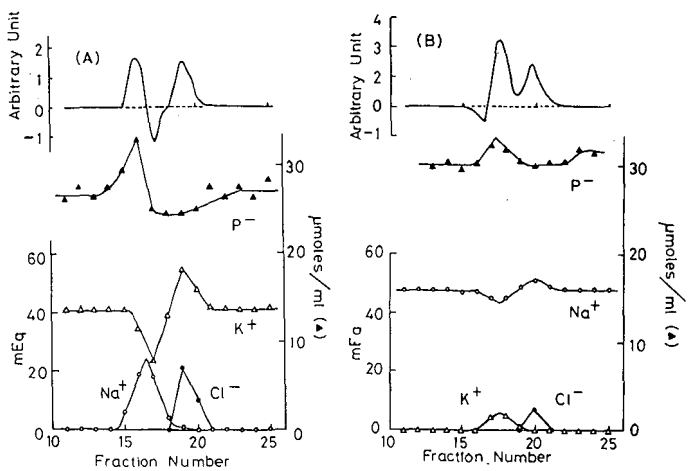

Fig. 3. Refractive index curves and elution profiles of each ion from column I, (A) when 0.68 *M* NaCl was eluted with potassium buffer, and (B) when 0.20 *M* KCl was eluted with sodium phosphate buffer.

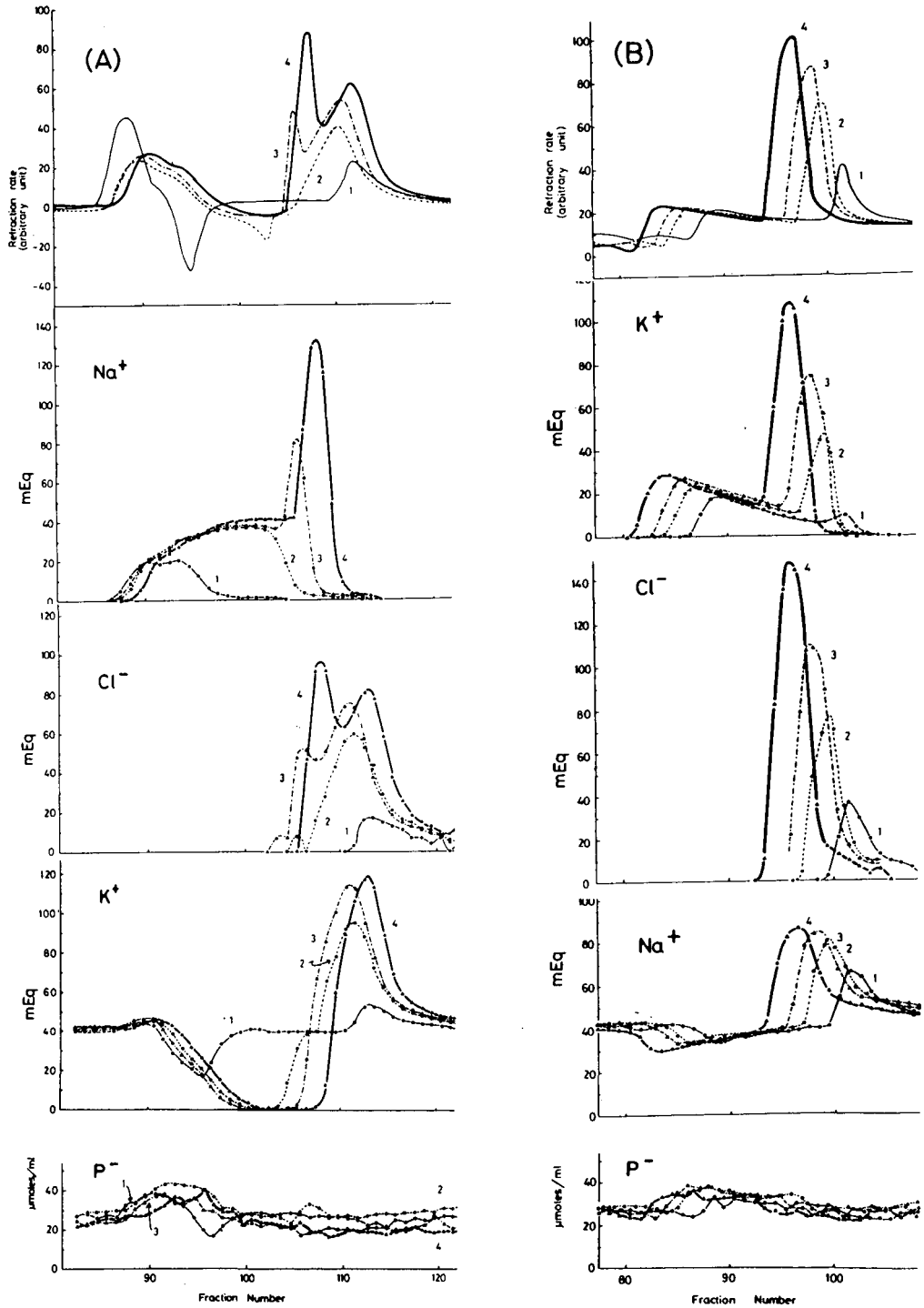

Fig. 4. Refractive index curves and elution profiles of each ion from column II, (A) when various concentrations of NaCl were eluted with potassium phosphate buffer and (B) when various concentrations of KCl were eluted with sodium phosphate buffer. Concentrations (*M*): NaCl: 0.72 (1), 1.44 (2), 2.16 (3), 2.87 (4); KCl: 0.56 (1), 1.13 (2), 1.69 (3), 2.25 (4).

4A). The Cl^- was thus split into two peaks: one which accompanied the potassium peak and the other which accompanied the Na^+ in the spike.

A similar experiment was performed with various concentrations of KCl eluted with sodium phosphate buffer (Fig. 4B). The refractive index curves differed from those obtained in the previous system. At the lowest sample concentration (0.56 *M*), the K^+ was distributed over many fractions and made a small broad spike where the Cl^- accompanied it. Thus, most of the K^+ and Cl^- from a sample were separated. The K^+ in the earlier fractions was accompanied by P^-. The Na^+ from the eluent was apparently excluded from the earlier potassium area to the later fractions where it made a peak. When the sample concentration increased, the elution volume of the K^+ decreased and the potassium spike became higher. In this system, the latter spike appeared in about the same fractions as the sodium peak. Therefore, the Cl^- accompanied both the potassium spike and the sodium peak.

Effects of pH and buffer concentration on the elution profile

When 0.56 *M* KCl was eluted from column II with sodium phosphate buffer (pH 6.0) the elution volume of the K^+ increased (Fig. 5B), compared with that obtained when the same sample was eluted with sodium phosphate buffer (Fig. 5A).

When 0.56 *M* KCl was eluted with 0.125 *M* sodium phosphate buffer, the K^+ did not spread and the elution volume of the Cl^- increased. The K^+ and Cl^-, therefore, were completely separated from each other (Fig. 5C).

Elution profile of $^{22}Na^+$ in an heterocationic system

In order to examine whether the higher salt concentration in the sample (rather than the eluent) was responsible for the association of the sample's cation with the P^- from the eluent, a solution containing an extremely low concentration of $^{22}NaCl$ ($5.5 \cdot 10^{-9} M$) was eluted with potassium phosphate buffer. The radioactivity was eluted within a sharp peak in early fractions (Fig. 6). From this result and those shown in Figs. 3A and 4A, it was concluded that the phenomenon was independent of the salt concentration in the sample.

Elution profile of $^{22}Na^+$ in an homocationic system

In homocationic systems, the cation and the anion from the sample were apparently eluted together in the late fractions. However, we hypothesized that the same ion-exchange reaction that occurs in heterocationic systems also occurs in homocationic systems. To confirm this, $^{22}NaCl$ was added to the cold NaCl solution and eluted with sodium phosphate buffer. The Na^+ and Cl^- appeared mainly in the late fractions, but the radioactivity appeared in the early fractions (Fig. 7). Even when the low concentration of $^{22}NaCl$ ($5.5 \cdot 10^{-9}$ *M*) was used as a sample, the $^{22}Na^+$ was eluted in the early fractions (Fig. 6).

We conclude from these results that not only in heterocationic systems but also in homocationic systems the cation from the sample was eluted in the earlier fractions and the cation from the eluent in the later fractions. However, since the cations from the sample and the eluent were the same, the negative peak of the eluent's cation was cancelled by the positive peak of the sample's cation as illustrated in Fig. 10. Although we have never performed the experiment in the other homocationic system (KCl–potassium phosphate buffer system), the same rule would be expected to operate in that system as well.

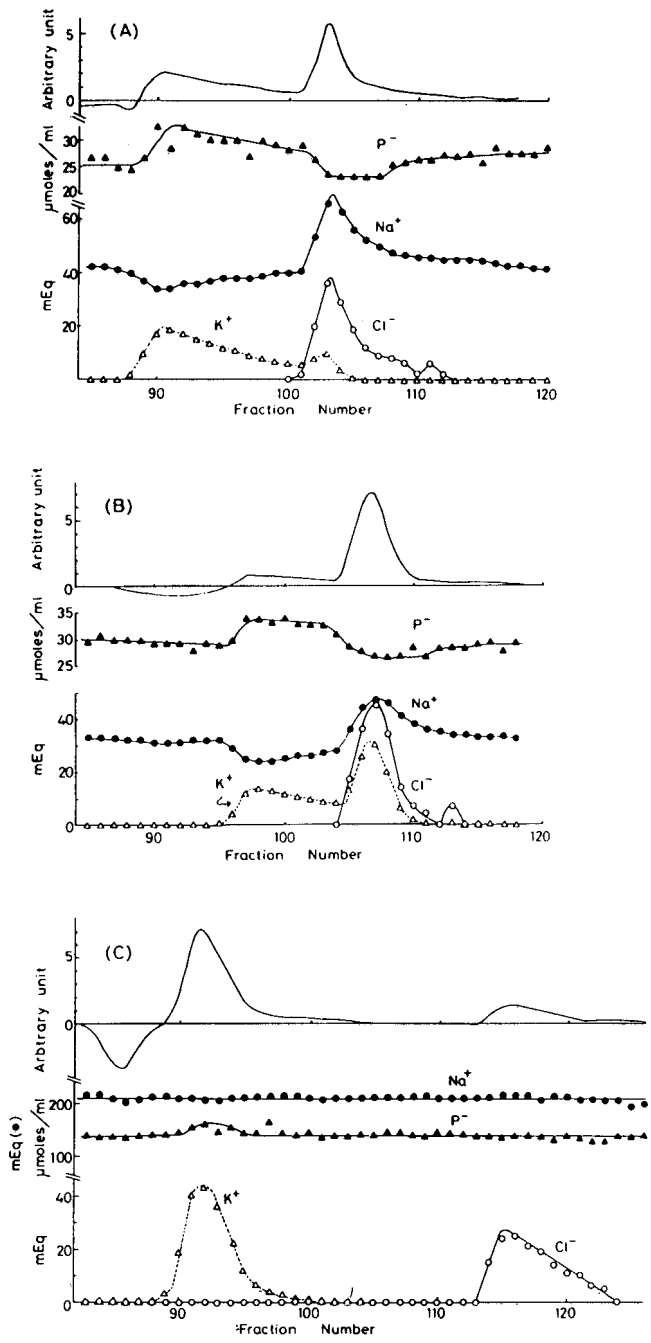

Fig. 5. Refractive index curves and elution profiles of each ion when 0.56 M KCl was eluted from column II, (A) with sodium phosphate buffer, (B) the same buffer (pH 6.0) and (C) 0.125 *M* sodium phosphate buffer.

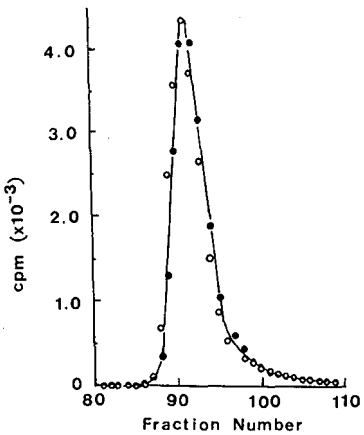

Fig. 6. Combined elution profiles of $^{22}Na^+$ obtained in two independent experiments, *i.e.*, $^{22}NaCl$–potassium phosphate buffer (○) and $^{22}NaCl$–sodium phosphate buffer (●) systems.

Sephadex G-25 column

When 1.13 *M* KCl was eluted with sodium phosphate buffer from a Sephadex G-25 column, the cation and anion from the sample were eluted in almost identical fractions (Fig. 8). This seems to show that the pore size of Sephadex G-15 is particularly suitable for the occurrence of the ion-exchange reaction.

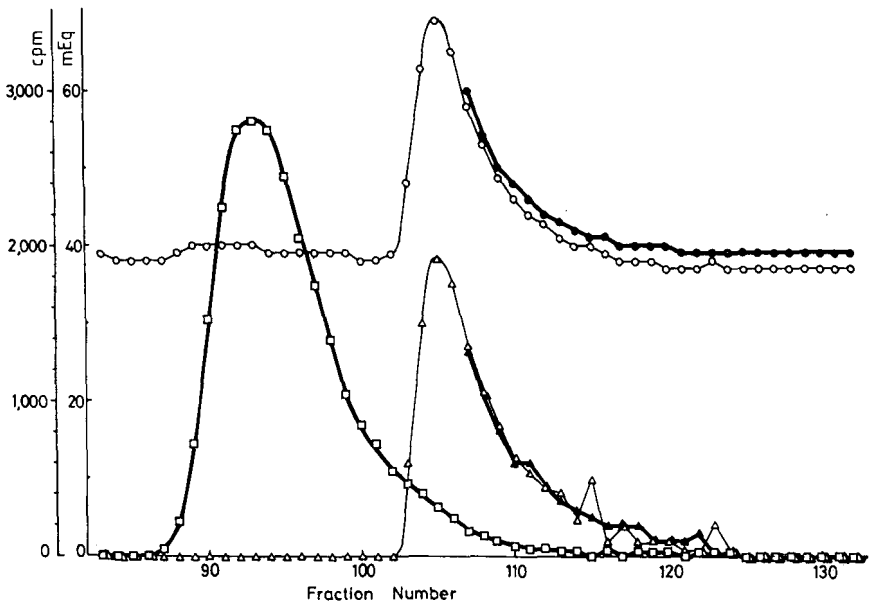

Fig. 7. Combined elution profiles of Na^+ and Cl^- obtained in two independent experiments: (1) sample, 0.72 *M* NaCl solution; eluent, sodium phosphate buffer Na^+ (○), Cl^- (△); (2) sample, $^{22}NaCl$ added to the same sample solution as in (1); eluent, sodium phosphate buffer, $^{22}Na^+$ (□), Na^+ (●) and Cl^- (▲) determined only for the fractions having low or no radioactivity.

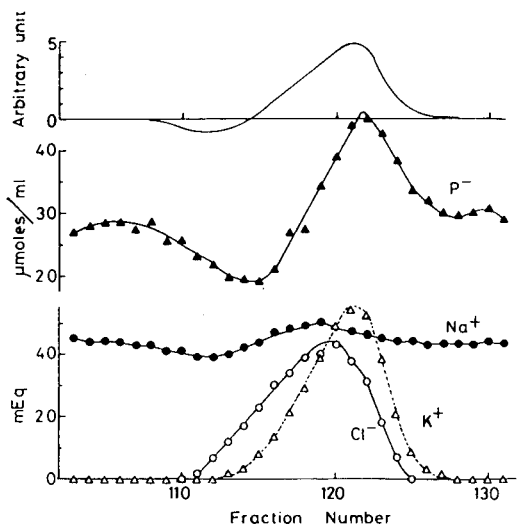

Fig. 8. Refractive index curve and elution profiles of each ion when 1.13 *M* KCl was eluted with sodium phosphate buffer from a Sephadex G-25 column.

DISCUSSION

In this study we used NaCl or KCl as a sample and sodium phosphate or potassium phosphate buffer as an eluent and observed that the cation from the sample accompanied by P^- from the eluent was eluted in earlier fractions, and Cl^- from the sample accompanied by the eluent's cation was eluted in later fractions in both homocationic and heterocationic systems (Fig. 2–7). This phenomenon was independent of the concentration of the sample salt (Fig. 6). On the other hand, when NaCl and/or KCl was eluted with distilled water, the bulk of the cation and anion from a sample salt were eluted together and the ion pair Na^+Cl^- was eluted slightly earlier than K^+Cl^- (Fig. 1). Therefore, the differential elution of the cation and anion from a sample described above was assumed to be caused by the interactions between the ions derived from the sample and the eluent.

Since Na^+ was eluted earlier than K^+ in the NaCl–potassium phosphate buffer system (Figs. 3A, 4A) and K^+ was eluted earlier than Na^+ in the KCl–sodium phosphate buffer (Figs. 3B, 4B), the elution volume of each cation was independent of the size of the molecule. Since the Na^+ from the sample was associated with the P^- in one heterocationic system (Figs. 3A, 4A), and the K^+ from the sample was associated with the P^- in the other (Figs. 3B, 4B), no preferential association of a cation with P^- was observed, and since the elution volumes of Na^+ and K^+ were reversed in the two heterocationic systems (Figs. 3, 4) no preferential adsorption of a cation to the gel matrix was observed. However, P^- was always eluted earlier than Cl^- and their elution sequence was not reversed in the two heterocationic systems (Figs. 3, 4).

We therefore tried to explain the ion-exchange reactions based on the phenomenon that P^- is eluted earlier than Cl^-. For convenience of interpretation, the gel phase can be divided into two phases according to the penetrability of P^- as described

by Ogata *et al.*[7] The hydrated Na^+, K^+ and Cl^- which are smaller than hydrated P^- can penetrate into both phase I and phase II, hydrated P^- only into phase II. Thus P^- is eluted earlier than Cl^-. Before the sample is applied, some of the Na^+ or K^+ from the eluent remains in phase II contrary to the principle of electrical neutrality. Thus, some of the cation and the P^- from the eluent are separated topographically. Therefore, when the sample is applied, the Cl^- from the sample is promptly taken up by the phase I cation from the eluent; the cation from the sample associates with the P^- in phase II which has lost its counter ion. The ion pair Na^+P^- or K^+P^- thus formed is eluted in earlier fractions than Na^+Cl^- or K^+Cl^-. This mechanism explains the phenomenon we observed.

A second possibility is that, after the sample is applied to the column, Cl^- from the sample is eluted more slowly than P^- from the eluent due to some mechanism (discussed later). Then, the cation–Cl^- pair will meet the cation–P^- pair continuously during the elution and the ion-exchange reaction occurs, between the two ion pairs and continues until all of the cation from the sample is replaced by the cation from the eluent. Thus, the cation from the sample which associates with P^- would be eluted rapidly, the cation from the eluent which associates with Cl^- more slowly (Fig. 9). This mechanism also explains the phenomenon we observed. It is more plausible, because the cation and anion from the eluent are not separated topographically contrary to the principle of electrical neutrality.

Based on these mechanisms, we explain the phenomena we observed as follows.

The refractive index curve showed a negative peak between two positive peaks in the NaCl–potassium phosphate buffer system and a small negative peak followed by two positive peaks in the KCl–sodium phosphate buffer system (Fig. 3)

This occurred because in the NaCl–potassium phosphate buffer system the ion pair Na^+P^- was eluted more rapidly than K^+P^-; a low ion-concentration area (negative peak) was formed between the two ion pairs. On the other hand, in the KCl–

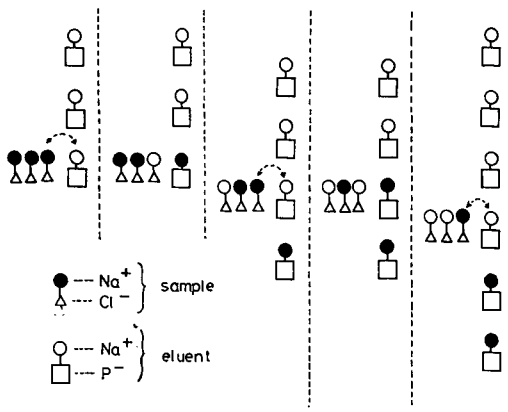

Fig. 9. Hypothetical scheme of the mechanism of the ion-exchange reaction. The time course is shown of the reaction when NaCl is eluted with sodium phosphate buffer: P^- is eluted more rapidly than Cl^-, hence a cation-exchange reaction occurs between the sample and the eluent, *i.e.*, Na^+ from the sample accompanies P^- from the eluent and is eluted more rapidly than the Cl^- from the sample which is associated with the cation from the eluent.

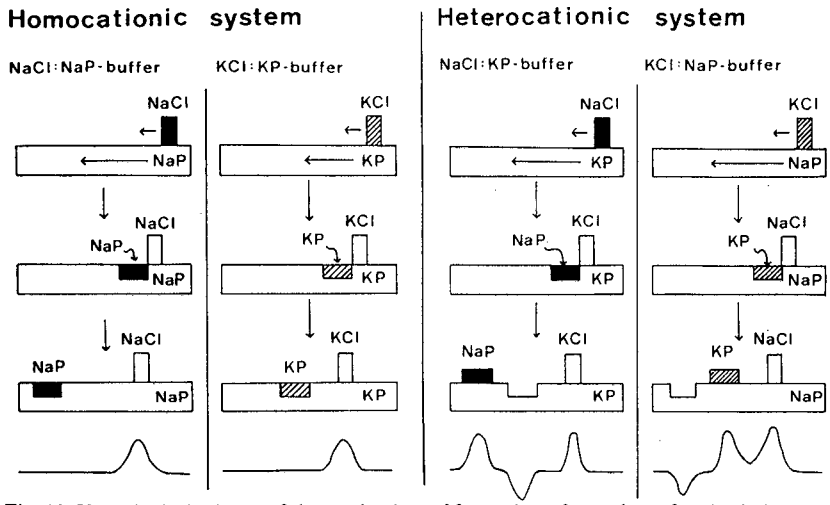

Fig. 10. Hypothetical scheme of the mechanism of formation of complex refractive index curves in homocationic and heterocationic systems.

sodium phosphate buffer system, the ion pair K^+P^- formed by the ion-exchange reaction was eluted now more slowly than the Na^+P^-. Therefore, the low ion-concentration area (negative peak) appeared in front of the ion pair K^+Cl^-. These behaviours of the ion pairs in heterocationic systems are illustrated in Fig. 10.

When an high concentration of sample salt was used in the heterocationic system, the cation from the sample spread to the later fractions (Figs. 4A and B)

The spreading can be explained as follows. The higher the concentration of the sample salt, the longer is the time needed to replace the cation from the sample with the cation from the eluent; the result is spreading. Ogata *et al.*[7] observed the spreading of magnesium ion from magnesium chloride eluted with sodium sulphate. However, they only observed the elution behaviour of Mg^{2+} and did not observe the other ions used. Therefore, they could not explain the mechanism of the spreading. This phenomenon can also be explained by the mechanism described above.

When the eluent concentration increased, the spreading of the cation from the sample decreased and the elution volume of Cl^- increased (Fig. 5C)

The spreading of the cation from the sample decreased because the time required for ion exchange is less due to the smaller difference between the salt concentration of the sample and the eluent.

The elution volume of Cl^- increased because the higher the ion concentration, the lower is the degree of hydration of both the ions and the gel matrix as assumed by Eaker and Porath[15]. This phenomenon is similar to that observed by Neddermeyer and Rogers[4] and Ueno *et al.*[16]

When extremely high concentrations of the sample salt were used in the heterocationic system, the sample's cation made a spike (Fig. 4A and B)

The spike fractions contained cation not associated with P^- entirely, but with Cl^-.

In NaCl–potassium phosphate buffer, the concentration of Na^+ in the spread was higher in the later fractions and the sodium spike did not appear at lower concentrations (0.72 and 1.44 M) of NaCl (Fig. 4A); in KCl–sodium phosphate buffer, the concentration of K^+ in the spread was lower in the later fractions and the potassium spike appeared even with the lowest concentration (0.56 M) of KCl used (Fig. 4B)

These elution profiles indicate that NaCl ionizes efficiently to the maximum level throughout under the ionic strength, while KCl ionizes at a fixed rate, resulting in a decrease of the amount of K^+ as the unionized KCl decreases.

The sodium spike and potassium peak were in different fractions in the NaCl–potassium phosphate buffer system (Fig. 4A), and in about the same fractions in KCl–sodium phosphate buffer (Fig. 4B)

Since in the NaCl–potassium phosphate buffer system, the ion pair K^+Cl^- formed was eluted more slowly than the sample (Na^+Cl^-) they were separated. In the KCl–sodium phosphate buffer system the ion pair Na^+Cl^- was expected to be eluted slightly earlier than the sample ion pair K^+Cl^-. However, the two ion pairs were eluted together, as if they were prevented from separating.

When acidic buffer was used, the elution volume, especially of the cation from the sample, increased (Fig. 5B)

Yoza and Ohashi[17] and Ueno *et al.*[6] showed that the elution volume of metal ions eluted with an acidic eluent was different depending on the anion used in the eluent. This was assumed to be due to the different adsorbability of the anions to the gel matrix.

The phenomenon we observed, however, might be ascribed to the decreased dissociation efficiency of both the sample and eluent; this results in a decreased efficiency in replacing the cation from the sample with the cation from the eluent.

In both homocationic and heterocationic systems, the negative peak of P^- was observed in chloride fractions and positive peak of P^- in the earlier fractions (Figs. 2, 3 and 5)

This phenomenon indicates that when P^- entered into the chloride region in the column, it passed through the region quickly, making a negative peak in the region and a positive peak in the earlier fractions. A possible mechanism is that Cl^- in the Sephadex beads excludes P^- from the beads, and the phase of the beads to which P^- can penetrate became smaller. Yoza described a similar phenomenon[1] and attributed it to the Donnan exclusion effect[1,16]. We do not know yet which mechanism is correct.

Saunders and Pecsok[13] described an ion-exchange reaction, *i.e.*, when a solution containing equal concentrations of barium chloride and potassium perchlorate is eluted with distilled water from Bio-Gel P-2 (100–200 mesh), an ion-exchange reaction occurs between the two sample salts, and KCl is eluted first, followed by barium perchlorate. They explained this phenomenon by partition of the ions, because the K_D values corresponding to the two peaks correlate well with those predicted for KCl and $Ba(ClO_4)_2$.

However, the mechanism of the ion-exchange reaction we observed is based on the assumption that P^- is eluted earlier than Cl^- from Sephadex G-15. The experimental results we obtained[18] indicate that this is the case. The differential elution of

P^- and Cl^- is possibly caused by the lower adsorbability of P^- than Cl^- on the Sephadex. Sinibaldi and Lederer[8] observed the adsorption of inorganic ions other than P^- and Cl^- on Sephadex G-25 and LH-20 in some eluents. The second possibility is that since Sephadex is considered as an inert support of the aqueous portion of the eluent just as the paper in paper chromatography is, the differential elution of P^- and Cl^- is possibly due to the different partition of P^- and Cl^- to the water which is bound on the Sephadex[19]. The third possibility is that P^- and Cl^- are eluted differentially by the molecular sieving function of the gel, *i.e.*, the ionic size of the hydrated P^- is sufficiently large to be eluted earlier than the hydrated Cl^-. That the ion-exchange reaction did not occur in a Sephadex G-25 column (Fig. 8) seems to show that the third possibility is plausible. Whatever the mechanism is, the P^- from the eluent is eluted earlier than Cl^- from the sample, and a cation-exchange reaction occurred between the sample and eluent. Therefore, in the case where the cation and anion from a sample are eluted differentially, one should consider ion-exchange reaction between the sample and eluent as a possible mechanism.

CONCLUSION

When sodium chloride or potassium chloride was eluted with sodium or potassium phosphate buffer from Sephadex G-15 the cation from the sample was accompanied by the anion from the eluent (P^-) and eluted in earlier fractions, and the cation from the eluent was accompanied by the anion from the sample (Cl^-) and eluted in later fractions. This cation-exchange reaction was assumed to occur by the differential elution of P^- and Cl^-.

This mechanism would raise a general rule, *i.e.*, cation-exchange reaction occurs between the sample and the eluent when anions from the sample and the eluent are eluted differentially due either to the different adsorbabilities of the anions on the Sephadex, partition of the ions on the Sephadex or the molecular sieving function of the Sephadex.

ACKNOWLEDGEMENTS

The authors are indebted to Professor Tsutomu Ohashi at Kanazawa Medical University, Professor Akira Uehara at Faculty of Science, Kanazawa University and Professor Motoichi Miyazaki at Department of Hygienic Chemistry, Faculty of Pharmaceutical Science, Kanazawa University. Our thanks go to the members of our laboratory for their discussions and to Miss Naoko Kawara for her help in preparing this manuscript.

REFERENCES

1 N. Yoza, *J. Chromatogr.*, 86 (1973) 325.
2 E. R. Nightingale, Jr., *J. Phys. Chem.*, 63 (1959) 1381.
3 T. Deguchi, A. Hisanaga and H. Nagai, *J. Chromatogr.*, 133 (1977) 173.
4 P. A. Neddermeyer and L. B. Rogers, *Anal. Chem.*, 41 (1969) 94.
5 B. Z. Egan, *J. Chromatogr.*, 34 (1968) 382.
6 Y. Ueno, N. Yoza and S. Ohashi, *J. Chromatogr.*, 52 (1970) 321.
7 T. Ogata, N. Yoza and S. Ohashi, *J. Chromatogr.*, 58 (1971) 267.

8 M. Sinibaldi and M. Lederer, *J. Chromatogr.*, 107 (1975) 210.
9 N. Yoza, T. Ogata and S. Ohashi, *J. Chromatogr.*, 52 (1970) 29.
10 T. Deguchi, *J. Chromatogr.*, 108 (1975) 409.
11 P. A. Neddermeyer and L. B. Rogers, *Anal. Chem.*, 40 (1968) 755.
12 W. Brown and K. Chitumbo, *J. Chromatogr.*, 63 (1971) 478.
13 D. L. Saunders and R. L. Pecsok, *Anal. Chem.*, 40 (1968) 44.
14 C. Fiske and Y. Subbarrow, *J. Biol. Chem.*, 81 (1926) 629.
15 D. Eaker and J. Porath, *Sep. Sci.*, 2 (1967) 507.
16 Y. Ueno, N. Yoza and S. Ohashi, *J. Chromatogr.*, 52 (1970) 469.
17 N. Yoza and S. Ohashi, *J. Chromatogr.*, 41 (1969) 429.
18 T. Okada, M. Miyakoshi, M. Inoue, Y. Nakabayashi and K. Teraoka, in preparation.
19 J. Sherma and G. Zweig, in G. Zweig and J. R. Whitaker (Editors), *Paper Chromatography and Electrophoresis*, Vol. II, Academic Press, London, 1971, pp. 6–29.

Journal of Chromatography, 481 (1989) 315–322
Elsevier Science Publishers B.V., Amsterdam — Printed in The Netherlands

CHROM. 21 773

ION CHROMATOGRAPHIC ELUTION BEHAVIOUR AND PREDICTION OF THE RETENTION OF INORGANIC MONOVALENT ANIONS USING A PHOSPHATE ELUENT

MASAHIRO MARUO, NAOKI HIRAYAMA and TOORU KUWAMOTO*
Department of Chemistry, Faculty of Science, Kyoto University, Kitashirakawa-Oiwake-Cho, Sakyo-ku, Kyoto 606 (Japan)
(First received April 10th, 1989; revised manuscript received July 6th, 1989)

SUMMARY

For the prediction of the retention times of inorganic anions with a phosphate eluent, Jenke's model was modified by using the elution system coefficients as a new concept instead of the calculated selectivity coefficients and measured effective column capacity as in Jenke's method. The capacity factors of analytes were precisely determined by using the modified calculation equation over a wide range of pH.

INTRODUCTION

Ion chromatography has been rapidly developed as an analytical method for inorganic and some organic anions and theoretical considerations have been also reported on the separation process, which is based on the partition of an analyte between the eluent and the ion-exchange resin[1–4]. For example, Gjerde *et al.*[5] and Haddad and Cowie[6] found theoretically the capacity factor of an analyte under a fixed charge ratio of analyte anion to eluent anion and fixed concentration of the eluent.

On the other hand, Hoover[7] interpreted theoretically the chromatographic retention data for phosphate and arsenate as a function of pH in carbonate–hydrogencarbonate eluents. Four premises were proposed, as follows: (1) the reduced retention volume of the analyte is equal to the volumetric distribution of the analyte; (2) the effective column capacity is expressed by the sum of adsorbed eluent anions; (3) electroneutrality is maintained during the elution process; and (4) for every pair of ionic species in the system, there is a constant selectivity coefficient corresponding to the concentration equilibrium for the exchange reaction. Moreover, Jenke and Pagenkopf[8,9] studied the retention behaviour of inorganic anions with phthalate eluents by using Hoover's model and obtained the selectivity coefficients by substituting the effective column capacity and experimental retention time into a modified equation. The reduced retention volume was calculated by using above-mentioned coefficients. In addition, a comparison of calculated with experimental retention times was carried out. However, it was difficult to obtain the same values of the effective exchange column capacity, because the measurements could not

0021-9673/89/$03.50

be performed under the same conditions. Accordingly, the selectivity coefficients were not correctly obtained.

On the basis of the above, we investigated the method for the prediction of the retention times of analyte anions with a phosphate eluent by using a modified Hoover equation, in which the empirically calculated elution system coefficients are used. It was found that the modified equation is useful for establishing the possibility of the separation of sample anions.

EXPERIMENTAL

Apparatus

The chromatographic system consisted of a Tosoh CCPD double plunger pump, a Rheodyne 7520 injection valve (sample injection volume 1 μl), a Shimadzu SPD-6AV UV detector (cell volume 0.6 μl) and a stainless-steel microbore column (120 mm $\times$ 0.5 mm I.D.) packed with Tosoh TSKgel IC-Anion-PW (particle size 10 μm, exchange capacity 30 μequiv./ml bed). The eluent flow-rate was 20 μl/min.

Eluents and standard solutions

Phosphoric acid (1 *M*), sodium dihydrogenphosphate and sodium hydroxide stock eluent solutions were prepared by dissolving special-grade reagents in deionized, distilled water, diluting to the appropriate volume and deaerating at a water-jet pump and by ultrasonic vibration.

Standard 1000 ppm (as each anion) sample solutions were prepared by dissolving sodium nitrate, sodium nitrite [pK_a = 3.14 (ref. 10)], sodium bromide, sodium bromate and sodium selenite [pK_{a_1} = 2.64, pK_{a_2} = 8.26 (ref. 10)] in distilled, deionized water. All solutions were prepared from analytical-reagent grade salts. Working standard solutions were obtained by diluting the stock solutions with the phosphate eluent.

RESULTS AND DISCUSSION

Theory; modification of Hoover's equations

According to Hoover's premises, the following equilibria should hold on the ion-exchange resin with a phosphate eluent [pK_{a_1} = 2.10, pK_{a_2} = 7.20, pK_{a_3} = 12.38 (ref. 10)] in the pH range 4.7–9.6:

$$K_1 = [\text{R–S}][\text{H}_2\text{P}^-]/[\text{R–H}_2\text{P}][\text{S}^-] \quad (1)$$

$$K_2 = [\text{R–S}]^2[\text{HP}^{2-}]/[\text{R}_2\text{–HP}][\text{S}^-]^2 \quad (2)$$

where K_1 and K_2 denote the ion-exchange equilibria constants between the monovalent phosphate anion (H_2P^-) and sample anion (S^-) and between the divalent anion (HP^{2-}) and the sample anion on the ion exchange resin (R).

The exchange capacity of an ion-exchange resin is expressed as follows:

$$\text{Cap} = [\text{R–H}_2\text{P}] + 2[\text{R}_2\text{–HP}] + [\text{R–S}] \quad (3)$$

where Cap denotes the ion-exchange capacity and [R–S] is neglected because the concentration of the analyte is very small. Substitution of eqns. 1 and 2 into eqn. 3 provides

$$\text{Cap} = [H_2P^-][\text{R–S}]/K_1[S^-] + 2[HP^{2-}][\text{R–S}]^2/K_2[S^-]^2 \quad (4)$$

The capacity factor (k') of an analyte anion and the total concentration ($[P_T]$) of the eluent are expressed by

$$k' = q[\text{R–S}]/[S^-] \quad (5)$$

$$[P_T] = [H_2P^-] + [HP^{2-}] \quad (6)$$

where q is the phase ratio.

The dissociation constant, K_{a_2}, of the phosphate eluent is expressed as a function of $[H^+]$ by

$$K_{a_2} = [H^+][HP^{2-}]/[H_2P^-] \quad (7)$$

Substitution of eqns. 5, 6 and 7 into eqn. 4 provides

$$[P_T]^{-1} = [1/(K_1q\text{Cap})]\{[H^+]/(K_{a_2} + [H^+])\}k' + [2/(K_2q^2\text{Cap})]\{K_{a_2}/(K_{a_2} + [H^+])\}k'^2 \quad (8)$$

By use of the elution system coefficients [$C_1 = 1/(K_1q\text{Cap})$ and $C_2 = 2/(K_2q^2\text{Cap})$],

$$[P_T]^{-1} = C_1\{[H^+]/(K_{a_2} + [H^+])\}k' + C_2\{K_{a_2}/(K_{a_2} + [H^+])\}k'^2 \quad (9)$$

At a given pH value,

$$[P_T]^{-1} = C_1'k' + C_2'k'^2 \quad (10)$$

If the charge number of analyte anion is n,

$$[P_T]^{-1} = C_1''k'^{1/n} + C_2''k'^{2/n} \quad (11)$$

As a result, if $[P_T]$, K_{a_2} and the pH of the eluent are fixed, C_1' and C_2' can be determined empirically by using the observed k', which is a measurable value under the defined conditions.

Concentration of phosphate eluent

Fig. 1 shows the dependence of the concentration of the phosphate eluent on the capacity factor of the nitrate anion. Although the relationship between the concentration of the eluent and the capacity factor is estimated to be nearly linear at pH 5.20 of the eluent ($[H_2P^-]$:$[HP^{2-}]$ = 99:1) because the dominant species in the eluent is monovalent phosphate, the observed relationship was curved, as shown in the figure. Moreover, although the slope of plots of $\log k'$ *versus* $-\log[P_T]$ represents the ratio of

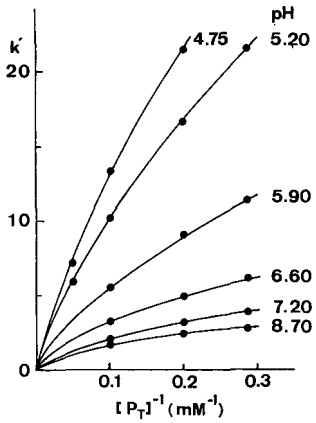

Fig. 1. Dependence of the capacity factor of nitrate on the concentration of phosphate eluent.

the charge of the sample anion to that of the eluent anion (according to Gjerde *et al.*[5]), the measured value at pH 5.20 was 0.71 compared with the calculated value of 0.99. At pH 7.20, the measured value of the slope was 0.46 compared with the calculated value of 0.67. These facts show that the divalent phosphate anion is very strongly retained in the column compared with the monovalent phosphate anion. Therefore, even if the ratio of the concentration of divalent phosphate anion to that of total phosphate in the eluent is small, the influence of the divalent anion on the retention time of the sample anion cannot be neglected because the measured value of the slope was smaller than the calculated value. The relationship between k' and $[P_T]^{-1}$ on the other anions was almost the same as that of nitrate ion.

pH of phosphate eluent

Fig. 2 shows the dependence of the pH of the phosphate eluent on the capacity factors of analyte anions. The capacity factors of the analytes decreased rapidly with increasing pH in the pH range studied, in which the divalent to monovalent

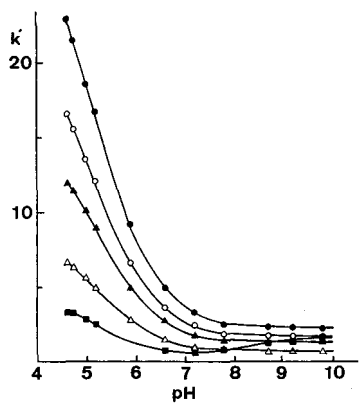

Fig. 2. Dependence of the capacity factor on the pH of the eluent. Sample: (●) nitrate; (○) bromide; (▲) nitrite; (△) bromate; (■) selenite. Eluent: 5 m*M* phosphate.

concentration ratio of phosphate anions is very small, and the intensified elution power is maintained above pH 7, where the monovalent anion is converted into the divalent anion.

Calculation of the elution coefficients C_1 and C_2

To calculate C_2 in eqn. 9, the simultaneous equations were solved by selecting two different pH values (A, B) of the eluent. The C_2 values obtained are given in Table I. As can be seen, if pH(B) is 8.70 or 9.20, C_2 of nitrate is 0.038 regardless of pH(A) in the range 4.75–9.20. At pH(B) 9.60, the C_2 values become large. This may be caused by the influence of trivalent phosphate formed at increasing pH. Finally, C_2 values were obtained easily at pH 8.70–9.20, because the elution power of the monovalent phosphate anion is very weak at high pH and the first term of eqn. 9 can be neglected.

C_1 values obtained by solving simultaneous equations were influenced considerable, especially at high pH. Accordingly, C_1 had to be determined at low pH in order to make the second term of eqn. 9 as small as possible. In practice, C_1 values were obtained by substituting the C_2 value at pH 8.70 into eqn. 9. The results are given in Table II. From these results, it was concluded that a pH of the eluent lower than 5.00 is to be preferred (the pH of the eluent is 2.2 smaller than the pK_{a_2} value of phosphate).

From eqn. 9, the following relationship between C_1 and C_2 is obtained: $C_1 = 1/(K_1 q\mathrm{Cap})$ and $C_2 = 2/(K_2 q^2 \mathrm{Cap})$ from eqn. 9;

$$C_1^2/C_2 = \tfrac{1}{2}(K_2/K_1^2)\,(1/\mathrm{Cap})$$

$$= \tfrac{1}{2}([\mathrm{R\text{–}H_2P}]^2[\mathrm{HP^{2-}}]/[\mathrm{R_2\text{–}HP}]\,[\mathrm{H_2P^-}]^2)\,(1/\mathrm{Cap})$$

$$= \text{constant} \qquad (12)$$

where K_2/K_1^2 is the selectivity coefficient between monovalent and divalent phosphate anions on the ion-exchange resin, which is the same as the term K_E in Jenke's

TABLE I

C_2 VALUES (l/mmol) OBTAINED BY SOLVING THE SIMULTANEOUS EQUATIONS

Sample: nitrate; P_T = 5 m*M*.

pH (A)	*pH (B)*						
	4.75	*5.20*	*6.60*	*7.20*	*8.70*	*9.20*	*9.60*
4.75	–	0.029	0.036	0.036	0.038	0.038	0.041
5.20		–	0.036	0.036	0.038	0.038	0.041
6.60			–	0.036	0.038	0.038	0.041
7.20				–	0.038	0.038	0.042
8.70					0.038[a]	0.038	0.042
9.20						0.038[a]	0.044
9.60							0.041[a]

[a] Determined by neglecting the first term in eqn. 9.

TABLE II

C_1 VALUES (l/mmol) OBTAINED BY USING C_2

P_T = 5 m*M*.

pH	*Sample*			
	NO_3^- ($C_2 = 0.038$)	Br^- ($C_2 = 0.072$)	NO_2^- ($C_2 = 0.13$)	BrO_3^- ($C_2 = 0.41$)
4.62	0.0065	0.0090	0.012	0.022
4.75	0.0065	0.0090	0.012	0.023
5.00	0.0064	0.0087	0.012	0.021
Av. (pH = 4.62–5.00)	0.0065	0.0089	0.012	0.022
5.20	0.0057	0.0078	0.011	0.020
5.90	0.0059	0.0081	0.011	0.020
6.60	0.0042	0.0038	0.008	0.024

TABLE III

C_1, C_2 AND C_1^2/C_2 FOR EACH SAMPLE

Sample	C_1 (l/mmol)	C_2 (l/mmol)	C_1^2/C_2 (l/mmol)
NO_3^-	0.0065	0.038	0.0011
Br^-	0.0089	0.072	0.0011
NO_2^-	0.012	0.13	0.0011
BrO_3^-	0.022	0.41	0.0012
$HSeO_3^-$	0.049	0.93[a]	0.0026

[a] C_2 value of selenite was determined at pH 7.20.

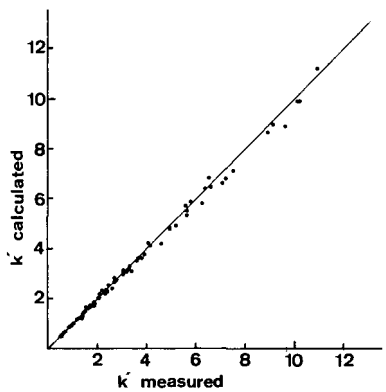

Fig. 3. Comparison of measured and calculated capacity factors by eqn. 9. $k'_{calc.s}$ of each sample (nitrate, bromide, nitrite and bromate) was calculated by using C_1 and C_2 as shown in Table III. The pH used is one of 4.62, 4.75, 5.00, 5.20, 5.90, 6.60, 7.20, 7.80, 8.70, 9.20 and 9.60, and the eluent concentration is one of 3.5, 5, 10 and 20 m*M*. $k'_{meas.s}$ values were measured under the same conditions as $k'_{calc.s}$.

equation[9]. C_1^2/C_2 values are obtained by using above-mentioned C_1 and C_2 values. The results are given in Table III. As can be seen, the C_1^2/C_2 values for each sample were approximately the same, except for that of selenite. The C_1 and C_2 values of selenite were not obtained accurately, because the charge number of selenite varies under acidic and basic conditions. As mentioned above, if the total concentration and the pH of the eluent are fixed under the same chromatographic conditions, k' can be evaluated by using the elution system coefficients C_1 and C_2.

In the calculation of k', the C_2 value obtained at pH 8.70 and the average value of C_1 obtained at pH below 5.00 were used. Fig. 3 shows the comparison of calculated and measured capacity factors. The measured and calculated values agree well in the pH range 4.62–9.60; the average relative error is 2.5%

It is concluded that, if C_1 and C_2 are determined experimentally, k' for analytes over a wide range of pH and concentrations of the eluent can be precisely predicted.

Chromatograms

On the basis of the above results, the separation of nitrate, bromide, nitrite, bromate and selenite was undertaken by using the conditions 5 m*M* phosphate eluent, pH 5.20 and flow-rate 20 μl/min. The chromatograms obtained are shown in Fig. 4.

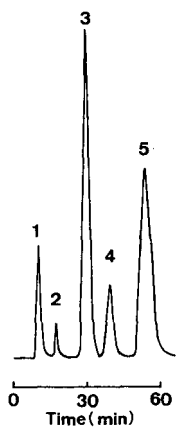

Fig. 4. Chromatograms of inorganic anions. Sample: 1 = selenite; 2 = bromate; 3 = nitrite; 4 = bromide; 5 = nitrate. Eluent: 5 m*M* phosphate (pH 5.20). Wavelength: 210 nm. Flow-rate: 20 μl/min.

ACKNOWLEDGEMENT

The authors gratefully acknowledge financial support from the Nippon Life Insurance Foundation.

REFERENCES

1 P. R. Haddad and A. L. Heckenberg, *J. Chromatogr.*, 300 (1984) 357.
2 T. H. Jupille and D. T. Gjerde, *J. Chromatogr. Sci.*, 24 (1986) 427.
3 J. S. Fritz, *Anal. Chem.*, 59 (1987) 335A.
4 J. S. Fritz, *J. Chromatogr.*, 439 (1988) 3.
5 D. T. Gjerde, J. S. Fritz and G. Schmuckler, *J. Chromatogr.*, 186 (1979) 509.
6 P. R. Haddad and C. E. Cowie, *J. Chromatogr.*, 303 (1984) 321.
7 T. B. Hoover, *Sep. Sci. Technol.*, 17 (1982) 295.
8 D. R. Jenke and G. K. Pagenkopf, *Anal. Chem.*, 56 (1984) 88.
9 D. R. Jenke, *Anal. Chem.*, 56 (1984) 2674.
10 A. J. Dean, *Lange's Handbook of Chemistry*, McGraw-Hill, New York, 13th ed., 1985.

Journal of Chromatography, 481 (1989) 323–330
Elsevier Science Publishers B.V., Amsterdam — Printed in The Netherlands

CHROM. 21 817

DETERMINATION OF TRACE LEVELS OF TOTAL CARBONATE-CARBON BY INDIRECT PHOTOMETRIC ION CHROMATOGRAPHY WITH NITROGEN PURGING

KAZUICHI HAYAKAWA*, SACHIE KITAMOTO, NOBORU OKUBO, SEIJI NAKAMURA and MOTOICHI MIYAZAKI
Faculty of Pharmaceutical Sciences, Kanazawa University, 13-1 Takara-machi, Kanazawa-shi 920 (Japan)
(Received May 8th, 1989)

SUMMARY

Purging with nitrogen substantially prevented atmospheric carbon dioxide from dissolving in the eluent used in indirect photometric ion chromatography. Total carbonate-carbon at trace levels could be determined as hydrogencarbonate by this method. By using an analytical column (250 × 4.6 mm I.D.) packed with MCI SCA-02 and $5.0 \cdot 10^{-4}$ *M* sodium hydrogenphthalate–$1.5 \cdot 10^{-4}$ *M* N-2-hydroxyethylpiperazine-N'-2-ethanesulphonic acid (HEPES) (pH 6.5) as the eluent, hydrogencarbonate was detected as a negative peak at 250 nm. The detection limit (signal-to-noise ratio = 2) was $1.4 \cdot 10^{-11}$ mol ($7 \cdot 10^{-7}$ *M* with an injection volume of 20 μl) and the calibration graph was linear from $3.0 \cdot 10^{-11}$ to $3.8 \cdot 10^{-9}$ mol ($r = 0.994$). The coefficient of variation was less than 2% on injection of $4 \cdot 10^{-10}$ mol. Total carbonate-carbon at levels as low as 10^{-4}–10^{-6} *M* level could be determined accurately. The errors in the analysis of practical samples by the method without nitrogen purging are demonstrated.

INTRODUCTION

Carbon dioxide plays important roles as carbonic acid, hydrogencarbonate and carbonate in biological fluids, liquid foods and environmental water samples[1–3], and an accurate and sensitive method for the determination of total carbonate-carbon is required. Atmospheric carbon dioxide causes serious problems both in the use of ultra-pure water and in the sensitive determination of anions.

For the sensitive determination of aqueous total carbonate-carbon, flow-injection analyses based on an ultraviolet (UV)–visible absorption detector[4,5] and optical sensors with pH-sensitive fluorescent dyes[6,7] have been developed. However, these methods could not determine both total carbonate-carbon and other anions simultaneously. Ion exclusion chromatography with conductometric detection, which was effective for weak acids such as carboxylic acids, has also been used for the determination of total carbonate-carbon[8,9]. Recently, a modified ion exclusion chromatographic method with two enhancement columns after the analytical column

0021-9673/89/$03.50

has been reported[10]. Although the sensitivity of the method is high, the enhancement columns must be regenerated when exhausted.

Indirect photometric ion chromatography (IPIC) based on indirect photometric detection[11] has been used in the determination of anions and cations with a conventional high-performance liquid chromatographic system[12–14]. It was reported that IPIC could detect hydrogencarbonate when the eluent pH was maintained nearly neutral[15]. Although total carbonate-carbon at concentrations higher than 10^{-4} *M* could be determined in samples such as tap water and river water[16,17], lower concentrations could not be determined accurately. When a trace amount of sodium hydrogencarbonate was injected into an IPIC system using an eluent that had not been treated to remove atmospheric carbon dioxide, the negative peak (decrease in UV absorbance) observed was smaller than expected, whereas a small positive peak was observed at the same retention time on injection of deionized water. This peak at the retention time of hydrogencarbonate, which is termed the "carbonate-system peak" in this paper, disturbed the determination of hydrogencarbonate at low levels. Atmospheric carbon dioxide dissolved in the eluent was considered to be the cause.

It is necessary to remove this interference due to carbon dioxide in the sensitive and accurate determination of total carbonate-carbon. Purging with an inert gas[18] and gas headspace treatment[19] have been reported to remove gases such as oxygen from mobile phases. We found that gas purging also removed carbon dioxide from eluents for IPIC. This paper describes the effect of nitrogen purging on the determination of total carbonate-carbon by IPIC.

EXPERIMENTAL

Chemicals

Sodium hydrogenphthalate and N-2-hydroxyethylpiperazine-N′-2-ethanesulphonic acid (HEPES) were purchased from Tokyo Kasei (Tokyo, Japan) and Wako (Osaka, Japan), respectively. All other chemicals were of analytical-reagent grade. Water was purified with a Millipore (Bedford, MA, U.S.A.) Milli-Q system. "Deionized water" in this paper means water just after repurification with this system.

Instrumentation

The HPLC system for IPIC consisted of a Jasco (Tokyo, Japan) 880-PU pump, a Rheodyne (Cotati, CA, U.S.A.) 7125 injector with a 20-μl loop, a Jasco 860-CO column oven, a Jasco 870 UV absorbance detector and a Jasco 805-GI graphic integrator. A Jasco 880-51 on-line degasser was also used. The nitrogen purging system consisted of a nitrogen gas bomb (purity over 99.99%), a gas washing bottle (glass, inner volume 200 ml) that contained 150 ml of water and an eluent reservoir (glass) with a gas purging filter. A schematic diagram of the system is shown in Fig. 1.

Operating conditions

An analytical column (250 × 4.6 mm I.D., stainless steel) and a guard column (50 × 4.6 mm I.D., stainless steel) were packed with MCI SCA-02 (styrene–divinylbenzene copolymer with an anion-exchange capacity of 0.01 mequiv./g and a particle size of 20 μm) (Mitsubishi Chemical, Tokyo, Japan). The eluent was $5.0 \cdot 10^{-4}$ *M* sodium hydrogenphthalate–$1.5 \cdot 10^{-4}$ *M* HEPES the pH of which was

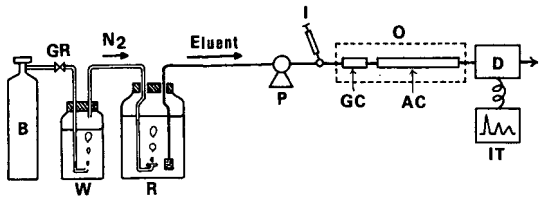

Fig. 1. Schematic diagram of IPIC with the nitrogen purging system. B = Nitrogen gas bomb; GR = gas regulator; W = gas washing bottle; R = eluent reservoir; P = pump; I = injector; O = column oven; GC = guard column; AC = analytical column; D = UV detector; IT = integrator.

adjusted to 6.5 ± 0.1 with sodium hydroxide. The eluent was treated with a 0.40-μm nylon membrane filter before use. Nitrogen was purged into the eluent continuously at a flow-rate of 50 ml/min during the experiment. The columns were equilibrated overnight with this nitrogen-purged eluent before use. The flow-rate of the eluent was 1.0 ml/min, the columns were kept at 40°C and the detection wavelength was 250 nm. Under these conditions, hydrogencarbonate, chloride and sulphate, which were standard anions, were separately determined as negative peaks at 6.0 min (capacity factor $k' = 0.8$), 7.7 min ($k' = 1.3$) and 12.9 min ($k' = 2.9$), respectively.

RESULTS AND DISCUSSION

According to Henry's law, the mass of a slightly soluble gas that dissolves in a definite mass of a liquid at a given temperature is very nearly directly proportional to the partial pressure of that gas, according to the following equation[20]:

$$CO_2(g) \overset{K_P}{\rightleftharpoons} CO_2(aq.) \tag{1}$$

where K_P is the Henry's law partition constant for carbon dioxide. In aqueous solution, carbon dioxide exists in three forms, carbonic acid (H_2CO_3), hydrogencarbonate (HCO_3^-) and carbonate (CO_3^{2-}), as indicated by the equation

$$H_2CO_3 \overset{K_1}{\rightleftharpoons} H^+ + HCO_3^- \overset{K_2}{\rightleftharpoons} 2H^+ + CO_3^{2-} \tag{2}$$

where pK_1 is 6.34 and pK_2 is 10.25[21]. In the eluent of pH 6.5 which was used in this work, the main species are HCO_3^- and H_2CO_3. H_2CO_3 in eqn. 2 is calculated as CO_2(aq.) in eqn. 1 and does not act as an anion in an anion-exchange column.

Let us consider here that the eluent contains hydrogencarbonate at the trace level and make the simplification that sample hydrogencarbonate elutes as a square pulse peak from an analytical column as shown in Fig. 2. If C_E and C_B are the concentration of UV-absorbing eluent anions and that of background hydrogencarbonate in the eluent, respectively, the total anion concentration in the effluent before the sample injection is $C_E + C_B$ and is constant. When the sample hydrogencarbonate peak is eluted at a concentration C_S, the increase in hydrogencarbonate concentration in the

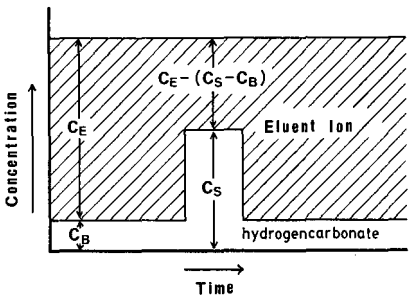

Fig. 2. Elution profile model for hydrogencarbonate.

effluent is given by $C_S - C_B$. Therefore, the signal (A_{S-E}) on the baseline is given by the equation

$$A_{S-E} = [C_E - (C_S - C_B)]\,A_E + C_S A_B - C_E A_E - C_B A_B$$

$$= (C_S - C_B)\,(A_B - A_E) \tag{3}$$

where A_E and A_B are the absorbance of eluent species and that of hydrogencarbonate, respectively. Eqn. 3 is simplified into the following equation as A_B is zero at 250 nm:

$$A_{S-E} = -(C_S - C_B)A_E \tag{4}$$

Eqn. 4 indicates that the signal is negative when C_S is higher than C_B, positive when C_S is lower than C_B and there is no signal when C_S is the same as C_B. If the eluent does not contain hydrogencarbonate ($C_B = 0$), the carbonate-system peak is not observed on injection of deionized water. Eqn. 1 suggests that carbon dioxide might be eliminated from an eluent with a decrease in its atmospheric partial pressure. The pressure can be decreased by displacing air to another gas. Nitrogen is readily available for purging an eluent and is advantageous from safety and economic points of view, although an inert gas such as argon or helium might be equally effective.

Fig. 3 shows chromatograms obtained by using $5.0 \cdot 10^{-4}$ *M* sodium

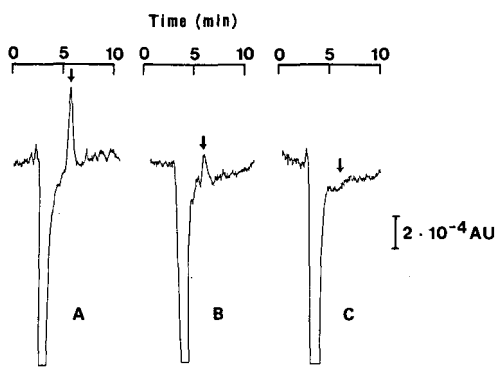

Fig. 3. Chromatograms of carbonate-system peak on injection of deionized water. The eluent was treated as follows: (A) none; (B) through an on-line degasser; (C) by the nitrogen purging system. The arrow indicates the position of the carbonate-system peak.

hydrogenphthalate–1.5 · 10^{-4} *M* HEPES (pH 6.5) as the eluent treated in the three different ways. Deionized water was injected as a sample. A positive peak (carbonate-system peak) was detected at 6.0 min without any treatment (Fig. 3A); the peak height decreased on passing through an on-line degasser as commonly used in HPLC (Fig. 3B); and the peak was not detected on using the nitrogen purging system (Fig. 3C). These results show that the nitrogen purging effectively prevents atmospheric carbon dioxide from dissolving in the eluent. Similar results were obtained when benzoate and benzenesulphonate eluents were tested. In the present system, a gas washing bottle was used to saturate the dry gas with water vapour and to wash out small amounts of contaminants from gas so as not to disturb the baseline stability.

Another interference from atmospheric carbon dioxide was observed in the preparation of hydrogencarbonate solutions. Dilute sodium hydrogencarbonate standard solutions were prepared by two different procedures. In the first series, a vial (inner volume *ca.* 26 ml) containing a small stirring bar was filled with deionized water under a nitrogen atmosphere and immediately stoppered with a silicone-rubber septum. After an aliquot of 0.1 *M* sodium hydrogencarbonate stock solution had been added to the vial by a microsyringe through the septum, the mixture was stirred for 2 min. In the second series, water was stirred overnight aerobically in a polyethylene bottle without a cap. Dilute sodium hydrogencarbonate solution was prepared with this water in a vial without a septum. Plots of peak area *vs.* amount injected for the two series are shown in Fig. 4. The former was a straight line ($r = 0.994$) from 3.0 · 10^{-11} to 3.8 · 10^{-9} mol (A), whereas the latter was curved (B). Line A could be used to represent dilute standard hyrogencarbonate solution. The difference between the two graphs might be due to the atmospheric carbon dioxide dissolved in the water. Therefore, the former procedure was used in subsequent experiments.

The coefficient of variation for the determination of hydrogencarbonate was less than 2% on injection of 4 · 10^{-10} mol. The determination error was as small as those of

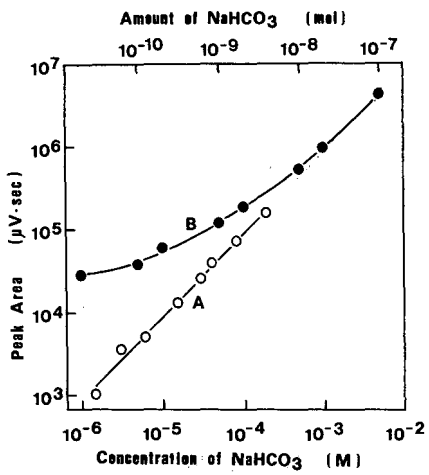

Fig. 4. Influence of atmospheric carbon dioxide on the calibration graphs for sodium hydrogencarbonate. Sodium hydrogencarbonate solutions were prepared in silicone rubber-stoppered vials with deionized water (A) and in open vials with air-equilibrated water (B).

TABLE I

DETERMINATION ERRORS OF THREE ANIONS

Anion	*Amount* (10^{-10} *mol*)[a]	*Coefficient of variation (%)* ($n = 5$)
Hydrogencarbonate	200	0.57
	20	1.4
	4	1.5
Chloride	200	0.50
	20	1.9
	2	1.5
Sulphate	200	0.20
	20	2.0
	2	3.4

[a] Injection volume, 20 μl.

chloride and sulphate, which were not affected by atmospheric carbon dioxide (Table I). The detection limit (signal-to-noise ratio = 2) of hydrogencarbonate was $1.4 \cdot 10^{-11}$ mol ($7 \cdot 10^{-7}$ *M* on injection of 20 μl). This value is more than ten times smaller than that obtained by the modified ion exclusion IC method, which gave the lowest limit in recent reports[10].

The concentration of total carbonate-carbon determined by IPIC without the nitrogen purging system is lower than the real concentration. The error is not negligible as the amount injected is small. Table II shows the results of the determination of total carbonate-carbon in aqueous samples by IPIC with and without the nitrogen purging system; the differences are given as relative values. Deionized water showed a negative peak with nitrogen purging but a positive peak without purging. The relative differences for air-bubbled water and for rain water were 37% and 13%, respectively. With an increase in concentration, the value becomes too small to be distinguished

TABLE II

ANALYTICAL RESULTS FOR TOTAL CARBONATE-CARBON BY INDIRECT PHOTOMETRIC ION CHROMATOGRAPHY (A) WITH AND (B) WITHOUT NITROGEN PURGING

Sample	*Concentration* (10^{-5} *M*)[a]		*Relative difference* [100 (*A* − *B*)/*A*] (%)
	A	*B*	
Deionized water	0	[b]	–
Air-bubbled water	3.0	1.9	37
Rain water	6.0	5.2	13
Tap water	43.3	42.4	2.1
River water	49.5	49.8	−0.6

[a] Mean values ($n = 3$).
[b] Positive peak.

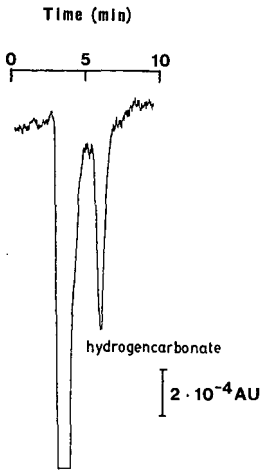

Fig. 5. Typical chromatogram of air-equilibrated water.

from the determination error. This was the reason why the value was positive (2.1%) for tap water but negative (−0.6%) for river water.

Total carbonate-carbon in air-equilibrated water could be determined by the present method, as shown in Fig. 5. The concentration was $1.2 \cdot 10^{-5}$ M when line A in Fig. 4 was used as a calibration graph. On the other hand, the concentration of carbon dioxide in air-equilibrated water can be calculated as

$$CO_2(aq.) = 3.9 \cdot 10^{-2} \cdot 0.03 \cdot 10^{-2}$$

$$= 1.17 \cdot 10^{-5}\ M \quad (5)$$

as the Henry's law partition constant (K_p) of carbon dioxide is $3.9 \cdot 10^{-2}$ M per atom at 20°C and the concentration of carbon dioxide in air is 0.03% (v/v). This close agreement between the observed and calculated values indicates the reliability of the present method for the determination of low levels of carbonate-carbon.

REFERENCES

1 B. A. Shapiro, R. A. Harrison and J. R. Walton (Editors), *Clinical Application of Blood Gases*, Year Book Med., Chicago, IL, 1977, pp. 1–39.
2 H. Forssell and L. Olbe, *Scand. J. Gastroenterol.*, 20 (1985) 767–774.
3 K. Tabata, E. D. Jacobson, M. Chen, R. F. Murphy and S. N. Joffe, *Gastroenterology*, 87 (1984) 396–401.
4 M. A. Kenny and M. H. Cheng, *Clin. Chem.*, 18 (1972) 352–354.
5 J. M. Hicks, F. T. Aldrich and M. Iosefsohn, *Clin. Chem.*, 22 (1976) 1868–1871.
6 Z. Zhujum and W. R. Seitz, *Anal. Chim. Acta*, 160 (1984) 305–309.
7 C. Munkolm and D. R. Walt, *Talanta*, 35 (1988) 109–112.
8 K. Tanaka, *Bunseki Kagaku*, 30 (1981) 358–362.
9 J. R. Kreling and J. DeZwaan, *Anal. Chem.*, 58 (1986) 3028–3031.
10 K. Tanaka and J. S. Fritz, *Anal. Chem.*, 59 (1987) 708–712.

11 H. Small and T. E. Miller, *Anal. Chem.*, 54 (1982) 462–469.
12 M. Miyazaki, K. Hayakawa and S. Choi, *J. Chromatogr.*, 323 (1985) 443–446.
13 K. Hayakawa, T. Sawada, K. Shimbo and M. Miyazaki, *Anal. Chem.*, 59 (1987) 2241–2245.
14 K. Hayakawa and M. Miyazaki, *LC · GC, Mag. Liq. Gas Chromatogr.*, 6 (1988) 508–512.
15 K. Hayakawa, H. Hiraki and M. Miyazaki, *Bunseki Kagaku*, 34 (1985) T71–T76.
16 K. Hayakawa, C. Yoshioka and M. Miyazaki, *Hokuriku-Koshueisei-Gakkaishi*, 12 (1985) 14–18.
17 T. Hironaka, M. Oshima and S. Motomizu, *Bunseki Kagaku*, 35 (1987) 503–507.
18 J. Doehl, *J. Chromatogr. Sci.*, 26 (1988) 7–11.
19 R. Slingsly, *J. Chromatogr.*, 371 (1986) 373–382.
20 Chemical Society of Japan, *Shin-Jikkenkagaku-Koza*, Vol. 1, Maruzen, Tokyo, 1975, p. 227.
21 Japan Society for Analytical Chemistry, *Bunseki-Kagaku Data Book*, Maruzen, Tokyo, 1983, p. 122.

Journal of Chromatography, 481 (1989) 331–342
Elsevier Science Publishers B.V., Amsterdam — Printed in The Netherlands

CHROM. 21 774

THIN-LAYER CHROMATOGRAPHIC BEHAVIOUR OF SOME STYRYL CYANINE DYES DERIVED FROM PYRIDINE

LALIT N. PATNAIK*[a], B. N. PATTANAIK, M. MOHANTY and A. SATAPATHY
Department of Chemistry, Ravenshaw College, Cuttack 753 003, Orissa (India)
(First received March 7th, 1989; revised manuscript received June 26th, 1989)

SUMMARY

The chromatographic R_M values for some styryl cyanine iodides derived from pyridine were obtained by thin-layer chromatography using propanol–water–acetic acid solvent systems in various proportions. Linear free energy relationship studies were carried out with some electronic, steric and lipophilic parameters, either singly or in combination with each other. The results indicate that the steric factor has the greatest influence on the chromatographic behaviour. An attempt was made to establish the nature of dye–substrate adsorption by correlation with the theoretical charge densities (CNDO/2 and INDO).

INTRODUCTION

In the past few years, several reports have appeared on the potential usefulness of organic dyes in a number of devices such as photovoltaics, dye lasers and photo- and thermochromic materials. As most of these applications require dyes of exceptionally pure quality, the analytical chemistry of dyes, particularly rapid methods for determining their purity and identity has become of considerable importance. Chromatographic methods (particularly paper and thin-layer chromatography) continue to be popular in this respect. In addition chromatographic methods can also be valuable aids in constitutional analysis and for particular applications chromatographic data can be correlated with activity (*e.g.*, photovoltaic properties). In this context, we have studied the thin-layer chromatographic (TLC) behaviour of some styryl cyanine dyes, which are under investigation for their photovoltaic properties. The dye types studied are shown in Scheme 1.

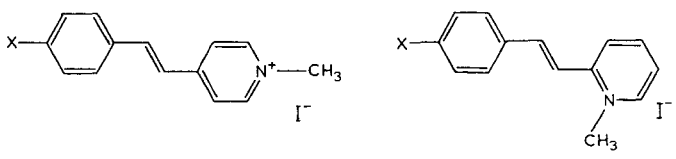

Scheme 1. Structures of 4-linked pyridine styryl dyes (left) and 2-linked pyridine styryl dyes (right). X = $N(CH_3)_2$; OCH_3; OH; CH_3; H; Cl; and NO_2.

[a] Present address: State Prevention and Control of Pollution Board, 118/A, Nilakantha Nagar, Unit-VIII, Bhubaneswar 751012, Orissa, India.

0021-9673/89/$03.50

TABLE I
R_F AND R_M VALUES

Dyes	*Mole fraction of water*	*Substituent*													
		$N(CH_3)_2$		OCH_3		OH		CH_3		H		Cl		NO_2	
		R_F	R_M	R_F	R_M	R_F	R_M	R_F	R_M	R_F	R_M	R_F	R_M	R_F	R_M
4-Linked	0.445	0.09	1.028	0.06	1.190	0.08	1.091	0.07	1.138	0.07	1.138	0.06	1.190	0.04	1.388
pyridine Styryl	0.548	0.16	0.718	0.13	0.830	0.14	0.804	0.12	0.859	0.11	0.921	0.11	0.921	0.07	1.114
	0.618	0.24	0.502	0.18	0.652	0.20	0.583	0.19	0.642	0.16	0.706	0.18	0.663	0.10	0.954
	0.669	0.27	0.437	0.22	0.555	0.26	0.461	0.26	0.461	0.23	0.528	0.23	0.537	0.14	0.778
	0.708	0.39	0.202	0.26	0.461	0.32	0.324	0.30	0.361	0.28	0.413	0.30	0.368	0.17	0.684
2-Linked	0.445	0.08	1.067	0.06	1.218	0.06	1.163	0.05	1.279	0.04	1.313	0.06	1.190	0.03	1.479
pyridine Styryl	0.548	0.16	0.730	0.11	0.905	0.13	0.848	0.13	0.831	0.11	0.889	0.12	0.875	0.06	1.163
	0.618	0.24	0.495	0.19	0.632	0.22	0.555	0.22	0.537	0.22	0.555	0.21	0.564	0.10	0.954
	0.669	0.26	0.445	0.19	0.642	0.22	0.546	0.20	0.602	0.19	0.622	0.22	0.555	0.11	0.889
	0.708	0.21	0.564	0.17	0.684	0.19	0.622	0.18	0.673	0.16	0.718	0.19	0.622	0.09	0.99

Attempts were also made to study the structure–adsorption behaviour in the framework of linear free energy relationships (LFER). Reports on this aspect of dyes appear to be very scanty.

EXPERIMENTAL

R_F values of styryl dyes derived from 2- and 4-linked pyridine were determined by TLC using silica gel G (TLC grade, Merck) as sorbent. The TLC plates (20 × 10 cm) were prepared by coating them with a silica gel slurry (20 g of silica gel in 50 ml of water) to a thickness of 0.25 mm. The TLC plates were dried at room temperature and then activated at 110°C for 15 min.

The chromatographic chambers were saturated with the appropriate composition of water–*n*-propanol–acetic acid (saturation time, 24 h; temperature of the chamber, 30°C). Initial experiments with water–*n*-propanol mixtures resulted in the formation of streaks, which could be avoided by the addition of acetic acid at a concentration below 2%. The presence of acetic acid was taken into account in calculating the mole fraction of water, at different values of which the R_F values are reported below.

The activated plates were spotted with the dye solution in acetone and then conditioned in the solvent-saturated chromatographic chamber for 10–15 min before development started. All the experiments were carried out in duplicate. The spots were detected in an iodine chamber and the R_F values were measured.

RESULTS AND DISCUSSION

Chromatographic parameters

The theoretical basis for the relationship between R_F values and chemical structure was first proposed by Consden *et al.*[1]. Subsequently, Martin[2] deduced that for ideal solutions the partition coefficient, P, of a substance A between two phases is related to the free energy required to transport 1 mole of A from one phase to another.

Bate-Smith and Westall[3] introduced the term R_M, defined as

$$R_M = \log\left(\frac{1}{R_F} - 1\right) \tag{1}$$

Boyce and Milborrow[4] investigated the theoretical basis for the relationship between the partition coefficient and R_M values and pointed out that the R_M value for a substituent is a free energy-related term analogous to π used by Hansch and Fujita[5], and consequently it is possible to correlate R_M with other free energy-related terms. There have been various reports of a very good correlation between R_M and π values[6]. It was pointed out, however, that R_M cannot be considered as an expression of the true partition coefficient as it does not take into account the ratio of the cross-sectional areas of the mobile and stationary phases[7]. We therefore carried out some of the correlations using log R_F. It was found, however, that there is hardly any significant difference between the results obtained with log R_F and R_M. The following discussions therefore pertain to the results obtained with R_M.

Solvent effects

R_F values were determined at five different compositions of water–*n*-propanol–acetic acid. The R_F values were found to increase with increasing water content, *i.e.*, with increasing solvent polarity (Table I) and the correlation of R_M with the mole fraction of water (x) was excellent for 4-linked pyridine-substituted styryl dyes. With the 2-linked pyridine dyes the R_F values increased with increasing water content up to a certain point and then decreased. For different substituted compounds this point was reached at different mole fractions of water. However, a value of 0.708 seems to be the limit beyond which the R_F values decrease in all instances. This observation indicates that perhaps there is a change in the retention mechanism. Similar observations have been reported in connection with the reversed-phase chromatographic behaviour of steroids[8,9]. The correlation of R_M of the 2-linked pyridine dyes with x up to a value of 0.708 was found to be satisfactory (Table II).

Linear free energy relationships

The reported correlations between chromatographic behaviour and π may be interpretated as the transport process being the step that determines the chromatographic activity[10]. Such correlations, however, do not preclude the possibility that the electronic properties and the steric arrangement of the molecule could also be important factors for interaction with the stationary phase in partition chromatography. In other words, it should be established which of the lipophilicity, electronic factors and stereochemistry of the molecules is the most important factor with regard to the chromatographic activity, either individually or combined. Accordingly, we studied four types of correlations:

(i) correlations with Hammet or related substituent parameters that are supposed to reflect the polar and/or resonance effects of the substituents[11];

(ii) correlations with the lipophilic parameter[5];

(iii) correlations with Taft's[12] E_s and Charton's[13–15] ν steric parameters;

(iv) correlations with combinations of (i) or (ii) with the steric parameters in (iii).

Correlations were carried out with the following equations:

for single-parameter correlations:

$$R_M \text{ (or log } R_F) = as + b \tag{2}$$

TABLE II

CORRELATION RESULTS WITH $R_M = ax + b$

x = Mole fraction of water.

Substituent	*4-Linked pyridine styryl dyes*				*2-Linked pyridine styryl dyes*			
	S	*R*	*a*	*b*	*S*	*R*	*a*	*b*
$N(CH_3)_2$	0.051	0.993	−2.963	2.248	0.124	0.938	−2.184	1.965
OCH_3	0.039	0.995	−2.738	2.374	0.111	0.950	−2.22	2.143
OH	0.013	0.999	−2.894	2.382	0.120	0.946	−2.312	2.128
CH_3	0.017	0.999	−3.002	2.486	0.168	0.916	−2.487	2.271
H	0.035	0.996	−2.797	2.413	0.175	0.913	−2.52	2.325
Cl	0.030	0.998	−3.101	2.589	0.119	0.951	−2.419	2.207
NO_2	0.017	0.999	−2.682	2.587	0.107	0.948	−2.099	2.350

for two-parameter correlations:

$$R_M \text{ (or log } R_F) = as_1 + bs_2 + c \quad (3)$$

where s, s_1 and s_2 are appropriate substituent parameters.

Single parameter correlations

Very poor correlations were obtained with both dye series with Hansch and Fujita's lipophilic parameter π (Table III).

As has already been pointed out, the parameter R_M, which is assumed to be a measure of lipophilic character, has been shown to correlate well with π for a large number of systems. The lack of any correlation in this study may be due to one or more of the following reasons. The transport process perhaps is not the most crucial factor in the chromatographic behaviour. The chromatographic process evidently is not analogous to the octanol–water system and the low correlation between π and R_M may be due to the electronic effects of the substituent. As the dyes are ionic in nature, they are likely to undergo dissociation in the aqueous–organic chromatographic system. It has been pointed out earlier that an R_M–π correlation is valid only if the degree of dissociation is taken into account. One way to meet the problem of the effect of dissociation is to include the Hammet σ constant in the correlation equation[16].

Correlations with polar substituent parameters

Correlations were attempted with four types of electronic parameters:

(i) the original Hammet σ constants derived from substituted benzoic acids;

(ii) σ_p^+, derived from the solvolysis of dimethyl diphenyl carbinyl chlorides in 90% aqueous acetone at 25°C[17];

(iii) σ_p^-, obtained from the reaction of phenols and anilines[18];

(iv) σ^0, derived by averaging values from selected reactions involving substrates in which a methylene group has been interposed between the reaction centre and the substituent to prevent an overestimation of direct conjugation effects[19–21].

The results in Tables IV and V indicate that the correlations are poor, or at the most fair in a few instances. Particular attention may be drawn to the results with σ_p^+. The poor quality of the correlation with this parameter would lead one to believe that the adsorption process perhaps does not involve an electron-deficient centre and hence not an electron-rich bonding site on the silica gel. If this were true, a substantial

TABLE III

CORRELATION RESULTS WITH $R_M = a\pi + b$

Mole fraction of water (x)	*4-Linked pyridine styryl dyes*				*2-Linked pyridine styryl dyes*			
	S	*R*	*a*	*b*	*S*	*R*	*a*	*b*
0.445	0.114	0.5391	−0.036	1.180	0.128	0.5123	−0.022	1.268
0.548	0.124	0.5075	−0.016	0.904	0.124	0.6241	−0.078	0.897
0.618	0.142	0.5386	−0.045	0.688	0.158	0.4727	−0.113	0.660
0.669	0.123	0.5846	−0.060	0.538	0.132	0.5873	−0.066	0.625
0.708	0.136	0.5900	−0.070	0.417	0.145	0.5845	−0.071	0.699

TABLE IV
CORRELATION RESULTS WITH $R_M = as + b$ FOR 4-LINKED PYRIDINE STYRYL DYES

s	*Mole fraction of water (x)*	*S*	*R*	*a*	*b*	$\hat{R}^2$
σ	0.445	0.049	0.931	0.224	1.181	0.88225
	0.548	0.023	0.987	0.259	0.900	
	0.618	0.055	0.945	0.286	0.691	
	0.669	0.059	0.921	0.247	0.545	
	0.708	0.085	0.866	0.252	0.427	
σ^+	0.445	0.0.70	0.854	0.133	1.213	0.76670
	0.548	0.036	0.969	0.169	0.940	
	0.618	0.071	0.907	0.181	0.734	
	0.669	0.082	0.842	0.145	0.580	
	0.708	0.102	0.796	0.149	0.463	
σ^0	0.445	0.047	0.938	0.251	1.160	0.86707
	0.548	0.034	0.972	0.281	0.877	
	0.618	0.058	0.938	0.315	0.664	
	0.669	0.054	0.933	0.280	0.522	
	0.708	0.083	0.872	0.283	0.403	
σ^-	0.445	0.058	0.903	0.116	1.202	0.84515
	0.548	0.019	0.992	0.141	0.924	
	0.618	0.053	0.950	0.157	0.717	
	0.669	0.068	0.893	0.129	0.568	
	0.708	0.088	0.854	0.134	0.450	

TABLE V
CORRELATION RESULTS WITH $R_M = as + b$ FOR 2-LINKED PYRIDINE STYRYL DYES

s	*Mole fraction of water (x)*	*S*	*R*	*a*	*b*	$\hat{R}^2$
σ	0.445	0.076	0.859	0.220	1.266	0.78003
	0.548	0.068	0.904	0.253	0.909	
	0.618	0.102	0.872	0.314	0.622	
	0.669	0.080	0.905	0.302	0.603	
	0.708	0.086	0.875	0.271	0.709	
σ^+	0.445	0.074	0.868	0.150	1.300	0.67299
	0.548	0.090	0.823	0.148	0.945	
	0.618	0.130	0.778	0.176	0.665	
	0.669	0.098	0.800	0.144	0.669	
	0.708	0.099	0.830	0.168	0.749	
σ^0	0.445	0.082	0.833	0.233	1.247	0.77860
	0.548	0.060	0.926	0.291	0.885	
	0.618	0.088	0.905	0.368	0.591	
	0.669	0.082	0.865	0.270	0.612	
	0.708	0.085	0.880	0.303	0.684	
σ^-	0.445	0.064	0.904	0.129	1.288	0.76836
	0.548	0.074	0.884	0.133	0.933	
	0.618	0.111	0.846	0.163	0.651	
	0.669	0.083	0.861	0.131	0.657	
	0.708	0.082	0.887	0.150	0.735	

improvement in the correlation should have been observed with σ_p^-. However, although there is an improvement with respect to σ_p^+, the correlations are still far from satisfactory. We therefore conclude that the polar factors alone cannot adequately account for the substituent effect on the chromatographic behaviour of the dyes.

Tables VI and VII give the results of the correlations with σ and π. Considering that the same number of data points are used for the two-parameter correlations, the apparent improvement in the correlations (increased average $\hat{R}^2$ values) is only marginal and not much significance need be attached to this, as is evident from the F values (the significance of the correlations being less than 95% in almost all instances).

Correlation with steric parameters

In an attempt to find a possible connection between lipophilicity and steric substituent constants, Tichy[10] reported that the steric constants E_s and v have the greatest chance of being independent of lipophilic substituent constants. As no correlation was found between the present set of chromatographic data and the lipophilic substituent constant π, we attempted a correlation of R_M (or log R_F) with E_s and v in preference to other steric and sterimole parameters.

Charton's[13–15] steric substituent constant, v, is based on the van der Waals radii and is defined by

$$v_X = r_X - r_H = r_X - 1.20 \tag{4}$$

TABLE VI

CORRELATION RESULTS WITH $R_M = a\pi + bs_2 + c$ FOR 4-LINKED PYRIDINE STYRYL DYES

s_2	*Mole fraction of water*	S	R	a	b	c	F	$\hat{R}^2$
σ	0.445	0.046	0.941	−0.011	0.182	1.172	5.155	0.9030
	0.548	0.061	0.938	−0.006	0.259	0.898	4.882	
	0.618	0.055	0.964	−0.028	0.285	0.685	8.296	
	0.669	0.052	0.960	−0.032	0.245	0.537	7.837	
	0.708	0.066	0.948	−0.037	0.250	0.417	5.915	
σ^+	0.445	0.066	0.872	−0.040	0.155	1.192	2.116	0.9074
	0.548	0.016	0.996	−0.044	0.177	0.930	82.834	
	0.618	0.050	0.970	−0.074	0.195	0.717	10.614	
	0.669	0.059	0.948	−0.085	0.160	0.561	5.915	
	0.708	0.085	0.972	−0.095	0.165	0.441	11.407	
σ^0	0.445	0.053	0.946	−0.009	0.248	1.158	5.677	0.8936
	0.548	0.037	0.978	0.015	0.287	0.880	14.653	
	0.618	0.067	0.946	−0.011	0.311	0.662	5.677	
	0.669	0.057	0.952	−0.031	0.269	0.515	6.449	
	0.708	0.089	0.903	−0.040	0.269	0.394	2.945	
σ^-	0.445	0.057	0.939	−0.040	0.118	1.191	4.970	0.922
	0.548	0.010	0.998	−0.022	0.142	0.918	166.167	
	0.618	0.042	0.979	−0.051	0.158	0.704	15.375	
	0.669	0.054	0.957	−0.065	0.131	0.551	7.256	
	0.708	0.078	0.927	−0.075	0.136	0.431	4.073	

TABLE VII
CORRELATION RESULTS WITH $R_M = a\pi + bs_2 + c$ FOR 2-LINKED PYRIDINE STYRYL DYES

s_2	*Mole fraction of water (x)*	S	R	a	b	c	F	$\hat{R}^2$
σ	0.445	0.086	0.880	−0.010	0.219	1.264	2.228	0.8231
	0.548	0.103	0.849	−0.042	0.251	0.899	1.721	
	0.618	0.083	0.946	−0.061	0.310	0.606	5.677	
	0.669	0.084	0.907	−0.035	0.238	0.625	3.092	
	0.708	0.068	0.950	−0.038	0.269	0.699	6.171	
σ^+	0.445	0.065	0.934	−0.038	0.111	1.285	4.556	0.8834
	0.548	0.053	0.962	−0.104	0.166	0.922	8.275	
	0.618	0.086	0.941	−0.143	0.201	0.633	5.155	
	0.669	0.077	0.924	−0.091	0.161	0.649	3.893	
	0.708	0.075	0.938	−0.10	0.185	0.726	4.882	
σ^0	0.445	0.095	0.853	0.004	0.231	1.248	2.088	0.8612
	0.548	0.052	0.964	−0.048	0.275	0.874	8.762	
	0.618	0.079	0.951	−0.075	0.342	0.574	6.307	
	0.669	0.049	0.964	−0.031	0.269	0.515	8.762	
	0.708	0.089	0.903	−0.040	0.269	0.394	2.945	
σ^-	0.445	0.070	0.924	−0.027	0.129	1.281	3.898	0.8983
	0.548	0.045	0.973	−0.084	0.136	0.911	11.681	
	0.618	0.074	0.957	−0.119	0.166	0.620	7.189	
	0.669	0.073	0.932	−0.071	0.134	0.639	4.377	
	0.708	0.067	0.952	−0.077	0.153	0.715	6.441	

where r_X and r_H are the van der Waal radii of X and H groups, respectively. For tetrahedral substituents such as methyl and *tert.*-butyl, the calculated values of the minimum van der Waal's radii were used. The results of the correlations of v and E_s with R_M for both series of dyes are given in Table VIII.

All correlations with E_s (Table VIII) were very poor. The E_s values are derived from kinetic data and there can be two possibilities for the failure: first, the E_s parameters may not have been correctly defined and may contain not only steric but also electrical effects[13–15]; second, they may be inapplicable in the pesent context as they do not correctly represent the "shape" in the particular environment under study.

On the other hand, although Charton's v parameter has been reported basically with the same properties and limitations, we found that in the present instance correlations of R_M with v are fairly satisfactory and much superior to those obtained with E_s (Table VIII). As the values are derived from van der Waals radii, it is reasonable to suppose that they represent a purer form of the steric parameters.

The results of the combination of a polar (σ) or a lipophilic (π) parameter with v are presented in Tables IX and X.

With the same number of data points, as expected there is an increase in the correlation coefficients. The improvement in the correlations, however, can be concluded from the F values, most of which represent the 95% significance level. Inclusion of a polar or lipophilic parameter leads to similar correlation results. This further corroborates our contention that the steric factor is predominant in the chromatographic behaviour.

The adsorption properties of silica gel are known to be determined by the

TABLE VIII
CORRELATION RESULTS WITH $R_M = av + b$ AND $R_M = aE_s + b$

Dyes	*Mole fraction of water (x)*	$av + b = R_M$				$aE_s + b = R_M$			
		S	*R*	*a*	*b*	*S*	*R*	*a*	*b*
4-Linked pyrydine styryl	0.445	0.032	0.972	−0.027	1.167	0.044	0.671	0.060	1.065
	0.548	0.041	0.959	−0.029	0.886	0.061	0.581	0.012	0.851
	0.618	0.022	0.992	−0.035	0.672	0.049	0.625	−0.045	0.712
	0.669	0.035	0.973	−0.031	0.529	0.051	0.578	−0.006	0.517
	0.708	0.038	0.974	−0.034	0.408	0.057	0.646	−0.064	0.476
2-Linked pyridine styryl	0.445	0.048	0.946	−0.029	1.251	0.060	0.729	−0.116	1.396
	0.548	0.027	0.986	−0.033	0.892	0.035	0.634	−0.034	0.916
	0.618	0.044	0.978	−0.043	0.599	0.042	0.579	−0.008	0.579
	0.669	0.029	0.984	−0.034	0.616	0.041	0.721	−0.075	0.700
	0.708	0.028	0.931	−0.036	0.688	0.032	0.838	−0.107	0.814

TABLE IX
CORRELATION RESULTS WITH $R_M = av + bs_2 + c$ FOR 4-LINKED PYRIDINE STYRYL DYES

s_2	*Mole fraction of water (x)*	*S*	*R*	*a*	*b*	*c*	*F*	$\hat{R}^2$
σ	0.445	0.034	0.967	−0.016	0.058	1.166	9.604	0.9648
	0.548	0.018	0.995	−0.009	0.185	0.895	66.167	
	0.618	0.021	0.995	−0.029	0.057	0.675	66.167	
	0.669	0.039	0.978	−0.027	0.035	0.531	14.653	
	0.708	0.045	0.976	−0.044	−0.09	0.404	13.391	
σ^+	0.445	0.038	0.960	−0.021	0.009	1.166	7.837	0.9661
	0.548	0.013	0.997	−0.015	0.099	0.915	110.611	
	0.618	0.017	0.996	−0.030	0.039	0.684	82.834	
	0.669	0.040	0.977	−0.032	−0.008	0.527	13.995	
	0.708	0.037	0.984	−0.042	−0.052	0.393	20.335	
σ^0	0.445	0.036	0.963	−0.016	0.059	1.161	8.887	0.9609
	0.548	0.031	0.984	−0.012	0.176	0.879	20.335	
	0.618	0.024	0.993	−0.032	0.030	0.671	47.120	
	0.669	0.038	0.978	−0.026	0.054	0.527	14.653	
	0.708	0.038	0.983	−0.045	−0.116	0.413	19.109	
σ^-	0.445	0.037	0.975	−0.027	0.002	1.168	12.835	0.9727
	0.548	0.011	0.998	−0.009	0.103	0.913	166.167	
	0.618	0.019	0.996	−0.028	0.038	0.682	82.834	
	0.669	0.040	0.977	−0.033	−0.010	0.527	13.995	
	0.708	0.035	0.985	−0.045	−0.060	0.392	21.723	
π	0.445	0.036	0.963	−0.023	0.014	1.167	8.887	0.9570
	0.548	0.038	0.976	−0.031	0.033	0.893	13.391	
	0.618	0.022	0.994	−0.036	0.013	0.675	55.056	
	0.669	0.038	0.978	−0.030	−0.012	0.526	14.653	
	0.708	0.041	0.980	−0.034	−0.015	0.405	16.168	

TABLE X
CORRELATION RESULTS WITH $R_M = av + bs_2 + c$ FOR 2-LINKED PYRIDINE STYRYL DYES

s_2	*Mole fraction of water (x)*	S	R	a	b	c	F	$\hat{R}^2$
σ	0.445	0.053	0.957	−0.034	−0.043	1.249	7.256	0.9692
	0.548	0.027	0.990	−0.035	−0.021	0.891	32.834	
	0.618	0.045	0.984	−0.053	−0.102	0.594	20.335	
	0.669	0.018	0.996	−0.047	−0.125	0.610	82.834	
	0.708	0.022	0.995	−0.048	−0.100	0.684	66.167	
σ^+	0.445	0.084	0.886	−0.045	−0.110	1.219	0.113	0.9431
	0.548	0.031	0.987	−0.037	−0.032	0.883	25.142	
	0.618	0.030	0.993	−0.055	−0.089	0.573	47.120	
	0.669	0.023	0.994	−0.041	−0.053	0.600	55.056	
	0.708	0.029	0.991	−0.042	−0.031	0.680	36.538	
σ^0	0.445	0.048	0.965	−0.042	−0.139	1.256	9.027	0.9524
	0.548	0.031	0.987	−0.032	0.013	0.892	25.142	
	0.618	0.092	0.931	−0.046	−0.036	0.601	4.337	
	0.669	0.011	0.999	−0.049	−0.157	0.622	332.833	
	0.708	0.019	0.996	−0.050	−0.131	0.694	82.834	
σ^-	0.445	0.054	0.955	−0.024	0.027	1.258	6.911	0.9697
	0.548	0.028	0.990	−0.039	−0.033	0.883	32.834	
	0.618	0.031	0.992	−0.060	−0.090	0.576	41.167	
	0.669	0.020	0.995	−0.045	−0.060	0.601	66.167	
	0.708	0.029	0.991	−0.044	−0.035	0.679	36.538	
π	0.445	0.051	0.960	−0.031	0.028	1.258	7.837	0.9684
	0.548	0.027	0.990	−0.031	−0.027	0.886	32.834	
	0.618	0.03	0.993	−0.040	−0.048	0.589	47.120	
	0.669	0.032	0.987	−0.033	−0.013	0.613	25.142	
	0.706	0.030	0.990	−0.036	−0.013	0.686	32.834	

number of hydroxyl groups on the surface[22], which in turn implies that the binding site on the silicagel surface is possibly the hydroxyl group through hydrogen bonding. Now we need to address the question of what the state of the substrate molecules is, *i.e.*, whether on the silica gel substrate adsorptions take place in a point-to-point manner or whether it is some kind of surface-to-surface stacking. Although more elaborate experiments must be designed in order to answer this question unequivocally, we would like to draw a broad, qualitative conclusion from our theoretical (quantum mechanical PCILO) studies on the conformation of these dyes. It has been observed with 4-linked pyridine dyes that the deviation of the end groups (benzene and pyridine) from coplanarity decreaes in the order $N(CH_3)_2 > OH > H > CH_3 > NO_2$. With 2-linked pyridine dyes the deviation from coplanarity is much more pronounced in terms of both the twist angle and the energy barrier with respect to the planar conformation. The deviation from coplanarity decreases approximately in the order $OH > H > CH_3 \approx N(CH_3)_2 > NO_2$. We find that the R_F values vary approximately in the reverse order, that is, the less planar a molecule is, the more strongly it is adsorbed by silica gel (lower R_F value) and *vice-versa*. From this we may perhaps preclude the possibility of surface-to-surface stacking, and hence a relatively smaller influence of the degree of planarity on the chromatographic behaviour of the dyes.

TABLE XI

CORRELATION RESULTS WITH $R_M = a(\text{CNDO}/2) + bv + c$ AND $R_M = a(\text{INDO}) + bv + c$

Substituents included in these correlations are $N(CH_3)_2$, OH, CH_3, H and NO_2. The value for $N(CH_3)_2$ was obtained by extrapolation from the best correlations in Table VIII.

Dyes	*Mole fraction of water (x)*	*a(CNDO/2) + bv + c = R_M*					*a(INDO) + bv + c = R_M*				
		S	*R*	*a*	*b*	*c*	*S*	*R*	*a*	*b*	*c*
4-Linked	0.445	0.014	0.9987	0.052	−0.027	1.144	0.014	0.9987	0.034	−0.028	1.146
pyridine styryl	0.548	0.023	0.9971	−0.197	−0.033	0.911	0.023	0.9970	−0.148	−0.033	0.905
	0.618	0.023	0.9977	−0.139	−0.037	0.695	0.023	0.9977	−0.106	−0.037	0.691
	0.669	0.046	0.9864	0.187	−0.026	0.498	0.047	0.9861	0.136	−0.026	0.605
	0.708	0.019	0.9985	−0.035	−0.037	0.397	0.019	0.9985	−0.035	−0.037	0.396
2-Linked	0.445	0.019	0.9981	−0.500	−0.037	1.342	0.024	0.9972	−0.350	−0.036	1.317
pyridine styryl	0.548	0.022	0.9977	0.207	−0.030	0.852	0.022	0.9978	0.159	−0.031	0.858
	0.618	0.046	0.9924	0.549	−0.030	0.521	0.048	0.9918	0.402	−0.031	0.540
	0.669	0.003	0.9996	−0.053	−0.035	0.624	0.004	0.99994	−0.037	−0.035	0.622
	0.708	0.025	0.9971	−0.024	−0.034	0.712	0.025	0.9971	−0.020	−0.034	0.712

From the correlation results with σ_p^+ and σ_p^-, we had earlier concluded that perhaps an electron-rich centre is involved in the chromatographic binding with silica gel (evidently an –O–H $\cdots$ X type of hydrogen bonding). To test this hypothesis, correlations were carried out with ν in combination with the electron densities (obtained by CNDO/2 and INDO methods). The excellent results obtained (Table XI) bear out this possibility.

ACKNOWLEDGEMENTS

The authors are grateful to the Department of Atomic Energy and the Council of Scientific and Industrial Research, Government of India, for financial assistance.

REFERENCES

1 R. Consden, A. H. Gordon and A. J. P. Martin, *Biochem. J.*, 38 (1944) 244.
2 A. J. P. Martin, *Biochem. Soc. Symp.*, 3 (1949) 4.
3 E. C. Bate-Smith and R. G. Westall, *Biochim. Biophys. Acta*, 4 (1950) 427.
4 C. B. C. Boyce and B. V. Milborrow, *Nature (London)*, 208 (1965) 537.
5 C. Hansch and T. Fujita, *J. Am. Chem. Soc.*, 86 (1964) 5175.
6 E. Tomlinson, *J. Chromatogr.*, 113 (1975) 1.
7 G. L. Biagi, A. M. Barbaro, M. C. Guerra, G. C. Forti and M. E. Fracasso, *J. Med. Chem.*, 17 (1974) 28.
8 J. Draffehn, K. Ponsald and B. Schonecker, *J. Chromatogr.*, 216 (1981) 69.
9 N. El Taylor, H. Van de Waterbeemd and B. Testa, *J. Chromatogr.*, 320 (1985) 293 and 305.
10 M. Tichy, *Int. J. Quantum Chem.*, 16 (1979) 509.
11 N. B. Chapman and J. Shorter (Editors), *Advances in Linear Free Energy Relationships*, Plenum Press, New York, 1972.
12 R. W. Taft, in M. S. Newman (Editor), *Steric Effects in Organic Chemistry*, Wiley, New York, 1956, p. 556.
13 M. Charton, *J. Am. Chem. Soc.*, 97 (1975) 1552.
14 M. Charton, *J. Org. Chem.*, 41 (1976) 2217.
15 M. Charton, *J. Org. Chem.*, 42 (1977) 3531; and references cited therein.
16 M. Kuchar, B. Brunova, V. Rejholec and V. Rabek, *J. Chromatogr.*, 92 (1974) 381.
17 H. C. Brown and Y. Okamoto, *J. Am. Chem. Soc.*, 80 (1958) 4979.
18 A. I. Biggs and R. A. Robinson, *J. Chem. Soc.*, 81 (1961) 388.
19 R. W. Taft, *J. Phys. Chem.*, 64 (1960) 1805.
20 R. W. Taft, S. Ehrenson, I. C. Lewis and R. E. Glick, *J. Am. Chem. Soc.*, 81 (1959) 5352.
21 H. Van Bakkum, P. E. Verkade and B. M. Wepster, *Recl. Trav. Chim. Pays-Bas*, 78 (1959) 815.
22 H. Schweppe, in K. Venkataramn (Editor), *The Analytical Chemistry of Synthetic Dyes*, Wiley-Interscience, New York, 1977, p. 25.

Journal of Chromatography, 481 (1989) 343–351
Elsevier Science Publishers B.V., Amsterdam — Printed in The Netherlands

CHROM. 21 763

APPLICATION OF FREE FLOW ELECTROPHORESIS TO THE PREPARATIVE PURIFICATION OF BASIC PROTEINS FROM AN *E. COLI* CELL EXTRACT

REINHARD KUHN[a] and HORST WAGNER*
Fachrichtung Anorganische Analytik und Radiochemie, Universität des Saarlandes, D-6600 Saarbrücken (F.R.G.)
(First received March 3rd, 1989; revised manuscript received June 26th, 1989)

SUMMARY

The application of free flow electrophoresis (FFE) to the purification of a basic protein from a complex protein mixture was investigated. For this purpose lysozyme (E.C. 3.2.1.17) from hen egg white, serving as a model for a basic protein, was added to a crude *E. coli* cell extract and reisolated. For three techniques of FFE (zone electrophoresis, isoelectric focusing and field step electrophoresis), suitable electrolyte systems were developed. The purity, purification factor, recovery and throughput were determined for the optimized experiments. A combination of field step electrophoresis and zone electrophoresis gave the best purification factor (9.5) and the highest recovery (95%). The purification factors achieved in zone electrophoresis and isoelectric focusing were comparable to each other and ranged from 3.5 to 4.75. In isoelectric focusing, 94% of the enzyme activity was recovered. Zone electrophoresis gave recoveries of 82% and 87%, respectively. Purities of more than 95% were achieved with all the techniques described. With the exception of zone electrophoresis, all the techniques effected a concentration of the enzyme during the separation. Zone electrophoresis and field step electrophoresis were very simple in application.

INTRODUCTION

With the developments in biotechnology in recent years, the requirements placed on the purity of proteins for pharmaceutical applications have increased considerably. New and efficient methods for the preparative purification of proteins had to be developed in order to reduce the cost of large-scale production. In addition to the commonly used purification techniques based on precipitation or chromatography, electrophoresis takes advantage of two individual characteristics of proteins, *viz.*, the mobility in an electric field depending primarily on the charge of the molecules and the isoelectric point.

[a] Present address: Analytical Research and Development, Pharma Division, Sandoz Ltd., Basle, Switzerland.

0021-9673/89/$03.50

For the purification of small amounts, a flat-bed electrophoresis system was developed, running in the zone electrophoresis[1] or the isoelectric focusing[2] mode. Sepharose or agarose was recommended as a stabilizing gel to minimize gravitational and diffusional instabilities. After the electrophoretic run, the gel has to be sliced and the proteins must be eluted from each slice.

For the purification of small ions and also for living cells or particles, free flow electrophoresis (FFE), pioneered by Hannig[3–5] as zone electrophoresis, was developed in the last two decades. Despite the advantages of this method, such as continuous use and the absence of carrier materials, which improve the recovery of active proteins, FFE has not been popular for the purification of biopolymers in the milligrams to grams range. With the development of new techniques[6–9], including isoelectric focusing (IEF), field step electrophoresis (FSE) and isotachophoresis (ITP), allowing higher sample throughputs at higher resolutions, FFE has become more and more interesting for application in research and industry. Additionally, these new techniques concentrate diluted sample compounds after the separation. An extensive overview of the technique and applications of FFE is given in ref. 10.

This paper demonstrates the suitability of FFE techniques for the purification of a basic protein from a crude *E. coli* protein extract. Lysozyme, as a model for interesting pharmaceutically active proteins with low molecular weights and high p*I* values such as the interleukins, was added to an *E. coli* protein extract and reisolated in a single step.

EXPERIMENTAL

Chemicals

All chemicals were of analytical-reagent grade unless indicated otherwise.

Arginine, aspartic acid, glutamine, glycine, hydrochloric acid, potassium chloride, potassium sulphate, *Micrococcus luteus* lyophil. cells and urea were purchased from Serva (Heidelberg, F.R.G.). E. coli cells were cultivated by BASF (Ludwigshafen, F.R.G.). All other substances were obtained from Merck (Darmstadt, F.R.G.).

Analytical methods

The enzymatic activity of lysozyme was determined according to Shugar[11] by measuring the change in turbidity of a *Micrococcus luteus* suspension at 450 nm and 25°C, using a Hitachi Model 100-60 photometer. The total protein concentration was determined by measuring the absorbance at 280 nm with chicken egg albumin as a standard[12]. For the measurement of pH and conductivity a WTW 530 pH meter and a WTW LF 521 conductimeter, respectively, from WTW (Lauda, F.R.G.) were employed.

Preparation of the sample

About 20 g of *E. coli* cells were suspended in 100 ml of 0.1 mol/l Tris–HCl (pH 7.0). After cell breakage by sonification and removal of the cell debris by centrifugation, 0.4% polyethyleneimine was added to the supernatant to precipitate the polynucleic acids. The resulting suspension was stirred for 30 min at room temperature and the precipitate was centrifuged. The conductivity of the sample solution was

reduced by dialysis against 0.1 mol/l glycine. The addition of lysozyme to the protein mixture caused precipitation, which could be prevented by adding at least 5 mol/l urea or 0.02 mol/l potassium sulphate.

Electrophoresis apparatus

The FFE apparatus and the operating conditions have been described in detail elsewhere[13].

RESULTS AND DISCUSSION

Although basic proteins tend to adsorb to supporting media in chromatography, they easily aggregate with oppositely charged proteins in free solutions, as was observed for the lysozyme with *E. coli* proteins. To achieve successful separations of lysozyme from the contaminating proteins, these hydrophilic protein interactions had to be suppressed by using inorganic salts or, *e.g.*, urea[14,15].

If lysozyme was added to a crude *E. coli* cell extract, precipitation of the enzyme with *E. coli* proteins could be observed. The addition of urea at concentrations of nearly 5 mol/l or potassium sulphate at more than 0.02 mol/l to the *E. coli* protein mixture prevented the precipitation of lysozyme with bacterial proteins or led to the dissolution of already precipitated proteins. The dependence of the enzyme solubility on the concentration of urea and potassium sulphate is illustrated in Fig. 1.

Zone electrophoresis

The electrophoretic mobility of proteins depends strongly on the pH of the dissolving medium. Investigations on mobility in zone electrophoresis (ZE) at different pH values revealed the general shape of the mobility curve for a protein in a polyacrylamide gel. With a decrease in pH from 11 (p*I* of lysozyme) to 7.5, the mobility of the enzyme increased steadily and changed only slightly at pH values lower than 7.5. The separation of lysozyme from contaminating *E. coli* proteins by ZE

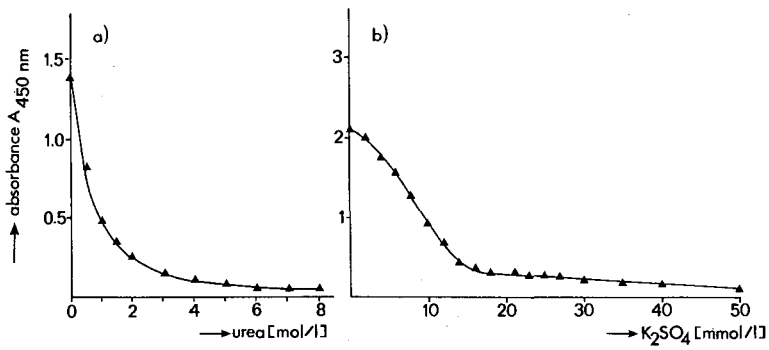

Fig. 1. Solubility of the lysozyme–*E. coli* protein complex depending on the concentration of (a) urea and (b) potassium sulphate. Solid lysozyme at a concentration of 2 mg/ml was dissolved in the dialysed *E. coli* cell extract with a protein concentration of (a) 14 and (b) 20 mg/ml and a conductivity of 0.4 mS/cm. After the addition of the various amounts of urea and potassium sulphate, the turbidity of the solution was determined by measuring the absorption at 450 nm.

succeeded very easily at pH 7.5 (Fig. 2). As most of the bacterial proteins had p*I* values below 7.5, they migrated towards the anode whereas lysozyme moved towards the cathode, with the consequence that almost all contaminating proteins could be separated. In many experiments two lysozyme peaks with equal biological activities were measured. Neither separation by polyacrylamide gel electrophoresis (PAGE) nor the A_{450}/A_{280} ratio gave any indications of different enzyme structures.

The peak shape of the lysozyme bands showed sharp fronting, whereas the bacterial proteins migrated as a surprisingly narrow band. The latter peak shape might have its origin in the high concentration of urea, which probably supports ionic interactions between the proteins. This assumption is also confirmed by the experiment but with potassium sulphate instead of urea as the solubilizing agent (Fig. 3). As the power supply used was limited to a maximum current of 0.2 A, the voltage and the flow-rate had to be changed compared with the experimental conditions given in Fig. 2. Potassium sulphate enhanced the polarity of the background electrolyte and probably induced the breakage of ionic protein interactions of the *E. coli* proteins, resulting in a broad peak shape ranging over more than 30 fractions.

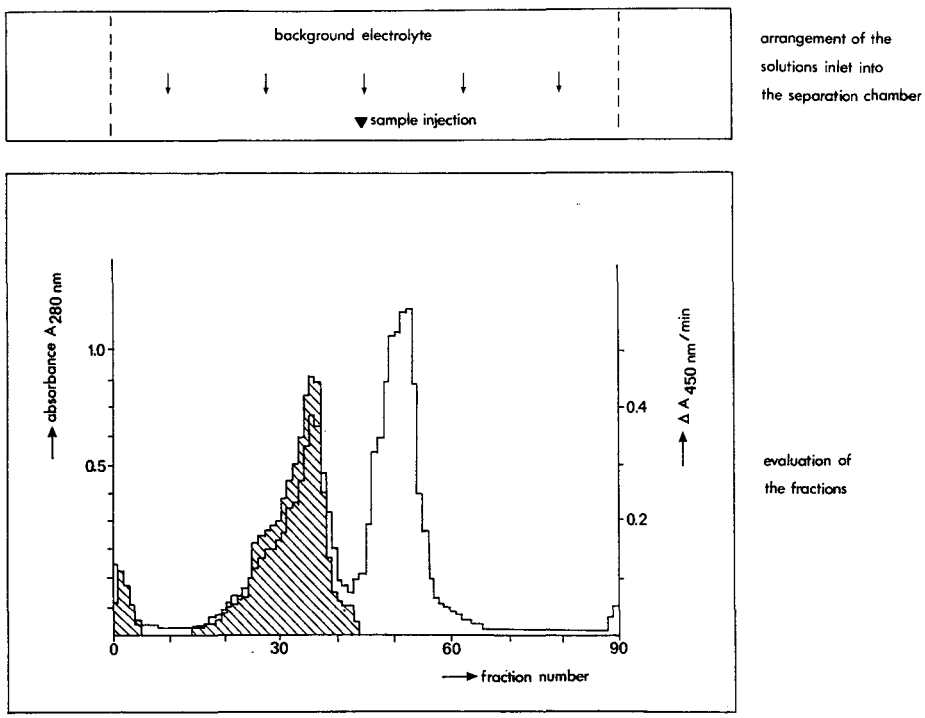

Fig. 2. ZE of lysozyme containing *E. coli* proteins. All solutions contained 5 mol/l urea. The top panel shows the inlet configuration and the lower panel shows the distribution of the enzyme activity (dashed area, as ΔA_{450}/min) and the total protein distribution (as A_{280}). The background electrolyte consisted of 0.01 mol/l Tris, adjusted to pH 7.5 with hydrochloric acid. The sample contained 10 mg/ml lysozyme and 28 mg/ml bacterial proteins. The field strength was 60 V/cm. The flow-rate was 190 ml/h and the sample was injected at 2 ml/h.

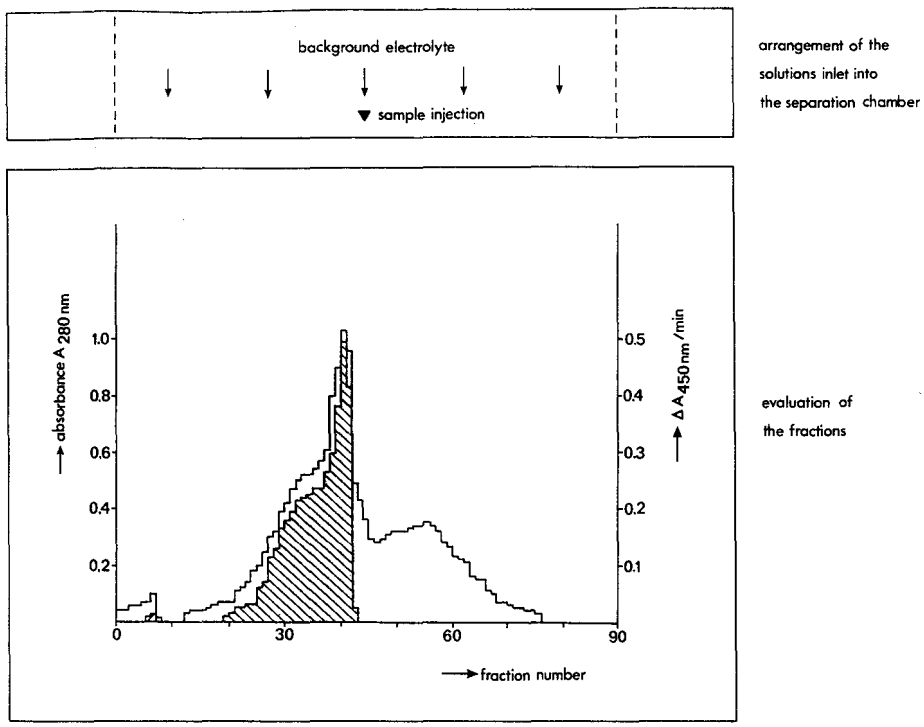

Fig. 3. ZE of lysozyme containing *E. coli* proteins. The top panel shows the inlet configuration and the lower panel shows the enzyme activity (dashed area, as ΔA_{450}/min) and the total protein distribution (as A_{280}). All solutions were adjusted to 0.02 mol/l potassium sulphate. The background electrolyte was prepared according to Fig. 2. The sample contained 10 mg/ml lysozyme and 18 mg/ml bacterial proteins. The field strength was 45 V/cm. The flow-rate was 100 ml/h and the sample was injected at 1 ml/h.

Isoelectric focusing

In addition to the recycling isoelectric focusing apparatus (RIEF) of Bier and Egen[16], which operates batchwise, Manzoni[17] developed IEF in a stepwise pH gradient running in the continuous mode. On pumping simple buffer solutions as parallel liquid films through the separation chamber there arises a stepwise pH profile according to the different pH values of the buffers. The migration of the enzyme within the pH step is based on the same principle as the migration in ZE. However, as in ZE almost the total transportation of charges is taken over by the ground electrolyte (carrier electrolyte), the migration velocity of the sample compounds, depending on the ionic strength of the buffer, is decreased compared with that in stepwise IEF. The focusing effect of this technique in only a few fractions allows one to add the sample as a broad zone into the top of the chamber. High ionic strengths of the sample solutions are unnecessary in this technique, because the sample compounds participate to a great extent in the transportation of current in the dosing zone of the sample. Shorter residence times or pH values with lower enzyme mobilities can be adjusted.

The separation of the enzyme from the bacterial protein mixture succeeded when using a cathodic buffer solution of pH 12.3 and a residence time of 7 min (Fig. 4). Most

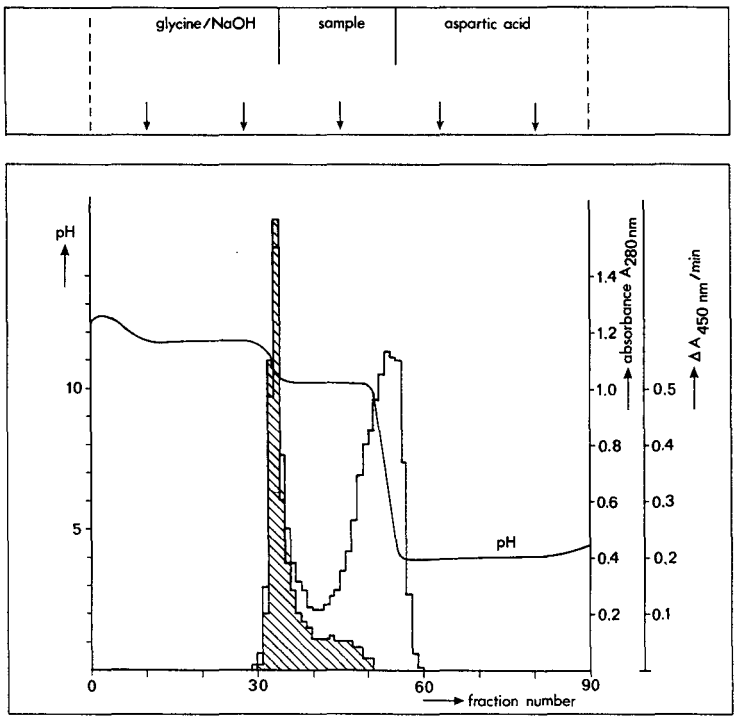

Fig. 4. IEF of 0.01 mg/ml lysozyme containing 0.3 mg/ml *E. coli* proteins. The arrangement of the inlet system is given at the top and the evaluation of the fractions is shown below; the dashed area indicates the enzyme activity as ΔA_{450}/min and the total protein concentration is given as A_{280}. All buffers contained 5 mol/l urea. Arginine–glutamine (0.03 mol/l each), pH 10.0, served as solvent for the sample. The concentration of glycine was 0.05 mol/l, adjusted to pH 12.3 with sodium hydroxide; the anolyte was 0.03 mol/l aspartic acid, pH 3.7. At a field strength of 30 V/cm the flow-rate was adjusted to 215 ml/h.

of the enzyme activity was well focused on few fractions and only weak tailing remained. Longer residence times in order to remove this tailing decreased the slope of the pH interfaces and diminished the concentration factor of the enzyme.

Field step electrophoresis

FSE is a simple and powerful technique for the concentration of diluted samples[18] and for these investigations it was often used to increase the protein concentration in fractions after the separation. The concentration factors depended on the zone width of the sample and could reach values of 10–20.

As the resolution of this technique was low for the purification of lysozyme, it was combined with ZE, as illustrated schematically in Fig. 5. In the separation buffer between the sample zone and the catholyte the sample compounds could be separated according to their different mobilities. The optimized experimental results are shown in Fig. 6. Nearly all the lysozyme was found in only three fractions. The enzyme was five-fold more concentrated than the injected sample and almost free from contaminants.

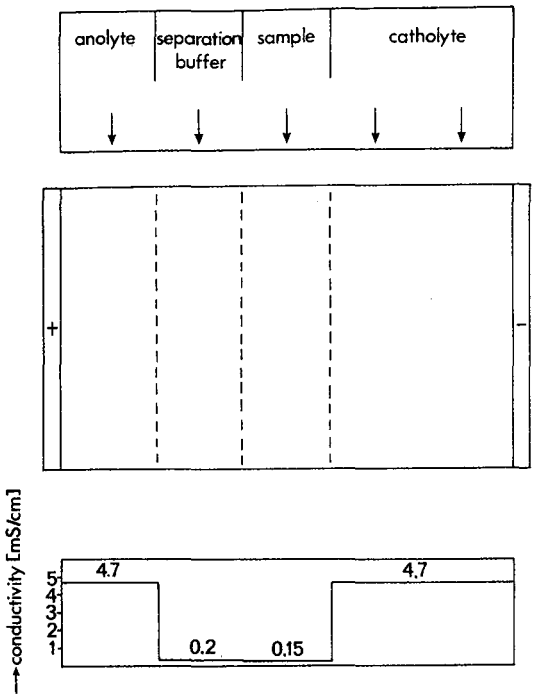

Fig. 5. Schematic representation of FSE combined with ZE. Above: the inlet system with anolyte and catholyte characterized by high conductivities, the separation zone with a conductivity adjusted according to the mobilities of the sample compounds and the sample solution with low conductivity. Below: conductivity profile across the separation chamber.

Comparison of results

All optimized experiments described abive were evaluated in terms of the purification factor, recovery, throughput and purity. The results are summarized in Table I.

All methods gave very high purities, irrespective of the purity of the sample before the separation. The recovery of enzyme activity was the highest for the focusing techniques IEF and FSE + ZE, but ZE also gave high recoveries of more than 80%. The combination of FSE and ZE achieved the best results. As no problems arise with protein precipitations, samples of much higher concentration than in IEF can be separated. ZE provided a low throughput of the sample volumes but, owing to the dilution of the sample compounds during the separation, high protein concentrations could be employed. Also, this technique was easy to apply. IEF was limited with regard to the concentration of the sample compounds because of the low solubility of the proteins at their isoelectric points. The resolving power of IEF is lower than that of the combined FSE and ZE. Separations of lysozyme from *E. coli* proteins can probably be performed with inorganic salt solutions instead of urea, as demonstrated with potassium sulphate in ZE.

Concerning chromatographic techniques for protein purification, FFE should

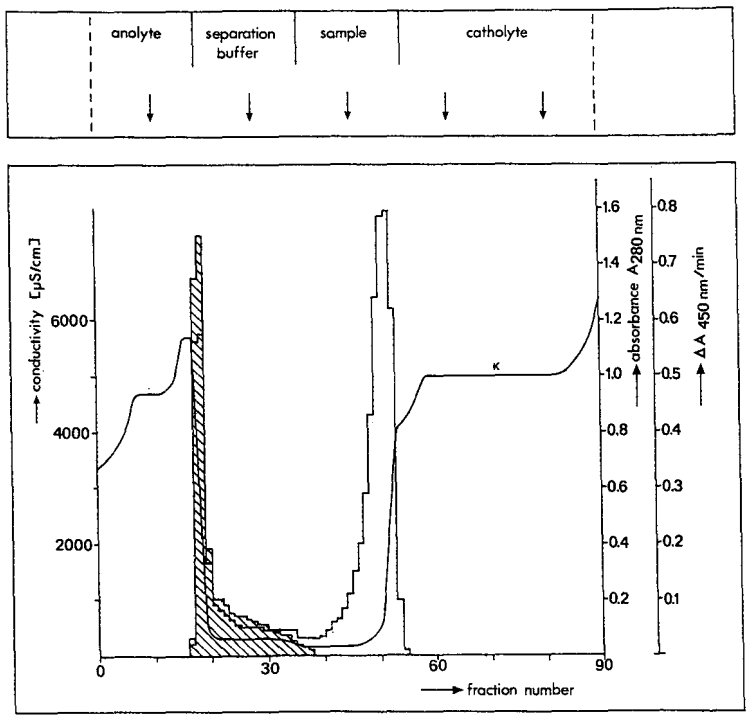

Fig. 6. FSE combined with ZE of lysozyme containing *E. coli* proteins. The top panel shows the inlet configuration and the lower panel shows the enzyme activity (dashed area, as ΔA_{450}/min) and the total protein distribution (as A_{280}). All solutions contained 5 mol/l urea. The anolyte and catholyte was Tris (0.1 mol/l) adjusted to pH 7.6 with hydrochloric acid, conductivity 4.7 mS/cm; the separation buffer was Tris (5 mmol/l)–HCl, pH 7.7, conductivity 0.17 mS/cm. The sample buffer was Tris (3 mmol/l)–HCl, pH 7.6, conductivity 0.15 mS/cm, with 0.17 mg/ml lysozyme and 1.5 mg/ml bacterial proteins. Field strength, 45 V/cm; flow-rate, 300 ml/h.

TABLE I

PURIFICATION OF LYSOZYME FROM CONTAMINATING *E. COLI* INTRACELLULAR PROTEINS BY ZE, IEF AND FSE COMBINED WITH ZE

Method	*Purification factor*[a]	*Recovery*[b] *(%)*	*Throughput (ml sample/h)*	*Purity*[c] *(%)*
ZE (urea)	3.7	87	2[d]	>95
ZE (K_2SO_4)	3.5	82	1[d]	>95
IEF	4.75	94	43	>95
FSE + ZE	9.5	95	60	>95

[a] Purification factor: purity after the separation/purity before the separation.
[b] Recovery: enzyme activity after FFE/enzyme activity before FFE × 100 (%).
[c] Purity: mg lysozyme/mg total protein × 100 (%).
[d] For ZE the protein concentration of the sample can be chosen as high as possible, as the sample will be diluted in the elctrophoretic run.

not been regarded as a competing but, owing to the different separation mechanisms, as a complementary technique within a purification scheme. For this purpose FFE is distinguished by high recoveries, high separation power and easy application.

ACKNOWLEDGEMENTS

We thank Dr. Horn and Dr. Hillen, BASF, Ludwigshafen, for the cultivation of *E. coli* bacteria. We are also grateful to Dipl.-Chem. S. Hoffstetter for many valuable discussions and B. Ranker for examination of the manuscript. This work was supported by the Bundesminister für Forschung and Technologie, F.R.G., Förderkennzeichen 03 188 08 A7.

REFERENCES

1 R. A. Scopes, *Protein Purification, Principles and Practice*, Springer, New York, Heidelberg, Berlin, 1982, p. 166.
2 W. F. Goodman and J. N. Baptist, *J. Chromatogr.*, 179 (1979) 330.
3 K. Hannig, *Electrophoresis*, 3 (1982) 235.
4 K. Hannig, *Fresenius' Z. Anal. Chem.*, 181 (1961) 244.
5 K. Hannig, *Angew. Chem.*, 75 (1963) 1129.
6 G. Schmitz, A. Boettcher, H.-G. Kahl and T. Bruening, *J. Chromatogr.*, 431 (1988) 327.
7 H. Wagner and V. Mang, in F. M. Everaerts (Editor), *Analytical Isotachophoresis*, Elsevier, Amsterdam, 1981, p. 41.
8 H. Wagner, V. Mang, R. Kessler, A. Heydt and R. Manzoni, in H. Hirai (Editor), *Electrophoresis '83*, Walter de Gruyter, Berlin, 1984, p. 283.
9 H. Wagner and R. Kessler, *GIT Labor-Med.*, 7 (1984) 30.
10 H. Wagner, R. Kuhn and S. Hoffstetter, in H. Wagner and E. Blasius (Editors), *Praxis der elektrophoretischen Trennmethoden*, Springer, Berlin, New York, Heidelberg, 1988, pp. 223–278.
11 D. Shugar, *Biochim. Biophys. Acta*, 8 (1952) 302.
12 B. L. Williams and K. Wilson, *Praktische Biochemie*, Georg Thieme, Stuttgart, 1978.
13 R. Kuhn and H. Wagner, *Electrophoresis*, 10 (1989) 165.
14 H. Netter, *Theoretische Biochemie*, Springer, Berlin, Göttingen, Heidelberg, 1959.
15 T. E. Creighten, *J. Mol. Biol.*, 129 (1979) 235.
16 M. Bier and N. B. Egen, in H. Haglund, J. G. Westerfeld and J. T. Ball (Editor), *Electrofocus '78*, Elsevier, New York, 1979, p. 35.
17 R. Manzoni, *PhD Thesis*, Universität des Saarlandes, Saarbrücken, 1985.
18 A. Heydt and H. Wagner, *J. Virol. Methods*, 19 (1988) 13.

Journal of Chromatography, 481 (1989) 352–357
Elsevier Science Publishers B.V., Amsterdam — Printed in The Netherlands

CHROM. 21 885

Note

Series of novel flavanones identified by gas chromatography–mass spectrometry in bud exudate of *Populus fremontii* and *Populus maximowiczii*

W. GREENAWAY* and S. ENGLISH
Department of Plant Sciences, University of Oxford, South Parks Road, Oxford OX1 3RA (U.K.)
E. WOLLENWEBER
Institut für Botanik der Technischen Hochschule, D-6100 Darmstadt (F.R.G.)
and
F. R. WHATLEY
Department of Plant Sciences, University of Oxford, South Parks Road, Oxford OX1 3RA (U.K.)
(First received June 8th, 1989; revised manuscript received August 15th, 1989)

We are investigating the chemotaxonomy of poplar species by analysis of their bud exudate composition[1], and initial work has established that the exudate is a complex mixture containing several previously unidentified compounds[1–5]. During preliminary analyses of bud exudate of *Populus fremontii* S. Wats and *P. maximowiczii* Henry, we noted a number of novel flavonoid aglycones which formed a series related to pinobanksin-3-acetate. We here describe this series.

EXPERIMENTAL

Reagents and materials

Ethyl acetate (nanograde) was from Mallinckrodt (St. Louis, MO, U.S.A.).

Poplar bud exudate

Bud exudate of *P. maximowiczii* was obtained from a specimen (identification code SF) at the Alice Holt Lodge, Forestry Commission (Farnham, U.K.). Specimen SF originated from Yamabe (Hokkaido, Japan) and was derived from material collected by Professor B. Lindquist. The bud exudate of *P. fremontii* was collected from a specimen at Fort Verde State Historic Park near Camp Verde, AZ, U.S.A.

Sample preparation and gas chromatography–mass spectrometry (GC–MS)

These were carried out as previously described[5].

RESULTS

Analysis by GC–MS allowed the separation and identification of the compounds in the bud exudates as their trimethylsilyl (TMS) derivatives. We here report

0021-9673/89/$03.50

the compounds chromatographing in the region of 24–30 methylene units (MU) which are primarily chalcones, flavones and flavanones (Fig. 1, Table I). During initial analyses of the data in this region we noted in both *P. fremontii* and *P. maximowiczii* bud exudates a series of previously undescribed flavanones related to pinobanksin-3-acetate (5,7-dihydroxy-3-acetyloxyflavanone). The mass spectrum of the bis-TMS derivative of pinobanksin-3-acetate is very similar in its initial fragmentation to that of underivatized pinobanksin-3-acetate[6], excepting that the bis-TMS derivative has an initial loss of a methyl from a TMS group (Fig. 2). In both cases there are characteristic losses involving $COCH_2$ or $OCOCH_3$ groups prior to further fragmentation of the molecule. Subsequent analyses of the mass spectra of TMS derivatives of flavonoids in which the acetate was replaced by a butanoate, for example the acetate and butanoate of 8-hydroxygalangin-7-methyl ether isolated from ferns[7], demonstrated that the

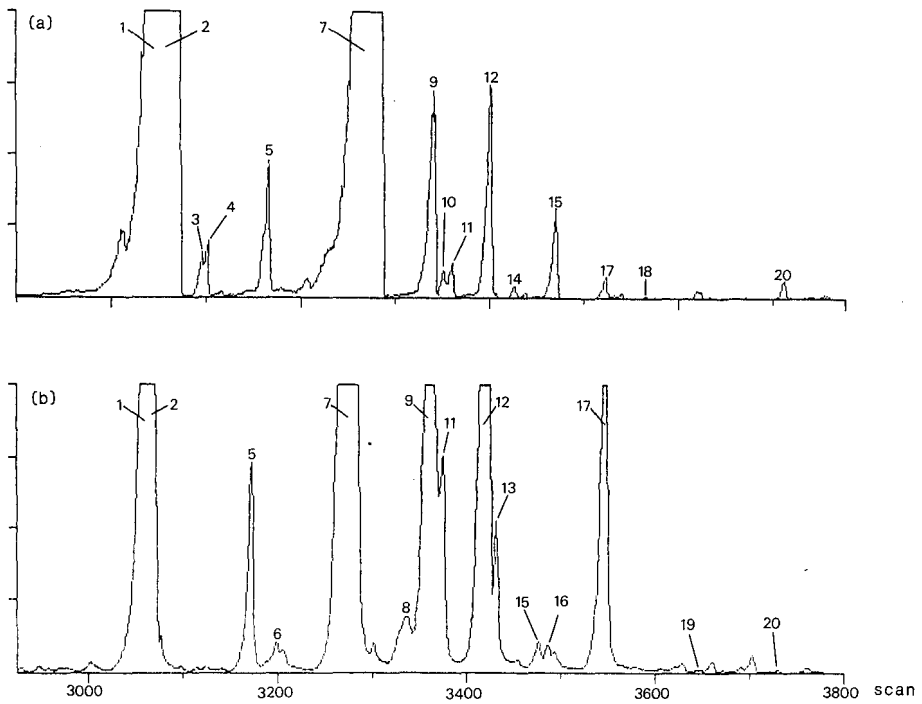

Fig. 1. Reconstructed ion chromatograms of bud exudate from *P. fremontii* (a) and *P. maximowiczii* (b), scans 2900–3800 (24–30 MU). For peak identification see in Table I; peak 8 = *trans*-caffeic acid benzyl ester; peak 16 = an unsaturated C_{18} hydrocarbon.

fragmentation patterns were almost identical after the initial loss of methyl from a TMS group and the subsequent loss of the acetate or butanoate substituent.

The series of flavanones we report here, which are related to pinobanksin-3-acetate, again produce spectra which are almost identical after the loss of a methyl from a TMS group and the substituent group at the 3-position. The substituent is represented in the mass spectra by a peak at *m/z* 43 (CH_3CO), *m/z* 57 (C_2H_5CO), *m/z* 71 (C_3H_7CO), *m/z* 85 (C_4H_9CO) or *m/z* 99 ($C_5H_{11}CO$). We therefore conclude that

TABLE I

FLAVONOIDS IDENTIFIED IN *P. FREMONTII* AND *P. MAXIMOWICZII* BUD EXUDATE

Peak numbers correspond to those given in Fig. 1. GC retention times in methylene units (MU; defined by Dalgliesh *et al.*[12]) are given to two decimal places to indicate the elution sequence of peaks which chromatograph closely. Factors such as concentration of the compound concerned and/or the characteristics of a particular GC column are liable to affect the chromatography, and for general purposes the MU figures are probably reliable to only a single decimal place.

Peak No.	*Chemical name*	*MU*	*Number of TMS groups*	*Total ion current*[a]	
				P. fremontii	*P. maximowiczii*
1	5,7-Dihydroxyflavanone	24.92	2	11.2	5.4
2	2',4',6'-Trihydroxychalcone[b]	24.99	3	35.8	14.6
3	7-Hydroxy-5-methoxyflavanone[c]	25.24	1	0.3	–
4	2',4'-Dihydroxy-6'-methoxychalcone	25.28	2	0.4	–
5	3,5,7-Trihydroxyflavanone	25.77	3	1.5	3.2
6	5,7-Dihydroxyflavone[d]	26.02	1	–	0.6
7	5,7-Dihydroxy-3-acetyloxyflavanone[e]	26.34	2	36.2	27.4
9	5,7-Dihydroxyflavone[d]	27.04	2	2.6	15.1
10	5,7-Dihydroxy-3-methoxyflavone	27.08	2	0.2	0.7
11	5,7-Dihydroxy-3-propanoyloxyflavanone[f]	27.10	2	0.3	2.5
12	3,5,7-Trihydroxyflavone	27.45	3	2.3	15.2
13	A dihydroxymethoxyflavone M^+ at *m/z* 428	27.66	2	–	1.2
14	A dihydroxymethoxyflavanone M^+ at *m/z* 430	27.69	2	0.1	–
15	5,7-Dihydroxy-3-butanoyloxyflavanone[f,g]	28.01	2	0.9	0.4
17	5,7-Dihydroxy-3-pentanoyloxyflavanone[f,g]	28.30	2	0.2	7.4
18	2',4',6',4-Tetrahydroxychalcone	28.54	4	<0.1	–
19	5,7-Dihydroxy-3-hexanoyloxyflavanone[f,g]	29.30	2	<0.1	<0.1
20	5,7-Dihydroxy-3-hexanoyloxyflavanone[f,g]	29.68	2	0.1	<0.1

[a] The total ion current generated depends on the characteristics of the compound concerned and is not a true quantitation (see ref. 2).

[b] This may be an overestimate, as some flavanones may be partially converted to the corresponding chalcones during sample preparation and/or analysis (see ref. 2).

[c] We are not aware of previous identification of this compound (alpinetin) in poplar bud exudates.

[d] 5,7-Dihydroxyflavone (chrysin) was seen as both the mono-TMS and the bis-TMS derivatives.

[e] We have previously found this compound in *Populus* × *euramericana* bud exudate (peak 75)[2], but could not then identify it.

[f] We believe this to be a previously unidentified flavanone.

[g] We do not know whether the substituents at the 3-position are linear or branched.

these compounds differ only in the acid with which pinobanksin (3,5,7-trihydroxyflavanone) is esterified in the 3-position.

We identified pinobanksin derivatives esterified in the 3-position with CH_3COOH, pinobanksin-3-acetate (7)[a]; C_2H_5COOH, pinobanksin-3-propanoate (11); C_3H_7COOH, pinobanksin-3-butanoate or pinobanksin-3-isobutanoate (15); C_4H_9COOH, pinobanksin-3-pentanoate or pinobanksin-3-methylbutanoate (17), $C_5H_{11}COOH$, pinobanksin-3-hexanoate or pinobanksin-3-methylpentanoate (19, 20). The structures of these compounds are shown in Fig. 3 and their initial

[a] The numbers in parentheses refer to peak numbers in Table I and Fig. 1.

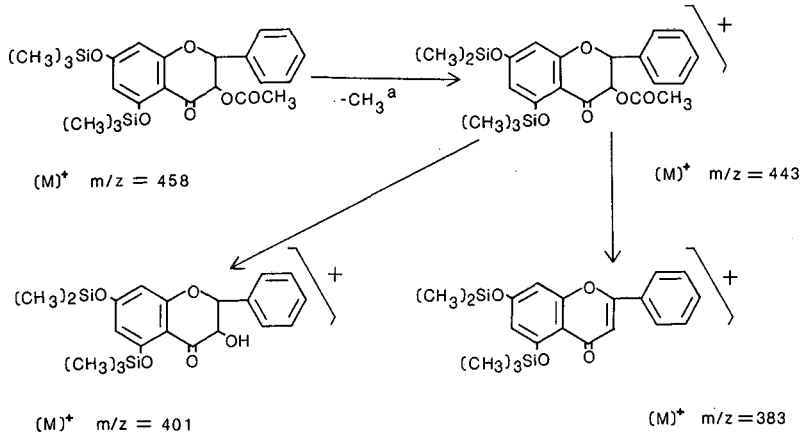

Fig. 2. Initial fragmentations at 70 eV of the bis-TMS derivative of pinobanksin-3-acetate. The use of deuterated silylation reagent confirms that the methyl group is lost from a trimethylsiloxy group although we do not know which. Demethylation of the 7-trimethylsiloxy is shown as an example.

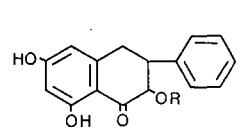

	Peak No.
R = $COCH_3$	7
R = COC_2H_5	11
R = COC_3H_7	15
R = COC_4H_9	17
R = COC_5H_{11}	19,20

Fig. 3. Structures of the series of novel flavanones related to pinobanksin-3-acetate. Peak numbers refer to Fig. 1 and Table I.

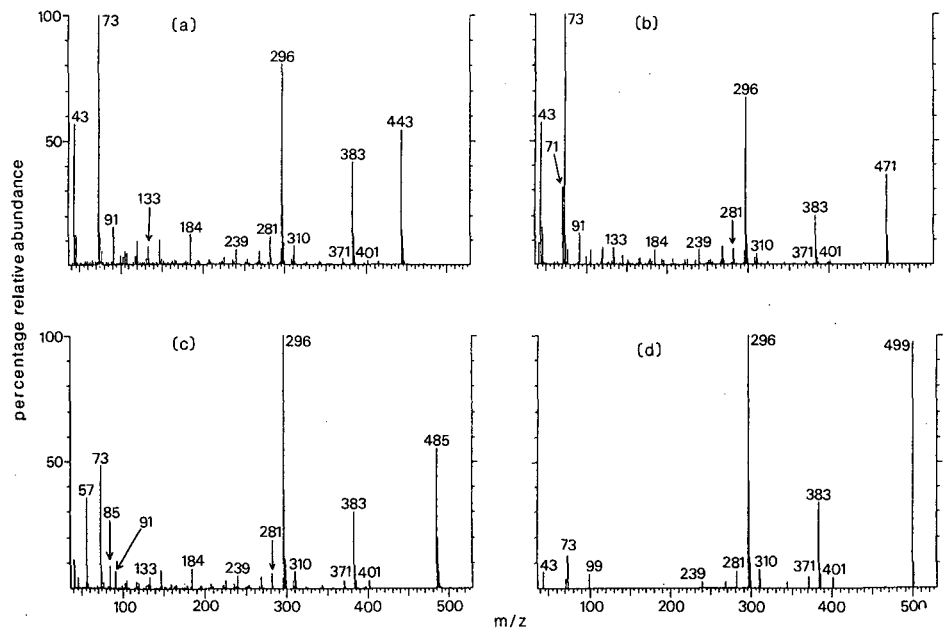

Fig. 4. Mass spectra recorded at 70 eV of the bis-TMS derivatives of: (a) pinobanksin-3-acetate, $[M]^+$ at m/z 458; (b) pinobanksin-3-butanoate (or isobutanoate), $[M]^+$ at m/z 486; (c) pinobanksin-3-pentanoate (or methylbutanoate), $[M]^+$ at m/z 500; (d) pinobanksin-3-hexanoate (or methylpentanoate), $[M]^+$ at m/z 514. Spectra (a), (c) and (d) were recorded from *P. maximowiczii* and spectrum (b) was recorded from *P. fremontii*. Spectrum (d) is of low intensity as the compound concerned is present in low quantities.

TABLE II

INITIAL MS FRAGMENTATION PATTERN OF PINOBANKSIN (3,5,7-TRIHYDROXY-FLAVANONE) DERIVATIVES ESTERIFIED AT THE 3-POSITION

Compound	*Peak No.*[a]	*m/z*	*Fragment*	*Composition*
R1	7	443	$[M-15]^+$	$M-CH_3$ (from TMS)
		401	$[M-57]^+$	$M-CH_3-COCH_2$
		383	$[M-75]^+$	$M-CH_3-H-OCOCH_3$
R2	11	457	$[M-15]^+$	$M-CH_3$ (from TMS)
		401	$[M-71]^+$	$M-CH_3-COC_2H_4$
		383	$[M-89]^+$	$M-CH_3-H-OCOC_2H_5$
R3	15	471	$[M-15]^+$	$M-CH_3$ (from TMS)
		401	$[M-85]^+$	$M-CH_3-COC_3H_6$
		383	$[M-103]^+$	$M-CH_3-H-OCOC_3H_7$
R4	17	485	$[M-15]^+$	$M-CH_3$ (from TMS)
		401	$[M-99]^+$	$M-CH_3-COC_4H_8$
		383	$[M-117]^+$	$M-CH_3-H-OCOC_4H_9$
R5	19, 20	499	$[M-15]^+$	$M-CH_3$ (from TMS)
		401	$[M-113]^+$	$M-CH_3-COC_5H_{10}$
		383	$[M-131]^+$	$M-CH_3-H-OCOC_5H_{11}$

[a] These numbers refer to the peak numbers in Fig. 1 and Table I.

fragmentation pattern in Table II; the mass spectra of pinobanksin esterified at the 3-position with CH_3COOH, C_3H_7COOH, C_4H_9COOH and $C_5H_{11}COOH$ are shown in Fig. 4.

DISCUSSION

The bud exudates of *P. fremontii* and *P. maximowiczii* are distinctive in that they contain large quantities of pinobanksin-3-acetate (peak 7). This implies that the enzyme responsible for acetylating pinobanksin in the 3-position is very active in these poplars. We suggest that either this enzyme has a low affinity for other acids or other acids are present in low amounts compared to acetic acid.

We do not know whether the C_4, C_5 and C_6 acids used for esterifying the 3-hydroxyl group of pinobanksin are linear or branched chain although all are saturated. The MU retention times (Table I) indicate that the substituent in peak 19 is branched chain (pinobanksin-3-methylpentanoate) whilst in peak 20 it probably is not (pinobanksin-3-hexanoate). We also deduce that the substituent in peak 17 is probably branched chain and therefore represents pinobanksin esterified in the 3-position with either 2-methylbutanoic acid or 3-methylbutanoic acid. Previous results from *P. nigra* L. bud exudate[4] have shown that caffeic acid forms esters with 2-methylpropanol, 2- or 3-methylbutanol and 4-methylpentanol and we suggest that the acids corresponding to these alcohols will be present in some bud exudates and therefore available for esterifications.

A number of flavonoid esters have been previously reported, including several acetates and butanoates[7,8], pinobanksin-3-cinnamate[9], chrysin-7-benzoate[10] and 3-angeloyloxy-8-methoxy-5,7,4′-trihydroxyflavanone together with the corresponding ester with a pentanoic acid[11]. We here extend this list of known flavonoid esters.

ACKNOWLEDGEMENT

We thank F. Topliffe for collecting the bud exudate of *P. fremontii.*

REFERENCES

1 W. Greenaway, J. May and F. R. Whatley, *J. Chromatogr.*, 472 (1989) 393.
2 W. Greenaway, T. Scaysbrook and F. R. Whatley, *Proc. R. Soc. London, Ser. B*, 232 (1987) 249.
3 E. Wollenweber, Y. Asakawa, D. Schillo, U. Lehmann and H. Weigel, *Z. Naturforsch., C: Biosci.*, 42 (1987) 1030.
4 W. Greenway, E. Wollenweber, T. Scaysbrook and F. R. Whatley, *Z. Naturforsch., C: Biosci.*, 43 (1988) 795.
5 W. Greenaway, E. Wollenweber, T. Scaysbrook and F. R. Whatley, *J. Chromatogr.*, 448 (1988) 284.
6 E. Wollenweber, M. Chadenson and M. Hauteville, *Z. Naturforsch., C: Biosci.*, 28 (1973) 638.
7 E. Wollenweber, J. Favre-Bonvin and M. Jay, *Z. Naturforsch., C: Biosci.*, 33 (1978) 831.
8 E. Wollenweber, *Phytochemistry*, 24 (1985) 1493.
9 C. Scheele, E. Wollenweber and F. J. Arriaga-Giner, *J. Nat. Prod.*, 50 (1987) 181.
10 F. J. Arriaga-Giner, E. Wollenweber and D. Hradetzky, *Z. Naturforsch., C: Biosci.*, 41 (1986) 946.
11 P. Proksch, M. Breuer, A. Mitsakos and H. Budzikiewicz, *Planta Med.*, 53 (1987) 334.
12 C. E. Dalgliesh, E. C. Horning, M. G. Horning, K. L. Knox and K. Yarger, *Biochem. J.*, 101 (1966) 792.

Journal of Chromatography, 481 (1989) 358–362
Elsevier Science Publishers B.V., Amsterdam — Printed in The Netherlands

CHROM. 21 821

Note

Determination of anatoxin-a, the neurotoxin of *Anabaena flos-aquae* cyanobacterium, in algae and water by gas chromatography–mass spectrometry

KIMMO HIMBERG
Technical Research Centre of Finland, Food Research Laboratory, Biologinkuja 1, SF-02150 Espoo (Finland)
(Received May 8th, 1989)

Cyanobacteria, or blue-green algae, are known to include several potentially toxin-producing species. A toxic cyanobacterial bloom was first reported in 1878 to have caused deaths of domestic animals which had been drinking water containing bloom[1]. Toxic blooms have been verified in at least twenty countries thereafter, with several poisonings of both domestic and wild animals[2]. There are also indications that cyanobacterial toxins may pose a potential health risk for man. Sometimes they are even able to contaminate raw water sources; there are reports of cases where they have affected human health through domestic water use[3,4].

Several different types of toxins have been described[2]. Two of the most typical groups are hepatotoxic cyclic peptides and alkaloid neurotoxins. The only compound from the latter group that has been thoroughly characterized is anatoxin-a, or 2-acetyl-9-azabicyclo[4.2.1]non-2-ene (Fig. 1), produced by *Anabaena flos-aquae*. Toxic strains of *Anabaena* have previously been reported in Canada[5] and Finland[6].

Several methods for the determination of cyanobacterial hepatotoxins have been published[7–9]. Studies of methods for the determination of cyanobacterial neurotoxins has been less intensive; to my knowledge, only one report concerning the determination of anatoxin-a has been published[10].

The aim of this work was to develop a sensitive, simple, reliable and highly selective method for the determination of anatoxin-a in algae and in water and thus make it possible routinely to control potential hazard situations in raw water sources and recreational waters during *Anabaena* blooms. In order to obtain high sensitivity and selectivity, a low-resolution quadrupole mass spectrometer working in the selective ion monitoring (SIM) mode was used as a detector.

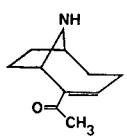

Fig. 1. Structure of anatoxin-a.

0021-9673/89/$03.50

EXPERIMENTAL

Materials

The algal material was collected on August 19th, 1986, from a bloom in Lake Säyhteenjärvi, Artjärvi, southern Finland. The material gave typical symptoms of anatoxin-a poisoning when suspended in physiological sodium chloride solution and injected intraperitoneally into mice. Its anatoxin-a content was later shown to be 4.4 mg/g of lyophilized algal material[6].

Cyanobacteria used as blank samples were collected from Lake Pitkäjärvi, Espoo, southern Finland. The bloom consisted mainly of *Aphanizomenon* and was shown to be non-toxic by mouse bioassay.

The algal materials were freeze-dried in an Atlas pilot-scale freeze-dryer.

The organic solvents and other chemicals used were of analytical-reagent grade (Merck, Darmstadt, F.R.G.) or pesticide grade (Mallinckrodt, Paris, KY, U.S.A.). Kieselgel 60 plates (20 × 20 cm, 0.25 mm layer thickness; Merck) were used for thin-layer chromatographic (TLC) purification of anatoxin-a. Millex-HV filters (0.45 μm) and Sep-Pak silica cartridges (both from Millipore/Waters, Milford, MA, U.S.A.) were used in sample preparation.

Preparative purification of anatoxin-a

The preparation of anatoxin-a standards was performed by modifying the methods of Devlin *et al.*[5] and Abstrachan and Archer[10] in the following way. A 16.5-g amount of lyophilized algae was suspended in 1.5 l of distilled water and, after adjusting the pH to 5 with hydrochloric acid, the suspension was left to equilibrate overnight. It was then clarified by centrifuging at 10 000 rpm (9200 *g*) for 10 min and the clear solution was diluted to 2.5 l and adjusted to pH 10.5. The toxin was then concentrated into a 30 × 1.5 cm I.D. XAD-2 column, which had first been washed consecutively with distilled water, acetone and 0.01 *M* sodium carbonate solution. The dilute toxin solution was poured slowly through the column, which was then washed with 2 l of sodium carbonate solution. The toxin was eluted with 200 ml of 0.01 *M* hydrochloric acid–ethanol solution which was then evaporated in a rotary evaporator to *ca.* 15 ml. A similar volume of distilled water was added and the solution was washed with two 30-ml volumes of *n*-hexane. After adjusting the pH to 11 with sodium hydroxide solution, anatoxin-a was extracted four times with 40 ml of chloroform and then back-extracted from the combined chloroform solutions with three 50 ml-volumes of 0.001 *M* hydrochloric acid. The yellowish solid material obtained by drying the solution was further purified by TLC with methanol–chloroform (1:4) as eluent. The zone of R_F = 0.2–0.4 containing anatoxin-a was scraped off and boiled in acidic methanol under reflux for 2 h. Anatoxin-a was again extracted from the alcohol solution as described previously and the dried material (*ca.* 20 mg) used for the analytical standards.

Method for determining anatoxin-a in algal material

The algae are freeze-dried. The leafy material thus formed is homogenized and mixed thoroughly and an aliquot of 20 mg placed in a centrifuge tube for analysis. A 10-ml volume of methanol and 0.1 ml of concentrated hydrochloric acid are added and the suspension is mixed thoroughly and extracted in an ultrasonic bath for 15

min. The suspension is centrifuged, the extraction step repeated and the combined solutions filtered through a Millex-HV filter. The solution is then evaporated nearly to dryness in a Kuderna–Danish evaporator. The residue is dissolved in 1 ml of chloroform, 1 ml of concentrated acetic acid and 0.5 ml of acetic anhydride are added, the solution is mixed gently and the test-tube closed tightly. The mixture is then left to react overnight (16 h) at 50°C. The excess of reagent and the solvent are again evaporated nearly to dryness in a Kuderna–Danish evaporator (no smell of acetic acid should be detectable) and the residue is dissolved in 1 ml of chloroform. The solution is transferred into a Sep-Pak silica cartridge, which is cleaned with 7.5 ml of acetone–chloroform (5:95). Acetylanatoxin-a is finally eluted with 2 ml of methanol, which is then concentrated under a gentle stream of nitrogen to about 100 μl and chloroform is added to a final volume of 1 ml. This solution is used for gas chromatographic–mass spectrometric (GC–MS) analysis.

Method for determining anatoxin-a in water

A 12-ml volume of 0.25 *M* sodium carbonate solution is added to 100 ml of water and the solution is mixed thoroughly. It is then extracted three times with 100 ml of chloroform and the combined chloroform solutions are concentrated to about 10 ml in a rotary evaporator. A 5-ml volume of methanol and 0.1 ml of concentrated hydrochloric acid are added and the solution is mixed thoroughly and concentrated nearly to dryness in a Kuderna–Danish evaporator. The derivatization step is per-

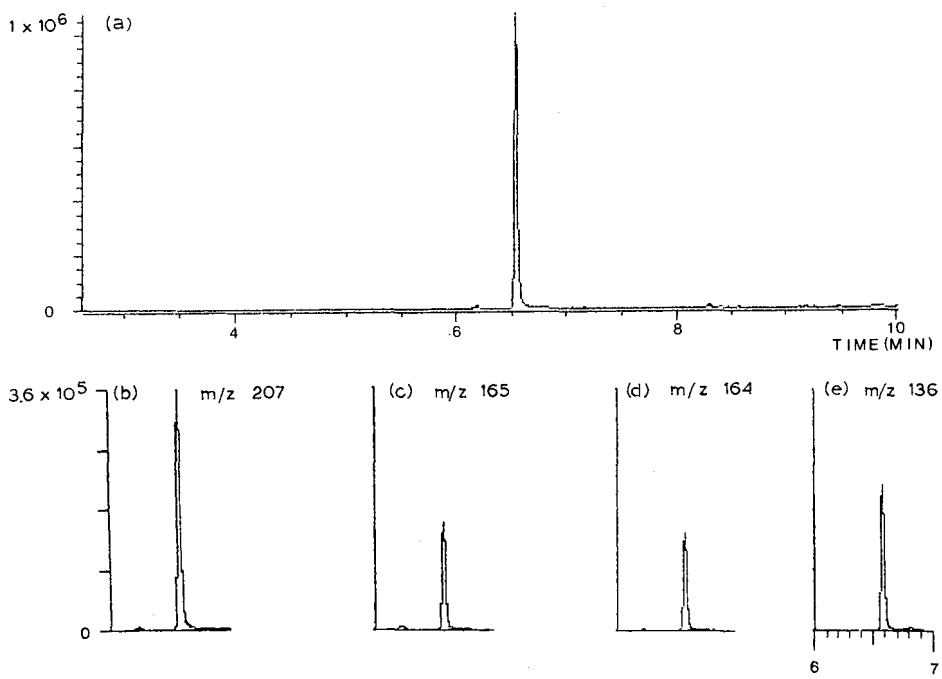

Fig. 2. Typical GC–MS traces from a run with an *Anabaena flos-aquae* sample. Top, total ion chromatogram; below, ion chromatograms with four monitored ions.

formed as above, although with relatively clean waters the Sep-Pak purification is normally not necessary.

GC–MS analysis

A GC–MS system consisting of a Hewlett-Packard 5790 gas chromatograph, an HP 5970B mass-selective detector and an HP 59970C ChemStation data system was used in the determination step. The column was 15 m × 0.2 mm I.D. with HP-1 cross-linked methylsilicone as stationary phase with a 0.33-μm film thickness (Hewlett-Packard, Avondale, PA, U.S.A.). Helium was used as the carrier gas at an injector pressure of 0.5 kg/cm^2 and the oven was temperature programmed from 80 to 275°C at 15°C/min. The volume injected was 1 μl, splitless time 45 s and the injector temperature 240°C. Ions of m/z = 207, 165, 164 and 136 were used for monitoring anatoxin-a. A typical group of ion chromatograms is presented in Fig. 2.

RESULTS AND DISCUSSION

The adequacy of the extraction step was checked by doubling the solvent volumes and by performing a second extraction from samples that had already been treated. The linearity of the method for anatoxin-a in algal material was tested by mixing various amounts of dried *Anabaena* and non-toxic *Aphanizomenon*. The anatoxin-a contents of these mixtures were determined in triplicate. Fig. 3 shows the detector signal as a function of amount of anatoxin-a injected; the test runs were performed with samples containing 1–20 mg of *Anabaena* in a 20-mg sample. The concentration range was selected to cover the most typical concentrations of anatoxin-a in Finnish *Anabaena* blooms[6]. The limit of determination (LOD) lies far below these concentrations at the level of 0.1 ng of anatoxin-a injected assuming a signal-to-

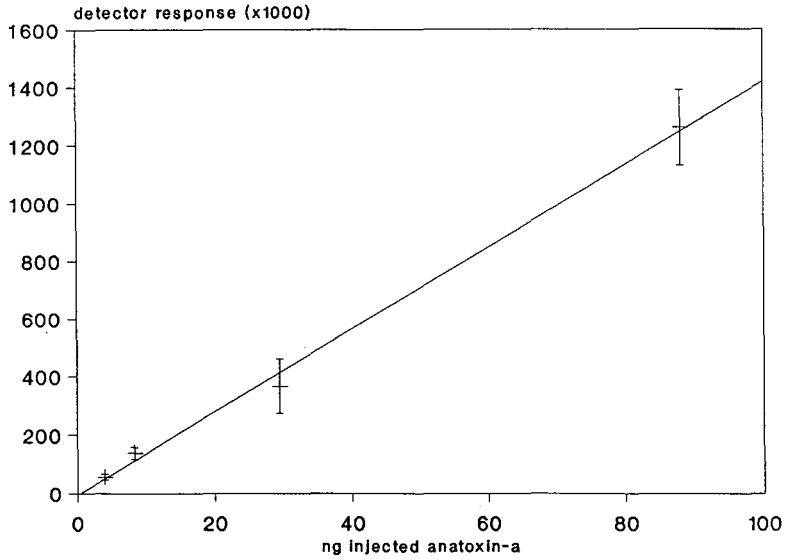

Fig. 3. Detector response (m/z 207) as a function of amount of anatoxin-a injected. Average of triplicate determinations ± S.D.

noise ratio of 100:1 at m/z 207, which is considered satisfactory regarding the natural background from the samples. The LOD corresponds to a concentration of 5 μg/g in dry algal material, an extremely low value for typical blooms, or 1 μg/l in water.

Cases in which anatoxin-a has to be determined in water samples are rare. In natural waters it should only be present in connection with an *Anabaena* bloom and then the algae themselves can be examined. However, if a bloom exists in a raw water source and the water treatment procedure does not include an effective filtration step, there is a possibility of finding anatoxin-a in the treated water also[11]. It is in such a situation that a method is needed for determining anatoxin-a in water.

The methods described above have been used in this laboratory for routine determinations of anatoxin-a in samples of algal blooms and in investigations concerning the behaviour of anatoxin-a in commonly used raw water treatment procedures, the results of which will be published elsewhere[11]. They have proved to fulfil the original aims of simplicity, selectivity and sensitivity and therefore it is expected that they could fill a need also in other laboratories concerned with research on the aqueous environment.

REFERENCES

1 G. Francis, *Nature (London)*, 18 (1878) 11.
2 W. W. Carmichael, C. L. A. Jones, N. A. Mahmood and W. C. Theiss, *CRC Crit. Rev. Environ. Control*, 15 (1985) 275.
3 I. R. Falconer, A. M. Beresford and M. T. C. Runnegar, *Med. J. Aust.*, 1 (1983) 511.
4 P. R. Hawkins, M. T. C. Runnegar, A. R. B. Jackson and I. R. Falconer, *Appl. Environ. Microbiol.*, 50 (1985) 1292.
5 J. P. Devlin, O. E. Edwards, P. R. Gorham, N. R. Hunter, R. K. Pike and B. Stavric, *Can. J. Chem.*, 55 (1977) 1367.
6 K. Sivonen, K. Himberg, R. Luukkainen, S. Niemelä, G. Poon and G. Codd, paper presented at the *First Biennial Water Quality Symposium: Microbiological Aspects, Banff, Alberta, Canada, August 29th–September 2nd, 1988*, Abstracts, p. 10.
7 H. W. Siegelman, W. H. Adams, R. D. Stoner and D. N. Slatkin, in E. P. Ragelis (Editor), *Seafood Toxins*, ACS Symposium Series, No. 262, American Chemical Society, Washington, DC, 1984, p. 407.
8 T. Krishnamurthy, W. W. Carmichael and E. W. Sarver, *Toxicon*, 24 (1986) 865.
9 J. A. O. Meriluoto and J. E. Eriksson, *J. Chromatogr.*, 438 (1988) 93.
10 N. B. Abstrachan and B. G. Archer, in W. W. Carmichael (Editor), *The Water Environment: Algal Toxins and Health*, Vol. 20, Plenum Press, New York, 1981, pp. 437–446.
11 K. Himberg, L. Hiisvirta, R. Luoma and A.-M. Keijola, in preparation.

Journal of Chromatography, 481 (1989) 363–367
Elsevier Science Publishers B.V., Amsterdam — Printed in The Netherlands

CHROM. 21 822

Note

Determination of the enantiomeric composition of γ-lactones in complex natural matrices using multidimensional capillary gas chromatography

ALEXANDER BERNREUTHER
Lehrstuhl für Lebensmittelchemie, Universität Würzburg, Am Hubland, D-8700 Würzburg (F.R.G.)
NORBERT CHRISTOPH
Landesuntersuchungsamt für das Gesundheitswesen Nordbayern, Theaterstr. 23, D-8700 Würzburg (F.R.G.)
and
PETER SCHREIER*
Lehrstuhl für Lebensmittelchemie, Universität Würzburg, Am Hubland, D-8700 Würzburg (F.R.G.)
(Received June 6th, 1989)

It is generally recognized that chiral discrimination is an essential principle of odour perception[1], and the determination of enantiomeric composition of aroma compounds is therefore very important in flavour analysis[2].

γ-Lactones are widely used as intermediates in the synthesis of natural products and are important, widespread aroma compounds[3,4]. Recently, sensory characteristics of several optically pure γ-lactones have been described[5]. Owing to the importance of this class of compounds in flavour chemistry, there have been a number of publications dealing with their chiral analysis. Recently, direct enantiomer separation of γ-lactones on chiral stationary phases has been described, *e.g.*, using both capillary (high-resolution) gas chromatography (HRGC)[6] and high-performance liquid chromatography (HPLC)[7,8]. However, results for the chiral evaluation of naturally occurring γ-lactones in plant tissues, *e.g.*, fruits, are scarce[9–12] owing to the difficulties in determining their enantiomeric composition in a complex natural matrix. In order to avoid laborious sample preparation and preseparation, multidimensional capillary GC (MDGC) has been recommended[13,14]. Extending our recent work on the chirality evaluation of secondary alcohols from banana fruit using MDGC with achiral and chiral columns[15], this paper reports the use of MDGC for the determination of the enantiomeric composition of γ-lactones in various fruits.

EXPERIMENTAL

Fruits

Fresh mangoes (from Venezuela) and yellow passion fruits (from Columbia) and deep-frozen apricots, peaches, raspberries and strawberries (all purchased in the local market) were used.

0021-9673/89/$03.50

Sample preparation

Deep-frozen fruits were thawed, stone fruits were stoned and passion fruits were peeled. After addition of 1 l of distilled water to 2.5 kg of fruit pulp and homogenization in a Braun blender (3 min), centrifugation (40 min, 3000 *g*) was carried out. The supernatants were continuously extracted over 36 h using pentane–dichloromethane (2:1) (40°C). The extracts were dried over anhydrous sodium sulphate and carefully concentrated to approximately 0.2 ml using a Vigreux column (45°C).

Optically pure reference substances

(*R*)- and (*S*)-4-alkylated γ-lactones were obtained from racemic references (γ-pentalactone to γ-dodecalactone; Roth, Karlsruhe, F.R.G.) by semi-preparative HPLC separation on a Hibar Chiraspher column (RT 250-4; 250 × 4 mm I.D.; particle diameter 5 μm; Merck, Darmstadt, F.R.G.) as recently described[8].

Capillary gas chromatography–mass spectrometry (HRGC–MS)

A Hewlett-Packard HP 5890A gas chromatograph coupled by an open-split interface to an HP 5970B mass-selective detector with an HP 300 data system was used. The apparatus was equipped with a J & W DB-Wax capillary column (30 m × 0.32 mm I.D.; film thickness 0.25 μm). Splitless injection [200°C; split opened (1:13) after 0.3 min] was employed. The column temperature was programmed from 40 to 250°C at 3.5°C/min. The carrier gas was helium at 1.4 ml/min, the temperature of the ion source and all connecting parts was 200°C and the electron energy was 70 eV. The selected ion monitoring (SIM) mode using *m/z* 85, 56 and 100 for γ-lactone detection was used.

Multidimensional gas chromatography (MDGC)

A Siemens Sichromat 2 double oven gas chromatograph with split injection (250°C; 1:55) and flame ionization detectors on ovens 1 and 2 (both at 250°C) was used. Preseparation was achieved in oven 1 on a BC SE-54 fused-silica capillary column (25 m × 0.25 mm I.D.; film thickness 0.2 μm). The temperature was programmed from 80 to 280°C at 5°C/min and held isothermally at 280°C for 20 min. A "live" switching device[16] in oven 1 was used to perform effluent cuts on column 2 in oven 2 [Pyrex glass capillary, Lipodex B (Macherey, Nagel & Co.), 25 m × 0.25 mm I.D.). The temperature was isothermal at 100°C for 10 min, then programmed from 100 to 180°C at 2°C/min and held isothermally at 180°C for 10 min. Cuts of 30 s were selected for each γ-lactone separately. Nitrogen was used as the carrier gas at 0.42 ml/min in oven 1 and 0.67 ml/min in oven 2. The flow-rates for the detector gases were 27 and 31 ml/min of hydrogen and 268 and 280 ml/min of air for ovens 1 and 2, respectively. Injection volumes of 0.5–2 μl were used.

Results of qualitative analyses were verified by comparison of MDGC retention data for authentic racemic and optically pure γ-lactones.

RESULTS AND DISCUSSION

First, the high capacity of Lipodex B [hexakis(3-O-acetyl-2,6-di-O-pentyl)-α-cyclodextrin] for the enantioseparation of γ-lactones[17] was confirmed under MDGC conditions. The α values obtained are given in Table I. In accordance with recent

TABLE I

SEPARATION FACTORS OBTAINED FOR HOMOLOGOUS CHIRAL 4-ALKYLATED γ-LACTONES (ALKYL CHAIN LENGTHS FROM C_1 TO C_8) UNDER MDGC CONDITIONS (SE-54/LIPODEX B)

γ-Lactone	*α-Value*	*γ-Lactone*	*α-Value*
γ-Pentalactone	1.154	γ-Nonalactone	1.028
γ-Hexalactone	1.126	γ-Decalactone	1.023
γ-Heptalactone	1.046	γ-Undecalactone	1.020
γ-Octalactone	1.030	γ-Dodecalactone	1.022

information[6], the order of elution, established with optically pure reference compounds, was (*R*) before (*S*). A detection limit of approximately 1 μg/ml was calculated.

In the aroma extracts obtained from the fruits studied (apricot, mango, passion fruit, peach, raspberry and strawberry), the occurrence of γ-lactones was checked by HRGC–MS using SIM. In MDGC analyses, their identities were verified by comparison of their HRGC retention data on two columns using authentic racemic and optically pure reference compounds. For the enantiomeric differentiation of natural γ-lactones on the chiral column, for each γ-lactone detected in the fruits a 30-s cut was performed according to the retention time. A representative example is shown in Fig. 1, in which the preseparation of peach volatiles on SE-54 without cutting and the enantiomeric separation of γ-decalactone on Lipodex B with cutting are outlined. All γ-lactones present in the above-mentioned fruits were investigated in a similar manner. The results are summarized in Table II.

For the composition of γ-lactones in the fruits studied, earlier elaborated data from the TNO list[18] were confirmed. However, in apricot γ-penta- and γ-heptalactone and in strawberry γ-penta-, γ-nona- and γ-undecalactone were additionally detected in trace amounts for the first time.

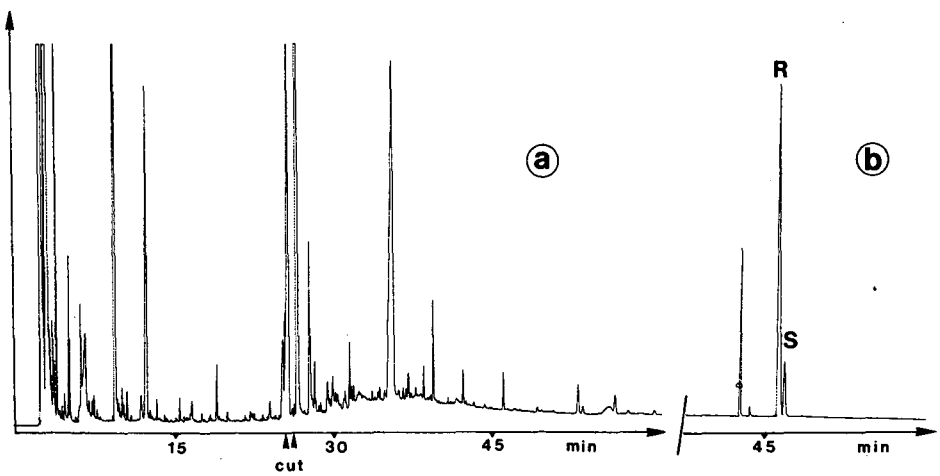

Fig. 1. MDGC separation of peach volatiles. (a) Preseparation on SE-54. (b) Enantiomeric separation of γ-decalactone on Lipodex B with cutting (25.5–26.0 min). See Experimental for details.

TABLE II

OCCURRENCE AND ENANTIOMERIC COMPOSITION OF CHIRAL 4-ALKYLATED γ-LACTONES IN DIFFERENT FRUITS

γ-Lactone	*Fruit*[a]	*(R)- (%)*	*(S)- (%)*	*Enantiomeric excess (%)*
γ-Pentalactone	AP	78.6	21.4	(*R*)-57.2
	MA	tr[b]	tr	—
	PE	73.4	26.6	(*R*)-46.8
	ST	40.1	59.9	(*S*)-19.8
γ-Hexalactone	AP	90.2	9.8	(*R*)-80.4
	MA	26.4	73.6	(*S*)-47.2
	PA	65.5	34.5	(*R*)-31.0
	PE	90.2	9.8	(*R*)-80.4
	RA	31.9	68.1	(*S*)-36.2
	ST	41.7	58.3	(*S*)-16.6
γ-Heptalactone	AP	81.8	18.2	(*R*)-63.6
	MA	tr	tr	—
	PA	32.4	67.6	(*S*)-35.2
	PE	33.5	66.5	(*S*)-33.0
	ST	34.2	65.8	(*S*)-31.6
γ-Octalactone	AP	89.1	10.9	(*R*)-78.2
	MA	53.4	46.6	(*R*)-6.8
	PA	59.1	40.9	(*R*)-18.2
	PE	86.8	13.2	(*R*)-73.5
	RA	39.9	60.1	(*S*)-20.2
	ST	66.2	33.8	(*R*)-32.4
γ-Nonalactone	AP	83.7	16.3	(*R*)-67.4
	MA	73.3	26.7	(*R*)-46.6
	PA	92.6	7.4	(*R*)-85.2
	PE	84.6	15.4	(*R*)-69.2
	ST	63.6	36.4	(*R*)-27.2
γ-Decalactone	AP	94.3	5.7	(*R*)-88.6
	MA	65.8	34.2	(*R*)-31.6
	PA	91.3	8.7	(*R*)-82.6
	PE	87.4	12.6	(*R*)-74.8
	ST	97.9	2.1	(*R*)-95.9
γ-Undecalactone	PE	81.2	18.8	(*R*)-62.4
	ST	tr	tr	—
γ-Dodecalactone	AP	100.0	0.0	(*R*)-100.0
	MA	100.0	0.0	(*R*)-100.0
	PA	97.6	2.4	(*R*)-95.2
	PE	96.3	3.7	(*R*)-92.6
	ST	98.3	1.7	(*R*)-96.6

[a] AP = apricot; MA = mango; PA = passion fruit; PE = peach; RA = raspberry; ST = strawberry.

[b] tr = Traces (enantiomeric discrimination not possible).

Concerning the enantiomeric distribution of γ-lactones in fruits, only a few studies have been carried out, *e.g.*, on nectarine[10], strawberry[11], peach[12] and mango[19]. Except for the enantiomeric composition of γ-octalactone in mango, the

previous findings were confirmed, *i.e.*, the occurrence of optically pure γ-deca- and γ-dodecalactone in strawberry, with an (*R*)- to (*S*)- ratio of approximately 88:12, and prevalence of the (*R*)-enantiomer of γ-decalactone in peach and mango. The discrepancy found for γ-octalactone in mango may be caused by varietal differences.

In general, in all fruits, the enantioselectivity increased with increasing chain length of γ-lactones (Table II). Whereas γ-dodecalactone was found to be present in approximately pure optical (*R*)-form in the fruits under study, shorter chained γ-lactones such as γ-pentalactone to γ-octalactone mainly showed large variations in the enantiomeric compositions. The biogenetic reason for this fact is not clear. At least two different enzyme systems or pathways in fruits, which potentially compete and lead to different enantiomeric ratios of γ-lactones, can be assumed[10].

REFERENCES

1 G. Ohloff, *Experientia*, 42 (1986) 271.
2 A. Mosandl, *Food Rev. Int.*, 4 (1988) 1.
3 J. A. Maga, *CRC Crit. Rev. Food Sci. Nutr.*, 8 (1976) 1.
4 G. Ohloff, *Fortschr. Chem. Org. Naturst.*, 35 (1978) 431.
5 A. Mosandl and C. Günther, *J. Agric. Food Chem.*, 37 (1989) 413.
6 A. Mosandl, U. Palm, C. Günther and A. Kustermann, *Z. Lebensm.-Unters.-Forsch.*, 138 (1989) 148.
7 E. Francotte and D. Lohmann, *Helv. Chim. Acta*, 70 (1987) 1569.
8 M. Huffer and P. Schreier, *J. Chromatogr.*, 469 (1989) 137.
9 R. Tressl and K. H. Engel, in P. Schreier (Editor), *Analysis of Volatiles*, Walter de Gruyter, Berlin, New York,1984, p. 322.
10 K. H. Engel, in P. Schreier (Editor), *Bioflavour '87*, Walter de Gruyter, Berlin, New York, 1988, p. 75.
11 G. Krammer, O. Fröhlich and P. Schreier, in P. Schreier (Editor), *Bioflavour '87*, Walter de Gruyter, Berlin, New York, 1988, p. 89.
12 M. Feuerbach, O. Fröhlich and P. Schreier, *J. Agric. Food Chem.*, 36 (1988) 1236.
13 G. Schomburg, H. Husmann, L. Podmaniczky and F. Weeke, in P. Schreier (Editor), *Analysis of Volatiles*, Walter de Gruyter, Berlin, New York, 1984, p. 121.
14 S. Nitz, H. Kollmannsberger and F. Drawert, in P. Schreier (Editor), *Bioflavour '87*, Walter de Gruyter, Berlin, New York, 1988, p. 123.
15 O. Fröhlich, M. Huffer and P. Schreier, *Z. Naturforsch.*, in press.
16 G. Schomburg, F. Weeke, F. Müller and M. Oreans, *Chromatographia*, 16 (1983) 87.
17 W. A. König, S. Lutz, C. Colberg, N. Schmidt, G. Wenz, E. von der Bey, A. Mosandl, C. Günther and A. Kustermann, *J. High Resolut. Chromatogr. Chromatogr. Commun.*, 11 (1988) 621.
18 H. Maarse and C. A. Visscher (Editors), *Volatile Compounds in Food, Qualitative Data*, Suppl. 1–5, TNO–CIVO, Zeist, 5th ed., 1987.
19 R. Tressl, K. H. Engel and W. Albrecht, in S. Nagy, J. A. Attaway and M. E. Rhodes (Editors), *Adulteration of Fruit Juice Beverages*, Marcel Dekker, New York, 1988, p. 67.

Journal of Chromatography, 481 (1989) 368–372
Elsevier Science Publishers B.V., Amsterdam — Printed in The Netherlands

CHROM. 21 748

Note

Determination of panaxytriol, a new type of tumour growth inhibitor from Panax ginseng, by capillary gas chromatography

HISASHI MATSUNAGA, MITSUO KATANO, HIROSHI YAMAMOTO, MASATO MORI and KATSUMI TAKATA*

Hospital Pharmacy and Department of Surgery, Saga Medical School, Nabeshima-Sambonsugi, Nabeshima-machi, Saga 840-01 (Japan)

and

MASATOSHI NISHI

Faculty of Pharmaceutical Science, Setsunan University, Nagaotouge-cho, Hirakata, Osaka 573-01 (Japan)

(First received March 13th, 1989; revised manuscript received June 26th, 1989)

Panax ginseng is known for its unique antitumour therapeutical effect[1]. During a series of studies aimed at isolation of the tumour growth inhibitory substance from Panax ginseng, we found a substance, a polyacetylenic alcohol, which inhibits tumour cell growth in a dose-dependent fashion *in vitro*[2,3]. Data from infrared (IR), proton and carbon-13 nuclear magnetic resonance and high-resolution mass spectra were identical with those of authentic panaxytriol, heptadec-1-ene-4,6-diyne-3,9,10-triol, previously described by several investigators[4,5].

In order to examine the mechanism of cell growth inhibition caused by panaxytriol, it is important to develop an assay method for panaxytriol. We describe in this paper a gas chromatographic (GC) method for its quantitation by silylation.

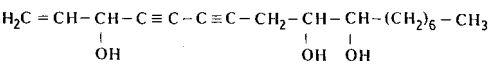

Fig. 1. Chemical structure of panaxytriol.

EXPERIMENTAL

Materials and reagents

A powder of the root of Panax ginseng C. A. Meyer was provided by Nikkan Korai Ninjin (Kobe, Japan). The root material is commonly used in Japan for treatment of various diseases as a commercial medicinal drug by the name of Korean Red Ginseng Powder. The isolation of panaxytriol from Korean Red Ginseng Powder has been described previously[2,3]. Briefly, the powder was extracted with ethyl acetate, and the extracts were separated by silica gel chromatography. Panaxytriol-rich fractions were collected and panaxytriol was purified by crystallization from distilled water. The chemical structure of isolated panaxytriol was verified by comparison with IR, proton and carbon-13 nuclear magnetic resonance and high-resolution mass

0021-9673/89/$03.50

spectra in the literature[4,5]. The purity of panaxytriol was confirmed by two-dimensional thin-layer chromatography (TLC). Briefly, TLC was performed on high-performance silica gel 60 plates (10 cm × 10 cm; E. Merck, Darmstadt, F.R.G.). The plate was first developed with ethyl acetate. When the solvent front had migrated about 8 cm, the plate was dried in air for 15 min and developed in the second dimension with ethyl acetate–*n*-hexane (1:1, v/v); the solvent front was again allowed to move about 8 cm. The spots were detected by spraying the plates with concentrated H_2SO_4 and by heating.

Bis(trimethylsilyl)trifluoroacetamide (BSTFA) was obtained from Gasukuro Kogyo (Tokyo, Japan). The internal standard, 1-docosanol, was obtained from Gasukuro Kogyo and a solution containing 20 μg/ml in chloroform was prepared.

Panaxytriol was dissolved in RPMI 1640 culture medium containing 10% foetal calf serum (Gibco Lab., NY, U.S.A.).

All other chemicals were of reagent grade and were used without further purification.

Instrumentation

An Hitachi gas chromatograph Model 663-30 equipped with a flame-ionization detector (Hitachi, Tokyo, Japan) and moving needle solvent-cut sample injection (MNSCSI) (Gasukuro Kogyo) was used for all analyses[6]. MNSCSI was used for increasing the sensitivity by concentrating the sample on the tip of the needle.

The column used was a flexible fused-silica capillary coated with OV-1701 (50 m × 0.25 mm I.D., d_f 0.15 μm; theoretical plates, 3806 per metre; Gasukuro Kogyo). The injection and detector temperatures were set at 250°C, while the column temperature was kept at 250°C. Helium was used as the carrier gas and make-up gas at flow-rates of 1.1 and 35 ml/min, respectively. The flow-rates of air and hydrogen were adjusted to 400 and 40 ml/min, respectively. A splitting ratio of 68:1 was used.

Gas chromatography–mass spectrometry (GC–MS) measurements were carried out with a JEOL JMS-D300, operated in the electron impact (EI) mode. The ionization voltage and ionization current were 30 eV and 0.3 mA, respectively; the injection port and separator temperatures were 250°C, the interface temperature 200°C and the electron multiplier voltage 1500 V, respectively. EI mass spectra were taken by continuously scanning the mass range m/z 50–500 every 1.0 s.

Extraction and derivatization

A 50-μl volume of internal standard (1-docosanol, 20 μg/ml, in chloroform) was transferred to extraction tubes and dried at 40°C under a stream of nitrogen. A 1.0-ml panaxytriol-containing culture medium was added to the residue, and mixed. Ethyl acetate (5 ml) was added and vortex-mixed for 30 s. The mixture was vigorously shaken mechanically at approximately 280 strokes per min for 10 min at room temperature. After centrifugation at 1500 *g* for 10 min, the organic phase was transferred to a 10-ml glass tube and concentrated under a stream of nitrogen at 40°C. The concentrated material was transferred to a micro-glass tube and dried. Then, 10 μl of triethylamine and 10 μl of BSTFA were added to the dry residue for derivatization of panaxytriol and 1-docosanol. The micro-glass tube was sealed and heated at 60°C for 60 min. After silylation, an 1.0-μl aliquot was adhered to the needle surface of the injector. After evaporating the solvent, the sample was injected onto the column.

Calibration graph

Various amounts (0.25, 0.5, 1.0 and 2.0 μg) of panaxytriol were added to 1.0-ml aliquots of blank culture medium. All the samples were extracted and analyzed using the procedure described above. The calibration graph was obtained by plotting the peak height ratio of the silylated panaxytriol derivative to the silylated internal standard.

Reproducibility

Six samples of culture medium each containing 0.5, 1.0 or 2.0 μg/ml of panaxytriol were prepared. All the samples were extracted and analyzed using the procedure described above. The intra- and interassay coefficients of variation (C.V.) were determined by replicate analysis.

RESULTS AND DICUSSION

The reaction time of the silylation was examined over the range of 30–120 min at 60°C. Many extraneous peaks were observed using 120 min, and only weak peaks for 30 min. Thus, it was determined that the optimum reaction time was 60 min.

In order to verify the structure of the trimethylsilyl (TMS)-panaxytriol derivative, we measured its spectrum by use of GC–MS (Fig. 2). The weak molecular ion m/z 494 (M^+) and m/z 479 ($M^+ - 15$) were observed. Consequently, silylated panaxytriol was shown to contain three trimethylsilyl groups. Similarly the structure of the internal standard, 1-docosanol, derivative was measured by use of GC–MS. The weak molecular ion m/z 398 (M^+) and m/z 383 ($M^+ - 15$) were observed. The silylated internal standard was shown to contain one trimethylsilyl group.

Chromatograms obtained from blank culture medium and culture medium containing 2.0 μg of silylated panaxytriol derivative and 1.0 μg of silylated internal standard are shown in Fig. 3. The retention times of silylated panaxytriol and silylated internal standard were 9.4 and 11.4 min, respectively.

No interfering peaks were observed in the extracts of culture medium containing

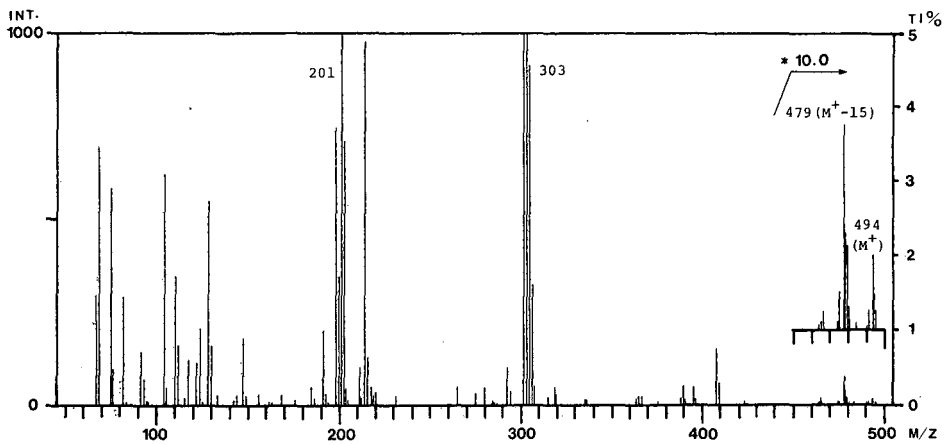

Fig. 2. Mass spectrum of the silylated panaxytriol.

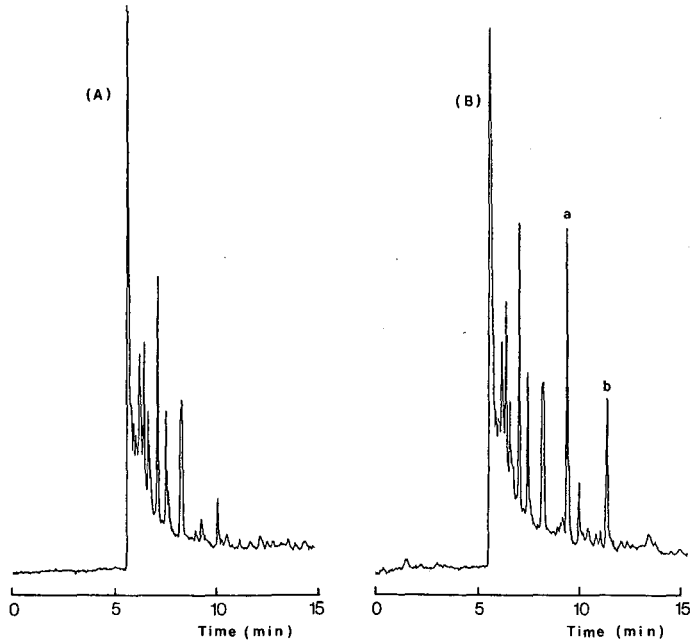

Fig. 3. Chromatograms of (A) blank culture medium and (B) culture medium containing 2.0 μg silylated panaxytriol and 1.0 μg silylated 1-docosanol. Peaks: a = silylated panaxytriol; b = silylated 1-docosanol, internal standard.

foetal calf serum and silylated panaxytriol and silylated internal standard.

This method allowed us to detect the silylated panaxytriol derivative at a concentration as low as 0.125 μg/ml (signal-to-noise ratio >3).

The ratio of the peak height of silylated panaxytriol to that of the silylated internal standard plotted against the drug concentration was linear between 0.25 and 2.0 μg/ml, with a correlation coefficient of 0.998.

The intra- and interassay data are shown in Table I. The intraassay reproducibility of silylated panaxytriol (n = 6, C.V. = 6.5–9.5%) was satisfactory in the concentration range of 0.5–2.0 μg/ml. On the other hand, the interassay reproducibility of silylated panaxytriol (n = 6, C.V. = 1.4–8.0%) was also satisfactory in the

TABLE I

THE INTRA- AND INTERASSAY COEFFICIENTS OF VARIATION FOR PANAXYTRIOL (n = 6)

Concentration (μg/ml)	*Intraassay*		*Interassay*	
	Mean ± S.D.	*C.V. (%)*	*Mean ± S.D.*	*C.V. (%)*
0.5	0.66 ± 0.063	9.5	0.55 ± 0.044	8.0
1.0	1.02 ± 0.068	6.5	0.95 ± 0.059	6.2
2.0	2.16 ± 0.015	7.0	2.03 ± 0.029	1.4

concentration range of 0.5–2.0 μg/ml. The recovery of panaxytriol from culture medium to which 2.0 μg/ml had been added was 89.56 ± 2.99% ($n = 5$). The recovery of 1-docosanol from culture medium was 98.4 ± 5.3% ($n = 5$).

In conclusion, a specific GC method has been developed for the analysis of panaxytriol in solution containing serum. The use of a fused-silica capillary column coated with OV-1701 permitted the selective determination of panaxytriol as its silylated derivative. It was also shown that MNSCSI is very useful for the straightforward and reproducible determination of panaxytriol. In addition, the sensitivity of silylated panaxytriol determination with MNSCSI, under the optimum conditions, was about five times higher than that with a conventional split injector system.

The present method of analysis of panaxytriol may be useful for studies of the biological properties of this compound such as its antitumour action and metabolism.

ACKNOWLEDGEMENT

The authors are indebted to Dr. J. Tadano and Mr. S. Kawasaki for analytical data.

REFERENCES

1 K. D. Lee and R. P. Huemer, *Jpn. J. Pharmacol.*, 21 (1971) 299.
2 M. Katano, H. Matsunaga and H. Yamamoto, *J. Jpn. Surg. Soc.*, 89 (1988) 971.
3 M. Katano, H. Yamamoto and H. Matsunaga, *Proc. 5th International Ginseng Symposium*, Korea Ginseng and Tobacco Research Institute, Seoul, 1989, in press.
4 I. Kitagawa, M. Yoshikawa, M. Yoshihara, T. Hayashi and T. Taniyama, *Yakugaku Zasshi*, 103 (1983) 612.
5 S. C. Shim, H. Y. Koh and B. H. Han, *Phytochemistry*, 22 (1983) 1817.
6 P. M. J. van den Berg and Th. P. H. Cox, *Chromatographia*, 5 (1972) 301.

Journal of Chromatography, 481 (1989) 373–379
Elsevier Science Publishers B.V., Amsterdam — Printed in The Netherlands

CHROM. 21 752

Note

Determination of tropospheric phosgene and other halocarbons by capillary gas chromatography

K. BÄCHMANN* and J. POLZER
Institut für Anorganische Chemie und Kernchemie, TH Darmstadt, Hochschulstraße 4, D-6100 Darmstadt (F.R.G.)
(First received March 7th, 1989; revised manuscript received June 7th, 1989)

Large amounts of halogenated hydrocarbons have been released into the atmosphere in recent years. Since these compounds are responsible for the destruction of the stratospheric ozone layer and contribute to the "greenhouse effect", it is necessary to investigate the chemical reaction cycles in which the halocarbons are involved.

Phosgene has been identified as an atmospheric decomposition product of several chlorinated hydrocarbons, for example CH_2Cl_2, $CHCl_3$, CCl_3CH_3, C_2HCl_3 and C_2Cl_4[1]. Because of the well known high toxicity of phosgene and its role as a reactive intermediate product in the troposphere it is important to develop sensitive analytical detection methods. This compound is also assumed by some authors[1,2] to accumulate in the troposphere.

Most existing analytical methods are not suitable for measuring phosgene at concentrations relevant to tropospheric conditions. There are a few wet chemical methods using the reaction of phosgene with a suitable reagent solution to form a product for spectrophotometric detection. These methods were often used to monitor the threshold limit value (TLV) (0.1 ppmv) at industrial working places. However, due to interferences, lack of specificity and large sample volumes they are less favoured for tropospheric trace determination of phosgene[3]. Infrared spectrophotometry suffers from similar problems and provides satisfactory results only for concentrations above 0.025 ppmv phosgene[4].

Priestley *et al.*[5] reported the determination of phosgene in air with gas chromatography with electron-capture detection (GC–ECD) using an aluminium column packed with 30% dodecyl phthalate coated on GC 22 super support (100–120 mesh). Singh[2] improved the method and presented the first results of phosgene detection in the area of Los Angeles. He found phosgene concentrations between 21 and 61 pptv also using a gas chromatograph equipped with an aluminium column packed with 30% dodecyl phthalate coated on Chromosorb P (100–120 mesh). The main problem of the analysis is the heterogeneous decomposition of phosgene on the active column sites. In order to prevent losses of phosgene it is necessary to precondition or pretreat the column and to carry out frequent calibrations[6]. Additionally, Singh used a gas chromatograph specially equipped with dual electron-capture detectors in series and applied "pulsed flow coulometry" in order to extrapolate to the phosgene concentration for a zero retention time on the column[7].

0021-9673/89/$03.50

Recently Hendershott reported upon a solid sorbent sampling procedure for phosgene and other chloroformates in combination with a GC–flame ionization detection (FID) system. He collected these compounds on a di-*n*-butylamine coated solid sorbent, whereby a detection limit of 0.002 ppmv for phosgene was achieved (40 l sample). The drawbacks are the large sampling volume and the time-consuming collection process and sample preconditioning.

This investigation describes a method which avoids significant losses of phosgene by use of chemically inert tubes, a capillary column and a careful enrichment step and analytical procedure. The high resolution of the capillary column allows the separation and simultaneous detection of other ECD-sensitive compounds. The method can be adapted easily for collecting samples in the field.

EXPERIMENTAL

Apparatus

A Siemens gas chromatograph (Model Sichromat 1) equipped with an electron-capture detection was used and prepared for a low temperature gradient. The apparatus was fitted with a fused-silica capillary column (50 m × 0.32 mm I.D., 0.53-μm coating of SE-30 CB, Macherey and Nagel). The carrier gas was helium (99.996%, Messer Griesheim), additionally purified in cryo- and adsorption traps; flow-rate 2.5 ml/min. Nitrogen was used as the make-up gas to provide proper ECD operation.

The transfer of the air sample on to the column was accomplished by a six-port valve (Valco). The valve was connected to the column with a deactivated fused-silica capillary column (2 m × 0.32 mm I.D., Macherey and Nagel) and a zero dead volume fitting. The deactivated fused-silica capillary column was used to cryofocus the analytes at the temperature of liquid nitrogen before separation on the column. This is necessary to provide sharp peaks. Separation on the column was performed with a temperature programme (−30°C for 7 min, raised at 25°C/min to 200°C).

During our investigations a packed column was also tested: a Perkin-Elmer Model F 22 gas chromatograph was equipped with a PTFE column (1.6 m × 1/8 in. I.D.) packed with 30% dodecyl phthalate coated on Chromosorb P. The enrichment and transfer of the sample was as described.

Analytical procedure

Air samples were collected by a system of two pumps as shown in Fig. 1. Ambient air (60 ml/min) was sucked through the PTFE loop at the trapping temperature of −196°C. The resulting sub-atmospheric pressure avoided condensation of oxygen. The volumes of air sampled during the enrichment procedure varied between 0.3 and 1 l, depending on the amount of trace compounds present in the air.

The humidity of the atmosphere has to be removed to avoid possible interferences of the electron-capture detector; furthermore, water shortens the lifetime of the deactivated capillary column used to cryofocus the analytes. Drying was performed in a glass tube (13 cm × 1.5 cm I.D.) filled with magnesium perchlorate (Fluka).

Cryogenic enrichment of the trace compounds was realized in a stainless-steel covered PTFE loop (70 cm × 1/8 in. O.D., 1/16 in. I.D.) at −196°C. Resistance heating of the stainless-steel cover was used for regulating the desorption process. After flushing the cryogenic trap with helium to remove oxygen, the carrier gas was

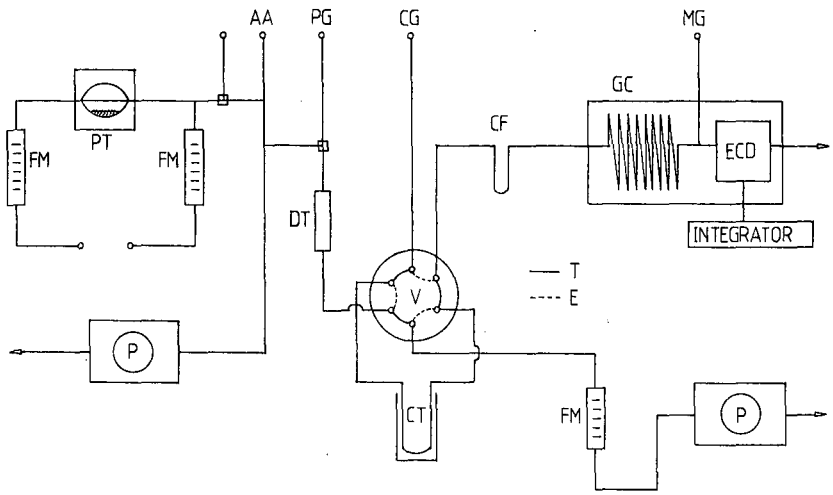

Fig. 1. Analytical system: FM = flow-meter; PG = purge gas (N_2); PT = permeation tube; AA = ambient air; CG/PG = carrier gas/purge gas (He); DT = drying tube; V = six-port valve; P = pump; CT = cold trap; CF = cold focussing; T = transfer; E = enrichment; GC = gas chromatographic system; MG = make-up gas.

conducted by the six-port valve through the PTFE loop. Analytes were vaporized by resistance heating of the stainless-steel cover. Before separation and detection the compounds were cryofocused at −196°C as mentioned above.

Calibration

The calibration had to be carried out completely identically to the sample collection procedure in order to compensate for possible losses of phosgene during the analysis. The phosgene standard was generated with a PTFE permeation tube kept at constant temperature. The purge gas was purified nitrogen at a flow-rate of 11 ml/min. All gas flows were controlled by flow meters. The content of phosgene in the nitrogen was determined with ion chromatography (IC) as a reference method. Phosgene was hydrolysed in impingers filled with water and determined as the chloride.

For GC calibration the purge gas was diluted in ambient air which was conducted through a trap filled with sodium hydroxide-coated charcoal (Merck) in order to decompose phosgene. So the phosgene concentration of the whole gas flow was reduced to the levels expected in the troposphere.

Enrichment and analysis were carried out analogous to the analysis of air samples described above. The amounts of phosgene were varied by changing the sampling volume.

Field measurement

Sample collection in the field was realized in a PTFE loop at the temperature of liquid nitrogen. Dried ambient air was sucked with a flow-rate of 60 ml/min through the cryogenic trap, then the loop was closed by two PTFE stop-cocks. The sample was kept under liquid nitrogen until it was subjected to GC analysis in the usual way.

RESULTS AND DISCUSSION

Fig. 2 presents two chromatograms containing characteristic compounds in air samples. In Fig. 2a trace compounds were separated using a capillary column, in Fig. 2b using a packed column.

Advantages resulting from the use of the capillary column are as follows. (1) High resolution; simultaneous detection of other chlorinated hydrocarbons is possible. (2) Analysis can be carried out using low temperatures (−30°C) during separation to prevent losses of phosgene. (3) Small sample volumes are required, therefore short sampling times are possible. (4) Conditioning or pretreatment of the column is not necessary. The careful enrichment and analytical procedure as well as

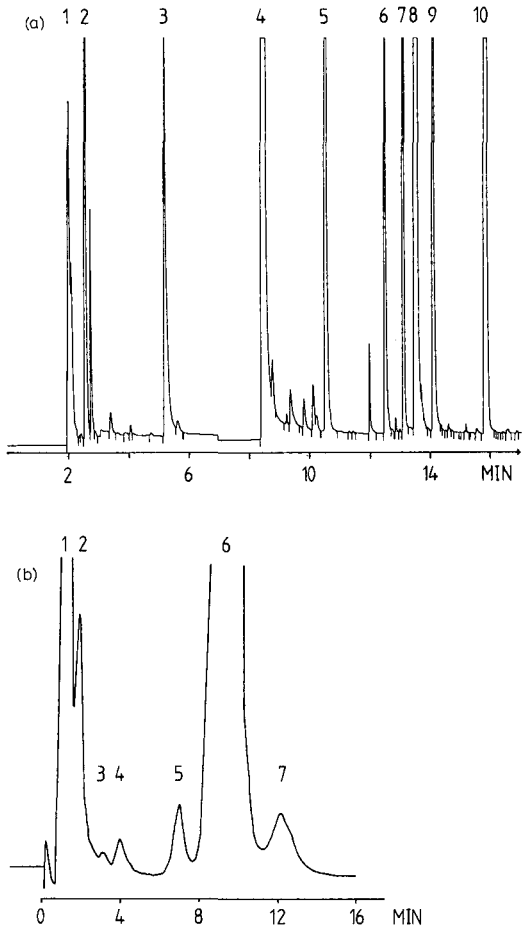

Fig. 2. (a) Gas chromatogram of an air sample (0.6 l, Darmstadt) on a capillary column with a temperature programme. Peaks: 1 = O_2/$CHClF_2$; 2 = CCl_2F_2; 3 = $COCl_2$; 4 = CCl_3F; 5 = CCl_2F–$CClF_2$; 6 = $CHCl_3$; 7 = CCl_3–CH_3; 8 = CCl_4; 9 = CCl_2 = CHCl; 10 = CCl_2 = CCl_2. (b) Gas chromatogram of an air sample (12 l, Darmstadt) on a packed column, 20°C isothermal. Peaks: 1 = O_2; 2 = $CHCl_2F$; 3 = $CHCl_3$; 4 = unknown; 5 = $COCl_2$; 6 = CCl_3F; 7 = CCl_2F–$CClF_2$.

the use of the chemically inert capillary column avoid significant losses of phosgene.

Cryogenic preconcentration of the trace compounds at −196°C proved to be an excellent method for trapping phosgene. PTFE loops filled with silylated glass balls (40–60 mesh) caused heterogeneous decomposition of phosgene on the glass surface. Detection was possible only when an empty PTFE loop was used. The efficiency of the method was tested with two traps in series. The second loop did not contain any compounds. Phosgene could be kept for several hours at −196°C without losses due to decay or adsorption.

Magnesium perchlorate used for drying proved to be inert to phosgene. No loss of phosgene during drying was observed. About 25 air samples were collected before a change of the magnesium perchlorate was necessary. A nafion dryer (Perma Pure, Model MD 250-48 F) was also tested. Its drying capacity was sufficient only for one sample. Due to adsorption of aldehydes and ketones on the nafion membrane, water was no longer removed effectively. A tedious cleaning procedure consisting of heating and outgassing the dryer while purging with purified nitrogen was necessary. If the cryogenically trapped compounds contained water the column was blocked temporarily by ice until the starting column temperature of −30°C was increased.

The separation on the column was obtained by a temperature programme. Phosgene should pass through the column in a short time at low temperatures.

The peak identities of the several compounds were determined by comparison of their retention times with those obtained of standard compounds. The standard deviation of the retention times was less than ± 0.01 min for most compounds (Table I). Additional chromatograms obtained with simultaneous ECD/FID detection were employed.

During calibration of phosgene an average reproducibility of ±8% of the single values (four repeat determinations) was achieved. Bearing in mind that the variation of the permeation rate lies in the same range, the reproducibility is acceptable[9,10]. Concentrations of phosgene down to 7 pptv are detectable in a sample volume of 1 l air (STP). The absolute detection limit is 30 pg phosgene (resulting from three times the standard deviation). Fig. 3 shows the calibration graph for phosgene.

The sample volume cannot be increased due to the fact that higher amounts of

TABLE I

STABILITY OF RETENTION TIMES

Compound	*Retention time (min)*	*Standard deviation, n = 10 (min)*
$O_2/CHClF_2$	2.243	0.013
CCl_2F_2	2.766	0.007
$COCl_2$	5.506	0.009
CCl_3F	8.562	0.008
$CCl_2F–CClF_2$	10.600	0.004
$CHCl_3$	12.521	0.003
$CCl_3–CH_3$	13.122	0.003
CCl_4	13.495	0.002
$CCl_2=CHCl$	14.112	0.003
$CCl_2=CCl_2$	15.622	0.003

TABLE II

CALIBRATION DATA FOR PHOSGENE

Amount of phosgene (pg)	*Area*	*Standard deviation, n = 4 (%)*
36.5	3426	11.3
46.8	7379	11.5
54.3	15 344	10.8
62.3	18 677	8.3
77.7	42 457	9.1
93.2	79 621	6.0
108.7	95 609	5.4
139.1	182 201	5.8
217.3	417 861	7.5

atmospheric CO_2 will block the column. In this case the retention times vary over a wide range and the chromatograms are not interpretable.

During our investigations the concentrations of phosgene found in air samples varied between 8 and 87 pptv during daytime, whereas night-time concentrations up to 143 pptv were determined. From the varying phosgene concentrations we measured over several days/nights, a tropospheric lifetime of a few months has to be assumed. Until now, lifetimes of a few years have been stated. Fig. 4 shows the diurnal variation of the concentrations of phosgene.

The analytical procedure described is a sensitive, simply applicable quantitative method for the determination of phosgene and other haloorganic compounds present in ambient air. This method is suitable for continuous monitoring of these compounds in the troposphere.

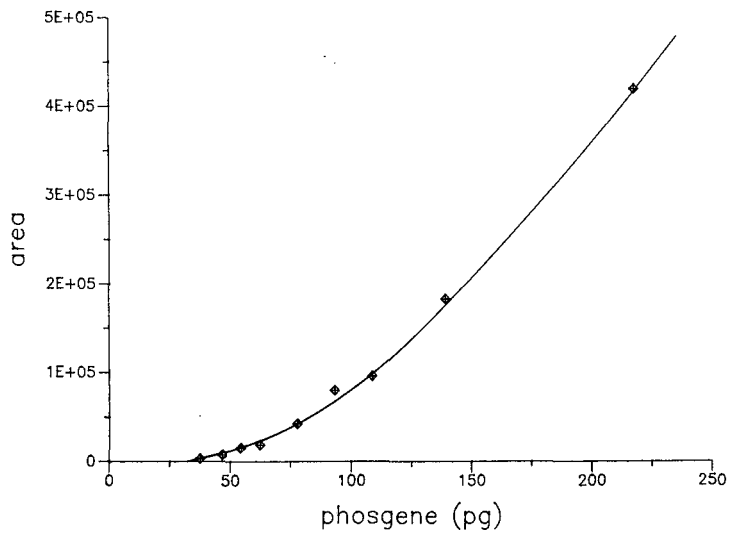

Fig. 3. Calibration graph for phosgene.

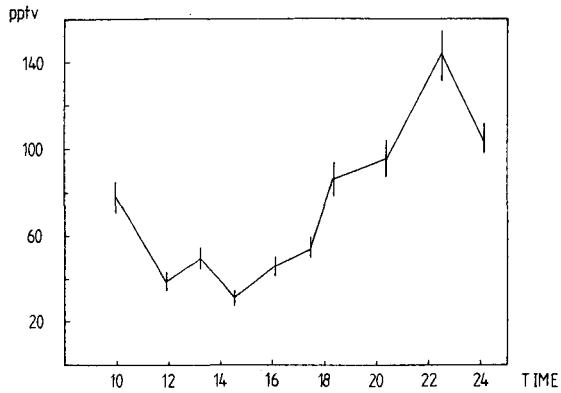

Fig. 4. Diurnal variation of phosgene.

ACKNOWLEDGEMENT

We are grateful to the BMFT (Förd. Nr. 0743133) for financal support.

REFERENCES

1 G. Helas and S. R. Wilson, personal communication.
2 H. B. Singh, *Nature (London)*, 264 (1976) 428.
3 P. C. Nigam and S. Prasad, *Indian J. Environ. Health*, 28 (1986) 218.
4 G. G. Esposito, D. Lilian, G. E. Podolak and R. M. Tuggle, *Anal. Chem.*, 49 (1977) 1774.
5 L. J. Priestley, F. E. Critchfield, N. H. Ketcham and J. D. Cavender, *Anal. Chem.*, 37 (1965) 70.
6 R. M. Tuggle, G. G. Esposito, T. L. Guinivan, T. L. Hess, D. Kilian, G. E. Podolak, K. G. Sexton and N. V. Smith, *Am. Ind. Hyg. Assoc.*, 40 (1979) 387.
7 H. B. Singh, D. Lilian and A. Appleby, *Anal. Chem.*, 47 (1975) 860.
8 J. P. Hendershott, *Am. Ind. Hyg. Assoc.*, 47 (1986) 742.
9 H. B. Singh, L. Salas, D. Lilian, R. R. Arnts and A. Appleby, *Environ. Sci. Technol.*, 11 (1977) 511.
10 A. W. Barendsz and G. van der Linden-Tak, *Fresenius' Z. Anal. Chem.*, 274 (1975) 207.

Journal of Chromatography, 481 (1989) 380–386
Elsevier Science Publishers B.V., Amsterdam — Printed in The Netherlands

CHROM. 21 841

Note

Chiral stationary phases via hydrosilylation reaction of N-acryloyl-amino acids

I. Stationary phase with one chiral centre for high-performance liquid chromatography and development of a new derivatization pattern for amino acid enantiomers

ROLF KUROPKA[a], BETTINA MÜLLER, HARTWIG HÖCKER and HEINZ BERNDT*
Lehrstuhl für Textilchemie und Makromolekulare Chemie, RWTH Aachen, Worringer Weg 1, D-5100 Aachen (F.R.G.)

(First received June 13th, 1989; revised manuscript received July 31st, 1989)

During the last decade, efforts have been made to achieve a better resolution of amino acid enantiomers by use of high-performance liquid chromatography (HPLC) with chiral stationary phases (CSPs). These developments are documented in several reviews[1–6]. Especially chiral diamide donor–acceptor CSPs, which have long been known in gas chromatography[7], seem to be very powerful[8].

In previous investigations we studied donor–acceptor CSPs containing the aromatic amino acid phenylglycine[9,10]. We found that these CSPs have a good enantioselectivity for several N^{α}-acylamino acid esters. Computer-aided energy calculations[10] indicated that one π–π donor–acceptor interaction and two hydrogen bonds interacting between amino acid derivatives and the CSP are essential for enantioselective recognition. We now report that it is possible to increase the separation factor, α, by strengthening one of the hydrogen bonds assumed to be essential for enantioselective molecular recognition.

In the literature, different methods of coupling have been used to link amino acids to a silica matrix. Coupling the amino acid via the C-terminus is more common (Pirkle-type columns), but N-terminal linking has the advantage that standard methods of peptide chemistry can be used to attach further groups at the C-terminus of the amino acid. Up to now coupling via the N-terminus of amino acids to the silica matrix has been achieved, *e.g.*, by derivatization with succinic anhydride and reaction with aminopropylsilica[11] or by derivatization of the amino acid with 10-undecenyl chloride, hydrosilylation of the olefin to give the chlorosilane derivative and coupling with silica[8].

Although the hydrosilylation reaction of olefins is well known[12], to our knowledge there have been no reports of the addition of hydrogensilanes to acryloylamides. For coupling a phenylglycine derivative via the N^{α}-terminus to a silica

[a] Part of the Ph.D. Thesis of R.K., RWTH Aachen, 1989.

0021-9673/89/$03.50

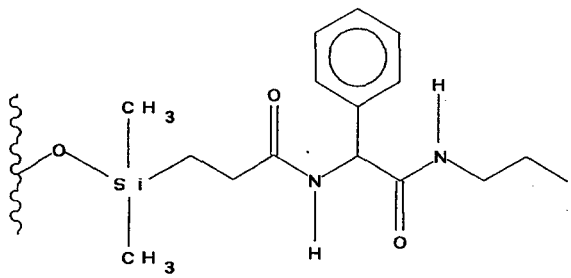

Fig. 1. Structure of the chiral stationary phase.

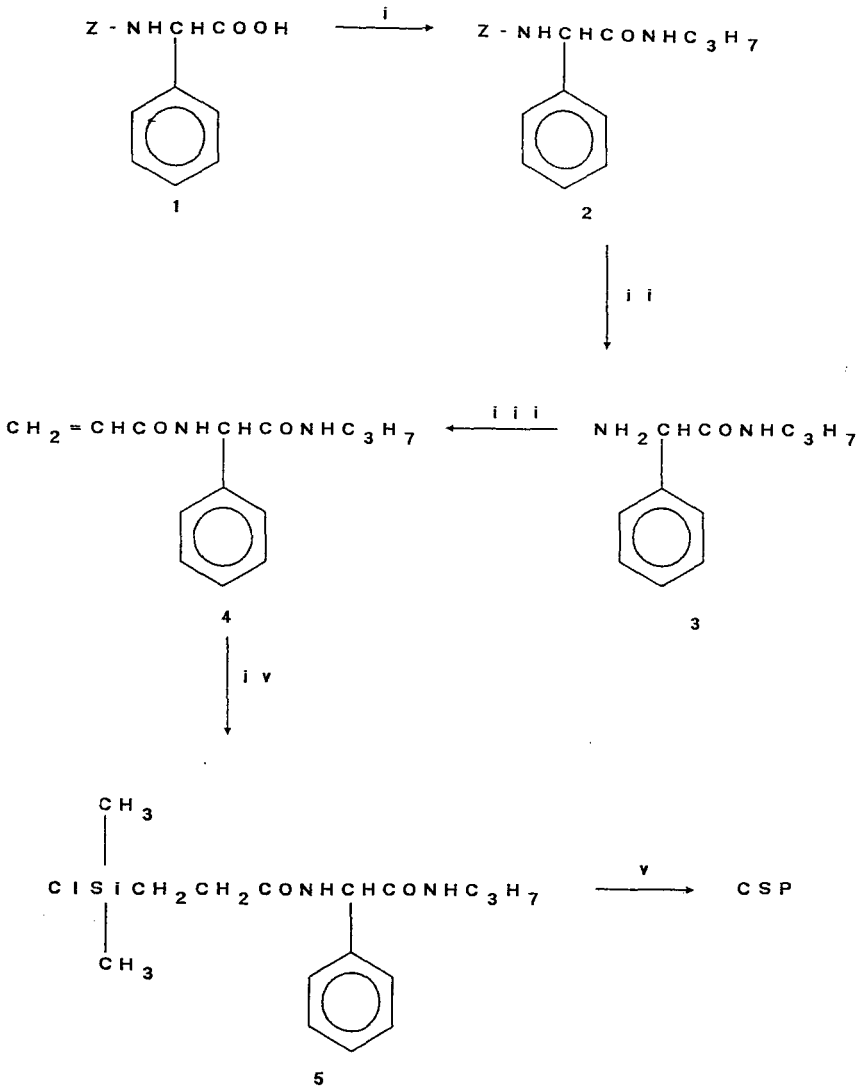

Fig. 2. Preparation of the CSP (according to ref. 15). Z = Benzyloxycarbonyl; i = mixed anhydride synthesis of **1** with propylamine; ii = catalytic hydrogenation of **2** over Pd–C; iii = reaction of **3** with acryloyl chloride; iv = hydrosilylation reaction of **4** with dimethylchlorosilane; v = coupling with Nucleosil Si 100-5 in pyridine.

matrix, the hydrosilylation reaction of acryloylamino acid derivatives is established to generate the CSP shown in Fig. 1.

EXPERIMENTAL

The scheme for the preparation of the CSP is shown in Fig. 2.

(*R*)-Phenylglycine, acryloyl chloride, dimethylchlorosilane, trimethylchlorosilane, hexachloroplatinic acid and propylamine were purchased from E. Merck (Darmstadt, F.R.G.). Nucleosil Si 100-5 was purchased from Macherey, Nagel & Co. (Düren, F.R.G.).

N^{α}-3,5-Dinitrobenzoylamino acid 2-propyl esters were synthesized according to ref. 13. The corresponding N^{α}-3,5-dinitrobenzoylamino acid propylamides, dimethylamides and diethylamides were obtained according to ref. 14. The acryloyl acid derivative of D-phenylglycine (**4**) was synthesized as shown in Fig. 2 according to ref. 15.

All new compounds showed the expected analytical and spectroscopic data (elemental analysis, ^{1}H NMR, ^{13}C NMR spectroscopy).

Preparation of the chiral stationary phase

All steps were carried out under a nitrogen atmosphere, avoiding any moisture. A 3.20-g (0.13-mol) amount of acryloyl-D-phenylglycylpropylamide (**4**), 4.50 g (0.48 mol) of dimethylchlorosilane and 100 mg of hexachloroplatinic acid were suspended in 120 ml of chloroform. After refluxing for 2 h, the solution was evaporated to dryness *in vacuo* (0.05 mbar). To a solution of the corresponding dimethylchlorosilyl derivative (**5**) in 50 ml of dry pyridine, 2.4 g of silica gel (dried for 24 h at 160°C and 0.05 mbar) were added and the mixture was stirred for 24 h at 40°C. The modified silica was end-capped by adding 4.0 ml of trimethylchlorosilane to the solution and stirring for 24 h at room temperature. The gel was collected by filtration through a G4 sintered-glass filter funnel, washed successively with methanol, chloroform, dichloromethane and dried *in vacuo* (0.05 mbar). Chromatographic columns (200 × 4.0 mm I.D.) were slurry-packed by conventional techniques. The CSP contained 0.54 mmol of chiral group per gram of gel (determined by elemental analysis).

Instrumental

HPLC experiments were carried out with a Perkin-Elmer (Überlingen, F.R.G.) Series 2B liquid chromatograph equipped with a Perkin-Elmer LC 55 variable-wavelength detector. Solvents were distilled and filtered through a G4 sintered-glass filter funnel before use. Solutes (0.2–0.5 mg/ml in ethyl acetate) were injected through a 10-μl sample loop. Chromatographic runs were performed at a flow-rate of 1 ml/min at room temperature.

RESULTS AND DISCUSSION

The hydrosilylation of an acryloylamino acid derivative with dimethylchlorosilane was successfully achieved with hexachloroplatinic acid as the catalyst. Dicyclopentadienylplatinum dichloride does not act as a catalyst (no hydrosilylation product). At least 60% of the resulting products were found to be the α-adduct to the

TABLE I

ENANTIOMER SEPARATION OF N^{α}-3,5-DINITROBENZOYLAMINO ACID 2-PROPYL ESTERS ON THE CSP

k'_D = Capacity factor for the D-isomer; k'_L = capacity factor for the L-isomer; α = separation factor. Mobile phase: 2-propanol–hexane (10:90).

Amino acid	k'_D	k'_L	α
Alanine	1.62	2.68	1.65
Valine	0.75	1.97	2.63
Leucine	0.90	1.95	2.17
Isoleucine	0.86	2.24	2.62
Phenylalanine	1.26	2.76	2.19
Phenylglycine	1.09	2.00	1.84
Tyrosine[a]	0.66	1.46	2.21
Serine	3.03	3.60	1.19
Threonine	2.14	2.50	1.17
Proline	1.05	1.05	1.00
Lysine	9.15	12.37	1.35
Glutamic acid	0.81	1.29	1.60

[a] Mobile phase: 2-propanol–hexane (30:70, v/v).

C=C bond according to ^{1}H NMR and ^{13}C NMR spectroscopy. Further, the propionic acid amide derivative was obtained as a result of hydrogenation. The chlorosilylamino acid derivative is sensitive towards moisture and light; its addition to silica should occur spontaneously.

The chromatography of N^{α}-3,5-dinitrobenzoylamino acid 2-propyl esters on the new CSP yielded excellent separation factors (Table I). In each instance investigated the L-enantiomer showed a stronger retention than the D-enantiomer. Racemic proline derivatives were not resolved.

TABLE II

ENANTIOMER SEPARATION OF N^{α}-3,5-DINITROBENZOYLAMINO ACID N-PROPYLAMIDES ON THE CSP

Mobile phase: 2-propanol–hexane (10:90, v/v).

Amino acid	k'_D	k'_L	α
Alanine	2.29	12.18	5.32
Valine	0.56	5.76	6.01
Leucine	0.88	5.80	6.58
Isoleucine	0.84	5.35	6.35
Phenylalanine	1.95	13.22	6.77
Phenylglycine	1.84	6.59	3.59
Tyrosine	6.70	Too strong interaction	
Serine	6.67	18.95	2.84
Threonine	3.25	10.95	3.37
Proline	3.08	2.71	0.88
Lysine	13.70	46.66	3.40
Tryptophan	4.53	34.46	7.60
Glutamic acid	3.53	6.53	1.85

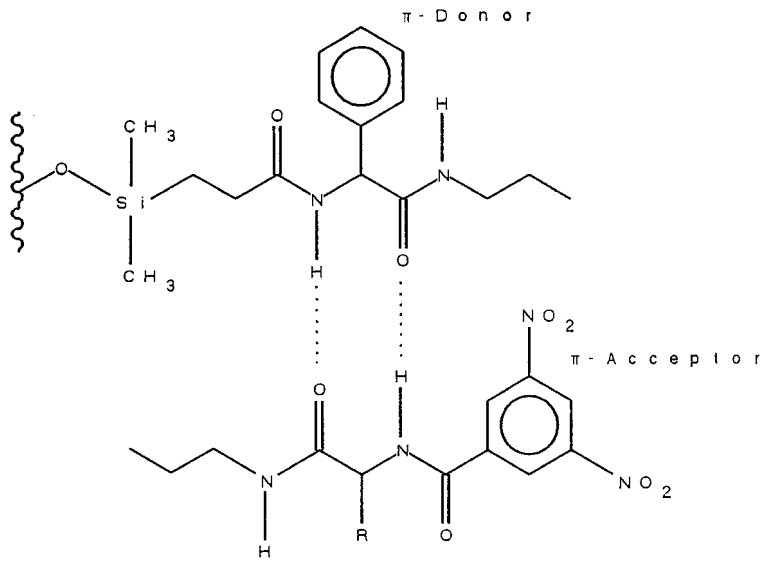

Fig. 3. Proposed adsorption complex of the CSP with N^{α}-3,5-dinitrobenzoylamino acid propylamides.

Although the reaction of D-phenylglycinepropylamide with acryloyl chloride does not generate a long spacer, the subsequent hydrosilylation leads to an efficient CSP. Obviously no marked distance between the chiral moiety and the silica matrix is necessary to achieve high enantioselectivity.

To study the influence of the derivatization pattern of the C^{α}-terminus of N^{α}-3,5-dinitrobenzoylamino acids on enantiomer separation, the chromatographic behaviour of the corresponding 2-propyl esters and propylamides was investigated. As shown in Table II, a dramatic increase in the separation factor was observed when the amides were used instead of the esters.

As indicated in Fig. 3, our previously proposed recognition model[10] gives an explanation of the phenomenon. We postulate that in the chiral diamide donor–acceptor stationary phase investigated, the more strongly retained enantiomer interacts with the CSP at least via two hydrogen bonds and a π–π donor–acceptor complex. The exchange of an ester group for an amide group at the C^{α}-terminus of the amino acid derivative increases the Lewis basicity of the carbonyl oxygen atom. As a consequence, the corresponding hydrogen bond between the solute and the CSP is strengthened, especially for the L-enantiomer, which shows a stronger retention than the D-enantiomer.

Changing the derivatization pattern of the analyte from N^{α}-3,5-dinitrobenzoylamino acid 2-propyl ester to N^{α}-3,5-dinitrobenzoylamino acid propylamide causes such a strong increase in the k'_L value (Tables I and II) that it becomes necessary to increase the concentration of 2-propanol in the mobile phase to 30% (Table III).

Derivatization of N^{α}-3,5-dinitrobenzoylamino acids to secondary amides leads to a further increase in the k'_L value, as shown in Table IV. In secondary amides the electron density of the carbonyl carbon atom is higher than in primary amides. The steric hindrance in C^{α}-diethylamides, however, results in lower k'_L values (Table V)

TABLE III

ENANTIOMER SEPARATION OF N^{α}-3,5-DINITROBENZOYLAMINO ACID N-PROPYLAMIDES ON THE CSP

Mobile phase: 2-propanol–hexane (30:70, v/v).

Amino acid	k'_D	k'_L	α
Alanine	0.51	2.84	5.60
Valine	0.27	1.71	6.30
Leucine	0.25	1.69	6.76
Isoleucine	0.22	1.61	7.30
Phenylalanine	0.54	3.54	6.60
Phenylglycine	0.47	1.56	3.34
Tyrosine	0.88	6.77	7.70
Serine	1.17	3.04	2.61
Threonine	0.70	2.22	3.16
Proline	0.53	0.53	1.00
Lysine	1.50	4.49	2.99
Tryptophan	0.63	4.56	7.27
Glutamic acid	0.51	0.95	1.85

TABLE IV

ENANTIOMER SEPARATION OF N^{α}-3,5-DINITROBENZOYLAMINO ACID DIMETHYLAMIDES ON THE CSP

Mobile phase: 2-propanol–hexane (30:70, v/v).

Amino acid	k'_D	k'_L	α
Alanine	0.91	4.13	4.52
Valine	0.34	2.36	6.91
Leucine	0.29	2.41	8.36
Isoleucine	0.27	2.24	8.19

than for the corresponding dimethylamides (Table IV). The increase in the k'_L values for the C^{α}-amides of dimethylamine emphasizes that the Lewis basicity of the corresponding carbonyl C^{α} atom is important for the strength of the diastereomeric complexes between the enantiomers of an analyte and a chiral selector, whereas the C^{α}-amide hydrogen is not involved in the chiral recognition mechanism.

TABLE V

ENANTIOMER SEPARATION OF N^{α}-3,5-DINITROBENZOYLAMINO ACID DIETHYLAMIDES ON THE CSP

Mobile phase: 2-propanol–hexane (30:70, v/v).

Amino acid	k'_D	k'_L	α
Alanine	0.44	1.85	4.21
Valine	0.18	1.15	6.34
Isoleucine	0.18	1.24	6.72

As shown in Table II, N^{α}-3,5-dinitrobenzoyl-D- and -L-prolinepropylamide are resolved with the CSP, but not with a baseline separation. Interestingly, the L-enantiomer is eluted first. As proline bears a secondary amino group, there is a lack of an α-amide proton which might effect an alternative mechanism of enantioselective recognition.

Coupling an additional chiral centre at the C-terminus of the CSP and its influence on the chromatographic behaviour of amino acid derivatives and other enantiomers will be considered in Part II. Further evidence of the mechanism of enantiomeric recognition will be obtained by computer-aided energy calculations for the reversible diastereomeric adsorption complexes.

ACKNOWLEDGEMENTS

We thank cand. chem. U. Eigendorf for excellent technical assistance and the Deutsche Forschungsgemeinschaft (Be 900/3-1) for financial support.

REFERENCES

1 W. H. Pirkle and T. C. Pochapsky, *Chem. Rev.*, 89 (1989) 347–362.
2 W. H. Pirkle and T. C. Pochapsky, *Adv. Chromatogr.*, 27 (1987) 73–127.
3 D. W. Armstrong, *J. Liq. Chromatogr.*, 7 (S-2) (1984) 353–376.
4 R. W. Souter, *Chromatographic Separation of Stereoisomers*, CRC Press, Boca Raton, FL, 1985.
5 S. G. Allenmark, *Chromatographic Enantioseparation*, Ellis Horwood, Chichester, 1988.
6 M. Zief and L. J. Crane, *Chromatographic Chiral Separation*, Marcel Dekker, New York, 1988.
7 W. A. König, *The Practice of Enantiomer Separation by Capillary Gas Chromatography*, Hüthig, Heidelberg, 1987.
8 A. Dobashi, Y. Dobashi, K. Kinoshita and S. Hara, *Anal. Chem.*, 60 (1988) 1985–1987.
9 G. Krüger and H. Berndt, *J. Chromatogr.*, 348 (1985) 275–279.
10 G. Krüger, J. Grötzinger and H. Berndt, *J. Chromatogr.*, 397 (1987) 223–232.
11 M. J. B. Lloyd, *J. Chromatogr.*, 351 (1986) 219–229.
12 J. L. Speier, J. A. Webster and G. H. Barnes, *J. Am. Chem. Soc.*, 79 (1957) 974–979.
13 G. Krüger, *Dissertation*, RWTH Aachen, 1986.
14 B. Müller, *Dissertation*, RWTH Aachen, 1987.
15 R. Kuropka, *Ph.D. Thesis*, RWTH Aachen, 1989.

Journal of Chromatography, 481 (1989) 387–390
Elsevier Science Publishers B.V., Amsterdam — Printed in The Netherlands

CHROM. 21 846

Note

Enantiomer separation of α-substituted γ-butyrolactones on the chiral polyacrylamide resin ChiraSpher®

S. HÜNIG* and N. KLAUNZER
Institut für Organische Chemie der Universität, Am Hubland, D-8700 Würzburg (F.R.G.)
and
K. GÜNTHER
Fa. Degussa AG, D-6450 Hanau (F.R.G.)
(Received July 21st, 1989)

Chiral butyrolactones substituted in the α-position have proved to be valuable synthetic intermediates, *e.g.*, in syntheses of chiral dialcohols[1], but the chiral analysis of these species has not been well studied. The determination of the enantiomer content through optical rotation[2] and proton magnetic resonance in the presence of a chiral solvent[3] or chiral shift reagents[4] have been found to be applicable to only a small number of these lactones.

For our studies on the enantioselective protonation of prochiral anions[5] we required a fast and reliable method for the chiral analysis of a series of α-substituted γ-butyrolactones. We have previously successfully demonstrated the high-performance liquid chromatography (HPLC) separation of similar compounds, the 1,3-dioxolanones **1a** and **b** and the O-substituted pantolactones **2a** and **b**[6], on the chiral acrylamide polymer ChiraSpher®[7], and have now extended this application to the above-mentioned α-substituted γ-butyrolactones **3–n** in Table I.

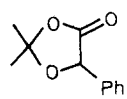

1a

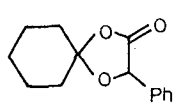

1b

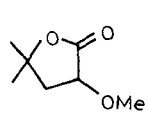

2a

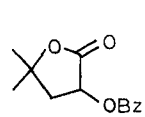

2b

As we wanted to compare the chromatographic properties of the α-alkylated with those of the γ-alkylated γ-butyrolactones, recently investigated by Huffer and Schreier[8], we did not optimize the separation of every lactone, but used a similar eluent to that given in the literature[8].

0021-9673/89/$03.50

EXPERIMENTAL

HPLC equipment

The chromatographic analysis was performed on a Hibar®-ChiraSpher® RT 250-4 column (250 × 4 mm I.D., d_p = 5 μm) or on a Hibar®-triacetylcellulose column (250 × 10 mm I.D., d_p = 10 μm) (both from Merck, Darmstadt, F.R.G.) at ambient temperature. The eluent was delivered with a Knauer 64 HPLC pump. The racemic mixture (30–60 μg) was applied with a Rheodyne 1265 injection valve with a 5-μl loop; the enantiomers were detected with a Soma S-3702 UV–VIS detector at 220 nm.

Light petroleum and *tert.*-butyl methyl ether were distilled prior to use. Dioxane and ethanol were of HPLC grade from Aldrich (Milwaukee, WI, U.S.A.).

Lactones

All α-substituted γ-butyrolactones, except **3a**, which is available from Aldrich, were prepared according to literature procedures. Compounds **3b**, **c** and **e** were synthesized according to Borne *et al.*[9]; the analytical data for **3b** and **c** were identical with those given by Zenk and Wiley[10] and those of **3e** were in accordance with the values given by Jedlinski *et al.*[11]. Compound **3d** was prepared according to Zenk and Wiley[10]. The lactones **3f–l** were prepared according to the procedure of Elad *et al.*[12]. The analytical data for **3f**, **i** and **k** agreed with those found by Rothstein[13]. α-Benzyl-γ-butyrolactone (**3m**) was synthesized according to Jahovac and Jones[4] and gave analytical data in agreement with those found by Flechtner[14]. α-Phenyl-γ-butyrolactone (**3n**) was prepared according to Andresen *et al.*[15] and showed analytical data in agreement with those found by the same group[16].

Prior to injection, all the lactones were purified by medium-pressure LC on silica gel with light petroleum–*tert.*-butyl methyl ether mixtures as eluent.

Assignment of the elution order was made according to Huffer and Schreier[8] by multiple injection of α-methyl-γ-butyrolactone (**3a**), determination of the optical rotation of the enriched fractions and comparison with the values found in the literature[17]. The elution order was found to be *S* before *R*. Transfer of the assignment to the other lactones seems to be valid from information obtained by enantioselective protonation studies[5].

RESULTS AND DISCUSSION

All the racemic mixtures of γ-lactones **3a–n** could be efficiently separated, as can be seen from the data in Table I.

Similarly to the γ-alkylated lactones[8], α-alkylated lactones show increasing separation factors and resolution with increasing chain length but decreasing capacity factors. If the eluent is modified (dioxane instead of *tert.*-butyl methyl ether), γ-butyrolactones with short alkyl chains (**3a–d**) are separated more efficiently. Those with longer alkyl chains (**3e–l**), however, suffer from a decrease in α and resolution. Special cases are α-benzyl- and α-phenyl-γ-butyrolactone, where the α values and the resolutions are very high, as also are the capacity factors. These two lactones are the only ones in the series investigated that can also be separated on a triacetylcellulose stationary phase. Probably the aromatic group favours chiral recognition on the chiral polyacrylamide as well as on the polysaccharide. In contrast to the γ-alkylated butyrolactones, the elution orders of **3m** and **n** are retained on triacetylcellulose.

TABLE I

RETENTION TIMES (t_R), CAPACITY FACTORS (k'), SEPARATION FACTORS (α) AND RESOLUTIONS (R) FOR THE SEPARATION OF α-SUBSTITUTED γ-BUTYROLACTONES ON CHIRASPHER®

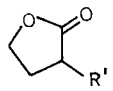

Eluent: hexane–*tert.*-butyl methyl ether–ethanol (4000:60:1); flow-rate, 1.2 ml/min.

Compound 3	*R' (min)*	*$t_R(S)$ (min)*	*$t_R(R)$*	*$k'(S)$*	*$k'(R)$*	α	*R*[a]
a	Methyl[b]	19.9	21.5	6.96	7.60	1.09	0.60
b	Ethyl[b]	14.1	15.3	4.64	5.12	1.10	0.81
c	Propyl[b]	11.9	13.4	3.76	4.35	1.16	1.07
d	Butyl[b]	10.3	11.07	3.12	3.70	1.19	1.65
e	Pentyl[c]	9.4	10.7	2.75	3.27	1.19	1.56
f	Hexyl	8.9	10.3	2.56	3.12	1.22	2.11
g	Heptyl	8.3	9.5	2.31	2.81	1.22	1.75
h	Octyl	8.0	9.3	2.19	2.71	1.24	1.52
i	Nonyl	7.6	8.8	2.03	2.51	1.24	2.05
j	Decyl	7.4	8.6	1.95	2.44	1.25	2.31
k	Undecyl	7.2	8.5	1.88	2.40	1.28	2.15
l	Dodecyl[c]	7.0	8.3	1.81	2.32	1.28	2.36
m	Benzyl [d]	33.0	36.5	7.35	8.03	1.09	2.01
n	Phenyl	44.8	59.1	16.92	22.64	1.34	3.20
n	Phenyl[e]	8.4	10.8	4.25	5.12	1.20	2.00

[a] The resolution was calculated from the width at the peak bottom according to Meyer[18].

[b] Hexane–dioxane (96:4) as eluent at a flow-rate of 0.7 ml/min provides better resolutions for **3a–d**, *e.g.*, for **3a** α = 1.10, R = 1.28.

[c] No separation could be achieved with triacetylcellulose; for unsuccessful separation of **3a** (R = Me) and **3d** (R = Bu) see ref. 19.

[d] Efficient separation could be achieved on triacetylcellulose; eluent 96% ethanol, flow-rate 1.1 ml/min (α = 1.47, R = 1.57).

[e] The slight tailing disappears with hexane–*tert.*-butyl methyl ether (3:2), flow-rate 1.2 ml/min; the lactone **3n** has previously been separated on triacetylcellulose[19], S elutes before R; assignment through optically enriched **3n**[20].

In general, the ChiraSpher® phase is much better suited for the separation of lactones than triacetylcellulose because of the wider scope of application and the faster and superior separations. By varying the substitution pattern, ring size and heteroatom(s) in the ring, a better understanding of the chiral interaction between organic substrate and ChiraSpher® may be achieved.

ACKNOWLEDGEMENT

Support from the Deutsche Forschungsgemeinschaft is gratefully acknowledged.

REFERENCES

1 A. I. Meyers and E. D. Mihelich, *J. Org. Chem.*, 40 (1975) 1186.
2 A. I. Meyers, Y. Yamamoto, E. D. Mihelich and R. A. Bell, *J. Org. Chem.*, 45 (1980) 2792.
3 W. H. Pirkle, D. L. Sikkenga and M. S. Pavlin, *J. Org. Chem.*, 42 (1977) 384.
4 J. Jahovac and J. B. Jones, *J. Org. Chem.*, 44 (1979) 2165.
5 U. Gerlach and S. Hünig, *Angew. Chem.*, 99 (1987) 1323; *Angew. Chem., Int. Ed. Engl.*, 26 (1987) 1283.
6 U. Gerlach, Th. Haubenreich, S. Hünig and N. Klaunzer, *Justus Liebigs Ann. Chem.*, 1989, 103.
7 G. Blaschke, in M. Zief and C. J. Crane (Editors), *Chromatographic Chiral Separations*, Marcel Dekker, New York, 1988, p. 179.
8 M. Huffer and P. Schreier, *J. Chromatogr.*, 469 (1989) 137.
9 R. F. Borne, H. Y. Aboul-Enein, J. W. Waters and J. Hicks, *J. Med. Chem.*, 16 (1973) 245.
10 C. Zenk and R. A. Wiley, *Synthesis*, (1984) 695.
11 Z. Jedlinski, M. Kowalczuk, P. Kurcok, M. Grzegorzek and J. Ermel, *J. Org. Chem.*, 52 (1987) 4601.
12 D. Elad, G. Friedman and R. R. Youssefyeh, *J. Chem. Soc. C*, (1968) 870.
13 B. Rothstein, *Bull. Soc. Chim. Fr.*, (1935) 80.
14 T. W. Flechtner, *J. Org. Chem.*, 42 (1977) 901.
15 B. D. Andresen, F. T. Davis, J. L. Templeton, R. H. Hammer and H. L. Panzik, *Res. Commun. Chem. Pathol. Pharmacol.*, 15 (1976) 21.
16 B. D. Andresen, F. T. Davis, J. L. Templeton, H. L. Panzik and R. H. Hammer, *Res. Commun. Chem. Pathol. Pharmacol.*, 18 (1977) 439.
17 H. G. W. Leuenberger, W. Bogath, R. Barner, M. Schmidt and R. Zell, *Helv. Chim. Acta*, 62 (1979) 455.
18 V. Mayer, *Praxis der Hochleistungsflüssigkeitschromatographie*, Diesterweg-Salle-Sauerländer, Frankfurt, 4th ed., 1986.
19 E. Francotte and D. Lohmann, *Helv. Chim. Acta*, 70 (1987) 1569.
20 N. Klaunzer, *Dissertation*, Würzburg, 1989.

Journal of Chromatography, 481 (1989) 391–396
Elsevier Science Publishers B.V., Amsterdam — Printed in The Netherlands

CHROM. 21 750

Note

Recovery of proteins and peptides with nanogram loads on non-porous packings

YOSUKE YAMASAKI*, TAKASHI KITAMURA, SHIGERU NAKATANI and YOSHIO KATO
Central Research Laboratory, Tosoh Corporation, Tonda 4560, Shinnanyo-shi, Yamaguchi 746 (Japan)
(First received May 17th, 1989; revised manuscript received June 23rd, 1989)

Non-porous packings were introduced by Horvath *et al.*[1] in 1967 and the operational variables were studied in detail for packings with fairly large particle sizes (*ca.* 50 μm in diameter)[2,3]. A major advantageous property of non-porous packings, *i.e.*, the absence of sample diffusion in pores that occur in porous packings, leads to rapid separation with high efficiency and resolution. In the last decade, the technology of packings for high-performance liquid chromatography (HPLC) has greatly advanced so that non-porous microparticles (1.5–7 μm in diameter) have been developed enabling the rapid separation of proteins and peptides[4–18] and nucleic acids[19,20] within 10 min.

Recently, it has become important to separate submicrogram amounts, *i.e.*, picomole or nanomole levels of proteins and peptides since quality control or on-line monitoring is required for invaluable biomolecules like recombinant products[21]. For this reason, the porous packings were examined as regards the quantitative recovery of nanogram amounts of proteins by reversed-phase chromatography (RPC)[22–25] and size-exclusion chromatography (SEC)[23,25] on microbore columns since the recovery is higher due to a smaller (packingweight)/(sample weight) ratio. Those columns, however, gave longer analysis times than conventional columns and, moreover, a sophisticated HPLC system equipped with a pump and a gradient mixer is necessary. In contrast to porous packings, another advantageous property of non-porous packings is the small surface area (< 5 m^2/g), which indicates the high recovery of sample with small loads. Hence, Burke *et al.*[6] reported the quantitative recovery of protein from nanogram loads on non-porous cation exchangers of 7 μm in diameter.

More recently, non-porous spherical resins of 2.5 μm in diameter have become commercially available as packed columns of TSKgel DEAE-NPR and SP-NPR for ion-exchange chromatography (IEC) and Octadecyl-NPR for RPC. Kato *et al.*[11,18] reported the quantitative recovery of proteins and peptides from microgram loads on these columns. In this paper, the quantitative recovery of proteins and peptides, and micropreparative separation of enzyme from nanogram loads, on these columns are described.

EXPERIMENTAL

All chromatographic separations were performed at 25°C with a high-performance liquid chromatograph consisting of a CCPM pump (Tosoh, Tokyo, Japan),

0021-9673/89/$03.50

a Model 7125 sample injector (Rheodyne, Cotati, CA, U.S.A.) with a 50-μl sample loop, an UV-8000 detector (Tosoh) operated at 215 or 220 nm (0.04–0.32 a.u.f.s.) for RPC, or an FS-8000 fluorescence detector (Tosoh) operated at 280 nm for excitation and 340 nm for emission (attenuation 3–16) for IEC, and an FBR-2 recorder (Tosoh). A line-filter with an 0.45-μm membrane was installed between the pump outlet and the sample injector. The dead volumes between the dynamic gradient mixer (volume 1.6 ml) and the injector and those of the tubings were kept to a minimum.

Proteins between 25 and 500 ng (10 ng/μl) were separated by a 10-min linear gradient from 0 to 0.5 *M* NaCl in 20 m*M* Tris–HCl (pH 8.0) by IEC on TSKgel DEAE-NPR (Tosoh), or a 10-min linear gradient from 0 to 0.5 *M* sodium sulphate in 20 m*M* acetate buffer (pH 5.0) by IEC on SP-NPR (Tosoh). Proteins and peptides between 12.5 and 500 ng were separated by a 10-min linear gradient from 0 to 80% acetonitrile in 5 or 100 m*M* $HClO_4$, or the same gradient from 15 to 80% in 5 m*M* $HClO_4$. All separations were performed by an high-pressure gradient system at a flow-rate of 1.5 ml/min. All columns were 35 mm × 4.6 mm I.D. The mass recovery of samples was determined by measuring the peak area of the eluate since the UV absorption and fluorescence intensity are proportional to the sample concentration in the eluent. Hexokinase activity was determined according to the standard procedures[26].

Cytochrome *c* was digested with N-tosyl-L-phenylalanine chloromethyl ketone (TPCK)–trypsin according to the standard procedures[27]. The protein (1 mg/ml) and TPCK–trypsin (5 mg/ml) were incubated at a substrate to enzyme ratio of 100:1 in 10 m*M* Tris–HCl (pH 8.3) containing 0.1 *M* sodium acetate and 0.1 m*M* calcium chloride at 37°C for 2 h. A 500-ng amount of the digest in 0.5 μl was directly injected into the column for RPC without terminating the reaction.

Ovalbumin (chicken egg) was obtained from Seikagaku (Tokyo, Japan) and mouse monoclonal antibody for human proline hydroxygenase (IgG_1) was from CosmoBio (Tokyo, Japan). Hexokinase was obtained from Oriental Yeast (Osaka, Japan) and all other proteins were from Sigma (St. Louis, MO, U.S.A.). All peptides were obtained from the Peptide Institute (Osaka, Japan).

RESULTS AND DISCUSSION

Table I summarizes the recovery of proteins and peptides with 400-ng loads obtained by IEC on TSKgel DEAE-NPR and SP-NPR, and by RPC on TSKgel Octadecyl-NPR. All proteins and peptides were recovered in high yields from submicrogram loads. The results obtained by IEC with 400-ng loads reveal are in good agreement with those obtained with 5-μg loads reported by Kato *et al.*[11], while IgG_1 showed slightly lower recovery.

Figs. 1 and 2 show the relationship between the sample loads and peak area of the eluate in the separation of proteins and peptides with less than 400-ng loads by IEC on TSKgel DEAE-NPR and SP-NPR, and by RPC on TSKgel Octadecyl-NPR. The sample loads showed good linearity with the peak area. As indicated in Table I, the recovery of the proteins from 400-ng loads were almost quantitative so that the proteins would also be recovered in high yields with more than 25-ng loads by IEC and with more than 12.5 ng by RPC, which suggests that the small surface area of non-porous resins contributes to the high recovery of the sample even when present in very small amounts.

TABLE I

RECOVERY OF PROTEINS AND PEPTIDES FROM 400-ng LOADS BY ION-EXCHANGE CHROMATOGRAPHY ON TSKgel DEAE-NPR AND SP-NPR AND BY REVERSED-PHASE CHROMATOGRAPHY ON TSKgel Octadecyl-NPR

Column	*Protein or peptide*	*Recovery (%)*
DEAE-NPR	Ovalbumin	103
	Soybean trypsin inhibitor	98
	IgG_1	89
SP-NPR	Lysozyme	94
Octadecyl-NPR	Ribonuclease A	95
	Insulin	94
	Cytochrome *c*	102
	Myoglobin	99
	Somatostatin	99
	Bradykinin	101
	Angiotensin I	106

As demonstrated above, it is evident that proteins and peptides can be recovered in high mass yields even with submicrogram loads. We also evaluated the recovery of enzymatic activity with submicrogram loads. Fig. 3 shows the micropreparative separation of crude hexokinase by IEC on TSKgel DEAE-NPR. The separation was

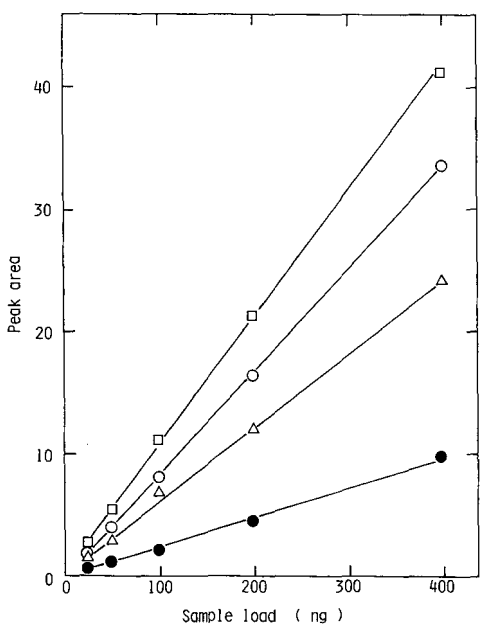

Fig. 1. Relationship between sample load and peak area of the eluate in the separation of proteins by IEC on TSKgel DEAE-NPR and SP-NPR. Proteins of ovalbumin (□), STI (○) and IgG_1 (△) were separated on TSKgel DEAE-NPR and lysozyme (●) was separated on TSKgel SP-NPR. Conditions as described in Experimental.

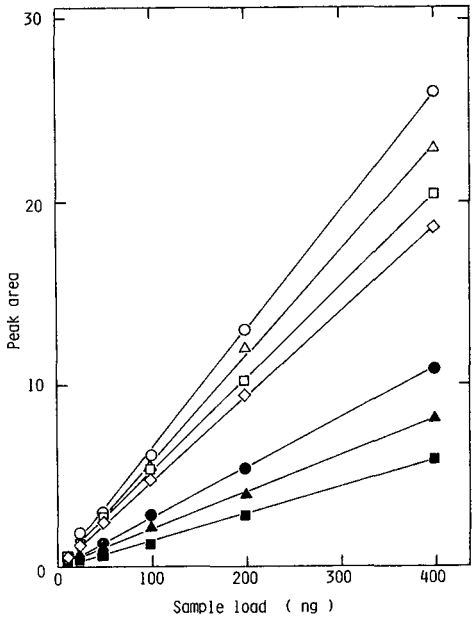

Fig. 2. Relationship between sample load and peak area of the eluate in the separation of proteins and peptides by reversed-phase chromatography on TSKgel Octadecyl-NPR. Proteins of ribonuclease A (○), cytochrome *c* (□), myoglobin (◇) and peptides of insulin (△), somatostatin (●), bradykinin (▲) and angiotensin I (■) separated on TSKgel Octadecyl-NPR. The conditions of chromatography were described in Experimental.

completed within 5 min and hexokinase was eluted at 4.1 min. The hexokinase fraction as indicated in the figure was collected with 80% recovery of hexokinase activity. The recovery of activity from the sample from 500-ng loads was fairly high, although that from 25 μg was slightly higher[11].

Fig. 4 shows the separation of proteins with 50-ng loads by RPC on TSKgel Octadecyl-NPR. The proteins were separated completely with high resolution within 6 min. Each peak was also sharp due to the small particle size (2.5 μm). Perchloric acid

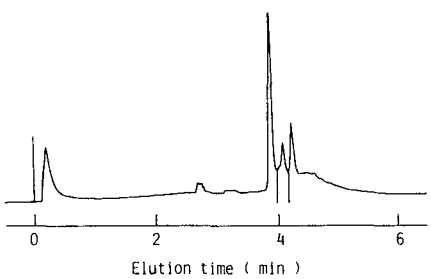

Fig. 3. Separation of hexokinase from nanogram loads by IEC on TSKgel DEAE-NPR. A 500-ng amount of crude hexokinase was separated by a 10-min linear gradient from 0 to 0.5 *M* NaCl in 20 m*M* Tris–HCl (pH 8.0) at a flow-rate of 1.5 ml/min. Recovery of activity was 80%.

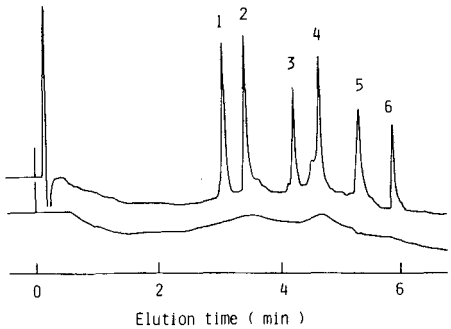

Fig. 4. Separation of a protein mixture from nanogram loads by RPC on TSKgel Octadecyl-NPR. A mixture containing 50 ng of each protein (1 = ribonuclease A; 2 = insulin; 3 = cytochrome *c*; 4 = lysozyme; 5 = transferrin and 6 = myoglobin) was separated by a 10-min linear gradient from 15 to 80% acetonitrile in 5 m*M* perchloric acid at a flow-rate of 1.5 ml/min and was detected by UV absorbance at 220 nm (0.04 a.u.f.s.). The trace of the blank gradient is also shown.

as a solvent seemed to give a better background compared with trifluoroacetic acid (TFA) when the submicrogram samples were separated by RPC[18].

Fig. 5 shows the monitoring of cytochrome *c* digested by TPCK–trypsin by RPC on TSKgel Octadecyl-NPR. The reaction mixture containing 500 ng proteins was directly injected into the column without termination of the reaction. Separation of the digest was completed within 7 min and many peptides derived from cytochrome *c* increased in peak height with time. This separation indicates rapid monitoring of enzymatic reaction and also suggests the application to peptide mapping of protein with submicrogram loads. Although Kalghatgi and Horvath[12] reported the same procedures previously with 10-μg sample loads, one-twentieth of the sample loads, *i.e.*, 500 ng was found to be enough for separation.

In conclusion, non-porous resins with 2.5-μm spherical particles yielded rapid separations of proteins and peptides with sharp peaks by IEC and RPC even though the sample loads were of the order of nanograms. Non-porous resin-packed columns

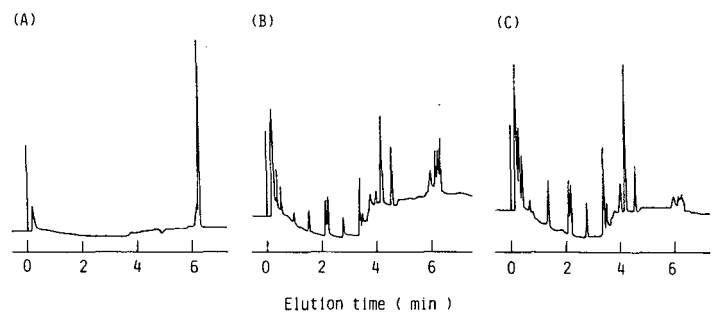

Fig. 5. Separation of tryptic digests of cytochrome *c* from nanogram loads by RPC on TSKgel Octadecyl-NPR. Cytochrome *c* was digested by TPCK–trypsin for 1 h (B) and 2 h (C). A 500 ng amount of cytochrome *c* (A) or the digests was separated by a 10-min linear gradient from 0 to 80% acetonitrile in 100 m*M* perchloric acid at a flow-rate of 1.5 ml/min and detected by UV absorbance at 215 nm on 0.32 a.u.f.s. in (A) and 0.08 a.u.f.s. in (B) and (C).

are applicable to conventional HPLC systems although microbore columns require sophisticated systems. Moreover, non-porous resins are chemically stalbe so that the separation by IEC at high pH, and column cleaning with sodium hydroxide, are possible although silica-based packings are unstable under such conditions. Non-porous resins, therefore are very useful not only for quality control, on-line monitoring, purity check of biomolecules like peptide mapping of recombinant products but also for micropreparative separation of active biomolecules.

REFERENCES

1 C. G. Horvath, B. A. Preiss and S. R. Lipsky, *Anal. Chem.*, 39 (1967) 1422.
2 C. Horvath and S. R. Lipsky, *J. Chromatogr. Sci.*, 7 (1969) 109.
3 C. Horvath and S. R. Lipsky, *Anal. Chem.*, 41 (1969) 1227.
4 D. J. Burke, J. K. Duncan, L. C. Dunn, L. Cummings, C. J. Siebert and G. S. Ott, *J. Chromatogr.*, 353 (1986) 425.
5 K. K. Unger, G. Jilge, J. N. Kinkel and M. T. W. Hearn, *J. Chromatogr.*, 359 (1986) 61.
6 D. J. Burke, J. K. Duncan, C. Siebert and G. S. Ott, *J. Chromatogr.*, 359 (1986) 533.
7 J. K. Duncan, A. J. C. Chen and C. J. Siebert, *J. Chromatogr.*, 397 (1987) 3.
8 G. Jilge, R. Janzen, H. Gieche, K. K. Unger, J. N. Kinkel and M. T. W. Hearn, *J. Chromatogr.*, 397 (1987) 71.
9 R. Janzen, K. K. Unger, H. Gieche, J. N. Kinkel and M. T. W. Hearn, *J. Chromatogr.*, 397 (1987) 81.
10 R. Janzen, K. K. Unger, H. Gieche, J. N. Kinkel and M. T. W. Hearn, *J. Chromatogr.*, 397 (1987) 91.
11 Y. Kato, T. Kitamura, A. Mitsui and T. Hashimoto, *J. Chromatogr.*, 398 (1987) 327.
12 K. Kalghatgi and C. Horvath, *J. Chromatogr.*, 398 (1987) 335.
13 F. D. Antia and C. Horvath, *J. Chromatogr.*, 435 (1988) 1.
14 M. A. Round and F. E. Regnier, *J. Chromatogr.*, 443 (1988) 73.
15 K. Kalghatgi and C. Horvath, *J. Chromatogr.*, 443 (1988) 343.
16 Y.-F. Maa and C. Horvath, *J. Chromatogr.*, 445 (1988) 71.
17 M. W. Dong, J. R. Gant and B. R. Larsen, *Biochromatography*, 4 (1989) 19.
18 Y. Kato, T. Kitamura, S. Nakatani and T. Hashimoto, in preparation.
19 Y. Kato, T. Kitamura, A. Mitsui, Y. Yamasaki and T. Hashimoto, *J. Chromatogr.*, 447 (1988) 212.
20 Y. Kato, Y. Yamasaki, S. Fukushige and K. Matsubara, *J. Chromatogr.*, (1989) in press.
21 S. Borman, *Anal. Chem.*, 59 (1987) 973A.
22 E. C. Nice, C. J. Lloyd and A. W. Burgess, *J. Chromatogr.*, 296 (1984) 153.
23 C. Flurer, C. Borra, S. Beale and M. Novotony, *Anal. Chem.*, 60 (1988) 1826.
24 M. A. Stadalius, M. A. Quarry and L. R. Snyder, *J. Chromatogr.*, 327 (1985) 93.
25 C. L. Flurer, C. Borra, F. Anderolini and M. Novotny, *J. Chromatogr.*, 448 (1988) 73.
26 B. E. P. Swoboda and V. Massey, *J. Biol. Chem.*, 240 (1965) 2209.
27 C. B. Kasper, in S. B. Needleman (Editor), *Protein Sequence Determination*, Springer, Berlin, New York, 1975, p. 114.

Journal of Chromatography, 481 (1989) 397–402
Elsevier Science Publishers B.V., Amsterdam — Printed in The Netherlands

CHROM. 21 843

Note

Rapid separation of α-amylases from barley by ion-exchange high-performance liquid chromatography on non-porous columns

ROBERT J. HENRY
Queensland Wheat Research Institute, P.O. Box 2282, Toowoomba, Qld. 4350 (Australia)
(First received January 24th, 1989; revised manuscript received July 28th, 1989)

α-Amylase (EC 3.2.1.1) is an important enzyme in biology and industry because of its central role in the hydrolysis of starch[1]. Multiple forms of α-amylase are found in many organisms due to the presence of isoenzymes[2] and possible post-translational modifications of the proteins[3]. The different forms of α-amylase in plants, especially the cereals wheat and barley, have been extensively studied because of their importance in hydrolysis of starch during germination, and the functional significance of these enzymes in the industrial utilisation of the grain[4].

Isoelectric focusing[5,6] is widely used to separate α-amylases but is difficult to quantify. α-Amylases from wheat and barley have been separated by ion-exchange chromatography on DEAE-cellulose[7,8] CM-cellulose[9] and CM-Sepharose[10] and more recently by chromatofocusing[5,11,12]. However, these separation techniques have been generally less resolving than electrophoretic methods and have been very slow. Omichi and Ikenaka[13] recently reported high-performance liquid chromatography (HPLC) of human salivary α-amylases using gel permeation, ion-exchange and chromatofocusing colums. However their study used colums containing porous media. Ion-exchange columns based upon non-porous packing materials have become available for protein separation[14]. These materials allow much faster flow-rates permitting more rapid separations.

This paper reports rapid separation of α-amylases from barley by high-performance ion-exchange chromatography on non-porous media.

MATERIALS AND METHODS

Sources of samples

Barley (cv. Grimmett) was partially malted by steeping and germination for 48 h as described previously[15]. The grain was immediately frozen by immersion in liquid nitrogen and then freeze-dried. The dry grain was ground using a laboratory mill 3100 (Falling Number) to pass a 0.8-mm screen and stored at −18°C.

Extraction of α-amylases

α-Amylase was extracted by stirring 7.5 g of ground barley in 75 ml of 50 m*M* sodium malate buffer pH 5.2, 2 m*M* calcium chloride, 50 m*M* sodium chloride, 3 m*M*

0021-9673/89/$03.50

sodium azide for 10 min at 4°C. In some extracts 2 m*M* phenylmethylsulphonyl fluoride was included. The supernatant was collected by centrifugation at 2000 *g* for 10 min at 4°C and concentrated by precipitation with 80% saturation ammonium sulphate. The precipitate was resuspended in 10 ml of 5 m*M* Tris buffer pH 8.6 containing 1 m*M* calcium chloride and stored frozen as 1-ml aliquots.

The sample was diluted (1 ml in 3 ml) filtered through a 0.45-μm membrane and de-salted on a 10-ml column of Bio-Gel P6 in 5 m*M* Tris pH 8.6, 1 m*M* calcium chloride.

High-performance liquid chromatography

The HPLC system was programmable with two pumps, a mixer, injection system, controller, variable-wavelength UV detector, fraction collector and a data station (Bio-Rad Model 402 gradient system). The system had a flow path of titanium rather than stainless steel.

Anion-exchange colums

Two anion-exchange columns were used, a Bio-Gel TSK DEAE-5-PW (diethylaminoethyl groups bound to G 5000 PW support) column of 75 × 7.5 mm I.D. and a non-porous MA7P cartridge of 30 × 4.6 mm I.D. Both columns were equilibrated in 5 m*M* Tris pH 8.6, 1 m*M* calcium chloride before sample injection.

α-Amylase assay

α-Amylase was assayed, following dilution with the extraction buffer, using dye-labelled starch substrate tablets (Pharmacia)[16]. Protein was monitored at 280 nm.

Isoelectric focusing

Isoelectric focusing was performed on Ampholine PAG plate gels pH 3.5–9.5 (LKB). Gels were run for 1.5 h at 30 W. The pH gradient was determined using p*I* markers and staining with Coomassie Blue.

α-Amylase was detected using Procion Red MX 2B starch impregnated paper[17]. Procion Red MX-2B React Red 1 (Polysciences) was reacted with soluble starch [American Society of Brewing Chemists (ASBC) for diastatic power][18]. Dyed starch was separated from unreacted dye by gel filtration on a 84 × 1.9 cm column of Fractogel TSK HW-40 (S) (Merck). Filter paper sheets (Whatman No. 4) 12 × 25 cm were soaked in a 0.5 mg/ml solution of Procion Red MX 2B starch containing 50 m*M* sodium chloride, 2 m*M* calcium chloride, 50 m*M* sodium maleate buffer pH 5.2, 3 m*M* sodium azide. The dry papers were pressed against the isoelectric focusing gels and incubated at 20°C for 30 min. The reaction was stopped by flooding the gel and paper with 1.0 *M* hydrochloric acid. α-Amylase bands appeared as white areas on a pink background. Amylases were also detected by incubating the isoelectric focusing gels in a solution of 1% soluble starch (ASBC for diastatic power) in 50 m*M* sodium chloride, 2 m*M* calcium chloride, 50 m*M* sodium maleate buffer pH 5.2, 3 m*M* sodium azide at 40°C for 20 min. Amylase bands were revealed as colourless bands on a blue background by staining with 0.04% iodine, 0.4% potassium iodide.

RESULTS AND DISCUSSION

DEAE-Resins

Separation of α-amylases from barley on a Bio-Gel TSK DEAE-5-PW column is shown in Fig. 1. Analysis of a sample and regeneration of the column for the next sample required about 1 h. Recoveries of α-amylase activity were high (82% in the example in Fig. 1). Two main peaks of α-amylase were observed with several minor components.

Non-porous colums

Separation of α-amylases from barley on a MA7P cartridge is shown in Fig. 2. This method was much more rapid allowing higher flow-rates with total analysis times of less than 10 min at 2 ml/min and less than 5 min at 5 ml/min (Fig. 3). Separation was improved by using a shallow gradient (Fig. 4) requiring about 10 min per sample.

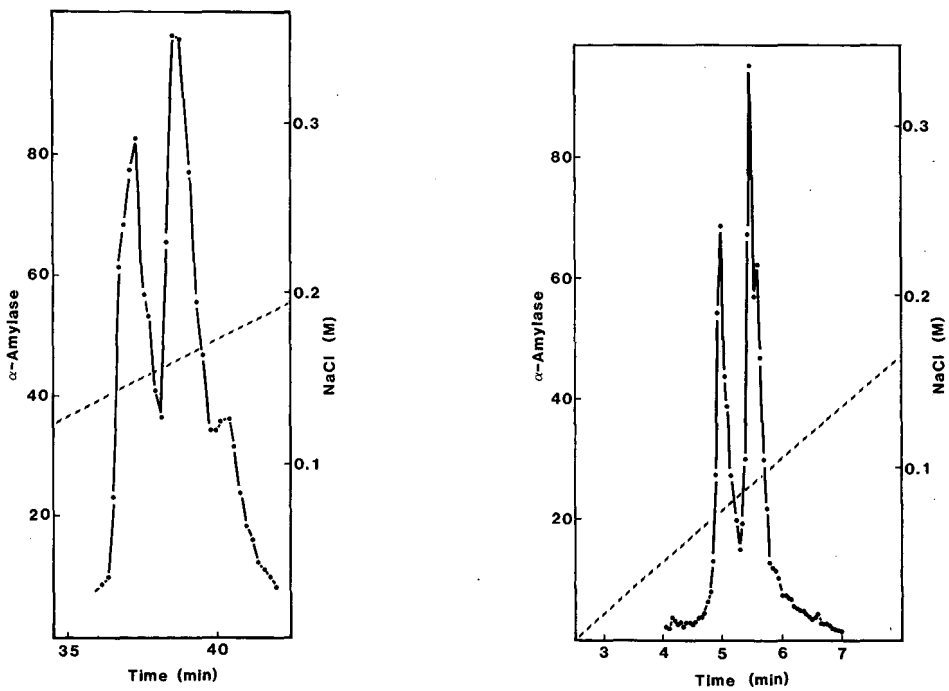

Fig. 1. Separation of barley α-amylases on a Bio-Gel TSK DEAE-5-PW anion-exchange column (75 × 7.5 mm). The sample (0.2 ml) was loaded in 5 m*M* Tris pH 8.6, 1 m*M* calcium chloride. The enzymes were eluted in a linear gradient from 0% to 80% Tris pH 8.6, 1 m*M* calcium chloride, 0.3 *M* sodium chloride between 15 min and 50 min at a flow-rate of 0.5 ml/min. Fractions collected were 0.125 ml. α-Amylase activity plotted in arbitrary relative units.

Fig. 2. Separation of barley α-amylases on a non-porous anion-exchange column (MA7P Cartridge, Bio-Rad, 30 × 4.6 mm). The sample (0.2 ml) was loaded in 5 m*M* Tris pH 8.6, 1 m*M* calcium chloride. α-Amylases were eluted in a linear gradient from 0% to 100% Tris pH 8.6, 1 m*M* calcium chloride, 0.3 *M* sodium chloride between 2.5 min and 12.5 min at a flow-rate of 2 ml/min. Fractions collected were 0.05 ml.

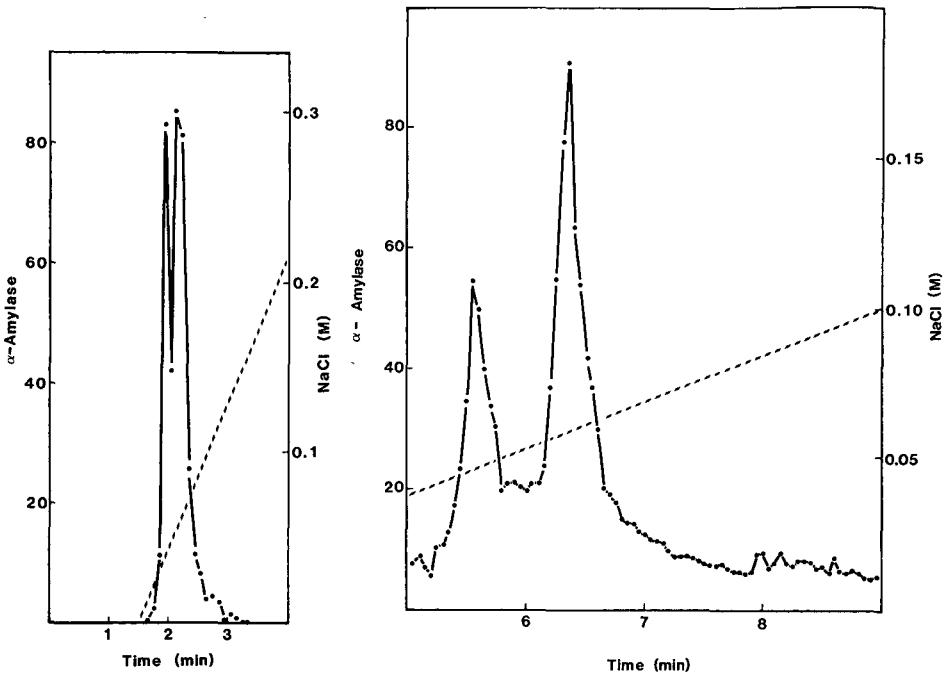

Fig. 3. Rapid separation of barley α-amylases on a MA7P cartridge. Conditions as for Fig. 2 except the gradient was between 1.5 min and 5 min, the flow-rate was 5 ml/min and fractions collected were 0.5 ml.

Fig. 4. Separation of barley α-amylases with a shallower gradient. Conditions were the same as in Fig. 2 with the gradient extended over twice the volume.

Recoveries of α-amylase activity were higher (90% in the example in Fig. 2) than with the DEAE-column. Most protein (more than 90% as assessed by the A_{280}) did not bind to these columns and was eluted before the gradient commenced. This resulted in a ten-fold purification of the α-amylase if all the fractions containing α-amylase were bulked.

Identity of α-amylases separated

The production of multiple forms of α-amylase by proteolytic degradation during isolation has been reported[3]. Inclusion of the protease inhibitor, phenylmethylsulphinyl fluoride, had very little effect on the elution profile. However, the isolation procedure used (4°C followed by ammonium sulphate precipitation) may protect against proteolysis and only two main components were detected. α-Amylase components reported may at least partially arise by proteolytic degradation of the two main isoenzymes as suggested by evidence produced by Hayes *et al.*[3] using electrophoretic analysis. The activity of α-amylase is apparently not always reduced by proteolytic action[3]. This retention of activity may explain the failure of many investigators to take steps to reduce proteolytic activity and as a result the very large number of forms of α-amylase often reported. Some heterogeneity can also be explained by the formation of α-amylase–inhibitor complexes[19]. The elution order and relative amounts

suggest that the first peak eluted may correspond to α-amylase III (a complex between α-amylase II and an inhibitor), the second, and largest peak, may be due to α-amylase II and the last minor component may be α-amylase I (Fig. 1).

Isoelectric focusing indicated that these samples contained two main bands of α-amylases between p*I* 6.7 and 5.5 with a minor band around p*I* 4.8. These correspond to α-amylases III (p*I* 6.1–6.9), II (p*I* 5.7–6.4) and I (p*I* 4.4–5.2). The proportion of α-amylase I is very low in barley. Chromatofocusing suggests that α-amylase I represents only 2.1% of total activity[5]. The major bands separated by HPLC must correspond to α-amylase II and III. Very small amounts of α-amylase (about 2.3% of total activity) probably corresponding to α-amylase I, were eluted in small peaks at higher salt concentrations (0.08–0.1 *M* NaCl, Fig. 4).

The identity of peaks was investigated by isoelectric focusing following concentration and de-salting of fractions from HPLC using Unicep-10 ultrafiltration cartridges (Bio-Rad). The results confirmed the predicted identities for the peaks but indicated that some peaks included a mixture of different forms of α-amylase. The first peak (5.5–6 min, Fig. 4) had a major band at p*I* 6.4 (α-amylase III); the second peak (6–6.5 min, Fig. 4) at p*I* 6.15 (α-amylase II) and the third (7.5–8 min, Fig. 4) at p*I* 4.8 (α-amylase I). However, small amounts of α-amylase III were detected in fractions collected between 6 and 7 min (Fig. 4).

DISCUSSION

Chromatography on non-porous anion-exchange columns provides a rapid and quantitative method for the analysis of multiple forms of α-amylase. The method may also have potential in the rapid purification of α-amylases. Affinity chromatography on cycloheptaamylose-Sepharose[20] and copper-iminodiacetic acid-Sepharose[21] has been used to purify α-amylases. Chromatofocusing has been used to separate isoenzymes in the purification of barley α-amylases[22]. The very rapid ten-fold purification on non-porous ion exchange columns reported here may be a useful step in any purification of α-amylase. Non-porous columns have several advantages, high flow rates are possible with good resolution and equilibration with solvents is rapid allowing fast recycling to the starting solvent for repeated analyses[23–25].

ACKNOWLEDGEMENTS

This work was supported by funds from the Australian Wheat Research Council and the Australian Barley Research Council. Robyn Coonan provided technical assistance.

REFERENCES

1 J. F. Robyt and W. J. Whelan, in T.A. Radley (Editor), *Starch and its Derivatives*, Chapman and Hall, London, 1968, p. 423.
2 A. H. D. Brown and J. V. Jacobsen, *Genet. Res., Camb.*, 40 (1982) 315.
3 B. Hayes, M. A. Harmey and H. Byrne, *J. Inst. Brew.*, 94 (1988) 253.
4 R. D. Hill and A. W. MacGregor, *Adv. Cereal Sci. Technol.*, 9 (1988) 217.
5 A. W. MacGregor, B. A. Marchylo and J. E. Kruger, *Cereal Chem.*, 65 (1988) 326.
6 B. A. Marchylo, L. J. Lacroix and J. E. Kruger, *Can. J. Plant Sci.*, 60 (1980) 433.

7 J. E. Kruger and R. Tkachuk, *Cereal Chem.*, 46 (1969) 219.
8 B. Marchylo, J. E. Kruger and G. N. Irvine, *Cereal Chem.*, 53 (1976) 157.
9 A. W. MacGregor, D. E. LaBerge and W. O. S. Meredith, *Cereal Chem.*, 48 (1971) 490.
10 E. Bertoft, C. Andtfolk and S. E. Kulp, *J. Inst. Brew.*, 90 (1984) 298.
11 B. A. Marchylo and A. W. MacGregor, *Cereal Chem.*, 60 (1983) 311.
12 B. A. Marchylo, A. W. MacGregor and J. E. Kruger, *J. Inst. Brew.*, 91 (1985) 161.
13 K. Omichi and T. Ikenaka, *Anal. Biochem.*, 168 (1988) 332.
14 D. Josic, W. Hofmann and W. Reutter, *J. Chromatogr.*, 371 (1986) 43.
15 R. J. Henry, *J. Sci. Food Agric.*, 42 (1988) 333.
16 R. J. Henry, D. J. Martin and A. B. Blakeney, *J. Cereal Sci.*, 5 (1987) 155.
17 L. Galleschi and J. M. Chapman, *Phytochemistry*, 24 (1985) 352.
18 W. F. Dudman and C. T. Bishop, *Can. J. Chem.*, 46 (1968) 3079.
19 C. A. Henson and J. M. Stone, *J. Cereal Sci.*, 8 (1988) 39.
20 M. P. Silvanovich and R. D. Hill, *Anal. Biochem.*, 73 (1976) 430.
21 V. Zawistowska, K. Sangster, J. Zawistowiski, J. Langstaff and A. D. Friesen, *Cereal Chem.*, 65 (1988) 414.
22 D. Lecommandeur, A. W. MacGregor and J. Daussant, *J. Chromatogr.*, 441 (1988) 436.
23 D. J. Burge, J. K. Duncan, L. C. Dunn, L. Cummings, C. J. Siebert and G. S. Ott, *J. Chromatogr.*, 353 (1986) 425.
24 D. J. Burke, J. K. Duncan, C. Siebert and G. S. Ott, *J. Chromatogr.*, 359 (1986) 583.
25 J. K. Duncan, A. J. Chen and C. J. Siebert, *J . Chromatogr.*, 397 (1987) 3.

Journal of Chromatography, 481 (1989) 403–410
Elsevier Science Publishers B.V., Amsterdam — Printed in The Netherlands

CHROM. 21 771

Note

Separation of rat liver HSP70 and HSP71 by high-performance liquid chromatography with a hydroxylapatite column

TAKUMI HATAYAMA*,[a], NAGAHISA FUJIO and MUNEHIKO YUKIOKA
Department of Biochemistry, Osaka City University Medical School, Osaka 545 (Japan)
YOSHIHIKO FUNAE
Laboratory of Chemistry, Osaka City University Medical School, Osaka 545 (Japan)
and
HIROAKI KINOSHITA
Second Department of Surgery, Osaka City University Medical School, Osaka 545 (Japan)
(First received March 7th, 1989; revised manuscript received May 26th, 1989).

Heat-shock proteins (HSPs) are induced in response to a broad range of environmental stresses, such as elevated temperature, amino acid analogues, transition metals and metabolic inhibitors (reviewed in refs. 1–3). HSPs with molecular weights of approximately 70 000, one of the major HSPs, are a family of evolutionally conserved proteins encoded by a conserved gene family. In mammalian cells, there seem to be two forms of these proteins, a constitutive form present at appreciable levels under normal conditions and an induced form, the synthesis of which is induced only by stress. These HSPs bind ATP tightly[4] and the property has been exploited to purify the HSPs[5]. Clathrin-uncoating ATPase was identified as a constitutive protein of the HSP70 family[6,7].

We have reported that the elevation of the body temperature of rats induces four HSPs with molecular weights of 70 000, 71 000, 85 000 and 100 000 (HSP70, HSP71, HSP85 and HSP100, respectively) in various tissues, with a concomitant induction of their corresponding mRNAs[8,9]. Among these HSPs of rats, HSP70 is a completely induced protein, whereas HSP71 is a constitutively expressed protein of the HSP70 family that exists abundantly in various tissues of rats. To obtain large amounts of an inducible protein and a constitutive protein of the HSP70 family for a study of their properties, liver tissue of rat may be better than cultured cells as a starting material.

In this paper, we describe a rapid method for the separation of HSP70 and HSP71 from rat liver by high performance liquid chromatography (HPLC) with a hydroxylapatite column.

[a] Present address: Department of Biochemistry, Kyoto Pharmaceutical University, Yamashina, Kyoto 607, Japan.

0021-9673/89/$03.50

EXPERIMENTAL

Materials

A hydroxylapatite column (KB-column, 100 × 7.8 mm I.D.) was obtained from Koken (Tokyo, Japan). DEAE-Sepharose CL-6B and ATP-agarose were obtained from Pharmacia (Uppsala, Sweden) and Sigma (St. Louis, MO, U.S.A.), respectively.

Animals

Male Sprague–Dawley rats weighing 220–240 g were purchased from the Shizuoka Agricultural Cooperative Association for Laboratory Animals and used at 7 weeks of age.

Preparation of HSP70 and HSP71 from rat liver

Whole-body hyperthermia of rats was brought about by elevation of the body temperature of the rats to 42°C for 15 min[8]. Livers (20 g) of rats killed 24 h after the hyperthermia were homogenized in 5 volumes of a buffer containing 20 m*M* Tris–acetate (pH 7.5), 20 m*M* sodium chloride, 0.1 m*M* EDTA and 0.1 m*M* dithiothreitol (buffer A). The homogenates were centrifuged for 10 min at 10 000 *g* at 4°C and the supernatant was further centrifuged for 1 h at 105 000 *g* at 4°C. The second supernatant (80 ml) was applied to a DEAE-Sepharose CL-6B column (60 × 2 cm I.D.) equilibrated with buffer A at 4°C. After the column had been washed with the same buffer, the proteins adsorbed were eluted with a linear gradient of 20–500 m*M* sodium chloride in the same buffer (500 ml). The eluted fractions containing HSP70 and HSP71 (50 ml) were adjusted to a magnesium concentration of 3 m*M* by the addition of 1 *M* magnesium chloride, and were applied to an ATP-agarose column (5 ml) equilibrated with 20 m*M* Tris–acetate (pH 7.5), 20 m*M* sodium chloride, 0.1 m*M* EDTA, 0.1 m*M* dithiothreitol and 3 m*M* magnesium chloride (buffer B) at 4°C. After the column had been washed with buffer B, proteins were eluted with buffer B containing 3 m*M* ATP. The fractions enriched in HSP70 and HSP71 (7.5 ml) were pooled and dialysed against 20 m*M* potassium phosphate buffer (pH 7.6) containing 0.1 m*M* dithiothreitol (buffer C) at 4°C.

High-performance liquid chromatography

Two Altex (Berkeley, CA, U.S.A.) pumps (Model 100) equipped with an Altex Model 420 solvent programmer and a UV-8 spectrophotometer (Tosoh, Tokyo, Japan) with an 8-μl flow cell were used.

The dialysed fractions from the ATP-agarose column were treated by HPLC with a hydroxylapatite column (10 × 0.78 cm I.D.) equilibrated with buffer C. After the column had been washed with the same buffer, the bound proteins were eluted with a linear gradient of 20–200 m*M* potassium phosphate in this buffer in 40 min at a flow-rate of 0.7 ml/min. Fractions containing HSP70 and HSP71 were pooled and dialysed against 20 m*M* potassium phosphate (pH 7.6), 0.15 *M* sodium chloride and 0.1 m*M* dithiothreitol (buffer D) at 4°C, and finally applied to the hydroxylapatite column for HPLC equilibrated with buffer D. The HSP70 and HSP71 were eluted separately with a linear gradient of 20–200 m*M* potassium phosphate in the same buffer in 60 min at a flow-rate of 0.7 ml/min.

One- and two-dimensional gel electrophoreses

For one-dimensional gel analysis, sodium dodecyl sulphate–10% polyacrylamide gel electrophoresis (SDS-PAGE) was carried out as described by Laemmli[10]. Two-dimensional gel electrophoresis was performed as reported by O'Farrell[11]. For the first dimension, the isoelectric focusing gel contained 1.6% pH 6–8 ampholites and 0.4% pH 3.5–10 ampholites. For the second dimension, SDS–10% polyacrylamide slab gels were used.

The separated proteins were stained with Coomassie brilliant blue. Molecular weight markers included phosphorylase b (92 500), bovine serum albumin (69 000), α-amylase (55 000), ovalbumin (45 000) and carbonic anhydrase (29 000).

Peptide mapping

Peptide mapping was performed as described by Cleveland *et al.*[12]. To 20 μl of each purified HSP at a concentration of 100 μg/ml, 5 μl of 0.25 *M* sodium hydrogencarbonate and 2.5 μl of *Staphylococcus aureus* V8 protease at various concentrations from 40 to 300 μg/ml were added, and proteolytic digestion was carried out at 30°C for 30 min. The reaction was stopped by the sample being boiled for 2 min, and the digest was separated by SDS-PAGE and detected by silver staining.

RESULTS AND DISCUSSION

Procedures have been developed for the purification of proteins of the HSP70 family from different cells and animals[5,13–15]. The proteins of the HSP70 family are purified rapidly by a two-step procedure involving DE-52 cellulose column chromatography followed by ATP-agarose affinity chromatography[5]; the latter is based on the tight binding of these proteins to ATP. However, the inducible protein and constitutive protein of the HSP70 family have similar physical properties, so these proteins are not separated by column chromatography on hydroxylapatite, DE-52 cellulose, DE-53 cellulose, DEAE-Sepharose, Sephacryl S-300, Bio-Gel P-300 or phenyl-Sepharose[13–15]. Isoelectric points of the inducible protein and constitutive protein of the HSP70 family from rats are 5.2 and 5.0, respectively, under non-denaturing conditions, and 5.8 and 5.6, respectively, under denaturing conditions[14]. By making use of the p*I* differences between these proteins, they can be separated from each other by preparative isoelectric focusing[14].

We established a method for purifying the HSP70 and HSP71 from the livers of rats that had been subjected to whole-body hyperthermia. These proteins were first recovered in the 150–180 m*M* sodium chloride eluate from DEAE-Sepharose Cl-6B column chromatography. The eluate was next chromatographied on an ATP-agarose column and an affinity-purified fraction contained mainly HSP70 and HSP71 with a main contaminating protein with a molecular weight of 54 000 and minor contaminating proteins with molecular weights of 45 000, 92 000 and 30 000. HSP70 and HSP71 were further purified, with removal of the contaminating proteins, by HPLC on a hydroxylapatite column (Fig. 1). These proteins were recovered in the 80–100 m*M* phosphate eluate. The second peak of A_{280}, which eluted at 110–130 m*M* phosphate, contained little protein but did contain ATP. Under the chromatographic conditions used, HSP70 seemed to be eluted slightly faster than HSP71 in the first peak, so we attempted to separate the two proteins more completely by adjustment of the chromatographic conditions.

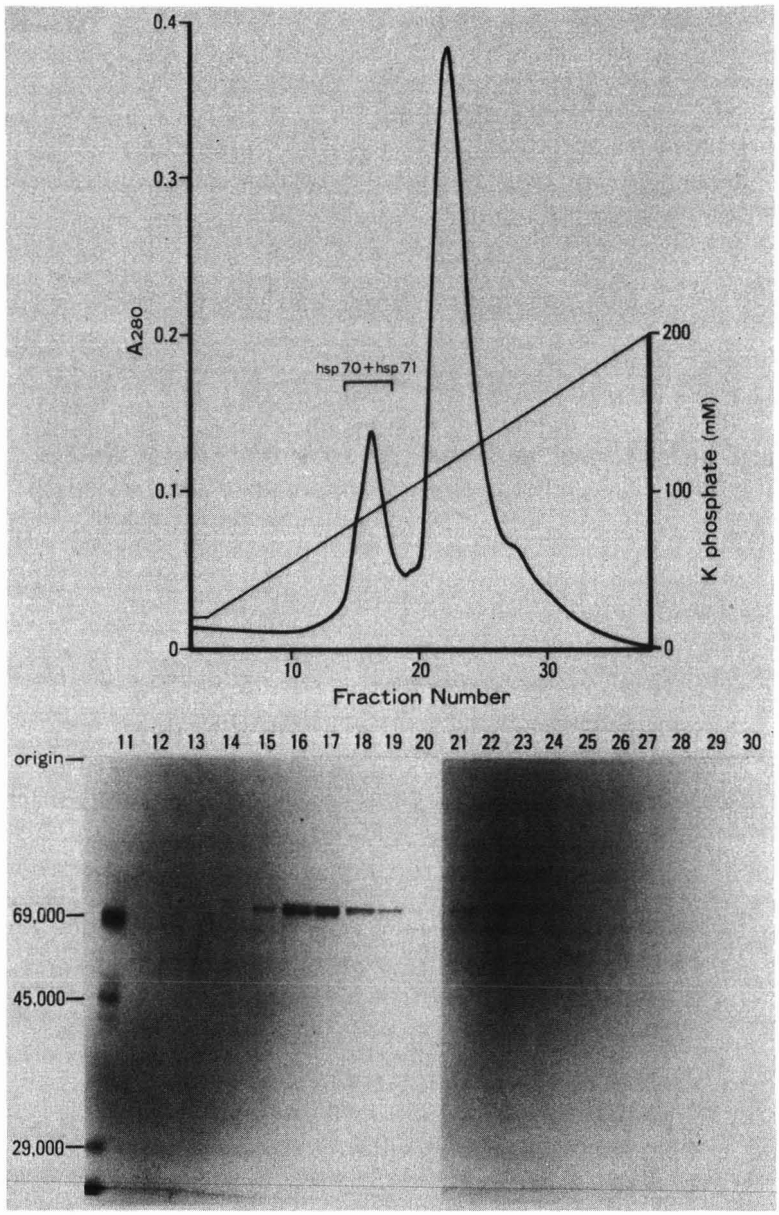

Fig. 1. Purification of HSP70 and HSP71 by HPLC with a hydroxylapatite column. Fractions containing HSP70 and HSP71 eluted from an ATP-agarose column were pooled and dialysed against buffer C. The solution was applied to a hydroxylapatite column equilibrated with buffer C. An elution profile of the column developed with a linear gradient of 20–200 m*M* potassium phosphate in buffer C is shown in the upper portion. In the lower portion is shown Coomassie blue staining of SDS–10% polyacrylamide gels loaded with 20 μl of each fraction. In this and subsequent figures, molecular weight markers are indicated on the left.

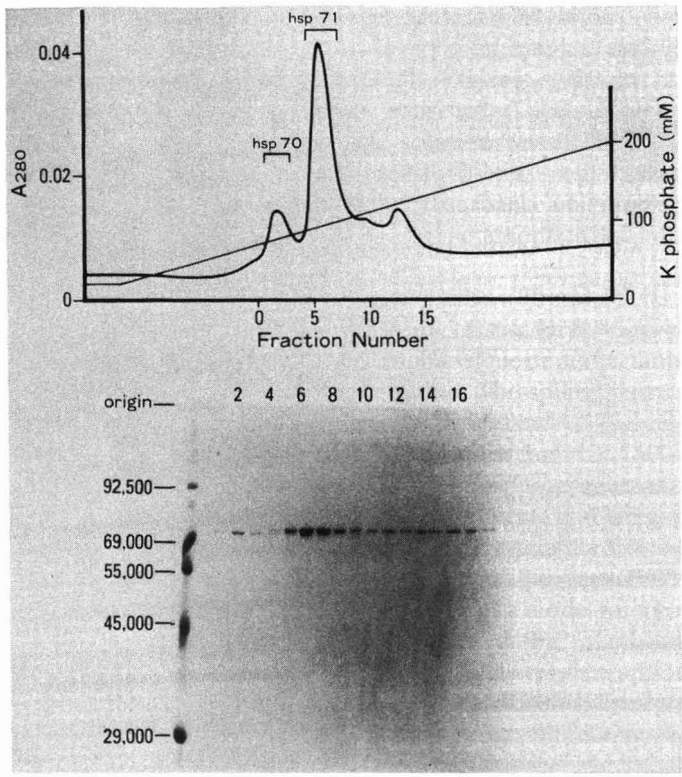

Fig. 2. Separation of HSP70 and HSP71 with a hydroxylapatite column in the presence of 0.15 *M* sodium chloride. Fractions containing HSP70 and HSP71 that eluted from the first hydroxylapatite column were dialysed against buffer D that contained 0.15 *M* sodium chloride and applied to a hydroxylapatite column equilibrated with buffer D. An elution profile of the column developed with a linear gradient of 20–200 m*M* potassium phosphate in buffer D is shown in the upper portion. In the lower portion is shown Coomassie blue staining of a SDS–10% polyacrylamide gel loaded with 20 μl of each fraction. The relative proportions of HSP70 and HSP71 are different in Fig. 1 and 2, because results obtained from different series of experiments are presented in each.

Fig. 2 shows an elution profile of HSP70 and HSP71 on rechromatography on a hydroxylapatite column with a potassium phosphate gradient in the presence of 0.15 *M* sodium chloride. Under these conditions, these proteins were separated from each other. HSP70 was eluted at 80 m*M* phosphate and HSP71 was eluted mainly at 90–110 m*M* phosphate, with tailing peaks eluting at 110–130 m*M* phosphate. HSP71 that eluted at the main peak and that which eluted at the tailing peaks were not different according to analyses by two-dimensional gel electrophoresis and by peptide mapping. Fractions containing HSP70 and HSP71, shown in Fig. 2, were pooled as purified HSP70 and HSP71.

When the purified proteins were analysed by two-dimensional gel electrophoresis, HSP70 and HSP71 gave nearly single spots on the gels (Fig. 3). When HSP70 and HSP71 were mixed with liver extract of heat-shocked rats, these proteins migrated

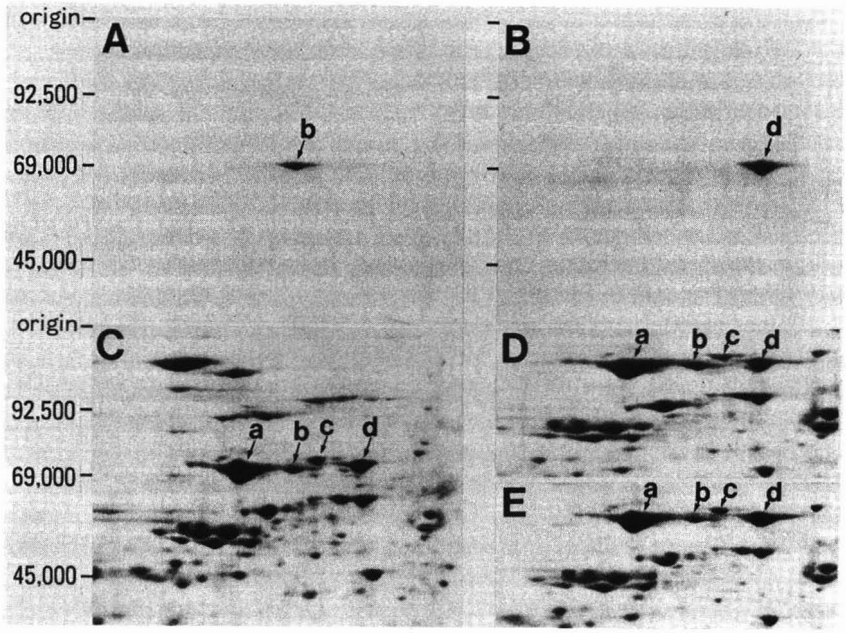

Fig. 3. Analysis of purified HSP70 and HSP71 by two-dimensional gel electrophoresis. Purified HSP70 (1 μg) (A), HSP71 (2 μg) (B), liver extract from heat-shocked rats (500 μg) (C), HSP70 (1 μg) + heat-shocked rat liver extract (500 μg) (D) and HSP71 (2 μg) + heat-shocked rat liver extract (500 μg) (E) were separated by two-dimensional gel electrophoresis. Isoelectric focusing gel for the first dimension was on the horizontal axis with the acidic end to the right. a, b, c and d indicate albumin, HSP70, a reference protein between HSP70 and HSP71, and HSP71, respectively.

identically with HSP70 and HSP71 in the extract on the two-dimensional gels. Fig. 4 shows the peptide mapping of these proteins. HSP70 and HSP71 gave similar but not identical peptide maps, indicating that the two proteins were different but highly homologous. Purified HSP70 and HSP71 which were incubated without protease migrated as double bands. As these HSPs without incubation migrated as a single band, as shown in Fig. 2, these HSPs seemed to degrade spontaneously *in vitro*, as reported by Mitchell *et al.*[16].

From 20 g of livers of heat-shocked rats, 0.4 mg of HSP70 was recovered. From 20 g of livers of untreated or heat-shocked rats, 0.6–0.7 mg of HSP71 was recovered. The purity of the final samples, determined by densitometry of the SDS–polyacrylamide gels stained with Coomassie blue, was higher than 95% in both instances.

The function of HSPs is not well understood, but there is much evidence of a correlation between the production of HSPs and the development of thermotolerance in various organisms[2,3]. The HSP70 family of proteins are found associated with the nuclei and nucleoli of cells during heat shock, and they seem to protect these structures and to facilitate the repair of heat-induced damage[17]. Some HSPs are expressed under normal physiological conditions and also at some stages of development of organisms[2,3], so HSPs probably have physiological functions. At present, a constitutive form of the HSP70 family is only identified as the same protein as a clathrin-uncoating ATPase[6,7]. Recently, facilitation of the translocation of

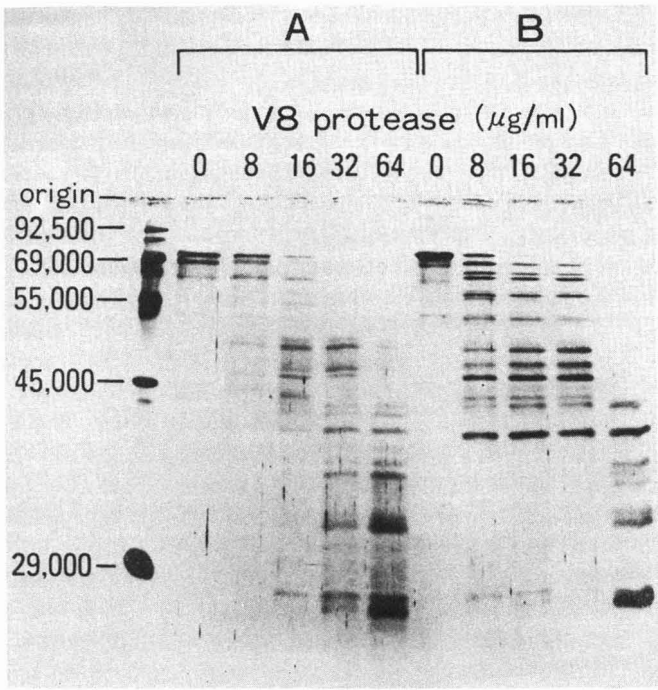

Fig. 4. Comparison of HSP70 and HSP71 by one-dimensional peptide mapping. Purified HSP70 (A) and HSP71 (B) were digested with various concentrations of *Staphylococcus aureus* V8 protease and analysed by SDS-PAGE.

secretory and mitochondrial precursor proteins by a subfamily of HSP70 in yeast cells has been reported[18,19]. It would be of interest to find whether the constitutive protein and inducible protein of the HSP70 family have the same or different functions. Rapid and large-scale preparations of both the inducible and the constitutive proteins of the HSP70 family by HPLC with a hydroxylapatite column may facilitate the study of the function of these heat-shock proteins.

ACKNOWLEDGEMENT

This study was supported in part by a Grant-in-Aid for Cancer Research from the Ministry of Education, Science and Culture, Japan.

REFERENCES

1 M. Ashburner and J. J. Bonner, *Cell*, 17 (1979) 241.
2 S. Lindquist, *Annu. Rev. Biochem.*, 55 (1986) 1151.
3 J. R. Subjeck and T. Shyy, *Am. J. Physiol.*, 250 (1986) C1.
4 M. J. Lewis and H. R. B. Pelham, *EMBO J.*, 4 (1985) 3137.
5 W. J. Welch and J. R. Feramisco, *Mol. Cell. Biol.*, 5 (1985) 1229.
6 E. Ungewickell, *EMBO J.*, 4 (1985) 3385.
7 T. G. Chappell, W. J. Welch, D. M. Schlossman, K. B. Palter, M. J. Schlesinger and J. E. Rothman, *Cell*, 45 (1986) 3.

8 N. Fujio, T. Hatayama, H. Kinoshita and M. Yukioka, *J. Biochem.*, 101 (1987) 181.
9 N. Fujio, T. Hatayama, H. Kinoshita and M. Yukioka, *Mol. Cell. Biochem.*, 77 (1987) 173.
10 U. K. Laemmli, *Nature (London)*, 227 (1970) 680.
11 P. H. O'Farrell, *J. Biol. Chem.*, 250 (1975) 4007.
12 D. W. Cleveland, S. G. Fischer, M. W. Kirschner and U. K. Laemmli, *J. Biol. Chem.*, 252 (1977) 1102.
13 W. J. Welch and J. R. Feramisco, *J. Biol. Chem.*, 257 (1982) 14949.
14 P. T. Guidon and L. E. Hightower, *Biochemistry*, 25 (1986) 3231.
15 P. T. Guidon and L. E. Hightower, *J, Cell. Physiol.*, 128 (1986) 239.
16 H. K. Mitchell, N. S. Petersen and C. H. Buzin, *Proc. Natl. Acad. Sci. U.S.A.*, 82 (1985) 4969.
17 H. R. B. Pelham, *EMBO J.*, 3 (1984) 3095.
18 R. J. Deshaies, B. D. Koch, M. Werner-Washburne, E. A. Craig and R. Schekman, *Nature (London)*, 332 (1988) 800.
19 W. J. Chirico, M. G. Waters and G. Blobel, *Nature (London)*, 332 (1988) 805.

Journal of Chromatography, 481 (1989) 411–415
Elsevier Science Publishers B.V., Amsterdam — Printed in The Netherlands

CHROM. 21 806

Note

Separation of homologues of methyl ester and 3-O-acetyl methyl ester derivatives of the corynomycolic acid fraction from *Corynebacterium pseudotuberculosis*

THUIOSHI IONEDA
Instituto de Química, B9T, Universidade de São Paulo, C. Postal 20780, 05508 São Paulo (Brazil)
(First received April 16th, 1989; revised manuscript received July 18th, 1989)

Mycolic acids are high-molecular-weight α-branched, β-hydroxylated fatty acids that characteristically undergo pyrolytic cleavage between the C-α–C-β linkage. The resulting fatty acid unit (merofatty acid) bears the α-branch and the first two carbon atoms of the whole molecule (R_1–CH_2–COOH). On the other hand, the fatty aldehyde unit (meraldehyde) corresponds to the main chain of mycolic acid less the first two carbon atoms, and therefore displays a carbon chain from methyl terminal to C-β(R_2–CHO) (Fig. 1). The number of carbon atoms of the α-branch centre either around C-16, as in representatives of the genera *Artrobacter*[1], *Brevibacterium*[2], *Corynebacterium*[3], *Nocardia*[4] and *Rhodococcus*[5,6], or C-24, in *Mycobacterium tuberculosis*[7], and C-22 in the majority of representatives of the genus *Mycobacterium*[8].

In general, the α-branch is represented by an alkyl group, and an alkenyl group may occur in small proportions. For example, the corynomycoldienic acid fraction and a small proportion of the corynomycolenic acid fraction from *C. diphtheriae* and *C. pseudotuberculosis* under pyrolysis liberate the monounsaturated fatty acid unit in which the double bond is located at C-9.

The β-unit displays progressive structural complexity with increasing chain length. Thus, the approximately C_{32} mycolic acids (corynomycolic acids) have either a saturated or a monounsaturated hydrocarbon chain with a double bond at C-9 from the carbonyl group of the meraldehyde unit[2,9]. The approximately C_{40} mycolic acids (short-chain nocardomycolic acids) contain in the β-unit a carbon chain of about C_{24}–C_{32}, and in *R. rhodochrous* only saturated and monounsaturated hydrocarbon chains have been reported[5,10]. However, approximately C_{50} mycolic acids (nocardic acids[4] or nocardomycolic acids) show an approximate chain length in the range C_{34}–C_{40} in which up to four double bonds may be found[11]. Therefore, the structure of the β-chain unit and also the amount of the corresponding homologue respond to the

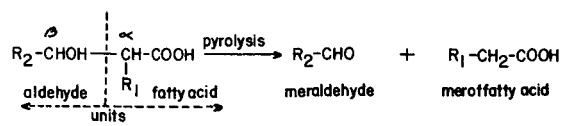

Fig. 1. Scheme of pyrolytic fragmentation of mycolic acids.

0021-9673/89/$03.50

complexity of composition of the nocardic acid fraction from *N. astéroides*. Similar reasoning can be applied to approximately C_{60} mycolic acids (long-chain nocardomycolic acids)[6] found in *R. bronchialis*[6], *R. aurantiacus* and *R. sputi*[12].

For approximately C_{80} mycolic acids, the structure of the β-unit becomes more complex, and in addition to the occurrence of double bonds in the hydrocarbon chain, there may be an additional side-chain from the introduction of a methyl or cyclopropyl group[13]. Moreover, other functional groups may be present, such as carbonyl and methoxyl[14].

Although a great deal of work has been done on mycolic acids, the investigation of procedures for the isolation of individual mycolic acids on the basis of the number of carbon atoms is limited. An interesting method is the separation of *p*-bromophenacyl mycolates into their homologues by reversed-phase column liquid chromatography (LC)[15,16]. However, the development of alternative procedures was thought to be of interest in order to provide another means of isolating individual homologues from a complex mixture of mycolic acids as methyl ester or O-acetyl methyl ester derivatives.

In this paper, the separation of C_{30}, C_{31}, C_{32} and C_{34} mycolic acids from *C. pseudotuberculosis* as methyl ester or 3-O-acetyl methyl ester derivatives by reversed-phase LC is described.

EXPERIMENTAL

All reagents were of analytical-reagent grade; commercial and analytical-reagent grade solvents were distilled before use. LiChrosorb-grade solvents were obtained from E. Merck (Darmstadt, F.R.G.).

Crude methyl corynomycolate from *C. pseudotuberculosis* was prepared essentially as described[17], and the methyl corynomycolate fraction was obtained by repeated crystallization using methanol. The corynomycolic acid fraction was obtained from methyl corynomycolate after alkaline hydrolysis[18], followed by preparative thin-layer chromatography (TLC) (solvent C, see below) and subsequent LC on silicic acid (Carlo Erba, Milano, Italy) [eluted with 40% (v/v) diethyl ether in *n*-hexane]. A standard corynomycolic acid fraction was from *C. diphtheriae*[18].

TLC was carried out either on plates coated in the laboratory with silica gel H (Merck) or on plastic sheets precoated with silica gel 60 F_{254}, layer thickness 0.2 mm (Art. No. 5735, Merck). The developing solvents were (A) *n*-hexane–diethyl ether–acetone–acetic acid (70:10:10:1), (B) *n*-hexane–diethyl ether–acetone–acetic acid (70:20:5:1), (C) *n*-hexane–diethyl ether–acetone–acetic acid (70:30:11:1) and (D) chloroform–acetone–methanol–water (50:60:2.5:3) (all proportions by volume). The precoated sheets were developed overnight in solvent D, then air dried in a hood; the solvent-free plates were kept in the original box and used without further heat activation.

The TLC plates were developed at room temperature (23–26°C) without previous chamber saturation.

Detection of spots on the plates was carried out under iodine vapour or by spraying with 20% (w/v) potassium dichromate in 10% (v/v) sulphuric acid and heating the plates at 110°C for approximately 10 min.

LC was carried out using a Perkin-Elmer (Norwalk, CT, U.S.A.) Series 2/2 pump with a Rheodyne 7125 injection port and a syringe-loading sample injector (20 μl

loop). The mobile phase was ethanol–distilled water–acetonitrile (90:10:5, v/v/v) containing 5% (v/v) of *n*-hexane (for methyl corynomycolate) or ethanol–distilled water (90:10, v/v) containing 20% (v/v) of *n*-hexane (for 3-O-acetyl methyl corynomycolate), at a flow-rate of 1 ml/min.

A stainless-steel column (250 mm × 4.6 mm I.D.) containing Spherisorb octadecylsilane–silica gel (ODS, 5 μm) was obtained from Spectra-Physics (Santa Clara, CA, U.S.A.). The detector was an SP-8400 variable-wavelength ultraviolet–visible spectrophotometer from Spectra-Physics, set at 215 nm. An SP-4100 integrator (Spectra-Physics) was used, the chart speed was set at 0.5 cm/min and attenuation 4 was used. For preparative purposes (with methyl corynomycolate), several runs were carried out by collecting 15 drops/min using an LKB (Bromma, Sweden) 7004 drop counter connected to an LKB Ultrorac 7000 fraction collector; each cycle was started from the same tube. Fractions corresponding to the most abundant homologue were concentrated to dryness with a stream of nitrogen in a hood. The white powdery residue was dissolved in a small volume of benzene and submitted to analytical chromatography for purity determination.

RESULTS AND DISCUSSION

The TLC behaviour of the methyl corynomycolate derivative from corynomycolic acid fraction of *C. pseudotuberculosis* is shown in Table I. It migrates with an R_F value that is intermediate between those of the unesterified form and the O-acetylated derivative. The melting point, refractive index and specific optical rotatory power are given in Table I, and compared with those of the acid and the 3-O-acetyl derivative.

Separation of the methyl corynomycolates fraction by LC on octadecylsilane–silica gel into homologues (methyl esters of C_{30}, C_{31}, C_{32} and C_{34} corynomycolic acid) with increasing retention times was achieved (Fig. 2, trace A). The component attributed to the methyl ester of C_{31} corynomycolic acid was inferred by plotting the logarithm of retention time against the number of carbon atoms in the mycolic acids. On the basis of the detector response and of the percentage peak area, the components accounted for approximately 13.1, 2.3, 80.6 and 4.1%, corresponding to methyl C_{30}, C_{31}, C_{32} and C_{34} corynomycolate, respectively. Previous studies on the composition of the saturated corynomycolic acid fraction from *C. pseudotuberculosis* as O-acetyl

TABLE I

TLC BEHAVIOUR AND PHYSICO-CHEMICAL CHARACTERISTICS OF CORYNOMYCOLIC ACID FRACTION FROM *C. PSEUDOTUBERCULOSIS* AND OF METHYL- AND 3-O-ACETYL METHYL ESTER DERIVATIVES

For the composition of mobile phases A–C, see Experimental. n_D of immersion oil (E. Merck) = 1.514.

Preparation	R_F			*Characteristics*		
	A	*B*	*C*	*m.p. (°C)*	n_D	$[\alpha]_D^{25}$
Corynomycolic acid	0.21	0.11	0.31	68–70	–	+ 6.4
Methyl corynomycolate	0.48	0.31	0.54	56–58	–	+11.4
3-O-Acetyl methyl corynomycolate	0.62	0.50	0.64	–	1.453	+16

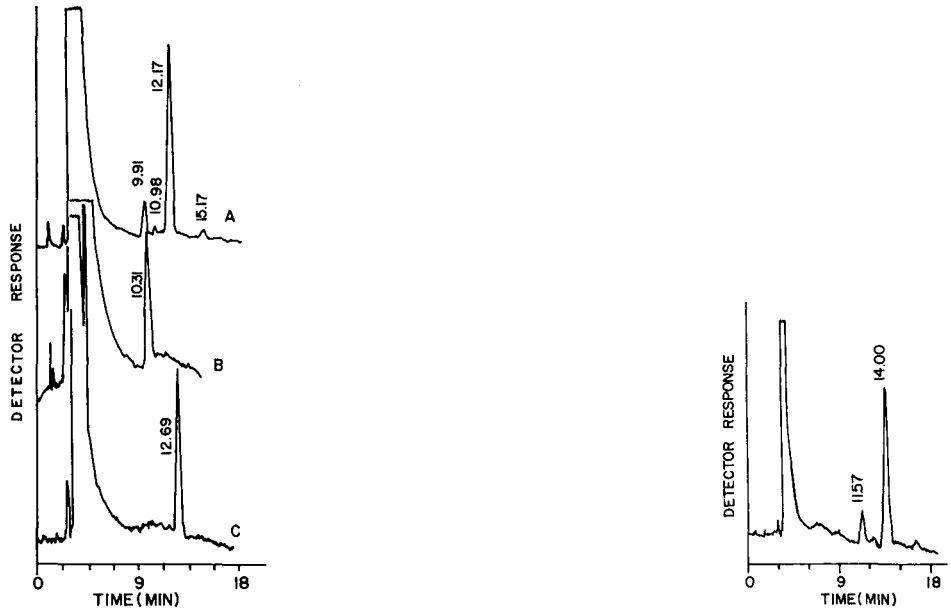

Fig. 2. Separation of methyl ester derivative of corynomycolic acid fraction from *C. pseudotuberculosis* into homologues (trace A) by reversed-phase LC on an octadecylsilane–silica gel column (250 mm × 4.6 mm I.D.). The peaks at 9.91, 10.98, 12.17 and 15.17 min correspond to the methyl ester of C_{30}, C_{31}, C_{32} and C_{34} corynomycolic acid, respectively. Trace B, methyl C_{30} corynomycolate; trace C, metyl C_{32} corynomycolate. Solvent: ethanol–water–acetonitrile (90:10:5, v/v/v) containing 5% (v/v) of *n*-hexane at a flow-rate of 1 ml/min. Detection at 215 nm.

Fig. 3. Separation of 3-O-acetyl methyl ester derivative of the corynomycolic acid fraction from *C. pseudotuberculosis* into homologues by reversed-phase LC on an octadecylsilane–silica gel column (250 mm × 4.6 mm I.D.). Solvent: ethanol–water (90:10, v/v) containing 20% (v/v) of *n*-hexane at a flow-rate of 1 ml/min. Detection at 215 nm.

methyl ester derivatives by gas chromatography combined with mass spectrometry showed mainly the homologues of C_{30}, C_{32} and C_{34} corynomycolic acids[17].

By carrying out several runs, the preparation of a single fraction was possible (Fig. 2, traces B and C; fractions corresponding to methyl C_{30} and C_{32} corynomycolate, respectively). In a similar way, 3-O-acetyl methyl corynomycolate can be separated into homologues by using reversed-phase LC (Fig. 3).

The derivatization procedure used to date for separating homologues of mycolic acids by reversed-phase LC involves the reaction of the carboxyl group with *p*-bromophenacyl bromide, the resulting *p*-bromophenacyl ester derivatives emerging from the column being detected at 254 nm. This technique was used for the separation of homologues of mycolic acids from *M. tuberculosis* $H_{37}Ra$[16] and *M. smegmatis*[15]; recently the usefulness of the same method for identifying the group of mycolic acids from C_{32} to C_{80} was shown, and the utilization of this procedure to classify clinical isolates was proposed[19].

The possibility of detecting methyl mycolate at 215 nm adds an alternative option for the isolation of homologues from a complex mixture of methyl ester derivatives of longer mycolic acids.

ACKNOWLEDGEMENTS

This work was supported by grants from FAPESP, FINEP and CNPq. Thanks are due to Mr. E. T. de Almeida and Mr. R. U. Gameiro for valuable assistance and to Mrs. L. Ribeiro for typing the manuscript.

REFERENCES

1 T. Suzuki, K. Tanaka, I. Matsubara and S. Kinoshita, *Agric. Biol. Chem.*, 33 (1969) 1619.
2 H. Okazaki, H. Sugino, T. Kanzaki and H. Fukuda, *Agric. Biol. Chem.*, 33 (1969) 764.
3 J. Pudles and E. Lederer, *Bull. Soc. Chim. Biol.*, 36 (1954) 759.
4 G. Michel, C. Bordet and E. Lederer, *C.R. Acad. Sci.*, 250 (1960) 3518.
5 T. Ioneda, E. Lederer and J. Rozanis, *Chem. Phys. Lipids*, 4 (1970) 375.
6 L. Alshamaony, M. Goodfellow, D. Minnikin and H. Mordarska, *J. Gen. Microbiol.*, 92 (1976) 183.
7 F. H. Stodola, A. Lesuk and R. J. Anderson, *J. Biol. Chem.*, 126 (1938) 50.
8 A. H. Etemadi, *PhD Thesis*, University of Paris, 1965.
9 D. W. Thomas, A. K. Matida, C. L. Silva and T. Ioneda, *Chem. Phys. Lipids*, 23 (1979) 267.
10 M. C. Z. Teixeira, T. Ioneda and J. Asselineau, *Chem. Phys. Lipids*, 37 (1985) 155.
11 C. Bordet and G. Michel, *Bull. Soc. Chim. Biol.*, 51 (1969) 527.
12 M. Tsukamura and I. Yano, *Int. J. Syst. Bacteriol.*, 35 (1984) 364.
13 A. H. Etemadi, R. Okuda and E. Lederer, *Bull. Soc. Chim. Fr.*, (1964) 868.
14 A. H. Etemadi, *C.R. Acad. Sci. Ser. C*, 263 (1966) 1257.
15 P. A. Steck, B. A. Swartz, M. S. Rosenthal and G. R. Gray, *J. Biol. Chem.*, 253 (1978) 5625.
16 N. Qureshi, K. Takayama, H. C. Jordi and H. K. Schnoes, *J. Biol. Chem.*, 253 (1978) 5411.
17 T. Ioneda, C. L. Silva and D. W. Thomas, *Chem. Phys. Lipids*, 24 (1979) 1.
18 T. Ioneda, M. Lenz and J. Pudles, *Biochem. Biophys. Res. Commun.*, 13 (1963) 110.
19 W. R. Butler, D. G. Ahearn and J. O. Kilburn, *J. Clin. Microbiol.*, 23 (1986) 182.

Journal of Chromatography, 481 (1989) 416–420
Elsevier Science Publishers B.V., Amsterdam — Printed in The Netherlands

CHROM. 21 765

Note

Isolation of the aromatic heptaenic antibiotics trichomycin A–F by high-performance liquid chromatography

TADAAKI KOMORI* and YUKIYOSHI MORIMOTO
Research and Technology Group, Fujisawa Pharmaceutical Co., Ltd., Kashima, Yodogawa-ku, Osaka 532 (Japan)
(First received March 15th, 1989; revised manuscript received July 4th, 1989)

Aromatic heptaene antibiotics possess a large lactone ring containing a hydroxylated portion, seven conjugated double bonds, an amino sugar and a characteristic aromatic moiety. Aureofungi, candicidin, DJ 400, hamycin, levorin, lucknomycin, partricin and trichomycin belong to this group. Trichomycin was the first member to be discovered[1,2].

Trichomycin, a potent and clinically useful antifungal drug, especially as the trichomonacide, is produced by *Streptomyces hachijoensis* from a soil on the Pacific Island, Hachijo Jima, Japan. Two compounds, trichomycin A and B, were first isolated from the *Streptomyces* by counter-current distribution methods[3]. The structure of the major constituent, trichomycin A, was tentatively deduced on the basis of chemical degradations[4]. It is surprising that the antibiotic has always been considered to be a mixture of only two components, trichomycin A and B.

However, it was subsequently reported that trichomycin is a mixture of more than ten components as determined by high-performance liquid chromatography (HPLC) by Helboe *et al.* in 1980[5], and that it is a complex mixture of ten components by thin-layer chromatography (TLC) and sixteen components by HPLC by Thomas and Newland in 1986[6]. None of these methods, however, appeared suitable for preparative-scale application. Our more recent detailed HPLC studies on the antibiotic indicated that it consists of more than seventeen closely related compounds and made possible the separation of the trichomycin complex into trichomycin A–F.

These studies were concerned with the isolation of six components, trichomycin A–F, representing about 65–75% of the total trichomycin.

The structure of trichomycin A, the major component, is shown in Fig. 1[7].

EXPERIMENTAL

Materials

A mixture of trichomycin was obtained from the extracts of the mycelial cake of *Streptomyces hachijoensis*.

Flash liquid chromatography

Flash liquid chromatography (FLC) was carried out on a Yamazen FMI-C

0021-9673/89/$03.50

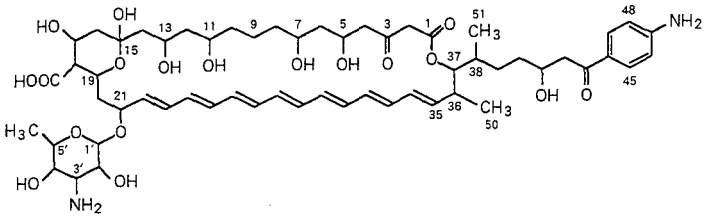

Fig. 1. Structure of trichomycin A.

instrument with a Yamazen Prep UV-1OV spectrophotometric detector. A silica gel column consisting of a 30 × 3 cm I.D. glass column packed with Fuji gel CQ-3 (particle size 30–50 μm) (Fuji Gel Hanbai) was used. The mobile phase consisted of the lower phase of a chloroform–methanol–water (2:2:1) mixture. Samples of 15 ml of solutions containing 80 mg of trichomycin in the same solvent were usually charged on to the column. Chromatography was carried out at a flow-rate of 4.0 ml/min with UV–VIS detection at 360 nm. Generally, two peaks were obtained, as shown in Fig. 3. The first fraction included trichomycin B and F and the second included trichomycin A, C, D and E. Each fraction was submitted to preparative HPLC.

Analytical HPLC

HPLC was carried out with a Hitachi 635 instrument with a Shimadzu SPD-1 spctrophotometric detector. A Nucleosil 5C8 column (particle size 5 μm; Macherey, Nagel & Co.) of dimensions 150 × 4 mm I.D. packed with C_8 reversed-phase silica was used. A 3-μl volume of solution containing 1 mg/ml of sample in dimethylformamide was usually injected. The mobile phase was acetonitrile–(phosphate–citrate buffer) (32.5:67.5, pH 4.6). The buffer was prepared from 33.47 g of $Na_2HPO_4 \cdot 12H_2O$ and 11.18 g of citric acid in 1 l of water. Chromatography was carried out at a flow-rate of 1.0 ml/min with UV–VIS detection at 360 nm.

Preparative HPLC

HPLC was carried out on a Hitachi 635 instrument with a Shimadzu SPD-1 spectrophotometric detector. A μBondasphere C_{18} column (particle size 5 μm; Waters Assoc.) of dimensions 150 × 19 mm I.D. was used. The mobile phase was acetonitrile–(phosphate–citrate buffer) (34.5:65.5, pH 4.75). A 0.2-ml volume of DMF solution containing 2 mg of trichomycin obtained from FLC was usually injected. Chromatography was carried out at a flow-rate of 4.0 ml/min and the column pressure ranged from 95 to 98 kg/cm^2, with detection at 355 nm. The peaks corresponding to trichomycin A–F were cut out manually in the following order: 76–80 ml (trichomycin C), 92–96 ml (D), 100–107 ml (E), 110–149 ml (A), 150–175 ml (B) and 215–255 ml (F). Each fraction was concentrated *in vacuo* in the dark until there was no odour of acetonitrile. The concentrate was extracted twice with 20% of its volume of *n*-butanol. The *n*-butanol extracts were washed twice with water and then concentrated *in vacuo*, adding water, to given an opaque solution, in the dark. The precipitated fine yellow powder was filtered off, washed throughly with water in order to desalt it and dried *in vacuo* over P_2O_5. Rechromatography was carried out to increase the purity as required.

The operating conditions are given in Figs. 2 and 3.

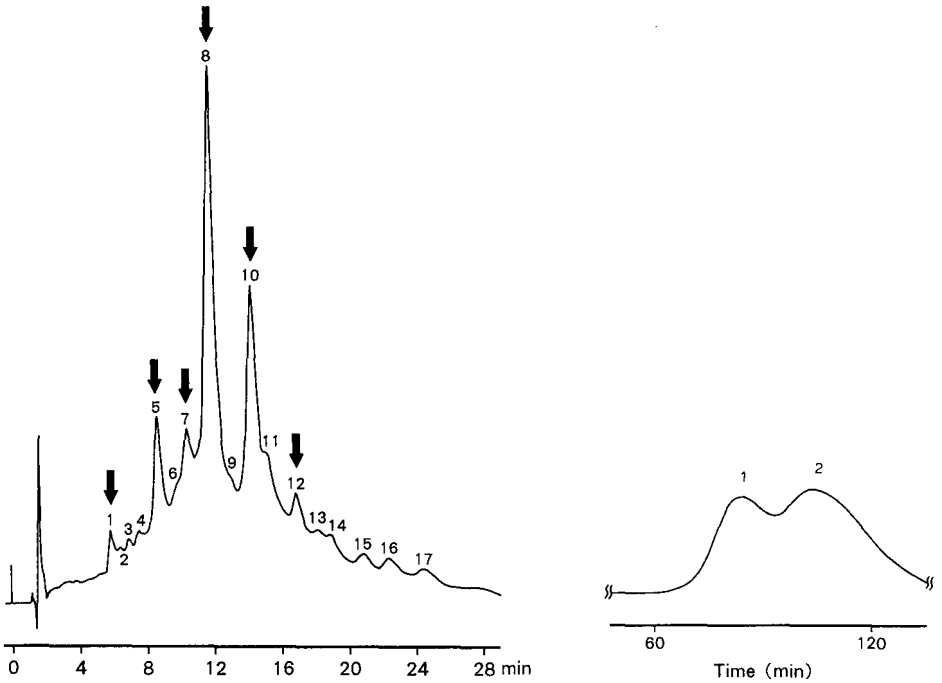

Fig. 2. Chromatogram of trichomycins by HPLC. Column: Nucleosil 5C8, 5 μm (150 × 4 mm I.D.). Mobile phase: acetonitrile–(phosphate–citrate buffer) (32.5:67.5, pH 4.6). Detection: 360 nm. Flow-rate: 1.0 ml/min. The isolated components are shown by arrows. Peaks: 1 = trichomycin C; 5 = trichomycin D; 7 = trichomycin E; 8 = trichomycin A; 10 = trichomycin B; 12 = trichomycin F.

Fig. 3. Chromatogram of trichomycins by FLC. Column: silica gel (Fuji gel CQ-3). Mobile phase: the lower phase of a chloroform–methanol–water (2:2:1) mixture. Detection: 360 nm. Flow-rate: 4.0 ml/min. Peaks: 1 = trichomycin B and F; 2 = trichomycin A, C, D and E.

Assay and testing procedures

Antibiotic potency was measured by a microbiological cylinder-plate method[8].

RESULTS AND DISCUSSION

Fig. 2 shows a chromatogram of a mixture of trichomycins. Seventeen peaks were completely resolved on the Nucleosil 5C8 column. Good resolution of the antibiotic was obtained with acetonitrile–(phosphate–citrate buffer) (32.5:67.5, pH 4.6) as the solvent at a flow-rate of 1.0 ml/min.

These results prompted us to use a similar solvent system for the preparative isolation of the main components from a mixture of trichomycins. The desired main components were concentrated by chromatography on alumina and silica gel, followed by FLC on silica gel with the lower phase of a chloroform–methanol–water (2:2:1) mixture. The components studied divided into two groups. One group

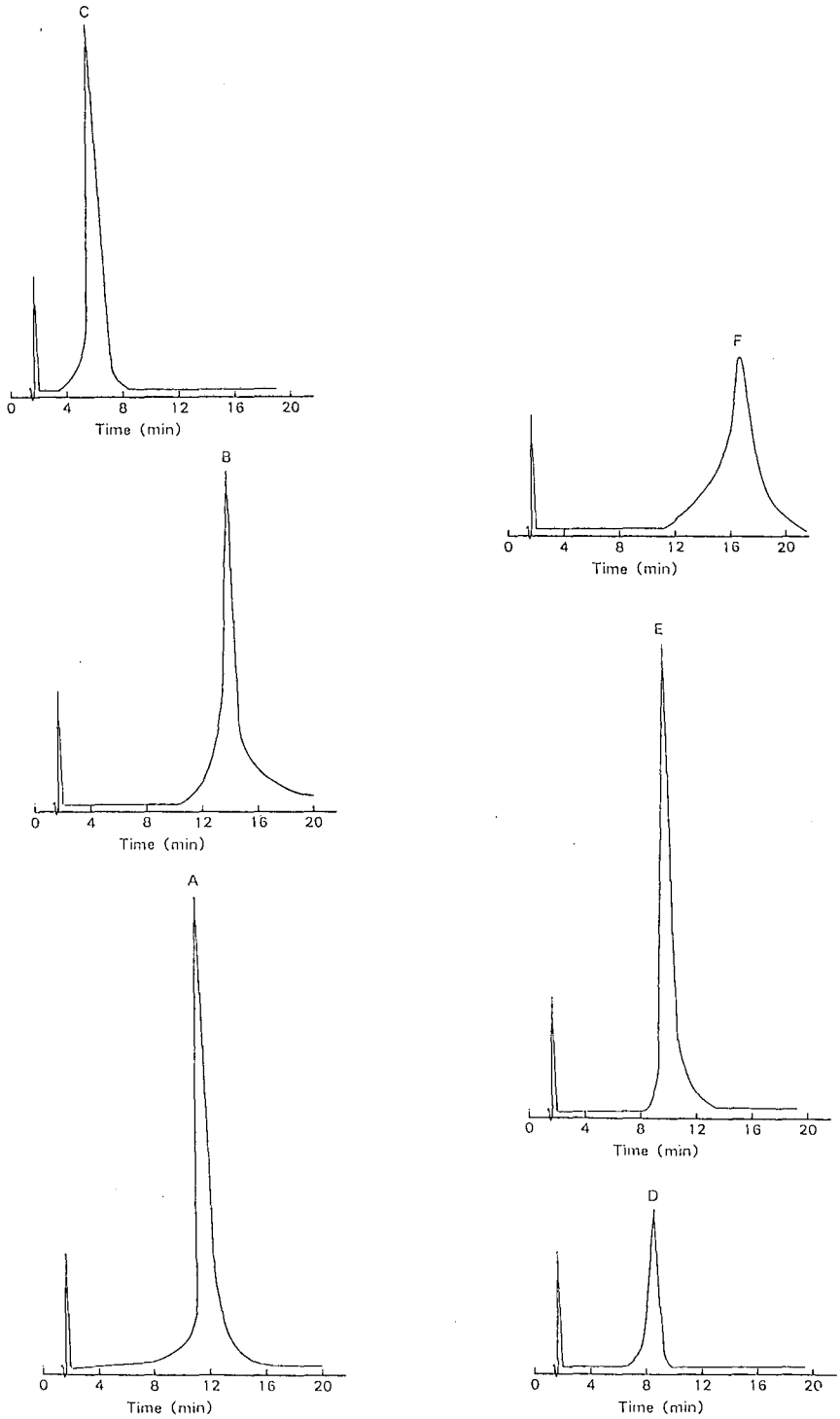

Fig. 4. Chromatogram of trichomycin A–F after isolation by preparative HPLC. Chromatographic conditions as in Fig. 2.

contained trichomycin B and F, and the other trichomycin A, C, D and E. Each fraction was submitted to preparative HPLC on μBondasphere C_{18} with acetonitrile–(phosphate–citrate buffer) (34.5:65.5, pH 4.75).

In conclusion, six main components of trichomycin, shown by arrows in Fig. 2, were isolated simultaneously by preparative HPLC. Although trichomycin A–F were effectively separated by only one procedure, a more satisfactory result was obtained by rechromatography under the same conditions. A chromatogram of trichomycin A–F after preparative HPLC is shown in Fig. 4.

A major advantage of this system is therefore that it has made it possible to clarify the structures and characterization of trichomycin A–F and other closely related compounds. The HPLC method reported here is also very suitable for the analysis and preparation of polyene macrolides.

The structure determination of trichomycin A[7] and B[9] and the properties of trichomycin A–F will be described elsewhere[9].

Trichomycin A, the major component, possesses the greatest potency against diverse fungi and yeasts, and exhibits a lower minimum inhibitory concentration against many kinds of candidas and trichomonas than amphotericin B and ketoconazole, a well known antifungal drug.

ACKNOWLEDGEMENT

The authors thank members of the Analytical Research Laboratories for bioassay measurements.

REFERENCES

1 S. Hosoya, N. Komatsu, M. Soeda, T. Yamaguchi and Y. Sonoda, *J. Antibiot. Ser. B*, 5 (1952) 564.
2 S. Hosoya, S. Ogata, N. Hamamura, M. Soeda, S. Nakazawa and N. Komatsu, *J. Antibiot. Ser. B*, 9 (1956) 172.
3 H. Nakano, *J. Antibiot., Ser. A*, 14 (1961) 71.
4 K. Hattori, *J. Antibiot., Ser. B*, 15 (1962) 39.
5 P. Helboe, M. Thomsen and S. H. Hansen, *J. Chromatogr.*, 189 (1980) 249.
6 A. D. Thomas and P. Newland, *J. Chromatogr.*, 354 (1986) 317.
7 T. Komori, Y. Morimoto, M. Niwa and Y. Hirata, *Tetrahedron Lett.*, 30 (1989) 3813.
8 H. Umezawa (Chairman), *Minimum Requirements for Antibiotic Products of Japan (English Version)*, Yakugyo Jiho, Tokyo, 1986, pp. 891-895.
9 T. Komori and Y. Morimoto, *J. Antibiot.*, in press.

Journal of Chromatography, 481 (1989) 421–427
Elsevier Science Publishers B.V., Amsterdam — Printed in The Netherlands

CHROM. 21 851

Note

Reversed-phase high-performance liquid chromatographic assay for camptothecin and related alkaloids

B. L. POEHLAND*, N. TROUPE, B. K. CARTÉ and J. W. WESTLEY
Research and Development Division, Department of Biomolecular Discovery, Smith Kline and French Laboratories, P.O. Box 1539, King of Prussia, PA 19406-0939 (U.S.A.)
(First received March 6th, 1989; revised manuscript received July 20th, 1989)

The potent antitumor alkaloid camptothecin **1** (Fig. 1), a component of *Camptotheca acuminata* (family Nyssaceae), a tree indigenous to China, was first described over twenty years ago[1]. Since then a number of hydroxyl and methoxyl derivatives have been reported, which exhibit similar levels of activity[2,3], and in addition a number of structurally related compounds have been isolated[4]. Despite problems of insolubility and toxicity there persists a significant level of interest in the mechanism of action of camptothecin[5].

In conjunction with our interest in water-soluble derivatives of camptothecin antineoplastics[6] approximately 2 l of alkaloid-enriched extract of *C. acuminata* were obtained for the purpose of investigating the possible presence of naturally occurring polar camptothecins which might exhibit appreciable aqueous solubility. We were also interested in the identification and isolation of any known campthotecin analogues which would be useful as bioassay standards or starting material for synthetic transformations. A suitable high-performance liquid chromatographic (HPLC) assay was essential for achieving these objectives.

Due to anticipated requirements for high sensitivity and solvent programming, a reversed-phase assay employing acetonitrile–water was selected because of its reduced baseline displacement of the gradient profile compared to methanol–water

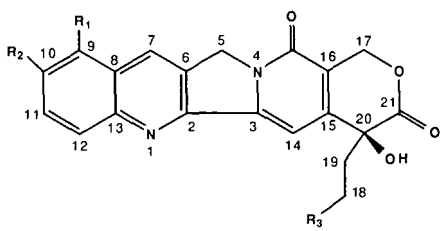

1. $R_1 = R_2 = R_3 = H$
2. $R_1 = R_3 = H$, $R_2 = OH$
3. $R_1 = OCH_3$, $R_2 = R_3 = H$
4. $R_1 = R_3 = H$, $R_2 = OCH_3$
8. $R_1 = R_2 = H$, $R_3 = OH$

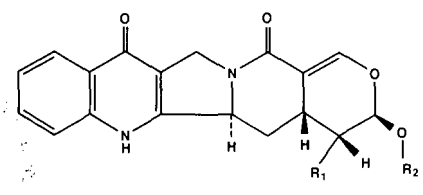

5. $R_1 = CH{=}CH_2$, R_2 = ß-D-(+)glucose
6. $R_1 = CH_2CH_3$, R_2 = ß-D-(+)glucose
7. $R_1 = CH{=}CH_2$, $R_2 = CH_3$

Fig. 1. Structures discussed in the text.

0021-9673/89/$03.50

systems. We wish to report the chromatographic analysis of the compounds we encountered in our work, including a novel analogue whose structure elucidation is reported elsewhere[7].

EXPERIMENTAL

Apparatus

Liquid chromatography was carried out on a Beckman/Altex instrument (San Ramon, CA, U.S.A.) equipped with two 110A solvent metering pumps, a 420/421 gradient programmer, a Hewlett-Packard (Palo Alto, CA, U.S.A.) 3390A integrator, a Perkin-Elmer (Norwalk, CT, U.S.A.) ISS-100 autosampler with a 50-μl sample loop and custom timing interface[9], and a Schoeffel/Applied Biosystems (Westwood, NJ, U.S.A.) SF770 Spectroflow monitor set at 270 nm (0.04 u.a.f.s.). A Whatman (Hillsboro, OR, U.S.A.) Partisil-10 ODS-3 C_{18} reversed-phase column (25 cm × 4.6 mm I.D.) was used at ambient temperature with a flow-rate of 2.0 ml/min and nominal pressure drop of 2000 p.s.i.g. (13.8 MPa). Standard materials were weighed on a Cahn (Cerritos, CA, U.S.A.) Model 29 electrobalance.

Starting material

Sample FB-12100B (1900 g) was received from Polysciences (Warrington, PA, U.S.A.) as an opaque viscous liquid containing suspended solids. This was the concentrate from the final one-third of the eluate from a large scale Amberlyst 15 column using 0.25% ammonia in isopropanol as the eluent. The starting material for this column (365 cm × 30 cm) was an isopropanol extract of sawdust from 24 000 pounds ($10.9 \cdot 10^3$ kg) of *C. acuminata* logs. The isopropanol extractions were performed by Madis Labs. (Hackensack, NJ, U.S.A.) using trees obtained from the USDA Plant Introduction Center (Chico, CA, U.S.A.).

Reagents and standards

Unless otherwise indicated, all chemicals used were ACS reagent grade. Water used in preparing the HPLC solvent system was obtained from an in-house Milli-Q water purification system (Millipore, Bedford, MA, U.S.A.). Acetonitrile for the HPLC system was Baker HPLC grade used directly without filtration. Silica used for column chromatography was from Merck (Darmstadt, F.R.G.) silica gel 60 70–230 mesh, and Sephadex LH-20 chromatography gel was obtained from Pharmacia (Uppsala, Sweden). Authentic samples of camptothecin **1**, 10-hydroxycamptothecin **2**, 9-methoxycamptothecin **3**, and 10-methoxycamptothecin **4** were supplied by the National Cancer Institute. The 18-hydroxy analogue **8** was isolated and identified by comparison of its spectroscopic and physical properties with published data[8]. Glycoside **5** was isolated and structural assignment made by analysis of physical and spectroscopic data[7]. The hydrogenated derivative **6** and methoxy hydrolysate **7** were prepared synthetically from **5**.

HPLC of camptothecin standards

Camptothecin and its 10-hydroxy and 9- and 10-methoxy analogues were each dissolved in acetonitrile at a concentration of 100 μg/ml and filtered through a 0.45-μm filter before use. A 25-μl aliquot of each compound was injected in a variety

of HPLC systems employing various concentrations of acetonitrile–water and acetonitrile–water acidified with 0.1% trifluoracetic acid. The acidified solvent systems were quickly abandoned due to excessive retention.

Aqueous isocratic systems emplying more than about 40% acetonitrile caused the standards to elute close to the solvent front and failed to adequately resolve the individual components. Several linear gradient solvent programs were evaluated to increase retention and improve resolution, and the gradient program below was found optimal for best resolution within a reasonable analysis time: beginning time 0.0 min, 15% acetonitrile–water isocratic for 1.0 min; beginning time 1.0 min, 15% acetonitrile–water increasing linearly to 25% acetonitrile–water over 10 min; beginning time 11.0 min, 25% acetonitrile–water isocratic for 14 min; beginning time 25.0 min, 25% acetonitrile–water decreasing linearly to 15% acetonitrile–water over 1.0 min; at time 30.0 min, stop program (ready for next injection).

To establish a basis for quantitation the standard materials were dried under high vacuum for 48 h, and their purity assumed to be 100% since each standard gave only a single peak when individual injections were made under the HPLC conditions described above. A stock solution of the standards was prepared by weighing out 1.00 mg of each compound and dissolving in 10.0 ml acetonitrile to give a standard mixture with a concentration of 100 μg/ml of each component. This solution was filtered through a 0.45-μm filter and stored at 4°C. A suitable aliquot of the standard mix was placed in each of three autosampler vials which were sealed before injection.

The system was calibrated for single-point quantitation by analyzing the chromatograms produced by two injections from each vial using the HPLC conditions described above. Measured peak areas and retention times for each standard were averaged and divided by the concentration to generate a response factor whose inverse was programmed into the integrator as a multiplication factor. For subsequent injections the integrator quantitated the standards peaks and printed results directly in units of concentration (μg/ml). When the standards were injected following calibration, the reported concentrations were within 1% of the programmed values (external standard method). At the beginning and end of each day of routine assays, standard injections were made to monitor calibration accuracy. Calibration was observed to deteriorate gradually over a period of weeks; fresh standards were prepared and the system recalibrated when calibration error exceeded 10%.

HPLC assay of isolation fractions

The HPLC conditions established for the camptothecin standards were used to evaluate fractions generated by the isolation scheme summarized in Fig. 2. Sample solutions were filtered through a 0.45-μm filter before injection, and quantitative results were reported as the average of two injections per sample.

Unknown peaks appearing in the HPLC standard profile were roughly quantitated by comparing their peak areas to that of the closest standard. Concentrations of camptothecin **1** and the 10-hydroxy analogue **2** in isolation fractions were determined by direct readout of sample concentration. Sample solutions were diluted as necessary to bring peak response on scale. No peaks corresponding to the methoxy derivatives **3** and **4** were observed in any of our extracts, and all of the isolated compounds were obtained with estimated purity better than 98% (single peak using the standard HPLC conditions).

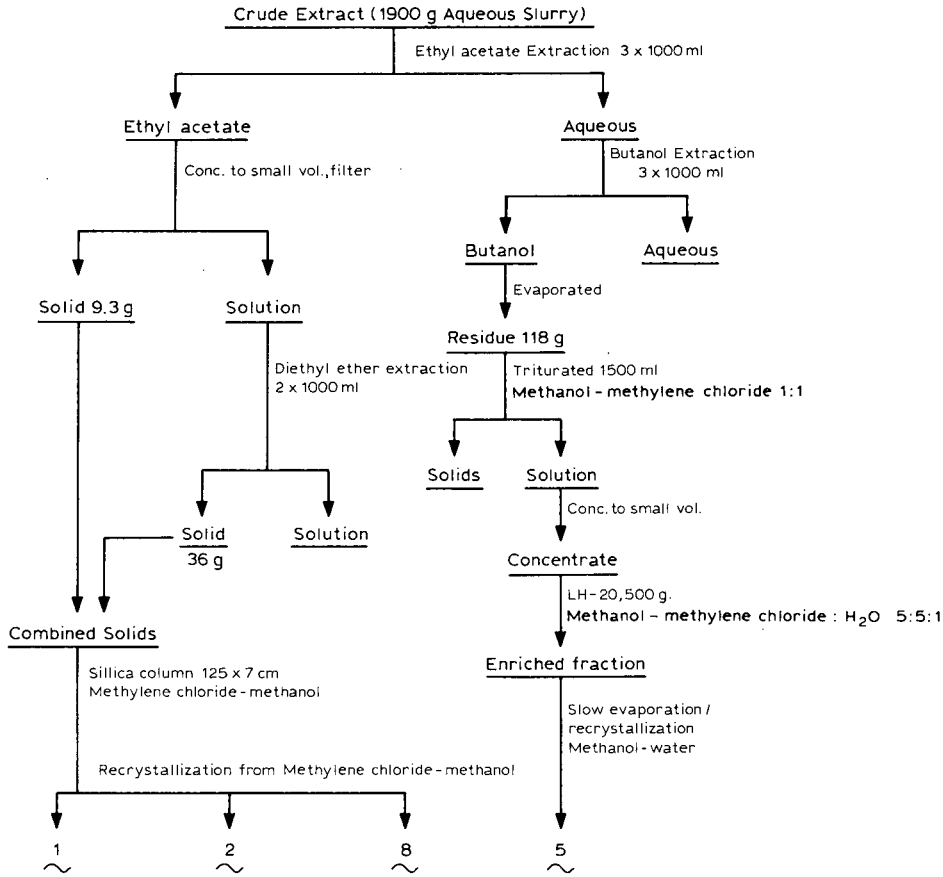

Fig. 2. Simplified purification scheme for camptothecin alkaloids. Numerals refer to structures in Fig. 1.

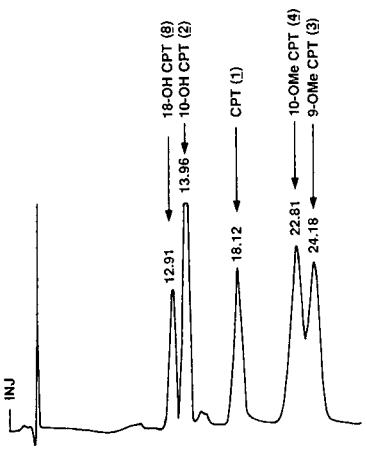

Fig. 3. Reversed-phase chromatographic profile of standard camptothecins.

The first unknown peak to appear in the reversed-phase HPLC profile of the standard camptothecins was the 18-hydroxy analogue **8**, obtained from a silica column fraction of the ethyl acetate soluble portion of the crude extract. This peak was monitored in the purification scheme until its isolation as a single component. The pure material had the same retention time as the peak isolated from partially purified fractions, and comparison of its UV, IR, NMR and mass spectra with published data[8] confirmed its identity. In later assays this compound was incorporated as a standard, as seen in the standard HPLC profile of Fig. 3.

Peaks with retention times corresponding to those of camptothecin **1** and 10-hydroxycamptothecin **2** were similarly monitored until their isolation as single components, and the isolated materials coeluted upon coinjection with the respective standard materials. Their identities were also confirmed spectroscopically.

Purification of the novel glucoside **5** {[3*S*-(3α,4β,4α,5a*β*)]-4-ethenyl-3-(β-D-glucopyranosyloxy)-4,4*a*,5,5*a*,6,12-hexahydro-3H-pyrano-[3′,4′:6,7]indolizino[1,2–6]-quinoline-11,14-dione} from the aqueous portion of the crude extract was easily followed using the standard HPLC conditions because it eluted well ahead of all other components subjected to the assay. However, upon injection of the purified material the HPLC profile exhibited two peaks (Fig. 4A) whose profile remained essentially unchanged despite additional recrystallization. Subsequently it was observed that when the sample was prepared in water or methanol (instead of acetonitrile) the profile collapsed into a single peak whose retention time coincided with that of the later-eluting material (Fig. 4B).

Chemical transformation and HPLC assay of glycoside derivatives

Hydrogenation. The glycoside **5** (100 mg, 20 mmol) was added to 10 ml methanol containing 10 mg of catalyst (10% palladium on activated carbon) and stirred at room temperature under hydrogen atmosphere for 20 h. Filtration of the solution

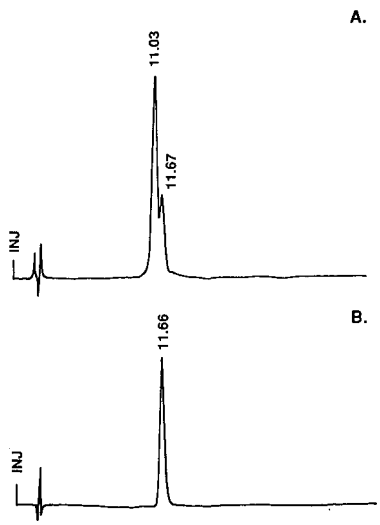

Fig. 4. Reversed-phase HPLC profiles of glycoside **5**. (A) Sample prepared in acetonitrile; (B) sample prepared in water.

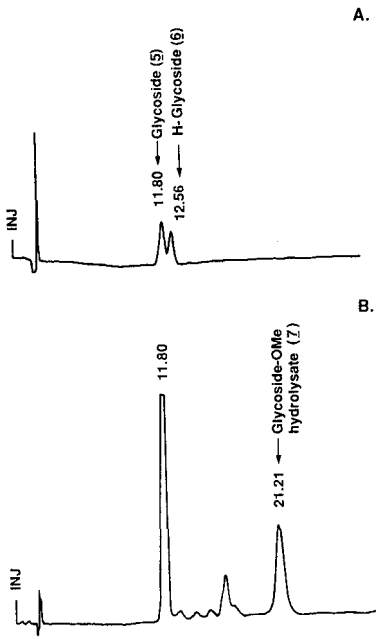

Fig. 5. Reversed-phase HPLC profiles of glycoside **5** reaction mixtures showing (A) the hydrogenated derivative **6** and (B) the O-methyl hydrolysate **7**.

yielded 30 mg of hydrogenated glycoside **6** whose structure was confirmed by NMR spectroscopy. Progress of this reaction was monitored using the standard HPLC conditions. Although chromatographic resolution was not as good as for the following methanolysis reaction, it was still sufficient to distinguish product from reactant (Fig. 5A) without modification of the assay.

Methanolysis. The glycoside **5** (50 mg, 10 mmol) was added to 10 ml methanolic 2 *M* HCl and stirred for 80 h at 70°C. Following evaporation of reaction solvent under nitrogen, the residue was taken up in 20% isopropanol–methylene chloride and filtered through silica gel to give a crude product. Final purification via semi-preparative HPLC (Dynamax C_{18}, 23% acetonitrile–water, 2.0 ml/min) yielded 6 mg of the methoxy aglycone **7**, confirmed by NMR spectroscopy. Using the standard HPLC conditions the course of this reaction was easily followed due to the high degree of resolution between the starting material **5** and the methanolysis product **7** (Fig. 5B).

RESULTS AND DISCUSSION

Retention times of all the camptothecins and related alkaloids subjected to the described HPLC assay are summarized in Table I. The ability of the assay to resolve these compounds was of immeasurable value to the success of our laboratory in isolating both known and novel camptothecins.

Solubility of camptothecins in acetonitrile was generally poor. The relatively dilute sample concentrations required by the assay are close to the upper limit of sample solubility required for reasonably reproducible quantitation. Due to the vola-

TABLE I

RETENTION TIMES OF CAMPTOTHECIN ALKALOIDS IN THE REVERSED-PHASE HPLC ASSAY

Compound	*No.*	$t_R(min)$
Glycoside	**5**	11.7
Hydrogenated glycoside	**6**	12.5
18-Hydroxycamptothecin	**8**	12.9
10-Hydroxycamptothecin	**2**	13.9
Camptothecin	**1**	18.1
Glycoside methoxy hydrolysate	**7**	21.2
10-Methoxycamptothecin	**4**	22.8
9-Methoxycamptothecin	**3**	24.1

tility of acetonitrile it was difficult to maintain accurate sample volumes, and on a daily basis a 10% variation in quantitation was tolerated. Small amounts of water or dichloromethane as required were added to samples to improve solubility. As long as the amount was low (< 10% of sample volume), no chromatographic problems were observed. Although methanol is a better solvent for the camptothecins, its use for sample preparation had to be judiciously applied as methanol tended to disrupt the chromatographic profile.

Although some additional investigation was undertaken to examine more closely the anomalous chromatographic behavior of the glycoside **5**, attempts to isolate and identify the two peaks were frustrated by their apparent interconversion according to the type of solvent to which the samples were exposed. However, these observations did not interfere with the ability of the assay to distinguish between the various camptothecins we sought to purify.

In summary, the HPLC assay reported here is a fast, convenient, and quantitative method for microscale analysis of camptothecins. The procedure resolves nine camptothecins including several novel structures and has proven useful for monitoring both natural product isolation and preparation of synthetic derivatives.

REFERENCES

1 M. E. Wall, M. C. Wani, C. E. Cook and K. H. Palmer, *J. Org. Chem.*, 88 (1966) 3888.
2 M. C. Wani and M. E. Wall, *J. Org. Chem.*, 34 (1969) 1364.
3 L. Long-ze, S. Chun-qing and X. Ren-sheng, *Act. Chim. Sin.*, 40 (1982) 86.
4 H. Xian-guo, J. Fu-xiang and Z. Qian-ru, *Act. Bot. Sin.*, 20 (1978) 76.
5 Y. H. Hsiang, R. Hertzberg, S. Hecht and L. F. Liu, *J. Biol. Chem.*, 260 (1985) 14873.
6 W. D. Kingsbury, R. P. Hertzberg, J. C. Boehm, K. G. Holden, D. R. Jakas, M. J. Caranfa, F. L. McCabe, L. F. Faucette, R. K. Johnson, R. W. Busby and S. M. Hecht, *Proc. Am. Assoc. Cancer Res.*, 30 (1989) 622–624.
7 B. K. Carté, C. DeBrosse, D. Eggleston, M. Hemling, B. L. Poehland, N. Troupe, J. W. Westley and S. M. Hecht, in preparation.
8 L. Z. Lin, J. S. Zhang, J. H. Shen, T. Zhou and W. Y. Zhang, *Act. Pharm. Sin.*, 23 (1988) 186.
9 B. L. Poehland, *Am. Lab. (Fairfield, Conn.)*, 16 (1984) 108.

Journal of Chromatography, 481 (1989) 428–433
Elsevier Science Publishers B.V., Amsterdam — Printed in The Netherlands

CHROM. 21 808

Note

Reversed-phase ion-pair high-performance liquid chromatographic separation and determination of tropane alkaloids in Chinese solanaceous plants

HE LI-YI, ZHANG GUAN-DE and TONG YU-YI
Institute of Materia Medica, Chinese Academy of Medical Sciences, 1 Xing Nong Tan Street, Beijing (China)
and
KAZUHIKO SAGARA, TOSHIYUKI OSHIMA* and TSUGUCHIKA YOSHIDA
Research Centre, Taisho Pharmaceutical Co., Ltd., 1-403, Yoshino-cho, Ohmiya-shi, Saitama 330 (Japan)
(First received March 28th, 1989; revised manuscript received July 10th, 1989)

Tropane alkaloids seem to be restricted to solanaceous plants. Hyoscyamine (I) and scopolamine (II) (Fig. 1) are tropane alkaloids and both have been used in clinical applications for a long time. Recently, two new tropane alkaloids, anisodamine [(−)-6-β-hydroxyhyoscyamine] (III) and anisodine (daturamine) (IV), were isolated in our institute from *Scopolia tangutica*. Both have distinct anticholinergic effects and can be used to cure various diseases[1–3].

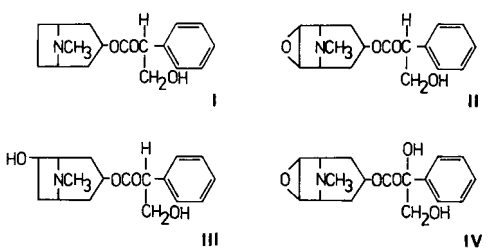

Fig. 1. Structures of the four tropane alkaloids. I = hyoscamine; II = scopolamine; III = anisodamine; IV = anisodine.

Scopolamine and hyoscyamine in crude drugs have been separated and determined by chromatographic techniques such as paper chromatography[4], thin-layer chromatography[5–7], gas chromatography[8,9] and high-performance liquid chromatography (HPLC)[10–13], but anisodine and anisodamine have been separated only by thin-layer chromatography and determined by spectrophotometry[5] or densitometry[6].

Recently, ion-pair HPLC has been applied to the determination of some natural compounds in plants[14–20]. We report here the application of reversed-phase ion-pair HPLC to the separation and determination of the above four tropane alkaloids in Chinese solanaceous plants.

0021-9673/89/$03.50

EXPERIMENTAL

Plant materials

Datura metel was collected in Shandong, Hunan and Guangdong, *Scopolia acutanglus* in Yunnan and *Scopolia lurida* and *Scopolia tangutica* in Qinghai and Tibet. These solanaceous plant samples were identified at the Institute of Materia Medica, Chinese Academy of Medical Sciences, Beijing, China.

Apparatus

The method was developed using a Shimadzu LC-6A liquid chromatograph, equipped with a Shimadzu UV spectrophotometric detector, a stainless-steel column (150 × 4 mm I.D.) packed with chemically bonded ODS silica gel (TSK gel 120 A, 5 μm; Toyo Soda, Tokyo, Japan), a Shimadzu CTO-6A column oven and a Sic Chromatocorder 11.

Reagents

Anisodine hydrobromide, anisoamine hydrobromide and scopolamie hydrobromide were isolated from *Scopolia tangutica* and identified by means of IR, NMR and mass spectrometers at the Institute of Materia Medica. Atropine as a standard for hyoscyamine was purchased from BDH (Poole, U.K.). Sodium dodecyl sulphate and sodium phosphate (monobasic) were purchased from Wako (Osaka, Japan), sodium decyl sulphate and sodium octyl sulphate from Kanto (Tokyo, Japan), and benzylamine hydrochloride from Tokyo Kasei (Tokyo, Japan). Methanol of chromatographic grade was used. All other reagents were of analytical-reagent grade.

Internal standard solution. A 0.2 mg/ml solution of benzylamine hydrochloride in methanol was prepared.

Standard solutions. Stock standard solutions of anisodine, anisodamine, scopolamine and atropine were prepared in separate flasks by dissolution in methanol to a final concentration of 1 mg/ml as the free base. A 0.2-ml volume of each stock solution was transferred into a 10-ml volumetric flask, 2 ml of the internal standard solution were added and the mixture was diluted to 10 ml with the mobile phase to give a working standard solution, containing 20 μg/ml of the alkaloid. Working standard solutions of 40, 60, 80 and 100 μg/ml were prepared in the same manner.

HPLC conditions

The mobile phase was 1/15 *M* sodium phosphate solution (adjusted to pH 3.5 with phosphoric acid)–methanol (48:52) containing 17.5 m*M* sodium dodecyl sulphate. The column temperature was maitained at 35°C and the flow-rate was 1.0 ml/min. The eluted substances were detected by a UV detector at 210 nm.

Assay procedure

A powered plank sample (0.5 g) was macerated with 10.0 ml of chloroform and 0.15 ml of 25% ammonia solution in a 50-ml glass-stoppered flask and left to stand overnight. A 2-ml volume of the chloroform layer were transferred into a 5-ml volumetric flask and evaporated to dryness on a boiling water-bath. A 1-ml volume of internal standard solution was added to the residual substance and the mixture was diluted to 5 ml with the mobile phase. A 10-μl volume of this solution was injected into

the HPLC system. The concentrations of anisodine, anisodamine, scopolamine and hyoscyamine in solanaceous plants were calculated from the peak-area ratios with respect to the internal standard.

Calibration graphs and detection limits

All calibration graphs for anisodine, anisodamine, scopolamine and atropine were obtained over the concentration range 20–100 μg/ml. The corresponding

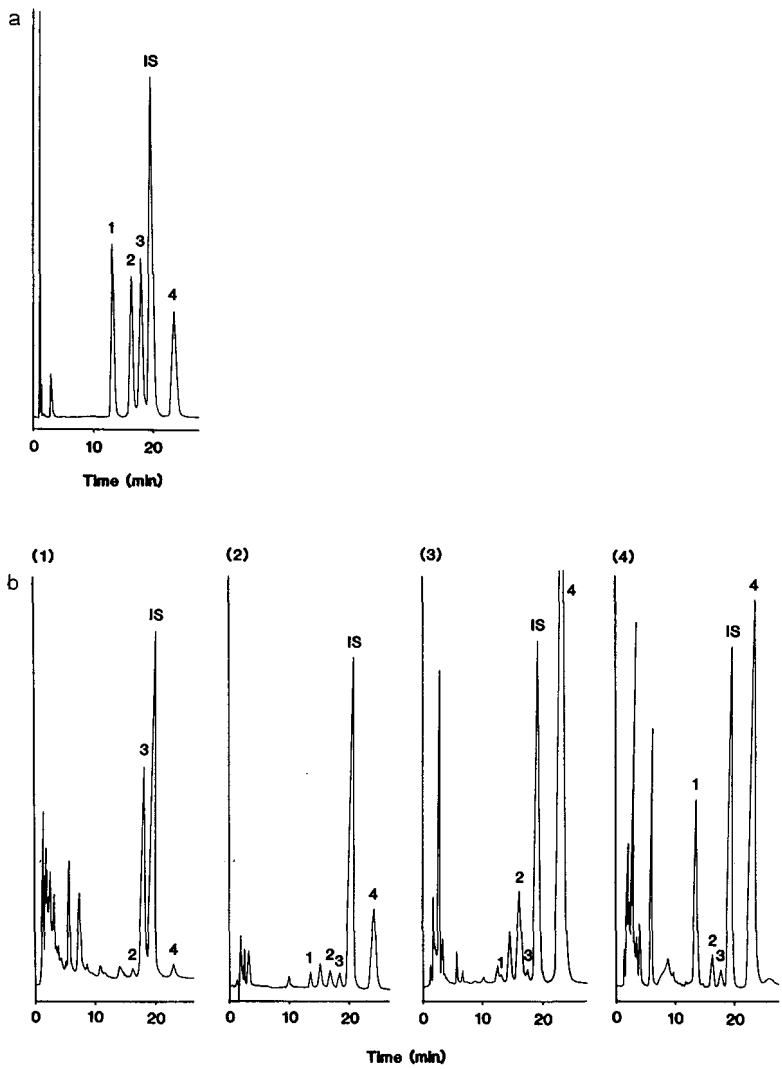

Fig. 2. Chromatograms of (a) standards and (b) plant samples. Plant samples: (1) *Datura metel* (Shandong); (2) *Scopolia acutangulus* (Yunnan:Zhongdian); (3) *S. lurida* (Qinghai:Haibei); (4) *S. tangutica* (Tibet:Ningjing). Peaks: 1 = anisodine; 2 = anisodamine; 3 = scopolamine; IS = internal standard (benzylamine hydrochloride); 4 = atropine. Mobile phase, 1/15 *M* sodium phosphate (pH 3.5)–methanol (48:52) containing 17.5 m*M* SDS; flow-rate, 1 ml/min; temperature, 35°C.

regression equations were $y = 0.95088x - 0.003335$ ($r = 0.999$), $y = 0.85741x - 0.004591$ ($r = 0.999$), $y = 0.90446x - 0.00335$ ($r = 0.999$), and $y = 0.80049x - 0.002557$ ($r = 0.999$) and the detection limits were 9.0, 7.5, 10.0 and 8.0 ng, respectively, at a signal-to-noise ratio of 3:1 for the peak heights.

RESULTS AND DISCUSSION

HPLC conditions

Various parameters such as counter ion, pH, concentration of organic modifier and ionic strength of the buffer on the ion-pair HPLC mobile phase were examined.

Sodium octyl sulphate (C_8), sodium decyl sulphate (C_{10}) and sodium dodecyl sulphate (C_{12}; SDS) were selected as counter ions. The pH of the mobile phase was examined over the range 2.0–6.0. The four tropane alkaloids were separated completely when SDS was used at a final concentration of 17.5 m*M* at pH 3.5. The methanol concentration in the mobile phase and that of sodium phosphate in the buffer were fixed at 52% and at 1/15 *M*, respectively. The column temperature was kept at 35°C to maintain constant retention times.

To enhance the reproducibility of the analytical results, about 30 compounds were tested for their suitability as internal standards under the above conditions. Benzylamine hydrochloride gave the best results. Fig. 2a shows a chromatogram of the four tropane alkaloids and the internal standard, which were well separated from each other, with an elution time of less than 25 min.

TABLE I

RECOVERY DATA FOR THE FOUR TROPANE ALKALOIDS

Compound	*Added (μg)*	*Recovery*		*Mean recovery (%)*	*Standard deviation (%)*	*Coefficient of variation (%)*
		μg	*%*			
Anisodine	0.0775	0.0768, 0.0756	99.10, 97.57	98.07	2.81	2.70
	0.1550	0.1571, 0.1598	101.37, 103.11			
	0.1550	0.1486, 0.1482	95.98, 95.63			
	0.3100	0.3025, 0.2919	97.59, 94.17			
Anisodamine	0.0762	0.0805	105.64	102.46	2.99	2.92
	0.1524	0.1630, 0.1534	106.97, 100.69			
	0.1524	0.1529, 0.1584	100.32, 103.95			
	0.3048	0.3105, 0.2981	101.87, 97.79			
Scopolamine	0.0789	0.0810, 0.0829	102.66, 105.06	106.35	1.93	1.82
	0.1577	0.1656, 0.1692	104.99, 107.25			
	0.1577	0.1697, 0.1713	107.62, 108.62			
	0.3154	0.3425, 0.3344	108.60, 106.02			
Hyoscyamine	0.0837	0.0795, 0.0788	94.98, 94.18	99.08	4.28	4.32
	0.1676	0.1750, 0.1661	104.39, 99.09			
	0.3352	0.3244, 0.3521	96.79, 105.05			

TABLE II

RESULTS OF ANALYSIS OF PLANT SAMPLES

Sample	*Locality*	*Part*[a]	*Content (%)*			
			Anisodine	*Anisodamine*	*Scopolamine*	*Hyoscyamine*
Datura metel	Shandong	fl	–	0.005	0.290	0.052
	Hunan: Changde	fl	–	0.027	0.560	0.073
	Guangdong	fl	–	0.018	0.270	0.057
Scopolia acutangulus	Yunnan: Lijiang	rt	–	0.020	0.046	0.470
	Yunnan: Lijiang	rt	–	0.012	0.003	0.130
	Yunnan: Zhongdian	rt	0.034	0.035	0.036	0.270
S. lurida	Qinghai: Haibei	rt	0.070	0.145	0.021	1.20
	Tibet: Zhamu	l	–	0.008	0.034	0.80
	Tibet: Yandong	st	–	0.005	0.054	0.47
S. tangutica	Qinghai	rt	0.006	0.058	–	0.200
	Tibet	rt	–	0.088	0.016	1.300
	Tibet: Ningjing	rt	0.200	0.036	0.023	0.690

[a] fl = Flowers; rt = root; st = stem.

Extraction conditions

The methods using the mobile phase[13] and basic chloroform[6,7] as the extraction solvent for scopolamine and hyoscyamine in solanaceous plants were compared. The two methods gave the same extraction efficiency from the crude drugs, but fewer impurities were extracted by the latter and the baseline was better than with the former. Therefore, the basic chloroform extraction method was chosen.

Of the powedered sample, 0.5 g was weighed accurately and three different amounts of the standard solution of four tropane alkaloids were added. The mixture was extracted and assayed according to the above procedure. The percentages of standards recovered were calculated by the internal standard method. Table I summarizes the recovery results and the statistical evaluation for each alkaloid.

Analytical results

Fig. 2b shows the chromatogram obtained on applying ion-pair HPLC to four kinds of solaneous plants.

Table II gives the analytical results. The concentration of scopolamine in *Datura metel* was more than five times higher than that of hyoscamine. In this study, we found that *Datura metel* contains a small amount of anisodamine.

CONCLUSIONS

Reversed-phase ion-pair HPLC was applied to the simultaneous determination of anisodine, anisodamine, scopolamine and hyoscyamine in Chinese solanaceous plants. This method is simple, reproducible and sensitive, and involves an isocratic HPLC system. This is the first report of the separation of the four tropane alkaloids anisodine, anisodamine, scopolamine and hyoscamine by HPLC. This quantitative method can be used for quality control and systematic research on solanaceous plants.

REFERENCES

1 Department of Pharmacology, Institute of Materia Medica, Chinese Academy of Medical Sciences, *Chin. Med. J.*, No. 2 (1975) 133 and No. 11 (1975) 795.
2 Department of Pharmacology, Institute of Materia Medica, Chinese Academy of Medical Sciences, *Chin. Med. J.*, No. 53 (1973) 260.
3 Institute of Materia Medica, Chinese Academy of Medical Sciences, *Zhongcaoyao Tongxun*, 6 (1976) 10 and 7 (1976) 6.
4 A. Puech and J. L. Reffay, *Ann. Pharm. Fr.*, 27 (1969) 483.
5 B. L. Wu Chu, E. S. Kika, M. J. Soiomon and F. A. Crane, *J. Pharm. Sci.*, 58 (1969) 1073.
6 L. Y. He and Y. C. Chang, *Acta Pharm. Sin.*, 14 (1979) 421.
7 L. Y. He, *Zhongcaoyao*, 13 (1982) 13.
8 H. Mechler and H. W. Kohlenbach, *Planta Med.*, 33 (1978) 350.
9 M. Ylinder, T. Naaranlahti, S. Lapinjoki, A. Huhtikangas, M.-L. Salonen, L. K. Simola and M. Lounnasman, *Planta Med.*, (1986) 85.
10 S. Paphassarang and J. Raynand, *J. Chromatogr.*, 319 (1985) 412.
11 P. Duez, S. Chamart, M. Hanocq and L. Molle, *J. Chromatogr.*, 329 (1985) 415.
12 K.-H. Plank and K. G. Wagner, *Z. Naturforsch., Teil C*, 41 (1986) 391.
13 T. Oshima, K. Sagara, T. Yoshida, Y. Y. Tong, G. D. Zhang and Y. H. Chen, in preparation.
14 T. Misaki, K. Sagara, M. Ojima, S. Kakizawa, T. Oshima and H. Yoshizawa, *Chem. Pharm. Bull.*, 30 (1982) 354.
15 K. Sagara, T. Oshima and T. Misaki, *Chem. Pharm. Bull.*, 31 (1983) 2359.
16 K. Sagara, Y. Ito, T. Oshima, T. Misaki and H. Murayama, *J. Chromatogr.*, 328 (1985) 289.
17 K. Sagara, Y. Ito, M. Ojima, T. Oshima, K. Suto, T. Misaki and H. Itokawa, *Chem. Pharm. Bull.*, 33 (1985) 5369.
18 K. Sagara, T. Oshima and T. Yoshida, *J. Chromatogr.*, 403 (1987) 253.
19 K. Sagara, T. Oshima, S. Sakamoto and T. Yoshida, *J. Chromatogr.*, 388 (1987) 448.
20 K. Sagara, T. Oshima and T. Yoshida, *J. Chromatogr.*, 409 (1987) 365.

Journal of Chromatography, 481 (1989) 434–438
Elsevier Science Publishers B.V., Amsterdam — Printed in The Netherlands

CHROM. 21 755

Note

Rapid quantification of paraquat and diquat in serum and urine using high-performance liquid chromatography with automated sample pretreatment

ITSUHIRO NAKAGIRI*, KOUICHIRO SUZUKI, YUMIKO SHIAKU, YUMI KURODA, NOBUKATSU TAKASU and AKITSUGU KOHAMA

Department of Emergency and Critical Care Medicine, Kawasaki Medical School Hospital, 577 Matsushima, Kurashiki-shi, Okayama 701-01 (Japan)

(First received April 4th, 1989; revised manuscript received July 7th, 1989)

Many methods have been employed for the quantification of paraquat and diquat, bipyridylium herbicides, including colorimetry with an alkaline dithionite reaction[1,2], gas–liquid chromatography[3,4], thin-layer chromatography[5,6] and high-performance liquid chromatography (HPLC)[7–9]. Each of these methods, however, requires pretreatment to extract paraquat or diquat from a serum or urine sample before measuring it.

In the present study, we developed a new system in which an automated pretreatment apparatus is connected to ion-exchange HPLC. The automated pretreatment, using a column switching method, made measurement of paraquat and diquat with HPLC easier and faster. After injecting a microsample of serum or urine, pretreatment and measurement were carried out automatically.

METHODS

Standard reagents

Paraquat dichloride and diquat dibromide standards (Wako Junyaku, Japan) for the test of drug residuals were used. All other agents were of special reagent grade.

Apparatus

The following pieces of analytical apparatus were used: a pump (CCPM, Tosoh, Yamaguchi, Japan), an automatic pretreatment apparatus (PT-8000, Tosoh), an ultraviolet detector (UV-8000, Tosoh) and a data analyzer (Chromatocorder 12, Tosoh). Columns for gel filtration chromatography (TSK precolumn PW, 3.5 cm × 4.6 mm I.D., Tosoh) and for ion-exchange chromatography (TSK gel SP-2 SW, 25 cm × 4.6 mm I.D., Tosoh) were used as the preparation column and the analytical column, respectively. The chromatographic conditions were as follows: column temperature, room temperature; mobile phase for preparation, 0.1 *M* sodium perchlorate solution containing 5 m*M* sodium dihydrogenphospate adjusted to pH 3 with phosphoric acid; mobile phase for analysis, 0.2 *M* sodium dihydrogenphosphate solution adjusted to pH 3 with phosphoric acid, and acetonitrile–0.2 *M* sodium dihydrogen-

0021-9673/89/$03.50

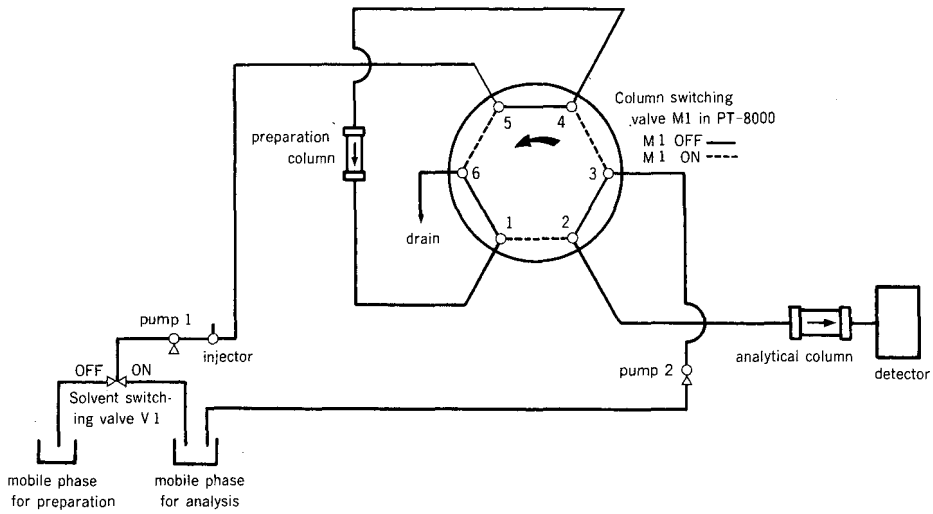

Fig. 1. Flow diagram of HPLC system with automatic sample preparation.

phosphate solution pH 3 (20:80, v/v); flow-rate, both 1.0 ml/min; detection wavelength, 290 nm.

Operation

A schematic drawing of the system detailing each component for analysis is shown in Fig. 1. A 50-μl sample was injected into the preparation column under a flow of the mobile phase for preparation (the solvent switching valve is off). Intensely hydrophilic components in the serum or urine are not retained in the preparation column, but are eluted and eliminated. Paraquat and diquat are retained in the column. The flow route was subsequently changed to that indicated by the dotted line by turning on the column switching valve in the automatic pretreatment apparatus as shown in Fig. 1. The mobile phase for analysis was directed to the analytical column by pump 2 and then redirected to the preparation column. Paraquat and diquat retained in the preparation column were extracted and transferred to the analytical column with the mobile phase for analysis. Then, with the solvent switching valve on

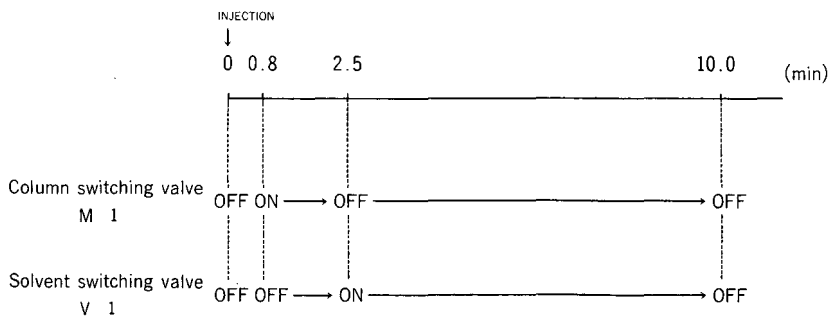

Fig. 2. Time program.

and the column switching valve turned back after 2.5 min of injection, the preparation column was washed with the mobile phase for analysis. When the solvent switching valve was again turned off after 10 min of injection, this column was recharged with the mobile phase for preparation.

In this manner, washing and recharging take place while the analysis is progressing. These procedures are performed by a program for turning the column switching valve and solvent switching valve in the automatic pretreatment apparatus off and on as shown in Fig. 2.

We examined the accuracy of this system for analyzing paraquat or diquat in serum or urine.

RESULTS AND DISCUSSION

Confirmation of deproteinization on the preparation column

Deproteinization on the preparation column was confirmed by using a serum sample containing 5 μg/ml each of paraquat and diquat (protein content 7.4 g/dl with albumin content 3.8 g/dl). Since highly hydrophilic protein is not retained in the

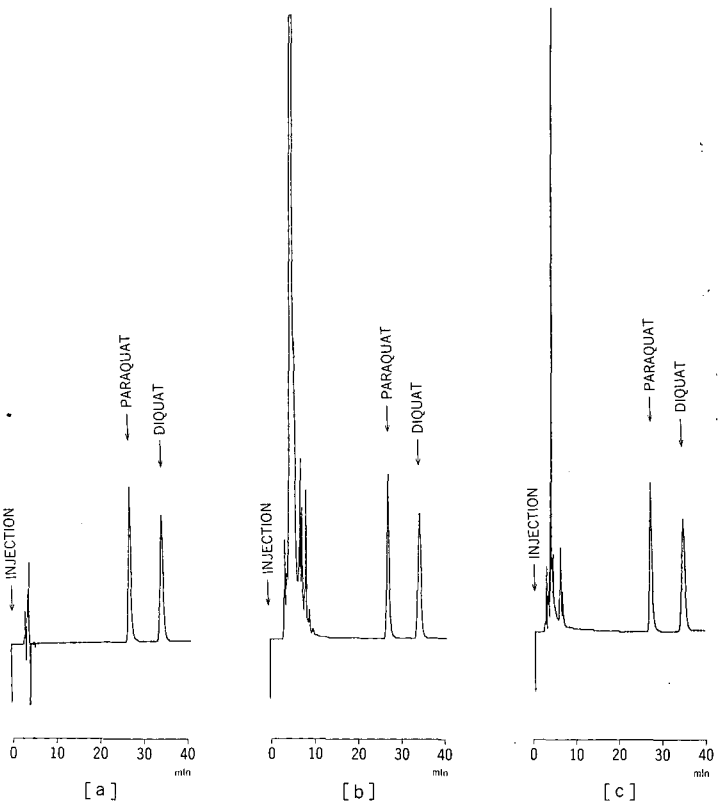

Fig. 3. Chromatograms of paraquat and diquat. (a) Standard paraquat (5 μg/ml) and diquat (5 μg/ml); (b) paraquat (5 μg/ml) and diquat (5 μg/ml) in serum; (c) paraquat (5 μg/ml) and diquat (5 μg/ml) in urine.

preparation column but is eluted and eliminated, we measured the amount of protein eluted using the method of Lowry *et al.*[10] with Folin-Ciocalteu reagent (Wako Junyaku). About 73% of the protein was detected in the waste fluid obtained after 10 min. The fractions containing paraquat and diquat, however, included no protein. These findings confirmed the satisfactory separation of paraquat and diquat from the protein of the serum sample.

Linearity of correlation between known and measured concentrations of paraquat or diquat

Paraquat dichloride and diquat dibromide were dissolved in 0.2 *M* NaH_2PO_4 in water to prepare 0.1–50 μg/ml standard solutions. Each calibration graph showed a good linear relationship between concentrations in standard solutions and those calculated from peak areas.

The relationships between the theoretical value, *i.e.* x (μg/ml), and the observed value, *i.e.* y (μg/ml), were: $y=0.983x + 0.011$, $r=0.999$ for paraquat; $y=0.938x + 0.009$, $r=0.999$ for diquat in the range of 0.1–1 μg/ml ($n=4$); $y=0.984x + 0.222$,

TABLE I

RECOVERY OF PARAQUAT AND DIQUAT BY THE AUTOMATIC SAMPLE PREPARATION METHOD

	Standard in water (μg/ml)	*Found (μg/ml)*	*n*	*C.V. (%)*	
Paraquat	20	19.65[a] ± 0.14	5	0.71	
	10	10.10[a] ± 0.10	5	0.99	
	1	0.93[a] ± 0.01	5	1.07	
Diquat	20	19.66[a] ± 0.13	5	0.66	
	10	10.28[a] ± 0.16	5	1.56	
	1	0.98[a] ± 0.02	5	2.04	
	Standard in serum (μg/ml)	*Found (μg/ml)*	*n*	*C.V. (%)*	*Recovery (b/a) · 100 (%)*
Paraquat	20	20.02[b] ± 0.13	5	0.64	101.9
	10	10.10[b] ± 0.24	5	2.38	100.0
	1	0.96[b] ± 0.03	5	3.13	103.2
Diquat	20	19.79[b] ± 0.15	5	0.76	100.7
	10	9.94[b] ± 0.18	5	1.81	96.7
	1	0.97[b] ± 0.03	5	3.09	99.0
	Standard in urine (μg/ml)	*Found (μg/ml)*	*n*	*C.V. (%)*	*Recovery (c/a) · 100 (%)*
Paraquat	20	19.59[c] ± 0.13	5	0.66	99.7
	10	10.09[c] ± 0.07	5	0.69	99.9
	1	0.99[c] ± 0.03	5	3.03	106.5
Diquat	20	19.71[c] ± 0.29	5	1.47	100.3
	10	10.02[c] ± 0.19	5	1.90	97.5
	1	0.95[c] ± 0.02	5	2.11	96.9

$r=0.999$ for paraquat, and $y=0.996x + 0.297$, $r=0.999$ for diquat in the range of 1–50 μg/ml ($n=6$).

Recovery rate and simultaneous reproducibility of this system

Fig. 3 shows chromatograms of paraquat (5 μg/ml) and diquat (5 μg/ml) in the standard solution, serum and urine.

The recovery rate and simultaneous reproducibility of our system are given in Table I. Recovery rates of paraquat and diquat in pooled human serum or urine were obtained by dividing values measured in the pooled samples by those in the authentic standards, multiplied by 100. The analytical recoveries and the coefficients of variation (C.V.s) for the three different concentrations (1, 10 and 20 μg/ml) ranged from 96.7 to 106.5% and from 0.64 to 3.13%, respectively.

The recovery rate and reproducibility were excellent.

CONCLUSIONS

Samples obtained from living organisms generally include a wide range of substances from higher, *e.g.*, proteins to lower molecular weight, *e.g.*, amino acids. Direct injection of a serum sample into an analytical column hence results in a clogging condensation on the column, leading to an increase in intracolumnar pressure, fluctuation of the chromatogram baseline and changes in the retention time and tailing of the peak. We must therefore pretreat a serum sample to measure paraquat and diquat. The pretreatment procedure requires time, and, in addition, has been an obstacle to measuring paraquat and diquat automatically with HPLC. Because our system includes a pretreatment apparatus, measurement of paraquat or diquat is automatically carried out after injecting a microsample of serum or urine into an injection port. This can provide quick and important information for the physician.

REFERENCES

1 J. Knepil, *Clin. Chim. Acta*, 79 (1977) 387.
2 A. F. Fell, D. R. Jarvie and M. J. Stewart, *Clin. Chem.*, 27 (1981) 286.
3 S. Ukai, H. Hirose and S. Kawase, *J. Hyg. Chem.*, 19 (1973) 281.
4 C. J. Soderquist and D. C. Crosby, *Bull. Environ. Contam. Toxicol.*, 8 (1972) 363.
5 G. S. Tadjer, *J. Forensic Sci. Soc.*, 12 (1967) 549.
6 C.W. Sharp and E. M. Lores, Jr., *J. Agric. Food Chem.*, 22 (1974) 458.
7 Y. Kawano, J. Audino and M. Edlund, *J. Chromatogr.*, 115 (1975) 289.
8 J. J. Miller, E. Standers and D. Webb, *J. Anal. Toxicol.*, 3 (1979) 1.
9 L. Needham, D. Paschal, Z. J. Rollen, J. A. Liddle and D. D. Bayse, *J. Chromatogr. Sci.*, 17 (1979) 87.
10 O. H. Lowry, N. J. Rosebrough, A. L. Farr and R. J. Randall, *J. Biol. Chem.*, 193 (1951) 265.

Journal of Chromatography, 481 (1989) 439–444
Elsevier Science Publishers B.V., Amsterdam — Printed in The Netherlands

CHROM. 21 793

Note

High-performance liquid chromatographic determination of phenoxyalkanoic acid herbicides using iron(II) 1,10-phenanthroline as a mobile phase additive

MANAR FAYYAD*, MOHMOUD ALAWI and TARAB EL-AHMAD
Chemistry Department, University of Jordan, Amman (Jordan)
(First received April 12th, 1989; revised manuscript received July 10th, 1989)

The increasing agricultural consumption of chlorinated phenoxy acid herbicides has led to greater possibilities of contamination of soil, water and food by their residues and their phenolic metabolites. This class of herbicides is considered to be moderately toxic, whereas their chlorinated phenolic metabolites are highly toxic to man and to aquatic organisms[1]. Therefore, the development of methods for the determination of this class of compounds is essential. Among other methods, chlorinated phenoxy acid herbicides can be determined spectrophotometrically[2–4], either directly or after derivatization of the phenols with 4-aminoantipyrine, which results in cleavage of the ether linkage. Differential pulse polarography has been used for the determination of phenoxy acids after nitration[5]. Chromatographic methods[6–8], including paper, thin-layer and gas–liquid modes, are also used for determination of this class of compounds. A great disadvantage of these methods is that derivatization is required before measurement. Liquid chromatography[9–15] using normal- and reversed-phase columns can also be used for the separation of phenoxy acids, with UV detection at 254 or 280 nm. At these wavelengths, however, many compounds may absorb, making detection non-selective.

In this work, the separation and selective detection of phenoxy acids was achieved by an indirect photometric high-performance liquid chromatographic (HPLC) method using $Fe(phen)_3^{2+}$ as a mobile phase additive. The ion-pairing reagent $Fe(phen)_3^{2+}$ has previously been used for the separation and indirect photometric detection of inorganic anions such as Cl^-, Br^- and I^-[16] and organic acid anions such as acetate, succinate and citrate[16]. In these studies, the stationary phase was modified by adding $Fe(phen)_3^{2+}$ to the mobile phase. As it is hydrophobic, $Fe(phen)_3^{2+}$ is adsorbed on the reversed stationary phase to form a double layer composed of $Fe(phen)_3^{2+}$ and its counter anion[17]. The type of analyte interaction mechanism was classified as an ion-interaction mechanism[18], where the analyte anion competes with the counter ion provided by the buffer or electrolyte anions. The separated analyte anions can be detected indirectly at the absorption maximum of $Fe(phen)_3^{2+}$ (510 nm), because absorbance within the analyte band differs from the background absorbance provided by the $Fe(phen)_3^{2+}$ salt-containing mobile phase.

Several factors cause the $Fe(phen)_3^{2+}$ concentration and thus absorbance to

0021-9673/89/$03.50

change within the analyte band: (1) the type of stationary phase, which affects the amount of $Fe(phen)_3^{2+}$ retained; (2) the concentration of $Fe(phen)_3^{2+}$; (3) the percentage of organic solvent in the mobile phase, which affects the separation; (4) the pH of the mobile phase, especially when the analyte anions are derived from weak acids; and (5) the concentration of salts and the ionic strength of the mobile phase, which affect both the amount of $Fe(phen)_3^{2+}$ retained and the direction of the peaks.

In this work, these parameters were optimized for the separation and indirect detection of 2,4-dichlorophenoxyacetic acid (2,4-D), 2,4-dichlorophenoxybutytric acid (2,4-DB) and 2,4,5-trichlorophenoxyacetic acid (2,4,5-T).

EXPERIMENTAL

Reagents

$Fe(phen)_3SO_4$ solution (ferroin) was obtained from Fluka. The inorganic salts used were of analytical grade. 2,4-D, 2,4-DB and 2,4,5-T were analytical standards obtained from Supelco. Organic solvents were of LC quality. LC-quality water was obtained by passing doubly distilled water through a LiChroprep RP-C_8 (40–63 μm) column (Merck). LiChrosorb RP-C_{18} and RP-C_2 (7 μm) prepacked columns (250 × 4.6 mm I.D. were obtained from Knauer.

Instrumentation

The HPLC instrumentation was obtained from Beckman and consisted of a Model 114M solvent-delivery system, Model 340 injection organizer with 20-μl sample loop, Model 165 multiscanning UV–VIS detector, Model 420A controller and an SP 4270 integrator (Spectra-Physics).

Procedure

Stock solutions (1000 ppm) of 2,4-D, 2,4-DB and 2,4,5-T were prepared by dissolving weighed amounts of the acids in acetonitrile. Solutions containing 800, 600, 400, 200, 100, 50, 10, 5 and 2.5 ppm of the acids were prepared by appropriate dilution of aliquots of the stock solutions with acetonitrile. Sample aliquots of 20 μl were introduced by syringe. Mixed mobile phase solvents are expressed as percent by volume. Mobile phases containing 68.0, 34.0, 25.5, 17.0 and 8.5 μM $Fe(phen)_3^{2+}$ were prepared by adding 1.36, 0.68, 0.51, 0.34 and 0.17 ml of a 0.025 M solution of $Fe(phen)_3SO_4$ to 500 ml of methanol–water (40:60). Mobile phases containing salts were prepared by dissolving the appropriate amounts of sodium sulphate or sodium chloride in 500 ml of 40% (v/v) methanol–water mobile phase which was 34 μM in $Fe(phen)_3^{2+}$. The chromatographic runs were performed at two pH values: at pH 7, which was the pH obtained on mixing the mobile phase constituents, and at pH 3, which was obtained by dropwise addition of 0.1 M sulphuric acid to the mobile phase.

Column breakthrough volumes were determined by passing a $Fe(phen)_3^{2+}$-containing mobile phase of known concentration through the column at a constant flow-rate until the colour of $Fe(phen)_3^{2+}$ appeared in the effluent, as indicated by a sharp increase in the detector response, which was monitored at 510 nm where $Fe(phen)_3^{2+}$ has maximum absorbance. The amount of $Fe(phen)_3^{2+}$ retained was calculated from the breakthrough volume and the concentration of $Fe(phen)_3^{2+}$ in the mobile phase.

Columns were conditioned prior to use with the desired mobile phase by passing at least 150 ml (flow-rate 1 ml/min) of mobile phase more than the volume required to reach breakthrough. The flow-rate was 1 ml/min and the inlet pressure between 1000 and 1500 p.s.i., depending on the mobile phase. Detection was performed at 510 nm. Capacity factors (k') were calculated from $k' = t_R - t_R^0/t_R^0$, where t_R is the retention time of the analyte peak (min) and t_R^0 is the retention time of the solvent peak (min).

RESULTS AND DISCUSSION

The parameters that affect the separation and indirect detection of 2,4-D, 2,4-DB and 2,4,5-T using $Fe(phen)_3^{2+}$ as a mobile phase additive were optimized.

Stationary phase and column conditioning

Two types of reversed stationary phases were tried, RP-C_2 and RP-C_{18}. The amount of $Fe(phen)_3^{2+}$ retained on the stationary phase can be calculated from the volumes of $Fe(phen)_3^{2+}$ solution required to saturate the column. For this purpose, the $Fe(phen)_3^{2+}$ solution was pumped through the column until the column effluent showed the presence of $Fe(phen)_3^{2+}$, as noted by the appearance of an orange colour and an increase in the detector absorbance. A 7-μmol amount of $Fe(phen)_3^{2+}$ was needed to equilibrate the RP-C_{18} column, whereas 17 μmol were required with the RP-C_2 column.

Although RP-C_2 and RP-C_{18} are both of low polarity, RP-C_2 has the higher polarity owing to its shorter carbon chain. This difference in polarity might be responsible for differences in the retention of $Fe(phen)_3^{2+}$, which although hydrophobic, carries two positive charges, leading to greater interaction with the stationary phase of higher polarity. As $Fe(phen)_3^{2+}$ carries two positive charges, the number of

TABLE I

VARIATION OF PEAK AREAS WITH $Fe(phen)_3^{2+}$ CONCENTRATION IN THE MOBILE PHASE

Compound	*Concentration of $Fe(phen)_3^{2+}$ (μM)*	*Peak area (arbitrary units)*
2,4-D	8.5	2.00
	17.0	2.34
	26.0	2.52
	34.0	3.12
	68.0	3.10
2,4-DB	8.5	1.40
	17.0	1.50
	26.0	1.82
	34.0	2.30
	68.0	2.29
2,4,5-T	8.5	1.77
	17.0	1.81
	26.0	1.96
	34.0	2.44
	68.0	2.44

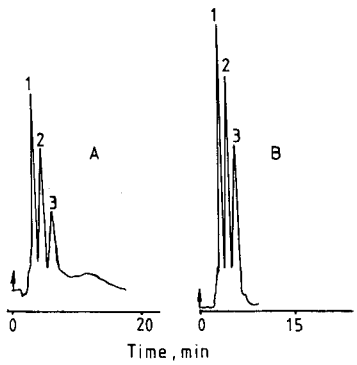

Fig. 1. Chromatograms of 10 μg each of (1) 2,4-D, (2) 2,4,5-T and (3) 2,4-DB. Column, RP-C_2; detection, 510 nm. Mobile phase: (A) 17 μM $Fe(phen)_3^{2+}$ and (B) 34 μM $Fe(phen)_3^{2+}$ in methanol–water (40:60, v/v).

available anion-exchange sites is $7 \times 2 = 14$ μequiv. with RP-C_{18} and $17 \times 2 = 34$ μequiv. with RP-C_2. Hence RP-C_2 has a greater capacity than RP-C_{18} to exchange analyte anions. Further, less solvent and a shorter time were required to clean the RP-C_2 column to remove retained $Fe(phen)_3^{2+}$. Also, under the above experimental conditions no analyte anion exchange could be detected when using the RP-C_{18} column. For these reasons, the RP-C_2 column was used in subsequent work.

Concentration of $Fe(phen)_3^{2+}$

Increasing the concentration of $Fe(phen)_3^{2+}$ in the mobile phase results in an increase in the peak areas of the three acids (Table I). Fig. 1 shows chromatograms of a mixture of the three acids in the presence of 17 and 34 μM of $Fe(phen)_3^{2+}$. The optimum $Fe(phen)_3^{2+}$ concentration when using methanol–water (40% v/v) as the mobile phase was found to be 34 μM. Lower concentrations resulted in a decrease in the peak areas of the three phenoxy acids. Although higher concentrations result in an increase in anion-exchange sites, eventually a level is reached where additional $Fe(phen)_3^{2+}$ will repel the retained $Fe(phen)_3^{2+}$. This occurs because $Fe(phen)_3^{2+}$ is a divalent cation and builds up surface charge. Also, if higher concentrations of $Fe(phen)_3^{2+}$ are used, it will become more difficult to offset the detector electronically.

Percentage of organic modifier in the mobile phase

Methanol and acetonitrile were used as organic modifiers. Increasing the percentage of methanol or acetonitrile in the aqueous mobile phase decreased the retention time of the phenoxy acids (Table II). The effect of adding an organic modifier to the mobile phase (water) is to decrease the polarity compared with pure water, which leads to a decrease in the retention time on a reversed-phase column. In this work, acetonitrile was used rather than methanol as the organic modifier because the retention times are shorter and lower pressures are obtained for acetonitrile at the same flow-rates.

pH of the mobile phase

Theoretically, a pH range of 2.0–9.0 over which $Fe(phen)_3^{2+}$ is stable could be

TABLE II

VARIATION OF CAPACITY FACTORS (k') USING METHANOL–WATER AND ACETONITRILE–WATER IN DIFFERENT PROPORTIONS ON THE RP-C_2 COLUMN

Compound	*Methanol (%, v/v)*				*Acetonitrile (%, v/v)*		
	25	*30*	*40*	*45*	*20*	*27*	*30*
2,4-D	11.89	5.38	3.49	2.69	3.91	2.03	1.53
2,4-DB	34.00	16.01	5.67	3.99	7.05	2.45	1.98
2,4,5-T	23.90	10.82	4.41	3.39	13.77	4.63	2.68

used[19]. However, at low pH (*ca.* 3) the analyte anions could not be detected as they are derived from weak acids, which are slightly dissociated at such pH values. On the other hand, pH values higher than 7.5 could not be applied as the RP-C_2 column is silica based and cannot tolerate pH values higher than 7.5, which cause hydrolysis of the chemically bonded groups[20]. The pH of the mobile phase was therefore adjusted to 7, at which the stationary phase and the $Fe(phen)_3^{2+}$ solution are stable and the analyte anions could be detected.

Effect of ionic strength and counter anion selectivity

If the ionic strength of the mobile phase is increased, the amount of $Fe(phen)_3^{2+}$ retained increases, as indicated by the disappearance of the colour of the column effluent[18]. This was observed when mobile phases containing 100 and 200 μM sodium sulphate or 300 μM sodium chloride were used. When a mobile phase containing 150 μM sodium chloride was used, negative peaks were observed for the three acids (Fig. 2) at longer retention times. On increasing the ionic strength of the mobile phase, the amount of $Fe(phen)_3^{2+}$ retained on the column and hence the number of anion-exchange sites increase, leading to longer retention times of the analyte anions.

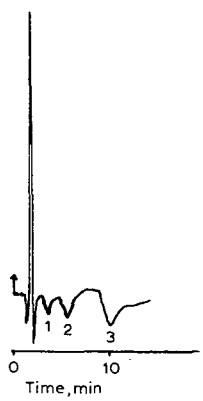

Fig. 2. Chromatogram of 100 μg each of (1) 2,4-D, (2) 2,4-DB and (3) 2,4,5-T. Column, RP-C_2; detection, 510 nm. Mobile phase: 34 μM $Fe(phen)_3^{2+}$ and 150 μM NaCl in methanol-water (40:60, v/v).

The negative peaks can be explained by assuming that chloride ions (counter anion) has a lower anion-exchange selectivity by mass action than the phenoxy acid anions, so the equilibrium amount of $Fe(phen)_3^{2+}$ retained increases and the $Fe(phen)_3^{2+}$ concentration decreases in the analyte band by an equivalent amount, leading to negative peaks when the analyte band passes through the detector[18].

Calibration and detection limits

For all three acids the linear working range was between 50 and 10 000 ng under the optimum chromatographic conditions, *i.e.*, RP-C_2 column and a mobile phase containing 34 μM $Fe(phen)_3^{2+}$ in 18:82, 20:80 and 28:72 (v/v) acetonitrile–water for 2,4-D, 2,4,5-T and 2,4-DB, respectively. The pH of the mobile phase is about 7 and no electrolytes are added to the mobile phase.

The detection limits were found to approach 50 ng for the three acids. The detection limit could be lowered by raising the pH of the mobile phase to increase the dissociation of the acids. This is possible only if another kind of column, such as poly(styrene–divinylbenzene), which can tolerate high pH values is used instead of the RP-C_2 column.

ACKNOWLEDGEMENT

We thank the office of the Dean of Scientific Research at the University of Jordan for financial support.

REFERENCES

1 R. W. Bovey and A. Young, *The Science of 2,4,5-T and Associated Phenoxy Herbicides*, Wiley, New York, 1980, pp. 301–345.
2 R. S. Banduski, *Bot. Gaz. (Chicago)*, 108 (1947) 446.
3 N. Gorden and M. Beroza, *Anal. Chem.*, 24 (1952) 1968.
4 S. Gottlieb and P. B. Marsh, *Ind. Eng. Chem.*, 18 (1946) 16.
5 A. Lechien, P. Valenta, H. W. Nürnberg and C. J. Patriarche, *Fresenius Z. Anal. Chem.*, 306 (1981) 156.
6 L. C. Mitchell, *J. Assoc. Off. Anal. Chem.*, 44 (1961) 720.
7 C. Feung, R. H. Hamilton and R. O. Mumma, *J. Agric. Food Chem.*, 21 (1973) 637.
8 J. F. Thompson, A. C. Walker and R. F. Moseman, *J. Assoc. Off. Anal. Chem.*, 52 (1969) 1623.
9 T. S. Stevens, N. E. Skelly and R. B. Ground, *J. Assoc. Off. Anal. Chem.*, 61 (1978) 1163.
10 J. F. Lawerence and D. Turton, *J. Chromatogr.*, 83 (1973) 439.
11 J. C. Van Darnme and M. Galoux, *J. Chromatogr.*, 190 (1980) 401.
12 A. D. Drinkwine, D. W. Bristol and J. R. Flecker, *J. Chromatogr.*, 174 (1979) 264.
13 N. E. Skelly, T. S. Stevens and D. A. Mapes, *J. Assoc. Off. Anal. Chem.*, 60 (1977) 868.
14 T. S. Stevens, *Adv. Chromatogr..*, 19 (1981) 91.
15 M. Armjad, R. H. Hamilton and R. O. Mumma, *J. Agric. Food Chem.*, 26 (1978) 971.
16 P. G. Rigas and D. J. Pietrzyk, *Anal. Chem.*, 59 (1987) 1388.
17 P. G. Rigas and D. J. Pietrzyk, *Anal. Chem.*, 58 (1986) 2226.
18 P. G. Rigas and D. J. Pietrzyk, *Anal. Chem.*, 60 (1988) 454.
19 A. A. Schilt, *Analytical Applications of 1,10-Phenanthroline and Related compounds*, Pergamon Press, Oxford, 1969, p. 103.
20 L. R. Snyder and J. J. Kirkland, *Introduction to Modern Liquid Chromatography*, Wiley, New York, 2nd ed., 1979.

Journal of Chromatography, 481 (1989) 445–451
Elsevier Science Publishers B.V., Amsterdam — Printed in The Netherlands

CHROM. 21 881

Note

Liquid chromatographic determination of N-methylcarbamate pesticides using a single-stage post-column derivatization reaction and fluorescence detection

B. D. McGARVEY
Agriculture Canada, Vineland Station, Ontario L0R 2E0 (Canada)
(Received June 13th, 1989)

The high-performance liquid chromatographic (HPLC) method for post-column derivatization and fluorescence detection of N-methylcarbamate pesticides introduced by Moye *et al.*[1] has been widely recognized for its sensitivity and selectivity for these compounds. Refined and collaboratively studied by Krause[2–6] and optimized by Engelhardt and Lillig[7], the method has achieved widespread acceptance and has been adopted by a number of laboratories for multiresidue analysis of N-methylcarbamate pesticides in foods. The number of N-methylcarbamates which may be analyzed by the method was expanded by De Kok *et al.*[8], who also introduced a simple cleanup method which can be applied to all types of crop samples.

The post-column derivatization technique consists of a two-stage reaction which converts the carbamate into a fluorescent derivative which is detected by a fluorescence detector. The first stage is hydrolysis of the carbamate molecule to release methylamine. This is accomplished by the introduction of an alkali solution, usually sodium hydroxide or potassium hydroxide, by means of a reagent delivery pump connected to the flow stream after the analytical column. The flow then passes through a reaction coil in a heater at 80–100°C where hydrolysis occurs. The second stage is derivatization of the released methylamine with *o*-phthalaldehyde (OPA) and 2-mercaptoethanol or 3-mercaptopropionic acid[9] to form a highly fluorescent substituted isoindole. This is accomplished using a second reagent delivery pump connected to the flow stream after the reaction coil.

Nondek *et al.*[10,11] explored the potential of replacing the use of alkali solution to hydrolyze the carbamates with a catalytic solid-phase reactor packed with an anion exchange resin. This approach eliminates one post-column reagent delivery pump and the attending mixing problems and flow pulsations. It also eliminates band broadening due to dilution of the analyte in the mobile phase. The cost of instrumentation is reduced, but this is partially offset by the cost of the solid-phase reactor. In spite of the potential advantages, this approach has not gained widespread acceptance.

This paper reports a simplification of the post-column derivatization technique which realizes the advantages of the solid-phase reactor technique by eliminating one post-column reagent delivery pump, but without the expense and potential problems of the solid-phase reactor. The method was evaluated for 11 commonly analyzed N-methylcarbamate pesticides. Results of this evaluation are presented here.

0021-9673/89/$03.50

EXPERIMENTAL

Materials

Analytical-grade standards of aldicarb, aldicarb sulfoxide and aldicarb sulfone were supplied by Union Carbide (Research Triangle Park, NC, U.S.A.). Oxamyl was supplied by E. I. du Pont de Nemours (Wilmington, DE, U.S.A.), carbofuran by FMC (Middleport, NY, U.S.A.) and carbaryl by City Chemical (New York, NY, U.S.A.). Methiocarb, bufencarb, methomyl and propoxur were supplied by Agriculture Canada, Laboratory Services Division (Ottawa, Canada).

Standard solutions were prepared by diluting 100 μg/ml stock solutions in methanol with HPLC-grade water to appropriate concentrations. Since oxamyl and propoxur were not well resolved from aldicarb sulfone and carbofuran, respectively, by the HPLC system used in this study, two series of mixed standards were used. One consisted of oxamyl and propoxur, and the other contained the remaining nine compounds.

Methanol, acetonitrile and water were HPLC-grade and obtained from J. T. Baker through Johns Scientific (Toronto, Canada). OPA and 2-mercaptoethanol were obtained from BDH (Toronto, Canada), and 3-mercaptopropionic acid from Aldrich (Milwaukee, WI, U.S.A.). Potassium hydroxide and sodium carbonate were obtained from Fisher Scientific (Don Mills, Canada).

The derivatization reagent was prepared by adding 10 mg OPA in 1 ml methanol to 400 ml 0.01 *M* potassium hydroxide solution in HPLC-grade water. This solution was degassed under vacuum with magnetic stirring, after which 0.05 ml 2-mercaptoethanol was added.

Instrumentation

A Hewlett-Packard 1090 liquid chromatograph equipped with a 79835A solvent delivery system, 79846A autoinjection module and 79847A autosampler was used. The injection volume was 10 μl and the flow-rate 1 ml/min. A mobile phase gradient of 20–80% acetonitrile in water over 16 min was employed. A Spherisorb 5 ODS-2 column (250 × 4.6 mm I.D.) was supplied by Phenomenex (Torrance, CA, U.S.A.). The single-stage post-column reactor, illustrated schematically in Fig. 1, consisted of the following. From a reservoir (A), the derivatization reagent was delivered at a rate of 0.6 ml/min by an SSI Model 350 pump equipped with a prime/purge valve (B)

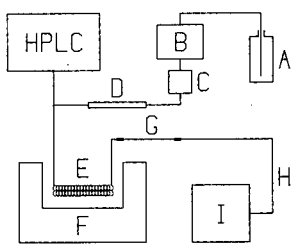

Fig. 1. Schematic diagram of post-column reactor. A = Derivatization reagent reservoir; B = reagent delivery pump equipped with prime/purge valve; C = pulse damper; D = spent PRP-1 column (to give back pressure to pulse damper); E = two delay tubes in series; F = hydrolysis heater; G = single-bead string reactor; H = 1 m × 0.5 mm I.D. PTFE tubing; I = fluorescence detector.

through a LO-Pulse pulse damper (C) connected to the flow stream from the HPLC column through a Valco zero volume tee. A spent 150 × 4.1 mm I.D. Hamilton PRP-1 column (D) inserted between the pulse damper and the tee provided back pressure which increased the efficiency of the pulse damper. The two streams were mixed in two knitted PTFE delay tubes (E) (3 m × 0.5 mm I.D., Supelco, Oakville, Canada) which were immersed in series in a 140°C dry bath consisting of glass beads in a Pierce Reacti-Therm heating module (Chromatographic Specialties, Brockville, Canada), hereafter called the reaction heater (F). The delay tubes were followed by a single-bead string reactor (G) and 1 m × 0.5 mm I.D. PTFE tubing (H) (both from Supelco) in which the flow stream cooled before it entered the flow cell of a Kratos FS 970 fluorescence detector (I). The excitation wavelength was 229 nm and a 418 nm emission filter was used. The chromatogram was recorded and integrated on a Shimadzu C-R3A Chromatopac (not shown in Fig. 1).

The following parameters were evaluated in order to optimize chromatographic peak heights of the carbamates: aqueous solution used to prepare the derivatization reagent; reaction heater temperature; delay tube length; choice of mercaptan in the derivatization reagent; and choice of organic mobile phase modifier.

RESULTS AND DISCUSSION

Selection of the optimum aqueous solution for the derivatization reagent made it possible to hydrolyze the carbamates and derivatize the released methylamine in a single step. Table I summarizes the relative peak heights of nine of the carbamates, using five derivatization reagent solutions of varying pH, normalized on the highest peak for each compound. While the 0.01 *M* sodium tetraborate solution (A) produced

TABLE I

EFFECT OF AQUEOUS SOLUTION USED TO PREPARE DERIVATIZATION REAGENT ON PEAK HEIGHTS OF 9 CARBAMATES (0.2 μg/ml EACH)

Solutions: A = 0.01 *M* sodium tetraborate, pH 9.2; B = 0.001 *M* potassium hydroxide, pH 9.5; C = 0.05 *M* sodium carbonate, pH 10.7; D = 0.01 *M* potassium hydroxide, pH 11.4; E = 0.06 *M* potassium hydroxide, pH 12.4. Reaction heater temperature 140°C.

Carbamate	*Relative peak heights (%)*[a]				
	A	*B*	*C*	*D*	*E*
Aldicarb sulfoxide	100	74	79	99	72
Aldicarb sulfone	100	79	72	91	66
Methomyl	39	17	91	100	85
3-Hydroxycarbofuran	100	77	68	95	59
Aldicarb	44	13	89	100	86
Carbofuran	100	63	61	84	56
Carbaryl	100	84	60	86	58
Methiocarb	100	82	56	85	43
Bufencarb	100	69	49	70	43
Mean	87	62	69	90	63

[a] Normalized on the highest peak (100%) for each compound.

the greatest number of maximum (100%) peaks (7 out of the 9 compounds tested), the peaks for methomyl and aldicarb were judged to be unacceptably low. The solution which produced the best peak heights overall, including the highest peaks for methomyl and aldicarb, was 0.01 *M* potassium hydroxide (D).

The method was evaluated at five reaction heater temperatures using the derivatization reagent prepared in 0.01 *M* potassium hydroxide. The results (Table II) indicate that methomyl and aldicarb exhibited the greatest resistance to hydrolysis, and the highest peaks for these compounds were obtained at the highest temperature studied. At 140°C seven of the eleven compounds exhibited their highest peaks, but the methomyl and aldicarb peaks were only about 60% of the maximum height obtained. However, since the absolute peak heights of methomyl and aldicarb at 140°C were comparable to those of the other compounds at the same temperature (see Fig. 2), the overall improvement in peak height at 150 and 160°C was not felt to be sufficient to justify using these higher temperatures. Based on these considerations it was decided to use a reaction heater temperature of 140°C. The single-bead string reactor positioned immediately downstream from the reaction heater provided adequate back-pressure to prevent boiling of the derivatization reagent/mobile phase mixture in the delay tubes.

Of all the carbamates studied, methomyl and aldicarb were most affected by the length of the delay tube (Table III). At a reaction heater temperature of 140°C the peak heights obtained for these two compounds were almost 90% higher with two delay tubes than with one. The peak heights for the other compounds were somewhat lower with two delay tubes than with one. Perhaps this was caused by band broadening due to diffusion of the analytes in the added volume. However, because of the significant improvement in peak height of methomyl and aldicarb, two delay tubes were used in the optimized single-stage reactor.

TABLE II

EFFECT OF REACTION HEATER TEMPERATURE ON PEAK HEIGHTS OF 11 CARBAMATES (0.2 μg/ml EACH)

Derivatization reagent prepared in 0.01 *M* aq. potassium hydroxide.

Carbamate	*Relative peak height (%)*[a]				
	100°C	*130°C*	*140°C*	*150°C*	*160°C*
Aldicarb sulfoxide	24	86	100	94	88
Aldicarb sulfone	32	94	100	95	91
Oxamyl	31	100	97	100	88
Methomyl	0	35	60	84	100
3-Hydroxycarbofuran	30	98	100	99	94
Aldicarb	0	34	59	82	100
Propoxur	21	97	100	98	98
Carbofuran	22	97	100	90	97
Carbaryl	52	99	100	98	97
Methiocarb	32	100	98	95	94
Bufencarb	26	97	100	98	94
Mean	23	85	92	94	95

[a] Normalized on the highest peak (100%) for each compound.

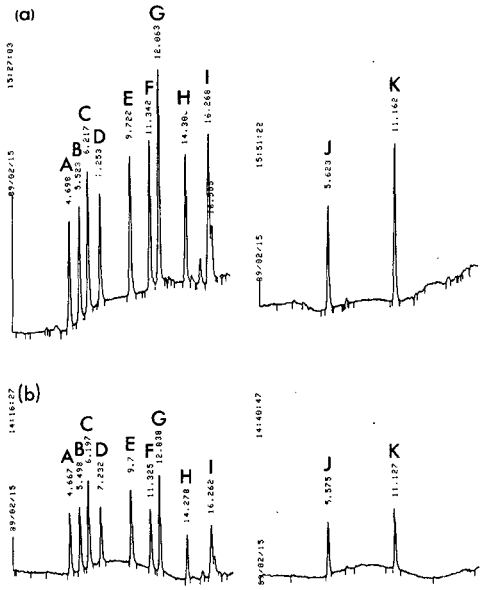

Fig. 2. Chromatograms of carbamate pesticides (0.2 μg/ml each): (a) single-stage method; (b) two-stage method. A = Aldicarb sulfoxide; B = aldicarb sulfone; C = methomyl; D = 3-hydroxycarbofuran; E = aldicarb; F = carbofuran; G = carbaryl; H = methiocarb; I = bufencarb; J = oxamyl; K = propoxur.

TABLE III

EFFECT OF LENGTH OF DELAY TUBE ON PEAK HEIGHTS OF 9 CARBAMATES (0.2 μg/ml EACH)

Derivatization reagent prepared in 0.01 *M* potassium hydroxide. Reaction heater temperature 140°C.

Carbamate	*Relative peak height (%)*[a]	
	One delay tube[b]	*Two delay tubes*[c]
Aldicarb sulfoxide	100	96
Aldicarb sulfone	100	95
Methomyl	53	100
3-Hydroxycarbofuran	100	86
Aldicarb	54	100
Carbofuran	100	85
Carbaryl	100	89
Methiocarb	100	84
Bufencarb	100	83
Mean	90	91

[a] Normalized on the highest peak (100%) for each compound.
[b] Approximate total length 3 m.
[c] Approximate total length 6 m.

TABLE IV

REPRODUCIBILITY OF RETENTION TIMES AND PEAK HEIGHTS OF 9 CARBAMATES (0.2 μg/ml EACH) USING THE SINGLE-STAGE POST-COLUMN DERIVATIZATION METHOD

Carbamate	*Coefficient of variation (%)*[a]	
	Retention time	*Peak height*
Aldicarb sulfoxide	0.18	1.08
Aldicarb sulfone	0.39	1.37
Methomyl	0.28	1.15
3-Hydroxycarbofuran	0.20	1.77
Aldicarb	0.21	2.14
Carbofuran	0.16	1.68
Carbaryl	0.20	3.42
Methiocarb	0.12	4.56
Bufencarb [b]	0.08	3.15

[a] Based on five consecutive 10-μl injections.
[b] Based on four injections only.

Acetonitrile and methanol were compared as modifiers of the aqueous LC mobile phase. A mobile phase gradient of 30–100% methanol in water over 16 min resulted in retention times which approximated those produced by the 20–80% acetonitrile gradient described earlier. The total peak height was about 90% higher when acetonitrile was used, indicating that the choice of organic mobile phase modifier made a significant difference in the performance of the method.

The choice of mercaptan in the derivatization reagent, either 2-mercaptoethanol or 3-mercaptopropionic acid (at the same concentration), did not have a significant effect on peak heights of the carbamates.

The reproducibility of the method in terms of coefficients of variation of both retention times and peak heights (Table IV) was adequate. The limit of detection was on the order of 0.1 ng analyte injected. Calibration curves for the carbamates were linear up to 5 ng analyte injected.

Fig. 2 illustrates chromatograms of the mixed standards obtained with the single-stage method (Fig. 2a) and the conventional two-stage method (Fig. 2b). The conditions used in the two-stage method were as follows. The hydrolyzing reagent (0.05 *M* aq. potassium hydroxide) was introduced at a flow-rate of 0.6 ml/min. The hydrolysis heater temperature was 140°C. The derivatizing reagent (5 mg OPA and 50 μl 2-mercaptoethanol in 200 ml 0.01 *M* aq. sodium tetraborate was introduced at a flow-rate of 0.6 ml/min. All other conditions were the same as those for the single-stage method. The total peak height for all the carbamates was 119% higher with the single-stage method than with the two-stage method at the same recorder attenuation.

The single-stage post-column derivatization method presented here is therefore an improvement over the conventional two-stage method in terms of both sensitivity and simplicity. The hardware requirements and cost are reduced and the daily operation is streamlined by the requirement of preparation of only one derivatization reagent.

REFERENCES

1 H. A. Moye, S. J. Scherer and P. A. St. John, *Anal. Lett.*, 10 (1977) 1049.
2 R. T. Krause, *J. Chromatogr. Sci.*, 16 (1978) 281.
3 R. T. Krause, *J. Chromatogr.*, 185 (1979) 615.
4 R. T. Krause, *J. Assoc. Off. Anal. Chem.*, 63 (1980) 1114.
5 R. T. Krause, *J. Assoc. Off. Anal. Chem.*, 68 (1985) 726.
6 R. T. Krause, *J. Assoc. Off. Anal. Chem.*, 68 (1985) 734.
7 H. Engelhardt and B. Lillig, *Chromatographia*, 21 (1986) 136.
8 A. de Kok, M. Hiemstra and C. P. Vreeker, *Chromatographia*, 24 (1987) 469.
9 P. Kucera and H. Umagat, *J. Chromatogr.*, 225 (1983) 563.
10 L. Nondek, U. A. Th. Brinkman and R. W. Frei, *Anal. Chem.*, 55 (1983) 1466.
11 L. Nondek, R. W. Frei and U. A. Th. Brinkman, *J. Chromatogr.*, 282 (1983) 141.

Journal of Chromatography, 481 (1989) 452–457
Elsevier Science Publishers B.V., Amsterdam — Printed in The Netherlands

CHROM. 21 736

Note

High-performance liquid chromatographic screening method for low levels of nicarbazin in eggs with off-line cartridge sample clean-up

M. H. VERTOMMEN*, A. VAN DER LAAN and H. M. VEENENDAAL-HESSELMAN
Poultry Health Institute, P. O. Box 43, 3940 AA Doorn (The Netherlands)
(First received January 9th, 1989; revised manuscript received May 27th, 1989)

Nicarbazin, a molecular complex of 4,4'-dinitrocarbanilide and 2-hydroxy-4,6-dimethylpyrimidine, has been in worldwide use from 1955 to control coccidiosis in poultry. In the Netherlands, nicarbazin is used as feed additive at a maximum level of 125 mg/kg for the prophylactic treatment of *ca.* 200 million broilers, representing 70% of the total annual production. A residual level of 4 mg/kg in uncooked chicken muscle, liver, skin and kidney is allowed by the U.S. Food and Drug Administration. The Dutch broiler industry attempts to eliminate nicarbazin residues by a compulsory withdrawal period of 9 days before slaughter.

Because of adverse effects on shell colour, yolk pigmentation and hatchability[1,2] the product is not used in layers and breeders. Because feed for both broilers and layers is produced in the same factory it is unavoidable that cross-contamination between different batches occurs and low levels of nicarbazin may be detected in feed for layers and breeders. This problem of carry-over is confirmed by the investigations of Friedrich *et al.*[3], among others. Investigations on the kinetics of nicarbazin in layers by Friedrich *et al.*[4] showed that even very low levels of nicarbazin in the feed result in detectable residues of nicarbazin in eggs.

In these studies the dinitrocarbanilide moiety of nicarbazin was analysed by the high-performance liquid chromatographic (HPLC) method of Malisch[5]. The Malisch procedure was developed for the determination of some 54 different substances in milk, eggs and meat, and has a detection limit for nicarbazin of *ca.* 5 μg/kg, with recoveries of 30–40% in 50-g test portions.

A practical disadvantage of this method is the low number of samples that can be analysed per day due to the time-consuming cleanup procedure. The need to analyse a larger number of samples at lower cost was the reason for developing a rapid screening method for nicarbazin in eggs.

MATERIALS AND METHODS

Reagents and standards

Water was purified with a Milli-Q system (Millipore, Bedford, MA, U.S.A.). The following reagents and solvents were used: acetic acid glacial (p.a. quality, Merck, Darmstadt, F.R.G.); acetonitrile (HPLC grade, Fisons, Loughborough, U.K.); sodium sulphate anhydrous (p.a. quality, Merck); *n*-hexane (Baker Grade,

0021-9673/89/$03.50

Baker, Deventer, The Netherlands); chloroform ("Baker Analysed", Baker); sodium acetate anhydrous (p.a. quality, Merck).

Nicarbazin standard (97.4%) was supplied by Merck, Sharp & Dohme (Haarlem, The Netherlands). For HPLC, a standard solution of nicarbazin in eluent (0.020 μg/ml) was prepared from a 50 μg/ml stock solution of nicarbazin in acetonitrile. For spiking, a standard solution of nicarbazin in water (1.25 μg/ml) was prepared from the same stock solution.

Spiking of egg material

To 49 g of blank homogenized whole egg, 1.0 ml of an aqueous standard solution of nicarbazin (1.25 μg/ml) was added by mixing on a magnetic stirrer for 10 min. From this material, containing a concentration of nicarbazin of 25 μg/kg, dilutions were prepared in blank whole egg material to obtain samples containing 2.5, 5.0, 10.0, 15.0, 20.0 and 25.0 μg of nicarbazin, respectively. To determine the recovery these materials were treated in the same way as the egg samples.

Sample preparation

Before analysis the total egg content was homogenized by shaking. The homogenate can be stored at 4°C for up to 4 days without measurable loss of nicarbazin content. For longer storage the samples can be kept at −20°C for several weeks.

For the extraction, 50 μl of 10% acetic acid solution was pipetted into a polystyrol tube. Using a 1-ml pipettor with a disposable tip, 1.0 g of sample was weighed into the tube and a magnetic stirring rod was added. While this was stirred on the magnetic stirrer (Model IKA, Combimag RCT) at maximum speed, 2.5 ml of acetonitrile were slowly added. The tube was closed with a stopper and stirring continued. After 4 min, 0.25 g of anhydrous sodium sulphate was added and stirring was continued for 2 min. The tube was centrifuged for 2 min at 3000 rpm (1400 *g*), on a Heraeus Minifuge. The supernatant was decanted into a glass centrifuge tube through a disposable funnel with a silanized glasswool plug (Baker). The sediment in the polystyrol tube was re-extracted with 2.5 ml of acetonitrile by stirring for 3 min at maximum speed. After centrifugation for 2 min at 3000 rpm, the supernatant was combined with the first extract through the funnel. The funnel was rinsed with 1 ml of acetonitrile. The combined extracts were evaporated to dryness under nitrogen, using a water-bath at 60°C.

Solid phase extraction (SPE) columns packed with 100 mg of Bond-Elut No. 601101 from Analytichem were washed twice with 1 ml of chloroform–acetonitrile (80:20) and once with 1 ml of chloroform, and finally air-dried before use. After evaporation the residue was redissolved in 1 ml of hexane-chloroform (50:50) and transferred to a pre-treated SPE column on a vacuum manifold (Alltech). The tube was rinsed with 1 ml of hexane-chloroform (50:50). The rinsing fluid was transferred to the SPE column without allowing it to run dry. After the liquid had flowed through, the column was dried by vacuum for 1 min. The column was then eluted with chloroform–acetonitrile (80:20), and the first 1 ml of the eluate was collected in a 1.5-ml glass autosampler vial. After evaporation to dryness under nitrogen at room temperature, 1.0 ml of the HPLC eluent was added. The vial was closed with a cap and the residue was dissolved by shaking on a Vortex mixer for 4 min.

HPLC conditions

The HPLC conditions were derived from those described by Malisch[5], Hoshino *et al.*[6] and Petz[7].

An HPLC system with an autosample (Promis, Spark Holland), a solvent-delivery pump (SF 400, Applied Biosystems), an UV–VIS detector (SF 783, Applied Biosystems) and an integrator (4290, Spectra Physics) was used. Sample volumes of 50 μl were injected.

The analytical column consisted of two cartridges (100 × 3.0 mm I.D.) packed with ChromSpher C_{18} (5 μm particle size) and was obtained from Chrompack. The guard column cartridge (10 × 2.1 mm I.D.) packed with pellicular RP (30–40 μm particle size) was also from Chrompack. The mobile phase was acetonitrile–acetate buffer (0.02 *M*, pH 4.8)–water (54:10:36). A flow-rate of 0.60 ml/min was used and nicarbazine was detected at 360 nm using a Kratos Model SF 783 UV detector.

The amount of nicarbazin in the samples was calculated by comparison of the peak height with that of the standard solution. The result was corrected for the recovery found in the spiked egg material.

RESULTS AND DISCUSSION

Chromatography

Chromatrograms from spiked and control samples and the standard are shown in Fig. 1.

Recovery

Samples spiked at 2.5, 5.0, 10.0, 15.0, 20.0 and 25.0 μg/kg were used in recovery experiments and in studies on the linearity of the photometric detector response. The results of the spiking experiments are shown in Table I. The linearity of the photometric detector response in presented in Fig. 2.

A good recovery for all the levels investigated and a low standard deviation for

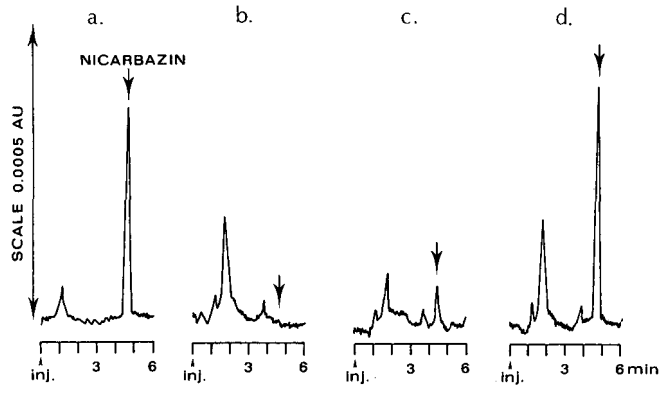

Fig. 1. Representative chromatogram from HPLC injections of (a) nicarbazin standard solution; (b) blank egg sample; (c) egg sample, spiked with 5 μg of nicarbazin per kg; (d) egg sample, spiked with 25 μg of nicarbazin per kg.

TABLE I

STATISTICAL SUMMARY OF ANALYSIS OF EGG MATERIAL SPIKED WITH SEVERAL LEVELS OF NICARBAZIN

Correlation coefficient for average content and spiking level: 0.99915.

Spiking level (μg/kg)	*n*	*Average content*	*Standard deviation*	*Coefficient of variation (%)*	*Mean recovery (%)*
2.5	4	2.91	0.65	22.41	116.4
5.0	5	4.41	0.67	15.11	88.2
10.0	5	9.21	0.38	4.08	92.1
15.0	5	14.03	0.28	1.96	93.5
20.0	5	18.40	0.37	2.00	92.0
25.0	8	22.31	0.53	2.39	89.0

the repeatability were obtained. The relationship between peak height and concentration of the analyte was linear in the range 2.5–25.0 μg of nicarbazin per kilogram of egg material.

Limit of detection

The use of the 5-μm ChromSpher C_{18} column and an UV detector such as the Kratos Model SF 783 was essential for sensitive detection of nicarbazin. With this combination of column and detector the detection limit, with the signal three times the noise level, was achieved with 125 pg of nicarbazin. This amount represents 2.5 μg of nicarbazin per kilogram of egg material.

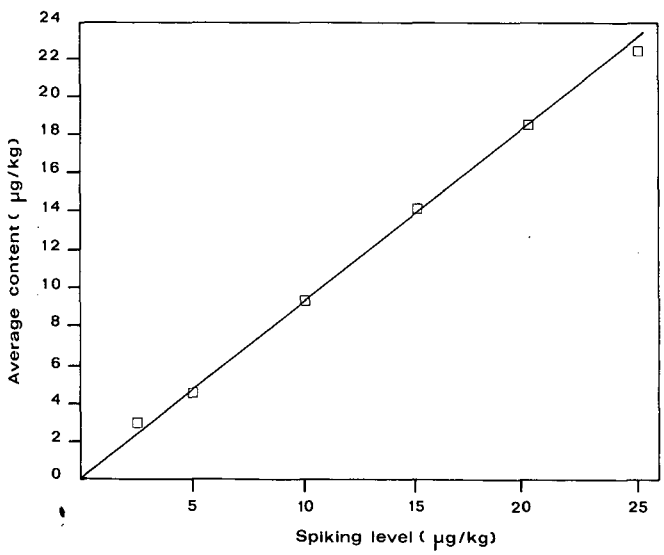

Fig. 2. Linearity of the photometric detector response to nicarbazin in spiked egg materials.

Extraction and cleanup

Working with the method of Haagsma and Van de Water[8] for the determination of sulphonamides in egg material, it was found that adding acetic acid to the sample, to adjust the pH, reduced the viscosity of the sample. This reduced viscosity made the sample more suitable for homogenizing with acetonitrile and improved the recovery.

Adding 0.25 g of anhydrous sodium sulphate to the homogenate is essential to remove part of the water, which makes evaporation to total dryness with nitrogen possible. Moreover, the sodium sulphate has a grinding effect, which possibly enhances partition of the egg material in the extraction fluid. Evaporation of the extract proved to be unavoidable, since only a part of the water from the sample could be removed by sodium sulphate during extraction. Moreover, evaporation of the extract to total dryness proved to be essential to obtain the proper polarity of the solution of the extracted material for further cleanup.

In experiments with different mixtures of chloroform and hexane, it was established that a 50:50 ratio of chloroform–hexane was optimal for dissolving the extracted material and prevented adsorption of egg matrix material on the SPE column as selectively as possible. Chloroform–acetonitrile (80:20) proved to be optimal for quantitative elution of nicarbazin in a small volume, minimizing co-elution of matrix material from the SPE column.

The need to evaporate twice during cleanup has little influence on the analysis time because of the small volumes involved. With simple equipment it is possible to evaporate several extracts simultaneously. The described cleanup procedure, in combination with a relatively short HPLC run time of 6.0 min, makes it possible for two technicians to analyse 30 samples per day.

During development of this method chromatograms of samples showed impurities from the SPE column material, but chromatograms were improved by washing as described. In present batches of SPE columns pretreatment has been proven to be less essential because of improvements in manufacture.

Applications

The procedure described has been used to determine the nicarbazin content of eggs obtained from hens fed with different levels of the anticoccidial drug in the feed. In accordance with the studies of Polin *et al.*[9] and Friedrich *et al.*[4] a maximum level of nicarbazin was detected *ca.* 8 days after first administration of the medicated ration. This finding was also in accordance with the results of the investigations of Anhalt[10] for other drugs.

The method was also used to screen several thousand samples from egg producers and exporters during a period of 2 years. In every case of positive findings a relation was found with carry-over of low levels of nicarbazin in the feedmill. Further research is being conducted to automate the method and to make it applicable to the analysis of nicarbazin in meat, feed and other matrices.

ACKNOWLEDGEMENT

The authors thank Drs. C. Fris for his help in editing this paper.

REFERENCES

1 W. H. Ott, A. M. Dickinson and A. C. Peterson, *Poultry Sci.*, 35 (1956) 1163.
2 D. H. Sherwood, T. T. Milby and W. A. Higgins, *Poultry Sci.*, 35 (1956) 1014–1019.
3 A. Friedrich, H. M. Hafez and H. Woernle, *Tierärztliche Umsch.*, 40 (1985) 190–199.
4 A. Friedrich, H. M. Hafez and H. Woernle, *Tierärztliche Umsch.*, 39 (1984) 764–772.
5 R. Malisch, *Z. Lebensm. Unters. Forsch.*, (1986) 385–339.
6 Y. Hoshino, M. Horie and N. Nose, *Jpn. J. Food Hyg.*, 23 (1982) 265–269.
7 M. Petz, *Z. Lebensm. Unters. Forsch.*, 176 (1983) 298–293.
8 N. Haagsma and C. Van de Water, *J. Chromatogr.*, 333 (1985) 256–261.
9 D. Polin, J. L. Gilfillan, W. H. Ott and C. C. Porter, *Poultry Sci.*, 33 (1956) 1367–1371.
10 G. Anhalt, *Arch. Geflügelkunde*, 41 (1979) 232–237.

Journal of Chromatography, 481 (1989) 458–460
Elsevier Science Publishers B.V., Amsterdam — Printed in The Netherlands

CHROM. 21 876

Note

High-performance liquid chromatographic separation of indandione rodenticides

JOEL E. HOUGLUM*, RICHARD D. LARSON and ROSE M. NEAL
*Chemistry Department and *College of Pharmacy, South Dakota State University, Brookings, SD 57007 (U.S.A.)*
(Received July 18th, 1989)

Chlorophacinone {2-[(*p*-chlorophenyl)phenylacetyl]-1,3-indandione}, diphacinone [2-(diphenylacetyl)-1,3-indandione], pindone (2-pivaloyl-1,3-indandione) and valone (2-isovaleryl-1,3-indandione) are used as anticoagulant rodenticides. These indandiones are available as concentrates, tracking powders or as ready-to-use baits on whole or crushed grain. There are published reports of high-performance liquid chromatographic (HPLC) separations of two[1–3] or three[4] of these indandiones, but no reports of an HPLC method that separates all four of these compounds. After attempting modifications of these reported procedures, we eventually developed a new procedure which utilizes a CN column with phosphoric acid in the mobile phase.

The purpose of this research, as a result of investigating the identity of a mislabelled sample, was to develop an HPLC method that could be used to separate all four of these indandione rodenticides so as to be able to identify which one is present in a sample of unknown or questionable content.

EXPERIMENTAL

Reagents and materials

Diphacinone was obtained from Beltsville Agricultural Research Center (Beltsville, MD, U.S.A.), chlorophacinone from EPA (Research Triangle Park, NC, U.S.A.) and pindone and valone from Bell Labs. (Madison, WI, U.S.A.).

Standard stock solutions were prepared in methanol at 500 μg/ml. Intermediate standard solutions were prepared at 5 μg/ml by dilution of 1 ml of stock solution to 100 ml with acetonitrile for chlorophacinone and diphacinone or bringing to volume with methanol–acetonitrile (1:3, v/v) for pindone and valone. Working standard solutions of 2.5 μg/ml were prepared from 5 ml of intermediate solution diluted to 10 ml with 0.2% (v/v) phosphoric acid.

The solvent to extract chlorophacinone and diphacinone was acetonitrile, whereas the extraction solvent for pindone and valone was methanol–acetonitrile (1:3, v/v).

Apparatus

The HPLC system consisted of an Alltech (5 μm) cartridge CN column (150

0021-9673/89/$03.50

mm × 4.6 mm I.D.) with a direct-connect CN guard column (10 mm × 4.6 mm), a Waters 6000 pump at a flow-rate of 1.5 ml/min, a Valco C6U injector with a 25-μl loop, an Isco V^4 variable-wavelength detector at 280 nm and a Varian Model 9176 chart recorder. The mobile phase consisted of acetonitrile–phosphoric acid solution (45:55, v/v). The phosphoric acid solution was 0.2% (v/v) in water. For samples injected at 2.5 μg/ml, the detector sensitivity was set at 0.01 absorbance units full scale for pindone and valone and at 0.005 absorbance units full scale for chlorophacinone and diphacinone.

Procedure

To prepare spiked samples, 1 ml of standard stock solution was added to 10 g ground corn to give 0.005% chlorophacinone or diphacinone, and 1 ml to 2 g ground corn to give 0.025% pindone or valone. The spiked bait was dried under a gentle stream of nitrogen and extracted with 100 ml of extraction solvent for 1 h on a mechanical shaker. After centrifugation for 5 min at 1500 rpm (500 *g*), 5 ml of the extract were diluted to 10 ml with 0.2% phosphoric acid, mixed and injected onto the HPLC system. Samples were injected in duplicate and bracketed with injections of the standard. The results were calculated based upon the relative average peak height of the sample and the standard.

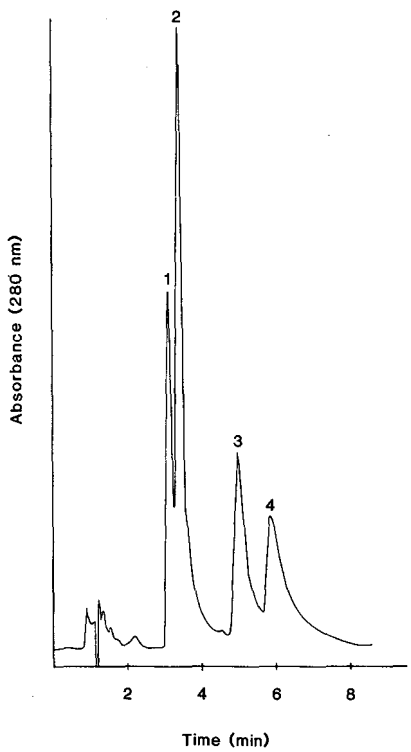

Fig. 1. High-performance liquid chromatogram of valone (1), pindone (2), diphacinone (3) and chlorophacinone (4) standards at a concentration range of 2–2.6 μg/ml on a 5 μm CN column (150 mm × 4.6 mm I.D.). Mobile phase, acetonitrile–0.2% phosphoric acid (45:55, v/v); flow-rate, 1.5 ml/min; UV detection, 280 nm.

TABLE I

MEAN RECOVERY OF INDANDIONES FROM SPIKED GROUND CORN

Results are from samples spiked in triplicate.

Compound	*Spiked level (%)*	*Mean recovery (%)*	*Coefficient of variation (%)*
Chlorophacinone	0.005	83.3	2.5
Diphacinone	0.005	96.3	3.8
Pindone	0.025	96.2	1.1
Valone	0.025	96.9	0.6

RESULTS AND DISCUSSION

Fig. 1 is a chromatogram of a mixture of valone, pindone, diphacinone and chlorophacinone standards with capacity factors of 2.5, 2.8, 4.6 and 5.6, respectively. Use of less than 0.2% phosphoric acid in the mobile phase caused a more pronounced broadening and tailing of the indandione peaks. Also, peaks were broader if the extracts and standards were not diluted with the phosphoric acid solution. Use of 0.5, 1.0 and 1.5% phosphoric acid did not improve the separation of the indandiones or change the retention times significantly and would likely decrease the longevity of the column.

The response was linear through the concentration range tested: 0.2–20 μg/ml. Least-squares linear regression analyses of the data gave correlation coefficients which ranged from 0.997 to 0.999 for the four indandiones.

As shown in Table I, the average recovery from spiked samples of ground corn ranged from 83.3% for chlorophacinone to 96.9% for valone. Even though acetonitrile has been reported by others to extract indandiones from baits[4,5], we found it necessary to add methanol to the extraction solvent to obtain good recovery of pindone and valone from spiked ground corn samples. The addition of methanol to the extraction solvent did not improve the percentage recovery of chlorophacinone nor did the use of a 2-h extraction. A similar recovery was obtained from the addition of chlorophacinone to wheat bait. Unspiked ground corn and wheat samples did not contain interfering peaks when extracted with either of the extraction solvents.

This method provides a convenient, isocratic HPLC system for the separation of these four indandione rodenticides and thus a means to identify the indandione in samples that are mislabelled or of unknown indandione content. Warfarin, another rodenticide, also separates from these indandiones and gives a sharp peak with a capacity factor of 1.9 (data not shown).

REFERENCES

1 B. R. Bennett and G. S. Grimes, *J. Assoc. Off. Anal. Chem.*, 65 (1982) 927.
2 G. Vigh, Z. Varga-Puchony and A. Bartha, *J. Chromatogr.*, 241 (1982) 169.
3 K. Hunter, *J. Chromatogr.*, 321 (1985) 255.
4 J. D. Reynolds, *Proc. Am. Assoc. Vet. Lab. Diagn.*, 23 (1980) 187.
5 B. J. Addison, *J. Assoc. Off. Anal. Chem.*, 65 (1982) 1299.

Journal of Chromatography, 481 (1989) 461–464
Elsevier Science Publishers B.V., Amsterdam — Printed in The Netherlands

CHROM. 21 667

Note

Reversed-phase high-performance liquid chromatography, a tool for the study of bichromophoric systems including polymethylenic linking bridges

JEAN-LUC DÉCOUT
Laboratoire d'Études Dynamiques et Structurales de la Sélectivité, Université Joseph Fourier, B.P. 53X, 38041 Grenoble Cedex (France)
BERNARD MOUCHEL
Service de RMN, Université de Lille I, 59655 Villeneuve d'Ascq Cedex (France)
and
JEAN LHOMME*
Laboratoire d'Études Dynamiques et Structurales de la Sélectivité, Université Joseph Fourier, B.P. 53X, 38041 Grenoble Cedex (France)
(First received October 25th, 1988; revised manuscript received June 7th, 1989)

The photochemical and photobiological properties of furocoumarins such as 5-methoxypsoralen **1** (5-MOP) and 8-methoxypsoralen **2** (8-MOP) have been extensively studied, notably with respect to their use in the phototherapy of skin diseases.

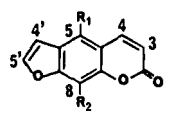

1: R_1=OCH_3, R_2=H, 5 MOP
2: R_1=H, R_2=OCH_3, 8 MOP

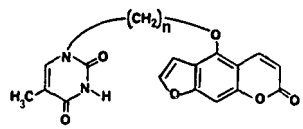

3: n = 2,3,4,5,6,12

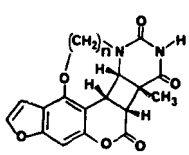

5: n = 2,3,4,5,6,12

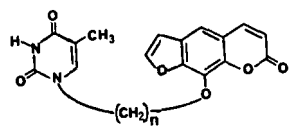

4: n = 3,4,5,6,12

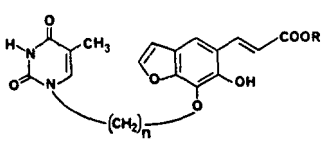

6: R = C_2H_5 ; n = 3,4,5,6,12
7: R = H; n = 3-6,12

0021-9673/89/$03.50

The biological effects are generally related to the photochemical reactions which occur with DNA. After intercalation of the psoralen ring between adjacent complementary bases, the 3, 4 or/and 4', 5' double bond of the drug can add to the 5, 6 olefinic bond of a pyrimidine, usually thymine[1,2]. The intermolecular psoralen-thymine photoreactions cannot be studied in solution due to the highly favoured psoralen photodimerization[3]. With this aim, we have prepared compounds **3** and **4** in which the two chromophores are linked by a flexible polymethylene chain. They represent two series of models related to the important drugs 5-MOP and 8-MOP. In dilute solution, the polymethylene link allows intramolecular ring–ring stacking interactions and competitive photoaddition of the 5,6 double bond of thymine onto the 3, 4 or 4', 5' psoralen double bond. The study of models of various chain lengths n = 2, 3, 4, 5, 12 provides a control of the geometric strains imposed by the chain. We report here an interesting application of reversed-phase liquid chromatography (RPLC) for the characterization of the photoproducts as a function of the chain length.

EXPERIMENTAL

Detailed procedures for the preparation and irradiation at 365 nm of the models have been previously reported[4,5].

Analytical conditions

The apparatus was a Waters Associates chromatographic system equipped with a Model 660 programmer, two M-6000 pumps and a dual wavelength detector (254 or 280 and 365 nm). The irradiated solutions were analyzed on a C_{18} reversed-phase column (packed with RP-18 Prolabo phase with a Touzart and Matignon apparatus) using a linear gradient of two solvents water and methanol (from 50 to 95% of methanol in 10 min then 95% methanol, 2 ml/min). Water (pH 6) and buffered water (pH 5, 0.02 M ammonium acetate–acetic acid) were respectively used in the 5- and 8-series. The absorption ratios at the two wavelengths of detection were measured to characterize each compound.

RESULTS AND DISCUSSION

The photoreactivity of models **3** (n = 2–5, 12) in the 5-series was first studied. The compounds were irradiated at *very low concentration* ($2 \cdot 10^{-5} M$)[a] to avoid the photodimerization. From each model, a very major photoproduct was formed (as monitored by HPLC analysis). The photoproducts with n = 2, 4 and 12 were isolated and characterized by ^{1}H NMR, mass spectrometry and X-ray crystallography[4]. All three products possess a *cis* cyclobutane ring resulting from regio- and stereoselective intramolecular photoaddition of the thymine double bond onto the 3,4 pyrone ring of psoralen. The HPLC characteristics of those adducts **5b**, **5d**, **5f** were examined: their capacity factors, k', were plotted *versus* the capacity factors of the corresponding starting compounds **3b**, **3d**, **3l** (Fig. 1). A remarkably good linear correlation was observed (r = 0.998). The photoproducts **5c**, **5e**, **5f** resulting from the corresponding

[a] The use of HPLC is critical for this study at the limits of detection (150–200 μl of solution injected).

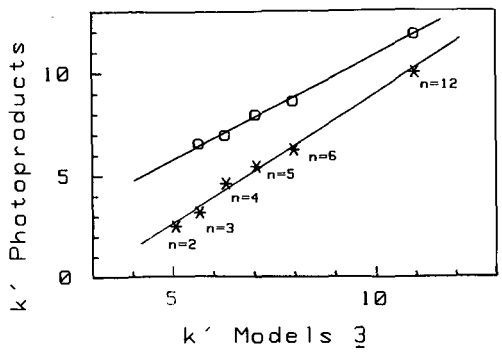

Fig. 1. Correlation between the RPLC capacity factors, k', of models **3** and the capacity factors of their photoproducts: intramolecular photoadducts **5** (*) and photodimers (O).

compounds **3c**, **3e**, **3f** were then examined. They were not isolated but their capacity factors were treated as previously, *i.e.*, they were plotted on the same graph as a function of the capacity factors of the starting compounds (Fig. 1). All points are remarkably localized on the same straight line ($r = 0.996$ for the six points).

The models **3** were then irradiated at a *more usual concentration* (10^{-3} *M*). From each model ($n = 3$–12)[a] a major photoproduct was formed. The photoproducts with $n = 4$ and 12 were identified by ^{1}H NMR spectroscopy as dimers resulting from a [2 + 2] photoaddition between the 3, 4 double bond of two psoralen rings[4]. As previously, the capacity factors of the photoproducts were plotted *versus* the capacity factors of the corresponding starting models **3**. All the five points obtained are again located on a straight line ($r = 0.998$).

Fig. 1 shows the remarkable relationships between the capacity factors of the two series of photoproducts, the intramolecular adducts **5** and the dimers, and the capacity factors of the parent compounds **3**.

The photoreactivity of models **4** ($n = 3$–6, 12) in the 8-series was studied at low concentration ($3 \cdot 10^{-5}$ *M*) in ethanol. From each model, a very major photoproduct was formed. The structure **6** resulting from a photolysis of the psoralen ring was assigned to the photoproducts with $n = 4$ and 12 (ref. 5). The capacity factors of all the observed photoproducts ($n = 3$–6 and 12) were plotted *versus* the capacity factors of the corresponding starting models **4** (Fig. 2). The localization of the five points on a straight line ($r = 0.999$) and the equality of the absorption ratios at the two wavelengths of detection led us to assign to each photoproduct the structure **6**. A similar photochemical study was realized in water and again HPLC allowed us to assign the same structure **7** to the major photoproduct observed after irradiation of each model **4** ($n = 3$–6 and 12, Fig. 2, $r = 0.999$)[5].

In each family of compounds possessing analogous structures, no good linear correlation was observed between log k' (capacity factor) and the number of methylenes in the linking chain. This is not unexpected as the HPLC analysis were not performed using isocratic elution. For practical reasons a linear gradient of solvents had to be used. However, for all the six families of compounds studied, remarkable good linear correlations were observed between the capacity factors of the com-

[a] No dimerization is observed for $n = 2$.

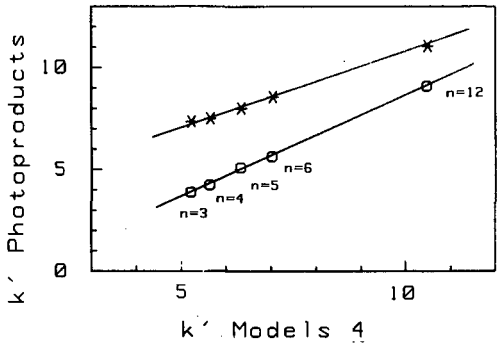

Fig. 2. Correlation between the RPLC capacity factors, k', of models **4** and the capacity factors of their photoproducts **6** (*) and **7** (○).

pounds *versus* the number of methylenes of their constitutive linking chain.

In conclusion, in each series of compounds, the capacity factors of the photoproducts are linearly related to the capacity factors of the irradiated compounds. Consequently, RPLC appears to be a powerful tool for the characterization and the study of bifunctional systems in which a polymethylene bridge of variable length separates the two functions. It should be especially useful for photochemical studies of bichromophoric systems which are currently the object of extensive investigations (for examples, see refs 6–12).

REFERENCES

1 E. Ben-Hur and P.-S. Song, *Adv. Radiat. Biol.*, 11 (1984) 131.
2 J. E. Hearst, S. T. Isaacs, D. Kanne, H. Rapoport and K. Straub, *Q. Rev. Biosphys.*, 17 (1984) 1.
3 P. Vigny, F. Gaboriau, L. Voituriez and J. Cadet, *Biochimie*, 67 (1985) 317.
4 J.-L. Décout, G. Huart and J. Lhomme, *Photochem. Photobiol.*, 48 (1988) 583.
5 J.-L. Décout and J. Lhomme, *Photochem. Photobiol.*, 48 (1988) 597.
6 J. J. McCullough, *Chem. Rev.*, 87 (1987) 811.
7 N. J. Leonard, *Acc. Chem. Res.*, 12 (1979) 423.
8 K. Golankiewicz, *Heterocycles*, 7 (1977) 1.
9 J. Gervais and F. C. De Schryver, *Photochem. Photobiol.*, 21 (1975) 71.
10 L. H. Leenders, E. Schouteden and F. C. De Schryver, *J. Org. Chem.*, 38 (1973) 957.
11 C. Kaneko, N. Katagiri, K. Uchiyama and T. Yamada, *Chem. Pharm. Bull.*, 33 (1985) 4160.
12 G. Wenska and S. Paszyc, *Can. J. Chem.* 66 (1988) 513.

Journal of Chromatography, 481 (1989) 465–470
Elsevier Science Publishers B.V., Amsterdam — Printed in The Netherlands

CHROM. 21 767

Note

Thin-layer chromatography on polyacrylonitrile

I. Effect of the *cis–trans* configuration of cobalt(III) complexes on their R_F values

T. J. JANJIĆ*, D. M. MILOJKOVIĆ, Ž. J. ARBUTINA, Ž. Lj. TEŠIĆ and M. B. ĆELAP
Faculty of Chemistry, University of Beograd, Studentski trg 16, P.O. Box 550, 11001 Belgrade (Yugoslavia)
(First received May 2nd, 1989; revised manuscript received June 19th, 1989)

Polyacrylonitrile is a chain polymer of acrylonitrile of the general formula $-[CH(CN)CH_2]_n-$. Owing to the mutual repulsion of cyano groups, the macromolecule gains a spiral chain conformation with occasionally formed hydrogen bonds between cyano groups and α-methyne hydrogens of adjacent chains[1].

At present, the most readily accessible are commercial polyacrylonitrile fibres consisting of different copolymers which contain at least 85% of acrylonitrile monomer[1]. Its world production is very high[1], which makes this material cheap and easily available.

Polyacrylonitrile belongs to specific sorbents with localized negative charges on nitrile groups[2]. It is very resistant at room temperature to the action of most organic solvents applied in chromatography and also to dilute solutions of acids and bases[3]. Hence we consider that polyacrylonitrile could be more widely applied in chromatography.

Polyacrylonitrile has so far been applied as a sorbent in thin-layer chromatographic separations in only one instance, namely, Hesse *et al.*[4] used it for the separation of some monosaccharides and dicarboxylic and sulphonic acids. However, they stated neither the method of preparation of the sorbent nor its characteristics. Therefore, in this work, we wanted to consider the possibility of its laboratory preparation and to determine its most important characteristics. In addition, we wanted to check the applicability of the prepared sorbent to the separation of some *cis–trans* isomeric cobalt(III) complexes.

EXPERIMENTAL

Preparation of the polyacrylonitrile sorbent

The procedure for the preparation of the polyacrylonitrile sorbent involves dissolution of 50 g of white PAN fibres (OHIS, Skoplje, Yugoslavia) in 2 l of concentrated nitric acid (ρ = 1.40 g/cm^3) at room temperature, followed by dropwise addition of the solution obtained to 6 l of water with vigorous stirring. The voluminous precipitate obtained is then filtered off under slightly reduced pressure, washed with

0021-9673/89/$03.50

water and ethanol and dried in a porcelain dish at 50°C with occasional stirring. The yield is quantitative. In order to separate larger particles, the dried powder is then finely ground and suspended in 1 l of 96% ethanol. The suspension is left to stand at room temperature for 10 min and then the part of the suspension above the sediment, which contains about 25 g of the sorbent, is decanted. The sediment is dried, ground and treated again as described above. The decanted suspension is left to stand overnight at room temperature, by which time a white precipitate has settled to the bottom. The main part of the ethanol above precipitate is gently decanted, and the remaining part is shaken and applied to chromatographic plates.

Apparatus and methods for the determination of sorbent characteristics

Electron microscope analysis was performed on a JEOL (Peabody, MA, U.S.A.) J. SM-35 scanning microscope.

X-ray diffraction analysis of the sorbent was carried out on a Philips (Wavre, Belgium) PW 1051 powder diffractometer.

Infrared spectra were recorded on a Perkin-Elmer (Norwalk, CT, U.S.A.) 457 spectrophotometer using the potassium bromide technique.

The distribution of sorbent particles according to their size was determined by means of a CILAS (Marcoussis, France) E 715 granulometer.

The pore volume of the sorbent was determined by centrifugation with *n*-nonane[5].

The ion exchange capacity of the sorbent was determined by volumetric analysis[6].

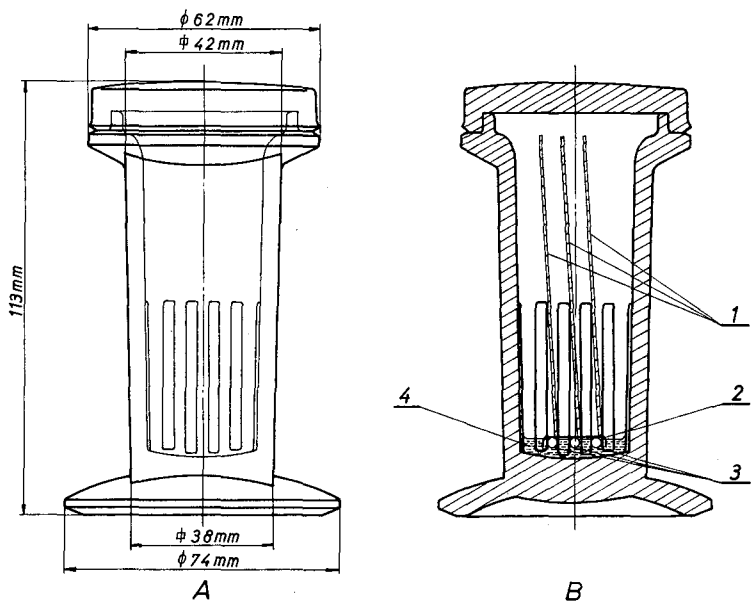

Fig. 1. Diagram of the apparatus. (A) Chromatographic chamber; (B) its cross-section. 1 = Microscopic plates; 2 = band made of Whatman 3MM chromatographic paper; 3 = glass rods; 4 = developing solution.

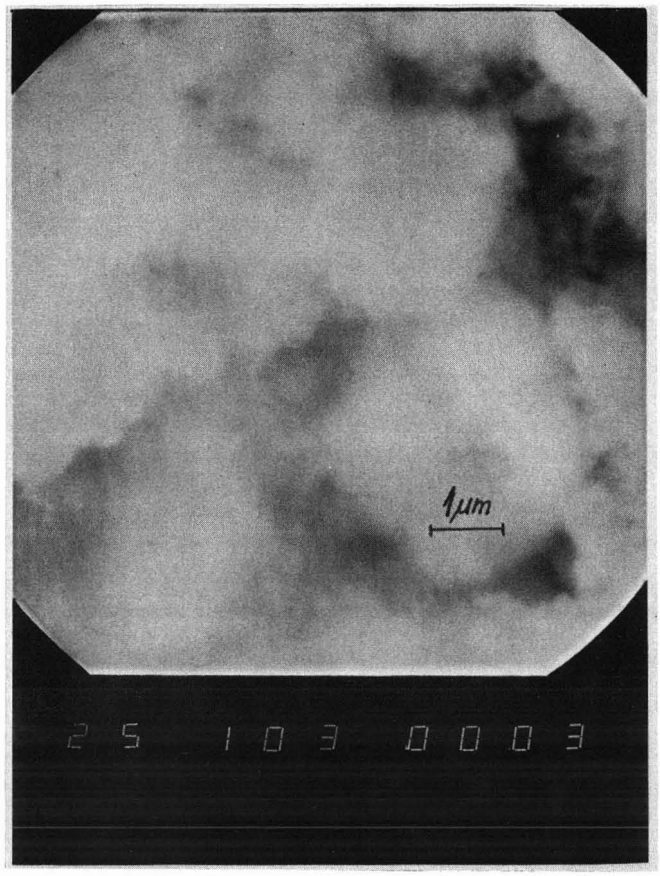

Fig. 2. Polyacrylonitrile sorbent examined by electron microscopy.

The specific surface area of the sorbent was determined, after drying at 70°C for 3 h, by the BET nitrogen adsorption method on a Flowsorb II 2300 apparatus (Micromeritics, Norcross, GA, U.S.A.).

For covering the plates with the sorbent, a Camag (Muttenz, Switzerland) hand-operated TLC plate coater was used.

Syntheses

All the investigated complexes were synthesized by described procedures (Table I).

Chromatographic data

Thin-layer chromatographic separations were carried out on microscope plates (26 × 76 mm); the layer thickness was about 0.25 mm. Before use, the plates covered with the sorbent were dried in air for about 1 h and then kept in a desiccator over calcium chloride. For each separation, 0.5 μl of a 0.01 *M* solution of the corresponding

TABLE I

$R_F \times 100$ VALUES OF THE INVESTIGATED COMPLEXES OBTAINED BY THIN-LAYER CHROMATOGRAPHY ON THE POLYACRYLONITRILE SORBENT

Complex[a]	*Isomer*	*Solvent*					*Ref.*[b]
		Water	*0.1% $KClO_4$*	*0.1% $HClO_4$*	*1% $KClO_4$*	*1% $HClO_4$*	
$[Co(NH_3)_4(NO_2)_2]^+$	*cis*	–	31	33	60	59	7, 8
	trans	–	45	54	76	69	7, 8
$[Coen_2(NO_2)_2]^+$	*cis*	–	27	38	50	53	9
	trans	–	43	52	70	69	9
$[Coen_2(NO_2)Cl]^+$	*cis*	–	34	27	52	52	10
	trans	–	49	33	64	67	10
$[Coen_2(SCN)Cl]^+$	*cis*	–	23	–	39	41	10, 11
	trans	–	37	–	47	55	10, 11
$[Coen_2(SCN)_2]^+$	*cis*	–	8	7	11	8	10, 11
	trans	–	20	18	24	23	10, 11
$[Cotn_2(NO_2)_2]^+$	*cis*	–	26	34	48	40	12
	trans	–	40	43	67	62	12
$[Copn_2(NO_2)_2]^+$	*cis*	–	33	25	46	50	13
	trans	–	50	43	72	70	13
$[Cotngly(NO_2)_2]$	*cis*	86	85	89	90	88	14
	trans	94	96	96	95	95	14
$[Cotn\beta\text{-}ala(NO_2)_2]$	*cis*	85	80	82	86	81	14
	trans	93	94	92	96	90	14
$[Coen\beta\text{-}ala(NO_2)_2]$	*cis*	89	87	79	88	84	14
	trans	96	95	92	99	94	14

[a] en = 1,2-Diaminoethane; tn = 1,3-diaminopropane; pn = 1,2-diaminopropane; glyH = glycine; β-alaH = β-alanine.
[b] Syntheses used.

Co(III) complex was used. The development of chromatograms was performed by the ascending method (Fig. 1). The developing time was 30–40 min, and the solvent front travelled about 5 cm. Detection was performed by keeping the plates for 10 min above 2 *M* ammonium sulphide solution. All investigations were carried out at room temperature (22 ± 1°C).

RESULTS AND DISCUSSION

Characteristics of the sorbent prepared

It has been established by electron microscopy that the sorbent prepared consists of grain-like particles grouped into agglomerates of different size (Fig. 2). On the basis of X-ray analysis, it can be concluded that the sorbent prepared is not completely amorphous, its pattern indicating a certain degree of an ordered structure.

Infrared spectra of the prepared sorbent and of ground PAN fibres used as the starting material were identical, which proves that no chemical changes take place in the course of sorbent preparation. The spectra clearly show the presence of carboxylic groups, which probably originate from comonomers possessing carboxylic groups (*e.g.*, itaconic acid[3]).

The mean particle size of the sorbent prepared was 4.7 μm; 80% of the particles had a diameter between 2 and 12 μm. The pore volume of the sorbent was 1.7 cm^3/g and its ion-exchange capacity was 1.0 mequiv./g. The specific surface area of the sorbent was 55 m^2/g.

From the above, it can be concluded that the polyacrylonitrile sorbent prepared fulfils all the conditions required for its successful application in thin-layer chromatography[15]. This is demonstrated by the fact that the isomer separations and spot shapes obtained were aproximately of the same quality as those which we obtained in a previous study[16] in which silica gel G-RS (Carlo Erba, Milan, Italy) was used.

Chromatographic separations

The R_F values obtained and the compositions of the solvent systems applied are given in Table I. To check the applicability of the sorbent prepared, seven pairs of *cis–trans* isomeric cobalt(III) complexes of the cationic type and three pairs of the neutral type were chromatographed. The solvent systems used were water and aqueous solutions of different electrolytes having concentrations of 0.1% and 1%, respectively. In all instances it was been established that the *trans* isomers exhibit higher R_F values than the corresponding *cis* isomers, which is in accordance with the previously established rule[16], obtained by chromatographing the isomers on silica gel with single solvents. This analogy exists in spite of the fact that silica gel contains on its surface localized positive charges, originating from protons of silanol groups, whereas polyacrylonitrile contains negative charges, originating from cyano groups[2]. On this basis, it may be concluded that the same regularity exists regardless of the adsorbent surface charge. In this connection, it may be assumed that the adsorption mechanism, involving hydrogen bond formation, is dominant in the chromatographic separation process. In the former instance hydrogen bonds would be formed between silanol protons of the silica gel and markedly electronegative atoms of the ligands, whereas in the latter instance, where hydrogen bonds between polyacrylonitrile and the complexes are concerned, hydrogen atoms from the ligands would be bonded to cyano groups of the sorbent.

As regards the mechanism of separation of the investigated cationic complexes, when potassium perchlorate was used as the solvent, it may be assumed that in addition to adsorption, cation exchange at carboxylic groups of the sorbent also takes place. For check this assumption, we carried out elution with perchloric acid solution in order to prevent the protolysis of the sorbent carboxylic groups and thus render impossible the process of ion exchange. As the results obtained were analogous to those obtained with a solvent system that contained no acid, it may be assumed that in both instances adsorption is the dominant separation mechanism. However, with complexes of the neutral type, only the adsorption separation mechanism may be involved.

Taking into consideration the nature of our sorbent, containing cyano groups with localized negative charges, and also carboxylic groups capable of exchanging cations, cationic complexes would be expected to be more strongly sorbed and to exhibit lower R_F values than neutral complexes, which was observed in all instances studied. The former consideration is supported by the fact that when water was used as the solvent the cationic complexes could not be chromatographed, as the spots were elongated from the start, whereas the complexes of the neutral type gave well defined spots. In addition, a comparison of R_F values obtained with solvent systems containing 0.1% and 1% solutions of the same electrolyte revealed that the elution capacity of 1% solutions was considerably higher than that of 0.1% solutions when cationic complexes were chromatographed. However, with neutral complexes this effect was insignificant.

It is concluded that the polyacrylonitrile sorbent can be applied to thin-layer chromatographic separations.

ACKNOWLEDGEMENTS

The authors are grateful to the Republic Fund for financial support, to Prof. I. Krstanović for recording and interpreting the X-ray patterns and to Mrs. Galebović for measuring the infrared spectra.

REFERENCES

1 *Römpps Chemie-Lexikon*, Franckh'sche Verlagshandlung, Stuttgart, 1966, VI ed., Band III, p. 5021; VIII ed., Band V, 1987, p. 3274.
2 A. V. Kiselev and J. Jasin, *Gas- und Flüssigadsorptionschromatographie*, Hüthig, Heidelberg, 1985, p. 37.
3 *Kratkaya Khimicheskaya Entsiklopediya*, Vol. IV, Sovetskaya Entsiklopediya, Moscow, 1965, p. 121.
4 G. Hesse, H. Engelhardt and R. Kaltwasser, *Chromatographia*, 1 (1968) 302.
5 N. G. Polyanskii, G. V. Gorbunov and N. L. Polyanskaya, *Metody Issledovaniya Ionitov*, Khimiya, Moscow, 1976, p. 208.
6 F. Gelferikh, *Ionity*, Izdatelstvo inostrannoi literatury, Moscow, 1962, p. 85.
7 F. H. Pollard, A. J. Banister, W. J. Geary and G. Nickless, *J. Chromatogr.*, 2 (1959) 372.
8 S. M. Jörgensen, *Z. Anorg. Allg. Chem.*, 17 (1898) 455.
9 A. Werner, *Chem. Ber.*, 44 (1911) 2445.
10 A. Werner, *Justus Liebigs Ann. Chem.*, 1 (1912) 386.
11 A. Werner, *Z. Anorg. Allg. Chem.*, 22 (1900) 91.
12 M. B. Ćelap, M. J. Malinar and P. N. Radivojša, *Inorg. Chem.*, 14 (1975) 2965.
13 T. E. MacDermott, *Inorg. Chim. Acta*, 3 (1969) 246.
14 M. B. Ćelap, M. J. Malinar and T. J. Janjić, *Rev. Chim. Miner.*, 13 (1976) 269.
15 S. Perri, R. Amos and P. Bryner, *Prakticheskoe Rukovodstvo po Zhidkostnoi Khromatografii*, Mir, Moscow, 1974, p. 59.
16 M. B. Ćelap, G. Vučković, M. J. Malinar, T. J. Janjić and P. N. Radivojša, *J. Chromatogr.*, 196 (1980) 59.

Journal of Chromatography, 481 (1989) 471–476
Elsevier Science Publishers B.V., Amsterdam — Printed in The Netherlands

CHROM. 21 766

Note

Effect of the chelate ring size of diamine cobalt(III) complexes on their R_F values obtained by paper chromatography

Ž. Lj. TEŠIĆ, T. J. JANJIĆ, M. J. MALINAR and M. B. ĆELAP*
Faculty of Chemistry, University of Beograd, Studentski trg 16, P.O. Box 550, 11001 Belgrade (Yugoslavia)
(Received May 12th, 1989)

The effect of the chelate ring size of diamine cobalt(III) complexes on their R_F values obtained by paper chromatography has so far been investigated only in one instance, in which Ćelap *et al.*[1] chromatographed 35 cobalt(III) complexes containing five- and/or six-membered ligands. By the use of ten solvent systems it was established that enlargement of the chelate ring causes an increase in the R_F values of metal complexes. A linear dependence was found between the R_M values and the number of five-membered rings substituted by the corresponding six-membered rings. Continuing these investigations, in this work we studied the effect of seven-membered rings of the diamine type.

EXPERIMENTAL

All the investigated complexes were prepared according to procedures reported in the literature (Table I). Chromatographic separations were carried out by the ascending method on Whatman No. 1 paper strips (23 × 3 cm), as described in detail previously[2].

RESULTS AND DISCUSSION

As can be seen from Table I, the effect of the chelate ring size of diamine ligands of cobalt(III) complexes was studied by chromatographing 21 cationic and neutral complexes. With the exception of tris(diamine) complexes, the investigated complexes contained, in addition to diamine, some of the following ligands: glycinato, (*R*)-alaninato and/or nitro ligands. Chromatographic separations were achieved with 14 solvent systems containing an organic component and water, and sometimes also an electrolyte (mineral acid or salt). The composition of the solvent systems applied is given in Table II. As can be seen from Table I, in all the instances studied the R_F values of metal complexes increased with enlargement of the chelate ring size. A linear dependence was also found between the chelate ring size and the R_M values of the investigated complexes (Figs. 1–4). In all the instances studied the straight lines had a negative slope.

From the above, it can be concluded that the earlier established rule[1], according

0021-9673/89/$03.50

TABLE I

R_F VALUES OF THE INVESTIGATED COMPLEXES OBTAINED BY PAPER CHROMATOGRAPHY

No.	*Isomer*	*Absolute configuration*	*Complex*[a]	*Ref.*	$R_F \times 100$[b]													
					1	*2*	*3*	*4*	*5*	*6*	*7*	*8*	*9*	*10*	*11*	*12*	*13*	*14*
1	*cis*-(NO_2), *trans*-(NH_2)-		$[Co(NO_2)_2glyen]$	3	30	58	63	52	40	63	69	86	41	38	26	67	82	–
2			$[Co(NO_2)_2glytn]$	4	43	66	79	64	49	75	82	94	51	51	42	78	87	–
3			$[Co(NO_2)_2glytmd]$	5	56	73	86	75	59	88	90	98	60	64	68	84	92	–
4	*trans*-(NO_2)-		$[Co(NO_2)_2glyen]$	5	22	33	52	47	32	50	62	82	25	30	16	63	69	–
5			$[Co(NO_2)_2glytn]$	4	30	48	61	55	45	68	73	90	36	45	25	68	78	–
6			$[Co(NO_2)_2glytmd]$	5	40	64	67	62	58	81	81	95	51	59	36	72	87	–
7	*cis*-(NO_2)-		$[Co(NO_2)_2en_2]^+$	6	23	43	70	44	49	19	71	91	38	44	68	67	86	11
8			$[Co(NO_2)_2tn_2]^+$	7	41	62	80	62	65	31	76	–	55	61	87	82	94	19
9			$[Co(NO_2)_2tmd_2]^+$	5	66	80	90	83	78	52	83	–	72	77	97	96	98	30
10	*trans*-(NO_2)-		$[Co(NO_2)_2en_2]^+$	6	13	29	49	38	45	5	61	90	28	32	60	56	77	5
11			$[Co(NO_2)_2tn_2]^+$	7	32	41	64	55	63	10	72	–	45	56	87	72	90	13
12			$[Co(NO_2)_2tmd_2]^+$	5	43	77	84	66	76	29	82	–	64	70	94	84	95	26
13			$[Coen_3]^{3+}$	8	21	10	62	56	–	13	75	64	36	14	36	63	60	16
14			$[Cotn_3]^{3+}$	8	32	15	76	71	–	22	80	94	52	51	45	72	76	24
15			$[Cotmd_3]^{3+}$	9	52	24	87	85	–	46	87	–	72	83	58	82	89	32
16	*cis*-(NO_2)-	$-(+)_{589}-$	$[Co(NO_2)_2(R\text{-ala})en]$	10	39	64	76	52	47	80	85	94	58	47	37	71	91	35
17			$[Co(NO_2)_2(R\text{-ala})tn]$	10	55	78	86	68	62	85	90	98	70	63	51	83	95	49
18			$[Co(NO_2)_2(R\text{-ala})tmd]$	5	68	87	94	79	75	90	94	–	79	73	66	93	98	64
19	*trans*-(NO_2)-	$-(-)_{589}-$	$[Co(NO_2)_2(R\text{-ala})en]$	10	48	67	77	57	50	82	87	96	60	51	39	75	94	38
20			$[Co(NO_2)_2(R\text{-ala})tn]$	10	64	81	88	74	66	87	91	–	72	66	55	86	97	51
21			$[Co(NO_2)_2(R\text{-ala})tmd]$	5	76	90	95	82	78	94	95	–	82	79	70	94	–	66

[a] glyH = glycine; *R*-alaH = (*R*)-alanine; en = 1,2-diaminoethane; tn = 1.3-diaminopropane; tmd = 1,4-diaminobutane.
[b] The compositions of the solvent systems are given in Table II.

TABLE II

SOLVENT SYSTEMS USED

No.	*Composition*	*Proportions*[a]
1	Isopropanol–water–conc. HNO_3	75:20:5 (v/v/v)
2	Ethyl acetate–ethanol–water	50:30:20 (v/v/v)
3	Acetone–water–conc. HNO_3	75:20:5 (v/v/v)
4	Ethanol–water–conc. HNO_3	75:20:5 (v/v/v)
5	Ethanol–water	80:20 (v/v)
6	Dioxan–water	80:20 (v/v)
7	Dioxan–water–KI	75:25:1 (v/v/w)
8	Phenol saturated with water	
9	Methanol–water–LiCl	90:10:5 (v/v/w)
10	Phenol–ethanol–water	10:70:20 (w/v/v)
11	Cyclohexanone–ethanol–water–KI	60:25:15:1 (v/v/v/w)
12	Tetrahydrofuran–water–conc. HNO_3	65:30:5 (v/v/v)
13	Pyridine–water–KI	80:20:1 (v/v/w)
14	Cyclohexanol–ethanol–water–conc. HNO_3	50:25:15:10 (v/v/v/v)

[a] v Refers to volume in millilitres; w refers to weight in grams.

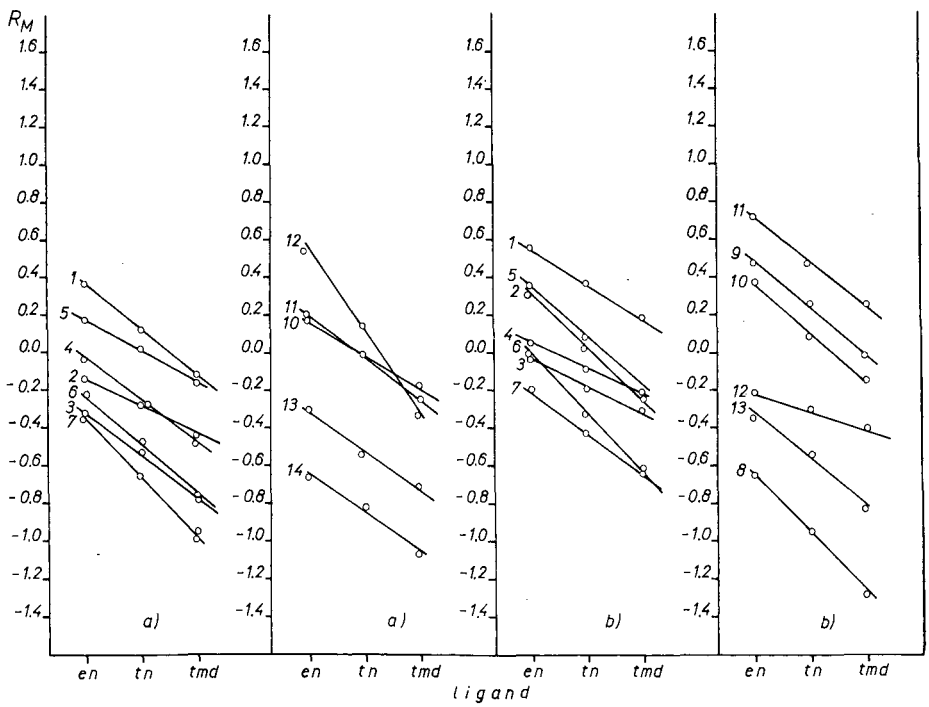

Fig. 1. Dependence of the R_M values on the chelate ring size of the following complexes (see Table I): (a) 1–3; (b) 4–6. The numbers on the lines refer to the solvent systems used (see Table II).

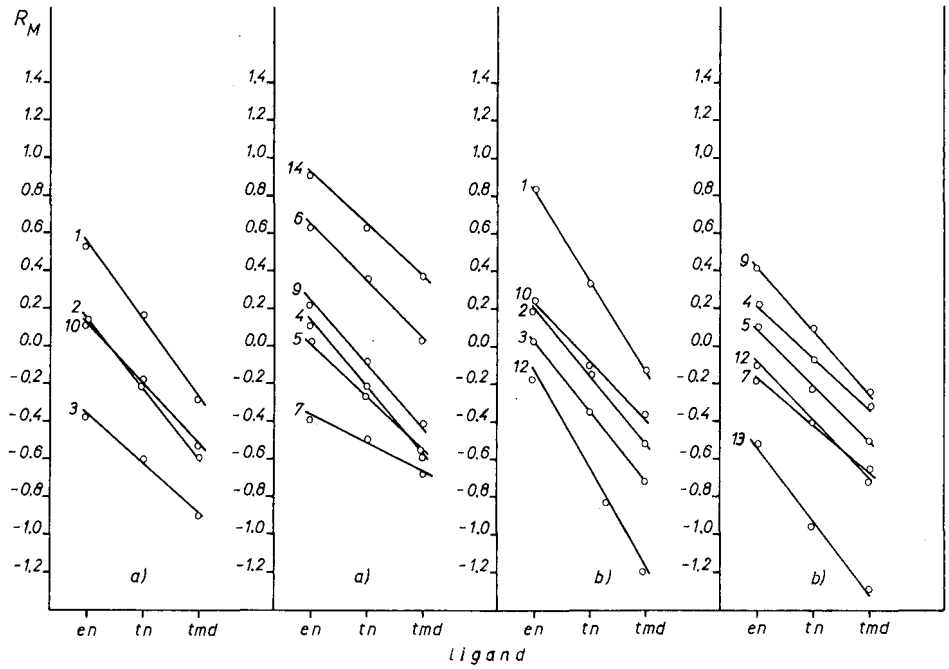

Fig. 2. Dependence of the R_M values on the chelate ring size of the following complexes (see Table I); (a) 7–9; (b) 10–12. The numbers on the lines refer to the solvent systems used (see Table II).

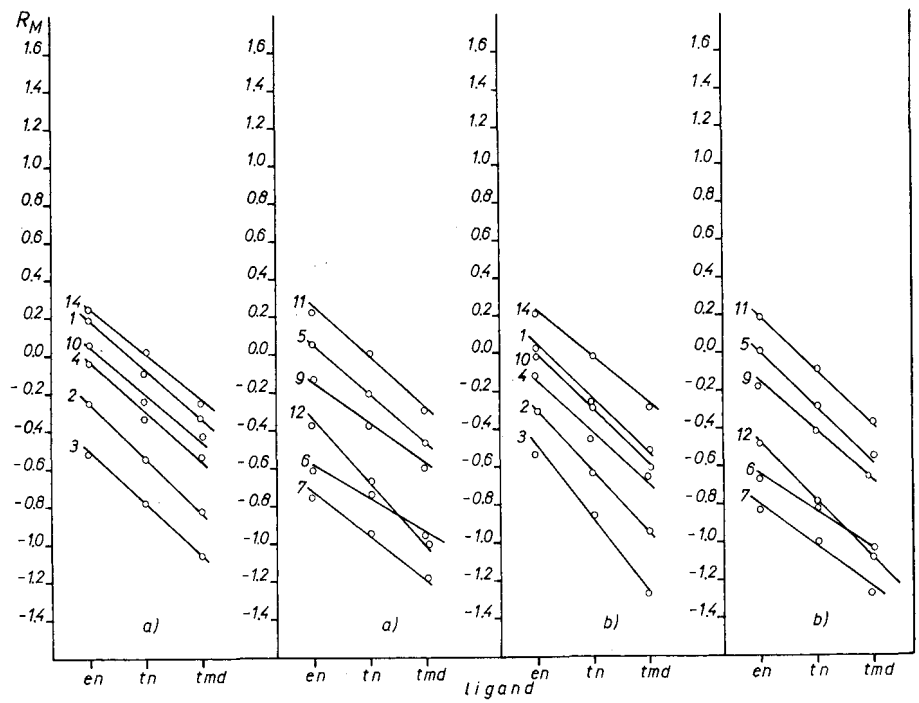

Fig. 3. Dependence of the R_M values on the chelate ring size of the following complexes (see Table I): (a) 13–15; (b) 16–18. The numbers on the lines refer to the solvent systems used (see Table II).

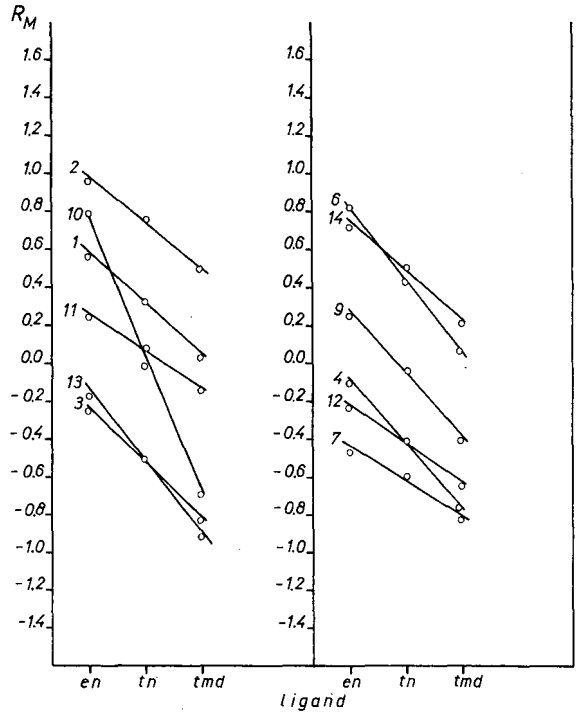

Fig. 4. Dependence of the R_M values on the chelate ring size of complexes 19–21 (see Table I). The numbers on the lines refer to the solvent systems used (see Table II).

to which the R_F values obtained by paper chromatography increase with enlargement of the chelate ring size of metal complexes, is valid also for seven-membered rings. It is worth mentioning that this regularity had already been established in thin-layer chromatographic separations on silica gel by the use of single-component solvent systems, with the exception of water[11]. As regards the mechanism of the separation on paper performed in this study it may be assumed that "normal" phase partition chromatography is involved, as it is known that analogous compounds possessing a larger hydrophobic part exhibit higher R_F values, owing to their greater solubility in the mobile phase[12]. Hence a new possibility is offered for the determination of the composition of the corresponding complexes.

ACKNOWLEDGEMENT

The authors are grateful to the Serbian Research Fund for financial support.

REFERENCES

1 M. B. Ćelap, M. J. Malinar, S. Sarić, T. J. Janjić and P. N. Radivojša, *J. Chromatogr.*, 139 (1977) 45.
2 T. J. Janjić, Ž. Lj. Tešić and M. B. Ćelap, *J. Chromatogr.*, 280 (1983) 382.
3 N. Matsuoka, J. Hidaka and Y. Shimura, *Bull. Chem. Soc. Jpn.*, 39 (1966) 1257.
4 M. B. Ćelap, M. J. Malinar and T. J. Janjić, *Rev. Chim. Miner.*, 13 (1976) 269.

5 R. Herak, M. J. Malinar, B. Prelesnik and M. B. Ćelap, *Book of Abstracts of the XXXI Gathering of Serbian Chemists, Beograd, 1989*, Serbian Chemical Society, Beograd, 1989, p. 30.
6 Y. Shimura, *J. Am. Chem. Soc.*, 73 (1951) 5079.
7 M. B. Ćelap, M. J. Malinar and P. N. Radivojša, *Inorg. Chem.*, 14 (1975) 2965.
8 F. Woldbye, *Proc. R. Soc. London, Ser. A.*, 297 (1967) 79.
9 J. Fujita and H. Ogino, *Chem. Lett.*, (1974) 57.
10 M. J. Malinar, R. Herak, M. B. Ćelap, N. Pavlović, S. Milić and D. Stojanov, *Glas. Hem. Druš. Beograd*, 46 (1981) 303.
11 G. Vučković, M. J. Malinar and M. B. Ćelap, *J. Chromatogr.*, 454 (1988) 362.
12 B. Fried and J. Sherma, *Thin-Layer Chromatography*, Marcel Dekker, New York, 2nd ed., 1986, p. 10.

Journal of Chromatography, 481 (1989) 477–479
Elsevier Science Publishers B.V., Amsterdam — Printed in The Netherlands

CHROM. 21 838

Letter to the Editor

2-Trichloromethylbenzimidazole, a selective chromogenic reagent for the detection of some azines on thin-layer plates

Addendum

Sir,

In a previous study[1], some azines were detected on thin-layer chromatographic (TLC) plates using their reaction with 2-trichloromethylbenzimidazole (TCMB). The structure of the product of the reaction of TCMB with pyridine shown here was suggested[1]. In this addendum, the analytical and spectral evidence that confirms this structure are presented.

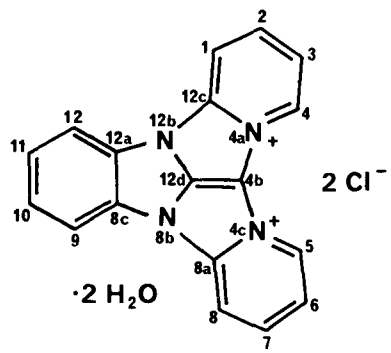

EXPERIMENTAL

4a,4c,8b,12b-Tetraazadibenzo[a,f]indano[1,2,3-cd]pentalene-4a,4c-diinium dichloride dihydrate

TCMB (234 mg, 1 mmol, freshly recrystallized from chloroform) was dissolved in pyridine (790 mg, 10 mmol, 99.8% chromatographic standard purity). An amaranth product was precipitated after several minutes. After 5 h, the solid product was filtered off and washed with diethyl ether and acetone and dried under vacuum over phosphorus pentoxide until the odour of pyridine had disappeared. The yield was 122 mg (31%); m.p. $>360°C$.

The crude product was purified by preparative TLC on precoated Polyamid 11 F_{254} aluminium sheets, 0.2 mm thick (Merck). The chromatograms were developed in acetic acid–water (1:9, v/v). The amaranth zone ($R_F = 0.51$) was scraped from the plate and eluted with methanol. The characteristics were as follows.

Elemental analysis: found, C 54.71, H 4.18, N 13.61, Cl 17.70; calculated for $C_{18}H_{12}N_4Cl_2 \cdot 2H_2O$, C 54.26, H 4.12, N 14.32, Cl 18.12%.

0021-9673/89/$03.50

Electron impact mass spectrometry (EI MS) (LKB 9000A, 70 eV, 250°C); *m/z* (intensity, %): 286 (1.0) 285 (23.8), M^+ 284 (100.0), 283 (64.1), M^{2+} 142 (1.1).

High-resolution EI MS (Finnigan-MAT 8200, resolution 7000): M^+ *m/z* 284, found 284.1056, calculated for $C_{18}H_{12}N_4$ 284.1062; M^{2+} *m/z* 142, found 142.0523, calculated for $C_9H_6N_2$ 142.0531.

Field desorption (FD) MS (Varian-MAT 711, J_E = 20 mA): *m/z* (intensity, %), 285 (33.5), M^+ 284 (100.0).

^1H NMR (Jeol JNM-100, 100 MHz, CH_3OH-d_4, hexamethyldisiloxane as internal lock, 25°C): δ (ppm), 6.5–9.6 (m).

IR (Specord IR-75, KBr pellets): ν (cm^{-1}), 3400sb (H_2O), 3090w, 3040w, 3015m (C–$H_{arom.}$), 1635s (C=N), 1630m, 1605s, 1590m, 1540m, 1510s (C=C and C=N of aromatic rings), 1460m, 1440m, 1390m, 1305w, 1205m, 1185m; 765m, 745s (2-substituted pyridie).

UV (Pye Unicam SP 700, CH_3OH): $\lambda_{max.}$ (nm) (log $E^{1\%}_{1cm}$), 210 (2.86), 240 (2.97), 350 (2.67), 520 (2.53).

The same procedure was repeated using pyridine-d_5 (of NMR solvent grade) and the deuterium-labelled product was obtained, with the following characteristics.

EI MS (70 eV, 20°C): *m/z* (intensity, %), 294 (6.1), 293 (34.6), M^+ 292 (100.0), 291 (27.3), 290 (61.9), 289 (10.0), 288 (11.3), M^{2+} 146 (9.9).

IR (KBr pellets): ν (cm^{-1}), 2700 mb (^2H_2O), 2270 m (C–$^2H_{arom.}$).

DISCUSSION

The proposed structure shown above is confirmed by the analytical and spectral data. The high polarity and m.p. of the examined compounds are indicative of an ionic structure.

In the mass spectra of the product (EI and FD), the molecular ion of the cationic fragment at *m/z* 284 (no chlorine) was found and its formula was determined as $C_{18}H_{12}N_4$ using high-resolution EI MS.

The formula $C_{18}H_{12}N_4Cl_2 \cdot 2H_2O$ was confirmed by elemental analysis. Therefore, the identified product must be a dication.

The molecular ion M^{2+} is converted into the base ion M^+ after the addition of an electron under EI ionization conditions: $M^{2+} + e^- \rightarrow M^+$. This phenomenon, characteristic of negative ionization MS, was also observed in the EI mass spectra of some dications, *e.g.*, diquat dibromide.

The UV and ^1H NMR spectra confirm the aromatic character of the molecule.

The band characteristics of aromatic C–H, C=C and C=N bonds was found in the IR spectrum. The bands typical of 2-substituted pyridines were present. No N^+–H band was observed.

In the EI mass spectrum of the deuterium-labelled compound, the M^+ ion of the octadeuterated derivative at *m/z* = 292 was observed. In the IR spectrum the bands characteristic of ^2H_2O and C–^2H were found.

The above evidence indicates that the structure shown is the most probable for the major product of the reaction of TCMB with pyridine.

ACKNOWLEDGEMENTS

The authors express their gratitude to Halina Jelin and Jerzy Zakrzewski for valuable assistance.

Institute of Industrial Organic Chemistry,
Annopo 16, 03-236 Warsaw (Poland)

LESZEK KONOPSKI*
BOLESŁAW JERZAK

1 L. Konopski and B. Jerzak, *J. Chromatogr.*, 363 (1986) 394–396.

(First received May 25th, 1989; revised manuscript received July 28th, 1989)

Journal of Chromatography, 481 (1989) 480–482
Elsevier Science Publishers B.V., Amsterdam — Printed in The Netherlands

CHROM. 21 657

Book Review

Natural products isolation, separation methods for antimicrobials, antivirals and enzyme inhibitors (*Journal of Chromatography Library Series*, Vol. 43), edited by G. H. Wagman and R. Cooper, Elsevier, Amsterdam, Oxford, New York, Tokyo, 1989, XIII + 619 pp., price Dfl. 285.00, US$ 139.00, ISBN 0-444-87147-0.

This book is an update of a previous volume published in 1978 (*Antibiotics: isolation, separation and purification*, edited by M. J. Weinstein and G. H. Wagman). It covers new material concerning the then known antibiotics and data on bioactive natural products discovered since.

Of 14 chapters, the first three concern solely chromatographic techniques and their applications in the field. A detailed description of instrumentation and techniques in counter-current chromatography is presented in Chapter 1. Specific examples of applications include a variety of natural products such as terpenoids, alkaloids and (mostly) antibiotics belonging to macrolides, sesquiterpenes, actinomycins, tetramic acids, quinoxalines etc.

In Chapter 2, detection methods are described for fermentation samples containing aminoglycoside, tetracycline, macrolide, oligosaccharide and nucleoside antibiotics.

In addition to classical extraction, separation and purification schemes, Chapter 3 is devoted to affinity chromatography and high-performance liquid chromatography (HPLC) in the purification of glycopeptide antibiotics such as vancomycins. Preparative reversed-phase separations of glycopeptides are presented. A very interesting chromatographic application of the biochemical mode of action of these antibiotics has been developed. Glycopeptide antibiotics kill bacteria by binding to peptidoglycan pentapeptide terminating in D-Ala–D-Ala, thereby inhibiting the extracellular peptidases which cross-link the bacterial peptidoglycans in the cell wall. This particular affinity for peptides was used as a basis for affinity column isolation procedures with D-Ala–D-Ala as the ligand and Affi-gel 10 as the support. New glycopeptide antibiotics have also been discovered using this principle.

In Chapter 4, nucleoside peptide antibiotics (nikkomycins and polyoxins) are described, including data on their isolation and properties. Methods based on paper chromatography (PC), paper electrophoresis (PE), thin-layer chromatography (TLC) and HPLC of these antibiotics are presented. Chemochromatography has been succesfully used for the separation of the homologous nikkomycin Z and X by adding sodium bisulphide (reacting specifically with the latter) to the mobile phase in HPLC.

Saframycin antibiotics and their detection, isolation and properties are considered in Chapter 5. Originally, the first members of the group were detected chromatographically (TLC) by means of an alkaloid reagent rather than usual biological assays. Some of them were later isolated from sponges (presumably produced by some symbiotic microorganisms). Among chromatographic techniques, TLC and HPLC of these antibiotics are included.

Chapters 6–8 are devoted to novel β-lactam antibiotics (cephabacins, monocyclic nocardicins and monobactams and also carbapenems). Applications of PC, PE, TLC and HPLC are richly documented in these chapters. Ion-exchange, partition gel and cellulose chromatography are extensively used in the isolation and purification of many β-lactams.

Antiparasitic macrocyclic avermectins are included in Chapter 9. TLC and HPLC assays have been widely used in their screening methods. Preparative HPLC and (mostly) Sephadex LH-20 chromatography have helped to separate the avermectin components.

The increasing use of chromatographic techniques in the field is stressed in Chapter 10 by the following statement: "Probably the most striking change to occur in the isolation of marine natural products since the publication of the preceding volume (*i.e.*, the afore mentioned Weinstein–Wagman book) is the heavy reliance placed upon high-performance liquid chromatography. Of the fifty-six sections devoted to marine-derived antibiotics in the previous volume, only one mentioned the use of HPLC. In the intervening years silica HPLC and bonded-phase RP-HPLC have become routine. Intermediate speed and efficiency column chromatographic techniques which have been used in various forms for years have now been optimized and published. Examples include flash chromatography (an outgrowth of short column chromatography), reversed-phase flash chromatography and vacuum liquid chromatography. These techniques serve as useful cleanup steps prior to HPLC and are often adequate to afford purified natural products" (p. 380).

Applications of reversed-phase and hydrogen-bonding HPLC and also immunoaffinity and Blue-Sepharose chromatography in purifications of interferons are presented in Chapter 11. Human leukocyte interferon synthesized by bacteria is now purified by employing immobilized monoclonal antibodies in immunoaffinity chromatography. Utilization of this, essentially, one-step purification procedure provided the first pure human interferon for clinical evaluation in 1981.

Enzyme inhibitors produced by microorganisms are extensively reviewed in Chapter 12. Applications of various techniques of liquid column chromatography (silica gel, ion-exchange, Sephadex, DEAE-Sephadex, etc.) in their isolation and purification are well documented.

In Chapter 13, alkaloidal glycosidase inhibitors from plants are described. The reason why they were discovered only relatively recently is that most of them do not react with reagents traditionally used to detect alkaloids in simple TLC and PC screens, nor can they be extracted into chloroform from aqueous alkaline solutions. Methods for their preliminary ion-exchange separations and gas chromatographic analysis (after trimethylsilylation) are also included.

"The final chapter is a futuristic essay indicating the challenges of the plant chemist to isolate minute amounts of natural products" (Preface). Those described in the chapter include germination stimulators, haustoria-inducing compounds, cell cycle-controlling hormones, tumorigenic substances and other morphogenic agents. Chromatographic methods have often been used in their isolation and characterization.

The volume has a list of abbreviations, a subject index and a list of numbered compounds. Regretfully, an author index is missing. Except for Chapters 8, 11 and 12, the most recent papers cited were published in 1987.

Being a multi-author volume and produced from camera-ready manuscript, the book has rather heterogeneous presentations of tables and illustrations but few typing errors were noted. The book has been written by expert scientists and can be highly recomended to workers in the field of bioactive natural products.

Bratislava (Czechoslovakia) VLADIMÍR BETINA

Journal of Chromatography, 481 (1989) 483
Elsevier Science Publishers B.V., Amsterdam — Printed in The Netherlands

CHROM. 21 840

Book Review

Gas chromatography and lipids, by W. W. Christie, The Oily Press, Ayr, 1989, 307 pp., price US$ 50.00, ISBN 0-9514171-0-X.

This book has been written as a complement to the author's earlier text on high-performance liquid chromatography and lipids. It takes note of the remarkable improvement in resolution attainable by gas–liquid chromatography (GLC) due to the availability of capillary columns fabricated from fused silica. The author has intended the book "for the laboratory bench and not the library shelf", yet has succeeded to write it in an easily readable form. Following a brief introduction to the structure, extraction and preliminary resolution of lipids (Chapter 2), and a general description of the theoretical aspects and instrumentation of GLC (Chapter 3), about 120 pp. are devoted to a most thorough coverage of the analysis of fatty acids, starting with preparation of derivatives (Chapter 4), GLC analysis (Chapter 5), isolation and identification by spectrometric and chemical degradation techniques (Chapter 6), and concluding with gas chromatography–mass spectrometry of fatty acids (Chapter 7). There is little that can be added to this discussion. It is followed by a less extensive coverage of the GLC analysis of lipids other than fatty acids (60 pp.), which includes the direct GLC resolution of molecular species of triradylglycerols and the diradylglycerol moieties of glycerophospholipids (Chapter 8) and indirect resolution of radylglycerols and ceramides based on application of complementary methods of analysis (Chapter 9). The book concludes with a chapter on miscellaneous GLC separations of lipids, dealing mainly with fatty alcohols and the hydrolysis products of ether lipids and long-chain bases. Again the coverage includes both historical and state-of-the-art methodology, which makes the reading more intelligible and interesting. Although the bibliography in all instances is extensive (over 1000 entries), it is not complete and the illustrations and citations used are selective and sometimes subject to argument. However, the incompleteness is acknowledged by the author as is the absence of a consistent effort in attributing scientific priority. These aspects of the research must be discovered by the reader by consulting the numerous reviews cited for background information. Since the advances in the field do not pause for reviews or books, certain areas of the discussion have already become outdated, while other areas have lived up to the expectations and projections of the author. The book is remarkably free of typographical and word-processing errors and is neatly printed.

In addition to the practical nature of the book, I wish to emphasize the sensible and thoughtful discussion of the rationale for analyzing intact molecular species, rather than just the fatty acids of lipids. Hopefully the arguments advanced and the practical feasibility demonstrated will convince more lipid chemists to undertake direct analyses of natural lipid mixtures, which previous authors and texts have failed to do. It should become apparent that it is difficult or impossible to uncover the biological function of a lipid structure after it has been destroyed by transmethylation. This book should encourage everyone to look beyond fatty acid analysis. I highly recommend the book for laboratory benches and library shelves alike.

Toronto (Canada) A. KUKSIS

Author Index

PUBLICATION SCHEDULE FOR 1989

Journal of Chromatography and Journal of Chromatography, Biomedical Applications

MONTH	J	F	M	A	M	J	J	A	S	O	N	D
Journal of Chromatography	461 462 463/1	463/2 464/1	464/2 465/1 465/2	466 467/1 467/2	468 469 470/1 470/2	471 472/1 472/2 473/1	473/2 474/1 474/2 475	476 477/1 477/2	478/1 478/2 479/1	479/2 480	481 482/1	–[a]
Bibliography Section		486/1		486/2		486/3		486/4		486/5		486/6
Biomedical Applications	487/1	487/2	488/1 488/2	489/1 489/2	490/1 490/2	491/1	491/2	492 493/1	493/2 494	495	496/1 496/2	497

[a]The publication schedule for further issues will be published later.

INFORMATION FOR AUTHORS

(Detailed *Instructions to Authors* were published in Vol. 478, pp. 453–456. A free reprint can be obtained by application to the publisher, Elsevier Science Publishers B.V., P.O. Box 330, 1000 AH Amsterdam, The Netherlands.)

Types of Contributions. The following types of papers are published in the *Journal of Chromatography* and the section on *Biomedical Applications*: Regular research papers (Full-length papers), Notes, Review articles and Letters to the Editor. Notes are usually descriptions of short investigations and reflect the same quality of research as Full-length papers, but should preferably not exceed six printed pages. Letters to the Editor can comment on (parts of) previously published articles, or they can report minor technical improvements of previously published procedures; they should preferably not exceed two printed pages. For review articles, see inside front cover under Submission of Papers.

Submission. Every paper must be accompanied by a letter from the senior author, stating that he is submitting the paper for publication in the *Journal of Chromatography*. Please do not send a letter signed by the director of the institute or the professor unless he is one of the authors.

Manuscripts. Manuscripts should be typed in double spacing on consecutively numbered pages of uniform size. The manuscript should be preceded by a sheet of manuscript paper carrying the title of the paper and the name and full postal address of the person to whom the proofs are to be sent. Authors of papers in French or German are requested to supply an English translation of the title of the paper. As a rule, papers should be divided into sections, headed by a caption (*e.g.*, Summary, Introduction, Experimental, Results, Discussion, etc.). All illustrations, photographs, tables, etc., should be on separate sheets.

Introduction. Every paper must have a concise introduction mentioning what has been done before on the topic described, and stating clearly what is new in the paper now submitted.

Summary. Full-length papers and Review articles should have a summary of 50–100 words which clearly and briefly indicates what is new, different and significant. In the case of French or German articles an additional summary in English, headed by an English translation of the title, should also be provided. (Notes and Letters to the Editor are published without a summary.)

Illustrations. The figures should be submitted in a form suitable for reproduction, drawn in Indian ink on drawing or tracing paper. Each illustration should have a legend, all the *legends* being typed (with double spacing) together on a *separate sheet*. If structures are given in the text, the original drawings should be supplied. Coloured illustrations are reproduced at the author's expense, the cost being determined by the number of pages and by the number of colours needed. The written permission of the author and publisher must be obtained for the use of any figure already published. Its source must be indicated in the legend.

References. References should be numbered in the order in which they are cited in the text, and listed in numerical sequence on a separate sheet at the end of the article. Please check a recent issue for the layout of the reference list. Abbreviations for the titles of journals should follow the system used by *Chemical Abstracts*. Articles not yet published should be given as "in press" (journal should be specified), "submitted for publication" (journal should be specified), "in preparation" or "personal communication".

Dispatch. Before sending the manuscript to the Editor please check that the envelope contains three copies of the paper complete with references, legends and figures. One of the sets of figures must be the originals suitable for direct reproduction. Please also ensure that permission to publish has been obtained from your institute.

Proofs. One set of proofs will be sent to the author to be carefully checked for printer's errors. Corrections must be restricted to instances in which the proof is at variance with the manuscript. "Extra corrections" will be inserted at the author's expense.

Reprints. Fifty reprints of Full-length papers, Notes and Letters to the Editor will be supplied free of charge. Additional reprints can be ordered by the authors. An order form containing price quotations will be sent to the authors together with the proofs of their article.

Advertisements. Advertisement rates are available from the publisher on request. The Editors of the journal accept no responsibility for the contents of the advertisements.

For Superior Chiral Separation

CHIRALCEL, CHIRALPAK and CROWNPAK are now available from DAICEL and include 15types of HPLC columns which provide superior resolution of racemic compounds.

Drugs directly resolved on our DAICEL columns are given as follows;

SUBSTANCE	α	column	SUBSTANCE	α	column	SUBSTANCE	α	column
Alprenolol	3.87	OD	Gauifenesin	2.40	OD	Oxapadol	complete resolution	CA-1
Amphetamine	1.2	CR	Hexobarbital	1.7	CA-1	Oxazepan	4.36	OC
Atenoloi	1.58	OD	Homatropine	3.13	OD	Oxazolam	1.67	OF
Atropine	1.62	OD	Hydroxyzine	1.17	OD	Oxprenolol	6.03	OD
Baclofen	1.39	CR	Indapamide	1.58	OJ	Perisoxal	1.33	OF
Carbinoxamine	1.39	OD	Ketamine	complete resolution	CA-1		1.27	OD
Carteolol	1.86	OD				Pindolol	5.07	OD
Chlophedianol	2.82	OJ	Ketoprofen	1.46	OJ	Piprozolin	1.7	CA-1
Chlormezanone	1.47	OJ	Mephobarbital	5.9	OJ	Praziquantal	complete resolution	CA-1
Cyclopentolate	2.47	OJ		2.3	CA-1			
Diltiazem	1.46	OD	Methaqualone	2.8	CA-1	Propranolol	2.29	OD
	2.36	OF		7.3	OJ	Rolipram	complete resolution	CA-1
	1.75	OG	Methsuximide	2.68	OJ			
Disopyramide	2.46	OF	Metoprolol	complete resolution	OD	Sulconazole	1.68	OJ
Ethiazide	1.54	OF				Suprofen	1.6	OJ
Ethotoin	1.40	OJ	Mianserin	1.75	OJ	Trimebutine	1.81	OJ
Fenoprofen	1.35	OJ	Nilvadipine	complete resolution	OT	Warfarin	1.96	OC
Glutethimide	2.48	OJ						

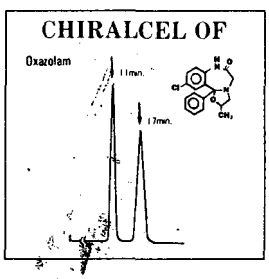

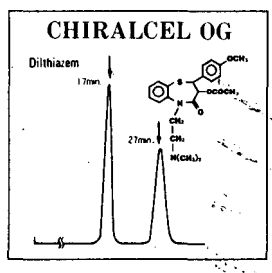

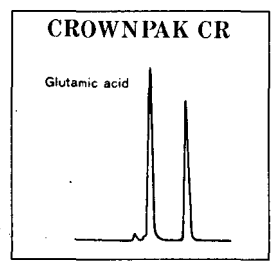

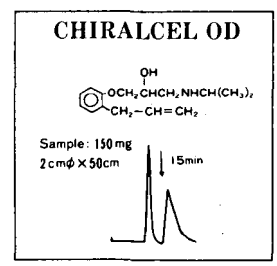

In addition to the drugs listed above, our chiral columns permit resolution also of the following: FMOC amino acids and Carboxylic acids, and Pesticides, for example Isofenfos, EPN and Acephate, and Synthetic intermediate 4-hydroxy cyclophentenone etc, Many other compounds besides these can be readily resolved.

▷ *Separation Service*

- A pure enantiomer separation in the amount of 100g~10kg is now available.
- Please contact us for additional information regarding the manner of use and application of our chiral columns and how to procure our separation service.

For more information about our Chiral Separation Service and Columns, please contact us!

DAICEL CHEMICAL INDUSTRIES, LTD.

8-1, Kasumigaseki 3-chome, Chiyoda-ku, Tokyo 100, Japan Phone: 03(507)3151 FAX: 03(507)3193

DAICEL (U.S.A.), INC.
Fort Lee Executive Park
Two Executive Drive, Fort Lee,
New Jersey 07024
Phone: (201)461-4466
FAX: (201)461-2776

DAICEL (U.S.A.), INC.
23456 Hawthorne Blvd.
Bldg. 5, Suite 130
Torrance, California. 90505.
Phone: 213-791-2030
FAX: 213-791-2031

DAICEL (EUROPA) GmbH
Königsallee 92a.
4000 Düsseldorf 1, F.R. Germany
Phone: (0211)134158
Telex: (41)8588042 DCEL D
FAX: (0211)879-8329

DAICEL CHEMICAL (ASIA) PTE.LTD.
65 Chulia Street #40-07
OCBC Centre, Singapore 0104.
Phone: 5332511
FAX: 5326454